

N.N.Maslov

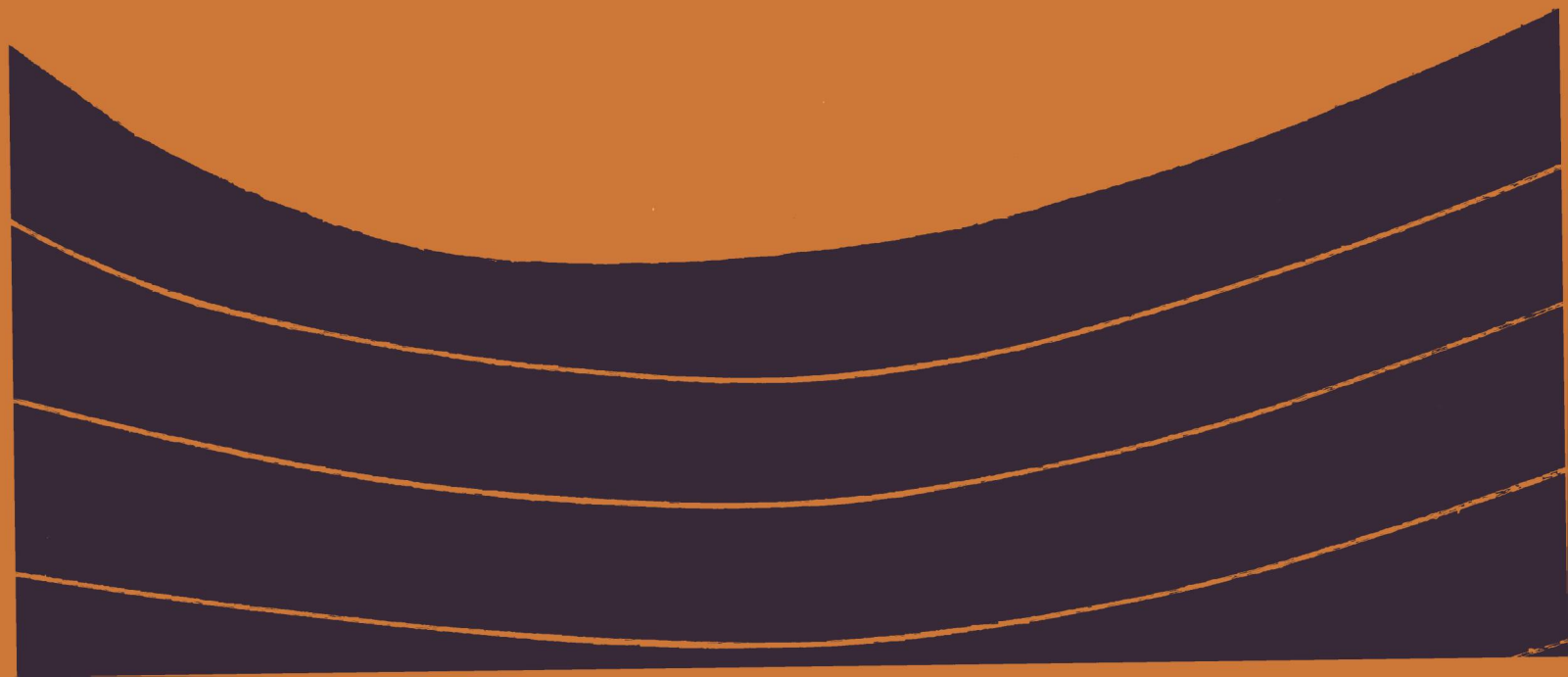
# Basic Engineering Geology

and

# Soil Mechanics

Mir Publishers

**Mir Publishers' books  
in foreign languages can be  
purchased or ordered through  
booksellers in your country  
dealing with  
V/O "Mezhdunarodnaya Kniga",  
the authorised exporters.**





# **BASIC ENGINEERING GEOLOGY AND SOIL MECHANICS**

**Н. Н. Маслов**

**Основы инженерной геологии  
и механики грунтов**

**Издательство «Высшая школа»  
Москва**

N. N. Maslov

**Basic  
Engineering  
Geology  
and  
Soil Mechanics**



**Mir Publishers Moscow**

**Translated from the Russian  
by V. V. Kuznetsov**

**First published 1987  
Revised from the 1982 Russian edition**

***Printed in the Union of Soviet Socialist Republics  
На английском языке***

**© Издательство «Высшая школа», 1982  
© English translation, Mir Publishers, 1987**



## **Preface**

Engineering geology and soil mechanics are disciplines concerned with the study and evaluation of environmental conditions at a purposed site where the designed structure is to be built and where its operating conditions are affected by the surrounding geological features.

By virtue of their subject matter both engineering geology and soil mechanics are general engineering disciplines. For college students specializing in transport technology they may provide a theoretical basis for such applied disciplines as road construction, construction of airfields, and the construction of bridges and tunnels.

The textbook is divided into four parts. Part One deals with elementary general geology. Part Two considers fundamentals of soil science for engineers. Part Three introduces elementary soil mechanics and Part Four, elementary engineering geology. This order of presentation mirrors the fact that the scientific basis of engineering geology is soil engineering and soil mechanics.

Both the theoretical and practical tasks faced by engineering geology can be solved based on natural and historical analysis utilizing field and laboratory investigations which, whenever possible, include physico-mechanical methods along with calculation formulae encompassing soil mechanics.

What makes the subject unique is that the physico-mechanical properties of soils and methods for their determination are studied from the viewpoint of engineering geology. Such an approach is justified by the obvious interconnection of these properties under particular natural conditions. It is important to note that in actual construction work undertaken in this country it is the engineering geological agencies that are fully responsible for studying the above properties and evaluating various design indices.

It was deemed unnecessary to add to the present book the impressive bulk of material of the last decade related to engineering geology and soil mechanics. This would have rendered the present volume excessively large and thus not expedient.

The ultimate goal of the author was to familiarize a beginning civil engineer with methods for solving problems relating to soil mechanics and

provide him with information that would be most likely to be of real use to him at the early stages of his engineering career. With this objective in mind the author made it a point to exclude all the data, conclusions and recommendations not verified in practice or of dubious importance, such as those which have not been proven by the nature of the phenomenon or ones that have no appreciable use.

Actual construction work has shown that due to a revolution in engineering methods young engineers should be taught a creative approach to tackling a particular engineering task. Hence the author's determination to make the book more than just a reference book covering a wide range of problems. Instead, he has restricted himself to a presentation of the major problems alone. For this reason, the author has endeavored to consider the theoretical aspects of the disciplines as they relate to practical tasks.

It would be appropriate to point out the great contribution made by Soviet scientists in the development and propagation of concepts bearing on engineering geology and soil mechanics. Credit must first be given to Academician G.O. Graftio who was the first to use and advance the ideas of engineering geology and soil mechanics resulting in the erection of unique engineering structures. Mention should also be made of Academician F.P. Savarensky whose activities did much to establish the Soviet school of engineering geology, connected with such notable men of science as I.M. Gersevanov, M.N. Goldshtein, I.V. Popov, E.M. Sergeev, N.A. Tsytovich and many more.

It is the author's pleasure to emphasize the important role played by my old co-worker, Assistant Professor and Candidate of Science (Geology and Mineralogy) M.F. Kotov in furthering a number of concepts proposed in the book. The author therefore extends sincere thanks to him. The author is also much indebted to Professor M.N. Goldshtein for his advice, assistance and courage in supporting a number of new procedures and theories which have been proposed in the present work.

The staff of the Leningrad Construction Engineering Institute (LISI) headed by Assistant Professor and Candidate of Science S.N. Sotnikov who reviewed the manuscript of the book have provided many useful suggestions and helped better arrange the material and elucidate some concepts outlined in the book. The author is deeply grateful to all of them. He also acknowledges the painstaking efforts undertaken by his constant assistant, Candidate of Science (Geology and Mineralogy) Z.V. Maslova-Pilgunova during the preparation of the manuscript for publication.

*N.N. Maslov*

# **Contents**

<b>Preface</b>	<b>5</b>
<b>Contents</b>	<b>7</b>
<b>Introduction</b>	<b>12</b>

## **Part One**

### **ELEMENTARY GENERAL GEOLOGY**

<b>Chapter 1. The Earth as a Cosmic Body, Tectonics</b>	<b>15</b>
Sec. 1.1. General Facts on the Structure of the Globe	15
Sec. 1.2. The Structure of the Earth's Crust	16
Sec. 1.3. The Role of Tectonic Phenomena in the Earth's Life	17
<b>Chapter 2. Tectonic Events</b>	<b>20</b>
Sec. 2.1. Tectonic Hypotheses	20
Sec. 2.2. Tectonic Epochs	22
Sec. 2.3. Forms of Tectonic Movements	23
<b>Chapter 3. Historical Geology in a Nutshell</b>	<b>27</b>
Sec. 3.1. General Characteristics	27
Sec. 3.2. Geochronology	28
Sec. 3.3. Some Facts from Historical Geology	33

## **Part Two**

### **ELEMENTARY ENGINEERING SOIL SCIENCE**

<b>Chapter 4. Igneous Rocks</b>	<b>42</b>
Sec. 4.1. Rock-Forming Minerals	42
Sec. 4.2. Characteristics of Igneous Rocks	44
<b>Chapter 5. Sedimentary Rocks</b>	<b>54</b>
Sec. 5.1. Origin of Sedimentary Rocks	54
Sec. 5.2. Principal Types of Sedimentary Rocks	55
<b>Chapter 6. Metamorphic Rocks</b>	<b>63</b>
Sec. 6.1. Metamorphism	63
Sec. 6.2. Principal Metamorphic Rocks	63
<b>Chapter 7. Areas of Distribution of Sedimentary Rocks</b>	<b>65</b>
Sec. 7.1. Marine and Continental Deposits	65
Sec. 7.2. Thickness of Strata	72

<b>Chapter 8. Regular and Irregular Bedding of Sedimentary Rocks and Soils</b>	<b>75</b>
Sec. 8.1. Regular Bedding	75
Sec. 8.2. Irregular Stratification	76
<b>Chapter 9. Jointing in Rocks</b>	<b>79</b>
Sec. 9.1. The Origins of Jointing	79
Sec. 9.2. Principal Types of Joints	81
<b>Chapter 10. Groundwater</b>	<b>87</b>
Sec. 10.1. The Origin of Groundwater	87
Sec. 10.2. The Level of Subsurface Waters	91
<b>Chapter 11. Coefficient of Permeability and Methods of Its Determination</b>	<b>96</b>
Sec. 11.1. A Coefficient of Permeability	96
Sec. 11.2. Methods for Determination of the Coefficient of Permeability	97
<b>Chapter 12. Physical Properties and Characteristics of Rocks and Soils</b>	<b>100</b>
Sec. 12.1. Class One and Class Two Index Characteristics	100
Sec. 12.2. Granulometric Rock (Soil) Composition. Classification Criteria	102
Sec. 12.3. Other Class Two Rock Indices. The Methods of Determination	106
<b>Chapter 13. Shearing Resistance of Rocks and Soils. Indices and Methods of Determination</b>	<b>119</b>
Sec. 13.1. Soil and Rock Strength	119
Sec. 13.2. Shearing Resistance in Grained (Cohesionless) Soils	125
Sec. 13.3. Shearing Resistance of Clayey Soils. General Characteristic. Methods of Study and Index Characteristics	138
Sec. 13.4. Strength and Shearing Resistance of Jointed Hard Rocks	149
<b>Chapter 14. Soil Compressibility. Its Origin and Characteristics. Methods of Determination</b>	<b>153</b>
Sec. 14.1. Soil Consolidation Induced by a Load	153
Sec. 14.2. Characteristics of Soil Compressibility	155
Sec. 14.3. Methods of Determinations of Characteristics of Soil Compressibility	163
<b>Chapter 15. Determination of Index Characteristics of Soils</b>	<b>170</b>
Sec. 15.1. Basic Concepts	170
Sec. 15.2. Abridged Methods for Determining Design Characteristics	171

### **Part Three**

### **BASIC SOIL MECHANICS**

<b>Chapter 16. The Behaviour of Soils in a Soil Mass in a State of Stress</b>	<b>176</b>
Sec. 16.1. Fundamental Concepts	176
Sec. 16.2. Forms of Expression of the State of Stress of the Soil Mass	181
<b>Chapter 17. Some Theoretical Facts Underlying Solutions of Problems Posed by Soil Mechanics</b>	<b>183</b>
Sec. 17.1. The Strength of Soils	183
Sec. 17.2. The Determination of Normal and Shearing Stresses in a Soil Mass	185
Sec. 17.3. Special Cases of the State of Stress of the Soil Mass	194
<b>Chapter 18. Three Phases of the Behaviour of the Subsoils of a Structure</b>	<b>195</b>
Sec. 18.1. General Considerations	195
Sec. 18.2. The Loss of Strength and Stability by the Foundation	198



<b>Chapter 19. Evaluation of the Strength of the Subsoil of a Structure Disregarding Normal Stresses</b>	<b>199</b>
Sec. 19.1. General Considerations	199
Sec. 19.2. A Safe Load	201
<b>Chapter 20. Evaluation of the Strength of the Subsoil of a Structure Taking into Account Normal Stresses</b>	<b>203</b>
Sec. 20.1. Criterion of the Limit Strength of a Soil	203
Sec. 20.2. Determination of the Angle of Maximum Inclination $\theta_{\max}$ . Loose Cohesionless Soils	205
Sec. 20.3. Evaluation of the Weight of the Soil Mass	207
Sec. 20.4. Lines of Simultaneous Rupture and Regions of Limit State of Stress	210
Sec. 20.5. Critical Safe $p_{saf}$ and Permissible Load	214
<b>Chapter 21. Critical Load when the Total Stability of the Subsoil of a Structure Must Be Ensured (Arching Phase)</b>	<b>221</b>
Sec. 21.1. Theoretical Solutions	221
Sec. 21.2. Semiempirical Relationships	223
<b>Chapter 22. Increasing Strength of Clayey Soils Induced by Consolidation with Time Under the Own Weight of a Structure</b>	<b>231</b>
Sec. 22.1. Pore Pressure and Filtrational or Primary Consolidation of Soils	231
Sec. 22.2. Consolidation Index $n$ and Its Significance	240
<b>Chapter 23. The Initial Pressure Gradient. Its Role in Limiting Consolidation of Clayey Soils</b>	<b>243</b>
Sec. 23.1. Introduction	243
Sec. 23.2. Theoretical Premises	245
<b>Chapter 24. The Hydrostatic and Hydrodynamic Effect</b>	<b>248</b>
Sec. 24.1. The Essence of the Phenomenon	248
Sec. 24.2. The Hydraulic Gradient as a Means of Hydrodynamic Action	249
Sec. 24.3. Conditions Resulting in Loss of Stability of Soils in Open Cuts	251
<b>Chapter 25. Settlement of Structures and Their Stability</b>	<b>254</b>
Sec. 25.1. Introduction	254
Sec. 25.2. Differential Settlement and Its Results	256
<b>Chapter 26. Principal Theoretic Premises to Predict Structure Settlement</b>	<b>262</b>
Sec. 26.1. Introduction	262
Sec. 26.2. Useful Formulae	265
<b>Chapter 27. Normal Stresses in the Subsoil of a Structure and Methods of Their Determination</b>	<b>272</b>
Sec. 27.1. Determination of Normal Stresses Under Conditions of a Plane Problem	272
Sec. 27.2. Determination of Normal Stresses in a Three-Dimensional Case	282
<b>Chapter 28. Methods of Predicting Settlement of Structures with a Consolidating Foundation Soil</b>	<b>285</b>
Sec. 28.1. Method of Summation	285
Sec. 28.2. Approximate Methods of Predicting Settlement of Structures	295
Sec. 28.3. Some General Conclusions from the Theory of Settlement of Structures	299
<b>Chapter 29. Forecasts of Time-Dependent Settlements of Engineering Structures</b>	<b>301</b>
Sec. 29.1. Consolidation of a Uniform Soil Mass	301
Sec. 29.2. Consolidation of a Stratified Soil Mass	304

<b>Chapter 30. Particular Cases of Forecasting Deformations of Foundations and Settlement of Structures</b>	<b>306</b>
Sec. 30.1. The Effect of the Lowering of the Water Table	306
Sec. 30.2. The Effect of Vibrations on a Sandy Subsoil	307
Sec. 30.3. Taking into Account the Anisotropy of the Subsoil	311
Sec. 30.4. Taking into Account the Stratified Pattern of the Soil Mass	312
Sec. 30.5. Taking into Account the Geological Features of the Subsoil	314
Sec. 30.6. Forecast of the Tipping of a Monolith Tower Type Structure	315
Sec. 30.7. The Behaviour of the Soil Under the Impact of a Rolling Wheel	318
Sec. 30.8. Cyclic Loads	321
<b>Chapter 31. Rheological Phenomena. Their Role in the Bearing Capacity and Time-Dependent Deformation of Clays</b>	<b>323</b>
Sec. 31.1. General Considerations	323
Sec. 31.2. Main Features of the Physico-Technical Theory of Creep Properties	328
Sec. 31.3. The Coefficient of Viscosity of Clays and Methods for Its Determination	335
Sec. 31.4. Long-Term Stability of Clay Slopes	337
<b>Chapter 32. Rheological Phenomena. Their Role in Performance of Retaining Structures</b>	<b>340</b>
Sec. 32.1. Classification Schemes	340
Sec. 32.2. Rheological Properties of the Foundation Soil of Retaining Walls	347
Sec. 32.3. Forecasting a Translational Slide of a Retaining Wall with Time	350
<b>Chapter 33. Rheological Events. Their Effect on Settlement of Structures</b>	<b>358</b>
Sec. 33.1. Introduction	358
Sec. 33.2. A Particular Case of Forecasting Settlement of a Structure on Un-saturated Soil	360
Sec. 33.3. The General Case	363

## Part Four

### BASIC ENGINEERING GEOLOGY

<b>Chapter 34. Classification of Rocks and Soils</b>	<b>367</b>
Sec. 34.1. The Principle of Classification	367
Sec. 34.2. Classification of Rocks and Soils	367
<b>Chapter 35. Swamp and Silty Deposits. Peat</b>	<b>370</b>
Sec. 35.1. Swamp and Silty Deposits (Muskeg Materials)	370
Sec. 35.2. Peat and Peat Deposits	372
<b>Chapter 36. Loess and Loessian Soils. Seasonal Changes in Bearing Capacity</b>	<b>377</b>
Sec. 36.1. General Characteristics	377
Sec. 36.2. Subsidence of Loess	380
Sec. 36.3. The Principle of Forecasting Subsidence	384
<b>Chapter 37. Glacial Deposits</b>	<b>387</b>
Sec. 37.1. The Composition of Glacial Deposits	387
Sec. 37.2. Glacial Deposits from the Viewpoint of Geotechnics	390
<b>Chapter 38. Permafrost. Soils in Permafrost</b>	<b>391</b>
Sec. 38.1. Introduction	391
Sec. 38.2. Construction in Permafrost Areas	398

<b>Chapter 39. Rock Weathering. Its Importance in Geotechnics</b>	<b>400</b>
Sec. 39.1. The Processes of Weathering. Eluvium and Its Geotechnical Characteristics	400
Sec. 39.2. Debris Formation. Talus Deposits and Their Role in Landslides	404
Sec. 39.3. Wind Action	406
Sec. 39.4. Soils. Formation of Soils	408
<b>Chapter 40. Mud Rock Flows</b>	<b>412</b>
Sec. 40.1. General Considerations	412
Sec. 40.2. Protective Measures	416
<b>Chapter 41. Karst Phenomena</b>	<b>417</b>
Sec. 41.1. General Considerations	417
Sec. 41.2. Conditions of Construction	420
<b>Chapter 42. Erosion. Its Effect on Road and Bridge Construction</b>	<b>424</b>
Sec. 42.1. Gully Erosion, or Gullying	424
Sec. 42.2. Erosion in River Valleys	426
Sec. 42.3. Formation of River Vallies	434
Sec. 42.4. Alluvial Deposits	438
<b>Chapter 3. Abrasion and Its Effect in Modern Conditions</b>	<b>445</b>
Sec. 43.1. Shaping of Shores of Seas and Lakes	445
Sec. 43.2. Transformation of Margins of Water Reservoirs	447
<b>Chapter 44. Landslides and Other Crustal Displacements</b>	<b>449</b>
Sec. 44.1. Introduction	449
Sec. 44.2. Causes of Landslides	453
Sec. 44.3. Possible Patterns of Disturbance of Slope Stability	456
Sec. 44.4. Stability Computations for a Slope or Hill Side	464
Sec. 44.5. Prevention of Landslides	479
<b>Chapter 45. Rheological Phenomena and Their Role in Creep Events</b>	<b>483</b>
Sec. 45.1. Conditions of Occurrence	483
Sec. 45.2. The Evaluation of Long-Term Stability of a Slope or Hill Side	484
Sec. 45.3. Prediction of the Intensity of Creep Deformation of a Sliding Slope	485
<b>Chapter 46. Seismic Events</b>	<b>490</b>
Sec. 46.1. General Characteristics	490
Sec. 46.2. Construction Conditions in Seismic Areas	497
Sec. 46.3. Seismic Stability of Saturated Sands	506
<b>Chapter 47. The Purpose and Types of Geotechnical Studies and Exploration</b>	<b>520</b>
Sec. 47.1. General Principles	520
Sec. 47.2. Types of Geotechnical Exploration	521
Sec. 47.3. Special Types of Geotechnical Studies	532
<b>Conclusion</b>	<b>545</b>
<b>Subject Index</b>	<b>547</b>

## **Introduction**

The unprecedented large-scale construction of transport facilities being undertaken in this country poses most complicated engineering tasks to the builders, especially with respect to utilization of the vast expanses of Siberia and the Soviet Far East. The putting through of major transport engineering structures and highways in these areas, usually in most inclement conditions, may be, as a rule, justified only on the condition of the efficient and extensive use of findings of engineering geology and soil mechanics.

The proper feasibility study for erecting big structures on any rock such as to rule out accidents is particularly important.

We use the historical method when dealing with natural phenomena. This directly applies to scientific investigations in the field of engineering geology and soil mechanics. Among these, to cite an example, is a theory of successive phases of tectonic inactivity and orogenesis in the formation and development of the earth's crust.

Any structure to be erected, including a transport facility, must possess proper stability and strength. Moreover, it should meet special deformability requirements. A structure being designed must concurrently satisfy the following conditions: it should be built at lowest possible costs in terms of money, manpower and time.

In order to successfully deal with all these problems, when designing a structure, it is necessary to determine and take into account the environmental conditions under which it will be constructed. These, notably, should include soils and rocks that will support the structure; their composition, state and properties and also the mode of their occurrence, thickness of individual layers, jointing of the hard rock mass etc.

The mode of occurrence of subsurface water and its regime in the soil mass being explored are an important component of the problem in hand. Yet the data on these separate items cannot aid in solving the entire problem. What proves of exceptional and sometimes crucial significance is the behaviour of soils and rocks under the effect of the weight of the structure being built, of the forces applied and the states of stress that appear in the soil mass.



In addition, a structure to be built may frequently be under the deleterious effect of one or more natural geological processes or phenomena known as geodynamic. These include, first and foremost, seismic phenomena (earthquakes), landslides and landfalls, collapses induced by the caving of the roofs of subterraneous voids etc.

The negative effect of the above phenomena on the structure in question may be avoided or lessened by taking requisite protective measures (active control). On the other hand it may prove in many cases better to apply simpler and cheaper methods of tackling the problem. For example, we can site the centre line of a bridge at other than a hazardous section of the bank of a river (passive control). Such a solution, however, can be effective if the phenomena in hand have been studied in advance and their likely influence on the structure being designed has been established.

*Engineering geology*, as a science and an applied discipline, studies general natural phenomena that must be taken into consideration when it is desired to design, build and operate an engineering structure, and geological processes and phenomena likely to affect adversely the structure concerned and interfere with the normal conditions of its operation.

The subject of engineering geology as an applied discipline includes a variety of problems most diversified in contents and important in essence. The natural conditions that obtain at a given job can be fully understood only after all the regularities of the particular geological processes and features have been determined and investigated.

These regularities can be referred to four principal types.

*The first regularity* suggests that the engineering and geological conditions of construction and operation of a structure are governed by the nature of the soils and rocks involved, their properties, mode of occurrence, subsurface water regime and also by the pattern and conditions of the likely effect of geodynamic processes and phenomena.

*The second regularity* suggests that the character and intensity of the occurrence of one or another geological process and phenomenon is determined by the peculiar features of the structure of the earth as a cosmic body. These primarily are: (1) the presence of a relatively thin hard outer shell of the terrestrial globe called *the crust* made up of rocks; (2) the occurrence in the inner reaches of the earth of complex processes that are responsible for the thermal and special physico-chemical regime of the earth's interior and for the processes that take place in the earth's crust by virtue of the latter's comparatively small thickness; (3) the effect of the external processes and phenomena associated with the activity of the atmosphere and surface waters on the crust-forming rocks and the earth's relief.

*The third regularity* consists in that the engineering geological properties of soils and rocks are determined by their composition, state and their structural and textural features.

*The fourth regularity* suggests that the composition and state of the rocks and soils, their structural and textural features and mode of occurrence are governed by the nature of the parent materials from which they originated, by origination conditions (*genesis*) and environment (*facies*) and by the character of the subsequent transformations of the particular rock or soil due to one or another geological (geodynamic) process and phenomenon.

As to soil mechanics, it is a science concerned with the conditions that lead to the disturbance of the strength and stability of structures and with the behaviour of the soil mass underlying engineering structures under the effect of forces acting on these. Conclusions from soil mechanics rely on the data furnished by engineering geological investigations. This discipline develops the array of mechanical and mathematical data for evaluating the stability and strength of soils and their deformations generally taking into account the time factor.

In fact, soil mechanics necessarily operates with ideal soils and rocks and uses approximate calculation formulae. The actual behaviour and properties of soils and rocks are much more diversified and complex than can be described by mathematical relationships. That is why in each particular job the conclusions from soil mechanics must be corrected by allowing for the actual natural conditions that can be studied by the methods of engineering geology. Thus the needed intimate connection between the two disciplines will be achieved.

# Part One

## Elementary General Geology

---

### Chapter 1

#### The Earth as a Cosmic Body. Tectonics

---

##### Sec. 1.1. General Facts on the Structure of the Globe

The appearance, occurrence conditions and construction properties of a rock or soil are governed by the character of the original products or rocks and by the conditions of their formation and subsequent action of consolidation, weathering, cementation and others. For this reason, the most reasonable pathway for studying the above aspects of evaluation of rocks and soils in terms of engineering geology is to gain an insight in the conditions of their origination and the agents acting on these rocks and soils that are directly connected with the earth's life.

The life of the planet Earth is determined by the following principal factors: (1) the presence of a solidified layer enveloping the globe said to be *the earth's crust (lithosphere)* composed of hard rocks; (2) the relatively small thickness and rigidity of the earth's crust; (3) complex processes are at work in the earth's bowels, beneath the crust, that determine the thermal and physico-chemical regime of the earth's interior; (4) the action of various physico-chemical processes related to the atmospheric activities on the crust-forming rocks and the earth's relief.

The age of the earth as a planet is now estimated to be 4.5 to 5 billion years. The earth's radius is about 6400 km. On the other hand, the thickness of the crust, according to geophysical findings, in particular, from the speed of propagation of seismic waves passing through the mass of the globe, does not exceed 30 to 40 km. In the Soviet Union (Caucasus Peninsula) and the USA attempts are being made to directly determine the crust's thickness by sinking superdeep boreholes. Thus, by 1980 the depth of a borehole reached some 10 km.

Such a thin shell, in practical terms, is unable to offer any appreciable resistance to various deformations that have been acting on the globe. The crust is being passively deformed in response to the deformations of the earth itself due to the processes and phenomena that occur in its interior which are termed *endogenic*.

At greater depths the pressure in the earth's interior and hence the temperature constantly rise to attain as much as 5 000 °C. The central part of the earth forms what is known as a core (inner and outer). The core is

about 3 000 km in diameter. The pressure there presumably attains 3.0 to 3.5 million at (0.3 to 0.35 million MPa).

As is known, the specific density of the globe as a whole, equal to 5.5, by far exceeds the bulk density of rocks (2.5 to 2.8) that compose the crust. It is only in the crust's lower strata that its value increases. Therefore the density of the globe's central part is expected to be much greater and amounts to 12, that is, close to the unit density of iron (Fe) and nickel (Ni). These figures are substantiated by geophysical evidence as well.

The above circumstance led, at one time, to an assumption that the core is composed of heavier elements (Ni, Fe, Mg) and, due to the great pressures and heat there, the material in the inner reaches of the earth is in a specific overheated elastic state of plastic viscosity. It has been by now established that the core lets pass longitudinal seismic vibrations (P-waves) and is impregnable to transverse vibrations (S-waves). This fact permits belief that the material forming the earth's core, at least, its outer shell, the inner core remaining hard, is in a specific overheated liquid state.

*The mantle* that encloses the core is very great in thickness and represents an intermediate zone between the core and the crust. According to the speed of propagation of seismic waves the mantle divides into *an upper* and *a lower mantle*. The chemical composition of the mantle is supposed to correspond to a well-known rock, basalt, which is in a less dense state in the upper mantle where Si, Fe, and Mg prevail that passes in the lower mantle to a denser state where Fe, Mg, Ni occur. It is there that catastrophic earthquakes originate.

### Sec. 1.2. The Structure of the Earth's Crust

The zone above the mantle is *the crust* or *lithosphere*. The lithosphere, in turn, divides into the upper granite belt where Si, Al, and Fe (sial) predominate, and the lower basalt belt. The oceanic crust differs from the continental in that it is thinner and lacks the upper granite layer.

The external layers of the earth's crust are composed by *sedimentary rocks* (e.g. clays, sandstones, limestones) formed by decomposition and disintegration, largely, of magmatic rocks 4 to 10 km in thickness. These rocks are underlain by what are known as *metamorphic rocks* (shales, gneisses, marble etc.) 5 to 10 km thick. These are rocks that originate from magmatic and sedimentary rocks transformed by the action of high temperatures and pressures inherent to orogenesis and volcanism. The mass of metamorphic rocks together with the granite layer provide *the crystalline foundation* of the continents.

These are the oldest of known rocks whose age is well over 3 billion years. Occasionally the rocks of the crystalline foundation may outcrop at the earth surface. Such areas are called *shields*. We know the Ukranian



shield (the Dnieper hydropower station region), the boundary zone of the Feno-Scandinavian shield fringes on some border areas of the Kola Peninsula and Karelia. Crystalline rocks have been revealed in the Leningrad area at a depth 200 m, near Moscow at 1 600 to 1 700 m and at the Kursk Region magnetic anomaly at 50 to 200 m.

The rocks composing the outer layers of the earth's crust are of crucial importance for an engineering and geological analysis since they inevitably provide a foundation for structures to be built.

### Sec. 1.3. The Role of Tectonic Phenomena in the Earth's Life

It is best to evaluate rocks and soils from the viewpoint of engineering geology by studying the conditions of their formation and the effect on them produced by various agents directly associated with the Earth's life. The action of *exogenic (external)* agents such as wind, heat and cold, atmospheric precipitation, running water and others on rocks and soils in the uppermost layers of the crust is evident. At the same time there is evidence suggesting that intensive *internal (endogenic)* processes are at work in the earth's inner reaches. They reveal themselves as grandiose volcanic eruptions, frequent earthquakes that occur at an annual rate of 100 thousand events including as many as 100 major events. These are accompanied by marine transgressions or regressions which fact testifies to the changes in the level of the continents with the passage of time and is responsible for the diverse deformations of the earth's crust and mountain building (orogenesis) as a result of the manifestation of *tectonic processes and phenomena*.

We can infer the scales of tectonic events from the fact that marine rocks containing remnants of marine organisms have been found as high as 4 km in the Andes and drift-wood has been detected on sea terraces on Novaya Zemlya at 400 m and higher. The mountain ranges of the Cordilleras and Andes, these crustal folds, extend along the western coasts of North and South America for more than 12 000 km, with mountain summits over 5 km high. Mount Chomolungma (Mt. Everest) in the Himalayas is almost 9 km high.

Huge areas of modern land were inundated by the sea (*marine transgressions*) in the geological past. About 100 million years ago vast regions of what is now the southern European part of the Soviet Union to today's Moscow and Western Europe (the Seine River basin and Rouen in France and Dover in England) were submerged in the Cretaceous. The waters later retreated (*marine regression*). The process of sinking of the earth's crust within the limits of Western Europe is still continuing which is suggested by



**Fig. 1.1.** The distribution of ancient and modern land in the region of the North Sea and the Atlantic Ocean. The submerged ancient sea is denoted by vertically shaded areas, black colour shows modern land

the advance of the sea in the low lying areas (Holland, France). The mouth areas and lower reaches of many rivers in Western Europe remain inundated until now (Fig. 1.1). The Black Sea is also due to the phenomenon of transgression.

We know of gigantic clefts in the earth's crust extending for some thousand km on the sea floor of the Pacific, Atlantic and Indian oceans with depths recorded attaining 11 km. These clefts or troughs provide a convincing proof of ruptures in the earth's crust and of displacements of individual continental blocks or lithospheric plates. These phenomena are in agreement with a theory of large-scale horizontal movements both of continental (continental drift) and oceanic blocks of the earth's crust.

The fairly close fit of the shorelines of West Africa and the eastern part of South America (Fig. 1.2) appears to provide convincing evidence in favour of the drift theory advanced by Alfred Wegener early in the present century.

A. Wegener argued for the existence in the past of a supercontinent that

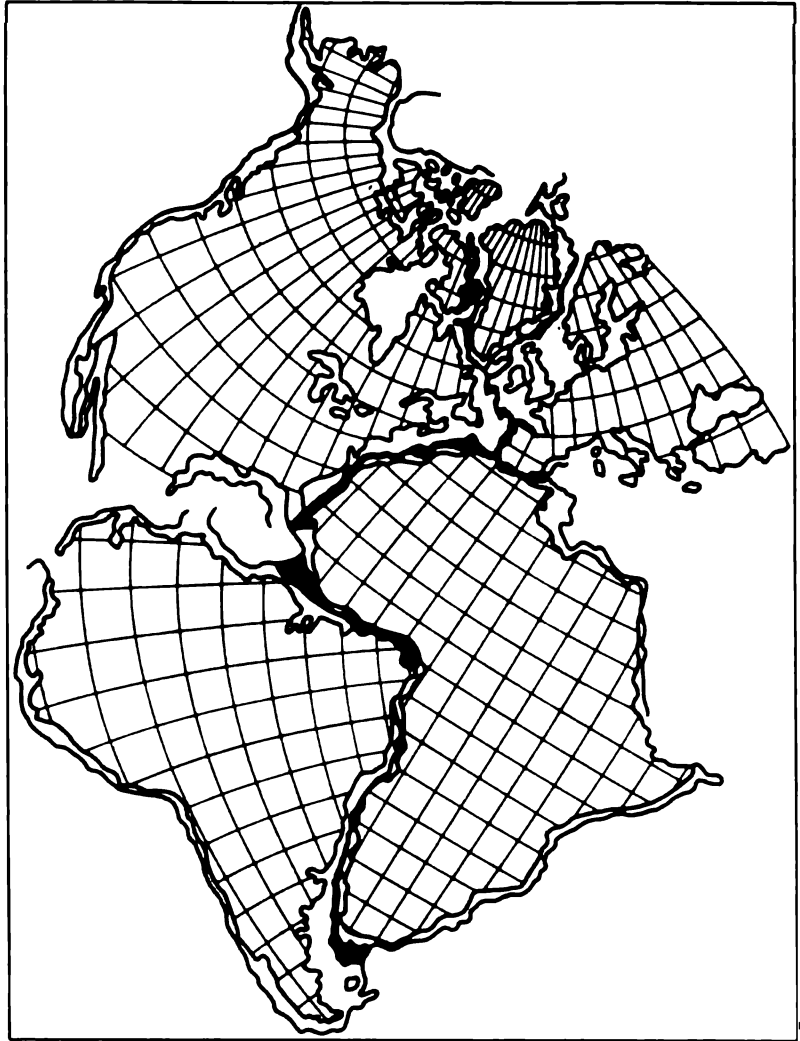


**Fig. 1.2.** A fit of the shorelines of South America and Africa as a proof to the drift theory

he called *Pangaea*. Later it separated and that portion of *Pangaea* that was to form North America and Eurasia began drifting westwards. This gave rise to the present Atlantic Ocean that was a thousand km wide and continued to expand.

The drift theory has been developing in the last decade in terms of displacements and subductions of the crustal blocks. This theory is validated by the many pieces of evidence that have by now been accumulated. It is believed that the plates of the lithosphere (rafts) are separated by deep cracks or troughs. Under definite conditions melted materials from the earth's inner reaches rush to the rupture zones pushing aside the plates (rafts) underlying the continents and thus causing a drift of these latter. It is assumed that it is by this mechanism that the Middle Atlantic oceanic ridge discovered in the last few decades has originated.

By using the drift theory we can also account for the numerous earthquakes and volcanic eruptions related with the fault zones and discontinuities in the continental plates, for the similarity between organic fossils on different continents, for the rich coalfields in the vicinity of the North and South Poles in Spitzbergen and in the Antarctic and for the magnetometric tests of rocks pointing to a migration of the earth's poles.

However, this hypothesis cannot be regarded to be fully valid.

It should be noted that the modern period of the earth's life is marked by relatively insignificant volcanic activities. In the earth's geological past volcanic events would have been colossal in scale. This can be derived from the huge layers composed of magmatic rocks. We may recall the solidified lava in India (Deccan Traps) which is 3 km thick and whose area is 650000 km<sup>2</sup> of the basaltic cover in the USA (Washington and Oregon States) which is 1000 to 1500 m in thickness and 500000 km<sup>2</sup> in area.

---

## Chapter 2

### Tectonic Events

---

#### Sec. 2.1. Tectonic Hypotheses

Before we continue to consider the laws that govern the similarity and the differences between the diversified rocks, their properties and conditions of occurrence we must first familiarize ourselves with tectonic hypotheses. Quite a number of these have been proposed. The problem, however, is so complicated that none can so far be considered as adequate.

What follows presents in very general terms one of such hypotheses which appears to us to be of interest from the standpoint of its approach and methodology. The principal points of this hypothesis are the following: (1) the structure of the earth is as outlined above (the uppermost shell is the earth's crust, the transition zone is the mantle with the core at the centre); (2) endogenic processes all display, to a degree, a thermal character; (3) there are overheated masses of fiery molten rocks (magma) at some places of the cover zone; (4) the earth's crust is relatively thin and insufficiently rigid.

The thermal nature of the events in question is to a certain degree validated by upwelling lavas with temperatures in excess of 1000 °C during volcanic eruptions and by the numerous hot springs that come up from the ground.

Suppose the earth is a sphere 4 m in diameter, then the earth's crust would be a veneer about 1 cm in thickness. Being thus thin, the earth's crust cannot in fact offer any significant resistance to all kinds of deformations acting on the globe. It is liable to deform due to *endogenic* processes and phenomena that occur in the earth's interior.

The accepted theory suggests that the earth whose age is believed to be 4.5 to 5 billion years presents an underdeveloped star (embryo star) since its

small size as a cosmic body prevents atomic reactions from fully revealing themselves in the earth's inner regions. These processes, however, do occur at the earth's centre which leads to a greater density of the core due to disruption of electron shells and "packings" of atoms of the core forming materials. Radioactive processes generate heat. This results in two oppositely directed actions associated with a decrease in the size of the globe because of the compression of the core and the increased volume of the globe due to thermal expansion.

The radioactive processes that are at work in the earth's bowels give rise to gradual accumulation of heat that expands with time toward the earth's surface. At some areas here (in particular, in extension zones with a relatively low pressure) overheated rocks may convert to fiery molten masses (magma) mentioned above.

Under certain conditions, due to pressure, magmatic melts may incorporate into the rock mass of the earth's crust and even erupt to its surface. These are *volcanic* events or volcanism. Such conditions will obtain whenever, with increased temperatures and an increase of the volume of the globe, the earth's crust, as it were, becomes too tight. This is followed by the appearance of fissures, fractures, chippings and other rupture deformations.

As it travels, magma comes in contact with different rocks and melting them it absorbs some products acquiring a specific composition. Magmatic masses, that have incorporated themselves in the bedrock or come to the outer surface as lavas devoid to some extent of their gases, cool and solidify. In this fashion *magmatic or igneous* rocks that differ in composition and structure form.

As a result of the lower density of the rocks of the earth's crust whose continental massifs are composed by granites (density 2.7), the continental cratons whose "roots" rest on a heavier layer, substrate (a variety of basalt with the density 3 to 3.5) appear to be floating on this subcrustal layer

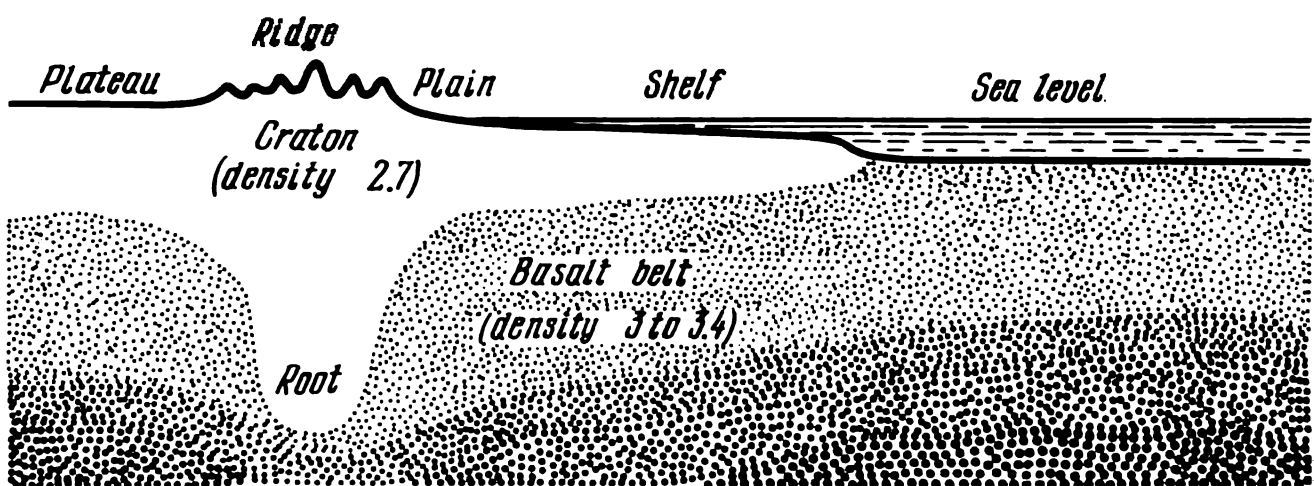


Fig. 2.1. Continental cratons and the floor of the World Ocean

much like slag at the surface of molten pigiron (Fig.2.1). Note that the scale in this figure is considerably distorted.

Under the effect of thermal expansion and the resultant loss in density of basaltic masses the continental massifs sink more into the basaltic belt. Naturally, this phenomenon may occasionally be accompanied by inundation of lower areas of land (*marine transgression*). The general rise in temperature in this period coupled to vast transgressions of the sea result in considerable amelioration of environmental conditions on the earth.

### Sec. 2.2. Tectonic Epochs

The period of the earth's life that we describe characterized by improvement of its thermal regime is considered as an epoch of *evolution* or *tectonic inactivity*. It is this period that witnesses all kinds of *exogenic* (external) agents revealing themselves. These primarily include weathering and erosion of prominent relief features (being a relic of the previous stage of orogenesis) leading to smoothing of relief (*denudation* processes).

With a lapse of time in geological terms weathering processes give rise to huge volumes of so-called weathering products. Part of these are carried by wind or running water and then deposited. By this mechanism *eolian* (e.g. loess) or *alluvial* depositions in the river valleys on continental areas originate.

Most of weathering products transported by rivers (including material that has been dissolved) are brought to the sea to be there deposited (sedimentation) and piled up (accumulation), frequently aided by biological agents. After a lengthy period of lithification these sediments convert to sedimentary rocks of marine facies (origin) different in their nature and properties. This is especially true of an epoch of tectonic inactivity when sediments accumulated on the sea floor at a particularly rapid rate.

After the heat stored in the globe's interior had been largely exhausted, a new phase in the earth's life began, an epoch of a so-called *tectonic revolution*.

According to the hypothesis in question, the cooling of the basaltic belt and a rise in its density cause the continental massifs to emerge. The sea thus retreats and land dries up. The land increases in area which, in turn, leads to further expansion of continental climatic conditions. As a result of it there is the onset of a cold period.

Owing to the cooling of the globe and outflow of magmatic materials from its interior the terrestrial globe undergoes *contraction*. Being not sufficiently rigid, the earth's crust tends to respond to the decreasing volume of the globe. As a result of an expanding outer surface due to the solidification of magmatic materials in the crustal fissures the crust warps, deforms

and develops folds. This was the beginning of an *epoch of orogenesis*, the formation of folded mountains. An analogy that suggests itself may be the appearance of folds on a too loose costume that would form if a too thin man wore it. This epoch provided the conditions that led to folded sedimentary rocks, crustal deformations: overlaps, shifts, upheavals, subductions and, finally, origination of mountain ranges and regions.

These zones and regions where extremely high pressures and temperatures developed and complicated physico-chemical processes occurred later provided ground for dynamic metamorphism of rocks. In this way metamorphic rocks, as it were, originated anew. The phase of mountain building was succeeded by a new phase of tectonic quiescence. Heat began to be accumulated in the inner reaches of the earth creating conditions that favoured a new phase of tectonic revolution. This process was repeated many times. During the geological life of the earth epochs of inactivity and orogenesis reversed regularly. Table 2.1 presents principal characteristics of epochs of tectonic inactivity (evolution) and mountain building (orogenesis).

Tabla 2.1

Main Characteristics of Tectonic Epochs

Natural phenomena	Epoch of	
	quiescence (evolution)	mount building (orogenesis)
Standing of continents	Low	High
Expansion of the sea	Transgression	Regression
Climate conditions	Tropical	Cold
Mountain building	Nonexistent	Intensive
Volcanism	Minor	Vigorous
Prevailing processes	Accumulation of precipitation	Denudation

### Sec. 2.3. Forms of Tectonic Movements

According to the form of movement tectonic events expressed in complicated and diverse crustal deformations can be divided into vertical (radial) and horizontal (tangential) ones.

*Vertical movements* are periodical slow uplifts and sinkings of some regions of the earth's crust or others. For this reason they are often termed vibrational, secular or epeirogenic movements. These are expressed primarily by the elevations of the regions concerned and the occurrence of sea transgressions and regressions (see Fig. 2.1).

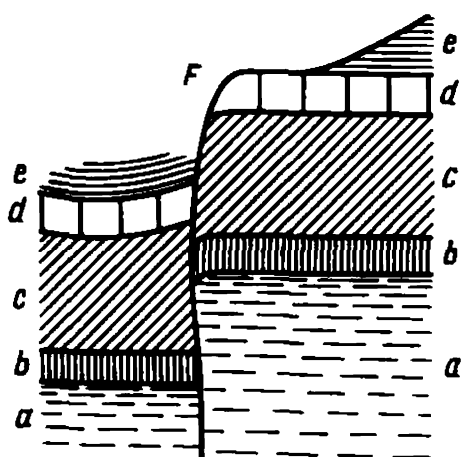


Fig. 2.2. Fault with a vertical dislocation of strata:

*F-F*—a profile of fault; *a*, *b*, *c*, and *d* are strata composed by different rocks

The rate of these upward and downward movements may attain 5 to 15 mm per year. In the course of geological epochs these movements eventually give rise to major changes in the coastlines. Thus, the oldest beach terrace on the Caucasian coast of the Black Sea is now at a height 900 m.

An example of the movements described can be provided by the geological history of the Volga River in the area of the Zhiguli Hills. In the age of reason the Volga River region underwent a major dome-like uplift to a height about 500 m. Later the Volga washed out this elevated mass to form a new valley. The valley then gradually sank by about 250 m and proved to be composed of younger deposits of the river. The subsequent period witnessed two more uplifts and two more sinkings whose amplitude, however, was less in value.

We can refer to quite a number of such examples, so the role of radial movements in formation of thick layers of deposited rocks and relief features is self-evident. Given definite conditions, *splits* and *fractures* occur in the earth's crust-forming masses that have experienced separate movements. This process results in *faults* (Fig. 2.2). In its pure form a fault is evidence of radial dislocation.

A combination of two or more faults gives rise to *step faults* (Fig. 2.3). A horst is an upheaval bounded by faults, and a graben is an oblong block

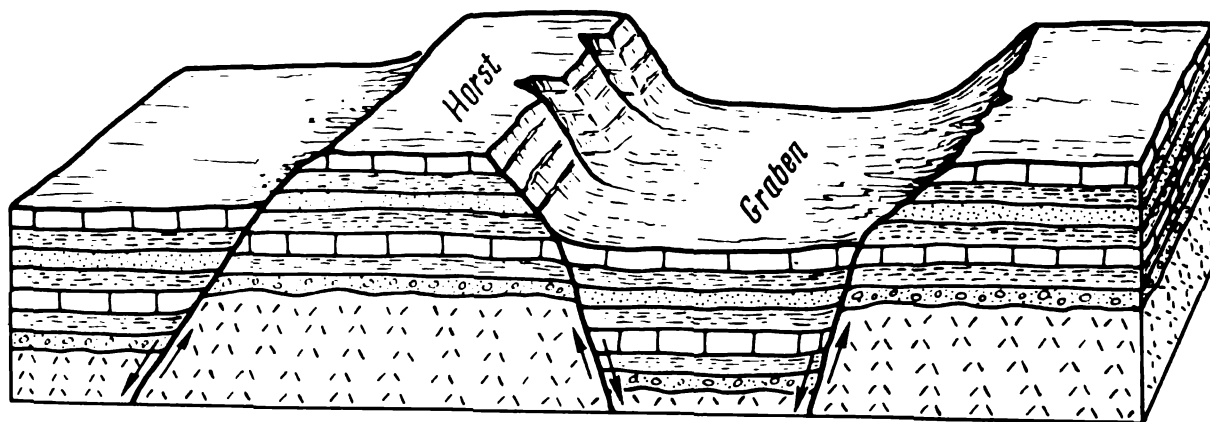


Fig. 2.3. Graben and horst



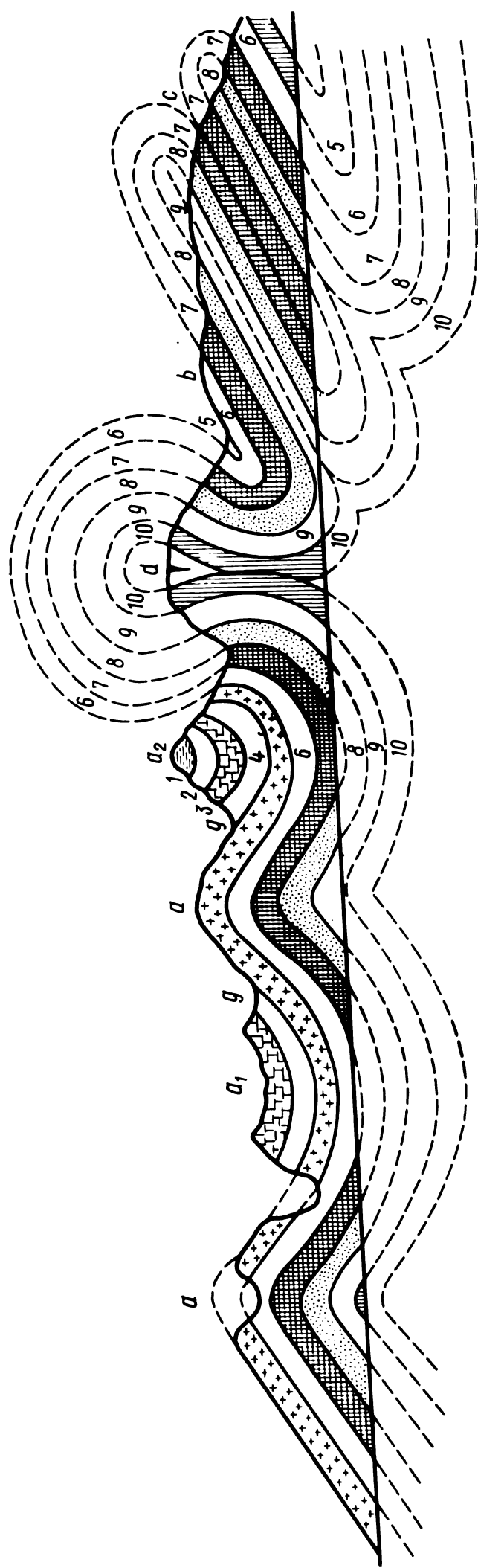


Fig. 2.4. Different fold types:

*a*—upright anticline; *c*—anticlinal recumbent; *d*—synclinalorium; *a<sub>1</sub>*, *a<sub>2</sub>*—upright synclines; *b*—inclined synclines. Figures indicate homogeneous strata

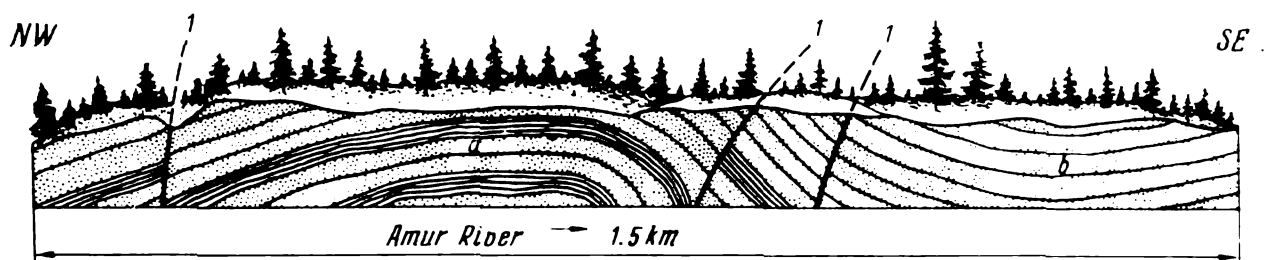


Fig. 2.5. Folded structure with erratic faults:

*a*—anticline; *b*—syncline; 1-1—faults

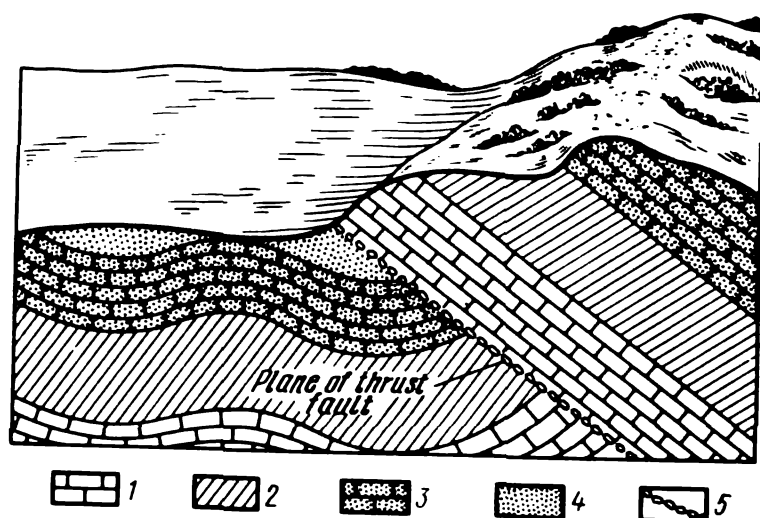


Fig. 2.6. Thrust fault:

1—limestone; 2—clays; 3—sandstones; 4—sand; 5—fault breccia

of the earth's crust that has dropped relative to the blocks on either side. Lake Baikal which is 1741 m deep may provide a specimen of a grandiose graben. There is evidence that the floor of Lake Baikal is still continuing to sink. This is, in particular, suggested by the presence of hot springs and frequent earthquakes that occur in the vicinity of the lake.

*Horizontal tectonic movements* are the cause of crumpling of the earth's crust, formation of folded structures, folded mountain chains. For this reason they are often called *tangential* or *orogenic*. It is in this fashion, for example, that the Urals and Caucasian ridge were generated. Depending on the type of their appearance there are two kinds of tangential movement: plicative and disjunctive, or rupture dislocations.

An example of a pure form of plication may be provided by a fold with a convex central part, called an *anticline*, and with a concave central part, called a *syncline* (Fig. 2.4).

Further formation of folds leads to disturbance in their original forms. There occur failures, ruptures, faults, overlaps etc. Such crustal deformations refer to rupture or disjunctive displacements.

A fold subjected to disjunctive displacements usually defies identification due to the effects of denudation such as weathering, water erosion,

ablation and can be revealed only after a detailed study of the geological features of a particular area (Fig. 2.5).

One of typical forms of disjunctive deformation is *a thrust fault* (Fig. 2.6). It is not uncommon that under conditions of vigorous orogenesis thrust faults are associated with displacements of whole mountainous massifs by hundreds of metres or even kilometres. Clearly, disjunctive dislocations accompanied by ruptures, faults or thrust faults interfere with the normal conditions of structure and occurrence of rocks and infrequently by disintegration along tectonic lines and in tectonic zones (*zones of fracture*).

---

## Chapter 3

### Historical Geology in a Nutshell

---

#### Sec. 3.1. General Characteristics

*Historical geology* is a branch of geology concerned with the earth's history. As it were, it reconstructs the order of geological events that have been occurring from the oldest times until present.

An adequate approach to the collection of evidence relating to the geological history of a particular area coupled to proper treatment of the findings obtained would permit an inquisitive researcher to infer much to predict the geological features of the building site and properties of the rocks that underlie it.

The discipline concerned with the geography of the geological past (i.e. reconstruction of facies) is called *paleogeography*. It provides an interface between historical and engineering geology.

It should be pointed out that methods of paleontology used for studying fossil remains of fauna and flora found in one layer of sedimentary rocks or another allows fairly reliable identification of the conditions in which a sediment was deposited and, in particular, of the depth of water basins, gas regime, the degree of water salinity and turbidity, temperature, specific conditions of accretion on the land etc.

An insight into the paleogeographic history of a particular area would largely facilitate prediction of the sedimented layer, its structure and properties of rocks composing it.

As is known, rock composition and natural properties that are responsible for the engineering geological characteristics of the rocks and their

mode of occurrence follow from the relevant facies and subsequent diagenesis (compaction of sediments) and metamorphism determined by the physiogeographical features of the given area.

Viewed in this context, historical geology offers an engineer vast possibilities. This analysis is especially facilitated by reconstruction of *tectonic phases* (orogenesis and evolution) in their historical sequence and the time of occurrence. It will be recalled that scientists refer these phases to definite physiogeographical conditions and assume them as resulting from the thermal regime of the terrestrial globe and of the level of the continents and the World ocean. In addition, we know that the mode of occurrence of rock layers may significantly vary in regions subject to orogenic processes.

We can determine the characteristics of the given area and its geological features if we identify the tectonic epoch (revolution or evolution) in which the rock mass in question was generated.

From the viewpoint of engineering geology it is of much importance to determine the time period in which tectonic phases occurred in this region of the earth's surface or another. This problem is the domain of *historical geology*.

The following phases of orogenesis are the best studied and important in terms of their effect: *Caledonian* Orogeny (Ordovician and Silurian); *Variscan* Orogeny termed also *Hercynian* Orogeny (Permian); *Kimmeridgian* (Jurassic); *Alpine* Orogeny (Quaternary).

The time period these phases occurred in is determined by the geological chronology or geochronology, for short.

### Sec. 3.2. Geochronology

Geochronology provides a system of dating of the events in the earth's history in a definite order (era, period, epoch, age). A geological time scale in Table 3.1 lists the principal stages in the earth's geological history.

*The epoch* corresponds to the time of deposition of rocks included in a definite subdivision of one system or another. The epoch is the third unit in the general geochronological scale and is in turn divided into *ages*. The epochs are named according to their temporal succession, i.e. Lower, Middle, Upper, or Lower and Upper. Thus, we may refer to Lower, Middle or Upper *Devonian*, *Carboniferous* etc. This time division may be designated by a corresponding index. For example, D<sub>2</sub> is a designation for Middle Devonian.

The table presented below is a brief outline of the paleogeographical events in the earth's life in eras.

Table 3.1

The Geological Time Scale (Abridged)

Era (geological group). Name and index	Period (rock system). Name and index	Epoch (rock-unit division). Name	Index	Duration of period, mln. yrs	Orogeny	Transgres- sion and regression	Volcanism
Archean AR	Division of local char- acter		AR	over 2600	Lauren- tian	?	Vigorous
			PR	200-2000	Huronian		
Protero- zoic PR							
	Cambrian Є	Lower Cambrian	Є <sub>1</sub>			Major trans- gression	Minor
		Middle Cambrian	Є <sub>2</sub>	70	Quiescence		
	Upper Cambrian		Є <sub>3</sub>				
	Ordovi- cian O	Lower Ordovi- cian	O <sub>1</sub>		Caledo- nian (in several phases)	Regression	Major
		Middle Ordovi- cian	O <sub>2</sub>	60			
		Upper Ordovi- cian	O <sub>3</sub>				
Paleozoic PZ						Transgres- sion	Minor

Table 3.1 (cont.)

Era (geological group). Name and index	Period (rock system). Name and index	Epoch (rock-unit division). Name	Index	Duration of period, mln. yrs	Orogeny	Transgres- sion and regression	Volcanism		
Paleozoic	Silurian S	Lower Silurian	S <sub>1</sub>	30	450	Regression	Major		
		Upper Silurian	S <sub>2</sub>						
	Devonian D	Lower Devonian	D <sub>1</sub>	60	Traces of Cale- donian orogeny	High-land standing	Minor		
		Middle Devonian	D <sub>2</sub>					Quiescence	Very large- scale- trans- gression
		Upper Devonian	D <sub>3</sub>						
	Carboni- ferous C	Lower	C <sub>1</sub>	75	Hercynian or Vari- scan	Large- scale trans- gression	Minor, at places major		
		Middle Carboni- ferous	C <sub>2</sub>						
		Upper Carboni- ferous	C <sub>3</sub>						
				350		Rapid regres- sion. Extensive expan- sion of more	Major		

	Permian P	Lower Permian	P <sub>1</sub>	50	300	Pro- nounced pre- domi- nance of land	Major
		Upper Permian <th>P<sub>2</sub></th> <td></td> <td></td> <td></td> <td></td>	P <sub>2</sub>				
	Triassic Tr	Lower Triassic	T <sub>1</sub>				
		Middle Triassic	T <sub>2</sub>	50	250	None	Minor
		Upper Triassic	T <sub>3</sub>			Kimmer- idgian	trans- gression
Mesozoic MZ	Jurassic Jr	Lower Jurassic	Jr <sub>1</sub>				
		Middle Jurassic	Jr <sub>2</sub>	50	200	Conti- nued Kimmer- idgian	Minor
		Upper Jurassic	Jr <sub>3</sub>				trans- gression
	Cretaceous K	Lower Cretaceous	K <sub>1</sub>				Minor
						Large- scale trans- gression	

Table 3.1 (concl.)

Era (geological group). Name and index	Period (rock system). Name and index	Epoch (rock-unit division). Name	Index	Duration of period, mln. yrs	Orogeny	Transgres- sion and regression	Volcanism
Cainozoic or Cenozoic KZ	Paleogene Pg	Upper Cretaceous	K <sub>2</sub>	70	Quies- cence	Immense- scale trans- gression	Very intensive
	Paleogene Pg <sub>1</sub> Eocene Pg <sub>2</sub> Oligocene Pg <sub>3</sub>			40	70	Trans- gression	Intensive
	Neogene Ng			25	Alpine folding	Regres- sion	Major
	Quater- nary Q or Anthro- pogene A	Lower Quater- nary	Q <sub>I</sub>	1.5-2.0	Alpine folding	Large- scale northern (boreal) trans- gres- sion.	Pro- nounced
		Middle Quater- nary	Q <sub>II</sub>			Other types of trans- gression are of minor scale	
		Upper Quater- nary Recent (Holocene)	Q <sub>III</sub>				

Note. Paleogene and Neogene are often classified as the Tertiary Tr. Foreign geologists generally present the geological succession in the reversed order, in conformity with stratigraphical succession—(Translator's Note).



**Sec. 3.3. Some Facts from Historical Geology**

I. *The Archean* (or *Archeozoic*) is the oldest era (or geological group) in the earth's geological history that lasted for about a billion years and witnessed origination of the earth's crust and appearance of early water and also deposition of huge layers of sedimented rocks.

All Archean rocks display intense dislocation and numerous granitic intrusions. The Archean rock group is typically composed of gneisses, various slates and quartzites greatly metamorphosed. Archean rocks display significant density and competence. If unweathered they provide excellent material as a foundation for various structures. In the USSR Archean rocks are exposed in Karelia, in the Kola Peninsula, in the southern European region of the country (Southern Russian crystalline shield) and in East Siberia. In particular the Dnieper dam is supported by granite-gneisses.

II. *The Proterozoic* is the second oldest era in the earth's geological history. It lasted about 600 to 800 million years. The epoch was characterised by a warm tropical climate, vast expansion of the sea where limestones accreted over huge areas.

Most Proterozoic rocks are typically sedimented material showing a more or less appreciable degree of metamorphism (metamorphic chists, phyllites, quartzites, conglomerates and marbles). Proterozoic rocks occur in Karelia, in the Urals, in Soviet Middle Asia and in the Altai Mountains.

III. *The Paleozoic* is the third era of the geological time scale that lasted 300 to 350 million years. This era is divided into the following periods: (1) *Cambrian* (C); (2) *Ordovician* (O); (3) *Silurian* (S); (4) *Devonian* (D); (5) *Carboniferous* (C); (6) *Permian* (P).

The Paleozoic era witnessed two vigorous orogenies: the Caledonian (Ordovician and Silurian) and the Hercynian Orogeny (Middle- and Upper-Carboniferous and Lower Permian). The Paleozoic displayed correspondingly phases of tectonic inactivity (evolution) as well typified by the low level of continental massifs and transgressions of the sea.

The Paleozoic climate was mainly characterized by tropical and subtropical conditions which were followed in orogenic times by continental conditions where general cold temperatures prevailed. An example of drastic deterioration of climatic conditions is provided by the Permian period in which a vigorous Hercynian orogeny occurred. A number of areas experienced glaciation in the period of peak activity of the Hercynian mountain-building phase and maximum uplift of the continents.

Paleozoic rocks display a pronounced diversification both of composition and the degree of metamorphism and of the mode of occurrence. Various limestones, marls and dolomites (marine facies) are very much abundant.

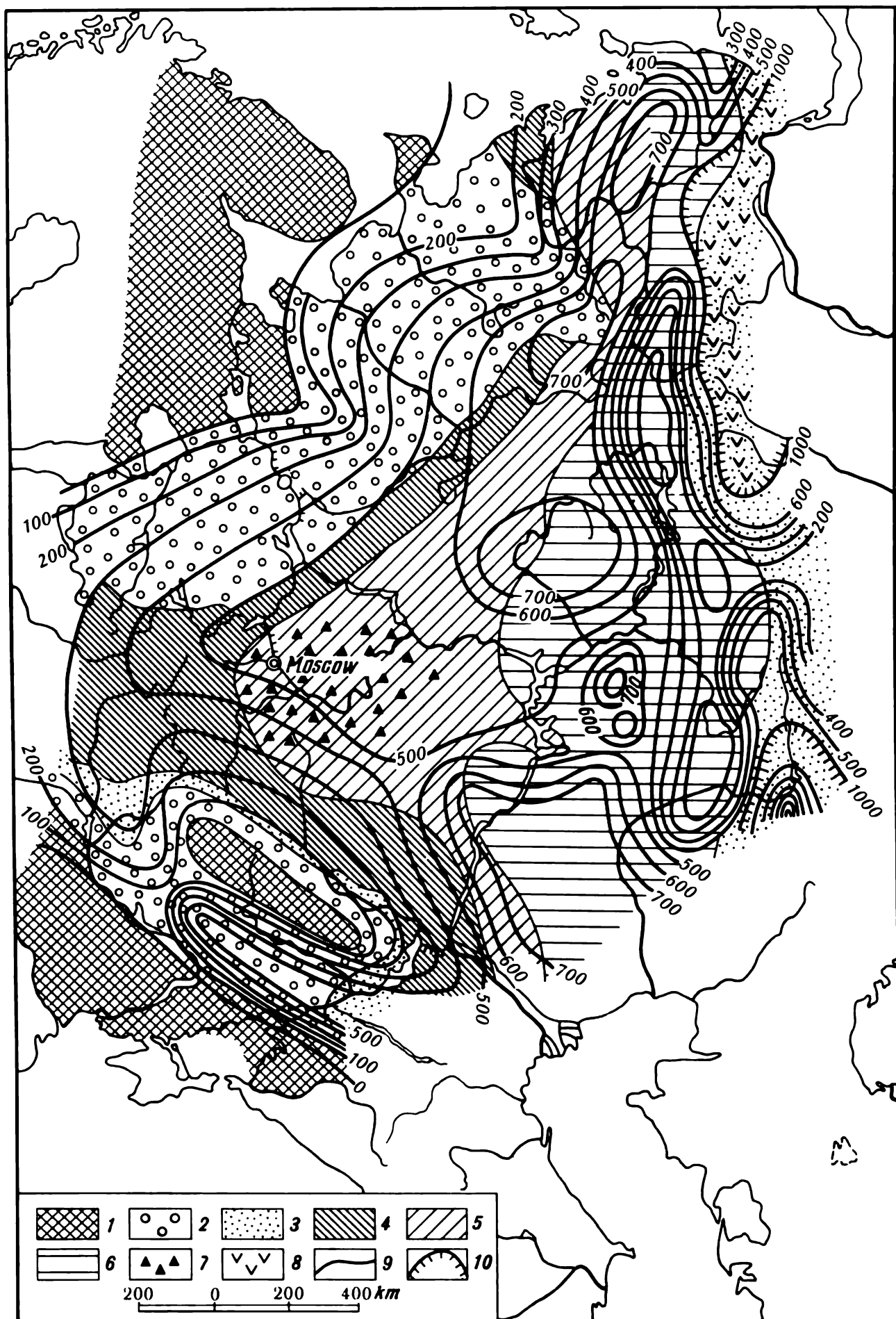


**Fig. 3.1. Facies of Famennian and thicknesses of Upper Devonian sediments of the Russian Platform:**

1—outwash regions; 2—red beds; 3—sands and clays; 4—clays, limestones and dolomites; 5—limestones and dolomites with interlayers of clays and marls; 6—limestones and dolomites; 7—gypsum; 8—igneous rocks; 9—100 m-interval isolines; 10—1000 m-interval isolines (after A.B. Ronov)

Paleozoic rocks are represented within the area of the continental platform (depending on the facies involved) by diverse clays, sands and soft sandstones (Figs. 3.1 and 3.2).

Stratification areas of the Paleozoic exhibiting pronounced dislocations are typically composed by different metamorphic rocks and at places by crystalline rocks and even gneisses.

IV. *The Mesozoic* is the fourth era in the geological succession. It consists of three periods: (1) Triassic (T); (2) Jurassic (Jr); (3) Cretaceous (Cr).

The Mesozoic era was marked by relative tectonic inactivity. The Jurassic period witnessed Kimmeridgian orogeny. This is why the Jurassic was largely typified by continental conditions, accumulation of continental facies deposits (coals) and shallow sea (black or dark-grey clays). Nevertheless the Mesozoic era had a warm uniform climate. Among Mesozoic sedimentation materials marine and continental deposits occur in approximately equal proportion. The most important of the former are argillaceous schists; various sandstones and marls are rather abundant; to a lesser degree, sandstones and conglomerates. This era's third period is characterized by white chalk which provides evidence of a large-scale marine transgression of the Cretaceous that gave rise to vast water basins



Fig. 3.2. Devonian sandstones of East Siberia showing plate parting

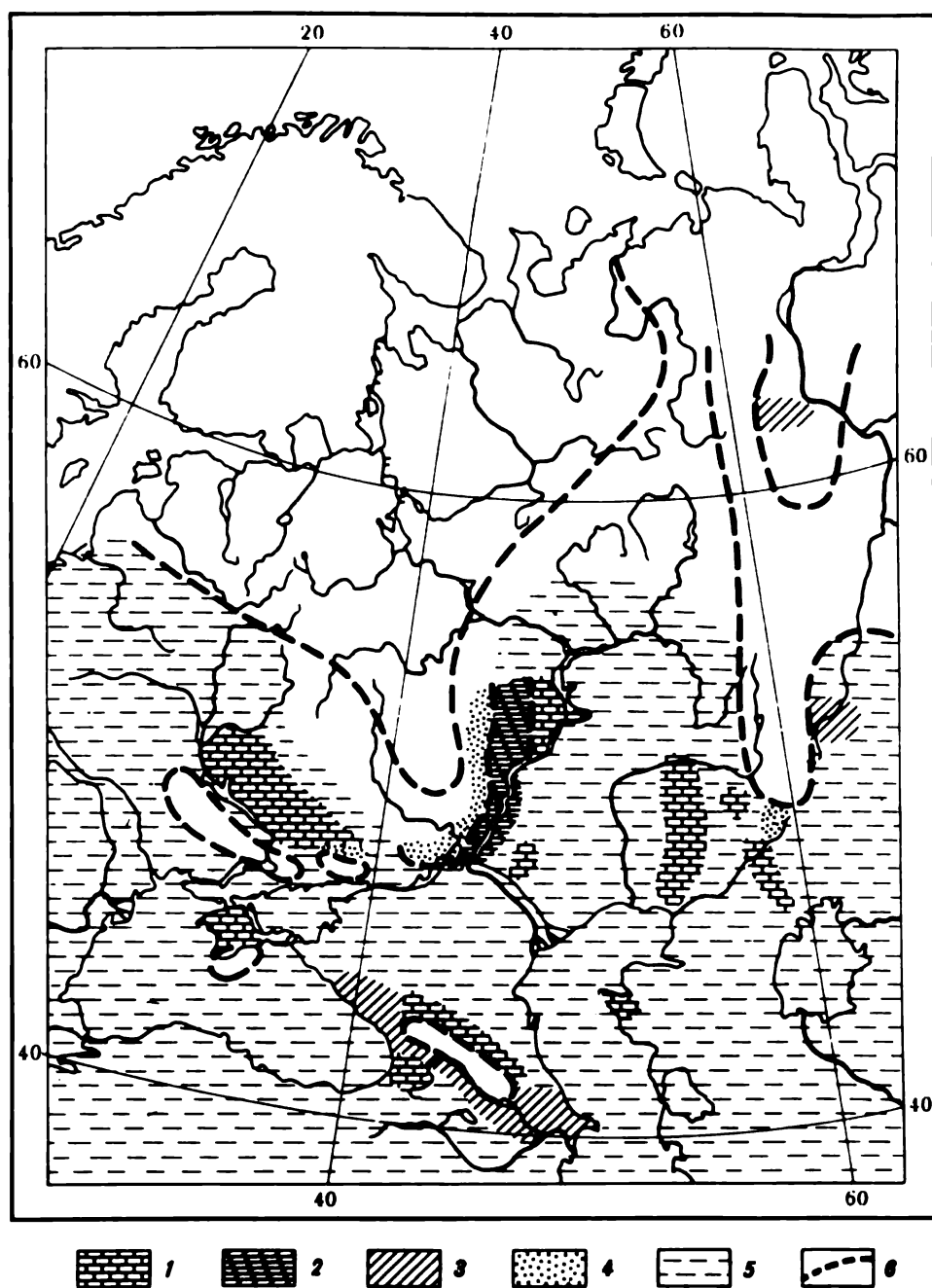


**Fig. 3.3.** Paleographic map of the Russian platform in the later half of the Upper Cretaceous (after N.P. Strakhov):

1—chalk; 2—clay marl rocks; 3—clays alternated by sand bands (flysch); 4—sands; 5—region of hypothetical formation of marine deposits; 6—probable boundary of expansion of the sea

within the area of continental massifs. Figure 3.3 illustrates the paleogeography of the epoch.

Sandstones, hardpans, limnetic marls and even argillaceous sandstones are prevalent of the continental facies rocks.

Mesozoic group deposits very often occur both in the European and Asiatic USSR. It should be pointed out that gigantic reptiles, dinosaurs (Greek for terrible lizards) widely spread over the earth in the Mesozoic that lasted 50 to 250 million years. Some specimens reached 25 m in length and 60 t in weight.

V. *The Cainozoic* (or *Cenozoic*) is the youngest era extending to the present. It includes *the Paleogene, Neogene* and *Quaternary*. It is this period that demonstrated vigorous, so-called Alpine orogeny which is associated with the appearance of the Alps, mountain ridges of the Caucasus, Crimea, Himalayas and other mountain ranges.

Very warm, almost tropical conditions existed during the early half of the Cainozoic (Paleogene). Later, as the Alpine Orogeny further developed, the conditions began to deteriorate. As to the climate of the Neogene, it was typified by pronounced cooling. It is then that the first symptoms of the future glacial epoch appeared.

As is known, up to the present time vast areas of Arctic lands (Greenland, Franz-Josef Land, Canadian Archipelago) and of the Antarctic are covered by thick ice sheets. The glacial shield that covers Greenland and Antarctic is at places 1.5 to 3 km and more in thickness. The area of Antarctic which is hidden under a sheet of ice is an impressive 14 million km<sup>2</sup>. Moreover, traces of oldest ice ages that occurred hundreds of millions of years ago have been discovered in other continents, including southern Africa. This evidence attests to the fact that the earth has experienced several ice ages.

During the last billion years which is less than a quarter of the earth's age, there have occurred at least four epochs when most of the terrestrial surface was ice-covered. We are living in the fourth of glaciation periods. A two km thick layer of ice buries Antarctic and Greenland, most of the Arctic ocean is ice-bound all the year round.

At least nine times within the last million years massive ice shields have advanced to North America and Europe. It took several thousand to ten thousand years for the glaciers to advance and retreat each time, although the climatic fluctuations that resulted in so tragic changes seem to have taken a much shorter time period, probably, some centuries. One dramatic jump from fairly warm climatic conditions directly to the cold of an ice age occurred in Greenland 89.5 thousand years ago. It appears that it took less than a hundred years. Previous snow that had not melted in cool summer was added to by new one, glaciers and ice sheets formed, the mountains of ice began to expand down to lower latitudes and descend downslope to the valleys.

During the last maximum glacial coverage the glacier crept far into North America, into the north of Europe and extended to part of north western Siberia. An impressive 2 km high ice mass moved relentlessly southwards. In so doing, it excavated the basins of Great Lakes, bulldozing the hills, carrying huge boulders and pushing before itself mountains of loose soil. On the American continent Canada proved to be all covered by ice.

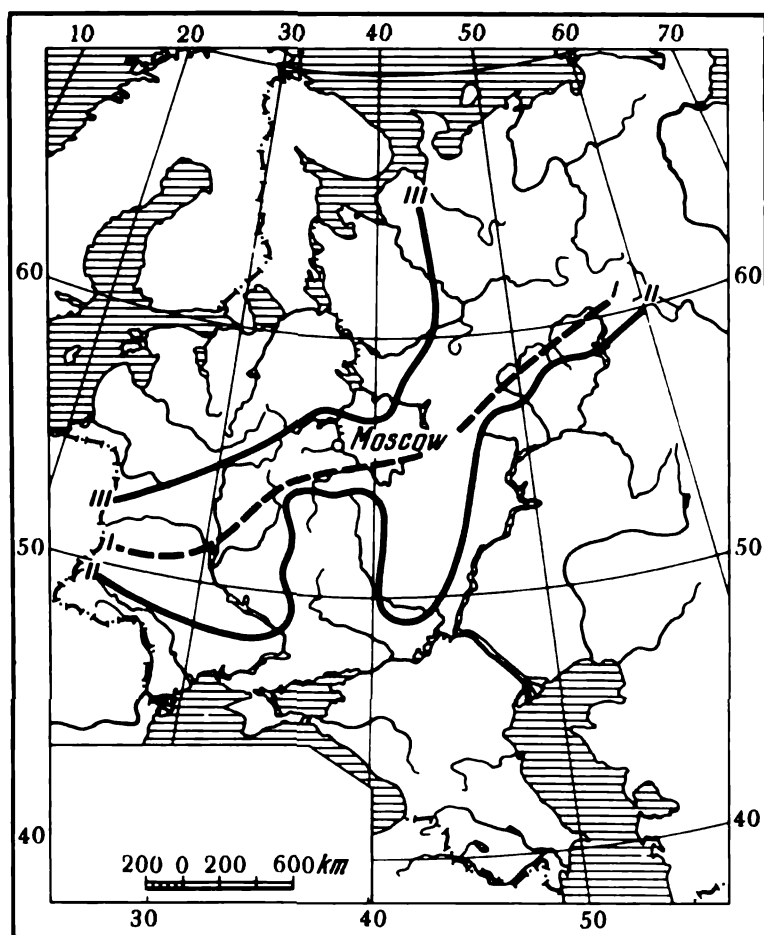


Fig. 3.4. Maximum hypothetical ice coverage in the principal stages of glaciations:

I—Likhvin; II—Dnieper; III—Valdai

The last ice sheet began to contract 14 to 18 thousand years back. A mere 8 thousand years has passed since the last ice shield melted in the region of the Scandinavian Peninsula, and hardly 6 thousand years since the time the permanent ice sheet disappeared in northern continental Canada. These both regions have not yet recovered from the enormous weight of the ice that weighed on them. At some places the surface in these areas heaves up at 20 cm per annum which, in particular, is demonstrated by a recent earthquake in a tectonically quiet region of the Gulf of Finland. Many scientists attribute it to the fact that the earth's crust reestablishes equilibrium once the huge pressure of the Scandinavian ice sheet has been removed whereas in south-eastern Estonia this equilibrium has already been attained.

Naturally, it is the last glaciation period that has been best studied. It began 500 thousand or, as others believe, a million years ago. The last traces of the ice age disappeared in the northern regions of the USSR about 12 thousand years ago.

The last ice age had four stages of Europe: Günz, Mindel, Riss and, finally, Würm. This glaciation period at the territory of the present USSR included three stages, namely *the Likhvin glaciation* (a counterpart to Mindel), *the Dnieper glaciation* (Riss) and the last, *Valdai glaciation*. The hypothetical zone of the expansion of these stages is shown in Fig. 3.4.

The glaciers melted in-between the glaciation periods. Such intervals are said to be *interglacial stages*. So, it is usual to describe thus the last but one interglacial stage between the Likhvin and the Dnieper glaciation.

As a result of general amelioration of the frigid climatic conditions the land freed from the ice sheet was partly inundated by transgressing seas during interglacial stages. These transgressions may have been due to the general low level of the continents that subsided at the time under the enormous weight of the glaciers and to the rise of the sea level as the ice melted. As some areas of the land were freed from ice vast lakes formed, and wide valleys were generated as the result of erosion.

The interglacial stage lasting tens or hundreds of thousands of years was succeeded by a new stage, that of glaciation.

It is possible to determine how far the glaciers expanded in one glaciation period or another from the presence of boulders composed of hard rocks alien to the particular areas along the southernmost limit of their penetration, i.e. ones that have been brought there by the glacier from Scandinavia.

The origin of the glaciation periods has not as yet been fully understood. A number of hypotheses have been proposed to account for these events including a climatic theory, Arrhenius's and Wegener's theories and a cosmic hypothesis.

*The climatic theory* stems from the fact that vast areas of land were covered by ice in the periods that immediately followed vigorous orogenic processes (tectonic revolutions) and loss of heat that resulted from these.

*The Arrhenius theory* accounts for glaciation stages by insufficient carbon dioxide content in the earth's atmosphere at certain periods of time because of waning of volcanism and dramatic spread of vegetation.

*The Wegener theory* refers glaciation of certain areas to the shift of the continents over the terrestrial surface. Such displacements could have caused continents to assume a more northern (or southern) position. This theory agrees with the fact that there is no fit between areas in Africa and Europe that were subjected to glaciation in the earth's geological past.

*The cosmic theory* presents a two-fold explanation of the glaciation periods. First, a change in the tilt of the terrestrial globe may have been the causative agent of glaciation. Second, what appears to be of more interest, the solar system, as it travelled across the galaxy, could have travelled through clouds of cosmic dust (nebulae). This must have led to lowered solar radiation and, consequently, to worldwide frigidity.

Let us resume considering the effect produced by the great glacier of the last ice age in this country. No traces of the Günz stage have been found in the USSR. The Likhvin glaciation has expanded insignificantly. The Dnieper glaciation that followed (counterpart of Riss) has had the greatest



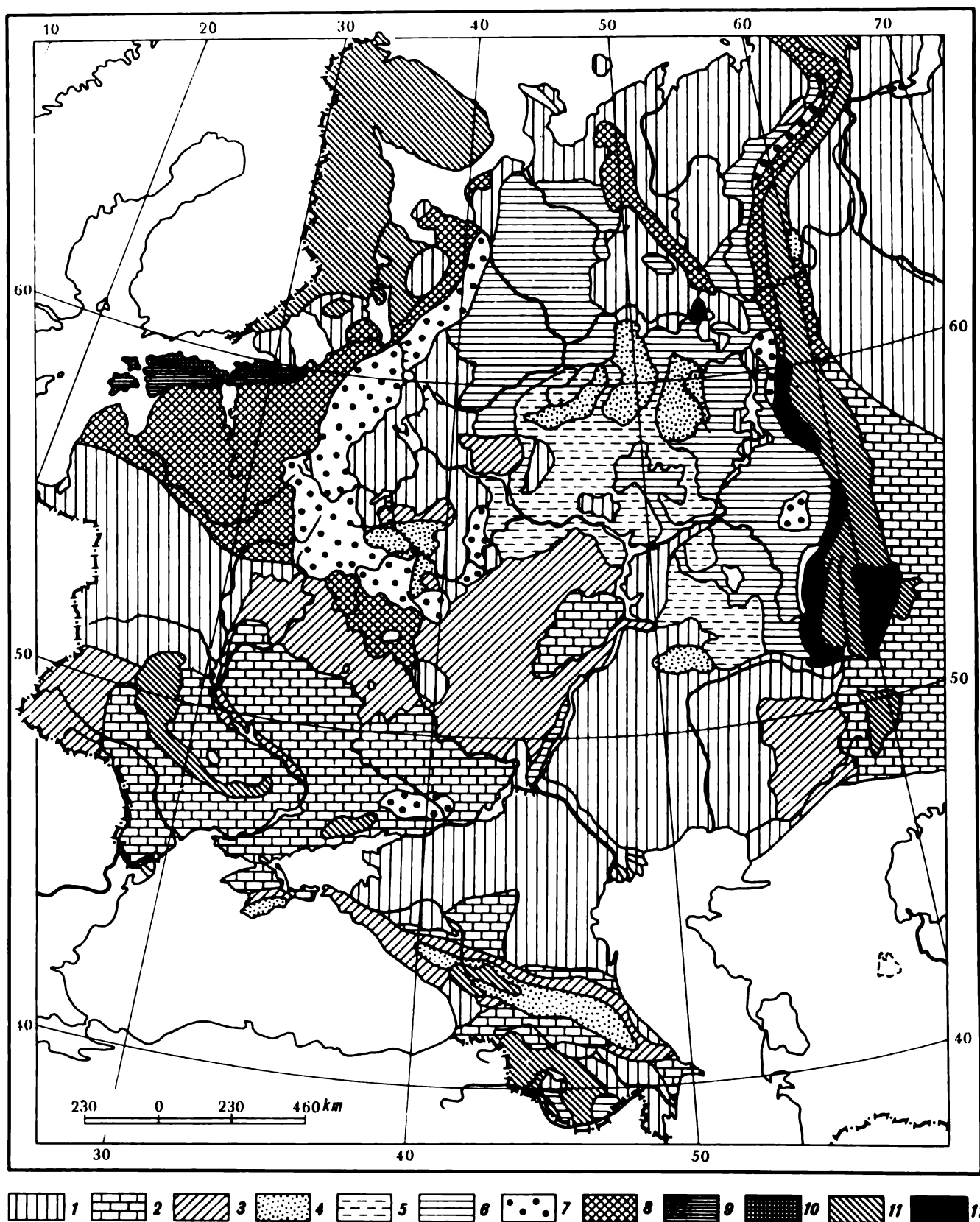


**Fig. 3.5.** Diagrammatic geologic map of the European part of the USSR:

1—post-Tertiary sediments; 2—Tertiary (Neogene and Paleogene); 3—Cretaceous; 4—Jurassic; 5—Permian Triassic sediments; 6—Permian; 7—Carboniferous; 8—Devonian; 9—Silurian and Ordovician; 10—Cambrian; 11-12—outcrops of magmatic rocks and crystalline schists (pre-Cambrian formations, metamorphic and ejected rocks)



effect and caused glacial deposits to be moved the farthest. This period saw vast areas of the European Soviet Union covered under a blanket of ice. Ice advanced as far as today's Dnepropetrovsk on the Dnieper and the mouth of the Medveditsa River, a tributary of the Don. The scale of the last, Valdai, glaciation (counterpart of Würm) was much smaller. The glacier only reached the Volga River's sources and the coasts of the White Sea.

As pointed out above, the origin of glaciations was mainly in the Scandinavian Peninsula and today's Bolshaya Zemlya Islands. As it advanced, the continental glacier did an enormous amount of work: it eroded the earth's surface carrying the disrupted rock material to sometimes appreciable distances. As the glacier encountered various crystalline and sedimentary rocks, these latter were added to the broken rocks the glacier was moving.

If the conditions prevented moving glaciers from being formed, huge masses of stagnant, "dead" ice accumulated in the corresponding climatic zones. This ice sheet did neither destructive nor constructive work. No glacial deposits are to be found in such regions. Such conditions, in particular, prevailed over vast areas of Siberian plains.

Figure 3.5 presents a schematic geological map of the European USSR showing the limits of expansion of sediments in different life periods of the earth.

Such maps do not indicate the overburden layers formed by quaternary deposits or those in the areas of expansion of pre-Quaternary (Tertiary and older) rocks. Where rocks belonging to this system or another prevail, it is usual to show in maps the age of pre-Quaternary rocks that occur the most closely to the earth's surface.

Naturally, deposits of a given system are underlain in each particular case at a definite depth by rocks of earlier origin according to the geologic column in a sequence described above. Not all of the previous formations may be represented in the geologic column. There may be gaps (hiatuses) which usually suggest that the area in question was that of land at the given period.

# Part Two

## Elementary Engineering Soil Science

---

### Chapter 4 Igneous Rocks

---

#### Sec. 4.1. Rock-Forming Minerals

All rocks and soils are aggregates of different minerals or broken remnants of the parent rocks. Rocks and soils differ in strength that is determined as these are worked. Rock materials are generally hard, like granite or limestone. For their manual working we use tools, such as a crowbar, a pick or resort to blasting operations. Soils usually include common sands, clays, peat and other materials that can be cut with a spade.

All rocks and soils differ in mineralogical composition that determines their chemical or salt composition and in state (density, humidity, weathering etc.) and also in *structural* and *textural* properties.

In the particular case structure is understood to be the peculiar properties of the internal structure of a rock or soil governed by the size and shape of minerals composing the rock (soil) and by the nature of bonds between their individual components, in particular, the degree of crystallization etc. The structure determines the appearance of a rock (soil), such as solidity, uniformity, stratification and porosity.

*Minerals* that compose rocks and soils are naturally occurring substances (compounds) or elements produced by complicated physico-chemical processes that are at work in the earth's crust. Of the known 3 000 minerals a mere 100 are of particular importance in formation and structure of rocks. These minerals are termed *rock-forming*.

Minerals differ in appearance and may occur in a crystalline or, less frequently, amorphous form or as an earth-like or glassy mass; in chemical composition, density, rigidity, foliation (ability to cleave, like mica, to develop smooth and even surfaces), cleavage plane and lustre.

There are standards to evaluate each of these properties. In particular, the hardness of minerals is measured with reference to what is called Mohs scale of hardness. It includes the softest (designated 1) mineral, talc, and the hardest (designated 10), diamond.

Reliable identification of a mineral sample generally calls for special techniques of analysis, special microscopes etc. We omit considering these problems since they are irrelevant to engineering geology.

Brief specifications of the most important rock-forming minerals are

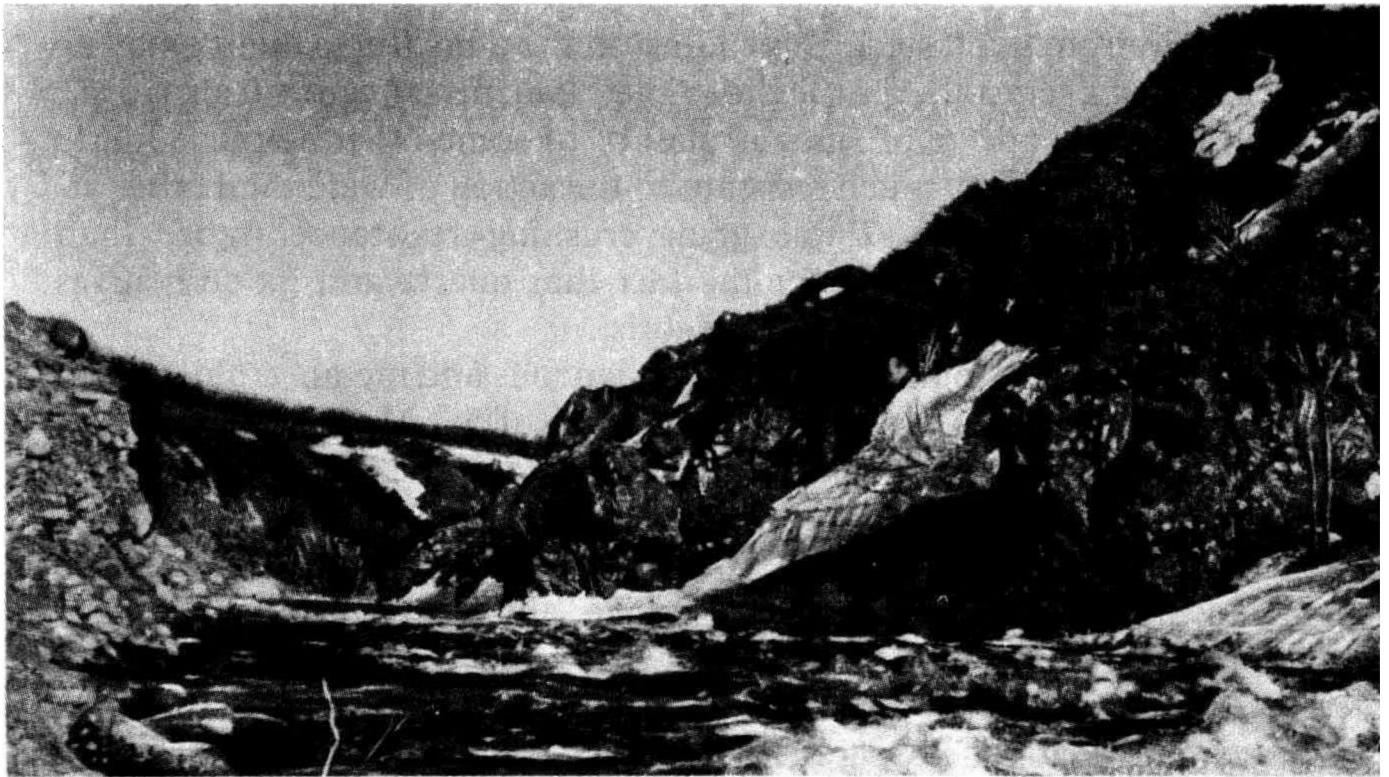


Fig. 4.1. Pre-Quaternary igneous rocks in the valley of the River Kronotskaya (photograph courtesy of the Leningrad Institute of Geology)

listed below when dealing with these rocks and soils or other which are divided, according to their origin, into igneous, sedimentary and metamorphic materials.

*Igneous rocks* are ones that have penetrated from the earth's interior to the surface or beneath the same as melted material and then cooled. They also include pyroclastic rocks ejected from volcanoes in explosive events.

*Sedimentary rocks* (known also as derivative, neptunic or stratified rocks) have been formed by consolidated sediment deposited from the water or air. These include products of weathering of all three species of rocks described above.

*Metamorphic rocks* are materials that have been changed from previously existing sedimentary (and, frequently igneous) rocks by the action of heat, pressure and associated physical and chemical activity.

Igneous rocks include granites, diabbases, porphyrites, basalts and many others (Fig. 4.1). Igneous rocks differ very much in chemical composition, structure and texture.

Clearly, the chemical composition of an igneous rock is determined by the composition of the minerals that constitute it. The particular rock species are mainly composed of oxides and silicates, main rock-forming minerals.

*Oxides* include *quartz*,  $\text{SiO}_2$ , free silica, one of the most abundant minerals. Its density is 2.65, it is fairly hard: quartz will easily scratch a

knife's blade from good steel. Depending on the admixtures quartz may be colourless (rock crystal), purple to violet (amethyst), grey (cainngorm, called also smoky quartz or smokestone) or of some other colour. Quartz and its varieties are very much resistant to the action of water and other atmospheric agents. They exhibit great crushing resistance (more than  $1\,000\text{ kg/cm}^2$ ). This accounts for the fact that quartz and its derivatives often occur in sedimentary rocks as debris.

*Silicates* are main components of most igneous and metamorphic rocks. These represent complex compounds made up of Si, Al, Fe, Ca, Mg, Na, K, O, H occurring as various salts of silicic acids. The most abundant of these are feldspars, micas, hornblende, augite.

According to their composition *feldspars* are divided into two major subgroups: (a) anorthoclases, richest in silica, and (b) plagioclases, that are less rich in silica.

Anorthoclases include potassium-sodium feldspars; plagioclases comprise sodium-calcium feldspars. Potassium feldspars occur chiefly as *orthoclase* ( $\text{K}_2\text{O} \cdot \text{Al}_2\text{O}_3 \cdot 6\text{SiO}_2$ ); sodium feldspars, as *albite* ( $\text{Na}_2\text{O} \cdot \text{Al}_2\text{O}_3 \cdot 6\text{SiO}_2$ ). Plagioclases notably occur as *anorthite* ( $\text{CaO} \cdot \text{Al}_2\text{O}_3 \cdot 2\text{SiO}_2$ ). Anorthoclases are characterized by light colouration (pale pink, pink yellow, reddish, less often white colour).

Plagioclases have greyish shades (greyish white, greyish green) and may be even bluish brown (Labrador spar, or labradorite).

The unit density of feldspars is 2.6 to 2.7, they are rather hard: similarly to quartz, they will scratch a knife from strong steel. It should be noted that under the action of atmospheric agents feldspars are fairly quickly eroded and decompose forming new compounds, in particular, kaolinite.

*Hornblende* that belongs to the amphibole group has the unit density 3.1 to 3.3 and is very hard: it will scratch a blade from a high carbon content steel. It is green and brown to black in colour. Hornblende is commonly found in igneous and metamorphic rocks. It is easily eroded forming more resistant minerals, such as serpentine, chlorite etc.

*Augite* (pyroxene group) has a density 3.2 to 3.6 and an appreciable hardness: it will also scratch a blade from hardened steel. It is dark green to black in colour. Augite is found in common igneous rocks.

*Micas*, such as *muscovite* (white mica) and *biotite* (black mica) are found in most igneous and metamorphic rocks. They often occur as scales in sedimentary rocks. Micas are fairly resistant to weathering.

#### Sec. 4.2. Characteristics of Igneous Rocks

Depending on chemical composition and silicon dioxide ( $\text{SiO}_2$ ) content, igneous rocks are classified as *ultraacidic*, *acidic*, *intermediate*, *basic* and *superbasic*.  $\text{SiO}_2$  content in acidic rocks is 65 to 75% (*granite* group), in in-

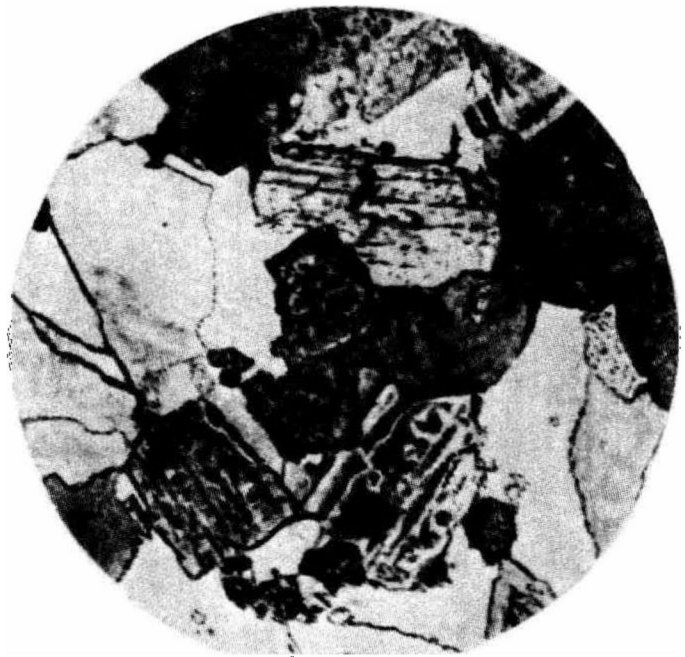


Fig. 4.2. Completely crystalline granular structure of a magmatic rock (magnification 46X)

intermediate rocks 52 to 65% (*syenite* and *diorite* groups), in basic rocks 52 to 65% (*gabbro* group). Ultraacidic and ultrabasic rocks that have a very limited distribution are not considered here.

Acidic rocks display increased quartz and potassium and sodium feldspars contents (orthoclase and microcline). Basic rocks are ones where sodium-calcium spars alternatively called plagioclases (albite, oligoclase, anorthite) typically occur.

Coloured minerals, such as hornblende, augite and biotite, that give these rocks dark colouration and higher bulk density are commonly found in basic rocks.

According to origin, conditions of formation and mode of occurrence igneous rocks fall into three classes: *plutonic* or *intrusive* rocks, *effusive* and, finally, *hypabyssal* igneous rocks (ones that rose from great depths and solidified as vein-like intrusions before they reached the surface).

Depending on the particular conditions that prevail, magmas of the same initial composition form different igneous rocks. So, diorite, an intermediate igneous rock, has resulted from the intrusive rock group; *porphyrites* (older rocks) and *andesites* (younger rocks) have originated from the effusive equivalent. Although of identical chemical composition, they differ in structure similarly to rocks of diverse groups.

In the course of slow cooling, typical for intrusive igneous rocks, magmas completely decrystallize as they pass to a solid state.

In this fashion plutonic (intrusive) rocks having a *completely crystalline (grained) structure* formed (Fig. 4.2). Granites, syenites, diorites and gabbro, different in chemical composition, are similar in this respect. Protrusions of magma solidify forming bodies of igneous rock that vary in shape: batholiths, laccoliths and different veined protrusions (Fig. 4.3).

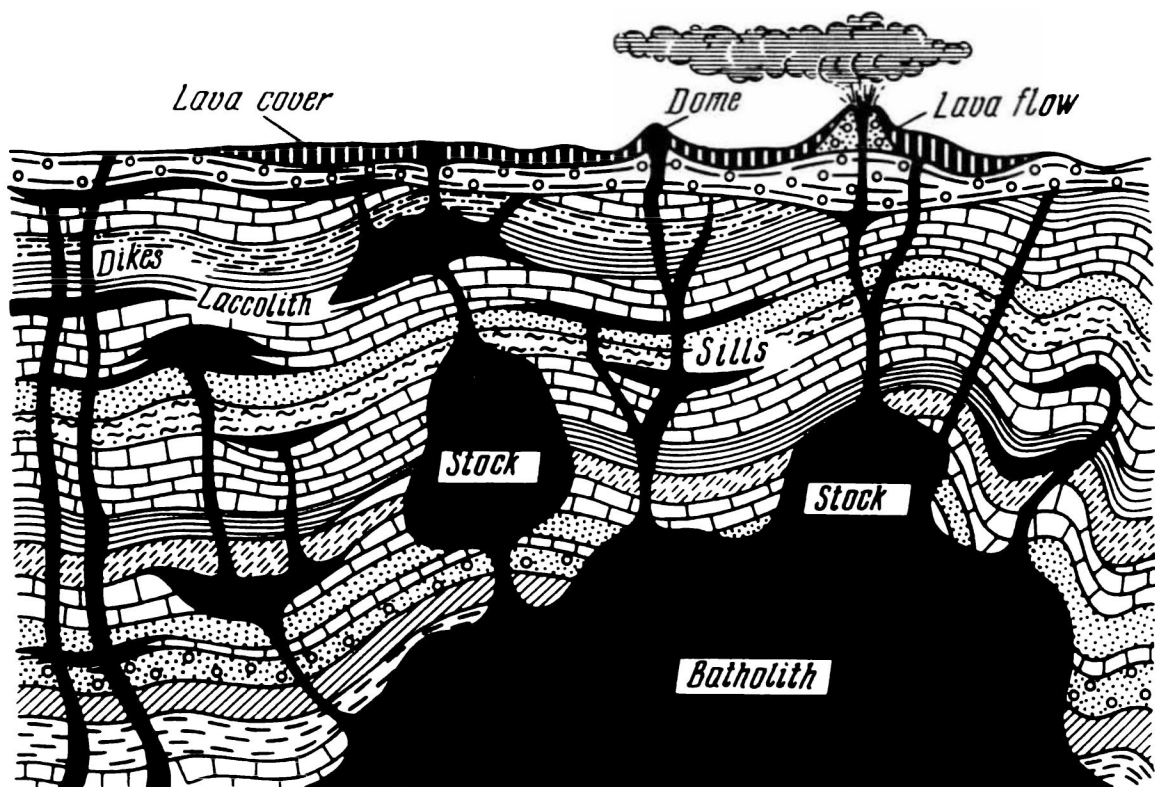


Fig. 4.3. Plutonic intrusive forms (after Yu.M. Vasilyev)



Fig. 4.4. "Ivan Razboinik" cliff in east Crimea. A keratophyre (equivalent of syenite laccolith after "liberation" due to washing out from the host mass of lava and tuff: (photograph by E.M. Dobrov)



A *batholith* is a body of intrusive igneous rock, 10 000 km<sup>2</sup> or more in area, that is exposed at the surface only if the overlying rocks (overburden) have been eroded. The thickness of a batholith may be enormous.

A *stock* is a batholith of a relatively small size.

A *laccolith* is a loaf-like body of intrusive rock, usually with a flat base. Laccoliths usually occur as magmatic bodies intruding into sedimentary rocks so that the overlying layers are noticeably lifted due to the effect of intrusion.

Examples of laccoliths as bodies of intrusive rock exposed after the host rocks have been eroded or washed out can be provided by Mt. Ayu-Dag (Bear Mountain) in the Crimea, by Mts. Mashuk, Beshtau and mountains in the vicinity of Mineral'nye Vody in the North Caucasus. A laccolith cliff called Ivan Razboinik (Ivan the Brigand) has a peculiar shape (Fig. 4.4).

A *veined shoot* is a crevice filled with magma branching from a larger body of intrusive rock. Most veined shoots are secant, i.e. cutting sedimentary rock strata at an angle. They are usually 1 to 3 m in thickness. A vertical veined shoot is termed a *dike*. As host rocks are eroded dikes often appear as collapsed fortress walls (Fig. 4.5).

*Veins*, or *layered intrusions*, occur less frequently. Unlike layered veins, layered intrusions which are bodies of igneous rock protruding between rock layers are usually very large in area. Such are, for example, *traps* known also as *trappides* or *trap rocks* (diabases and basalts) that occur in Siberia.

*Effusive magmatic activity* occurs as magma penetrates to the surface through crevices or as volcanic eruptions. In the former case magma transforms to lava at the surface, usually expanding over large areas and forming *lava fields*. This phenomenon is especially characteristic for melts of principal composition that display low viscosity and great mobility.

In contrast to the origin of lava fields volcanism is associated with outflow of denser acidic melts having lesser mobility and greater viscosity. Lava fields, especially basaltic, may vary from a few metres to 1 to 2 km in thickness and are then called lava plateaus (Deccan Plateau in India or ones in Oregon, USA).

The difference in the rate of magma cooling and in the speed at which magma loses its gases converting to lava led to the following principal varieties of effusive rock structure: porphyritic (Fig. 4.6), cryptocrystalline, glassy and porous texture indicating the conditions under which cooling proceeded the most rapidly.

*Porphyritic texture* shows more or less large individual crystals, usually of feldspars, imbedded in host mass, uncrystallized or weakly crystallized.

The structure of effusive rocks can, to a certain degree, provide evidence as to the thickness of a body of igneous rock. It is indeed known

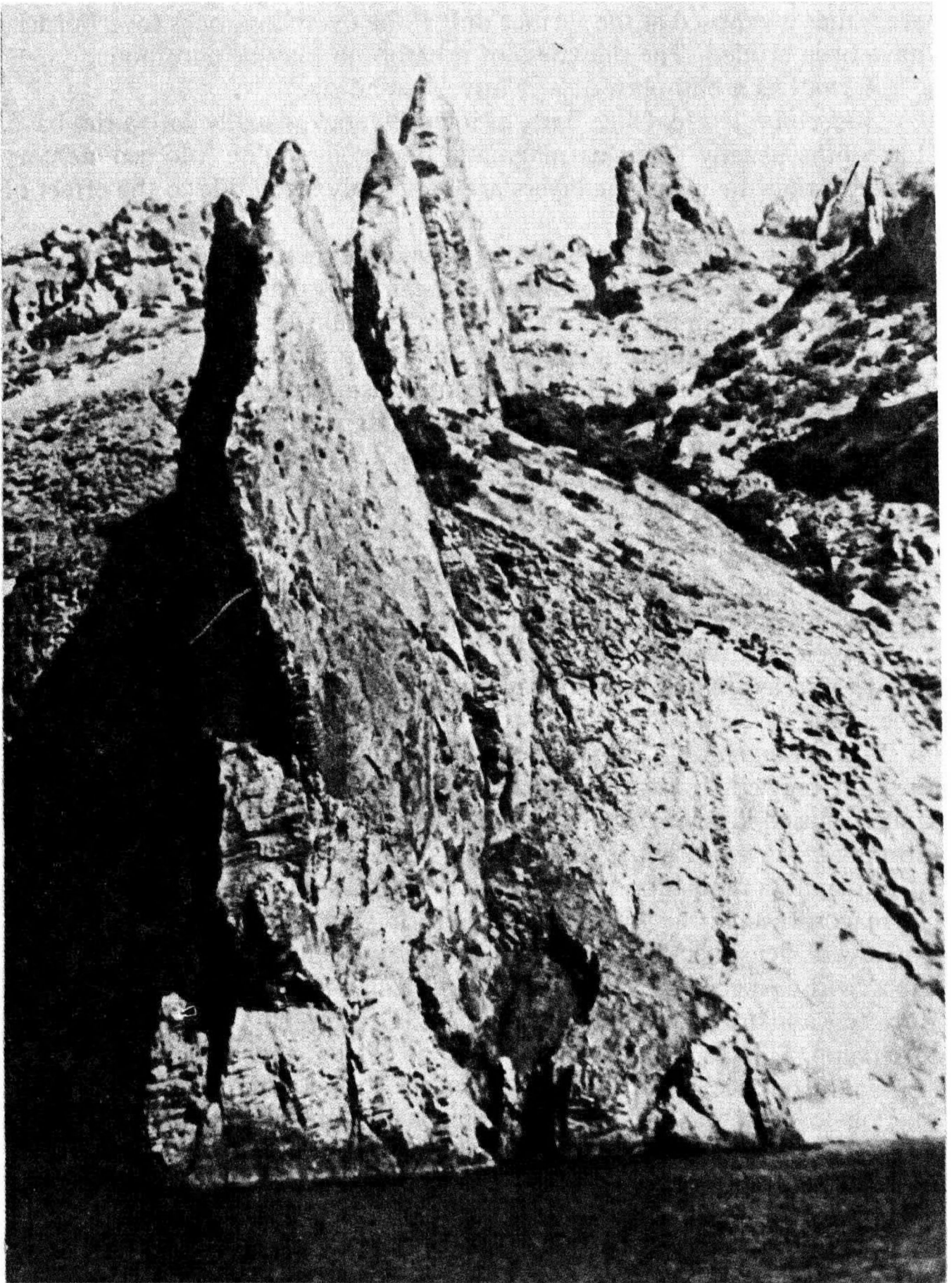


**Fig. 4.5.** A magmatic rock dike. The Crimea (photograph by E.M. Dobrov)



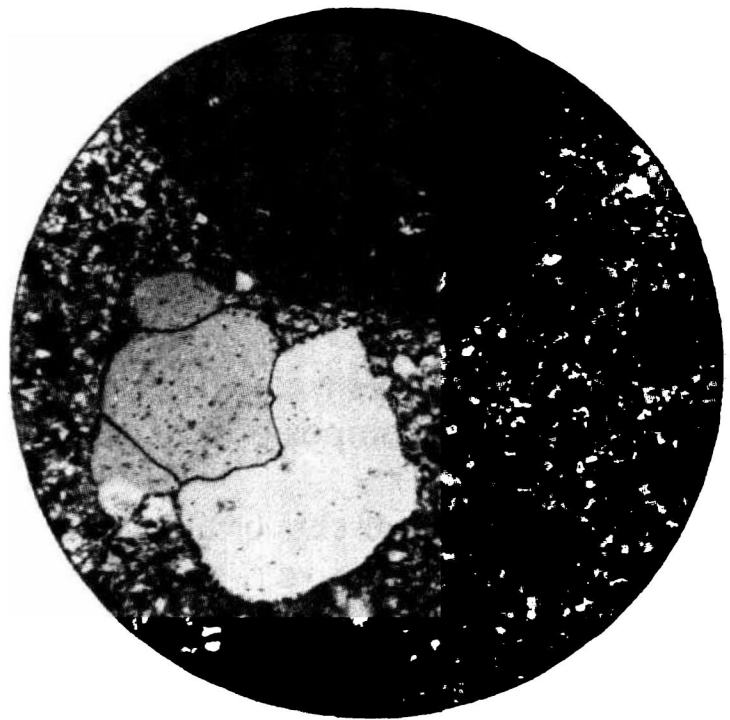


Fig. 4.6. Structure of an effusive rock (magnification 46X)

that a small body with a larger relative surface will cool more rapidly than a large one. Hence, effusive igneous rocks with porphyritic texture, the proof of relatively slow cooling of a body of igneous rock, point to its fairly large thickness.

*Vitreous* texture and, to a larger extent, porous texture suggest quite a different mechanism. Such textures were formed upon rapid cooling of magmas or lavas when magma could not have completely decrystallized before it solidified. In addition, *porous* and, to a greater degree, *spongy* texture resulted from the fact that as the effluent magma cooled it had been rapidly losing its gases. Such a texture is typical for basaltic slags and, especially, for pumices.

The thickness of a body of igneous rock is one of the principal factors that determine the bearing capacity of the bedrock. It should be kept in mind, however, that under definite conditions the thickness of igneous rocks may be insignificant, only a few centimetres. There are places where the effluent basaltic rock on volcano slopes is underlain by ice. The thickness of a body of igneous rock points, on the one hand, to the intensive rate and incorporation of magma into the crustal layers or solidified lava layers. On the other hand, it may attest to the viscosity of magma that, given specific conditions, may penetrate to minor fissures in the earth's crust. It is not uncommon that the decisive role in this process is played by viscosity of fiery-hot rock melt at a particular cooling stage. Naturally, it is the chemical composition of magma or lava that is the determining factor.

It appears that at the same temperature iron-rich melts possess the least viscosity, i.e. melts that form, as they cool, *basic* rocks enriched by iron-

containing minerals, such as augite, hornblende (amphibole), pyroxene and others. In contrast, silicate- and silica-rich melts which is typical of *acidic* rocks, cool more rapidly.

From what has been said it may be concluded that basic igneous rocks of dark colouration which are heavy and display necessarily undefined crystalline structure may, under certain conditions, be of a particularly small thickness. Such a structure is indicative of rapid cooling of a body of igneous rock.

Table 4.1 presents a classification of principal igneous rocks according to their chemical composition. It also gives some additional data on rocks of interest.

What follows presents brief characteristics of individual igneous rocks.

*Granite* is an intrusive rock with a complete crystalline structure of the acidic group (Fig. 4.7). It is widely distributed in the USSR. Granites generally occupy areas of several thousand km<sup>2</sup>. Most of major hydropower stations in the Soviet Union have been constructed on granites. Among these are the Krasnoyarsk, Bukhtarma, Dnieper, Upper Tuloma and other power stations. Granites are abundant in the southern Ukraine, Kola Peninsula, Siberia, in particular, in the region of the Kolyma River.

*Liparite* and *quartz porphyries* are, respectively, young and old granitic effusive rocks. They have porphyritic texture in which quartz and feldspar crystals are usually enclosed.



Fig. 4.7. Granites in the Kolyma River basin

Table 4.1

Classification of Igneous Rocks

Acidity	Acid content, %	Rocks		Colour	Fusibility	Principal mineralogical composition, %			Bulk density, t/m <sup>3</sup>
		intrusive (plutonic)	effusive (volcanic)			quartz	feldspars	coloured minerals	
Acid	> 65	Granites	Quartz porphyries, liparites, obsidian, pumice	Grey (less often dark-grey), pink, reddish	Refractory	15-40	40-60	5-10 (micas, hornblende)	2.6-2.7
Inter-mediate	65-52	Syenites	Porphyries, trachytes	Grey, dark-grey, reddish	Medium	None or negligible	85-90	10-15 (hornblende, augite, biotite)	2.7-2.95
		Diorites	Porphyrites, andesites	Grey, dark-grey, dark-green		About 70	About 30	(hornblende, augite, biotite)	
Basic	52-40	Gabbro	Diabases, basalts	Dark-grey, black, dark-green	Pronounced	None	50	50 (augite, hornblende)	2.8-3.1

**Obsidian** (volcanic glass) is a glassy rock of a grey to brown to jet-black colour. Also known as hyalopsite, Iceland agate, mountain mahogany. **Pumice** (also known as pumicite, volcanic foam) is a spongy glassy rock.

**Syenites** resemble in their appearance granites but differ from these latter by the absence of quartz and somewhat higher content of coloured minerals (see Fig. 4.4). Syenites are less abundant in the USSR than granites. They occur mostly in the vicinity of the Ukrainian crystalline massif and in the Urals (Mts. Blagodatnaya and Vysokaya, Nizhni Tagil). Sculptures were executed from syenites in ancient times, such as, for example, the sphynxes brought to the banks of the Neva River.

**Trachytes** as its older equivalent, *porphyry*, represent an effusive facies of syenite magma. Trachytes are generally light-coloured with a greenish shade.

**Diorite** is phaneritic (coarse-grained) plutonic rock with granular texture of a dark grey or greenish-grey colour, of medium acidic composition. Diorites generally occur as veins and are alternatively called black granites.

**Andesite** (extrusive volcanic rock) is an equivalent of diorite. Like basalts, andesites are the most abundant lavas and compose together with the latter vast volcanic nappes in the Caucasus and Kamchatka. Andesite is generally of a dark grey with a greenish shade. Porphyry is an old equivalent of andesite.

**Gabbro** is a group of basic medium and large-grained igneous intrusive rocks. They are dark-green and black coloured. Especially abundant in the Ukraine and Urals. Labradorite (or Labrador spar) that belongs to the gabbro group is a beautiful ornamental stone with a peacock's eye texture of a blue colour.

**Basalt** (Fig. 4.8) and its older equivalent, *diabase*, or *dolerite* are the most abundant rocks of an effusive facies of gabbro magma. Basalts and diabases are most frequently found in East Siberia (traps), in the Caucasus and Armenia where shoots of these rocks penetrate layers of clayey shales occasionally. Yet more frequently they occur as nappes. This rock group, after granites, has been best studied as a construction material. Diabases support the Bratsk, Ust-Ilim, Vilyui hydropower stations and others.

Basalts and diabases may be aphanitic to glassy in structure, depending on the thickness of a nappe. They are dark-grey and black coloured. It is not uncommon that basaltic mass rocks are separated by tuff streaks into individual layers indicating volcanic eruptions at different time periods.

**Pyroclastic rocks** are composed of fragmented volcanic products, including ashes (Fig. 4.9), ejected in huge amounts from volcanoes in volcanic eruptions. Ashes are deposited on land or sea floor and, following complicated lithification processes, form *tuffs*. These occupy an intermediate position between purely igneous and sedimentary rocks. Tuffs are very much abundant in younger volcanic areas (Armenia, Kamchatka).

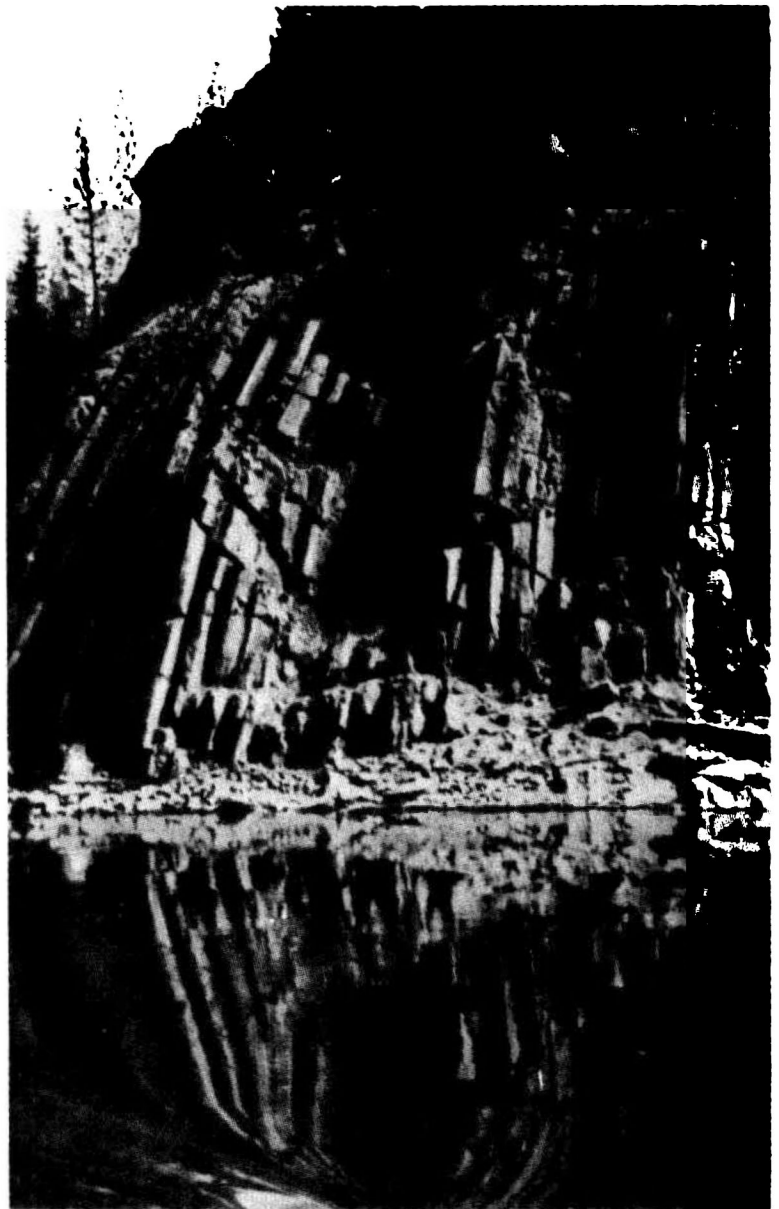


**Fig. 4.8.** Basalt columns in the bank of the Kolyma River

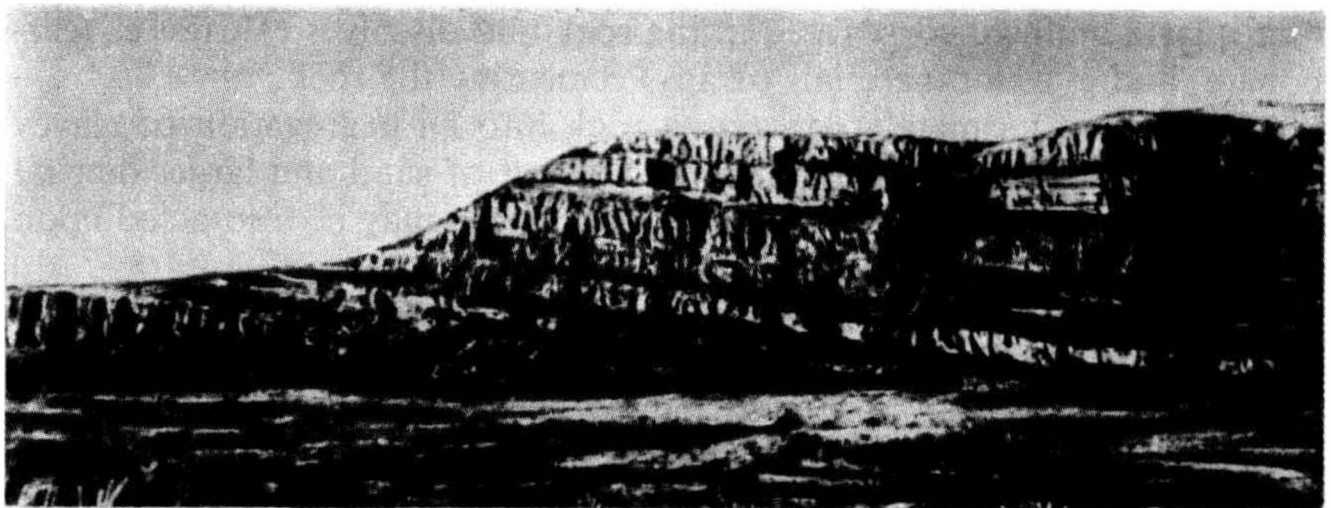


**Fig. 4.9.** Layered Devonian tuffs and tuffites. Eastern slopes of the South Urals

Tuffs of marine origin are known as *tuffites*. The so-called Artic tuff (Armenia), fine porous rock with numerous inclusions of volcanic materials is well known. This tuff species provides excellent construction material for buildings of minor height and for wall facing. Tuffs may often occur as nappes of huge areas.

---

## Chapter 5

### Sedimentary Rocks

---

#### Sec. 5.1. Origin of Sedimentary Rocks

Sedimentary rocks are rocks that are composed of consolidated particles which are the product of weathering and erosion of any previously existing rocks or soils often followed by cementation.

Weathering of rocks is due to the action of atmospheric agents and of physical and chemical processes.

Weathering of hard rocks generally occurs from disintegration of massive rock into ever diminishing rock fragments induced, e.g. by non-uniform heating and cooling (*physical weathering*). This process is enhanced by expansion of water frozen in fissures. Physical weathering is generally accompanied by *chemical weathering* (decomposition) as rock progressively disintegrates.

The action of water, oxygen and carbonic acid on a rock causes its decomposition, e.g. kaolinization, which converts the rock-forming feldspars and, in part, micas, to clay. The process in question loosens resistant quartz grains incorporated in the rock and dissolves calcareous (carbonate) and gypsum materials (if any) cementing the rock.

Weathering ultimately converts a rock into an aggregation of clayey materials containing in addition some amount of sand and larger detrital products, such as gruss and broken stone. Rocks may be also acted upon by various microorganisms and plant roots.

The formation of sedimentary rocks generally includes four stages: (1) physical and chemical disintegration and decomposition (*weathering*) of starting materials; (2) transportation by the water or air of debris as fragments of differently-sized fragments of starting materials and that of solutions resulting from chemical weathering; (3) deposition of products of physical weathering (rock fragments) and of chemical weathering (precipitation of salts from solutions) coupled to deposition of organic

remnants of animals and plants; (4) formation of rocks from loose material as it is compacted by the pressure of sedimented and overlying layers (*diagenesis*) and resulting from various soil-cementing physicochemical processes (*epigenesis*).

Such important mechanisms (see Introduction) as composition, state, conditions of occurrence and thickness of one sedimentary rock species or another are primarily governed by the composition of starting materials, by the nature of decomposition and disintegration products and by conditions under which sedimentation, accumulation and rock formation occurred.

The natural conditions typical of circumstances under which a rock formed are determined by the particular facies (marine, lagoonal, continental etc.). That is why we refer to sedimentary rocks of *marine* or *continental origin*, or, in short, marine and continental rocks.

With rare exceptions (glacial boulder-derived clays) sedimentary rocks occur in beds or layers called *strata* which is the result of the conditions of deposition that obtained at the particular time period.

In this country sedimentary rocks generally provide foundations for structures. Hence their importance in terms of engineering geology.

According to their origin (genesis) sedimentary rocks fall into three principal groups: (1) clastic (or detrital) rocks; (2) organogenic rocks; (3) chemical rocks.

### Sec. 5.2. Principal Types of Sedimentary Rocks

**Detrital rocks.** These are rocks formed from loosened hard products of physical and chemical weathering of starting materials remaining on the site of their accumulation or deposited after being transported by the water or air.

Detrital sedimentary rocks may be divided into the following types:

1. *Detrital rocks proper* subdivided into two groups: (a) incompetent at grained loose rocks (sands, gravel, shingles, gruss, crushed stone etc.); (b) cemented or compact rocks (sandstones, conglomerates, breccias).

2. *Clayey rocks*, frequently considered as constituting a self-sustained group, are in turn divided into non-compact (soft, clays, loams, sandy soils) and compact (argillites and aleurolites). Compaction of loose grained deposits typically occurs as a result of the action of natural cements (calcareous, siliceous, ferrous etc.). The strongest cementing material is siliceous, the weakest argillaceous. Calcareous and gypsum cements are of intermediate strength.

The degree of compression of a clayey rock associated with diagenesis is governed by the time and the weight of the overlying strata. For this reason it is the clays of earliest origin and found at a considerable depth that must



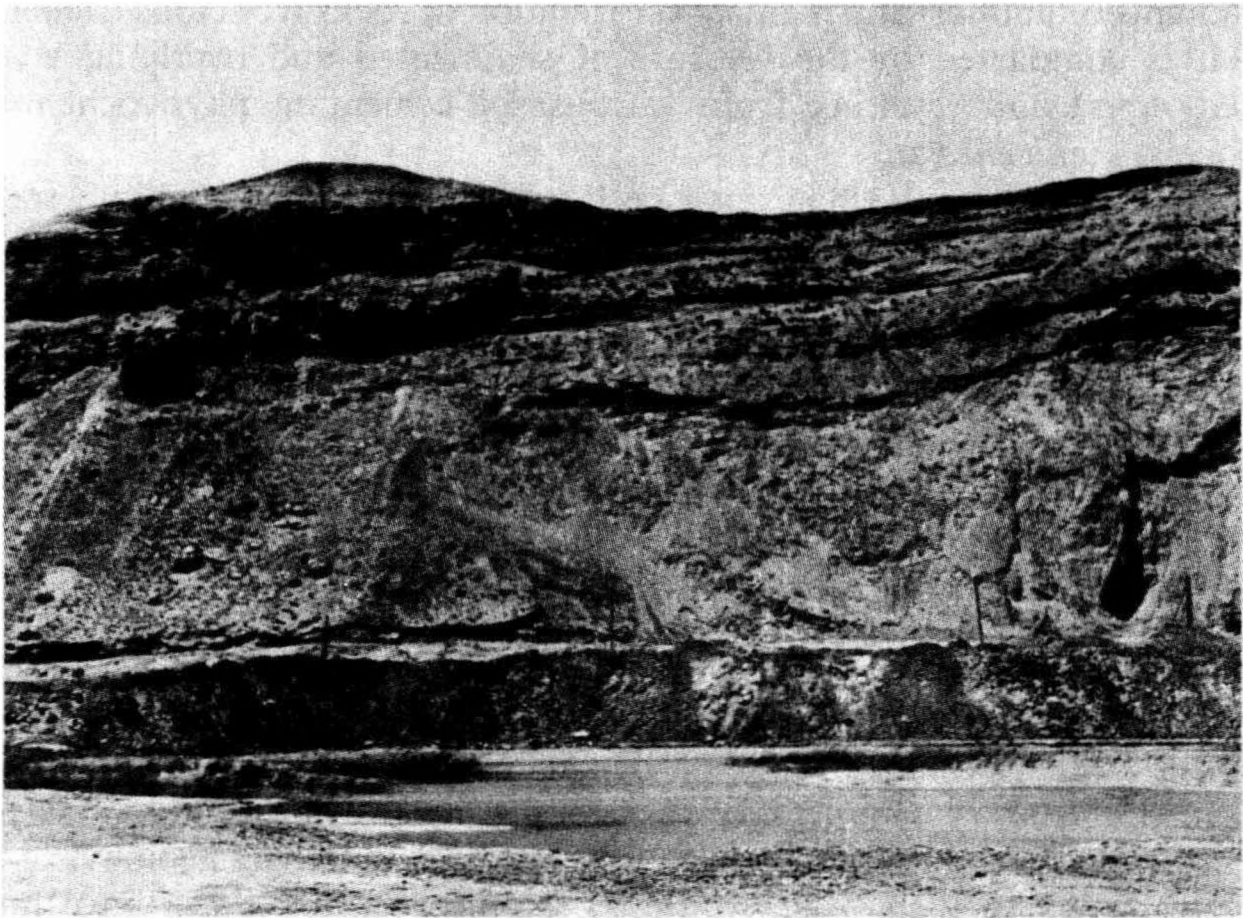


**Fig. 5.1.** Soil mass composed of deposits of clay with sand in the bank ledge of the Syr Darya River in the Kara-kum desert

prove the most compact and concurrently the hardest. Examples of such clayey rocks are argillites and (coarser-grained) aleurolites.

Detrital sedimentary rocks, such as gravel and sand or loose clayey deposits typically occur in younger deposited layers. They occur mostly in the littoral zones of modern seas and lakes and in the river valleys. Cemented detrital rock varieties, conglomerates, sandstones and argillites represent old deposits of the previous geological times yet originating under similar physiogeographical conditions. A general picture of structure of a massive rock composed of sands and clays and formed by successive strata of sedimented materials is given in Fig. 5.1.

**Petrographic and mineralogical composition** of detrital sedimentary rocks is universally similar to that of starting materials. Therefore, apart from such abundant rocks as quartz sands, broken stone, gravels and shingles, products of disintegration of igneous rocks, there occur, although much less frequently, feldspar (arkosic), olivine, calcareous and even slightly pervious gypsum sands, calcareous ballast, gravel and others.

What is typical of detrital rocks is pronounced porosity which may be as great as 40% or more (by contrast, porosity of igneous rocks is never greater than 1 to 3%).





Fig. 5.2. Mesozoic dense sandstones on the left bank of the Amur River

The group of detrital rocks proper includes: *shingles* with water-rounded hard rock fragments 20 to 200 mm in diameter; *rock debris* with angular non-eroded rock fragments of the same size; *gravel*, a deposit of rounded pebbles 2 to 20 mm in diameter; *gruss* with a loose accumulation of non-rounded fragmental products of the same size as in gravel; *sands*, loose materials with more or less rounded grains whose diameter range is 0.05 to 2.0 mm.

The most common of compact sedimentary rocks are: *sandstones*, sand grains bonded together by various agents (Fig. 5.2). The most rigid are siliceous sandstones. *Conglomerates* are cemented rounded rock fragments or pebbles (Fig. 5.3).

**Clayey soils and rocks.** This group includes soils and rocks incorporating clay minerals (kaolinite, montmorillonite, hydromica known also as hydrous mica etc.).

Clay rocks are the most abundant soils (about 50%) in the sedimentary rock group.

Loose clayey materials comprise *sandy loams* where clay particles less

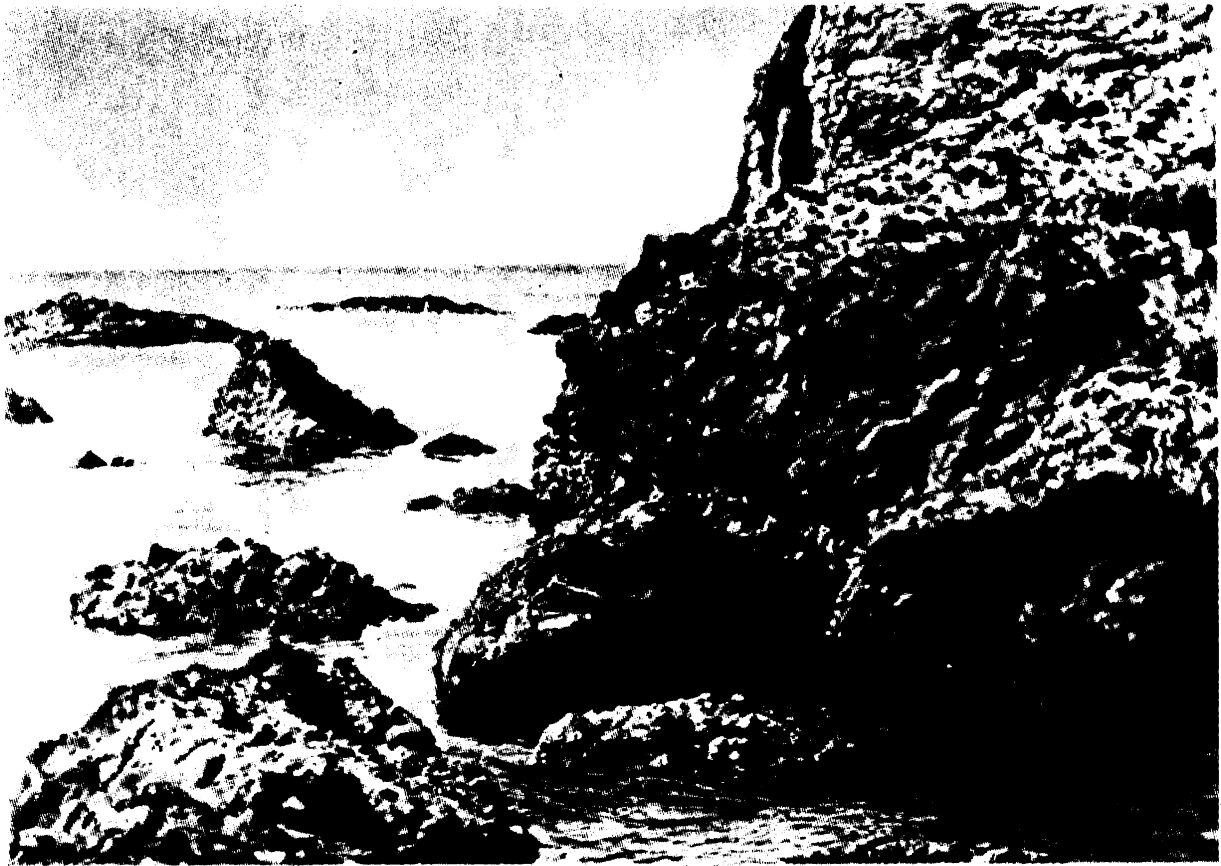


**Fig. 5.3.** Conglomerates rock mass on the Black Sea shore in the Crimea (photograph by E.M. Dobrov)



**Fig. 5.4.** Texture of Chasov Yar clay seen in an electronic microscope (22 000X). One can discern pores and a network of  $0.1-0.2\ \mu$  particles bounding larger hydromica aggregates up to  $2-3\ \mu$  in size

than 0.005 mm in diameter constitute 3 to 10%; *clayey loams* with clay content 10 to 30%; and *clays* with clay mineral content more than 30%. Apart from clay minerals that represent tiniest crystals with a diameter ranging from fractions to a few microns, clayey materials may include grains of quartz, feldspars etc.

Clay minerals together with other constituent minerals compose in clays complex systems (Fig. 5.4) including colloidal substances which, when affected by mechanical agents (say, by shaking), may dissociate and pass to a state of sol or suspension. Once the mechanical action has discontinued, the substance will again pass to a state of gel.

Clay minerals impart to clayey materials quite a number of important properties, essentially, plasticity (montmorillonite to the largest, kaolinite to the least degree, hydromicas producing an intermediate effect). They are subject to swelling and shrinkage, which is especially true for montmorillonites.

As geological time passes, colloidal systems age. This is suggested by the decreased plasticity of oldest clayey rocks, by the development in these of rigid irreversible bonds inherent to compact rocks.

**Aleurolites and argillites** are oldest compact dusty clayey rocks and clays, respectively. Unlike conventional clayey materials, these substances are fairly impervious and provide, in fact, semi-hard rocks.

The sedimentary rock group includes additionally quite a number of rocks of organic origin formed in water reservoirs due to the activities of diverse organisms. Of *organogenic rocks* the most abundant are *carbonate rocks*, notably, limestones (rock-forming mineral  $\text{CaCO}_3$ ), dolomite and marl. As pointed out, limestones are formed following the accumulation in the water of calcite shells of various molluscs or skeletons of marine organisms including corals.

Limestones and dolomites possess a high degree of structural strength and can thus provide support to the heaviest engineering structures. These rocks owe the above properties to cementation of organic remains by carbon dioxide lime ( $\text{CaCO}_3$ ) and to compaction due to the processes of diagenesis (Fig. 5.5).

*Dolomite* (or *dolostone*), in terms of its chemical composition, is a double salt of calcium and magnesium ( $\text{Ca, Mg}(\text{CO}_3)_2$ ). This material is generally considered a chemically derived sedimentary rock, since its origin is due to dolomitization of limestones by relevant solutions. Dolomite is a hard rock species endowed with a great bearing capacity.

*Marl* is crumbling earthy material composed of clay and magnesium and calcium carbonate. Calcite content range is 25 to 75%. Marl is a semi-hard rock (Fig. 5.6).

*Chalk* is a hard rock species formed from accumulated remains of

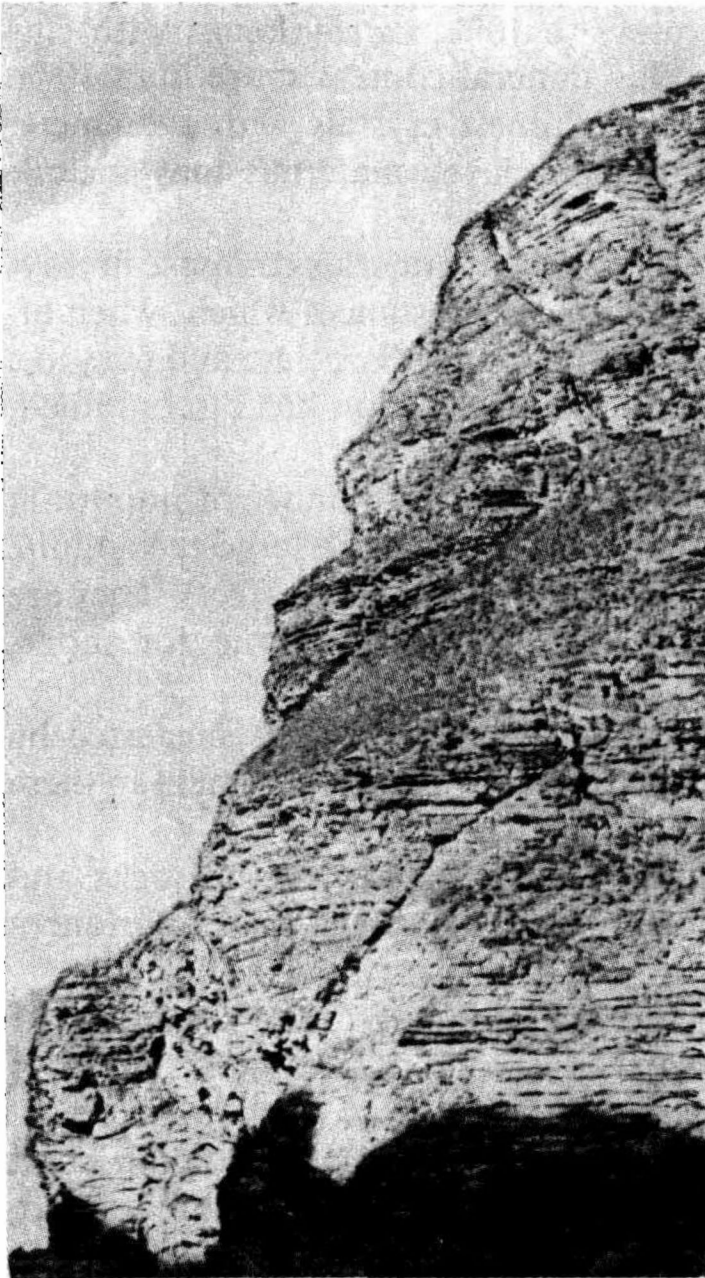


Fig. 5.5. A cliff composed of limestones exposed in the bank of the Sulak River (Daghestan)

tinest pelagic organisms. Similarly to limestones, chalk consists principally of calcite.

About 60 to 70% of chalk material is composed of skeletons of plankton organisms, such as foraminifers. The remaining part is composed of calcite, possibly, of chemical origin. Unlike limestones, chalk is not foliated and is weakly cemented. Clayey streaks often occur in chalk, and chalk may sometimes be contaminated by clayey admixtures. Chalk deposits can be found in a vast area from the steep banks of the Don River to the White cliffs of Dover in England.

The group of organogenic rocks includes also *siliceous rocks*, the principal of which are opoka and diatomite. *Opoka* is a flinty and calcareous hard rock consisting mainly of opaline silica (up to 90%) and hardened by the presence of organic remains, in particular, spicules of Echinodermata. It is a water-resistant semi-hard rock.



Fig. 5.6. Sarma (above) and Urzhum (below) clay marls occurring in the Gorky Region

*Diatomite* is a porous weakly cemented rock, formed from the siliceous coverings of tiny diatom algae also bonded by opaline silica.

When constructing a road, the civil engineer frequently deals with peat moors (peat bogs or peat beds). *Peat* should be regarded as an organogenic rock of the *phytogenic* (or vegetable origin) group. Peat forms in the process of slow decomposition of vegetable matter in stagnant water with small amounts of oxygen.

**Chemical sedimentary rocks** have been originated through natural evaporation and deposition of dissolved salts from seas and lakes. Such conditions arise in certain lakes and sea lagoons under conditions of enhanced concentration of aquatic solutions and lowered temperatures (water cooling in winter time). An interesting example is provided by winter-time precipitation of a valuable mineral, *mirabilite*, whose pure crystals are known as Glauber's salt ( $\text{Na}_2\text{SO}_4 \cdot 10\text{H}_2\text{O}$ ), in Kara-Bogaz-Gol Gulf in the Caspian Sea.

Chemical sedimentary rocks include first and foremost *gypsum* ( $\text{CaSO}_4 \cdot 10\text{H}_2\text{O}$ ), *anhydrite*  $\text{CaSO}_4$  (known also as cube spar), and *rock salt* or common salt consisting mainly of the mineral halite (sodium chloride  $\text{CaSO}_4$ ).



Fig. 5.7. Deposits of large-grained (lump) and fine salt alternated by clay lamina. The thickness of an annular layer is about 6 cm. Solikamsk

These rocks occur as deposits many tens and even hundreds of metres in thickness. A typical example can be provided by an anhydrite deposit with a gypsum “cap” (product of anhydrite hydration) in the vicinity of the city of Perm more than 400 m in thickness. There are cases when salt strata interchange with clay rock layers pointing to the conditions of salt deposition (Fig. 5.7).

Table 5.2 lists principal sedimentary rocks.

Table 5.

Most Important Sedimentary Rocks					
I. Detrital or Clastic Rocks			II. Rocks of Organic Origin		III. Chemical Rocks
clastic proper	loose	cemented	carbonate	flinty	
	Rock debris } Gruss } Shingle } Gravel } Sand	Breccia  Conglomerates  Sandstone	Limestones Dolomite Chalk Marl	Opoca Diatomite	Anhydrite Gypsum Rock salt
Clayey	Sandy loams } Loams } Clays }	Aleurolite Argillite			



---

Chapter 6**Metamorphic Rocks**

---

**Sec. 6.1. Metamorphism**

Igneous but generally sedimentary rocks, if subjected to high pressure and temperature in the earth's interior and to the chemical action of solutions and gases, form metamorphic rocks.

There are three types of such rock alteration: *contact*, *dynamic* and *regional metamorphism*.

*Contact metamorphism* results from the action of high temperature, gases and hot vapours on the adjacent rocks intruded by a magmatic body. Contact metamorphism thus reveals itself by melting the intruded rocks, on the one hand, and by recrystallization and consolidation of the rocks involved, on the other hand.

In zones of contact metamorphism clayey and sandy rocks convert to dense *hornblendes*, and sedimentary carbonate rocks to *skarns* found generally in ore deposits. Condensation of aqueous magma rocks rich in various materials leads to carbonization, chloritization and silicification of the fissure-filling material. The width of a belt of contact metamorphism rarely exceeds several kilometres.

*Dynamic metamorphism* occurs under conditions of high temperature and great pressures that accompany mountain building. The predominant process in formation of metamorphic rocks is dynamic metamorphism typically associated with the action of compressing forces.

**Sec. 6.2. Principal Metamorphic Rocks**

Metamorphism caused by volcanic events and mountain-building processes may lead to reconstitution in detrital rocks of their original structural bonds and durability. Loose quartz sands may then convert to its metamorphic variety, quartzite, a granoblastic rock of remarkable strength.

Clay rocks, that usually have low cohesion, under conditions of great pressure and heat acquire properties of hard rocks forming clay shales, phyllites, mica schists, and, finally, gneiss which is a typical hard rock.

*Argillaceous schists* are rocks (Fig. 6.1) associated with dynamic metamorphism that are most abundant in mountainous regions.

*Sandstones* when passing to marble as a purely metamorphic rock undergo a series of similar transformations starting from *calcareous schists* (Fig. 6.2).

*Marble* displays a typical crystalline structure. Such metamorphic rocks are termed *crystalline schists*.

Rocks that occur at deepest levels are especially subject to metamorphism. That is why typically metamorphic rocks are found in areas where deep rock strata have been uplifted due to orogenic processes and then exposed by eroding agents. Such conditions exist, in particular, in old mountainous regions as the Urals and Karelia etc.

Crystalline schists exhibit a specific capacity for *cleavage* resulting from great pressure. Such rocks as argillaceous schists may laminate forming thin layers.

It is generally the oldest rocks overlain by a thick overburden of the order of several kilometres in the earth's geological past and affected by greatest pressure and heat that undergo the most pronounced alteration due to metamorphism. The nearer the surface the less the effect of metamorphism.

Crystalline schists are especially abundant in the oldest rock strata.

Metamorphic bodies are often intruded by veins of igneous rocks and



Fig. 6.1. Shale sediment beds



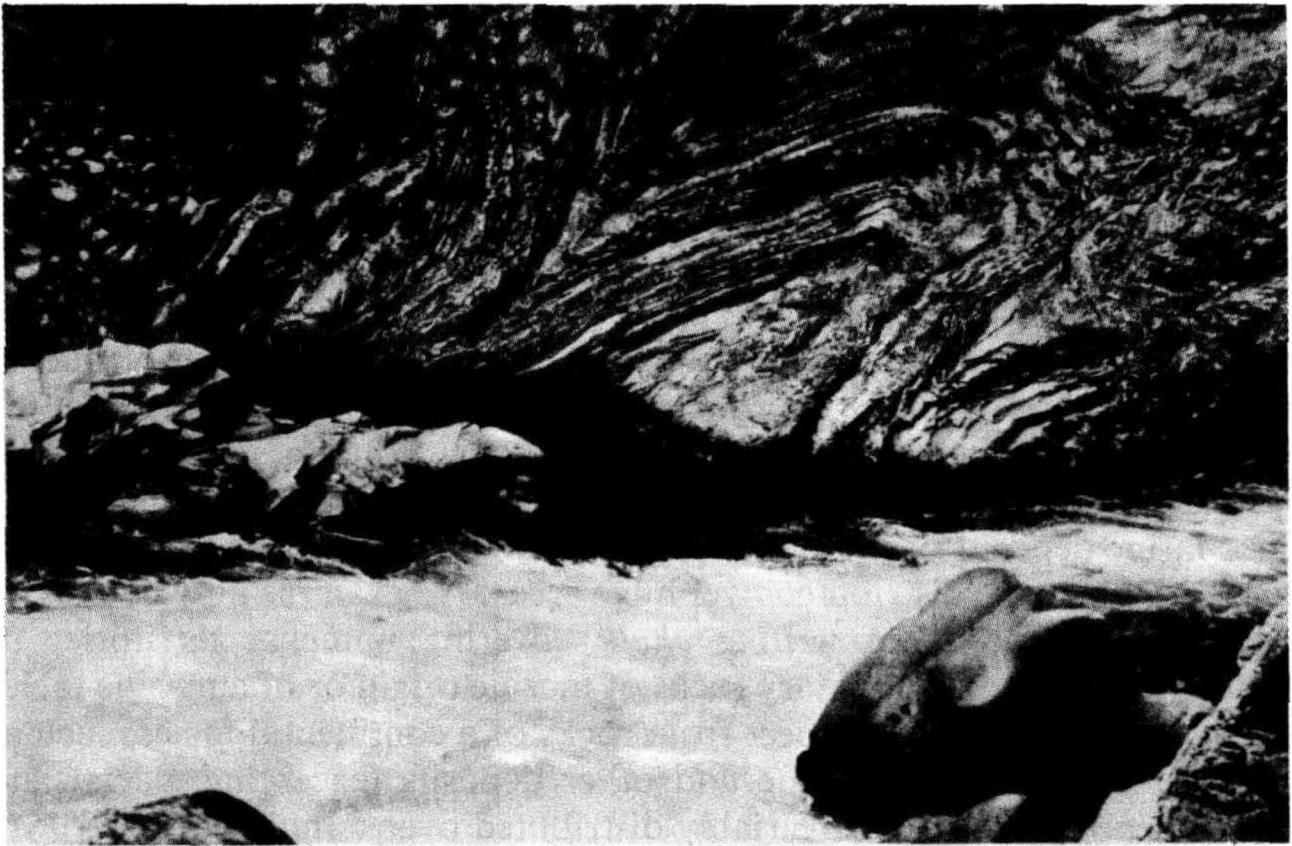


Fig. 6.2. Metamorphic lime slates exposed in the bank of the Belaya River

thus local contact metamorphism occurred, in turn, acting upon the former materials.

As contrasted to dynamic metamorphism directly associated with orogenic processes and the area they occurred in, regional or dynamic metamorphism affected vast territories without being related to magmatism or forbidding tectonic conditions. This type of metamorphism is believed to be due to huge crustal regions sinking to great depths where infernal temperatures prevail. This metamorphism must have given rise to gneissose granite of the Ukrainian crystalline massif, of the Baltic shield and others.

---

## Chapter 7

### Areas of Distribution of Sedimentary Rocks

---

#### Sec. 7.1. Marine and Continental Deposits

According to their origin, all sedimentary rocks are classified as *marine* and *continental* deposits (fluvial, alluvial, glacial etc.). Clearly, such

species will prevail in the geologic column as determined by the particular conditions under which they accumulated. So, the abundance of a given rock species (detrital, clayey, organogenic) in the mass of marine deposits would point to periods of marine transgressions (stages of tectonic evolution). On the other hand, continental deposit formation must have occurred at times when continents stood high above sea level during the Caledonian, Hercynian and Alpine orogenies.

If we wish to estimate the conditions of occurrence of marine deposits or others we must be aware of the area of their distribution, the sequence these layers are found in the rock mass of a definite species and age, the thickness of individual layers in the geologic column and their total thickness.

Marine deposits of the same species dating to one marine transgression or another may be distributed over huge areas. An example may be provided by vast deposits of *writing chalk* covering immense territories of southern Europe. Sedimentary rocks of marine origin or of a marine facies differ very much in this respect from rocks of a continental facies, such as alluvial, lacustrine, palustrine and other deposits (excepting glacial and eolian deposits) that are invariably distributed over a limited area.

When evaluating the area of distribution of rocks of a marine facies of a definite age, it will be borne in mind that the continental masses have been flooded at this or that geological time by the sea. Consequently, the rock mass constituting the land generally displays deposits formed during the respective marine transgressions.

This can be exemplified by Jurassic black clays found in Moscow and its vicinity which represent deposits of the shallow sea that at a distant time inundated this area serving as an abode to now extinct dinosaurs and pterodactyls. The great deposit of Crimean Yaila limestone with its kilometre-high cliff descending to the seashore in the southern Crimea evidences the fact that this mountainous region was in the past flooded by a warm sea inhabited by a multitude of organisms with calcareous skeletons.

It is also evident that not all marine transgressions that occurred have left a trace on each particular tract of land. It must be pointed out that in many instances the deposits of previous marine transgressions may have been transported by the subsequent transgressions or washed away by *denudation*, running water (*erosion*), wind action (*deflation*), glacial action (*exaration*), during the periods continents stood high above sea level. This is especially true of deposits formed by marine transgressions of minor thickness. It should be further noted that the hiatuses in the geologic column associated with one or another marine transgression have been typically associated with the elevated position of the continents in the earth's past.

Uplifts and sinkings of continental masses that had a more or less uniform pattern in periods of quiescence, whatever the site of occurrence, had at the same time various magnitude. Given such conditions, only definite land areas were simultaneously found below sea level on being inundated by the advancing sea in the respective transgression. However, there concurrently remained dry tracts of land where no deposits of the given marine facies could accumulate.

A typical example is provided by the territory of today's Leningrad. One can identify here Paleozoic deposits of marine transgression (Cambrian clays, and, in the adjoining region, Ordovician limestones) preceding the Caledonian orogeny that occurred about 500 million years ago. Since then to the latest time period (the recent 10 to 12 thousand years) the area occupied by what is today's Leningrad and its environs has represented land, waters of major transgressions that occurred in the Lower Carboniferous and Cretaceous (following Ordovician) bypassing the region in question. For this region younger Quaternary deposits overlie older Paleozoic rocks.

Another example may be provided by the area of today's Moscow and the adjacent regions. As a result of crustal uplift at an early stage of the *Alpine orogeny* the Cretaceous sea that had inundated the above-mentioned territory and deposited brownish-yellow sands (exposed in the Lenin Hills cliffs), about 100 million years ago retreated from this region forever. Therefore no traces of other marine transgressions or other rock units of a marine facies can be found here.

On the other hand, the same areas of continental lowland must have been periodically flooded at different times in the earth's history. As a result, the geologic column at the same site can display marine sedimentary rocks of different ages deposited in different, often subsequent, transgressions. So, in the Moscow region (Fig. 7.1) at the bottom of a geologic column, underlain by a crystalline stratum reached by boring at a depth 1648 m and composed of gneisses, deposits of a marine facies (conglomerates, sandstones and schists) Proterozoic and Cambrian clays are found. Ordovician and Silurian deposits do not occur here which suggests that for about 150 million years continental conditions prevailed in the given area resulting from crustal upheavals of the *Caledonian orogeny*.

Cambrian deposits are here immediately overlain by a mass of limestones, dolomites, marls and clays, all products of a later large-scale Medium-Devonian and Carboniferous marine transgression. The uppermost strata are composed of a mass of Jurassic clays overlain by sands of a littoral facies of a Cretaceous sea. Here one can trace deposits of a marine regression following a large-scale Carboniferous transgression with continental conditions prevailing in the Permian and Triassic (Hercynian

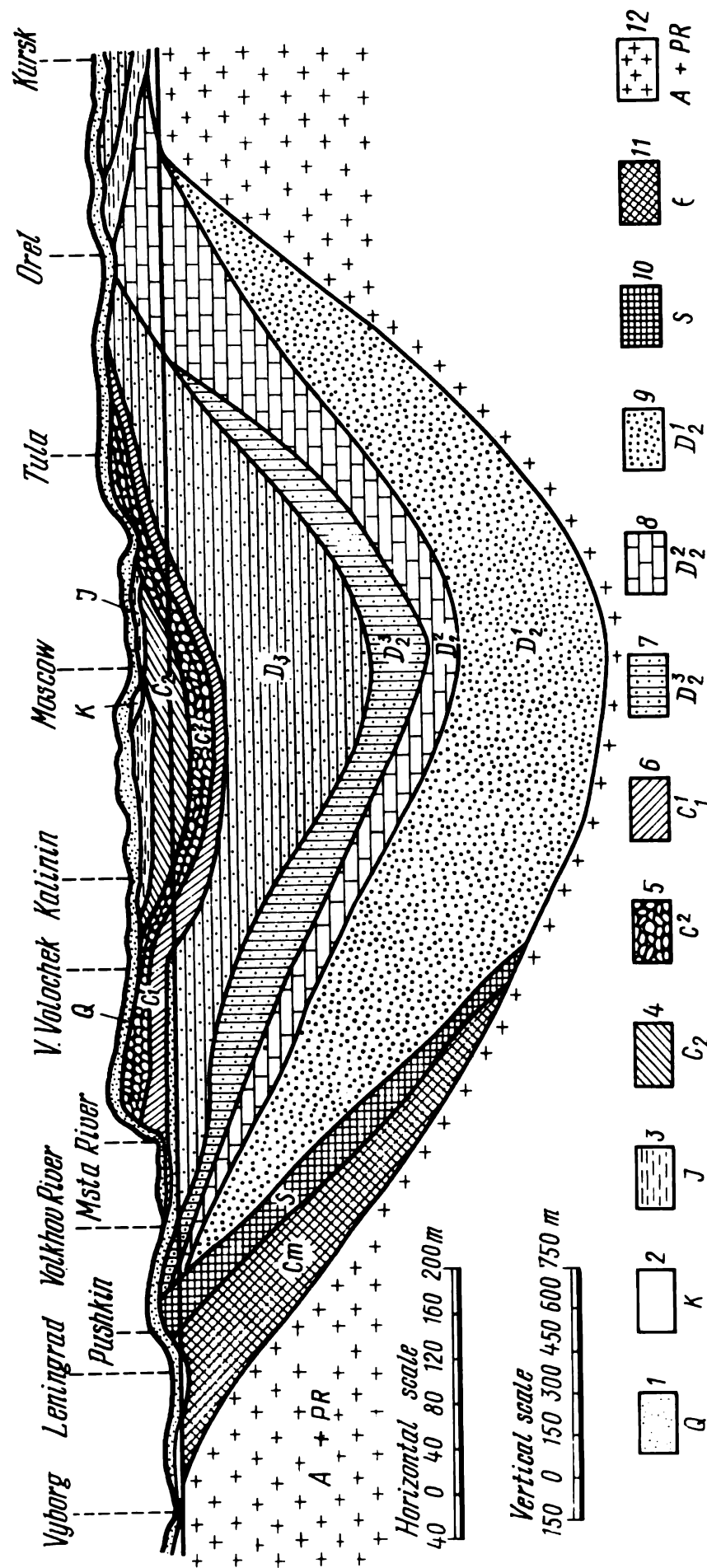


Fig. 7.1. Schematic geologic section of the Moscow synclinorium:

1—Quaternary deposits; 2—Cretaceous; 3—Jurassic; 4—Middle Carboniferous; 5—Rock-bearing stratum of the Carboniferous; 6—coal-bearing stratum of the Carboniferous; 7—upper strata of the Middle Devonian; 8, 9—lower strata of the Middle Devonian; 10—Silurian and Ordovician; 11—Cambrian; 12—Proterozoic and Archeozoic (or Archean)

orogeny) and with new evidence of a Jurassic and major Cretaceous transgression.

As a matter of fact, marine facies rock strata should have been alternated by rock layers corresponding to the elevated position of continents and marine regressions (continental facies rocks in the Ordovician-Silurian and Permian-Triassic). Such rocks, however, were mostly non-existing at that time since they could be easily washed away and transported by the waters of a subsequent marine transgression.

Two conditions may be responsible for this process: (1) continental deposits are almost always thinner compared with a mass of marine deposits; (2) they are generally fairly unstable and unconsolidated aggregations (sands, gravel, loams, sandy loams etc.). Such factors facilitate erosion and transport of continental facies deposits by marine transgressions.

Note also that marine transgressions and regressions are typically brought about by tectonic events. Alternatively, variations of the level of the World ocean, of the seas connected with it and, especially, of isolated in-land seas (like the Caspian Sea) could be conditioned by other causes, e.g. climatic ones. Such world-wide fluctuations of sea level are called *eustacy*. It is a known fact, for example, that huge ice masses piled up on land during the glaciation periods contributed to a marked drop of sea level. There is belief that if the ice caps of the Antarctic and Greenland that are 1 to 3 or 4 km in thickness melted the sea level would rise by 80 or 90 m. Vast areas of land including ones occupied by Leningrad, London and New York would then be submerged.

It should be also noted that the sea level of the Caspian is very much dependent on the inflow of the waters carried by the influent rivers, notably the Volga, Ural, Kura and Terek. We are now witnessing a lowered position of the Caspian which markedly changes its outlines as a result of the fact that its shoreline has been altering within the lifetime of a single generation. At the same time we can find traces of large-scale marine transgressions that occurred in the geological past in the Caspian depression area. The Akchagyl Sea flooded at that period vast areas of the Caspian depression and along the Volga River valley reaching today's towns of Kazan and Ufa.

What has been said above enables us to make three logical conclusions:

(1) marine facies rocks may occur at the same depth in the sedimentary rock mass, whatever the site;

(2) these rocks have undergone deformations mainly during deposit accumulation on the sea floor as a result of marine transgressions in the periods of tectonic evolution;

(3) marine facies rocks of different ages typically occur in the mass of sedimentary rocks.

*Continental* facies sedimentary rocks include alluvial, lacustrine, palustrine, eolian and glacial deposits. The area of distribution of both continental and marine facies sedimentary rocks is limited and is governed by the processes responsible for the accumulation of such deposits. What is more, chemical deposits of bitter salt lakes may only be found on the sites of existing or dried up, formerly salt-rich lakes. Peat deposits and silt deposits that often underlie the former, naturally, occur in the areas of distribution of peat bogs.

Alluvial deposits are generally composed of gravel and pebbles, sandy loams and loams that can be found within the basin of a given river, that is, commonly occur in a limited region. However, if we want to evaluate the conditions of distribution and occurrence of alluvial deposits, it must always be borne in mind that modern rivers differ in configuration from those of the geological past. A river valley may have older river channels differing by tens of metres in depth and not coincident with younger alluvial deposits. In addition, terraces can occur there at the sides of a river valley almost universally composed of fluvial deposits that serve as evidence of the past activities of the river at other levels. There are also so-called alluvial plains which may frequently occupy huge areas. Such plains are the result of meandering river channels.

Such conditions have been arising particularly easily during marine regressions when a given area, due to the activity of the sea, often proves to be ideally flattened out. So, alluvial plains formed in the eastern regions of the Volga basin area during the Upper Permian as a result of the Hercynian orogeny.

We may also refer to deposits of an alluvial plain in the West Siberian lowland. However, the area of distribution of alluvial deposits in the general case is strictly limited to the valley of each particular river.

*Eolian deposits* include, first and foremost, eolian loess deposits and eolian sands in sand dunes and barchans. Dunes are wind-blown mounds or ridges of sand typically found along sea-shores or, sometimes, river banks in narrow stretches. Barchans (barchanes or barkhans), sometimes tens of metres in height, are, in fact, sand dunes occurring in desert continental areas. They may cover appreciable areas as, for example, in the Kara-Kum desert.

*Eolian loess* is unconsolidated silt formed by precipitation of atmospheric dust, the finest product of rock weathering, or previously deposited material blown by wind. Under conditions of decreased air humidity dust may be suspended in the atmosphere for an indefinite time and be transported by wind action many hundreds and even thousands of kilometres away.

The area of distribution of loess is, in fact, limited by environmental

factors, such as the direction of prevailing winds and air humidity, that typically arose at a time these rock masses originated. Under such conditions loess rocks may cover fairly large territories. Note that loess rocks almost universally occur in Middle Asiatic republics of the USSR and occupy immense areas in southern continental Asia. Appreciable areas of the south European USSR are also covered by loess-like rocks. Strata of these rocks usually occurring at the top of the geologic column and overlying older rocks of other facies are ones that Soviet civil engineers have typically to deal with.

*Glacial deposits* can be found in this country no less frequently, yet in the central and north European regions. At certain moments in glaciation periods glacial lobes reached as far as today's Dnepropetrovsk and the Don River. Most of Western Europe was at some time covered by a sheet of ice. Glaciers especially occurred in mountainous regions.

Naturally, glacial deposits may be encountered only in areas that were formerly glaciated and in the adjoining regions. Glacial deposits typically originated in the Quaternary and they overlie older rock layers. Such deposits, usually in the uppermost strata, are very much distributed in the USSR.

It is not uncommon that the rock mass is composed of deposits formed during two or more marine transgressions at a given area of the earth's sur-



**Fig. 7.2.** Mass of limestones transgressively and unconformably overlying a suite of conglomerates



face spaced at intervals of many tens and even hundreds of millions of years. Such type of stratification is termed *transgressive*. Layers of each succeeding rock unit then generally overlie *an eroded* uneven surface of the previous rock unit (Fig. 7.2.). This suggests that in the interval between two transgressions the given areas represented land that had undergone a more or less lengthy denudation process.

### Sec. 7.2. Thickness of Strata

*The thickness* of the sedimentary rock mass is determined by the following factors: (1) duration of the period of deposition and accumulation of parental products giving rise to sedimentary rocks; (2) intensity of detrital product transport to the area of sediment accumulation and the process of accumulation of organogenic materials and the products of chemical decomposition; (3) presence of vast depressions where conditions were favourable for deposit accumulation and storage; (4) presence in the given area of sites of progressive sagging and flexing of crustal layers leading to formation of such depressions (*geosyncline areas*).

The marked thickness of the sedimentary rock mass (amounting to a few kilometres) which can be often observed stems from the fact that most geological events and transformations occurred within a span of time infrequently measured in terms of many hundreds of thousands or even millions of years. For example, accumulation of calcareous ooze on the sea floor providing parental material for limestones occurs at an annual rate of fractions of the millimetre or a few millimetres. Suppose that in our case such accumulation occurred at a rate of 1 mm of silt deposited per annum. Such seemingly an inappreciable rate would yield 1 000 m in a million years. There are cases when the sedimentary rock mass attains some tens of kilometres in thickness. We may refer to the coal deposits of the Donets Basin that are 10.6 km in thickness. Even given littoral deposits that composed this huge mass, it must have taken many millions of years for it to be formed.

Clearly, only in rare cases did the conditions of deposit accumulation remain unchanged for such lengthy time periods. Alterations of a sea's shoreline and, hence, increased or decreased depth of the sea basin as well as retreat of a given point from the shoreline must have influenced the character of material being deposited and, consequently, the type of resultant rocks.

The coal deposits of the Donets Basin, referred to the Carboniferous, are mainly composed of clay and sandy clay rocks alternated by sandstone and sometimes limestone strata with 120 to 150 limestone seams 0.5 to 10 m in thickness each. It took much less time for such limestone seams to be formed compared with the entire rock mass, yet thousands of years.



The thickness of individual layers and of the entire sedimentary rock mass, the intensity of accumulation (e.g. of parental material to a water basin), naturally, were acted on by the configuration and relief of the shoreline, by environmental factors and the distance of a point in question from the shoreline. Clearly that transport to the water basin of so-called *terrigenous material* (the product of mechanical washout of land), mainly sand and clayey ooze, will be the most pronounced under conditions of a large gradient of a river and a significant discharge, i.e. under conditions of mountainous relief of land and in periods abundant in atmospheric precipitations. Other conditions being equal, the intensity of accumulation of water-borne materials close to the shoreline representing the most coarse constituents of detrital material transported to a given water basin (pebbles, gravel, coarse-grained sands) will be the greatest.

Accumulation of clay and silt materials transported by currents to the open sea and frequently distributed over vast areas, vice versa, occurs at a much slower rate. However, other conditions remaining the same, the thickness of water-deposited sediments cannot exceed the depth of a given water basin or stream.

Since the depth of the sedimentary rock mass may amount to tens of kilometres, clearly, such a mass could have originated only following gradual subsidence and sag of the most incompetent elastic areas of the earth's crust, termed *geosynclines* (or *geoclines*), under the weight of the accumulating deposits. These areas, after a deformation of the terrestrial globe accompanied by a deformation of the earth's crust faulted and folded eventually, thus facilitating pronounced orogenic events.

The thick masses of alluvial deposits must have been generated only due to a gradual or marked lowering of certain areas of the terrain along the course of a river or at its mouth.

In particular, a similar event occurred in the channel of the Katun River which has a relatively thin layer of alluvial deposits, where at the same time there occur alluvial deposit areas in excess of 100 m in thickness.

A vivid illustration of this phenomenon is provided by the Zhiguli Hills region on the Volga River. Following a number of uplifts and sinkings of this region the Volga River scoured and then filled up by its sediments up to 250 m in thickness several river valleys that are now buried. The deepest of the valleys (as much as 140 m below sea level of today's Caspian Sea) corresponds to the washout and incised meander of the Volga cut in into a ridge of uplifted Carboniferous limestones. This upheaval, up to 500 m in height, that carried limestone strata and overlying Jurassic clays occurred late in the Tertiary.

It is also natural that the thickness of deposits accumulated in the seas that flood during marine transgressions of deeply cut land areas is the

largest in buried relief depression zones. An example of this can be provided by the mass of Tertiary (Kinelian) clays in the Volga River valley deposited during the Akchagyl transgression, in the depressions of old valleys of the Volga and Kama catchment areas inundated during the aforementioned transgression. The thickness of the Kinelian clay rock mass in the now buried valleys of the aforesaid rivers may sometimes exceed 100 m.

The thickness of eolian loesses proves to be far from uniform. Naturally, their thickness is the greatest in buried relief depressions where the dust deposited from the atmosphere and blown by winds was well preserved. Evidence is available that in some regions in China where such conditions obtain the loess rock mass is several hundreds of metres in thickness.

Rock composition may sometimes change gradually. For example, plastic clays, as sand content in these increases, gradually transform to fine-grained sands. A gradual change may be often observed as we pass from calcareous clays to marls. Such stratification pattern testifies to a gradual shallowness of a basin, and it is then difficult to identify individual layers.

The types of stratification where the boundaries between individual layers are distinct occur much more often. Limestones are then succeeded by clay schists which, in turn, are alternated by sandstones etc.

Such a pattern of strata arrangement attests to a fairly abrupt change in the conditions of deposit accumulation that were for a more or less lengthy time period relatively constant. The appearance of, say, gravel streaks in the mass of sandy alluvial deposits points to increased flow rates of water streams due to climate-induced increase in their discharge.

In the above example of the structure of the coal-bearing rock mass of the Donets Basin composed of clay and sandy clay rocks and, in part, limestones, up to 200 individual coal seams have been exposed not more than 1 to 2 m thick each. The formation of coal seams is due to the accumulation and burial of vegetable matter from the forests growing in the Carboniferous by the subsequent deposits. The composition and nature of deposits suggest that they originated partly on marshy lowland, partly in a shallow sea that flooded at times the land. This sequence of deposits indicates that 200 million years ago the sea advanced and retreated from here at least 120 to 150 times. Consequently, land submerged as many times below sea level and then again rose.

In the general case, limestones alternated in the mass of marine deposits by some other rocks can be accounted for not only by fluctuations of sea level and position of the shoreline. This could be also affected by such important factors as changes in salinity and temperature of the given water

basin as a biological medium. Finally, marine facies rocks could have in many instances been overlain by continental facies deposits, e.g. glacial or eolian ones. This would provide evidence of land regions emerging from below sea level for substantial geological periods, i.e. the earth passing to a new stage in its life.

---

## Chapter 8

### Regular and Irregular Bedding of Sedimentary Rocks and Soils

---

#### Sec. 8.1. Regular Bedding

What is specific for sedimentary rocks is their stratification, i.e. occurrence in strata or beds. Rocks that form such strata generally differ in conditions of deposition, in material and granulometric composition etc. There may be cases when strata of such rocks are composed of the same material and under the same conditions of deposition yet are separated by distinct separation planes of deposition or scouring which is observed in limestones. If a rock layer has a more or less uniform thickness and occupies a fairly large area it is called *a bed* (e.g. a bed of limestone, clay etc.).

Depending on conditions of deposition accumulation these beds may differ in thickness and incorporate diverse rocks, both fairly hard (limestones, sandstones etc.) and incompetent rocks (plastic clays, peat, quicksands etc.).

*The rock unit* is a complex of layers or a single layer of a more or less appreciable thickness (e.g. limestone rock unit, clay rock unit etc.).

If a layer of a rock is penetrated by a thin layer of a different rock, this is called *an intercalation*. Conformable bedding of a rock or soil attests to stable natural conditions of their formation. In this context we distinguish uniform (monolithic) structure of the rock unit of a foundation, certainly, within a definite depth governed by the size of the structure in hand.

More commonly structures have to be erected on a subsoil composed of layers of different depth. Then the soil mass is stratified or bedded.

If a layer or intercalation converges to the edges that are at a fairly short distance, it is termed *a lens*, if to one edge, *pinching out*. A lens may be formed by an incompetent material (e.g. peat), or, alternatively, by highly pervious rocks (e.g. gravels).

All the above forms and conditions of regular stratification of sedimentary rocks and soils may be essential for the service of the structure being erected at a particular site and thus be taken into account by the engineer as an important fact.

From the viewpoint of engineering geology the most durable and competent rocks formed in the geological past are of interest only in such cases when they occur at a relatively small depth. Therefore a possibility to predict with a certain degree of accuracy the conditions of occurrence of a rock bed underlying the foundation of an engineering structure from analysis of its tectonics may prove of much practical value.

### Sec. 8.2. Irregular Stratification

Let us recall the meanings of the terms “*the dip*” and “*the strike*” of a bed (Fig. 8.1).

The dip of a bed is the direction and magnitude of a bed’s inclination to the horizontal. The angle made between the inclined plane of the bed (seam) and the horizontal plane is called *an angle of dip* or a *true dip*. There are steeply inclined beds (Fig. 8.2) with the angle of dip of 45 to 90° and flat beds or seams with lesser angles of dip. The line of intersection of the horizontal by the plane of an inclined bed is termed *the strike*. The dip and the strike are always at mutual right angles.

In a fault there occurs only roughly vertical displacement of beds that constitute some rock unit without any significant alteration in conditions of their occurrence. But both wings of a fault (uplifting and falling) will inevitably contain a definite *bed* or *formation* of interest to us located at different depths.

Unlike faults, folded dislocation forms typically display inclined occurrence of beds without rupture of their continuity. In some cases folds are hardly noticeable. Under such conditions the bed is mildly inclined. There may be cases where folding reveals itself more dramatically in the central areas of folds with almost vertical dip of the layers (Fig. 8.3). It is not uncommon that a folded relief feature is disintegrated or worn down in part. Various layers may be exposed then at different areas of the earth’s surface that were previously buried at great depths and then uplifted to the top by folding and subsequent denudation (Fig. 8.4).

When designing a foundation for a proposed engineering structure it should be borne in mind that a fold is a geometrical body that obeys certain regularities. Of these the most interesting are regularities of alternating one layer by another throughout a fold. This makes it possible to predict the structure of the foundation and properties of rocks underlying this latter through studying the conditions of occurrence and alternating of beds in

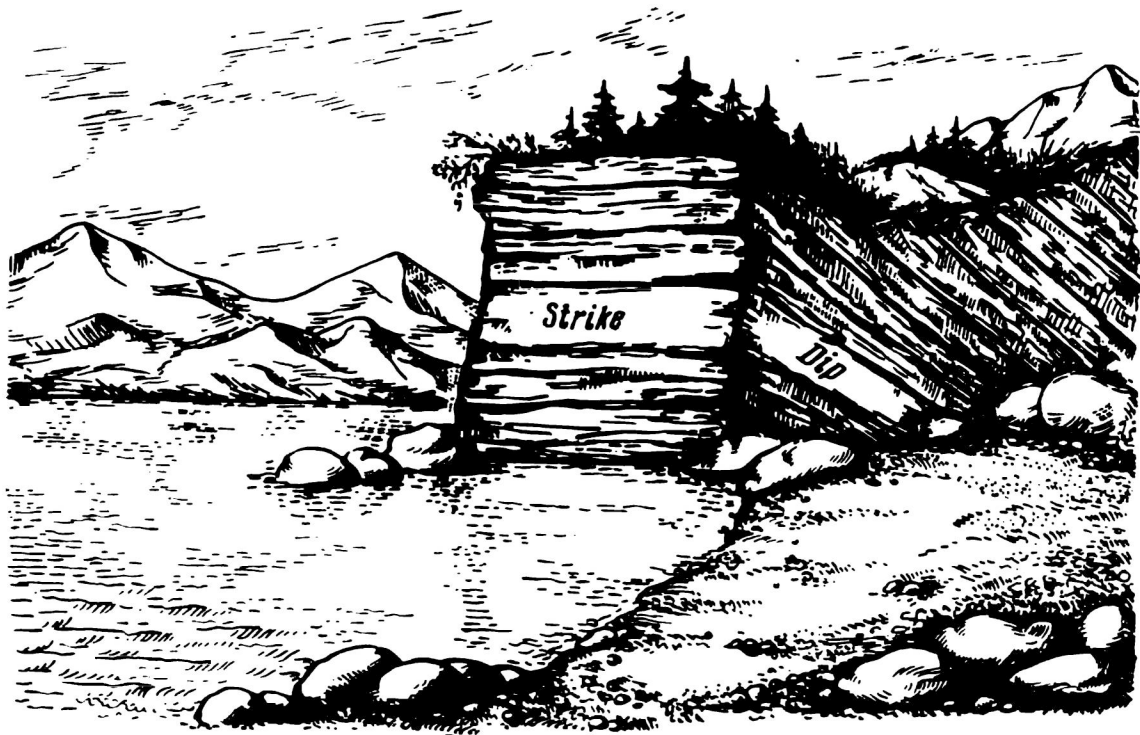


Fig. 8.1. Elements of occurrence of rock strata



Fig. 8.2. Steeply inclined limestone beds

exposed (e.g. eroded) elements of a fold followed by extrapolating the dip and the strike of these beds.

Intact sedimentary rocks typically exhibit *conformable* horizontal or almost horizontal occurrence in the overburden mass. Tectonic disloca-



**Fig. 8.3.** Upright lime marl beds. Tadjikistan



**Fig. 8.4.** Water-eroded fold. Outcrops of Upper Jurassic limestones. The Crimea

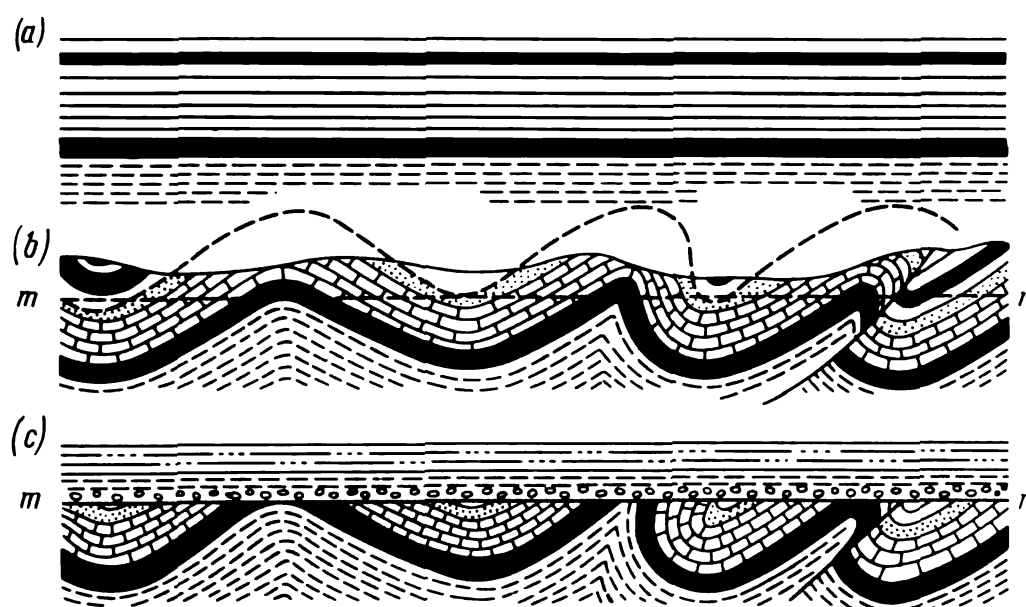


**Fig. 8.5.** Conformable (*a* and *b*) and unconformable (*c*) bedding:

*a*—horizontally bedded sediments; *b*—same, but located and folded and in part denuded; *c*—denudation reached the *m-n* plane followed by horizontal deposition of new series of deposits

tions of the overburden mass will disturb this position. Such unconformities, however, only occur in beds formed in periods that preceded and followed latest tectonic events that took place at the given area. In areas of past intensive tectonic activities one may well find horizontally stratified overburden layers overlying rocks that had been to some extent dislocated. What we observe then is unconformability in rock occurrence (Fig. 8.5).

---

## Chapter 9

### Jointing in Rocks

---

#### Sec. 9.1. The Origins of Jointing

The presence of jointed rocks in an area to be built up poses particularly difficult problems if it is required to construct a surface or subsurface structure (Fig. 9.1).

It is not uncommon that two areas of different geological structure are separated by a major disturbance of the earth's crust called *a fault* that can extend to a substantial depth and reach many hundreds of kilometres in length. Such faults appear at the surface as wide, long fissures termed *lines of fracture* and often veiled by subsequent processes.





**Fig. 9.1.** Fracture zone in a rock mass

Practically all masses formed by hard competent rocks and solidified clays display jointing. Joints may be of various origin, character, length, size and opening.

Fissures in a rock mass generally form a certain pattern obeying a definite regularity. Moreover, the rock mass or beds that compose it prove to be separated into rather large rock blocks with uneroded sharp edges that form generally dihedral angles close to right angles ( $70$  to  $90^\circ$ ). One of directions of a fissure frequently coincides with the stratification surface



(stratification fissure). Such fissures may often coincide with contacts of different rock beds composing the overburden (*bed fissures*). In such cases two other fissure systems will intersect the beds across the strike.

Consequently, a net of generally connecting fissures in a rock mass is responsible for *jointing* of the rock mass and separation of this latter into individual blocks (block jointing). Blocks are usually 20 to 40 cm, sometimes smaller or larger (up to several metres on the side).

The jointing is usually due to fissures of a limited extent.

The degree of opening of fissures in rocks may differ in a significant range varying from a hair breadth often invisible to the unaided eye to several tens of centimetres or metres (in the area of active weathering of the mass rock in excess of 1 m).

There are *gaping* (or free) and *replacement* fissures filled up by some minerals. As a rule, jointing of the rock mass increases the latter's permeability. If fissures are filled up by replacement clay materials, there is a decline in the rock mass's permeability.

The bedrock masses are often intruded by products of magmatism. This is how *veinous* igneous (veins of erupted rocks) intrusions appeared.

Fissures, especially in the rock mass composed of carbonate rocks (limestones, dolomites), are often filled up by calcite. Where gypsum and anhydrite deposits occur, the fissures in overlying clay and marl sediment layers frequently contain a variety of gypsum (selenite or spectacle stone) which is a product of sedimentation from underground water circulating in the rock mass.

In active weathering areas fissures may often be of the gaping type or filled up to an extent by materials of weathering of clay.

The degree of jointing of hard and semi-hard rocks, such as argillites, sandstones etc. may vary appreciably which directly affects the stability of the rock mass (e.g. in slopes) and permeability and, if the rock mass is submerged, its water-bearing capacity.

L. I. Neishtadt has proposed a *jointing void ratio* for qualitative evaluation of rock jointing. This is understood to be a ratio of the area of fissures in a definite cross section to the very area of the cross section expressed in per cent.

The value of this ratio generally defined by  $k_j$  determines the type of a rock. Weakly jointed rocks have  $k_j = 2$  to 5%; medium fissile rocks,  $k_j = 5$  to 10%; and rocks with pronounced jointing have  $k_j = 15$  to 20%.

## Sec. 9.2. Principal Types of Joints

Since there is an assortment of joints, Table 9.1 presents a scheme of approximate classification of joints according to their origin.

Table 9.1

The Classification Scheme of Fissures in Rock According to Their Genesis

I. Formation fissures (joints and shrinkage cracks)		II. Deformation fissures			III. Weathering fissures		
cooling	shrinkage	tectonic	pseudotectonic	mechanical	chemical	biological	
Fissures in igneous rocks	Fissures in clayey and carbonate rocks (sandstones and dolomites)	(a) Tension joints in folded constructions	(a) Chipping joints	(a) Drying fissures	(a) Decomposition fissures	(a) Bacteria-induced decomposition fissures	
		(b) Spalling fissures	(b) Subsidence fissures	(b) Temperature-induced (contraction and expansion) fissures	(b) Leaching joints	(b) Root fissures	
		(c) Fracture joints	(c) Swelling fissures			(c) Rocking fissures	
		(d) Fissures in fractures zones	(d) Entrainment fissures				
		(e) Seismic cracks					

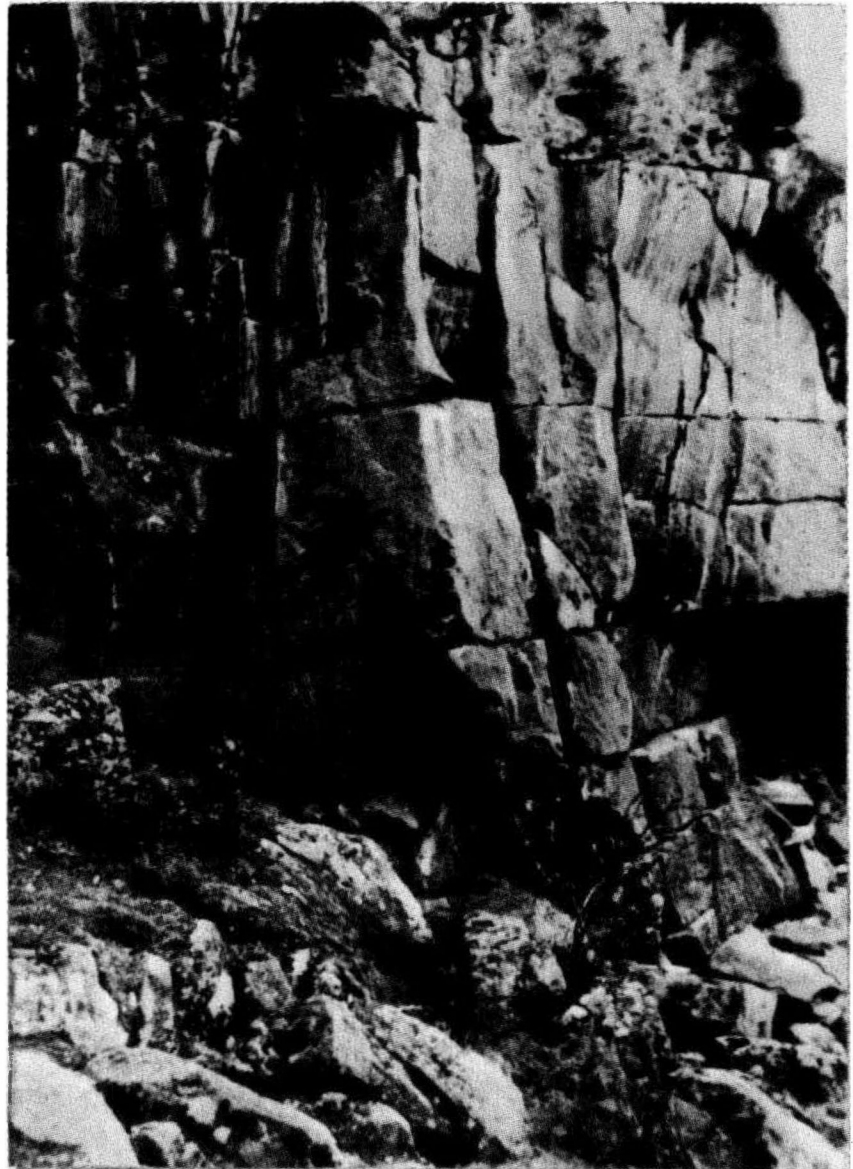


**Fig. 9.2.** Jointing in granites

In conformity with this classification scheme all joints in rocks fall into three classes. Class I includes **formation joints** (jointing and shrinkage); Class II includes **deformation joints**; Class III, **weathering joints**.

Joints in igneous rocks occur in conditions leading to contraction of products of magmatic activity as these cool.

This process causes the mass of erupted rock to be split into individual units or large blocks typical for the given rock species and called *jointing* (Fig. 9.2). Granites feature mattress-shaped or *parallelepipedal* jointing, basalts — *columnar jointing*.

Joints found in the mass of clayey or carbonate rocks are generally attributed to contraction following rock formation from excessively damp deposits (clay or calcareous silts). Limestones, in particular, are characterized by *slab parting* (Fig. 9.3).

Class II (*deformation joints*) includes fissures induced by deformations in the massive rocks, such as bending, tension, shear etc. The rock mass



**Fig. 9.3.** Slab parting in limestones

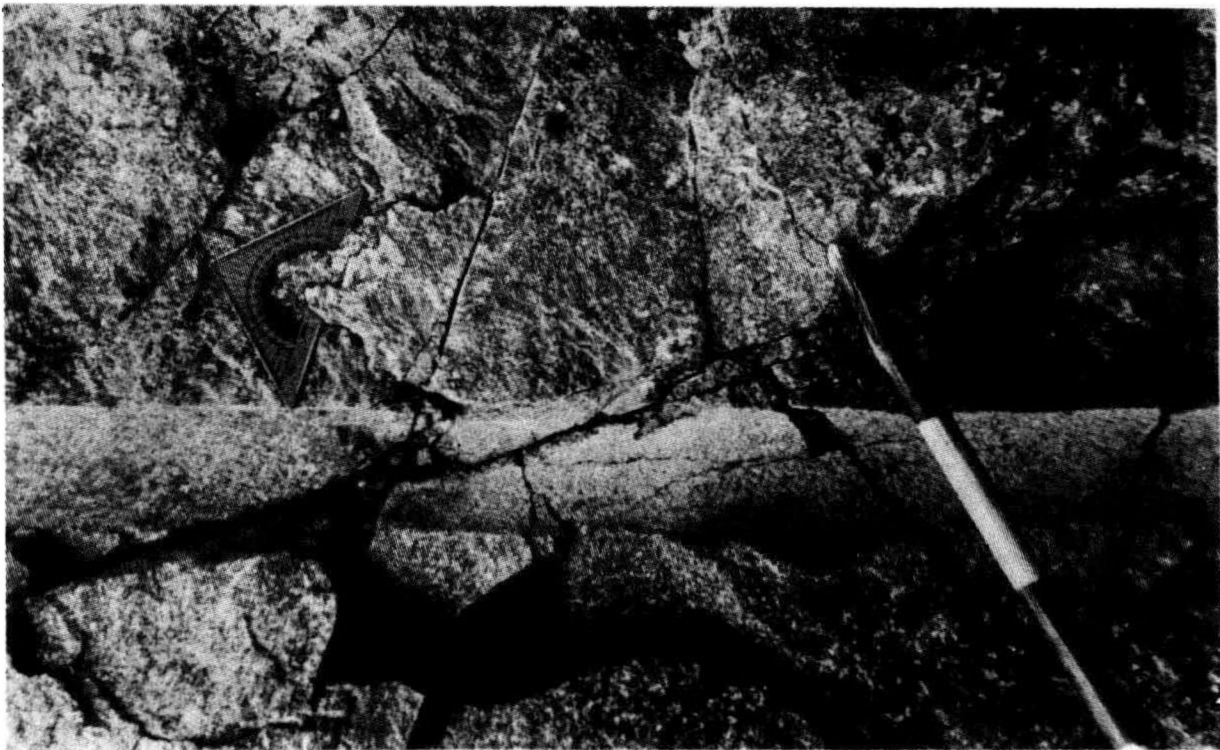


**Fig. 9.4.** Pattern of crossing deeply inclined and subhorizontal fissures in granites. The Dnieper Power Development (staff divisions spaced at 10 cm intervals) (photograph by V. Kalinchev)

may be deformed both by tectonic events (tectonic joints) and by other factors (pseudotectonic joints).

Tectonic joints typically appear in strongly dislocated areas. In other cases they prove less developed and may overlap, say, a system of stratification joints (Fig. 9.4).

Pseudotectonic joints include ones that appear in landslide hazardous slopes (*landslide, shear joints*).

*Subsidence joints or breaks* whenever there occur caving-in (e.g. in karst areas), subsidence due to undermining, melting of buried ice lenses or movement of a loess rock mass (e.g. along canal banks).

*Bulging joints* typically appear in areas where anhydride hydration occurred at deep crustal levels forming gypsum at the uppermost layers (gyp-

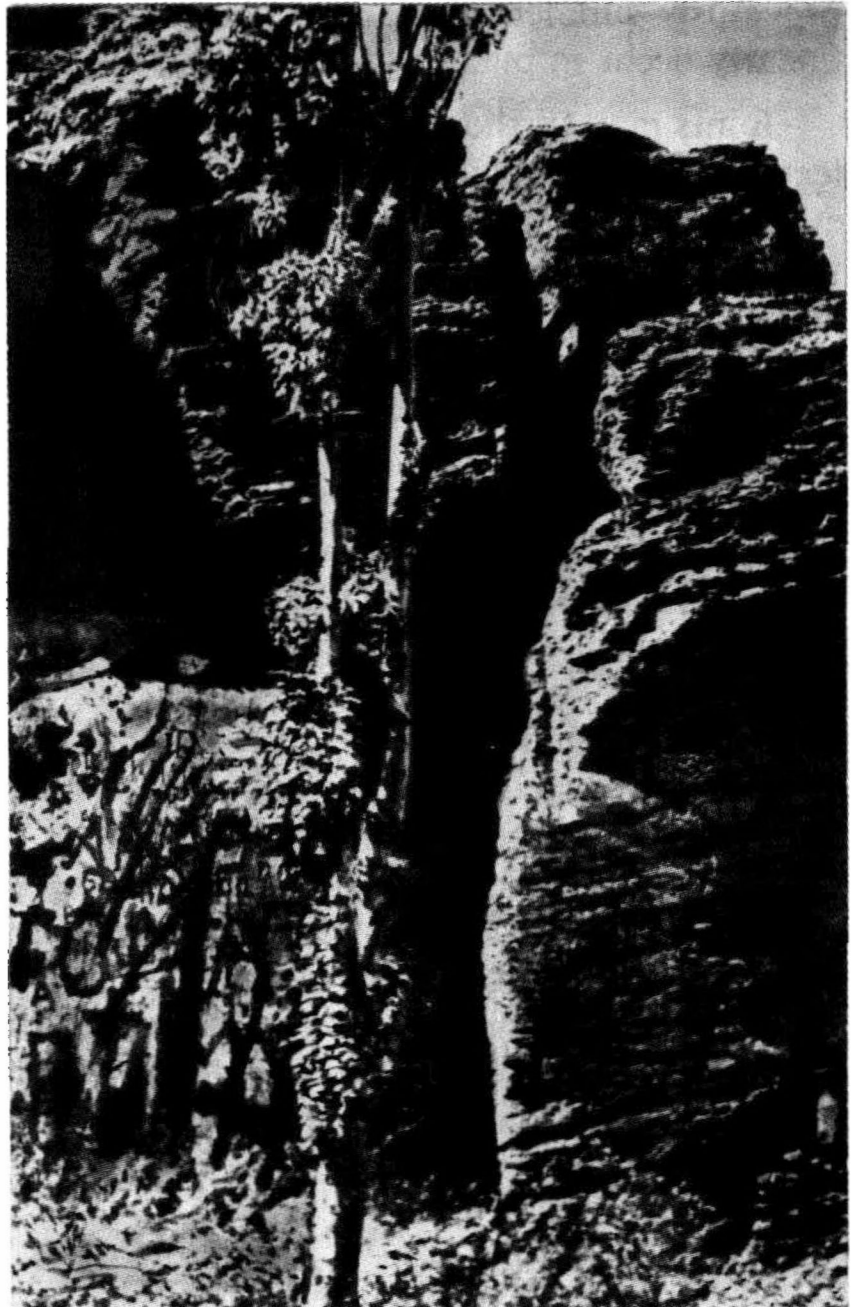


**Fig. 9.5.** Wide rift in a limestone rock mass

sum cap). Note that as anhydride transforms to gypsum it increases in volume up to 60%. Similar joints originate in an ice-rich rock mass as it freezes solid in permafrost regions.

*Entrainment joints* occur in the underlying rock mass in the case of a dislocation of the rock mass overlying it. Such conditions may have arisen in the crustal rock masses in previously glaciated areas.

*Weathering joints* (Class III) are commonly developed joints originally appearing due to other causes (Fig. 9.5). The degree of opening of these joints is very much dependent on various factors, such as physical, chemical and biological weathering.

As already reported, physical weathering occurs primarily due to changes in temperature (contraction or cooling joints, expansion joints induced by expansion of water freezing in the joints). This group also includes dessication joints that appear following intensive drying of previously submerged, usually clayey, rock mass. Such phenomena frequently occur in pits, in areas exposed to intense solar heat.

Joints may further develop by the action of various chemical processes leading to rock decomposition within their walls (*decomposition joints*) or even leaching under the effect of atmospheric (or meteoric) and ground waters. The latter joint variety typical of permeable rocks, such as limestones, dolomites, gypsum etc. may comprise a separate type of *leaching joints*. The weathering joint group includes also joints generated by pressure exerted by plant roots (*root joints*) or by trees rocked by wind (*rocking joints*).

Jointing of the rock mass into separate blocks decreases the stability of slopes and impairs the durability of structures being erected. Under such conditions steep slopes and hill sides will be subject to landslides and land slumps. Special hazard is presented by joints of substantial length that separate large rock blocks from the rock mass (tectonic rupture lines, shears etc.). When driving a tunnel or some other subterranean passage in a rock mass of pronounced jointing special care must be taken and strong timbering should be used.

Sheet jointing tends to decrease shear resistance of engineering structures. Pronounced jointing of the rock mass decreases its bearing capacity, calls for lesser permissible loads acting on a structure's foundation etc.

It is common occurrence that tectonic joints in a mass of permeable rocks trigger progressive opening due to water-induced rock leaching and development of karst phenomena.

---

## Chapter 10

### Groundwater

---

#### Sec. 10.1. The Origin of Groundwater

Ground or subsurface water is accumulated beneath the earth's surface in the pores of rocks, fissures, spaces and below the surface of the floor of water basins and streams.

*Pore water or moisture* is contained in the shingle, sand and gravel voids. Hard rocks mainly contain what is called *quarry or connate water* filling the cracks and joints\*.

In typically karst areas groundwater may occasionally fill karst cavities and voids forming subterranean rivers and lakes (*karst water*).

Increased inflow of groundwater to a pit excavated for a proposed structure or to a tunnel being driven dramatically deteriorates construction conditions.

Groundwater is an important causative agent giving rise to landslides and similar events that present a great hazard to transport routes, urbanized areas, industrial enterprises and land use features in such regions as South Kazakhstan, the Volga Region, the areas of the Crimea and Caucasus adjoining the coast of the Black Sea and other areas.

According to their origin, there are the following varieties of groundwater: infiltration, condensation, sedimentation, juvenile groundwater.

*Infiltration (or meteoric) water* accumulates chiefly due to atmospheric precipitation. Surface water in rivers and reservoirs soaking into the rock mass may also be included in this class.

*Condensation water* is due to condensation and precipitation of water vapours contained in the air that penetrate to the groundwater level, generally in desert areas.

*Sedimentation water*, which is of but partial value, is, in fact, water removed from rocks and soils on their consolidation.

*Juvenile water* (or magmatic water) is derived from or existing in molten magma and rising to the upper layers. Ascending juvenile water generally mixes up with meteoric water. On the other hand, the latter may soak down to large depths to be then mineralized by solutions present

---

\* In fact, that water which was buried concurrently with the igneous or sedimentary host rock is termed *connate water*.



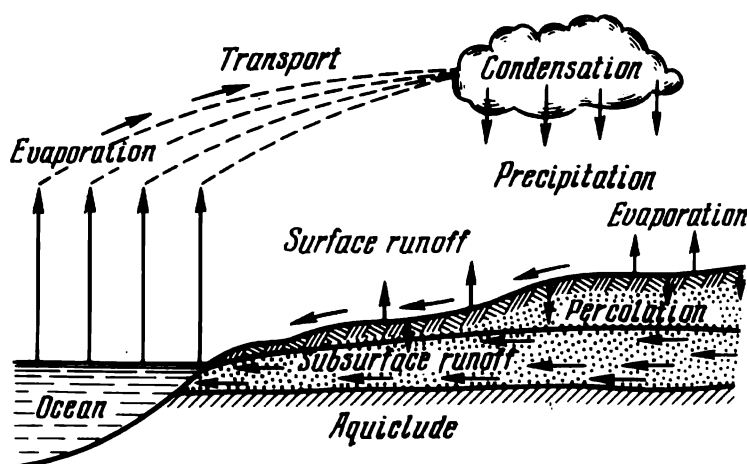


**Fig. 10.1.** The hydrological cycle and hydrogeological conditions in the upper part of the earth crust

there. *Mineral springs* thus originating have high mineral content and, often, increased temperature.

Juvenile water is of no practical importance for engineering hydrogeology, so what follows concerns primarily elucidation of mechanisms of groundwater of atmospheric (meteoric) origin.

Naturally, not all meteoric water falling on the land surface becomes groundwater. As is known, a definite fraction, as it evaporates, returns to the atmosphere as water vapours. Another fraction runs down the earth's surface supplying water to streams and rivers. Thus *runoff* occurs. It is only still another fraction of the meteoric water that replenishes groundwater by *soaking down* to the upper strata. Groundwater, in turn, gives extra water back to streams and rivers as springs.

With rare exceptions (*drainage-free areas*) all rivers flow eventually into the ocean. Extensive evaporation occurs there, especially in equatorial regions, under the effect of the sun's rays. Given definite conditions, precipitation occurs as rain, snow, hail etc. falling on the earth's surface. Thus the hydrologic cycle (or water cycle) takes place (Fig. 10.1).

The amount of precipitation reaching the ground varies considerably from one part of the earth's surface to another. In Atacama Desert (South America) it is 0 to 10 mm per annum, whereas in coastal areas of Hindustan it is up to 13 000 mm per annum. Precipitation falling on the territory of the USSR is in the range of 100 to 2 500 mm per annum (Batumi area).

Evaporation rate, generally measured in mm of water column, also changes in a wide range as governed by the afore-mentioned factors (in the European regions of the USSR 50 to 500 mm per annum).

*Surface runoff* of atmospheric water varies no less significantly. Runoff intensity may be determined from the so-called *coefficient of runoff* (or runoff coefficient). It is expressed in decimal fractions of unity and indicates the proportion of total precipitation within a given period of



time in a given catchment (drainage) area that feeds the rivers of this area (in the USSR it is 0.05 to 0.75).

Thus supply to groundwater by meteoric water soaking down to the rock and soil mass, apart from the amount of precipitation, depends on numerous local factors, such as climate, relief, the nature of crustal materials etc.

The upper crustal layers are divided into *an aeration zone* (unsaturated zone) and *a saturation zone*. As the name suggests, voids and pores in rocks are primarily filled by air in this zone. Naturally, the aeration zone coincides with the upper horizons. On the other hand, water may be existing in this zone in one form or another. This zone includes the following horizons: (1) with soil moisture; (2) with vadose water; (3) capillary fringe.

*The soil moisture horizon* has no free water. The presence of water here is only due to moisture in soils that compose the uppermost crustal layers.

The lower zone of aeration, may contain water as: (1) water vapour; (2) hygroscopic moisture; (3) pellicular moisture; (4) free or gravitational water; (5) solid water (ice) forming under definite environmental conditions.

*Water vapour* is contained in the aeration zone in pores free from water. Its transfer occurs due to different elasticity of vapours. Notwithstanding inappreciable moisture (or water) content in soils (about 0.001 of the mass of dry soil), water is of much importance for the moisture regime of the upper soil horizon and lower (aeration zone) levels, especially in prairies and deserts.

*Hygroscopic moisture* is strongly attached to particle's surfaces. As it is bonded with rock, heat is generated (wetting heat) which is the principal property of hygroscopic water that makes it different from other types of bound water. It cannot move from one particle to another, but, rather, escaping from a particle, converts to vapour. Hygroscopic water may result either from simple wetting of soil particles by water or by absorption of water vapours contained in soil pores by dry soil minerals. Whatever the mode of origination, it is always in equilibrium with the elasticity of pore water vapour, decreasing or increasing in volume as the air humidity decreases or increases.

Maximum amount of water absorbed by soil minerals accompanied by heat release is termed *maximum hygroscopic moisture* content. For clean sands it is fractions of a per cent, for clay rocks it may amount to 18% (7.9% for loess, 7.4% for Chernozem soils).

Aeration zone soils, as they occur in nature, have a moisture content generally exceeding maximum molecular water content. This increased soil moisture content results generally from meteoric water soaking down the rock layers in the aeration zone. In addition, pore water vapour under

definite conditions is condensed in the aeration zone layers and, as a result, soil grains adsorb film of water. If condensation continues sufficiently long it may increase moisture content until capillary water appears in the soil forming local or "suspended" accumulation of water in the aeration zone. This condensation process presents especial hazard to loess and loess-like loams; as the moisture content in these latter increases their stability drops conspicuously.

*Pellicular water* forms on the surface of soil particles, the thickness of the pellicles depending on the composition and size of individual particles. Unlike hygroscopic water, pellicular water is transported from one soil particle to another, from areas with greater thickness to those with lesser thickness.

Transport of pellicular water, independent of the force of gravity, occurs in various directions and is an important causative agent in properties of clay soils. It may also be responsible for frost-associated blisters in soils.

Maximum amount of pellicular water (including hygroscopic water) held in soil is *maximum molecular moisture capacity*. For clean sands it is 3 to 4%, for clayey soils it may attain 39 to 41%. Thus, most water in clayey soils is bound.

*Free water* in the aeration zone occurs, as already reported, either as capillary suspended water or slowly infiltrates downward (infiltration state) to eventually reach the groundwater level. If free water, as it soaks down to the aeration zone, encounters minor lenses of clay materials (confining strata or aquicludes), it may be trapped above these forming a "perched" water table.

This latter is of a temporary, generally seasonal, character. Water remains at this level until it penetrates in some way or another to lower levels thus feeding groundwater. As a result of evaporation the perched water dries up very often, since the depth of water here is generally insignificant. On the other hand, in spring and autumn characterized by much precipitation the water may accumulate at this level in large amounts, especially where the underlying impervious rocks form pockets.

If the perched water table is located close to the surface, swamps may be formed. What is specific for the perched water is that rocks underlying it are aerated, i.e. are in a state of incomplete saturation.

*The capillary fringe* is directly associated with groundwater, so rocks here are in a state of capillary saturation. Consequently, this variety of water is bound and suspended. By this virtue its contribution to the general water cycle is insignificant.

The thickness of the capillary fringe is governed by the size of the pores in rocks of this horizon. In clayey and loamy rocks the capillary fringe is the largest amounting sometimes to several tens of metres in thickness. In

fine sand layers it is within several metres, in coarse-grained sands some tens of centimetres. The upper surface of the capillary fringe does not remain constant in all times, rather, it varies following the fluctuation of groundwater table.

In *the saturated zone* (phreatic zone or zone of saturation), as the name suggests, rocks are almost completely saturated, i.e. all pores, fissures, cavities and voids in the rock mass are filled with water.

Subsurface water in the saturated zone can be classified as follows: ground (pressure-free) water, karst water and artesian (confined) water.

### Sec. 10.2. The Level of Subsurface Waters

The water in the zone of saturation contained in pervious rocks (aquifers) is groundwater or phreatic water.

The groundwater horizon is generally underlain by strata of impervious clayey rocks. These latter limit the thickness of the horizon and provide confining strata.

Unlike the perched groundwater, phreatic water is of substantial thickness. The level of groundwater may be subject to seasonal variations. These, however, are of minor extent and, in turn, affect the aquiferous level.

The upper surface of groundwater saturation is *the water table* or *the phreatic surface*. This provides a boundary between the zone of aeration and the saturated zone. The water table indicating the depth of occurrence of groundwater may vary depending on conditions of replenishment of groundwater irrespective of the type of overlying rocks or soils. Since there is a varying free surface of the water table, no pressure of water is built up in the groundwater.

This feature of groundwater is of much importance: the water table may be true level. In this case a sort of underground lake appears. This type of groundwater forms *a groundwater basin* or *reservoir*.

The upper surface of groundwater is generally inclined in some direction. The groundwater will, in this case, move toward where the water table falls. In this particular case groundwater flow occurs. Groundwater flow is usually directed to where draining relief features are inclined.

The gradient of the water table and, hence, the direction in which groundwater runs can be determined from the pattern of *groundwater contours* (Fig. 10.2) shown on the map. These are contour lines connecting points on the terrain where groundwater occurs at the same depth (in absolute or relative heights). Clearly, groundwater flows at right angles to the groundwater contours at a particular point on the terrain. Thus there appears on a plan a system of groundwater contours as *equipotential lines*

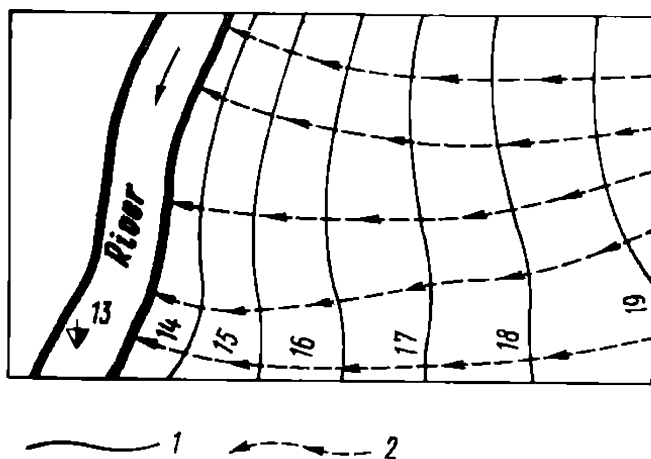


**Fig. 10.2.** Elements of subsurface flow in plan:

(1) equipotential (contour) lines (1)  
and flow lines (2)

and *flow lines* that are orthogonal to the former. Typically obeying the local topography, groundwater contours coincide with contour lines.

If groundwater occurs close to the earth's surface or appears on the surface the given area generally becomes waterbogged. In such cases groundwater is often connected with the surface *swamp water*.

Groundwater is replenished in part due to the condensation of the air water vapours but mainly due to meteoric water seepage (*infiltration*) into the soil and subsoil or, to a lesser extent, by pressure water from the lower strata rising to the upper levels. Conditions of distribution of groundwater are governed by today's geographic zones. The nearer the south, the greater is the depth of the groundwater level.

Other conditions being equal, the depth of the water table is determined by the amount of meteoric water falling onto the ground and seeping through it. Lesser amounts of precipitation and higher evaporation rate will result in lesser supply of groundwater. This is typical for southern regions. On the other hand, precipitation in northern regions is much greater whereas evaporation is usually negligible. Hence the high water table that almost reaches the ground surface which circumstance is responsible for the abundance of swamps in northern areas.

*Runoff* is also an essential factor. Since the northern regions of this country that in a not very distant past were the floor of the sea that later retreated represent flat country, runoff of meteoric water is being made very difficult here. This leads to precipitation standing on the ground surface and its penetration in excessive amounts into the soil mass.

*The drainage ratio* is an important factor determining the level of the water table, i.e. the greater the drainage, the lower the groundwater level. This is especially true of areas where river valleys cut deep into the rock mass and for places characterized by a distinct net of gullies or other erosion-induced features. Such conditions, in particular, obtain in the southern Ukraine, areas lying on the right bank of the Volga River, mountainous regions etc. Naturally, groundwater is best drained in the im-

mediate vicinity of the drain (e.g. a river valley) which typically leads to the lowest water table in the areas adjoining a river bank.

Northern areas of the USSR are slightly above sea level which provides here a base level of *erosion* and, concurrently, a base level of *drainage*. Under such conditions river valleys and erosion surfaces in general will inevitably be shallow. Naturally, groundwater will not be any noticeably drained here. This fact, in turn, is responsible for the high water table in such areas.

At the same time the water table generally fluctuates between seasons. As surface water increasingly penetrates to the aquifers at periods of greatest rainfall and snow melting the groundwater level rises, although with some retardation. This delay is due to a time taken by surface water to seep to the aquifer and flow to a point of interest to us. The level of seasonal variation of the water table may sometimes attain several metres in amplitude.

In the shoreline strip the groundwater level is primarily governed by the level of the water in the stream. The latter level dramatically increases during spring high floods. The drainage base level rises correspondingly as, consequently, does the water table.

This is how groundwater *pressure head* (or simply head) appears. Clearly, an increase in the groundwater level under conditions of water head is likewise retarded. This retardation is due to the fact that new rock volumes take time to be saturated by groundwater (Fig. 10.3). For some time this saturation process proceeds due to seepage of river water into the bulk rock and to the head of the groundwater flow. As the flood retreats and the drainage base level is lowered the groundwater level in the strip along the river banks gradually drops until it assumes its usual position.

It should be finally pointed out in high precipices groundwater may ap-

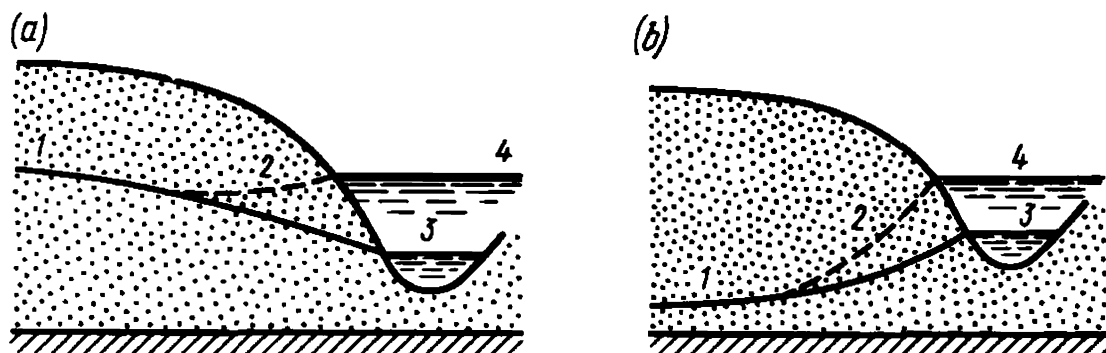


**Fig. 10.3.** Different modes of occurrence of surface and subsurface water:

*a*—subsurface water feeds the river (the river drains subsurface water); *b*—subsurface water is supplied by the river water seeping down the soil; 1—the water table in general conditions (prior to uplift pressure); 2—the water table after seepage of flood water; 3—the level of the river at low water; 4—same, at high water

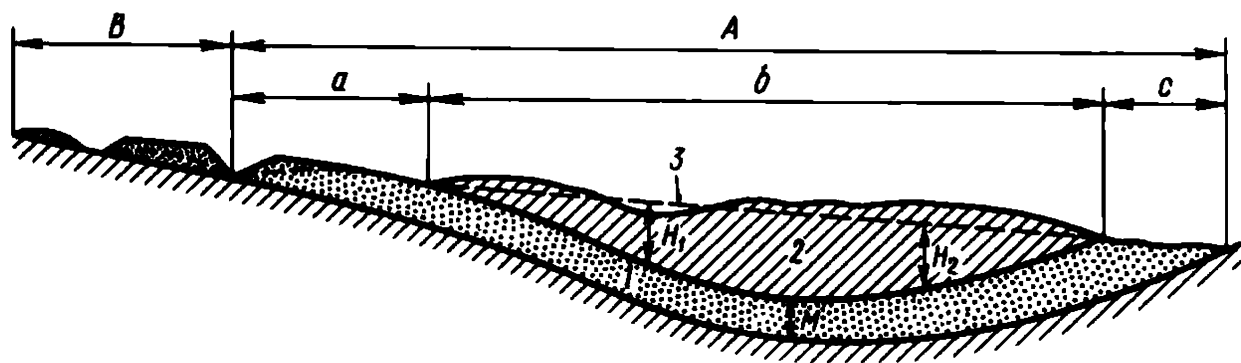


**Fig. 10.4.** Artesian aquifer (after A.M. Ovchinnikov):

1—water-bearing stratum; 2—impermeable rocks; 3—water table; A—the area of occurrence of artesian (confined water); a—water supply or intake (and, in part, runoff) area; b—pressure area; c—discharge area; B—boundary of the water table;  $H_1$ —positive head;  $H_2$ —negative head; M—thickness of the artesian aquifer

pear on the surface as springs at several levels. This is usually the case when there are several water tables separated by aquicludes.

The groundwater level in a particular area can be determined from *long-term observations in situ*.

Groundwater generally accumulates in the upper sedimentary layers, mainly in Quaternary and only partially in older formations. Aquiferous layers occurring at lower horizons generally exhibit certain peculiar features of their occurrence and regime.

An aquifer is typically bounded above and beneath by confining strata. Let us imagine that, due to a dislocation, this aquifer occurs along an inclined layer (Fig. 10.4). The intake area  $a$  where surface water infiltrates down a layer in question lies above the groundwater discharge area  $c$ . The aquiferous stratum is exposed at the ground surface or is overlain by a minor sedimentary layer that does not prevent underground water flow in the intake and discharge area.

Thus groundwater flows in the aquifers at a definite pressure determined by the difference in elevations of zones  $a$  and  $b$ . If such a pressure aquifer is located at a substantial depth it is called *artesian*. The imaginary line connecting any two points is the feeding area and the discharge one is called a *piezometric surface*.

The pressure head  $H$  at a point of an aquiferous stratum is determined by the difference between the piezometric level at a given point and the level of the roof of the aquifer.

Clearly, at a point of relief depression  $H_1$  the water at a pressure will freely outflow from a borehole. At a point of relief elevation  $H_2$  the water piezometric level will be below the earth's surface. In the area  $b$  the artesian level discharges due to outflow of subterranean water as *rising sources*.

The chemistry of subterranean water, primarily to determine its aggressiveness toward concrete structures is established from analysis in a special laboratory. When conducting chemical analysis take a sample of water *in situ* at least 2 litres in volume. Be sure that the water container is quite clean. When taking water samples for carbonic acid content and for that of  $\text{SO}_4$  ion, hydrogen sulphide, iron and organic materials, follow special instructions. The problems relating to the determination of aggressive action of subterranean water on one material or another are dealt with in special texts on construction materials.

In the general case it is customary to consider as the most suitable for construction purposes water with a reaction approximating a neutral one, the type of water that is not especially hard, has no free carbonic acid and with low sulphate content.

In volcanic regions hot springs, sources and, characteristically, geysers are very much abundant. Their temperature may exceed  $90^\circ\text{C}$ . These hot springs usually result from the occurrence at some depth of still hot magmatic materials emitting heat, vapours and gases.

As magmatic gaseous products and solutions rise from magmatic bodies to upper layers, they come in contact with subterranean water circulating in the bulk rock. As they do so they get rich in gases, in particular, in carbonic acid (Narsan water in the Caucasus), and minerals (mineral water). Hot springs are especially abundant in Kamchatka, warm sulphur springs in Tbilisi are also well-known.

Increased temperatures of subterranean water may sometimes be due to other than magmatic events. An example can be provided by hot springs in the Kuban region. Such phenomena are induced by water circulating in deep strata where increased temperatures prevail.

New vast deposits of subterranean hot water have been discovered in this country in the last few decades. If we mention only the West Siberian basin, these occur at an area of 3 mln  $\text{km}^2$ , temperatures occasionally reaching  $125^\circ\text{C}$ . Since 1967 subterranean hot water has been in extensive use for different purposes in the town of Makhachkala (heating of structures, hot water supply to laundries, baths etc.). There are cases when tunnels being driven meet with paths of hot springs common in young mountainous areas. Temperatures of such springs (often in excess of  $45^\circ\text{C}$ ) may be as much as  $80$  to  $85^\circ\text{C}$ . Thermal springs have also been discovered along the route of the Baikal Amur railway, in particular, in line with the Severo-Muisk tunnel, with temperatures up to  $52^\circ\text{C}$ . The springs are planned to be used for domestic needs.

Under such conditions tunnel driving becomes a complicated task. This especially so if a tunnel has to be driven through a mountain of substantial height. It is possible to approximately predict temperature to be expected at

one depth or another in the rock mass if we proceed from the principle of a geothermic step.

A *geothermic step* is the average depth of the bulk rock expressed in m at which the temperature of the surrounding medium will rise by 1 °C. For flat country the geothermic step is generally taken equal to 33 m. Under conditions of pronounced relief erosion providing better cooling for mountainous country the geothermic step is usually larger, about 40 to 42 m. To have better conditions of tunnel driving through solid rock it is a good plan to direct the tunnel's centre line where rock strata are steeply inclined.

Finally cases may occur where water with high mineral content, as it rises up fissures to the upper lying strata, due to lower pressures and temperatures, causes the solutes to be deposited on the fissure walls. Thus it is not uncommon that cracks and fissures in the bulk rock due to very old dislocations are completely filled by mineral materials, in particular vein quartz or calcite.

---

## Chapter 11

### Coefficient of Permeability and Methods of Its Determination

---

#### Sec. 11.1 A Coefficient of Permeability

Denoted by  $K$ , it finds wide application for hydrogeological calculations. It is a measure of a rock's permeability and depends on the rock's properties, primarily, mineral composition of the soil particles or grains and density and also on the properties of the percolating fluid and its state, notably, temperature determining its viscosity. Like velocity, the coefficient of permeability is measured in cm/s, m/d.

The magnitude of  $K$  is a function of the resistance offered by water passing through a rock (soil). As to the resistance, it is dependent on the degree of roughness of the walls of a conduit in which water flows and, mainly, on the size of the conduit. As the cross section of a conduit decreases the resistance to water flow rises dramatically. This is what accounts for the unusually low permeability of clay materials that have very fine particles and, consequently, very small pores.

Viewed in this context, it is clear that the degree of permeability of sands will increase with an increase in grain size and uniformity. In sands with grains very much different in size the pores of courser grains may in a more or less extent be filled by finer particles. In this case the coefficient of



permeability is determined by the pore size of finer material. So, clean gravel has this coefficient of very large magnitude.

By contrast, the coefficient of permeability of gravel with sand-filled pores may often prove less than that of the filling material. Clearly, of importance are the smoothness of grains and sand porosity which is also an essential factor in rock permeability.

Viscosity of water increases with greater water densities at lower temperatures. Under these conditions the resistance to water flow in the pores will also rise. This results in lesser seepage velocities and, accordingly, (fictitious) drop in the coefficient of permeability of the soil in question.

### Sec. 11.2. Methods for Determination of the Coefficient of Permeability

Clearly, it is possible to allow for the joint effect of diverse factors influencing the magnitude of the coefficient of permeability only by *in situ* investigation of the particular soil. However, we may well use in many cases any of an assortment of empirical formulae for rough estimation of sand permeability. These formulae rely on the relationship between a rock's coefficient of permeability and its granulometry. There are formulae proposed by Hasen, Slichter, Krüger, Kozeny, Zunker, Zamarin, Terzaghi and others.

Some of these formulae take into account the temperature of the percolating water, sand porosity, uniformity etc. Yet the determination of a sand's coefficient of permeability from its mechanical analysis is so approximated as to make it in many cases impossible to allow for all of these factors.

The following formula may be used for a rough evaluation of  $K$  for conditions that normally arise:

$$K = 1000d_{10}^2 \text{ m/d} \quad (11.1)$$

where  $d_{10}$  is the *particle size* in mm. The particle size is the diameter of grains of sand where finer particles take up 10% of the bulk volume of the sand in hand.

In many instances the above formula well approximates experimental data. For example, for  $d_{10} = 0.25$  mm  $K = 1000 \times 0.0625 = 62.5$  m/d. More reliable values of a coefficient of permeability of sand materials may be obtained experimentally in the laboratory or by *in situ* observations.

Figure 11.1 is a schematic drawing of a permeameter permitting fairly reliable results in laboratory investigations. Place the rock (soil) to be tested in glass container  $A$  which is  $75 \text{ cm}^2$  in cross-sectional area or more such that there remains some water above it. Insert sieves above and

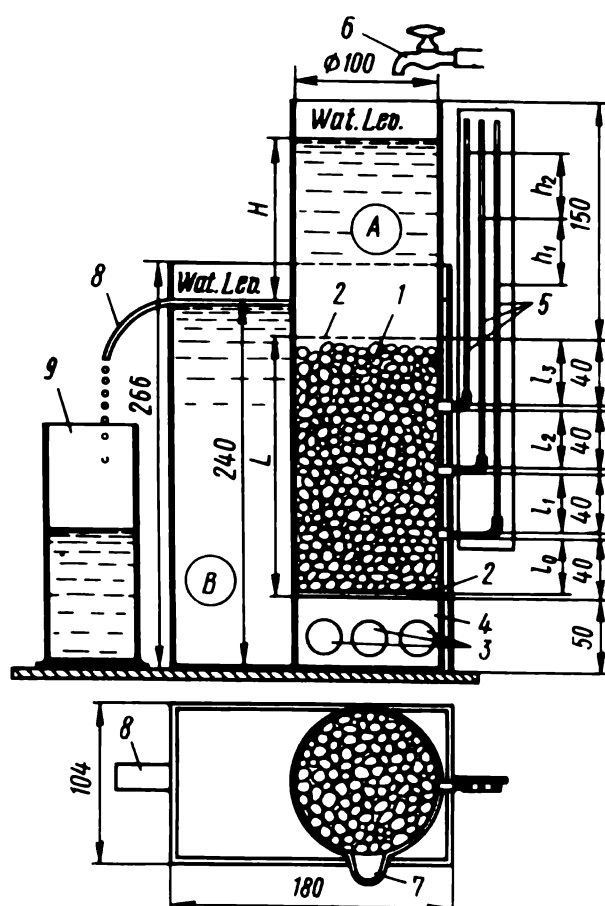


Fig. 11.1. Diagram of a filtration (permeability) apparatus:

1—soil being tested; 2—strains; 3, 4—apertures in the support; 5—piezometric tubes; 6—water cock; 7—extra drain; 8—drain controlling the level of the downstream bief; 9—measuring cylinder

beneath the sample. The lower sieve supports the sample and the upper one prevents washout by a stream of water from cock 6. The water head,  $H$ , is maintained due to the difference in water levels in containers A and B. The definite altitude of drain 8 ensures that the water in container B is constantly at the same level. The water level in container A is kept at the necessary height by manipulating the cock or using the several control drains located at different levels (not shown in the diagram). By varying this level and the height of the rock column in container A it is possible to conduct the test with any value of the average gradient

$$J_{av} = H/L$$

The calculated actual gradients  $J_{1_{calc}}$  and  $J_{2_{calc}}$  are determined, allowing for piezometer readings (the difference between readings  $h_1$  and  $h_2$ ) from the relationship  $F_i = h_i/l_i$  (see Fig. 11.1).

By knowing the cross section of the sample  $\omega$  and water discharge  $q$ , it is possible to find the seepage velocity  $v$  from the relationship  $v = q/\omega$ . Then the coefficient of permeability will be determined from the formula

$$K_f = v/J_f$$

Coefficients of permeability of clay materials, due to their exceptional permeability, are determined after studying their compression under a load

acting for a definite time period. This problem will be dealt with in what follows.

The coefficient of permeability of a definite depth of bulk rock is found more reliably by *in situ* tests by preserving the texture of the rocks and allowing for the natural mode of their occurrence.

Depending on the objectives in mind the experimental tests to determine the coefficient of permeability are divided into two groups: (1) to study the relationship between groundwater flow discharge and the drop in the water level in the bulk rock during pumping out of water from the main working and during observations of the water level in the boreholes; (2) to determine the actual (true) velocity of water infiltration ( $v_0$ ) in the rock in pores and fissures also depending on the gradient.

In the latter case the determination of the coefficient of permeability relies on a comparison of the groundwater in several workings spaced at definite intervals along the line of flow. In so doing, observe the velocity of water flowing from one working to an adjoining one using one type of *indicator* or another. As markers or labels use is made of various colouring agents (e.g. fluorescein), different salts (common salt, ammonium chloride etc.) whose presence in the water can be determined by chemical analysis or by measuring the changes in electroconductivity of subterranean water (Slichter's method). Labelling may be also provided by odoriferous materials (chloroform, kerosine etc.) and even cultures of harmless bacteria. Recently it became possible to study the regime of subterranean water by tracer technique.

*In situ* tests to determine coefficients of permeability are considered in detail in texts on hydrogeology (or geohydrology) as a science which studies subsurface water.

Average values of this coefficient,  $K$ , m/d, for some species of soils and rocks are presented below.

Permeability of rocks	$K$ , m/d
Almost impermeable rocks (clays, monolith rocks)	$< 5 \times 10^{-5}$
Extremely slightly permeable rocks (loams, coarse-grained sandy loams, sandstones without jointing etc.)	$5 \times 10^{-3}$
Weakly permeable rocks (sandy loams, clayey schists with minor jointing, sandstones, limestones etc.)	0.5
Permeable rocks (fine- and small-grained sands, jointed hard rocks)	5
Well permeable rocks (medium-grained sands, hard rocks with marked jointing)	50
Very well permeable rocks (coarse-grained gravelly sands, gravels, hard rocks with pronounced jointing)	500 and more

---

## Chapter 12

### Physical Properties and Characteristics of Rocks and Soils

---

#### Sec. 12.1. Class One and Class Two Index Characteristics

Physical, mechanical, hydromechanical characteristics are important from the standpoint of engineering geology and soil mechanics. Road construction needs thermophysical characteristics. Clearly, these properties are governed by the state and structure of the rock or soil in hand.

A soil's composition can be inferred from the bulk density of its constituents, from the grain size etc. In addition, important criteria of a rock or soil are its density, moisture content, consistency of a clayey soil etc.

To solve tasks faced by engineering geology and rock mechanics these properties should be represented in quantitative terms. Thus a science arose concerned with a complex of physical and mechanical indices of rocks and soils necessary for calculating and predicting a soil's behaviour under particular conditions. These index characteristics termed by us *Class One indices* include primarily the compressive strength of rocks and soils, their deformability and some others.

It is essential that these indices be determined in undisturbed samples, i.e. ones with *intact texture*. It is quite a problem to take such samples from the bulk rock. *In situ* sampling is done from an open working (trench, pit, adit), or, alternatively, from a large-diameter borehole using a sampler.

This operation is time- and labour-consuming. This leads to fewer *in situ* tests involving undisturbed specimens which is a disadvantage in view of a large spread of site investigations.

In such conditions it is of much importance to refer to *Class Two indices* that characterize rock composition, state and physical properties even if these indices have no direct use in soil investigations. What must be first emphasized is their intimate connection to mechanical characteristics of rocks. Moreover, Class Two indices may, as a rule, be determined from *disturbed samples*.

This latter fact permits a wide spectrum of specimen selection as engineering geological investigations are made, and, primarily, boreholes are drilled. Unlike undisturbed sampling, this kind of test is much less costly and samples taken are generally large in number. Taken together, all this makes it possible to more reliably establish Class One indices.

Note that Class Two indices may be used for a visual evaluation of engineering geological and, by extention, even mechanical properties of a rock or soil. At early stages of investigations this advantage may play a decisive role.

The geomechanical properties of one rock or another are governed by *rock composition, state and structure*. Naturally, many of rock and soil properties are determined by their composition. E.g. clay materials fall into rich and lean clays with a spectrum of intervening varieties. However, this characteristic alone, indicative of a rock's composition, is clearly insufficient even for a rough evaluation of properties of clays. E.g. it is a matter of experience that the strength of a dry clay is much greater than that of an excessively wet clay material. Hence a need in calculating the moisture content of the given rock that will in this case attest to its state.

Principal Class Two indices (physical characteristics) include composition, state and consistency index of clay rocks  $I_L$ . Rock composition may be: petrographic, mineralogic and chemical; granulometric  $d$ ; bulk density  $\rho_0$ .

A soil's plasticity indices are: the liquid limit  $W_L$ , plastic limit  $W_p$ , plasticity index  $I_p$ . A soil's state is characterized by moisture content  $w$ , compression index, porosity  $n$ , voids ratio  $e$ .

The consistency index of clay rocks  $I_L$  is also used.

A soil's compactness can be also determined from its bulk density (Class One index  $\rho_w$ ) concurrently taking into account the fact that rock

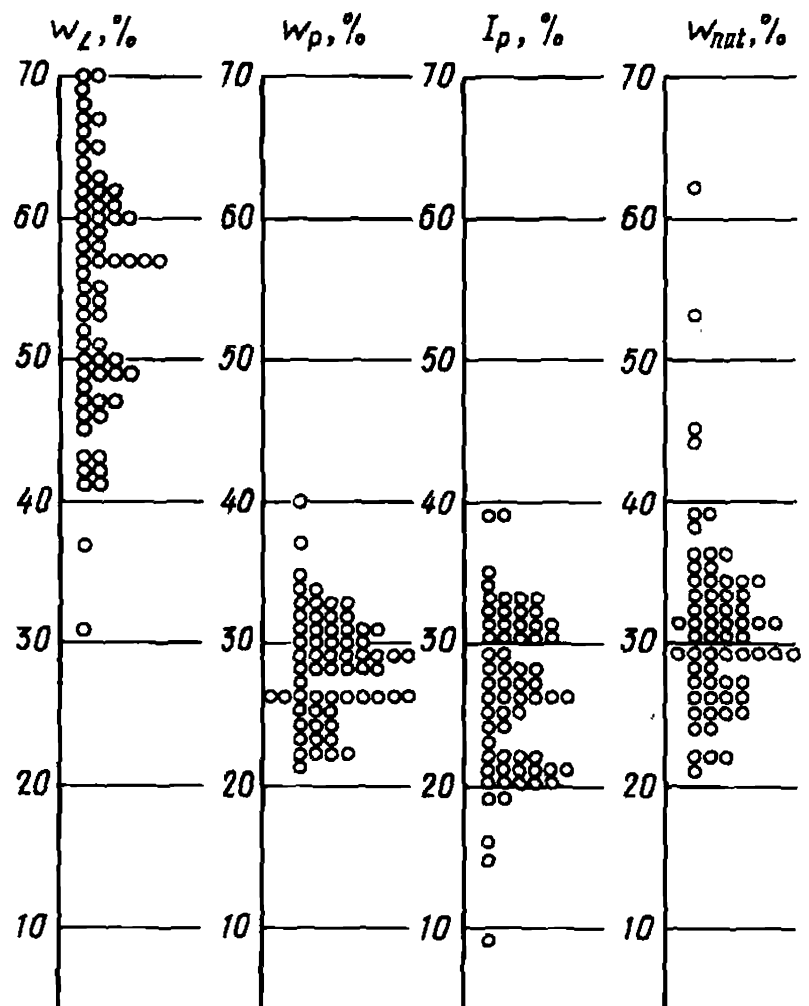


Fig. 12.1. Graphs of scattering characteristic water contents for sensitive deluvial clays occurring in the slope of Rabochy spusk street in the town of Ulyanovsk (submitted by Z.I. Rogozina):

$w_L$ —liquid limit;  $w_p$ —plastic limit;  $I_p$ —plasticity index;  $w_{nat}$ —natural moisture content. Average values on the median:  $w_L = 57.0\%$ ;  $w_p = 29\%$ ;  $I_p = 28\%$ ;  $w_{nat} = 31\%$

volume mass is governed not only by its density, but also by the moisture content and unit bulk densities of the soil's constituents.

As far back as the 1930s the present author proposed a hypothesis of continuous rock change even within the boundaries of an individual horizon in terms of composition, state and, consequently, properties ("from point to point"). The above fact can be better visualized from dispersion graphs (Fig. 12.1).

This type of graph may be used to treat any rock characteristic. (The graphs have no  $y$ -coordinates). The width of a graph may vary depending on ease of plotting and of use. The graph enables one to readily observe the number of tests taken and their quality (discrepancies), the degree of rock non-uniformity (from dispersion of trial points). It is especially convenient to compare findings obtained by different laboratories relating to some object when dispersion graphs of different indices are plotted on one common sheet. This method may be used for comparing rock properties from two separate building sites in terms of Class Two indices.

Taken together, one or another rock index may characterize a rock not from data furnished by individual tests but, rather, as a sort of *experimentally obtained aggregation* of their values.

Despite the apparent randomness in variation of these indices for the same rock species "from point to point", in terms of distribution they obey a definite regularity. This regularity is governed by the principles of the theory of probability and, in particular, generally obeys the Gaussian law of normal distribution. Practice shows that a deviation of soil indices from this law is not greater than discrepancies in indices of compression strength of construction concrete.

### Sec. 12.2. Granulometric Rock (Soil) Composition. Classification Criteria

To determine the granulometric composition of a soil the percentage of particles of one size or another is determined.

It would appear that the easiest method of determination of a soil's granulometric composition is by passing the soil through a set of standard sieves much like in studying the composition of a sand as a building material. This determination, however, has a disadvantage since the minimum particle size is limited by the insufficient (about 0.1 mm) fineness of sieve cloth and by the difficulty of separation of aggregations of fine fractions in a dry form into individual grains. For this reason it is customary to divide complete analysis of very fine-grained soils into two stages: (1) determination of percentage of grains more than 0.1 mm in diameter using a standard set of screens; (2) determination of percentage of

grains less than 0.1 mm in diameter by measuring the velocity of deposition of soil particles in water.

The former operation does not present any particular problem. Before the latter stage begins prepare the soil being tested by washing, lengthy boiling and rubbing in water to be sure that no minor particles remain stuck together. This operation is called *dispersion*. The aqueous medium in which clay mineral particles are suspended is called a *dispersion medium*, and hard particles, both visible and invisible to the unaided eye are *suspension* (or disperse phase). It may prove sometimes helpful to add some ammonia to the suspending medium for better soil dispersion.

The rate of particle precipitation from a dispersion medium is governed by the size and shape of grains, their bulk density and water viscosity determined, in turn, by its purity and temperature. The easiest of all methods of granulometric analysis of clay soils is the areometric method. For this reason it finds extensive use in laboratory investigations, especially so since granulometry of clay soils is an index of only relative value.

The areometric method relies on the measurement, using a special hydrometer, of the density of the dispersion medium containing 30 to 40 g of soil particles per 1 000 cm<sup>3</sup> varying with a lapse of time as the suspended soil particles are deposited. Hydrometer readings, allowing for requisite corrections, are converted to percentage data on particles of one size or another using a special nomogram. Make sure, however, that, prior to use, each hydrometer must be tared.

Soil analysis using techniques of Sabanin and Robinson that rely on sampling at definite time intervals specimens from the aqueous solution followed by determination of the dry residual through evaporation of the specimens and weighing require much time, labour and large amounts of distilled water. To adequately conduct such fine analysis care must be taken to exactly follow the procedures of such tests described in relevant instructions and manuals\*.

To facilitate the usage, the results of a rock's granulometric analysis are plotted on a semilogarithmic scale shown in Fig. 12.2. Each point on the curve indicates the percentage of particles less than the particular size in the rock (soil) being tested. The ratio of diameters corresponding to 60 and 10% of particle size contents is called a *coefficient of non-uniformity* suggested by Z. Hasen. If we define it by  $k_{n-u}$ , we may set up a relationship

$$k_{n-u} = d_{60}/d_{10} \quad (12.1)$$

The diameter  $d_{10}$  is said to be an *active* or *effective* diameter.

---

\* See, e.g. Chapovsky, E. G. *Laboratory Experiments Related to Soil Science and Soil Mechanics*. Moscow, 1975 (in Russian).

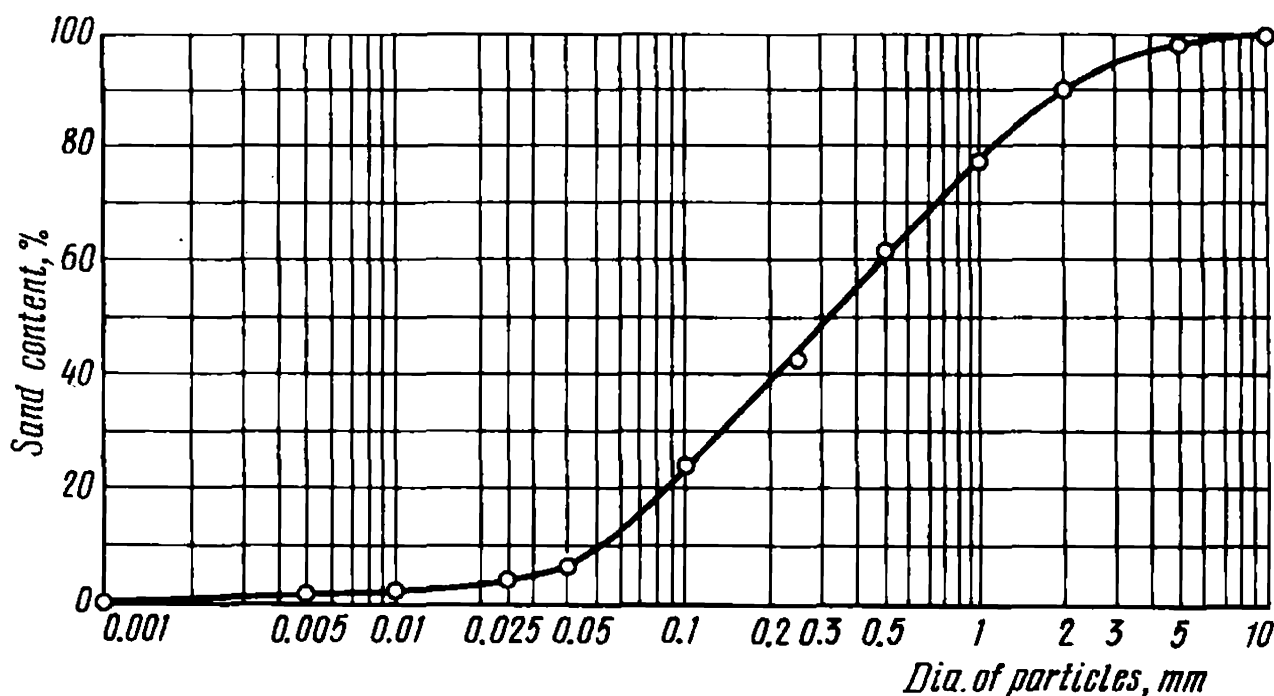


Fig. 12.2. Granulometric composition of sand fills of Dams No. 1 and 4 for particles:  $> 5$  mm—2.0%; 5 to 2 mm—7.5%; 2 to 1 mm—13.5%; 1 to 0.5 mm—15%; 0.5 to 0.25 mm—19.3%; 0.25 to 0.10 mm—18%; 0.05 to 0.1 mm—5.3%; 0.01 to 0.005 mm—1.4%;  $< 0.005$  mm—0.3%; coefficient of nonuniformity  $k_n = d_{60}/d_{10} = 9.6$

Depending on particle size, it seems appropriate to distinguish granulometric characteristics given in Table 12.1.

According to Table 2 in Chapter 15 of the Soviet Code of Practice SNiP II-15-74 grained rocks are divided into *detritus* and *sand rocks*. Detritus, in particular, includes boulders, pebbles and gravels (with particles more than 2 mm in diameter exceeding 50%).

Sand rocks, in turn, include *gravel*, *coarse-grained*, *medium-grained*, *fine-grained* and *powdered* rocks (rock flour). It is not uncommon that building practice refers rocks where particles 0.25 to 0.10 mm in diameter prevail to *fine-grained* sands. Still another group includes very fine-grained sands with prevailing particle size 0.10 to 0.05 mm.

According to Table 12.1, clay materials have particles less than 0.005 mm in diameter. If a loamy or a sandy loamy soil has particles 0.05 to 0.005 mm in diameter prevailing over coarser-grained particles (0.05 to 2.0 mm in diameter) the name of the soil is prefixed by the term “powdered”. So we often meet in building practice the term *light powdered sandy soil*. Loamy soils are abundant where sand particles prevail over powdered particles. Such soils are termed sandy or sabulous clays.

Lithological diagnostics of a soil (clay, loams or sandy loams, heavy or light-textured) does not need such a detailed particle size classification. In



Table 12.1

Classification of Granulometric elements

Rock name	Particle size, mm	Rock name	Particle size, mm
Boulders (rounded) and rocks (angular)	> 200	Large boulders	800
		Medium-size boulders	800-400
		Small boulders	400-200
Cobbles, pebbles (rounded) and rock debris (angular)	200-40	Cobbles and large-size rock debris	200-100
		Large-size pebbles and rock debris	100-60
		Small-size pebbles and rock debris	60-40
Gravel (rounded) and gruss (angular)	40-2	Large	40-20
		Medium	20-10
		Small	10-4
		Very small	4-2
Sand	2-0.5	Coarse-grained	2-1
		Large-grained	1-0.5
		Medium-grained	0.5-0.25
		Small-grained	0.25-0.1
		Fine	0.1-0.05
Silt	0.05-0.005	Coarse	0.05-0.01
		Fine	0.01-0.005
Clay	less than 0.005	Clayey	< 0.005

most cases it suffices to determine the percentage of particles contained in a rock: sand particles with grains more than 1 mm; those with grains 1 to 0.05 mm; powdered particles 0.05 to 0.005 mm; clay particles less than 0.005 mm in diameter.

If data on the content (in %) of clay particles in a rock are available, it is a good plan to use, especially at an early stage of soil investigations, the following abridged classification scheme.

The easiest method to determine the percentage of clay particles in a soil is to apply the so-called *in situ* technique.

Soil type	Percentage of clay particles			
Sand	up	to	3	
Sandy loam	from	3	to	12
Loam	from	12	to	18
Heavy-textured loam	from	18	to	25
Clay	more than			25

Clay particle content is then established from incremental volume of the soil sample in water induced by clay swelling using a special table or the following relation

$$x = 22.7\nu_0$$

where  $x$  is the content of clay particles in a soil;  $\nu_0$  is incremental volume per  $1 \text{ cm}^3$  of the original soil volume.

The above scheme of rough classification allowing for the clay content in a soil facilitates categorization of soils for road building practice.

### Sec. 12.3. Other Class Two Rock Indices. The Methods of Determination

**Rock particle density  $\rho_0$ .** It should be first pointed out that we mean the average bulk density of rock particles contained in a unit volume. The bulk density is a numerical measure of the mass of a rock cubic unit on the assumption that the rock in question has no pores. In the definition  $\rho_0$  this circumstance is denoted by a subscript  $\rho$  (previously known as specific weight).

It follows, then, that the determination of  $\rho_0$  consists in experimentally finding the volume of solid particles composing a certain amount of rock and the mass of the particles proper.

If we define the total volume of a definite quantity of particles (specimen skeleton) as  $V_{sk}$  and the mass of these particles as  $Q_{sk}$ , then the bulk density of the particles  $\rho_0$  will be found from the relation

$$\rho_0 = Q_{sk}/V_{sk} \quad (12.2)$$

It should be noted that the bulk density  $\rho_0$  is measured in  $\text{g/cm}^3$  or  $\text{t/m}^3$ . This follows from the above relationship.

The bulk density may differ from one rock to another in the range from 2.60 to 2.85  $\text{g/cm}^3$  and, most commonly, from 2.65 to 2.75  $\text{g/cm}^3$ . The bulk density of particles composing quartz sand is 2.65 to 2.66  $\text{g/cm}^3$ ; of sandy loams and loams 2.70 and 2.71, respectively; of clay materials 2.71 to 2.75  $\text{g/cm}^3$ .

The bulk density  $\rho_0$  is the mass of a substance per unit volume. The bulk density of a soil (rock) is governed by compactness and moisture content of the soil, of particles composing the given material, i.e. the value of  $w$ .

If we define the volume of a certain amount of a soil as  $V_w$ , and the mass of this soil quantity as  $Q_w$ , then the bulk density of the soil being tested will be

$$\rho_w = Q_w/V_w \quad (12.2')$$

The bulk density of a soil skeleton  $\rho_{sk}$  is understood to be the mass of the solid phase of the soil per rock unit volume. Differently speaking,  $\rho_{sk}$  is the mass of a rock cubic unit measured from its volume in the state of its natural (original) density (or compactness) and weighed after the material has been completely dried. The bulk density of a soil (rock) skeleton  $\rho_{sk}$  is connected with its bulk density  $\rho_w$  and moisture content  $w$  through the following relationship

$$\rho_{sk} = \rho_w / (1 + w) \quad (12.3)$$

where  $w$  is moisture content in fractions of unity.

For example, given  $\rho_w = 1.9 \text{ t/m}^3$  and  $w = 34\%$ , the soil skeleton mass density is

$$\rho_{sk} = 1.9 / (1 + 0.34) = 1.41 \text{ t/m}^3$$

As follows from the definition of the bulk density of a soil its determination is two-fold: first determine the volume of some quantity of a soil, then find the mass of this soil volume.

*The volume of a (monolith) sample of non-porous hard rock* can be easily and without incurring any noticeable errors or causing rock derangement established by immersing the rock specimen into water and measuring the volume of the water thus displaced. In so doing we may well refer to the familiar method of measuring the weight of a body from the loss of its weight upon being immersed in water due to the weight of the water thus displaced.

It is impossible to find the volume of a specimen of *clay soil* by directly immersing it into water: a clay specimen upon being wetted either disintegrates or swells absorbing water. It is necessary, before putting a clay soil specimen into water, to paraffine the specimen thus making it impervious.

When paraffining, take care that no air bubbles are entrapped between the soil and the paraffine coat. Then proceed with the test as described above. To find the volume of the clean soil subtract the volume taken by the paraffine from the total volume of the paraffine-coated soil. The volume of the paraffine can be easily determined by weighing the specimen before and after the coating and by allowing for the bulk density of paraffine usually close to  $0.9 \text{ t/cm}^3$ .

A very convenient method of determining the volume of a clay soil is to immerse the specimen into mercury followed by a measurement of the mercury thus displaced weighing this latter and allowing for the temperature correction. In this case no need arises to paraffine the specimens.

The bulk density of large-size *bound rock monoliths* can be established fairly accurately by directly measuring the specimen of a regular



Fig. 12.3. Sampling in the field by using a cutting cylinder

geometrical, say, cylindrical shape and then weighing it. For this end we often use a hollow cylinder without a bottom or cover and with a cutting edge. It is 5 to 15 cm in dia. and 2 to 5-10 cm high (Fig. 12.3). For sampling the cylinder is pushed into the soil. The volume of the specimen will in this case be determined from the inner volume of the cylinder.

It is permissible to find the bulk density of clay soil specimens with undisturbed texture finding concurrently the reference moisture content  $w$ . This latter is suffixed to the definition of the bulk density of a soil. For example, the subscript in  $\rho_{24} = 1.95 \text{ t/cm}^3$  indicates that with 24% moisture content  $1 \text{ m}^3$  of clay soil will weigh 1.95 t.

The bulk density of *wet clay soils* is generally within  $\rho_{sk} = 1.95$  to  $2.10 \text{ t/m}^3$ .

To find the volume of a *cohesionless sandy soil* presents some difficulty since no devices are available that would permit sampling without deranging the soil structure. It is usual, therefore, to determine the bulk density of a sand soil in two states, the most loose and the most compressed. In so doing, put the sand to be tested in a measuring vessel. Test the sand in dry form or immersed. To achieve looseness, carefully pour the soil in the vessel, and to achieve maximum compaction mix the soil until its volume remains unchanged or, alternatively, vibrate the dry soil with  $\rho_{sk} = 1.58$  to  $1.65 \text{ t/m}^3$ .

In most cases it is very easy to determine the volume of dry sand under conditions of maximum looseness. Fill a measuring vessel (e.g. a graduated

cylinder) with the sand until it is half filled. Cover its top with a hand, carefully incline the vessel to a horizontal position, then, as carefully, cause the vessel to resume its original position. Now measure the specimen's volume referring to the graduations.

**Moisture or water content  $w$ .** This index characteristic is known to be one of the most essential control determinations of clay rocks. The moisture content is the ratio of the quantity of water  $P_w$  contained in the soil's pores, expressed in percentage by weight, to the quantity of skeleton  $Q_{sk}$  (solid particles) of the soil in question, i.e.

$$w = 100P_w/Q_{sk}$$

In some cases the moisture content  $w$  may be expressed in fractions of unity.

The quantity of water  $P_w$  is found as a difference between the mass of the soil specimen when it has its original moisture content and when absolutely dry. The mass of solid (skeletal) particles is assumed to be similar to the latter phase's mass. Hence the procedure of moisture content determination by drying soil specimens in a drying cabinet.

The degree of rock pore filling is determined from a saturation coefficient (or soil moisture content) defined by the letter  $G$ . The numerical value of this coefficient is found from the relationship

$$G = w/w_0$$

where  $w$  is the soil's natural moisture content;  $w_0$  is the limit soil moisture content likely for the given rock (soil) porosity.  $w_0$  is generally called *a total moisture capacity*.

Naturally, with  $G = 1$  the pores of a rock are all saturated; with  $G < 1$  some amount of air or other gases is entrapped in the rock voids.

The total moisture capacity is calculated from this relationship

$$w_0 = 100(1/\rho_{sk} - 1/\rho_0)\rho_w \quad (12.4)$$

where  $\rho_{sk}$  is the bulk density of skeletal rock particles;  $\rho_0$  is the density of soil particles;  $\rho_w$  is the water density, 1.0 g/cm<sup>3</sup> or 1.0 t/m<sup>3</sup>.

**Example.** Let  $\rho_{sk} = 1.41$  t/m<sup>3</sup>;  $\rho_0 = 2.68$  t/m<sup>3</sup>;  $w = 30\%$ ;  $\rho_w = 1.0$  t/m<sup>3</sup>. Then

$$w_0 = 100 \left( \frac{1}{1.41} - \frac{1}{2.68} \right) 1.0 = 34\%;$$

$$G = 30/34 = 0.88$$

This means that not all the rock pores are water-filled.

The coefficient of saturation can also be found from a simpler formula stemming from the one mentioned above:

$$G = w\rho_0/(\varepsilon\rho_w) \quad (12.5)$$

where  $\varepsilon$  is the voids ratio;  $\rho_w$  is the water density (measured in the same units as the rock bulk density).

If the saturation coefficient  $G < 1$  the rock is called a *three-phase system* (mineral-composed skeleton, voids contain air or some other gas, and water in one phase or another). If the soil pores are fully saturated the soil is called a *two-phase system* (mineral-composed skeleton and water).

Depending on pore saturation in sandy and macroporous soils these may be classified as: dry and low moisture content soils with  $G \leq 0.5$ ; high moisture content soils with  $0.5 < G \leq 0.8$ ; saturated soils with  $0.8 \leq G \leq 1.0$ . In most cases it is possible with a degree of accuracy sufficient for practical purposes, to assume soils occurring below the water table as being completely saturated.

The moisture content  $w$  of naturally occurring clayey soils may vary in a wide range, usually 25 to 40% and greater. In the vicinity of Mexico City it is up to 300%.

**The optimum moisture content**  $w_{op}$  is one at which the maximum soil density relative to the skeleton bulk density  $\rho_{sk}$  is achieved under conditions of definite (standard) labour spent for its compaction.

According to USSR St.St. GOST 22733-77, standard compaction of a soil in a cylinder 100 mm in diameter and 127 mm high requires 40 shocks on a layer. The test procedure is described in the above mentioned manual and in instructions.

The concept of an optimum moisture content is referred to in order to find out the optimum conditions of clay soil compaction when doing earthwork.

**The plasticity and consistency of clayey soils.** Soil plasticity index characteristics are the *liquid limit*  $W_L$  (or  $LL$ ), the *plastic limit*  $W_p$  (or  $PL$ ), and the *plasticity index*  $I_p$ .

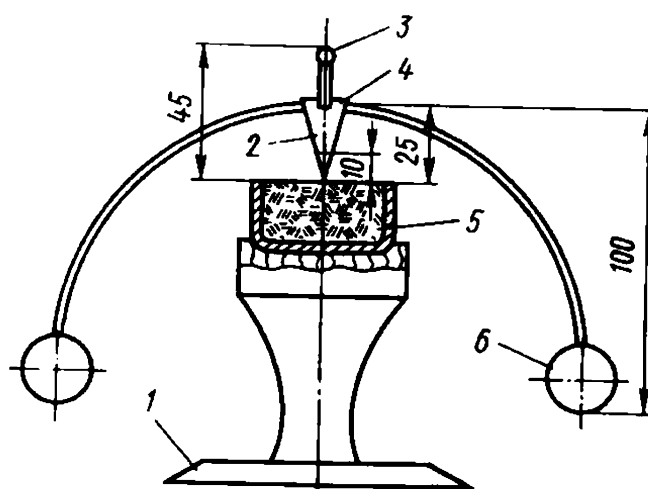
In order to find these soil characteristics we must determine the moisture content at which the particular clay will exhibit definite properties assumed to be standard for tests. The moisture content at which a standard balance cone (Fig. 12.4) in 5 s will sink into the soil mass by 10 mm due to its own weight is the liquid limit.

The plastic limit (or rolling limit) is the moisture content at which clay samples just begin to crumble when rolled out into threads of about 3 mm in diameter. The common error in this test is failure to prepare a standard size of a soil sample thread.

**The plasticity index**  $I_p$  (or  $PI$ ) is the difference between the liquid limit

Fig. 12.4. Balance cone for determining the liquid limit in soils  $\omega_\alpha$ :

1—stand; 2—circular mark; 3—handle; 4—cone 30°; 5—soil mass; 6—balance ball



(*LL*) and the plastic limit (*PL*), i.e.

$$I_p = W_L - W_p \quad (12.6)$$

So, given  $W_L = 28\%$  and  $W_p = 18\%$ , the plasticity index  $I_p$  is 10. The greater is the clay content in a soil, the greater is its plasticity index. At the same time we can have a definite idea of a soil's natural state if we compare the *in situ* moisture content with the plastic (*PL*) and liquid (*LL*) limits.

Clays and loams pass three stages: solid, plastic and liquid. It is assumed at this that the soil is in a solid stage if its *in situ* moisture content is less than the plastic limit, i.e.  $w < W_p$  (or *PL*). When a soil is in a plastic stage, its natural moisture content exceeds *PL*, yet does not exceed *LL*, i.e.  $W_p \leq w \leq W_L$ . Finally, a soil has passed to a liquid stage, if its original moisture content exceeds the liquid limit, i.e.  $w \leq W_L$ .

To have a numerical characteristic of the phase of a clay soil from its moisture content the relative consistency (or consistency index) is used. This characteristic, defined as  $I_L$ , is found from this relationship

$$I_L = \frac{w - W_p}{W_L - W_p} \quad (12.7)$$

Thus, a clayey soil with  $I_L < 0$  is in a solid stage, with  $0 \leq I_L \leq 1$  in a plastic stage, with  $I_L > 1$  in a liquid stage.

A more detailed consistency of a clayey soil may be established from the numerical values of  $I_L$  listed in Table 12.2.

In our opinion it is more convenient to express soil consistency in terms of a coefficient  $\alpha$  so as to avoid using negative quantities to express the degree of consistency which is a perpetual source of errors:

$$\alpha = \frac{W_L - w}{W_L - W_p} \quad (12.8)$$

Table 12.2

Values of Coefficients of Consistency of Clayey Soils

Consistency	$I_L$	Consistency	$I_L$
Hard	Less than 0	Soft plastic	0.50-0.75
Semi-hard	0.00-0.25	Liquid plastic	0.75-1.00
Stiff plastic	0.25-0.50	Liquid	More than 1.00

Clearly,  $\alpha$  and  $I_L$  are related as follows:  $\alpha = 1 - I_L$ .

Consequently, a soil's consistency may be expressed by means of these values of  $\alpha$ :  $\alpha > 1$  suggests a solid stage,  $\alpha = 0.75$  to  $1.0$ , to a semisolid stage;  $\alpha = 0.50$  to  $0.75$ , a stiff plastic stage;  $\alpha = 0.25$  to  $0.50$ , a soft plastic stage;  $\alpha = 0$  to  $0.25$ , liquid plastic stage;  $\alpha < 0$ , a liquid stage.

In the recent years foreign engineers determine the consistency of clays from the strength of a cylindrical sample as it is compressed longitudinally until a point of failure is reached according to data in Table 12.3.

Table 12.3

Consistency of Soils Determined from Their Strength

Consistency	Unconfined compression strength, kg/cm <sup>2</sup> (0.1 MPa)	Consistency	Unconfined compression strength, kg/cm <sup>2</sup> (0.1 MPa)
Very soft	Less than 0.25	Stiff	1-2
Soft	0.25-0.50	Very stiff	2-4
Medium	0.5-1.0	Extremely stiff	More than 4

Practical standards for designing foundations for buildings and structures (the Soviet Code of Practice SNiP II-15-74, Table 6) classify clayey soils depending on the plasticity index as follows:

Clayey soils	Plasticity index $I_p$
Sandy loam	$0.01 \leq I_p \leq 0.07$
Loam	$0.07 \leq I_p \leq 0.17$
Clay	$I_p > 0.17$

On the other hand, according to paragraph 2.9 of the Soviet Code of Practice SNiP II-15-74 clayey soils possess these consistency indices  $I_L$ :



Clayey soils		$I_L$
Sandy loam:		
solid		$I_L < 0$
plastic		$0 \leq I_L \leq 1$
liquid		$I_L > 1$
Loams and clays:		
stiff		$I_L < 1$
semi-stiff		$0 \leq I_L \leq 0.25$
stiff plastic		$0.25 < I_L \leq 0.50$
soft plastic		$0.50 < I_L \leq 0.75$
liquid plastic		$0.75 < I_L \leq 1$
liquid		$I_L > 1$

The road building practice often employs a soil classification presented in Table 12.4.

Table 12.4  
Soil Classification Used in Highway Construction Practice

Soil type	Soil Variety	Plas- ticity index	Sand particle content of 2.0-0.05 mm dia. grains	
			particle size, mm	weight, %
Clays	Fat	> 27	not classified	
	Silty (semifat)	17-27		< 30
	Sandy	17-27	2-0.05	> 40
Loams	Heavy silty	12-17	2-0.05	< 40
	Heavy	17-27	2-0.05	> 40
	Medium and light silty	7-12	2-0.05	< 40
	Light	7-12	2-0.05	> 40
Sandy loams	Heavy silty	1-7	2-0.05	< 20
	Silty	1-7	2-0.05	20-50
	Heavy	1-7	2-0.05	> 50
	Light	1-7	2-0.25	> 50
Sands	Silty (or powdered)	< 1	> 0.1	> 75
	Fine	< 1	> 0.1	< 75
	Medium-grained	< 1	> 0.25	> 50
	Coarse-grained	< 1	> 0.5	< 50
	Very coarse-grained	< 1	> 1.0	> 50

The road soil classification, apart from the plasticity index, takes into account the soil particle content. If a soil contains 20 to 50% of particles

larger than 2 mm in diameter, it is called *gravelly* for smooth particles and *coarse-grained* for rough particles.

**Soil density index characteristics  $\varepsilon$  and  $n$ .** The voids ratio  $\varepsilon$  is a characteristic of a soil's density. To assess the density of loose soils in building practice it is better to use another characteristic, called *porosity*, usually defined by  $n$  and expressed in per cent.

Porosity  $n$  is the ratio of the volume taken by pores to the total bulk of the soil, unlike *the voids ratio*  $\varepsilon$  which is the ratio of the volume of pores to that of soil skeletal particles.

For example, given that the volume of pores per  $1 \text{ m}^3$  in a soil is  $0.4 \text{ m}^3$ , and the volume of skeletal particles is  $0.6 \text{ m}^3$ , then

$$n = \frac{0.4}{0.4 + 0.6} 100 = 40\% \quad \text{and} \quad \varepsilon = 0.4/0.6 = 0.67$$

Conversion formulae from  $n$  to  $\varepsilon$  and vice versa have been derived taking into account considerations that follow. Assume that a unit volume of a soil (say,  $1 \text{ m}^3$ ) contains, in fractions of a unity,  $V_{sk}$  of skeletal material and  $V_n$  of voids (pores). Then  $V_{sk} + V_n = 1$ .

Proceeding from the very definition of the voids ratio  $\varepsilon$  we will have

$$\varepsilon = V_n/V_{sk} = n/(1 - n) \quad (12.9)$$

where  $(1 - n)$  is the volume of skeletal material in fractions of a unity.

Opening the parentheses in (12.9) with respect to  $n$ , we will get a second of the characteristics sought

$$n = \frac{\varepsilon}{1 + \varepsilon} \quad (12.10)$$

Apart from the bulk density of a soil,  $\rho_0$ , Eqs. (12.3) and (12.10) enable us to derive a number of conversion formulae listed in Table 12.7.

The easiest way to determine the porosity of coarse detrital rocks (pebble, cobbles, gravel) and coarse-grained sands is to determine the volume of water for rock void saturation. This method cannot be used for other rocks since air bubbles are entrapped in pores of the rocks as they are filled by water. In such case the porosity  $n$  and the voids ratio are calculated in terms of bulk density  $\rho_w$ , density  $\rho_0$  and moisture content  $w$  of the rock using this formula:

$$\varepsilon = \left[ \frac{\rho_0(1 + w)}{\rho_w} - 1 \right] \quad (12.11)$$

In the case of a saturated soil it is possible to derive a simpler formula relating the voids ratio  $\varepsilon$  to the soil's moisture content  $w$  through the densi-

ty of the soil particles. Indeed, stemming from the definition of the moisture content, and by virtue of (12.10), we may write

$$w = \frac{\varepsilon \rho_{wat}}{(1 + \varepsilon)[1 - \varepsilon/(1 + \varepsilon)]\rho_0} \quad (12.12)$$

where  $\rho_{wat}$  is water density.

In the above formula  $\varepsilon \rho_{wat}/(1 + \varepsilon)$  is the mass of the water contained in pores  $p$  of a definite quantity of a soil; at the same time the second and third terms of this formula represent the mass of the soil's hard particles with porosity  $n$ .

Some simplifications will yield

$$\varepsilon = w \rho_0 / \rho_{wat}$$

or, assuming in most engineering calculations the water density  $\rho_{wat} = 1.0$  (i.e.  $\rho_{wat} = 1.0 \text{ g/cm}^3$  or  $\rho_{wat} = 1.0 \text{ t/m}^3$ ), we will have

$$\varepsilon = \rho_0 w \quad (12.13)$$

The moisture content,  $w$ , is expressed in both formulae in fractions of a unity. Having determined  $\varepsilon$  using one method or another, it will be easy to find  $n$  referring to the above relationships.

The porosity of a *dry sand* can be best found from the relationship

$$n = (\rho_0 - \rho_{sk})/\rho_0 \quad (12.14)$$

The *voids ratio* of clayey soils, depending on their consistency, may vary within 0.6 to 0.8, yet may sometimes exceed these limits.

Transport construction extensively uses relative indices of soil compactness and moisture content. In particular, the degree of compactness is often assessed from the magnitude of the coefficient (standard) of consolidation determined by the formula

$$k = \rho_{sk} / \rho_{sk}^{max} \quad (12.15)$$

where  $\rho_{sk}$  is the mass density of soil skeletal particles under conditions of natural occurrence or in embankment;  $\rho_{sk}^{max}$  is the maximum mass density of these particles on standard consolidation.

The degree of wetting is evaluated by a coefficient of wetting which is the ratio of the soil's moisture content  $w$  to the soil's optimum moisture content on standard consolidation  $w_{op}$ :

$$k_{cons} = w / w_{opt} \quad (12.16)$$

The indices  $k$  and  $k_{cons}$  are needed for solving problems relating to machine soil compaction. The relative moisture content is also used as a

characteristic of the soil moisture content:

$$w_{rel} = w/w_{liq} \quad (12.17)$$

where  $w_{liq}$  is the soil moisture content at the liquid limit.

The porosity  $n$  of sandy gravelly soils is commonly close to 38 to 42%.

The relative density  $D$  of cohesionless soils may sometimes be found from the relationship

$$D = \frac{\varepsilon_{max} - \varepsilon}{\varepsilon_{max} - \varepsilon_{min}} \quad (12.18)$$

where  $\varepsilon_{max}$  and  $\varepsilon_{min}$  are, respectively, the maximum and minimum voids ratio of a soil in its loosest and most consolidated state;  $\varepsilon$  is the voids ratio of the soil in the particular state.

It may often prove more convenient to express the relative voids ratio in terms of the bulk density of the solid (skeletal) ( $\rho_{sk}$ ) constituents as an index of the soil's density or simply in terms of porosity  $n$ . Then

$$D = \frac{\rho_{sk.nat} - \rho_{sk.min}}{\rho_{sk.max} - \rho_{sk.min}} \frac{\rho_{sk.max}}{\rho_{sk.nat}} \quad (12.19)$$

$$D = \frac{n_{max} - n}{n_{max} - n_{min}} \times \left( \frac{1 - n_{min}}{1 - n} \right) \quad (12.20)$$

Given a relative density  $D$ , the corresponding unit weight  $\rho_{sk.D}$  will be equal to

$$\rho_{sk.D} = \frac{\rho_{sk.max} - \rho_{sk.min}}{\rho_{sk.max} - D(\rho_{sk.max} - \rho_{sk.min})} \quad (12.21)$$

As indicated by experience in construction, the looseness or denseness of sandy soils may be determined from the relative density  $D$  according to this scheme:

$D$	Density of sandy soil
0 to 0.20	extremely loose
0.20 to 0.40	Loose
0.40 to 0.60	Medium
0.60 to 0.80	Dense
0.80 to 1.0	Very dense

**Soil swelling tests.** The swelling capacity of a soil is a very important geomechanical characteristic of the soil. The test consists essentially in observing the part of a soil sample submerged in water on a metallic sieve.

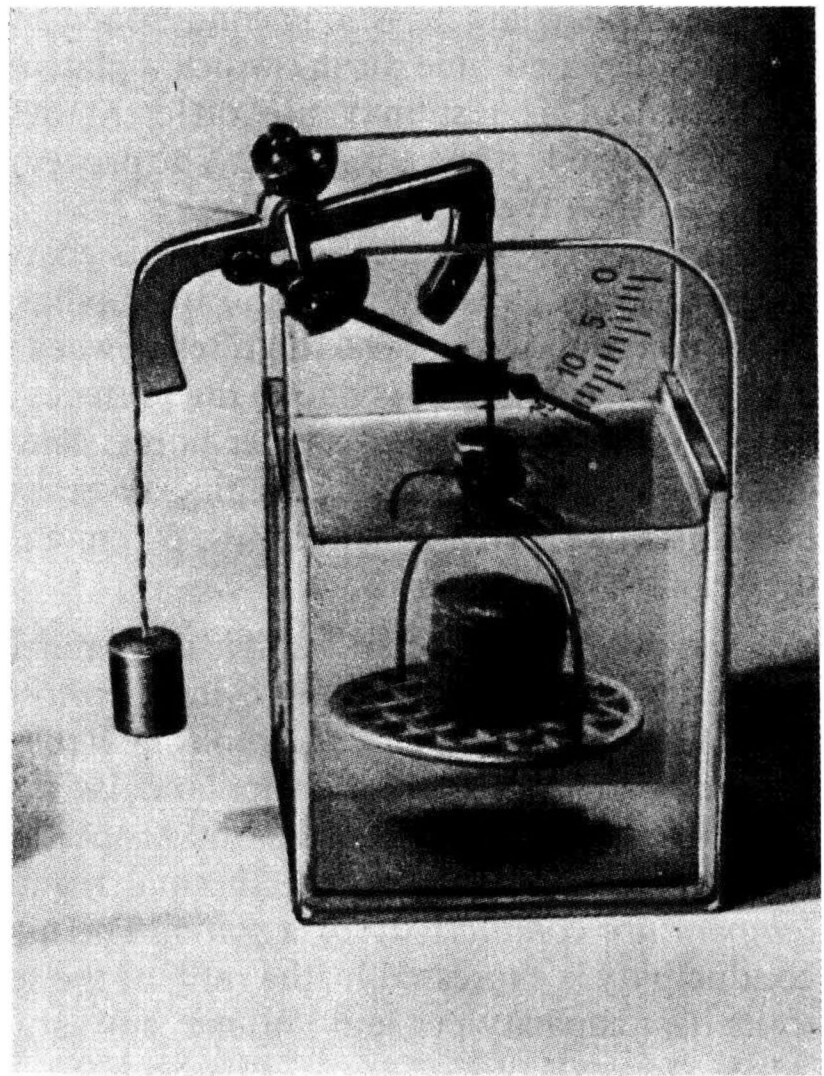


Fig. 12.5. ППГ-1 apparatus designed by the Neftekhimavtomatika factory to determine soil swelling capacity

This test uses devices of special design, e.g. a device that relies on the principle of a balance (Fig. 12.5).

**The shrinkage limit.** Shrinkage occurs when clay materials are drying out. They decrease in volume in so doing. As clay shrinks it passes to a stiff or semistiff stage. It develops fissures and rigid structural bonds are ruptured. The strength of the clay mass drops accordingly ( $c_c \rightarrow 0$ ). As a clayey soil reaches the shrinkage limit it becomes lighter in colour. This is ascribed to the limit of change of the soil volume and penetration of air into the soil. This test makes it possible to evaluate the soil's moisture content corresponding to the shrinkage limit on sample drying.

**The sticky limit.** Stickiness is the capacity of a soil to adhere to various materials with which it comes in contact. As soils are being worked, sticky soils may adhere to metallic parts and bodies of road construction and transport equipment thus complicating its use. Very sticky soils impede also the movement of vehicles. In all respects the stickiness is a negative soil characteristic, so, whenever necessary, the soil must be tested for this property.

The sticky limit is expressed numerically in grams per  $\text{cm}^2$  of area. It is determined by measuring the force needed to tear a metal plate pressed to

the soil. This characteristic is conditioned by the soil's moisture content, force applied and time during which a plate remains pressed to the soil being tested. This test may use different devices. A device designed by V.V. Okhotin is often employed. The procedure is described in the manual delivered with the device.

**Capillary rise of water in soils.** This characteristic is used to assess the water-carrying capacity of a soil or capillary action due to which water from the groundwater level migrates upward towards the free surface. The above property of soils is due to the presence of a system of capillary tubes interconnected by small diameter pores. The height of capillary rise is the greatest in pulverized soils attaining several meters at times. In clays this height is 1 to 1.5 m\*, in sands 40 to 50 cm and is the smaller, the larger are the grains of the soil in hand.

The capillary action of a soil is determined by observing saturation of a dry soil in a tube or bottomless cylinder whose lower end is put into a vessel filled with water. It is necessary to follow the alteration of the colour of the soil being saturated and the capillary rise rate.

**Thermal properties of soils.** Soil properties may change as their thermal regime varies. Moreover, the thermal regime is directly associated with *temperature conductivity of a soil  $a$* . The numerical value of temperature conductivity is expressed by the ratio of the soil's temperature conductivity to its heat capacity per unit volume, cm<sup>2</sup>/s:

$$a = \lambda / c_\delta$$

where  $\lambda$  is temperature conductivity, W/(m · K) (cal/cm × s × °C);  $c_\delta$  is specific heat capacity, J/K (cal/cm<sup>3</sup> × °C).

Soil thermal characteristics are governed by the soil's composition, state and temperature. The heat capacity of a wet soil is greater than that of a dry soil. The temperature conductivity of a saturated soil is approaching that of water.

Care should be always taken to exactly follow the relevant standards, regulations and specifications when conducting tests to determine physical properties of soils. In so doing, aids can well be used containing detailed description of laboratory tests of soils\*\*.

To conclude the Chapter, Table 12.5 presents the most important soil characteristics and their interrelations.

---

\* According to D. P. Krynine and W. R. Judd (*Principles of Engineering Geology and Geotechnics*. McGraw-Hill Book Company, Inc. 1957, p. 173), it may reach 30 or 40 ft or more in clays. — *Translator's note*.

\*\* See Reference at p. 103.

Table 12.5

Correlation Between the Most Important Soil Constants

No. Sym- bol	$\rho_0$	$\rho_w$	$\rho_{sk}$	$n$	$\varepsilon$	$w$
1 $\rho_0$	$\rho_0$	$\frac{\rho_w}{(1+w)(1-n)}$	$\frac{\rho_{sk}}{1-n}$	$\frac{\rho_{sk}}{1-n}$	$\rho_{sk}(1+\varepsilon)$	$\frac{G_\varepsilon}{w}$
2 $\rho_w$	$\rho_0(1-n)(1+w)$	$\rho_w$	$\rho_{sk}(1+w)$	$\rho_0(1-n)(1+w)$	$\frac{\rho_0(1+w)}{1+\varepsilon}$	$\frac{G_n(1+w)}{w}$
3 $\rho_{sk}$	$\rho_0(1-n)^{-1}$	$\frac{\rho_w}{1+w}$	$\rho_{sk}$	$\rho_0(1-n)$	$\frac{\rho_0}{1+\varepsilon}$	$\frac{\rho_w}{1+w}$
4 $n$	$\frac{\rho_0 - \rho_{sk}}{\rho_0}$	$1 - \frac{\rho_w}{\rho_0(1+w)}$	$\frac{\rho_0 - \rho_{sk}}{\rho_0}$	$n$	$\frac{\varepsilon}{1+\varepsilon}$	$1 - \frac{\rho_w}{\rho_0(1+w)}$
5 $\varepsilon$	$\frac{\rho_0 - \rho_{sk}}{\rho_{sk}}$	$\frac{\rho_0(1+w)}{\rho_w} - 1$	$\frac{\rho_0 - \rho_{sk}}{\rho_{sk}}$	$\frac{n}{1-n}$	$\varepsilon$	$\frac{\rho_0(1+w)}{\rho_w} - 1$
6 $w$	$\frac{\rho_w}{\rho_0(1-n)} - 1$	$\frac{\rho_w - \rho_{sk}}{\rho_{sk}}$	$\frac{\rho_w - \rho_{sk}}{\rho_{sk}}$	$\frac{\rho_w}{\rho_0(1-n)} - 1$	$\frac{\rho_w(1+\varepsilon)}{\rho_0} - 1$	$w$
7 $G$	$\frac{w\rho_0(1-n)}{n\rho_w}$	$\frac{w\rho_w}{n(1+w)\rho_w}$	$\frac{w\rho_{sk}}{n\rho_w}$	$\frac{w\rho_{sk}}{n\rho_w}$	$\frac{w\rho_0}{\varepsilon\rho_w}$	$\frac{w\rho_0}{\varepsilon\rho_w}$

Chapter 13

Shearing Resistance of Rocks and Soils.  
Indices and Methods of Determination

Sec. 13.1. Soil and Rock Strength

The strength of a soil or rock can be inferred from its shearing resistance. *The shearing resistance capacity* defined as  $s_{pw}$ , being the measure of specific shearing resistance per unit area is expressed in kg/cm<sup>2</sup> (Pa).

We should discriminate between the concepts of shearing resistance and shearing resistance capacity. Clearly resistance  $S$  to shearing in some soil volume followed by this latter shift along some surface of a unit area  $\omega$  will

be found from this relationship:

$$S = s_{pw}\omega \quad (13.1)$$

In the general form the shearing resistance capacity in soils may be represented by a formula proposed by N. N. Maslov (1941)

$$s_{pw} = p \tan \varphi_w + \Sigma_w + c_c \quad (13.2)$$

where  $p$  is the normal tension acting over a given area in the soil (rock) usually denoted without the subscript  $n$ ;  $\varphi_w$  is the angle of *internal friction* at moisture content  $w$ ;  $\Sigma_w$  is *the degree of cohesiveness* of soil colloids of a reversible character at moisture content  $w$ ;  $c_c$  is the true cohesion which is of an irreversible bond character.

In the given case and elsewhere,  $s_{pw}$ ,  $\Sigma_w$  and  $c_c$  are measured in units of tension. The respective subscripts in  $s$ ,  $\varphi$  and  $\Sigma$  indicate the dependence of all these indices under given conditions on the moisture content  $w$ , and, as to the shearing resistance capacity  $s_{pw}$ , in the general case, on the magnitude of normal tension  $p$  as well.

Thus a soil's shearing resistance capacity and, consequently, its strength are in the general case conditioned by: (1) forces of internal friction in the soil depending on the value of  $p$ ; (2) soil's apparent cohesion  $\Sigma_w$ ; (3) value of true cohesion  $c_c$ .

It should be borne in mind that in the given case and elsewhere  $s_{pw}$  of a soil corresponds to the limit shearing resistance of the soil on failure or flow of the soil's sample.

**Internal friction in soils.** It may be said that the origin of inner friction in loose cohesionless soils like sand is known to a definite extent. The surface of grains in loose soils is more or less rough. As soil particles are pressed together by compressive normal stress, friction forces appear between the particles that reveal themselves during mutual displacement.

Forces of friction, as shown by experience, are connected to definite limits to the normal stress through a linear relationship.

By defining specific force of friction as  $s_{fr}$  (it is measured in  $\text{kg/cm}^2$  (MPa)) we can write

$$s_{fr} = pf \quad (13.3)$$

where  $f$  is the coefficient of friction that in the given case is a characteristic of roughness of the sand grains.

As is known, the coefficient of friction may be expressed in terms of *the angle of friction*  $\varphi$ . Then Eq. (13.3) will take on this form:

$$s_{fr} = p \tan \varphi \quad (13.4)$$



Since friction originates inside a soil, the quantities  $f$  and  $\varphi$  are called, respectively, *the coefficient* and *the angle of internal friction* of the soil.

For sands and other grained soils (gravel, pebble, gruss, crushed rock) the angle of internal friction is governed by their density. The most evident index characteristic of a soil's density is its porosity expressed in per cent or fractions of unity. Then the above indices should be operated depending on the soil's density whose measure is  $n$ , i.e. by  $\varphi_n$  and  $f_n$ . In this case Eq. (13.4) will appear as

$$s_{fr} = p \tan \varphi_n \quad (13.5)$$

In the general case, especially when clayey soils are involved, the coefficient  $f$  and angle of internal friction  $\varphi$  may be dependent on the soil's moisture content  $w$ . Taking it into account, we may rewrite Eq. (13.4) as follows:

$$s_{fr} = p \tan \varphi_w \quad (13.6)$$

The last equation's right side exactly represents the first term of our principal relationship (13.2). However, when dealing with clayey soils, things get more complicated and internal friction must be considered in conjunction with other internal bonds that govern the strength of a clayey soil, i.e.  $\Sigma_w$  and  $c_c$ .

**True cohesion  $c_c$ .** This lends a soil a certain degree of stiffness and rigidity. This kind of cohesion is accounted for by rigid bonds between the soil particles.

True cohesion is especially strong in hard rocks and in fact responsible for competence of such rocks. Clayey soils exhibit this property to a much less extent. Incompetent soils like a loose sand or broken rock have no true cohesion. Grains of dense sands, sandy gravels and gravelly soils are often held together by sort of *interlocking between the grains*. This characteristic may be in this case considered as a type of true cohesion  $c_c$ . Rigid bonds in hard and cemented rocks lending to these latter the appearance of a solid have the character of electrical ionic bonds.

Rigid bonds in cemented rocks (sandstones, argillites etc.) have resulted from the *in situ* cementation by materials of one kind or another. True cohesion occurs in a rock, given definite conditions, on the crystallization of the material in hand, crystal intergrowth, and is accompanied by individual particles fusing together.

Structural bonds exhibit a definite degree of elasticity governing soil deformability and compressibility. However, a rupture of a soil's or rock's structures leads to the irreversible loss of the rigid structural bonds responsible for the degree of structural cohesion  $c_c$ . Hence bonds of true cohesion of a soil may be described as *irreversible*.

This is the main and dominant property of a soil's structural cohesion. The structural cohesion may be lost by relatively incompetent rocks following an excessive load (failure of structural skeleton), an irreversible shear, excessive moisture content of soils that have a relatively weak structural cohesion etc. In the last case the wedging effect of thickening water films enveloping soil particles results in *swelling* (or *bulging*) of clayey soils. These events, in turn, bring about the rupture of rigid structural bonds in the soil and, consequently, eventual loss by the clay mass of its strength and stability.

**Cohesion in clayey soils.** Cohesion  $\Sigma_w$ , typical of uncemented clayey soils irrespective of their consistency and mainly responsible for their strength is of a different nature than true cohesion. Depending on the amount of water clayey rocks may many times pass from a solid state to a semiliquid state and vice versa which can be observed, e.g. in spring and in autumn on sections of dirt roads covered by clay materials. When in a plastic state, a few clumps of clay can easily be compressed to form one larger uniform clump. This principle underlies the manufacture of air-dried bricks.

Plastic properties of clay are familiar to sculptors. Thus, unlike true cohesion  $c_c$ , apparent cohesion  $\Sigma_w$  is of a *reversible* character since it can be remolded. This property of bonds in question is due to the colloidal character of such materials.

It should be pointed out that the complex nature of strength of clayey soils has not as yet been fully understood. This problem is being considered here in very general terms\*.

The property of clayey soils to remold and swell is due to the presence of poorly investigated clay minerals that appear as tiny particles of a crystalline form. This mineral group includes the best studied species, reported above, kaolinite ( $\text{Al}_2\text{O}_3 \times 2\text{SiO}_2 \times 2\text{H}_2\text{O}$ ) and montmorillonite ( $\text{Al}_2\text{O}_3 \times 4\text{SiO}_2 \times n\text{H}_2\text{O}$ ).

With a large surface per unit area of the particles composing a soil the process of *adsorption* is of crucial importance. Owing to adsorption each mineral particle of a clay is enveloped by a film of water, as is assumed, due to the attraction by negatively charged clay particles of water molecules that have positively charged ends. Water molecules are *dipoles* that carry at one end a positive charge (oxygen atom) and at the other end a negative charge (two hydrogen atoms).

All fine particles composing a clay as well as the moisture filling tiniest

---

\* For a more detailed consideration of the question refer, e.g. to N. N. Maslov, *Fundamentals of Soil Mechanics and Engineering Geology*. Moscow, 1968 (in Russian).

pores in the soil and the film water enveloping soil particles are mutually connected thanks to the expression of specific physicochemical processes.

Electromolecular forces appearing at the interface between clay particles and water dipoles, especially in the first layer (of the order of 1 to 3 water molecules) have a very great magnitude, up to several thousand  $\text{kg}/\text{cm}^2$ . In this fashion films of tightly bound *adsorbed water* form at the surface of the particles.

With increased distance from the surface of a particle these molecular forces diminish rapidly. So, at some distance from the particle's surface layers of *loosely bonded water* appear that are to a certain degree subject to mechanical action. This layer of pore water is often termed *diffuse*.

About  $0.5 \mu\text{m}$  from the surface of hard particles the effect of electromolecular forces becomes zero. Free (gravitational) water prevails here.

The pellicular water connected with the particle surface blocks the narrowest passages, pores between the particles. This is what is responsible for practically total imperviousness of consolidated (non-jointy) clays. It should be kept in mind that molecules of even loosely bonded water may to a certain degree be slow to react to the action of pressure and, to cause them to move, increased head gradients are needed. Thus the concept of the initial hydraulic gradient originated (see Chapter 23).

Unlike pellicular (bound) water, *gravitational water*, if it is available in the soil pores, is free and, obeying the force of gravity, moves through the soil pores. Note that hydrostatic pressure may develop only in gravitational water. This type of water is characteristic of coarse-grained detrital soils as broken rock, pebbles and sands. On the other hand, film water is common in clayey soils, especially dense and fat varieties.

Pellicular water, as it flows, does not obey Darcy's Law. Rather, it flows in a soil due to the action of forces of molecular attraction or, possibly, electrical forces. Figuratively speaking, it creeps from particles covered by a thicker film to ones with a thinner film. If moisture in a soil is in small amounts it will mainly be hygroscopic and pellicular water, i.e. one that is adsorbed on the surface of the particles.

Rigidly bound water has properties distinct from ones in its common state. The density of rigidly bound water attains  $1.2$  to  $2.4 \text{ g}/\text{cm}^3$ . This water is capable of offering some resistance to shear and tension, it shows weak dissolving power, its freezing temperature ranges from  $-20$  to  $-193^\circ\text{C}$ , and boiling temperature is  $+200^\circ\text{C}$ .

When dealing with clayey soils, take into account the fact that the viscosity of bound water is greater than that of free water. The viscosity will be the greater, the thinner is the film covering a particle and bound by this latter (up to 5 to 17 compared with  $0.01 \text{ Pa}$  for free water).

The effect of bound water on clayey soils may cause different action, especially, on their strength. The nature of such soils is most complicated and is far from being completely understood. An important factor contributing to apparent cohesion  $\Sigma_w$  between individual clay particles is undoubtedly played by pellicular water held by the particles (rigidly and loosely bound water) and, to some extent, by intermolecular forces of electromagnetic origin (van der Waals forces). These latter forces are responsible for the mutual attraction of particles composing a clay with different degree depending on a number of factors.

Van der Waals molecular forces may be of a very large magnitude, yet reveal themselves when the intermolecular distances measured by a few molecule rows are very small. Differently speaking, in a soil exhibiting pronounced consolidation when the envelope of the pellicular water is ruptured there occurs a direct contact between the adjacent mineral grains. In usual conditions this requirement is satisfied only partially. Consolidation of a clayey soil by applying a load to it leads to a decrease of the thickness of the water pellicules on soil particles. Particles come closer to each other thus enhancing the efficiency of intermolecular forces.

On the other hand, added water content of a clayey soil results in increased layers of pellicular water covering soil particles. This increases distances between the particles which weakens cohesion between these latter.

Excessive saturation of a clay causes a practically total loss of cohesion and the soil's shearing resistance in this condition eventually approaches zero. Academician I. V. Grebenshchikov has at his time put forward a hypothesis of *colloidal water pellicules* on the surface of silicate and aluminosilicate particles composing clayey soils. According to this hypothesis the degree of plasticity of soils is directly associated with the nature and state of water colloidal pellicules.

A specific orientation of water molecules close to colloidal particles leads to eventual hardening of clayey soils.

During the immensely long time taken by the formation, in the course of diagenesis (consolidation) and epigenesis (cementation) of bedrocks (pre-Quaternary), the pellicular water envelopes pass through a process of *colloidal aging*. In so doing the thickness of the pellicular water decreases and the soil's moisture content drops. The soil loses its plasticity and acquires a certain degree of stiffness. According to findings of F. V. Chukhrov, at the moisture content 94 to 97.3% a gel of silicic acid appears as jelly and will quiver on shaking. At the same time, at a moisture content 74.2% it will be rubbed to powder.

Colloidal envelopes lose then their elasticity and capacity of mutual transformation on hydration and dehydration. Thus, a sort of petrification

occurs, internal colloidal bonds passing to strong bonds. Apparent cohesion  $\Sigma_w$  transforms to true cohesion  $c_c$  and the clay mass acquires a typical degree of hardness and stiffness.

The transition of cohesion forces  $\Sigma_w$  conditioned, as pointed out above, by the expression of intermolecular forces, to true cohesion forces  $c_c$  is accompanied by new events. As the transition proceeds, ionic bonds may convert to chemical bonds. Then the viscosity forces  $\Sigma_w$  pass to a force of true cohesion  $c_c$  conditioned by maximum possible closeness of the particles (fusion).

Powdered or even sand-size particles, if they are sufficiently abundant, constitute a skeletal structure, as it were, of a clayey soil. The excess of coarse fractions results in the fact that the clay filler does not, in fact, receive a fraction of the initial load which is almost completely imparted to the soil's skeleton. This accounts for the smaller compressibility of such clays and typical increased value of the angle of internal friction  $\varphi_w$ .

A rupture of this skeletal structure due to one external cause or another (e.g. shear, excessive load, concussion etc.) may bring about a dramatic drop in the soil's strength and shearing resistance (disturbed-structured soil).

**Internal bonds in different rocks and soils.** Certain types of internal bonds may prevail in a rock depending on its nature. At the same time other bonds may be suppressed or completely lose their importance.

Strong irreversible forces of true cohesion  $c_c$  prevail in *hard rocks* like granite or limestones. Internal bonds typical of a colloidal system are not exhibited by such rocks ( $\Sigma_w = 0$ ). Internal friction forces from an external load develop in such rocks on contact walls of joints typically traversing the rock mass.

Internal friction forces and, to a certain degree, true cohesion forces become the most important for *loose cohesionless rocks and soils* (sand, gravel, crushed rock etc.) that, e.g. carry the load of a structure.

The most conspicuous role in the strength of clayey soils is played by cohesiveness  $\Sigma_w$  although cases may occur where other components of a soil's shearing resistance, i.e. forces of internal friction and true cohesion may reveal themselves.

### Sec. 13.2. Shearing Resistance in Grained (Cohesionless) Soils

**The effect of granulometric composition and density.** As already pointed out, the shearing resistance of clean (non-argillaceous) grained or loose soils is mainly conditioned by the forces of internal friction and partly those of true cohesion. Other conditions being equal, the shearing resistance in cohesionless soils is strongly dependent on the density increas-

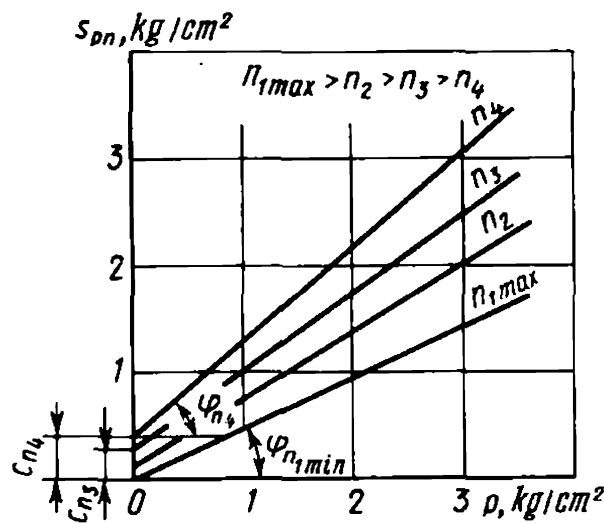


Fig. 13.1.  $s_p = f(p)$  relationship between the shearing capacity of granular soils and the load  $p$  at different densities referring to the porosity  $n$

ing with the latter. An important exception, however, will be the case of a likely decompression of a soil following its deformation (refer to what follows). At the same time, excepting special cases of dynamic stresses acting on a soil (considered later), the shearing resistance of clean cohesionless soils (e.g. various grain-size sands, gravel, pebbles, broken rock) depends on the soil’s moisture content only to a slight degree which has not practical importance.

As applied to these conditions, the principal equation (13.2) for grained (cohesionless) soils takes on the form:

$$s_{pn} = p \tan \varphi_n + c_n \tag{13.7}$$

where  $\varphi_n, c_n$  are, respectively, the angle of internal friction\* and true cohesion of the rock (soil) at the particular density (referring to porosity  $n$ ) of the particular material.

This equation was proposed by the French mathematician and engineer Coulomb in 1773.

The relationship (13.7) for a certain particular case is plotted in Fig. 13.1.

The true cohesion (or simply cohesion)  $c_n$  is revealed by grained soils only if they have a high degree of density and consolidation coupled generally to a low uniformity and is mainly conditioned by coherency of grains or interlocking of grains. The latter property is especially typical of dense cohesionless soils of non-uniform granulometric composition. It should be noted, by the way, that the stability of high abrupt river banks composed of sand conglomerates (gravel with sand-filled pores) commonly observed in mountainous rivers is mainly due to the pronounced interlocking of the grains specific for such soils.

\* Some authors prefer the term “angle of shearing resistance” (see Krynine, D. P. and Judd, W. R., op. cit., p. 55). — *Translator’s note.*

The degree of grain interlocking conditioned by the above factors may vary in a wide range in different conditions. In particular, coherency of sands ranges from 0 (extremely loose state  $n_{max}$ ) to 0.3-0.5 kg/cm<sup>2</sup> (dense sands). Nonuniform cohesionless soils incorporating coarser fractions (sandy soils with some gravel and cobbles) generally have a larger coherency sometimes attaining 1 or even 2 kg/cm<sup>2</sup>.

The angle of internal friction  $\varphi_n$  increases with a higher content of coarse and grained inclusions, roughness of soil grains and greater density. For the evaluation of a likely effect of the above factors on the magnitude of  $\varphi_n$  in sand and gravels the following empirical formula has been proposed by Hansen and Landborn:

$$\varphi_n = 30^\circ + \varphi_1 + \varphi_2 + \varphi_3 + \varphi_4$$

The correction values  $\varphi_1 - \varphi_4$  in this formula are given in Table 13.1. As we pass from a consolidated sand to a loose one the angle of internal friction may decrease by 7 to 12°.

Depending on the aforementioned factors the angle of internal friction

Table 13.1

Values of Corrections  $\varphi_1 - \varphi_4$  (grad)  
To Be Applied to Hansen and Landborn Formula

Properties of sand	Characteristic of sand and gravel	$\varphi_1$	$\varphi_2$	$\varphi_3$	$\varphi_4$
Roundedness	Poorly rounded grains	+ 1	—	—	—
	Averagely rounded grains	0	—	—	—
	Rounded grains	— 3	—	—	—
	Well rounded sands	— 5	—	—	—
Grain size	Sand	—	0	—	—
	Fine gravel	—	+ 1	—	—
	Medium and coarse gravel	—	+ 2	—	—
Uniformity	Very uniform sand	—	—	— 3	—
	Sand of medium uniformity	—	—	0	—
	Very nonuniform sand	—	—	+ 3	—
Density	Extremely loose	—	—	—	— 6
	Medium density	—	—	—	0
	Extremely dense	—	—	—	+ 6

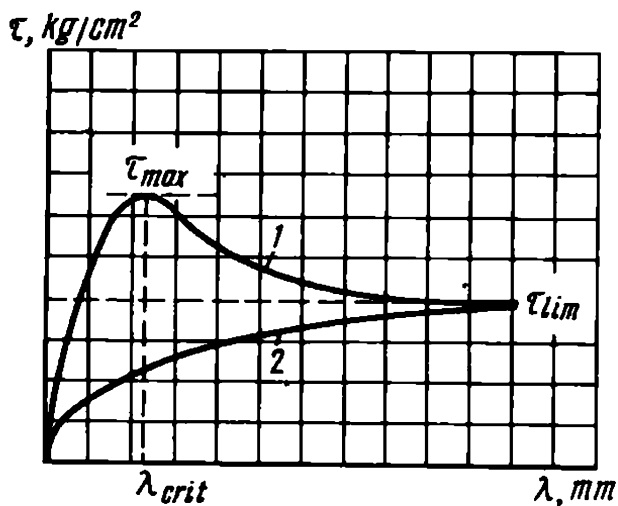


Fig. 13.2. Pattern of shear deformation (displacement  $\lambda$ ) and critical shearing stress

$\tau_{max}$  with  $p = \text{const}$ :

1—dense sand; 2—loose sand

may vary from one variety of cohesionless soil to another within a very large range: from 24 to 40° or even more.

We have repeatedly remarked that the shearing resistance in cohesionless soils increases in proportion to their specific density. This is true, however, only in the absence of decompression of the soil caused by a deformation due to a shearing stress. Such deformation may be accompanied by a migration of grains composing a soil from their seats occupied in the dense state of the soil and by the uplift of the surface of the clay mass.

This is illustrated by Fig. 13.2. Referring to this figure,  $\tau_{max}$  corresponds to a maximum shearing resistance which may develop in a dense cohesionless soil with minor shearing deformation (displacement of sample). As a soil is further displaced, the shearing resistance decreases due to progressive soil decompression and finally attains its maximum value  $\tau_{lim}$  corresponding approximately to the shearing resistance of the soil in an extremely loose state under conditions of a conspicuous deformation. It should be noted that the shearing resistance of cohesionless soils in this state increases gradually due to the enhanced shearing deformation induced by the resultant increase in their density (I.V. Yaropolsky, 1933).

Thus it is possible to use increased values of  $\varphi_n$  and  $c_c$  for dense cohesionless soils only in local conditions that rule out the above type of deformation of the bulk soil. The admixture of clay material in cohesionless soils decreases the angle of internal friction concurrently increasing the shearing resistance due to the apparent cohesion of the soil  $\Sigma_w$ . At this point the moisture content of the soil also becomes of practical importance. As will be shown later, the latter factor may under definite conditions play an essential role even in the absence of a clay material in the soil. This is especially true of the finest-grained varieties of cohesionless soils.

Within a definite moisture content (up to 34%) the angle of internal friction of even fine-grained sands does not change practically on wetting



and equals roughly  $30^\circ$ . As a soil is further excessively saturated, the angle of internal friction tends to dramatically decrease (to  $14^\circ$  and less).

This is directly associated with the thickness of pellicular water envelopes of soil particles under conditions of excessive moisture content owing to a progressive loss of the apparent cohesion and fewer contacts between the mineral particles themselves.

In practice such events often occur under conditions of decompression of such soil varieties and minor load. The process in question generally takes place in the upper layers in the bottom of an opencast or a submerged slope which flow as a result of it. Flow reveals itself more dramatically in quicksands, soils that easily pass to a semiliquid state.

It is commonly very fine-grained sands or silts that pass to a quicksand condition. According to A.F. Lebedev (or Lebedeff) there are *pseudo-quicksands* and *true quicksands*.

The two quicksand varieties are characterized by pronounced mobility. Under definite conditions they behave like a heavy viscous fluid. It appears that this state is accounted for by the total loss by the soils of compressive strength coupled to a drop in the shearing resistance down to zero. The nature of this phenomenon is different in pseudo- and true quicksands. The shearing resistance of pseudo-quicksands, whatever their condition, is described by Eq. (13.7)

$$s_{pn} = p \tan \varphi_n + c_n$$

The transition of pseudo-quicksands to a liquid state is invariably followed by loosening together with the loss of cohesion and inner friction in the soil as a result of the absence of a normal stress. This may be brought about by a dynamic stress on the soil and by seepage pressure (refer to Chapter 25). Viewed in this context, any variety of loose cohesionless soil may be described as a pseudo-quicksand that can pass to a liquid state with a drop of the normal stress to zero due to one cause or another (e.g. after an earthquake).

The process proceeds differently in true quicksands which, by virtue of their granulometric composition, occupy an intermediate position between finest-grained sands and clayey soils. Under this condition soil particles become covered by colloidal water pellicles with specific properties. With a sufficiently dense texture of the soil a certain degree of coherency  $\Sigma_w$  appears. Cohesion  $c_c$  may also reveal itself to a minor extent. Yet the composition of quicksands is fairly coarse, so pellicular water on the soil particles is of a relatively small thickness and bonds between them are weak. As a result, at a relatively small load the colloidal pellicles are easily disrupted and the particles touch each other.

Thence we may conclude that the shearing resistance of quicksands in a

dense state (bulk density up to  $2.2 \text{ t/m}^3$  at porosity  $n = 24$  to  $25\%$ ) may be described by the principal equation (13.2).

The picture changes dramatically on mechanical disruption of the true quicksand structure. Forcible disjunction and increase in distance between particles in the first place eliminate the cohesion of the soil  $c_c$ , if any.

The increased interstitial distances lead to weakened intermolecular bonds and to a dramatic drop in the apparent cohesion between the particles  $\Sigma_w$ . The particles are no longer in touch with each other which results in a conspicuous decrease in the angle of internal friction and, consequently, in the shearing resistance of true quicksands which may sometimes drop to zero.

Thus under *in situ* conditions true quicksands may possess a relatively high stability and bearing capacity. However, breakdown of their structure and deconsolidation lead to a total loss of positive properties and to liquefaction. This latter state may be caused by a shock, vibration, saturation by amounts of water in excess of the volume of the pores in the soil, e.g. under conditions of subsoil flow pressure or seepage pressure. The critical moisture content in quicksands is generally about 15 to 17%.

According to A.F. Lebedev the especially perfidious feature of quicksands, encountered in northern areas of this country, is conditioned by a protective colloid of organic origin (related to peat) facilitating the transition of a true quicksand to a liquid state.

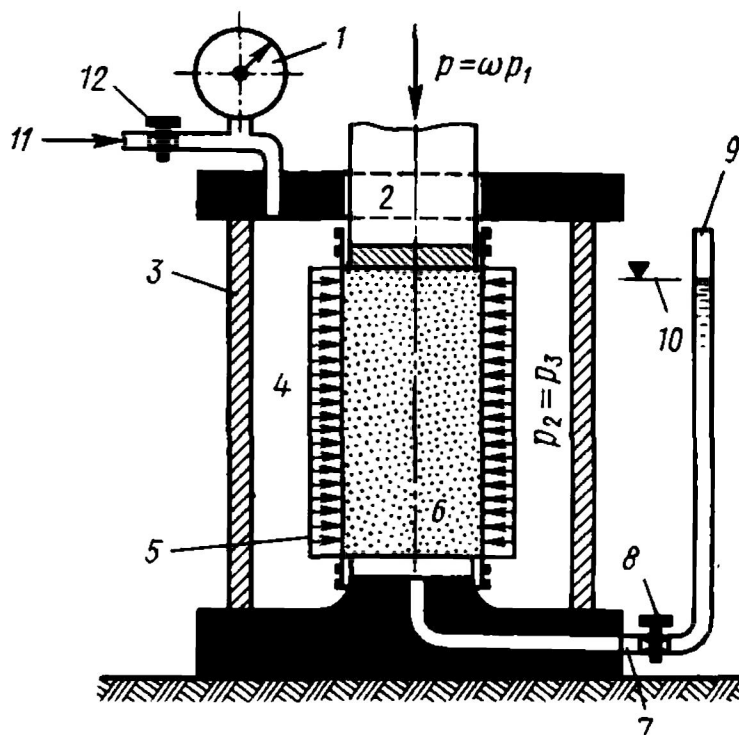
**Triaxial compression test of loose (cohesionless) soils.** The shearing resistance of a loose soil, especially one containing coarse-grained fractions can be best determined by a triaxial compression test. The test uses special apparatus. One type of such a sophisticated triaxial-test apparatus, called a *stabilometer*, is shown diagrammatically in Fig. 13.3, and a general view in Fig. 13.4.

The test is performed as follows. A specimen of the soil of a cylindrical shape with a height 2 to 3 times larger than its diameter is enclosed in a rubber cover. It is then placed in a chamber which is hermetically sealed. A vertical pressure  $p_1$  is applied to the specimen with an additional pressure  $p_2$  acting concurrently on its sides. The vertical (or axial) pressure  $p_1$  is produced by a force applied to the piston,  $P = p_1 \omega$ , where  $\omega$  is the area of the cross section of the soil specimen. The lateral pressure is imparted to the specimen by a fluid (water or glycerine) pumped to the cylinder of the apparatus at a pressure  $p_2$  using a special pump.

It is the purpose of the test to determine the magnitude of the vertical compression  $p_1$  under conditions of the soil failure at a definite value of lateral pressure  $p_2$ . Tests are performed under various conditions. However, one of the following requirements should be satisfied: (a) constant value of the lateral pressure  $p_2$  and gradual increase in compression

**Fig. 13.3.** Diagram of a stabilometer for triaxial tests of soils:

1—pressure gauge; 2—piston;  
3—cylinder from transparent material;  
4—space filled with fluid; 5—rubber sleeve;  
6—soil sample; 7—pipe;  
8—drain cock 1 for water squeezed out from the soil sample; 9—burette for measuring volume of sample;  
10—level of water; 11—pipe connected with pump; 12—cock 2



pressure until the soil specimen fails; (b) constant value of vertical pressure and gradual decrease in the lateral pressure  $p_2$  until the specimen fails.

Observe the specimen's failure looking through the transparent cylinder of the apparatus or refer to special instruments with which the triaxial compression machine is equipped. Samples 5 to 7 cm in diameter and 15 to

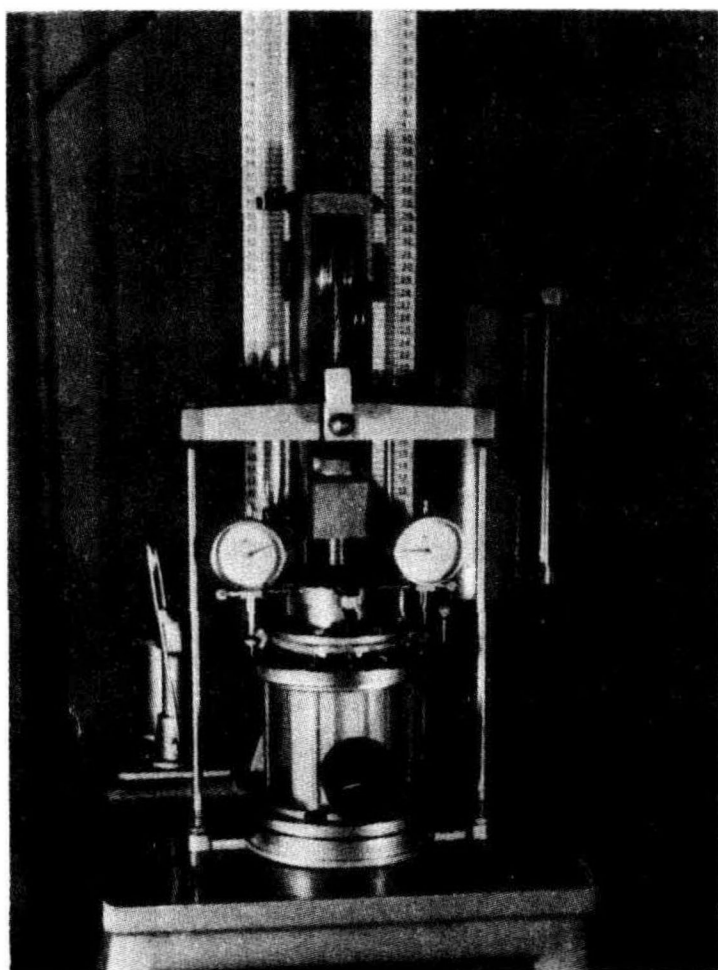


**Fig. 13.4.** General view of stabilometer designed by G.A. Andreev

20 cm high are commonly tested. However, when it is desired to test samples of cohesionless soils containing coarser materials (sandy gravelly soils with pebbles or even boulders) larger machines should be used. Note that the diameter of the sample must be 5 times the size of the largest subsidiary constituent.

The next stage of the test is to determine, from the obtained critical values of  $p_{1_{cr}}$  and  $p_{2_{cr}}$  corresponding to the sample's failure, the numerical values of the angle of internal friction  $\varphi_n$  and cohesion  $c_n$  followed by the calculation of  $s_{pn}$  using Eq. (13.7):  $s_{pn} = p \tan \varphi_n + c_n$ .

For this end a diagram is plotted in which circles of rupture are constructed. This diagram is known as Mohr's rupture diagram. In so doing it is assumed that the moment the sample fails in the stabilometer corresponds to its limit equilibrium under conditions of the all-around pressure due to the two principal stresses  $p_{1_{cr}}$  and  $p_{2_{cr}}$ .

First consider the cases when a cohesionless soil is in an extremely loose state and manifests no apparent cohesion. Equation (13.7) will then take on a simple form:

$$s_{pn} = p \tan \varphi_n \quad (13.8)$$

Clearly, the limit curve bending about Mohr's circles of stress plotted from  $p_{1_{cr}}$  and  $p_{2_{cr}}$ , provided that the above condition is observed, will represent a straight line in the coordinate axes  $s_{pn} = f(p)$  corresponding to Eq. (13.8). This line's slope will be  $\tan \varphi$  and will pass through the origin of coordinates. Under this condition the straight line in the given case of limit equilibrium will deflect from the abscissa axis at an angle equal to the angle of internal friction of the soil  $\varphi_n$ . This line is generally called the Mohr envelope.

Three circles of stress,  $A$ ,  $B$ , and  $C$ , are plotted in Fig. 13.5. The circles  $A$  and  $B$  have a point of contact with the Mohr envelope. The stresses  $p_1$  and  $p_2$ , and also  $p'_1$  and  $p'_2$  from which the Mohr circles have been plotted are numerically pairwise different. However, proceeding from the conditions of tangency of the Mohr envelope, the state of the samples in both cases must be considered to be limit and the stresses themselves critical ( $p_{1_{cr}}$  and  $p_{2_{cr}}$ ;  $p'_{1_{cr}}$  and  $p'_{2_{cr}}$ ).

The circle  $C$  is plotted using the stresses  $p'_{1'}$  and  $p'_{2'}$  which are much greater than the corresponding stresses  $p_1$  and  $p_2$  or  $p'_1$  and  $p'_2$ . Yet, despite this, since the circle  $C$  has no point of contact with the Mohr envelope, the soil sample must be considered in a state of a subcritical stress far from the point of failure.

The above diagram for the general case cannot be universally used since it is hard to determine in advance that the particular soil is in an extremely

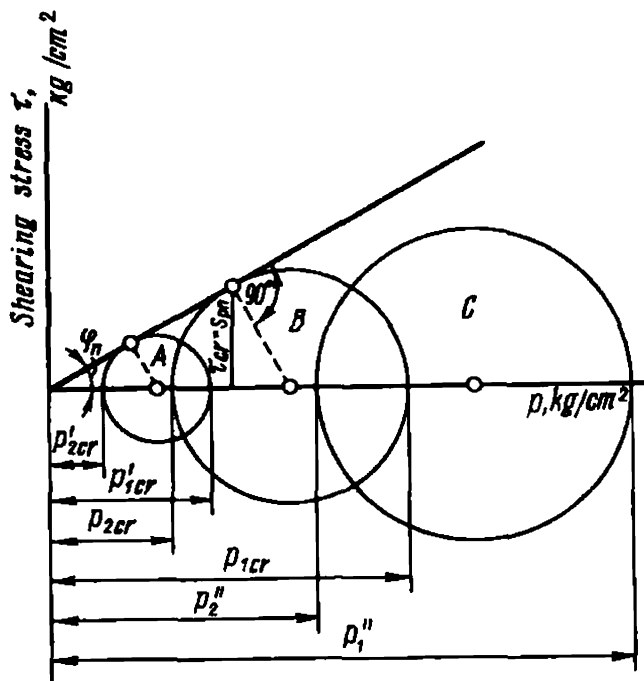


Fig. 13.5. Mohr circles of stress for a loose (cohesionless) soil ( $c = 0$ ):

circles A and B correspond to soil in a state of critical equilibrium; circle C—same, in a subcritical state

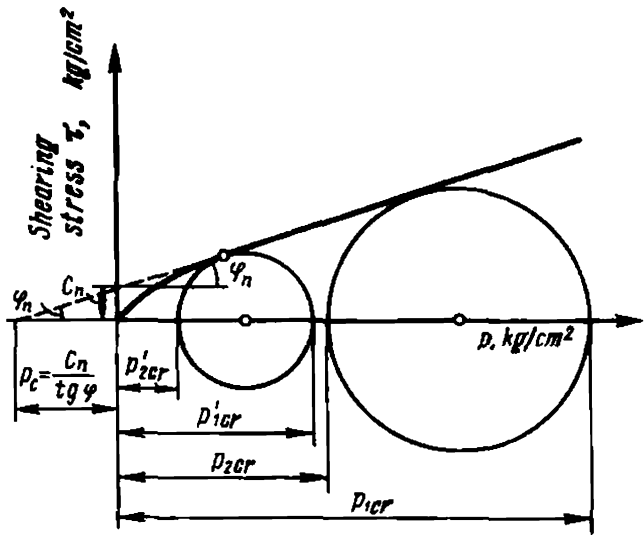


Fig. 13.6. Mohr envelope for soils with  $c \neq 0$

loose state at which apparent cohesion is zero. The general case illustrates Coulomb's equation (13.7). In order to apply this latter for practical purposes two unknowns should be found: the angle of internal friction  $\varphi_n$  and cohesion  $c_n$ . The numerical values of the two quantities are determined experimentally by successively performing, as described above, two tests on two soil samples with the same specified density (referring to porosity).

The two tests differ only in the initial values of the lateral stress  $p_{2cr}$  and  $p'_{2cr}$  and, consequently, critical (breaking) vertical or axial loads  $p_{1cr}$  and  $p'_{1cr}$ . It is evident that in the particular case two circles of stress must be plotted (Fig. 13.6). A tangent to the two circles may often cut off a definite segment on the ordinate axis. The equation for this tangent agrees with Coulomb's equation (13.7) for loose (cohesionless) soils.

Clearly, the tangent will then make with the horizontal coordinate axis an angle equal to the angle of internal friction  $\varphi_n$  concurrently intercepting a segment (free term of a linear equation) on the ordinate axis. A continuation of the tangent to the left until it dissects the abscissa axis will cut off a segment on this latter axis equal to

$$p_c = c_n / \tan \varphi_n$$

The critical state conditions are valid for this case, too, if we shift the origin of coordinates to the left by the value  $c_n / \tan \varphi_n$ .

The calculated value of each of the principal stresses,  $p_1$  and  $p_2$ , is thus increased by the same amount,  $c_n/\tan \varphi_n$ .

Clearly, due to cohesion, the failure of the specimen under the same lateral pressure  $p_2$ , other conditions being equal, should occur at a greater vertical (axial) load  $p_1$ .

Despite the apparent simplicity of the triaxial compression test (called also a triaxial shear test or cylinder test), this method is rarely used in construction engineering in this country. This is mainly due to the inadequacy of testing apparatus, especially, insufficient water-tightness necessary for producing the all-around pressure on the sample. In addition, the sample failure in the testing machine inaccurately simulates the shear stress in the soil mass *in situ*.

**Direct shear test.** The shearing resistance is generally determined by using a common direct-shear apparatus. Figure 13.7 is a schematic diagram of this apparatus. Its principal components are two separate frames or boxes each with a recess for the soil sample. The soil of a specified density (referring to porosity  $n$ ) is placed in the recess and a vertical load  $P_1$  is applied to it. The shearing load  $Q_1$  is applied to the upper frame of the apparatus which largely eliminates random results if the sample has minor inclusions. If we define the cross section of the sample as  $\omega$ , we will then have a normal compression stress  $p_1 = P_1/\omega$  and a shearing stress  $\tau_1 = Q_1/\omega$ .

Given a certain constant value of  $p_1$ , we gradually increase the shearing stress  $\tau_1$  until it reaches a critical value,  $\tau_{cr}$ , corresponding to the shear of the sample recorded by special devices, dial gauges. Under this condition the critical shearing stress  $\tau_{cr}$  corresponds to the soil's shearing resistance  $s_1$  at a load  $p_1$ . The test is then repeated at a different, generally higher load, and a new value of  $s_2$  is determined. By setting up two equations with two unknowns

$$s_1 = p_1 \tan \varphi_n + c_n \quad \text{and} \quad s_2 = p_2 \tan \varphi_n + c_n$$

and by solving them we find the quantities of interest to us,  $\varphi_n$  and  $c_n$ . To have a check the test is usually performed at three loads.

In practice engineers prefer a graphical solution of this set of equations

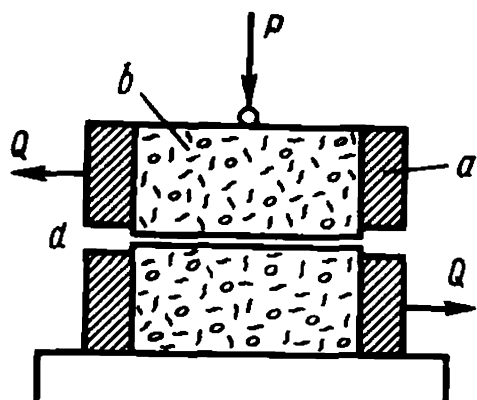
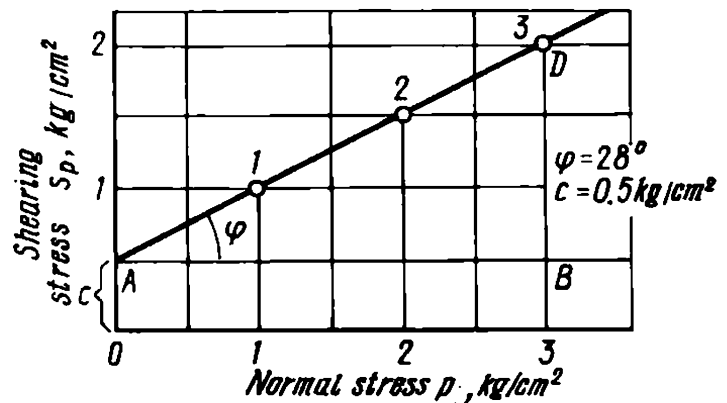


Fig. 13.7. Diagram of a direct-shear apparatus:  
 $a$ —frame;  $b$ —soil sample;  $d$ —gap;  $P$ —compressive stress;  
 $Q$ —shearing stress

Fig. 13.8. Graphical determination of characteristics of shearing resistance  $\varphi_n$  and  $c_n$  of sand in a direct shear test ( $s_{pn} = p \tan \varphi_n + c_n$ )



(Fig. 13.8). For this, a graph is plotted in an  $s = f(p)$  frame of reference with the same scale of stresses along the abscissa ( $p$ ) and the ordinate ( $s_p$ ) axis. Empirically found values of  $s_1, s_2, s_3$ , and  $s_4$  are plotted on the graph. These points are connected by a straight line, and the angle of its inclination to the horizontal corresponding to the angle of internal friction is measured as is the segment on the ordinate axis which is intercepted by the straight line drawn.

Thus the soil's cohesion,  $c_n$ , is determined. Depending on the size of the subsidiary material the size of the samples may vary and the area of their cross section may range from  $20 \text{ cm}^2$  to  $1 \text{ m}^2$ .

**The angle of repose of a loose soil.** When considering methods of determining the angle of internal friction  $\varphi_n$  for loose cohesionless soils we inevitably have to deal with *the angle of repose*,  $\varphi_0$ . It is defined as the angle between the (natural) slope of a heap of dry soil and the horizontal (Fig. 13.9). Let us take some constituent element of a weight  $P$  on the slope with an angle  $\varphi_0$  to the horizontal. Resolve this force into two components: a normal  $N$  and a tangential  $Q$ :

$$N = P \cos \varphi_0; \quad Q = P \sin \varphi_0$$

The force  $N$  acting along the contact surface of the selected unit block and the slope gives rise to friction forces:

$$T = N \tan \varphi_n = P \cos \varphi_0 \tan \varphi_n$$

As the angle of slope increases, the stability of the isolated constituent element on the slope's surface will decrease. At a certain value of the angle

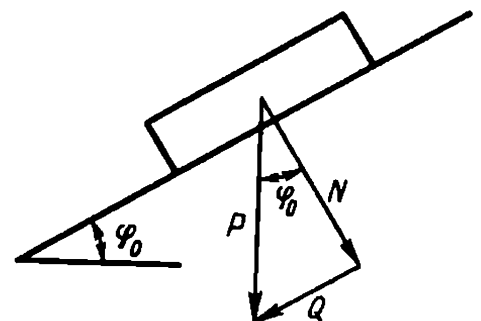


Fig. 13.9. Diagram for determining the angle of internal friction  $\varphi_n$  from the angle of repose  $\varphi_0$  of loose soils

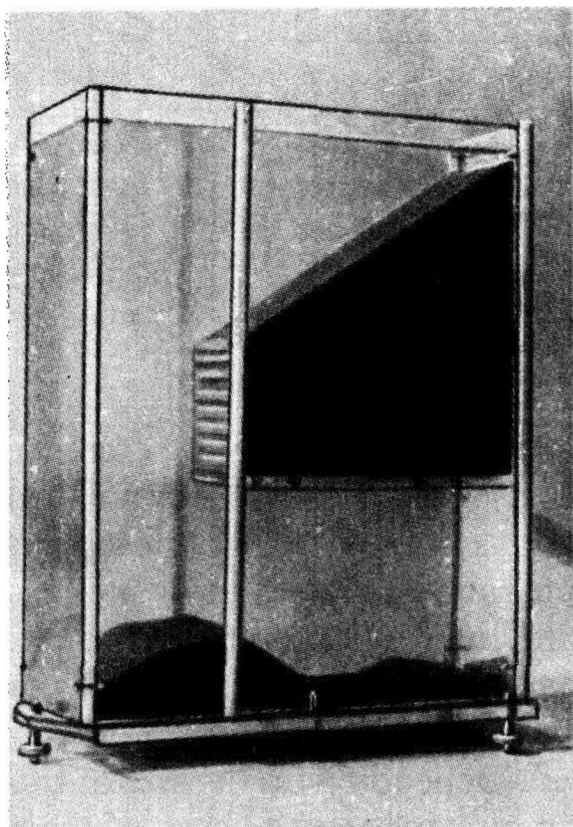


Fig. 13.10. Apparatus designed by V.G. Naumenko for determining the angle of repose  $\varphi_0$

of slope,  $\varphi_0$ , the element block will be in a state of limit equilibrium  $T = Q$ , i.e.

$$P \cos \varphi_0 \tan \varphi_n = P \sin \varphi_0$$

After the requisite simplifications and transformations we will have

$$\tan \varphi_n = \sin \varphi_0 / \cos \varphi_0 = \tan \varphi_0$$

whence

$$\varphi_0 = \varphi_n \quad (13.9)$$

Thus, in the case of a dry loose soil the angle between the horizontal and the angle of a heap of dry soil (angle of corresponding slope) proves to be equal to the angle of internal friction.

Let us consider briefly the determination of the angle of repose. In the field the angle  $\varphi_0$  is established by pouring the soil to form a cone. Laboratory tests use one kind of apparatus or another. One of the best apparatuses (Fig. 13.10) has been designed by V.G. Naumenko. The angle  $\varphi_0$  of a dry and submerged soil is measured from a slope that remains after the redundant soil mass has been removed. This condition is essential for a correct determination of the angle of repose. The advantage of the method is the independence of the test results of the personal errors, especially, when conducting a submerged soil test.



It should be finally pointed out that the angle of repose is equal to the angle of internal friction only when loose and cohesionless soils are involved. An increase in the angle of repose in other soil varieties is a direct result of cohesion bonds between soil particles, and under such conditions Eq. (13.9) is no longer valid. That is why it is impossible to determine the angle of internal friction in wet sands to say nothing of clayey soils from the angle of repose in the laboratory test conditions.

Approximate values of the angle of internal friction in common smooth-grained loose (cohesionless) soils devoid of apparent cohesion are listed in Table 13.2 after Table 1 in Appendix 2 of SNiP II-15-74 irrespective of the origin, age and moisture content of sands.

For average conditions the calculated angle of internal friction for sands may be taken equal to 30°. The minimum value of the angle of internal friction in pebbles with gravel under conditions of loose structure and minor tensions is generally  $\varphi = 40^\circ$  or somewhat more. In a more consolidated state ( $n = 20\%$ ) it may reach 50 to 55° (L.N. Rasskazov, 1936).

Grained soils located in the bedrock mass generally possess some cohesion (consolidated or precompressed sands) due to minor cementation. The angle of internal friction in such sands ranges from 30 to 35°. They display a slight cohesion (up to 0.3 kg/cm<sup>2</sup>). 0.25 to 0.05 mm fraction content in them is 90 to 95%. Under *in situ* conditions such soils exhibit strength and stability. If they are opened in a saturated state they display quicksand properties which is typically due to the seepage pressure.

Table 13.2

Standard Values of the Angle of Internal Friction  $\varphi^{loose}$ , grades, and of Specific Cohesion  $c^{loose}$ , kg/cm<sup>2</sup> (0.1 MPa) of Sandy Soils

Soil type	Soil constants	Values of constants at the voids ratios			
		0.45	0.55	0.65	0.75
Gravelly and coarse-grained	$\varphi^{loose}$	43	40	38	—
	$c^{loose}$	0.02	0.01	—	—
Medium-grained	$\varphi^{loose}$	40	38	35	—
	$c^{loose}$	0.03	0.02	0.01	—
Small-grained	$\varphi^{loose}$	38	36	32	28
	$c^{loose}$	0.06	0.04	0.02	—
Fines	$\varphi^{loose}$	36	34	30	26
	$c^{loose}$	0.08	0.06	0.04	0.02

### Sec. 13.3. Shearing Resistance of Clayey Soils. General Characteristic. Methods of Study and Index Characteristics

Depending on their origin, formation conditions, composition and density and moisture content ( $\varepsilon - w$ ) clayey soils may be grouped into stiff, semiplastic and plastic.

The natural properties of these clay varieties change correspondingly the equation describing their shearing resistance which in the general case (13.2) has this form:

$$s_{pw} = p \tan \varphi_w + \Sigma_w + c_c$$

*Stiff clayey soils* generally include old, to some extent cemented pre-Tertiary soils. These, as a rule, have pronounced strength. The apparent cohesion  $\Sigma_w$  of stiff undisturbed clays is generally suppressed by the true cohesion  $c_c$ . The angle of internal friction in these soils,  $\varphi$ , is only to a minor degree conditioned by the moisture content.

The shearing resistance of stiff clayey soils, in conformity with the above characteristic, can be described by the following equation

$$s_p = p \tan \varphi + c_c \quad (13.10)$$

The relationship is graphically shown in Fig. 13.11. As the true cohesion  $c_c$  increases the importance of internal friction for the strength of a soil gradually drops. The soil then acquires the properties of a solid rock.

In *semiplastic clayey soils*, apart from internal friction, the apparent cohesion  $\Sigma_w$  is important as is, though to a lesser extent, true cohesion  $c_c$ . The total shearing resistance in such soils,  $s_{pw}$ , is usually strongly dependent on the amount of water (consistency) in the soil. Hence, to evaluate the shearing resistance of a semiplastic clay the general form equation may be also used (13.2):

$$s_{pw} = p \tan \varphi_w + \Sigma_w + c_c$$

By defining the sum of the two free terms of this equation as the total

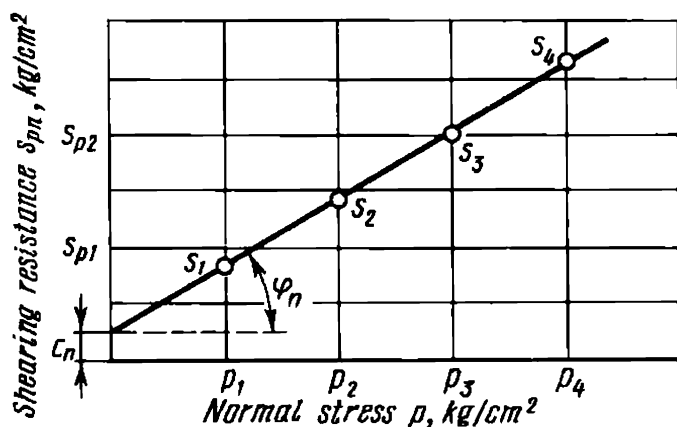
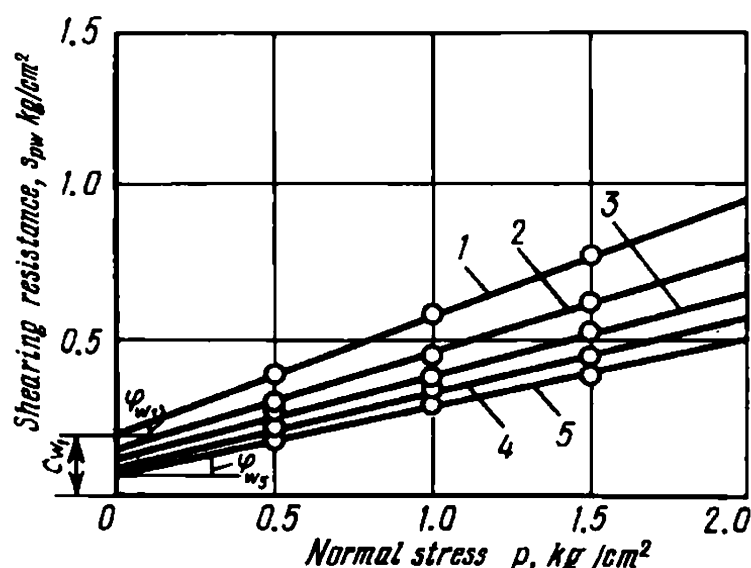


Fig. 13.11. Shearing resistance of stiff clays. Akchagyl bedrock clays. Minge-chaur

Fig. 13.12. Shearing stress of pseudoplastic loams in the form of  $s_{pw} = f(w, p)$ . Landslide deluvium in Ulyanovsk:

1— $w_2 = 30\%$ ; 2— $w_2 = 33\%$ ; 3— $w_3 = 35\%$ ; 4— $w_4 = 38\%$ ; 5— $w_5 = 41\%$ ;  
 $\varphi_{w1} = 22^\circ$ ;  $\varphi_{w2} = 16^\circ 45'$ ;  $\varphi_{w3} = 14^\circ$ ;  
 $\varphi_{w4} = 12^\circ 40'$ ;  $\varphi_{w5} = 12^\circ$



cohesion  $c_w$ , or

$$c_w = \Sigma_w + c_c \quad (13.11)$$

we can rewrite Eq. (13.2) which will take on this form often used in practice:

$$s_{pw} = p \tan \varphi_w + c_w \quad (13.12)$$

The relationship (13.12) is graphically presented in Fig. 13.12. The latter diagram is similar to that in Fig. 13.1. The only difference is that here and elsewhere, rather than density (referring to porosity) the soil's consistency  $w$  is used when clayey soils are involved. For each value of the soil's moisture content ( $w_1 - w_5$ ) the angle of internal friction,  $\varphi_w$ , is governed by the angle between the straight line  $s_{pw} = f_1(p)$  and the abscissa axis. The total coherency,  $c_w$ , for the same moisture contents is found from the length of the segment intercepted by the  $s_{pw} = f_1(p)$  line on the ordinate axis.

Having thus found the values of  $\varphi_{w1}$  and  $c_{w1}$  at different values of moisture content it becomes possible to plot, using these data, a diagram showing the relation between the angle of internal friction,  $\varphi_w$ , and the total coherency,  $c_w$ , on the one hand, and the moisture content,  $w$ , on the other hand (Fig. 13.13).

The relationship  $c_w = f_2(w)$  enables us to find for each value of the moisture content the respective soil's apparent cohesion  $\Sigma_w$ , from the difference

$$\Sigma_w = c_w - c_c \quad (13.13)$$

In the simplest case the value of  $c_c$  is found by extrapolating the  $c_w = f(w)$  curve, bearing in mind that the true cohesion,  $c_c$ , is dependent of the moisture content and remains constant (Fig. 13.13).

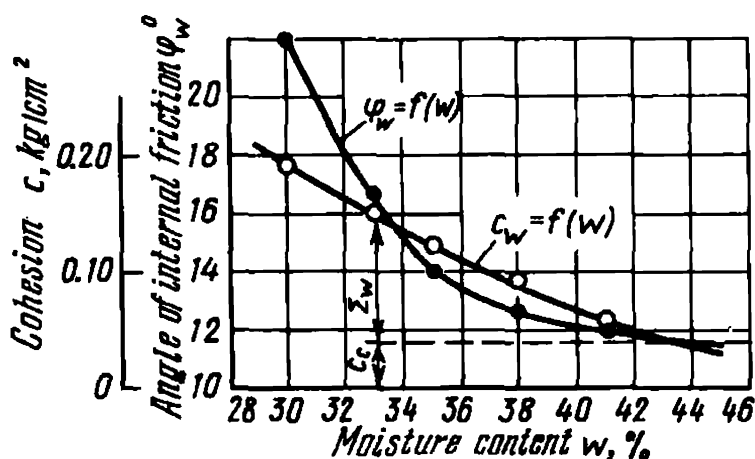


Fig. 13.13. Relationships  $\phi_w = f_1(w)$  and  $c_w = f_2(w)$  for pseudoplastic loams occurring in Ulyanovsk (referred to Fig. 13.12)

This technique yields good results provided that the inequality  $w_{max} > w_p$  is observed, where  $w_{max}$  is the peak moisture content of the sample and  $w_p$  is the moisture content equivalent to the load  $p$  in the test. Under conditions of the above constraint a method of split specimens is generally better. This method consists in comparing the shearing resistance of an undisturbed soil sample and that of a soil sample cut into two halves.

It is assumed, when conducting the test, that the friction resistance remains unchanged in either case and that the cohesion is lost at this, due to its severe character, in the zone of the sample's dissection and on the subsequent shear surface. Clearly, the difference between the values of the shearing resistance of the undisturbed sample and of the disturbed one will then correspond to the value of the true cohesion,  $c_c$ .

Much information can be obtained by determining the shearing resistance of undisturbed samples which preserve their original cohesion,  $c_c$ , and comparing the results with the shearing resistance of samples artificially prepared from the same soil with a disturbed structure yet of the same bulk density. The fact that the results of the two tests practically agree points to the absence in the soil of true cohesion forces ( $c_c = 0$ ), however great the total cohesion,  $c_w$ , may be.

Viewed in this context, of much interest are tests of boulder (moraine) clay having a very great density (bulk density is  $2.25 \text{ t/m}^3$ ). These tests have demonstrated that its pronounced cohesion is only due to its apparent cohesion,  $\Sigma_w$ . The diagrams in Figs. 13.12 and 13.13 show the results of testing a completely saturated soil ( $G \approx 1.0$ ).

As has been shown by the studies of V.D. Kazanovsky, the above regularities are valid also for clayey soils with a coefficient of saturation less than unity ( $G < 1.0$ ). However, not only the soil's moisture content but also its density must be taken into account. It emerged in these tests that the angle of friction  $\phi_w$  for such soils, unlike the total cohesion,  $c_w$ , is often found independent of the soil's density and is governed by its moisture content only. As applied to semiplastic clay varieties the diagram

in Fig. 13.13 is of much practical value. It permits the determination of design values of the angle of internal friction  $\varphi_w$  and total coherency  $c_w$  for a particular soil in any state of consistency. Thus, the specific property of semiplastic clays is the dependence of their shearing resistance on the load and consistency.

*Plastic clayey soils* include fresh heavy loams and, of course, fat clays usually having a soft plastic consistency. Colloidal pellicules in such soils are so thick as to rule out a direct contact between soil particles. This is the reason why the friction between the particles is practically approaching or equal to zero, and, consequently, the coefficient of friction and the angle of friction are zero ( $\varphi_w = 0$ ).

Clearly, under such conditions the shearing resistance of plastic clays proves independent of the load, too. On the other hand, as a result of the relatively young age of clayey soils under consideration, no cohesion practically exists in plastic soils, i.e.  $c_c = 0$ .

Stemming from the above, the shearing resistance of plastic clayey soils can be expressed by this abbreviated formula:

$$s_w = \Sigma_w \quad (13.14)$$

It follows that the shearing resistance in plastic clayey soils is only governed by their coherency and, for a given natural moisture content, is independent of the load. This is a typical characteristic of plastic clayey soils.

The values of the angle of internal friction,  $\varphi_w$ , apparent cohesion  $\Sigma_w$ , and cohesion between particles,  $c_w$ , should be determined taking into consideration the natural moisture content and the density of the particular soil.

The relationship  $s_{pw} = f_1(p)$  and  $s_w = f_2(p)$  for different values of soil moisture content making it possible to determine, according to Figs. 13.12 and 13.13, the relationships of interest to us:  $\varphi_w = f_3(w)$ ;  $c_w = f_4(w)$  and  $\Sigma_w = f_5(w)$ , are found from a series of tests at different loads,  $p_1, p_2, \dots, p_n$ . In these tests the soil samples are kept at definite loads and, consequently, compressed, for different time periods.

The consistency of the samples corresponding to one critical shearing resistance or another is established from the parts of the samples taken from the shear zone after the test. The early stage of treatment of the tested results involves a diagram plotted like one in Fig. 13.14. Points of  $s_{pw} = f(w)$  were obtained by tests at different loads,  $p$ . Next step is to transform the diagram shown in Fig. 13.14 to one shown in Fig. 13.12 which represents the relationship  $s_{pw} = f(p)$ . Further handling of the tested results follows the familiar procedure of the determination of values of  $\varphi_w$

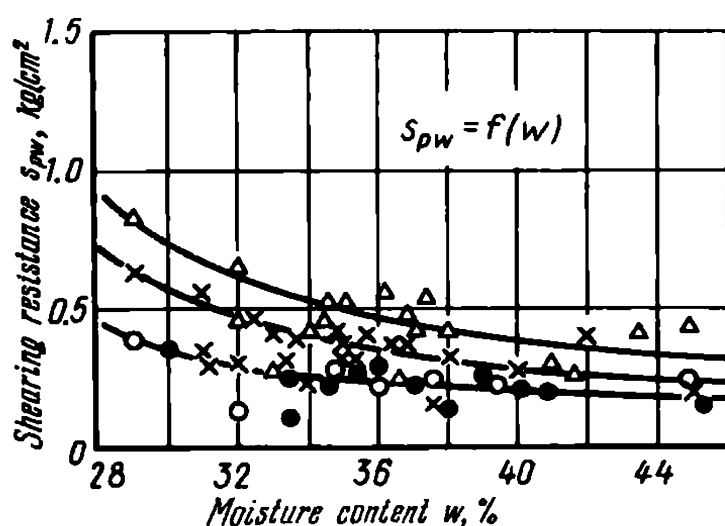


Fig. 13.14. Primary treatment of shearing tests to determine relationships  $\varphi_w = f_1(w)$  and  $c_w = f_2(w)$ . Plotting a graph  $s_{pwi} = f(p_i, w_i)$ . Pseudoplastic loams. Landslide deluvium in the Ulyanovsk area:

$$p_1 = 0.5 \text{ kg/cm}^2; p_2 = 1.0 \text{ kg/cm}^2; p_3 = 1.5 \text{ kg/cm}^2$$

and  $c_w$  depending on the given moisture content,  $w$ , and is concluded by plotting a graph of  $\varphi_w = f_3(w)$  and  $c_w = f_4(w)$  according to Fig. 13.13.

Given data on  $\varphi_w = f_3(w)$  and  $c_w = f_4(w)$ , say, in the form of a diagram shown in Fig. 13.13, we can easily find the resistance of semiplastic clays at one moisture content,  $w$ , or another for different loads  $p$  from the familiar equation  $s_{pw} = t \tan \varphi_w + c_w$ . As has been shown by V.I. Rudenko, the best consistency in the test data is achieved by expressing the shearing resistance in terms of *soil consistency* (Fig. 13.15).

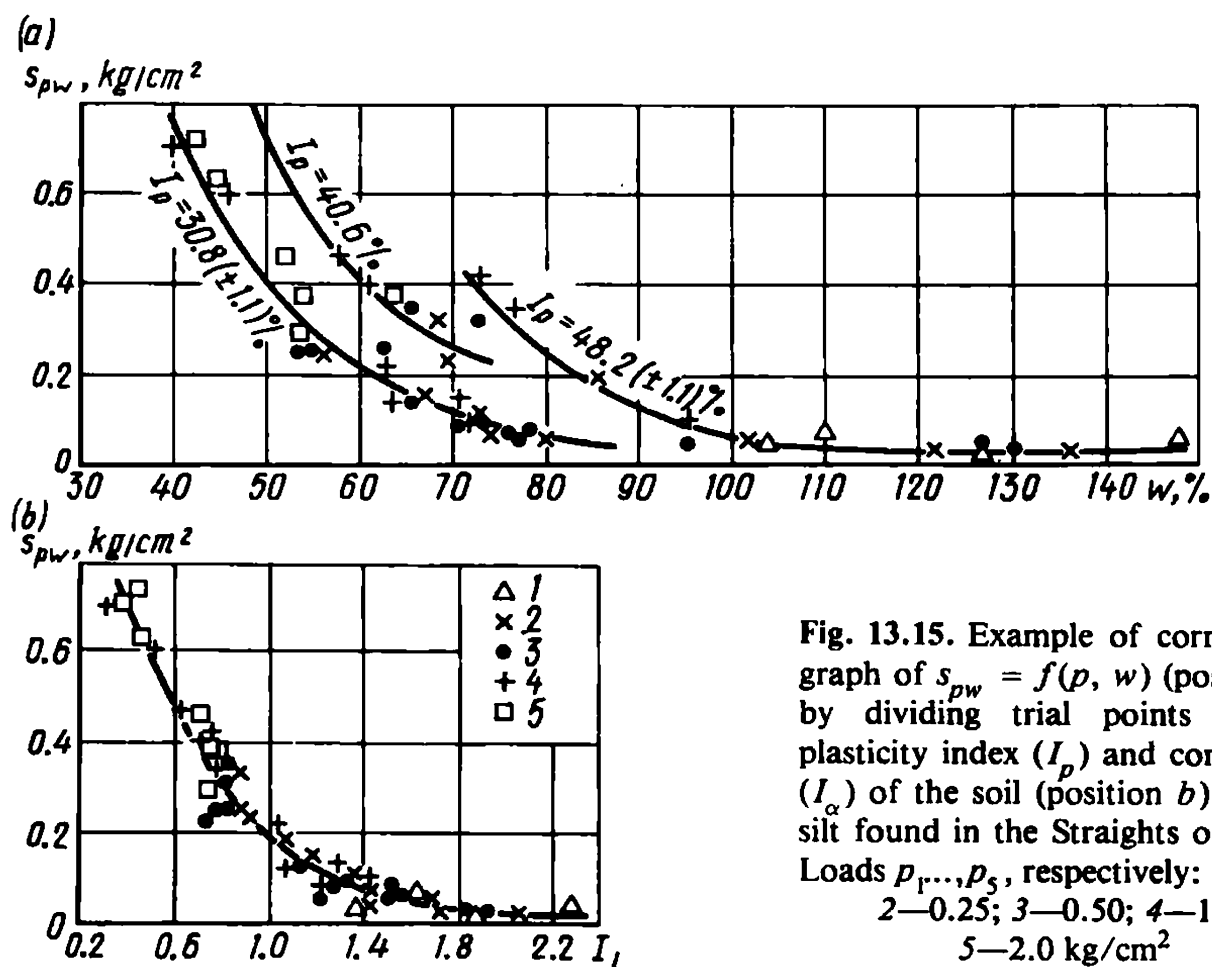


Fig. 13.15. Example of correcting a graph of  $s_{pw} = f(p, w)$  (position a) by dividing trial points by the plasticity index ( $I_p$ ) and consistency ( $I_\alpha$ ) of the soil (position b). Clayey silt found in the Straights of Kerch. Loads  $p_1, \dots, p_5$ , respectively: 1—0.10; 2—0.25; 3—0.50; 4—1.0; 5—2.0  $\text{kg/cm}^2$

To plot a diagram showing the relationship  $\varphi_w = f_3(w)$  and  $c_w = f_4(w)$  for semiplastic clays we must test for shearing resistance at least 9, but, better, 12 samples. This is due to the fact that no further averaging of the test results is thus needed.

Other methods of testing call for averaging of the test data which requires no less number of shear tests and, consequently, soil specimens. The treatment of the test data according to the procedure relying on the consistency is largely facilitated by the logarithmic nature of the relationship  $s_{pw} = f_1(w)$  and  $s_w = f_2(w)$ .

This regularity found by G.A. Andreev and substantiated by V.D. Kazarnovsky permits approximation of the test data by a straight line when plotting a diagram in a semilogarithmic frame of reference. This cuts down on the number of requisite determinations, facilitates more accurately plotting other diagrams that may be needed and validates extensive extrapolations. A need, however, may sometimes arise to determine the shearing resistance of both semiplastic and plastic clayey soils in the state of consistency critical for the given load.

A moisture content corresponding to a definite load  $p$  is termed an *equivalent* one and is denoted as  $w_p$ . In this case soil samples to be tested are compressed previously until they reach the equivalent density-moisture state,  $w_p$ , by subjecting them to the loads at which they will be then sheared.

Experience shows that the equation  $s_{pw} = f(p)$  at comparatively low loads is of a linear character corresponding to Coulomb's law, i.e.

$$s_p = p \tan \varphi + c \quad (13.15)$$

It must be borne in mind that, despite their apparent similarity there is essential difference between Eqs. (13.12) and (13.15).

The angle  $\varphi$  in Eq. (13.15) is indicative of the intensity rate of a soil's shearing resistance induced not only by the load but also by the increase in the coherency proper,  $\Sigma_w$ . On the other hand, in semiplastic soils it depends on the angle of internal friction,  $\varphi_w$ , increasing in proportion to the soil's density at a load.

By this token, the index  $\varphi$  determined allowing for the equivalent moisture content,  $w_p$ , in Eq. (13.15) should be called *an angle of internal friction and cohesion*. Clearly, for perfect sands this will be only an angle of friction, whereas for perfect plastic clays (with  $\varphi_w = 0$ ) only an angle of cohesion.

When testing specimens of plastic clayey soils the points of the relationship  $s_w = f(w)$  still corresponding to the moisture content of samples,  $w$ , from the shear zone for different loads,  $p_1, p_2, \dots, p_n$ , fall on the same curve (Fig. 13.16a).

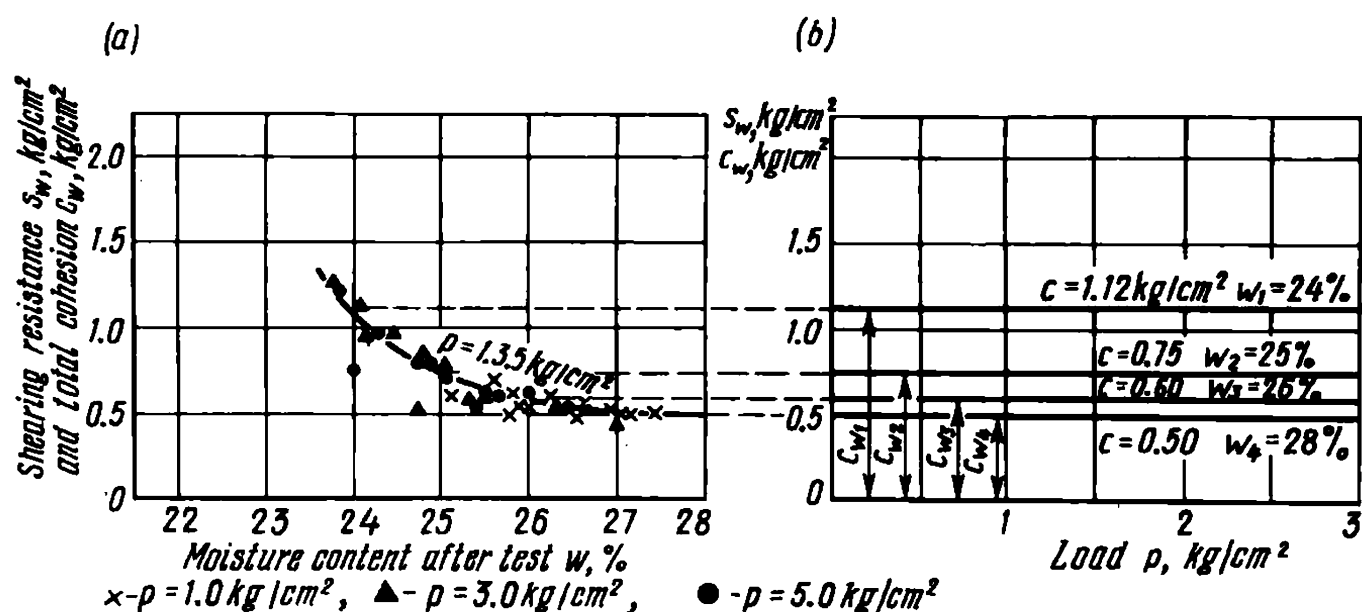


Fig. 13.16. Shearing resistance  $s_w$  and total cohesion  $c_w$  of plastic clays with  $\varphi_w = 0$  (heavy loams) as a function of moisture content  $w$  (a) and load  $p$  (b) at  $\varphi_w$

This validates the independence of the shearing resistance,  $s_w$ , of plastic clays, at some definite moisture content, of the load,  $p$ , and, consequently, substantiates the validity of the equations  $s_w = \Sigma_w$ . Clearly, under this condition the equations  $s_w = f_1(w)$  and  $\Sigma_w = f_2(w)$  agree, and the curve in Fig. 13.16 may be used to concurrently determine the shearing resistance,  $s_w$ , and the coherency,  $\Sigma_w$ , depending on the particular moisture content.

At a given density-moisture state the shearing resistance of such soils is independent of the load and is only governed by the value of

$$s_w = c_w \quad (13.16)$$

This statement is illustrated in Fig. 13.16b.

The shearing resistance of semiplastic and plastic clayey soils is sometimes better determined by *triaxial compression tests using a triaxial compression machine*. This is done, e.g. when it is desired to test the shearing resistance of much wetted clay soil masses with disturbed texture (remolded clays) used as filling material (clay fills) for filling gullets of bridge abutments and retaining wall fills or for earth works, such as road embankments, dams etc.

Evidently, the material to be tested may in the given case be considered as isotropic which is a prerequisite for testing using a triaxial compression machine. As has been shown by V. I. Rudenko of the Moscow Highway Construction Engineering Institute (MADI), the indices of the shearing resistance of such clayey soils as determined by a triaxial compression test and a direct shear test of samples with the same density-moisture ratio (*a sine qua non* condition!) are practically identical.



The test may be conducted in two variants: (1) with sample failure after complete consolidation at a given load (open shear); (2) under conditions preventing the escape of the moisture pressed out of the soil sample due to the load applied which means for saturated soils the absence of additional consolidation and the preservation in the soil samples of the initial density-moisture index (closed shear).

The results of such tests are handled as described above.

The use of characteristic indices referred to the complete consolidation of a soil under a load for engineering calculations may often lead to disastrous effects. To rule out such miscalculations commonly induced by overexaggerated design indices, foreign engineers generally apply indices  $\varphi_w$  and  $c_w$  determined by *undrained* tests called alternatively *quick* tests. Such determinations, however, may also be prone to errors. For example, additional soil consolidation during the test is not taken into account here.

Figure 13.17 is a general view of a shear test device designed by the present writer (constructed by Yu.Yu. Lurye), fairly popular in this country. The diameter of the sample to be tested by the device is  $\approx 7$  cm, the cross sectional area  $40 \text{ cm}^2$ .

In order to determine two unknown indices of the shearing strength of clayey soils (the angle of internal friction,  $\varphi$ , and cohesion,  $c$ ), the samples must be subjected to a shear by at least two different loads,  $p$ . A test generally calls for three or even four loads. To provide a vertical pressure metal plates or weights are used.

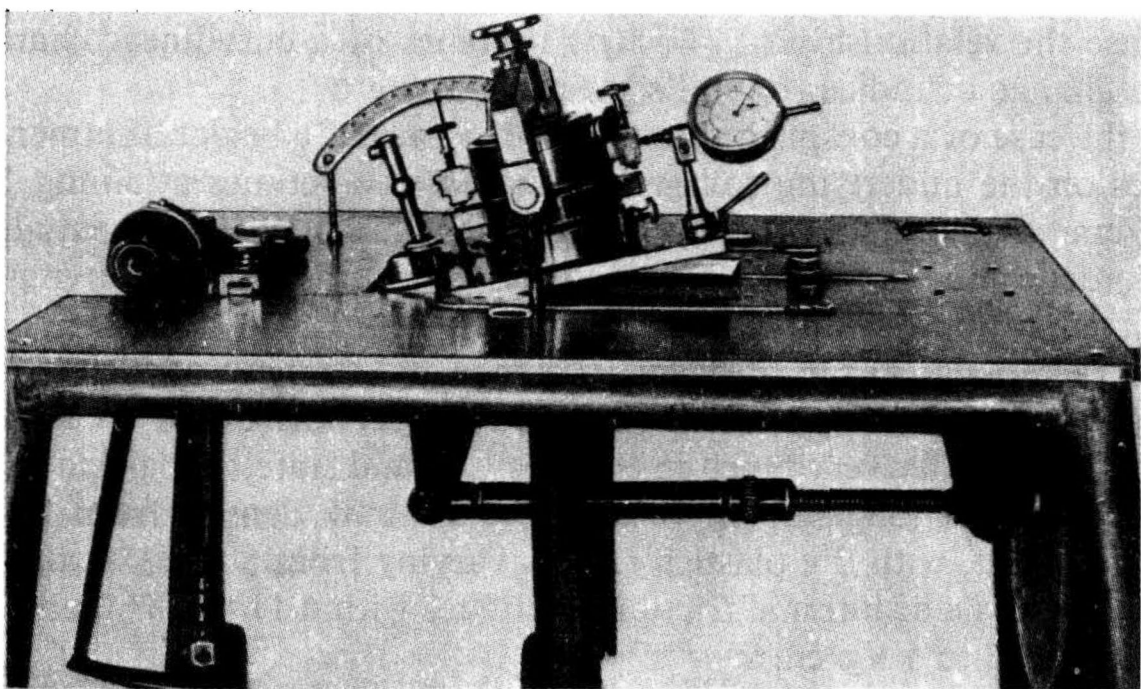


Fig. 13.17. General view of apparatus for shear tests of inclined samples designed by N.N. Maslov. Model MJIC-46

The shearing force may be imparted to a soil sample in two ways: (a) according to a scheme of an independent shearing force, using special levers; (b) according to a scheme of a shear of an inclined sample using the tangential component of the vertical load on the sample (a handwheel in the right-hand side of Fig. 13.17). Such a procedure is advantageous when a constant intensity of the sample deformation must be achieved.

In the test involving an independent shearing force the values of  $\varphi$  and  $c$  are determined according to the data presented in Fig. 13.8. In an inclined (shear) sample test the interpolation of the results obtained calls for the solution of at least two equations of this form:

$$\tan \varphi + \frac{c_1}{p_1} = \tan \alpha_{p_1}; \quad \tan \varphi + \frac{c}{p_2} = \tan \alpha_{p_2}$$

where  $p_1$  and  $p_2$  are normal stresses used for the test;  $\alpha_{p_1}$  and  $\alpha_{p_2}$  are critical angles of tilt of the working cylinder at which the shear occurred as recorded by dial gauges and measured using a special protractor at different loads  $p_1$  and  $p_2$ .

Note that if a soil is cohesive, the critical angles of tilt,  $\alpha_{p_1}$  and  $\alpha_{p_2}$ , are numerically equal to the *angles of shearing resistance*  $\psi_p$ . For loose cohesionless soils (at  $c = 0$ )  $\alpha_{p_1} = \alpha_{p_2} = \varphi$ .

It must be finally pointed out that the linear character of the dependence of the soils' shearing strength on the load is preserved only at relatively low loads,  $p$  (generally in the range of 0 to 4 kg/cm<sup>2</sup>). At greater loads the soils' density increase rate is inhibited as the load is increased. In this case the relationship  $s_{pw} = f(p)$  becomes of a curvilinear character with a change of indices of soil's shearing strength.

In the case of a conspicuous depth of the base of a bridge abutment the stresses on the underlying soil greatly increase sometimes attaining 12 to 15 kg/cm<sup>2</sup> or more. In order to preclude displacement it is essential that tests to determine the index characteristics of a soil's shearing strength be conducted at appropriate loads.

Characteristics of the shearing resistance and strength of different old soils may be provided by Jurassic clays (Oxfordian horizon) of the Moscow Region. They differ very much in composition and state. In particular, the moisture content ranges from 16 to 53%, the bulk density from 1.68 to 2.09 t/m<sup>3</sup>, and, with the plasticity index varying from 8 to 61%, the corresponding angle of internal friction fluctuates within 11 to 32°, and cohesion from 0.03 to 1 kg/cm<sup>2</sup>.

In the southern areas of the USSR the bedrocks are mainly composed of clayey soils of the Buchag layer (Paleogene series) which are over 50 m in thickness, have a hard or semihard consistency and the moisture content

20 to 24%. According to the index characteristics the soil of the area adjoining the Volga-Don canal can be classified as light and heavy sandy loams. The average angle of internal friction in these is 23 to 24°, and cohesion is about 0.50 kg/cm<sup>2</sup>.

Tests of Kievan marly clays of the same region having a semihard and hard consistency have yielded these results: the moisture content  $w = 34\%$ , the angle of friction is 20° and cohesion is 0.40 kg/cm<sup>2</sup>.

*Marly clays* have very specific properties. These are largely governed by carbonization and intactness: when unweathered, such clays, like marls, exhibit properties of semihard or even hard rocks. In this state their properties are mainly conditioned by jointing. Depending on the degree of carbonization, their compressive strength may vary in a very wide range, from several tens to several hundreds of kg/cm<sup>2</sup>.

Bedrock clays of a solid consistency have a definite texture (block-like and fragmentary) resultant from a directed tectonic or gravitational (in landslides) action. Such are, e.g. Lower Cretaceous soils of the Saratov, Volgograd and Maikop Regions. They are dissected under conditions of undisturbed occurrence into blocks 10 by 10 by 20 cm in size and angular fragments from a few mm to several cm. Clearly, the shearing resistance in this soil mass may prove many times less than in an individual small sample, especially, when the surface of the blocks is wetted by meteoric water.

In this respect are typical Maikopian clays of a semisolid and solid plastic consistency and an average moisture content 35 to 40% that feature microcracks. When precompressed, such clays typically have  $\varphi = 17^\circ$  and  $c = 0.35 \text{ kg/cm}^2$  (at a moisture content equivalent to the load applied). Yet the composition and state of Maikopian soils are very much diversified. In particular, the angle of true friction in soils occurring in the vicinity of the Mamai burial mound (in Volgograd) at a natural moisture content drops to  $\varphi_w = 0$  to 2°.

A classical example of plastic consistency clayey soils is provided by the late ice-age limnetic varved clays occurring in the Leningrad area. Half of this city is underlain by these clays. They are also very much abundant along the route of the dam being erected across the Gulf of Finland to protect Leningrad from inundations. Varved clays display a lowered density and an increased moisture content ( $\varepsilon = 0.8$  to 0.9 and  $w = 20\%$ ) and, consequently, a lowered shearing resistance ( $\varphi_w = 9$  to 12° and  $c_w = 0.10 \text{ kg/cm}^2$ ).

Hence the low bearing capacity, high deformability and tendency to rheologic events typical of these soils.

Despite all this, Leningrad engineers who have vast experience of construction on incompetent soils confidently build footings for various structures resting on varved clays.

An example of such clays of plastic consistency in the Volga Region is provided by so-called *Khvalynian* clays. Two varieties of these have a moisture content ranging from 34 to 38 and from 50 to 51%. These are generally soft plastic clays. At a natural moisture content the angle of true friction is  $\varphi = 2$  to  $2.5^\circ$ , cohesion is  $c = 0.20 \text{ kg/cm}^2$ .

The group of clayey soils with a liquid consistency primarily includes the freshest formations, such as deposited materials as weathering products with the composition typical of argillaceous rocks. Similar soils are most frequently found in younger and even modern marine deposits (Ioldian clays in the White Sea with the moisture content up to 105%), in limnetic and alluvial deposits found in the flood lands in the cut offs having a moisture content 170% or even more. With the bulk density  $\rho_w = 1.48 \text{ t/m}^3$  and less the true angle of friction in these soil varieties generally ranges from 0 to 2 to  $3^\circ$  with a cohesion within 0.05 to  $0.10 \text{ kg/cm}^2$ .

Clearly, unless appropriate measures are taken, such soils have practically no bearing capacity. Yet positive results may be achieved by such steps as an additional compression of the soil by applying a load to it. This is shown by a number of examples. One of these is the construction of the buildings of the Polytechnical Institute in Hanoi (DRV) that have been in operation for more than two decades without a failure.

The familiar varieties of clayey soils with a soft plastic, practically liquid consistency are marine silts found in the Azov Sea and in the north west of the Black Sea. These silts possess a practically zero bearing capacity which may be slightly increased by the admixture of crushed shells at the angle of friction approximately  $7^\circ$  and cohesion about  $0.05 \text{ kg/cm}^2$ . Even if piles are driven the foundation of an engineering structure cannot rest on such a soil if this latter has not been artificially compressed.

To conclude, for preliminary estimates Table 13.3 presents *design indices* of some of important varieties of clayey (cohesive) soils\*.

A more detailed table showing standard values of the angles of internal friction  $\varphi_{st}$  and cohesion  $c_{st}$  for Quaternary clayey soils in relation to soil consistency and of the corresponding voids ratios  $\varepsilon$  is provided by Table 2 of Appendix 2 of the Soviet Code of Practice SNIIP II-15-74.

---

\* This table has been compiled under the guidance of the present writer, basing on the statistical handling of several hundreds of engineering geologic records, by D.V. Shnitnikov, G.A. Andreev, Z.V. Pil'gunova and N.I. Kulenko and was first published in 1949 (*N.N. Maslov. Applied Soil Mechanics, Mashstroizdat, in Russian*). More than three decades of experience have validated the practical value of the data contained in the table.

Table 13.3

**Approximate Design Constants of Shearing Resistance  
in Clayey (Cohesive) Soils**

Consistency of soil	Clay		Loam		Sandy loam	
	$\varphi_w$ , grade	$c_w$ , kg/cm <sup>2</sup> (0.1 MPa)	$\varphi_w$ , grade	$c_w$ , kg/cm <sup>2</sup> (0.1 MPa)	$\varphi_w$ , grade	$c_w$ , kg/cm <sup>2</sup> (0.1 MPa)
Hard	22	1.00	25	0.60	28	0.20
Semi-hard	20	0.60	23	0.40	26	0.15
Semi-plastic	18	0.40	21	0.25	24	0.10
Soft plastic	14	0.20	17	0.15	20	0.05
Liquid plastic	8	0.10	13	0.10	18	0.02
Liquid	6	0.05	10	0.05	14	0.00

#### Sec. 13.4. Strength and Shearing Resistance of Jointed Hard Rocks

Hard rocks are endowed with a pronounced strength and, hence, low compressibility, a capacity to retain high steep slopes coupled to low permeability under conditions of minor jointing of the rock mass. On the other hand, rock ruptures and fragmentation may lead to a pronounced permeability.

The strength per unit volume of hard rocks is generally very great, of the order of hundreds and thousands of kg/cm<sup>2</sup>.

The compressive strength of individual fragments of igneous rocks is very great in effusive rocks and lower in intrusive rocks (respectively, 1 000 to 4 000 and 800 to 3 000 kg/cm<sup>2</sup>).

The hard rock mass is always dissected by a more or less complex system of cracks or fissures (jointing). Jointing is what largely governs the degree of the bearing capacity of hard rocks, slope stability, deformability and permeability.

Weathering may be another decisive factor affecting the latter properties, in particular, the shearing resistance at joints. The compressive strength of a rock mass weakened by jointing and weathering is, at best, 10% of the intact massive rock. So, *in situ* tests of the granites underlying the foundation of the Dnieper Hydro Power Station have shown their shearing strength to be only 8 to 9% of their compressive strength. The value of this index in Carboniferous limestones occurring in Moscow is 8%, in sandstones and argillites about 2 to 3%.

Weathering may penetrate in the hard rock mass to a depth of 5 to 7 m

and more. However, pronounced jointing and, especially, tectonic disturbances may increase this depth to 25 m and sometimes more\*.

If joints are conspicuous and are filled with some other material, the shearing resistance of the rock mass at fissures will also be governed by the type of filler (rock disintegration products under conditions of rock displacement along the joint plane, clayey material), its moisture content. Under definite conditions the shearing resistance of such rock mass may be very low, only several decimal fractions of  $\text{kg/cm}^2$ .

Unlike igneous rocks, metamorphic rocks, even in the bulk form, exhibit anisotropic properties conditioned by schistosity or foliation (e.g. in gneisses). Schistosity, especially, when coupled to weathering, results in a lowered shearing resistance.

Mechanical properties of metamorphic rocks, by virtue of their formation conditions and state, are very much diversified. Crystalline schists have an especially great strength. The compressive strength of quartzites may be  $6000 \text{ kg/cm}^2$  (600 MPa). A much less strength is manifested by sericite chlorite and quartz sericite shales found in the area of the Troitsk Hydro Power Station. Their compressive strength ranges from 138 to  $1135 \text{ kg/cm}^2$  and is on the average 300 to  $400 \text{ kg/cm}^2$  (30 to 40 MPa). Upon weathering these rocks lose their strength dramatically. So, the angle of friction of a weathering rock does not exceed  $20^\circ$  and may often prove much less. The cohesion drops to  $0.05 \text{ kg/cm}^2$ .

Clay shales, being a product of minor metamorphism affecting clayey soils, under conditions of continued and pronounced weathering may transform to a clayey mass with a very low strength and insignificant shearing resistance upon wetting.

At the same time, depending on their condition (weathering extent and moisture content) the mechanical properties and, in particular, shearing resistance of argillaceous shales may vary in a very wide range. The coefficient of friction in these rocks ranges from 0.25 to  $0.75 \text{ kg/cm}^2$ , cohesion from  $0.45$  to  $1.5 \text{ kg/cm}^2$  and more.

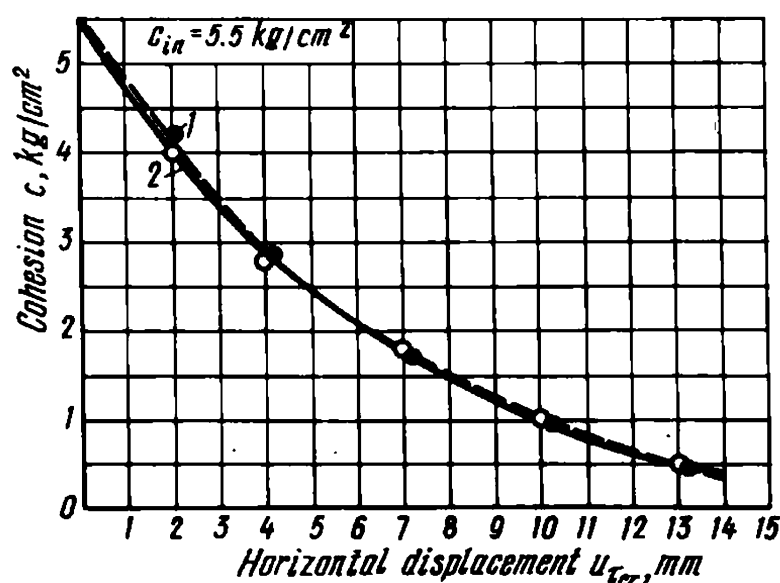
The porosity of limestones is generally only 1 to 3%, yet in loose-textured varieties it may be up to 15 to 25%, and in shell rocks it may attain 50 to 60%. Depending on the porosity, the bulk density of limestones may also vary within a wide range, from 2.0 to  $2.6 \text{ t/m}^3$ . Accordingly, their

---

\* A bed of granite had decayed at Washington, D. C., to a depth of 80 ft. so that it could be removed with pick and shovel. Elsewhere in the United States, limestone has been found decomposed to a depth of 200 ft. In Brazil, shales have been found disintegrated to a depth of 394 ft. below surface level. (R. L. Legget. *Geology and Engineering*. McGraw-Hill, N. Y. and L., 1939, p. 324). — *Translator's note*.

**Fig. 13.18.** Drop in cohesion over contact surface of fissure walls in a rock mass at deformation of displacement  $u_{\tau_{cr}}$ . Granite gneisses found in Naglu, Afghanistan:

1—theoretical curve using formulae:  
 $c_u = c_{in} - (a + b \ln u)$ ;  $c_{in} = 5.5 \text{ kg/cm}^2$ ;  $a = 4.5 \text{ kg/cm}^2$  and  $b = 2.0 \text{ kg/cm}^2$ ; 2—experimental curve



strength varies from several tens of  $\text{kg/cm}^2$  to  $1200 \text{ kg/cm}^2$  (120 MPa) in hard varieties of limestones and dolomites.

Limestones and dolomites typically occur in strata of different thickness. Limestones are invariably fissured. The voids ratio in these rocks is different, generally from 2 to 5%. Jointing rapidly decreases with the depth. For example, limestones in the area of the Chervak Hydro Power Station (the Chirchik River) at depths of 35 to 40 m exhibit only closed cracks. Commonly occurring thin layers of fat clays with an inappreciable shearing resistance may impair the generally high mechanical strength of carbonate rocks, especially flagstones. An example may be provided by some varieties of limestones of the Carboniferous plateau belonging to the Carboniferous System found in the Valdai Hills. The angle of internal friction at strata does not commonly exceed  $7^\circ$  and sometimes becomes zero.

Tectonic fissures in the massive rock are often filled by magmatic or hydrothermal veins. In this case the soundness of the rock mass, and, consequently, the latter's stability and bearing capacity are to a certain extent restored.

As has been demonstrated above, the shearing resistance in the jointed massive rock is conditioned by many factors. Even if fissures are not filled it may depend on the pattern of the joints, on the degree of rock soundness and the deformation of the massive rock under definite conditions.

Dislocations of rocks along joint planes may lead to detrimental results, such as progressive loss of the shearing resistance, due to cohesion operative here, which often becomes practically nonexistent (Fig. 13.18). In the particular case we observe the effect of smoothing of the surface of dislocation at which there occurs a progressing with time breakdown (failure and chipping) of protrusions on the fissure walls, the seat of pro-



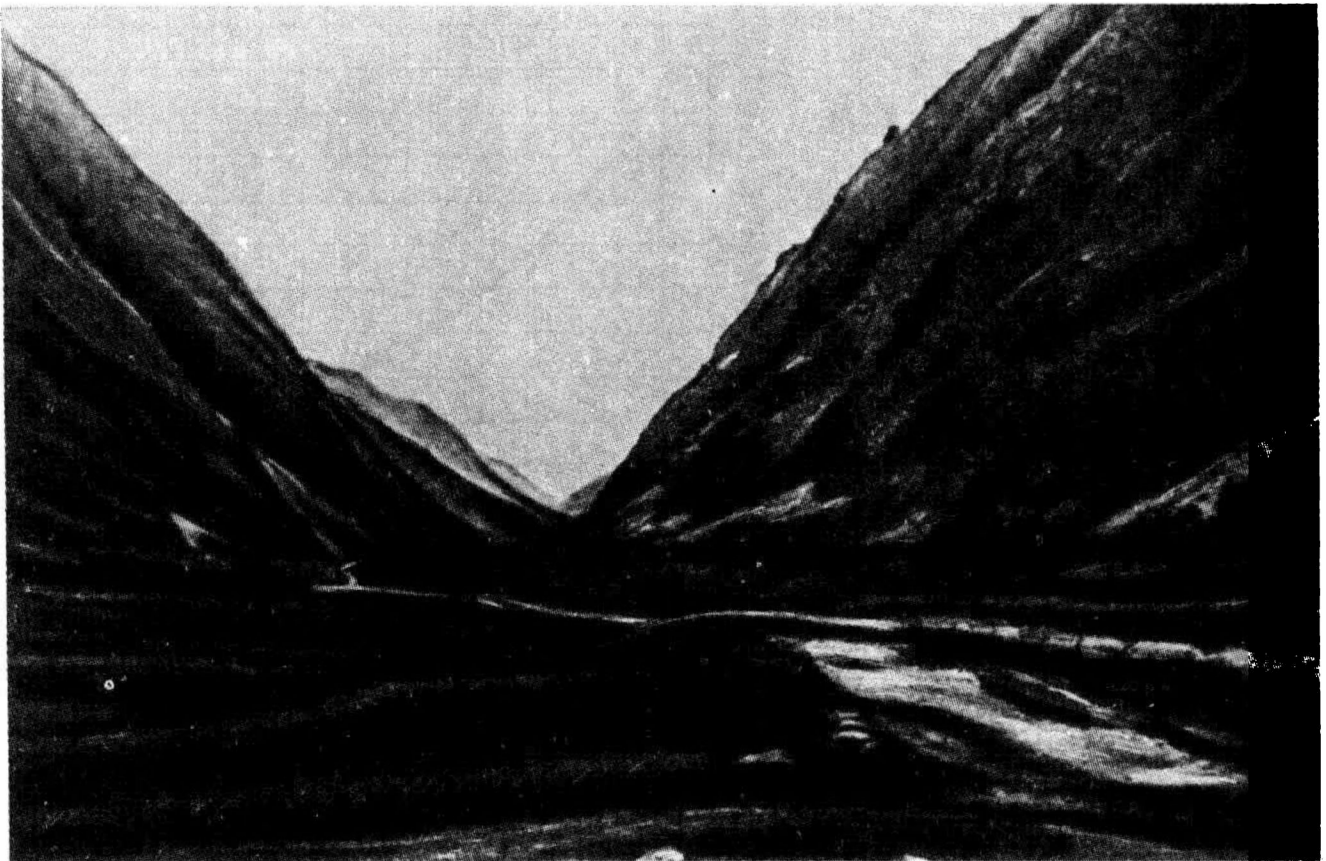


**Fig. 13.19.** Gorge in rock mass in the North Caucasus. Note the linear character of the slopes

nounced stresses concentration. The friction resistance and, accordingly, the angles of friction remain at this practically unchanged (T.V. Pavlishcheva, 1977-1978).

At comparatively low stresses the protrusions on the fissure walls are not chipped off and the deformation in a thrust will proceed under conditions of slippage along rough walls, the cohesion being practically zero. It is the friction, in fact, remaining unchanged that will again play the decisive role. This phenomenon can be revealed by shear tests in the field using loading plates.

Engineers are generally faced with difficulties when comparing and transferring the laboratory and field test results to the massive rock as a whole and when determining the desired index characteristics. This problem may be better understood by referring to morphology (origin and form) of fissures being developed by S. E. Mogilevskaya.

The small role of cohesion in fissures of the massive rock under conditions of rather free deformation and mutual displacement of individual blocks in the massive rock is attested to, in particular, by the almost linear character of slopes in hard rocks. As is known, in rocks with cohesion the slopes will have a curvilinear shape with the curvature rate increasing, particularly at the upper part of the slope (Fig. 13.19).



---

Chapter 14**Soil Compressibility. Its Origin and Characteristics.  
Methods of Determination**

---

**Sec. 14.1. Soil Consolidation Induced by a Load**

The compressibility of a soil is conditioned by the capacity of the soil voids to decrease in volume under a pressure. It is also assumed that in the given case the pore volume decreases due to a larger degree of packing of soil grains. The process invariably involves the mutual displacement of the grains which reveals itself as a type of *microshifts* of the soil particles.

Naturally, if a soil is saturated, i.e. all its voids are filled with water, the soil can be consolidated if only part of the water drains out of the pores. Differently speaking, the consolidation of such a soil is accompanied by a decrease in the moisture content. The time rate of the consolidation of clay materials is larger, the more viscous and impervious they are, i.e. the greater is their clay content and denser consistency. It follows thus that the greatest compressibility will be demonstrated by soils with the lowest shearing strength and density. A soil's compressibility is mainly governed by the presence or lack of internal rigid bonds.

For this reason, voids in materials with a high value of *cohesion*,  $c_c$ , prove practically incompressible. Among such materials are all hard rocks and cemented soils. A typical example is provided by pumice. The pores in this material are large in volume, yet, within the load range of interest to us, pumice may be considered as almost incompressible.

An increase in the applied load, however, may cause failure of the material, and its compression is then sure to occur.

The resisting effect of rigid bonds reveals itself in almost all materials, excepting, of course, loose ones. As a result, at a minor load such materials possess low compressibility. This property is especially pronounced in the bulk clay strata which generally have a fairly high degree of cohesion,  $c_c$ .

A gradual increase in pressure finally results in a sudden rupture of the soil's rigid bonds. A further increase in the load will cause a dramatic rise in the clay's compressibility. Such events are detected even in fairly old clay deposits. As a clayey soil is consolidated, the mineral particles come closer to each other, thus enhancing intermolecular forces, and, consequently, the apparent cohesion of the grains,  $\Sigma_w$ . Under conditions of a pressure-induced consolidation of clayey soils this circumstance brings about residual, *irreversible deformations*. These latter are greater, the less dense is the soil. Thus, after removal of the load the soil is not completely decom-

pressed. As a loose (cohesionless) soil is being compressed its grains become deeper and closer introduced in the soil's voids and tighter stuck there. Clearly, at a forceful compaction of a soil to a definite critical value of its density it is its irreversible fraction that prevails in the soil's compressive deformation.

The greatest role in the settlement of surface structures due to the pressure-induced consolidation of the foundation soil is played by the irreversible part of the deformation which is the domain of soil mechanics.

As the density of a soil is increased, its compressibility decreases leading to a definite decrease in the residual irreversible events and increase of its elastic component. If this condition obtains, we speak of the curvilinear character of the mechanical characteristic of soils subjected to a minor consolidation.

Thus we must *a priori* recognize the absence of the linear dependence of the compressive deformation for weakly consolidated soils. It would be appropriate to recall that the enhanced initial density of clayey soils may stem from: (1) dynamic metamorphism which is most typical of dislocated bulk masses and mountainous areas; (2) high pressure exerted by the overlying strata on the given horizon; (3) dessication (induced by climatic conditions or a low water table).

The effect of the pressure of the overlying layers can be due both to horizons occurring at a great depth and ones that overlay the particular horizon in the geological past, but are absent now.

It should be noted in addition that *the density of sands* is governed by quite different conditions: the regime of deposit accumulation (quiet or dynamic) and frequently seismic events. Under statistical conditions the density of sands is independent of the weight of the overburden strata or the structure itself due to the forces of internal friction, increasing in proportion to the increase in load, that are operative between sand grains. Therefore doubts as to whether a structure underlain by a sand deposit may settle are validated only under conditions of exceptional incompetence of the sand or likelihood of dynamic stresses acting on the sand mass.

We have so far been concerned with soil consolidation under conditions of *increased* load (normal stress).

It follows from the above that removal of part of the load from a soil will cause the process to be reversed. The voids volume will increase, and, as water will percolate, the moisture content of the soil will increase. In the long run the soil will *swell* (or heave).

The swelling will produce a conspicuous effect in excavating fairly large and deep (some tens of metres) open cuts.

### Sec. 14.2. Characteristics of Soil Compressibility

To be able to predict soil subsidence induced by an increased load, apart from the magnitudes of pressure causing this displacement, we must know definite index characteristics of the soil's compressibility. These latter are called *compression characteristics*.

We must know the relationship between the voids ratio,  $\varepsilon$ , and the pressure,  $p$ , written as  $\varepsilon = f(p)$ ; the value of the *coefficient of consolidation or compressibility*,  $a$ ; the *modulus of total soil deformation*,  $E_p$ ; the value of the relative deformation,  $e_p$ .

**The voids ratio-pressure  $p$  relationship.** It will be recalled that the *voids ratio*,  $\varepsilon$ , is the ratio of the void volume to the volume of the solid substance. Thus, the voids ratio,  $\varepsilon$ , referred to a definite load,  $p$ , is the measure of the soil's density at the given load. The voids ratio is a dimensionless characteristic.

It was Professor K. Terzaghi who proposed to express the measure of the load-induced compression of soils by a relationship between the voids ratio,  $\varepsilon$ , and the load,  $p$ :  $\varepsilon = f(p)$ .

The relationship in question is of a *logarithmic character* of this form

$$\varepsilon_p = \varepsilon_0 - \frac{1}{B} \ln(p + c) \quad (14.1)$$

where  $\varepsilon_p$  is the voids ratio at a load  $p$ ;  $\varepsilon_0$  is the voids ratio of the soil in its original state of density;  $B$  and  $c$  are parameters determined from experience.

The above equation is rarely used for practical purposes. Use is generally made of tabular data or, more commonly, *compression curves* are plotted. The general view of such a curve describing the relationship  $\varepsilon_p = f(p)$  is given in Fig. 14.1, where two branches are plotted. The *a* branch corresponds to a common compression curve that characterizes the soil's compressibility (compression branch).

The *b* branch is called the *soil's decompression, expansion or swelling branch*. The decompression branch indicates the change of the voids ratio,  $\varepsilon$ , in the given case, increase induced by the expansion of voids and likely

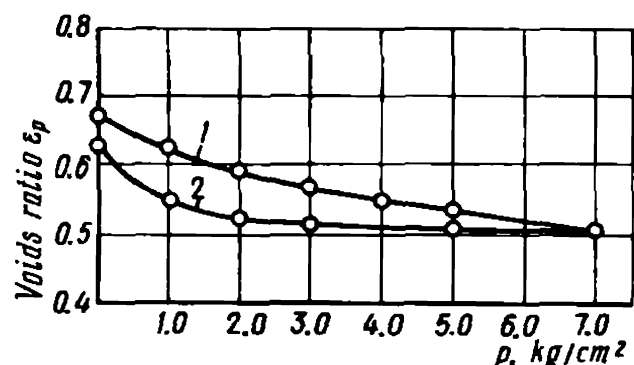


Fig. 14.1. Compression curves as an  $\varepsilon_p = f(p)$  relationship for alluvial loams at  $w = 26.2\%$ :

1—consolidation (loading) branch; 2—same, of decompression

additional saturation of the soil after removal of part of the load. The decompression curve is usually plotted only in special cases.

To determine the voids ratio,  $\varepsilon$ , referred to a definite load,  $p$ , we must in the general case know the density of the skeletal particles of the soil,  $\rho_0$ , as well as its bulk density,  $\rho_w$ , and moisture content,  $w_p$  (in fractions of unity) characteristic of this state. The ratio,  $\varepsilon_p$ , is then found from the following relationship:

$$\varepsilon_p = \frac{\rho_0(1 + w_p) - \rho_w}{\rho_w} \quad (14.2)$$

In a particular case, under conditions of *complete saturation* of the soil (degree of saturation  $G = 1.0$ ), the ratio  $\varepsilon_p$  is found from this equation:

$$\varepsilon_p = \rho_0 w_p \quad (14.3)$$

**Example.** The soil's density  $\rho_0 = 2.70$  (dimensionless quantity); moisture content at a load  $p = 3.0 \text{ kg/cm}^2$  is  $w_3 = 25\%$ .

At this load the voids ratio is found from Eq. (10.3):

$$\varepsilon_3 = 2.70 \times 0.25 = 0.670$$

As can be seen, the determination of the value of the soil compressibility from the relationship  $\varepsilon_p = f(p)$  by using (14.2) and, even in the simplest case, at a complete saturation of the soil ( $G = 1.0$ ) calls for a number of additional laboratory and computational operations (determination of the soil's moisture content, unit density and bulk density).

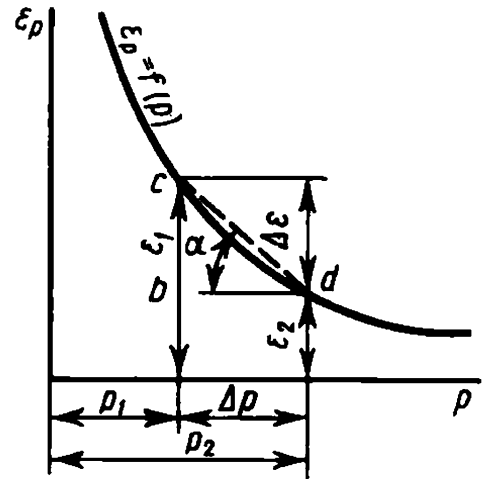
The application of the above relationship for calculations (e.g. for prediction of structure settlement) also involves much arithmetic. Moreover, the equation  $\varepsilon_p = f(p)$  lacks clarity and operates with quantities little known by the engineer. It must also be kept in mind that the measure of load  $p$ -induced soil compressibility is provided not by voids ratio,  $\varepsilon_p$ , itself, but, rather, by the variation in the voids ratio ( $\Delta\varepsilon$ ), caused by that load.

In addition, calculations of soil compressibility, using this method, invariably need tabular data or graphs. The impossibility to express the compressibility characteristic by some numerical quantity makes often the task too difficult. For this reason the equation  $\varepsilon_p = f(p)$  is seldom used in practice.

*The coefficient of consolidation,  $a$* , as an alternative form of expressing the compressive characteristic of soils proposed at his time by prominent scientist N.M. Gersevanov is, to a certain extent, devoid of these limitations.

The expression of soil compressibility in terms of the coefficient of consolidation,  $a$ , relies on the principle of straightening of the compression

Fig. 14.2. Expression of soil compressibility in terms of the coefficient of compressibility  $a$ ,  $\text{cm}^2/\text{kg}$



curve of the form  $\varepsilon_p = f(p)$  at some segment of the curve (Fig. 14.2). It represents  $\tan$  angle of inclination ( $\tan \alpha$ ) of the compression curve at a given point to the horizontal, i.e. at a given load  $p$ . Thus  $a = \tan \alpha$ .

The value of  $a$  for some point  $p_i$  on the compression curve can be found from the right-angled triangle  $cbd$ . Clearly,

$$a = \Delta\varepsilon/(\Delta p) \quad (14.4)$$

A substitution in the above equation of  $\Delta\varepsilon$  and  $\Delta p$  by the respective values of  $\Delta\varepsilon = (\varepsilon_1 - \varepsilon_2)$  and  $\Delta p = (p_2 - p_1)$  yields

$$a = \frac{\varepsilon_1 - \varepsilon_2}{p_2 - p_1} \quad (14.5)$$

Clearly, in Eq. (14.5)  $p_1$  and  $p_2$  denote the original and the consequent load, and  $\varepsilon_1$  and  $\varepsilon_2$  the respective voids ratios. As follows from Eq. (14.5), the measure of the coefficient of consolidation,  $a$ , is opposite to that of stresses, i.e. expressed in  $\text{kg}/\text{cm}^2$ .

Given  $a$ , we can write the following *approximate* formula for compression within some narrow range of loads  $p_1$  and  $p_2$ .

$$\varepsilon_2 = \varepsilon_1 - a(p_2 - p_1) \quad (14.6)$$

where  $\varepsilon_2$  is the sought value of the voids ratio for a definite load  $p_2$ ;  $\varepsilon_1$  is the original (known) voids ratio for the original load  $p_1$ .

Thus the coefficient of consolidation represents the measure of *a decrease* of soil porosity,  $\Delta\varepsilon$ , following an *increase* of load by  $\Delta p$ . This circumstance (reversed direction of the process) permits one to write  $a = -\Delta\varepsilon/(\Delta p)$  or proceed to differentials

$$a = -\frac{d\varepsilon}{dp} \quad (14.7)$$

The latter equation suggests, in theoretical terms, a variable

dependence of the mechanical soil characteristic on the load and, hence, is of much value.

The important advantage of  $a$  as one of compression characteristics is the possibility offered by it to express soil compressibility numerically. So, for  $p_1 = 1.0$  and  $p_2 = 3.0 \text{ kg/cm}^2$  along the compression branch of the compression curve (see Fig. 14.1) there are the values of  $\varepsilon_1 = 0.625$  and  $\varepsilon_2 = 0.570$ . Substituting these into Eq. (10.5) yields

$$a = \frac{0.625 - 0.570}{3.1 - 1.0} = 0.055 \text{ cm}^2/\text{kg}$$

Despite its obvious advantage, the method using the coefficient of consolidation is not, regrettably, free from limitations. Like the method relying on the voids ratio,  $\varepsilon$ , the given method lacks visuality.

The determination of  $a$  calls for the same subsidiary operations as that of  $\varepsilon$  followed by calculations using Eq. (14.5). Thus the application of  $a$  for predicting settlement means additional difficulty.

Depending on the value of  $a$ , the degree of soil compressibility may be roughly classified as follows:

Coefficient of consolidation $a$	Soil compressibility
< 0.001	Practically incompressible
0.001 to 0.005	Weak
0.005 to 0.01	Medium
0.01 to 0.10	High
> 0.10	Very high

**The expression of soil compressibility through the modulus of total deformation,  $E_p$ .** Experimental tests show that soil compressibility can also be expressed in terms of the modulus of total soil deformation,  $E_p$  ( $\text{kg/cm}^2$ ). In the given case  $E_p$  is an equivalent of the modulus of elasticity or Young's modulus,  $E$ , found, in conformity with the principal law of the theory of plasticity (Hooke's law) from the equation

$$E_p = p/e \tag{14.8}$$

where  $e$  is the relative deformation.

On the other hand, there is an essential difference between the modulus of deformation,  $E_p$ , as a measure of soil compressibility and Young's modulus. This difference stems from the distinct nature of soils as specific physical bodies.

We have already emphasized the role of residual deformation in soil consolidation. Unlike Young's modulus,  $E$ , the modulus of total deformation,  $E_p$ , invariably represents both the elastic and irreversible fraction of

the total soil deformation. This fact is revealed in the name of  $E_p$  as a modulus of total soil deformation. Moreover, as has been reported, the rate of soil compressibility, as the soil is consolidated under a load, does not remain unchanged but decreases with enhancing soil density. This results in the variation of the value of and in the dependence of  $E_p$  on the load,  $p$ , which is indicated by the subscript of the definition of  $E_p$ .

Thus  $E_p$  is connected with  $p$  through a definite functional relation:

$$E_p = f(p)$$

At the same time, as is known, when making calculations, Young's modulus,  $E$ , is assumed to be constant and independent of the load ( $E = \text{const}$ ). In view of the above properties of  $E_p$ , Eq. (14.8) for the determination of  $E_p$  at some specified value of  $p$  through the relative deformation,  $e_p$ , will take on this form:

$$E_p = p/e_p \quad (14.9)$$

This relation may be used for the determination of  $E_p$  in simplest terms, through  $p$  and  $e_p$ .

**Example.** A soil sample of a height  $h = 4$  cm at a load  $p = 0.75$  kg/cm<sup>2</sup> (0.075 MPa) has settled by  $\Delta h = 0.2$  mm. Determine the modulus of total deformation,  $E_{0.75}$ .

The relative deformation is

$$e_{0.75} = \Delta h/h = 0.2/40 = 0.005$$

Then, by virtue of Eq. (14.9), we will get

$$E_{0.75} = 0.075/0.005 = 125 \text{ kg/cm}^2 \text{ (12.5 MPa)}$$

According to the Soviet Code of Practice SNiP II-15-74 (Appendix 2, Tables 1 and 2),  $E_p$  for sandy soils, depending on the grain size and density, ranges from 100 to 500 kg/cm<sup>2</sup> (10 to 50 MPa). For clayey soils, depending on their genesis, consistency,  $I_L$ , and voids ratio,  $\varepsilon$ , the value of  $E_p$  may vary from 50 to 750 kg/cm<sup>2</sup>, the average value being 200 kg/cm<sup>2</sup> (20 MPa).

Calculations can use  $E_p$  in the above form, i.e. as some functional dependence on the load in conformity with Eq. (14.9). At the same time it may sometimes prove practicable to assume  $E_p$  to be constant for some soil variety ( $E = \text{const}$ ).

The assumption of the independence of  $E_p$  of  $p$  in general, including the value of the natural (normal) pressure  $p_{nat}$  is only little founded. The fact is that the allowance for this dependence in calculations with the purpose of predicting structure settlement by using the modulus of subsidence,  $e_p$ , described below, presents no difficulty.

**The modulus of subsidence (compressibility)  $e_p$ .** The general form of Eq. (14.9) suggests a possibility of directly using the relative deformation,  $e_p$ , as a measure of soil compressibility. It would rule out a need in all subsidiary determinations ( $\rho_0, \rho_w, w$ ) for calculations involved in the establishing of the voids ratio or modulus of deformation,  $E_p$ .

When determining  $e_p$ , at a load  $p$  ascertain experimentally the absolute value of the increment of the compression  $\Delta h$  of a sample with a height  $h$  and calculate then  $e_p$  from a simple equation

$$e_p = \Delta h/h \tag{14.10}$$

All intermediate operations are unnecessary.

As follows from Eq. (14.10), the modulus of subsidence is a dimensionless quantity. It may be used in practice in per cent or per mil ( $\text{‰}$ ). The latter measure is especially convenient. The subscript  $p$  in the definition,  $e_p$ , indicates the value of  $p$  to which the given value of  $e_p$  corresponds.

The modulus of soil subsidence demonstrates then the degree of deformation, i.e. the value of the compression in mm of a 1 m high column of soil to which an additional pressure,  $p$ , is applied. Equation (14.10) can thus be rewritten as

$$e_p = 1000 \Delta h/h \text{ mm/m} \tag{14.11}$$

The characteristic  $e_p$  has a definite engineering meaning and is easy to handle. Let  $e_2 = 20 \text{ mm/m}$ . It follows that a 1 m thick layer of the given soil after a load  $p = 2 \text{ kg/cm}^2$  has been applied to it will settle by 20 mm. Clearly, a settlement (or subsidence)  $\eta'$  for the case of a one-dimensional problem of the same soil (the load remaining the same) of a layer with a thickness  $h$  can be easily found from the equation

$$\eta' = e_p h \tag{14.12}$$

The relationship  $e_p = f(p)$  in a graphical form is also expressed by a compression curve (Fig. 14.3). Two branches are also plotted here, of

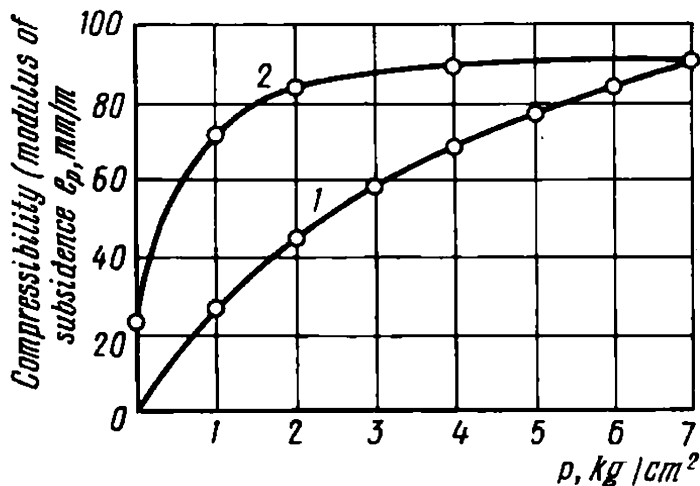
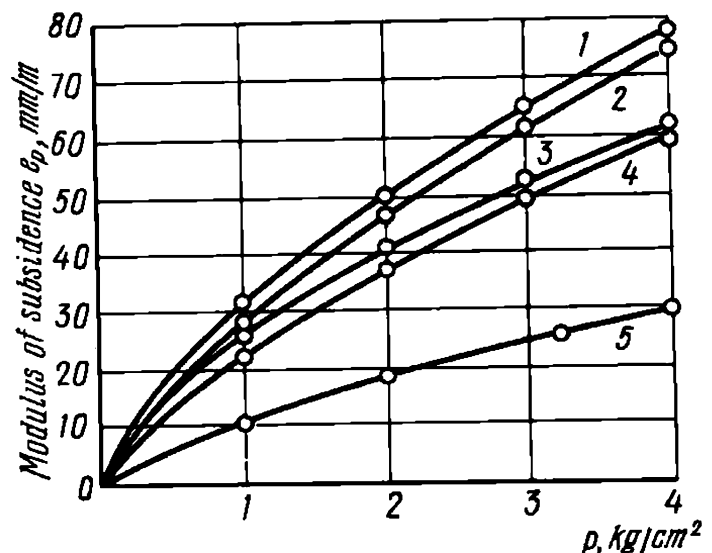


**Fig. 14.3.** Compression curves in the form of the relationship between the modulus of subsidence  $e_p$  and load  $p$ .  
Alluvial loams at  $w = 26.2\%$ :  
1—consolidation (loading) branch;  
2—decompression (unloading) branch



Fig. 14.4. Compression curves for Quaternary ancient lagoonal loams:

Nos of curves .....	1	2	3	4	5
Moisture content $w$ , % .....	32	29	27	28	24
Clay content $d$ , % ...	23	21	18	19	17
(content of fractions < 0.005 mm)					



which branch 1 corresponds to compression, branch 2 to decompression.

The diagram in Fig. 14.4 shows several compression curves of an  $e_p = f(p)$  form for old lagoonal loams of different clay content  $d$  (with grains less than 0.005 mm) and moisture content  $w$ . The diagram distinctly shows an increase in the compressibility of the soil with increasing its clay content and, consequently, moisture content.

The degree of soil compressibility referred to the value of the modulus of settlement  $e_p$  at  $p = 3 \text{ kg/cm}^2$  can be described by the following data:

Category of soil compressibility	Modulus of subsidence $e_p$ , mm/m	Compressibility
0	1	Practically zero
I	1 to 5	Weak
II	5 to 20	Medium
III	20 to 60	Increased
IV	60	Strong

The compression curves of the form  $\varepsilon_p = f_1(p)$  and  $e_p = f_2(p)$  are related through conversion formulae. These are deduced from the following considerations. Suppose a sample of some soil variety,  $h$  cm high, is being compressed at a load  $p$ , the specimen being enclosed in a metal ring preventing its lateral expansion. The cross sectional area of the sample  $\omega = \text{const}$ . The initial density is determined from the value of porosity  $n_0$ . Under a load the sample is being consolidated to reach a new density state with porosity  $n_p$ .

By taking into account Eq. (14.11) and expressing the relative deformation in per mil we obtain

$$e_p = 1000 \frac{\varepsilon_0 - \varepsilon_p}{1 + \varepsilon_0} \quad (14.13)$$

We can easily find the values of the modulus of subsidence,  $e_p$ , using this equation, from the specified values of the voids ratios  $\varepsilon_0$  and  $\varepsilon_p$  corresponding to the loads  $p_0$  and  $p$ .

At the same time, by solving Eq. (14.13) with respect to  $\varepsilon_p$ , we will have a formula making it possible to change the compression curve plotted as  $e_p = f_1(p)$  for an  $\varepsilon_p = f_2(p)$  curve. By taking into account the fact that the modulus of subsidence is expressed in per mil, we will have the following relationship:

$$\varepsilon_p = \varepsilon_0 - (1 + \varepsilon_0)(\Delta h/h)$$

(14.14)

The latter equation is used to determine the actual voids ratio  $\varepsilon_p$  at a load  $p$  in the course of compression test from the value of the initial voids ratio  $\varepsilon_0$  and the relative compression of the sample  $\Delta h/h$  under the given load.

Let us finally consider an example of determination of the compressibility of some definite soil variety by using different methods. Figure 14.5 presents the  $\varepsilon_p = f_1(p)$  and  $e_p = f_2(p)$  curves for an old lagoonal loam with the moisture content  $w = 29\%$  (curve 2 in Fig. 14.4). The data from which these curves have been plotted, together with compressibility constants determined by other methods, are listed in Table 14.1.

When plotting an  $e_p = f_2(p)$  compression curve in Fig. 14.5 through a voids ratio  $\varepsilon$  we have employed a transition formula (14.13). In particular, for the determination of the modulus of subsidence  $e_2$ , i.e. at a load  $p = 2 \text{ kg/cm}^2$  (0.2 MPa) we have

$$e_2 = 1\,000 \frac{0.866 - 0.778}{1.0 + 0.866} = 47.2 \text{ mm/m}$$

and at a load  $p = 4 \text{ kg/cm}^2$  (0.4 MPa) we have

$$e_4 = 1\,000 \frac{0.866 - 0.726}{1.0 + 0.866} = 75.3 \text{ mm/m}$$

Table 14.1

Characteristics of Compressibility of Ancient  
Lagoonal Loam by Different Methods

Load $p$ , kg/cm <sup>2</sup> (0.1 MPa)	Voids ratio $\varepsilon$	Coefficient of con- solidation $\alpha$ , cm <sup>2</sup> /kg	Modulus of sub- sidence $e_v$ , mm/m	Modulus of total deforma- tion $E_p$ , kg/cm <sup>2</sup>
0	0.866	—	—	—
1	0.818	0.048	25.8	39
2	0.778	0.040	47.2	42
3	0.750	0.028	62.6	48
4	0.726	0.024	75.3	53

Let us find the coefficient of consolidation  $a$  from Eq. (14.5) for the load range  $p_1 = 2 \text{ kg/cm}^2$  (0.2 MPa) and  $p_2 = 3 \text{ kg/cm}^2$  (0.3 MPa).

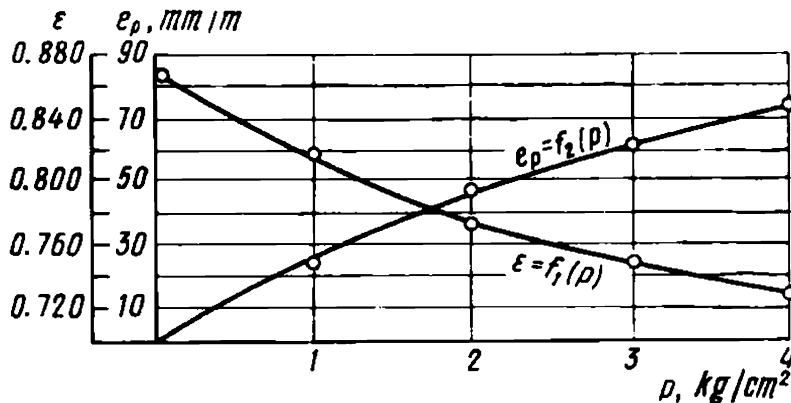


Fig. 14.5. Compression characteristics of ancient lagoonal loams presented in different forms (curve No. 2 in Fig. 14.4)

By substituting the corresponding values of  $\epsilon_p$  from Table 14.1 into this equation we obtain

$$a_3 = \frac{0.778 - 0.750}{3.0 - 2.0} = 0.28 \text{ cm}^2/\text{kg}$$

Let us, at last, find the modulus of total deformation  $E_p$  at a load  $p = 4 \text{ kg/cm}^2$  (0.4 MPa) from Eq. (14.9) bearing in mind that the modulus of subsidence  $e_4$  is expressed in per mil:

$$E_4 = 1000 \frac{4.0}{75.3} = 53 \text{ kg/cm}^2 (5.3 \text{ MPa})$$

### Sec. 14.3. Methods of Determination of Characteristics of Soil Compressibility

The test aimed at the determination of characteristics of soil compressibility consists in the observation of the linear pressure (subsidence  $\Delta h$ ) of a soil sample to which a load  $p$  is applied.

The soil sample is compressed in a closed ring, such that its lateral expansion is excluded (Fig. 14.6). The pressure is imparted to the sample by weights using levers through the medium of a pressure pad or loading piston in which a porous stone is inserted. The porous stone permits the moisture to be squeezed out of the loaded sample.

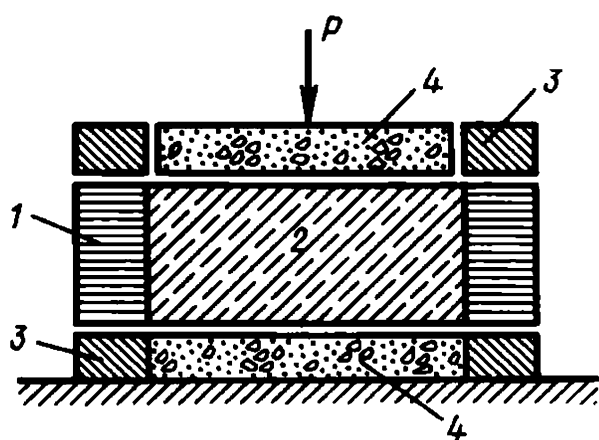


Fig. 14.6. Direct shear test:  
1—box; 2—soil sample; 3—ring; 4—porous stone;  
 $P$ —load

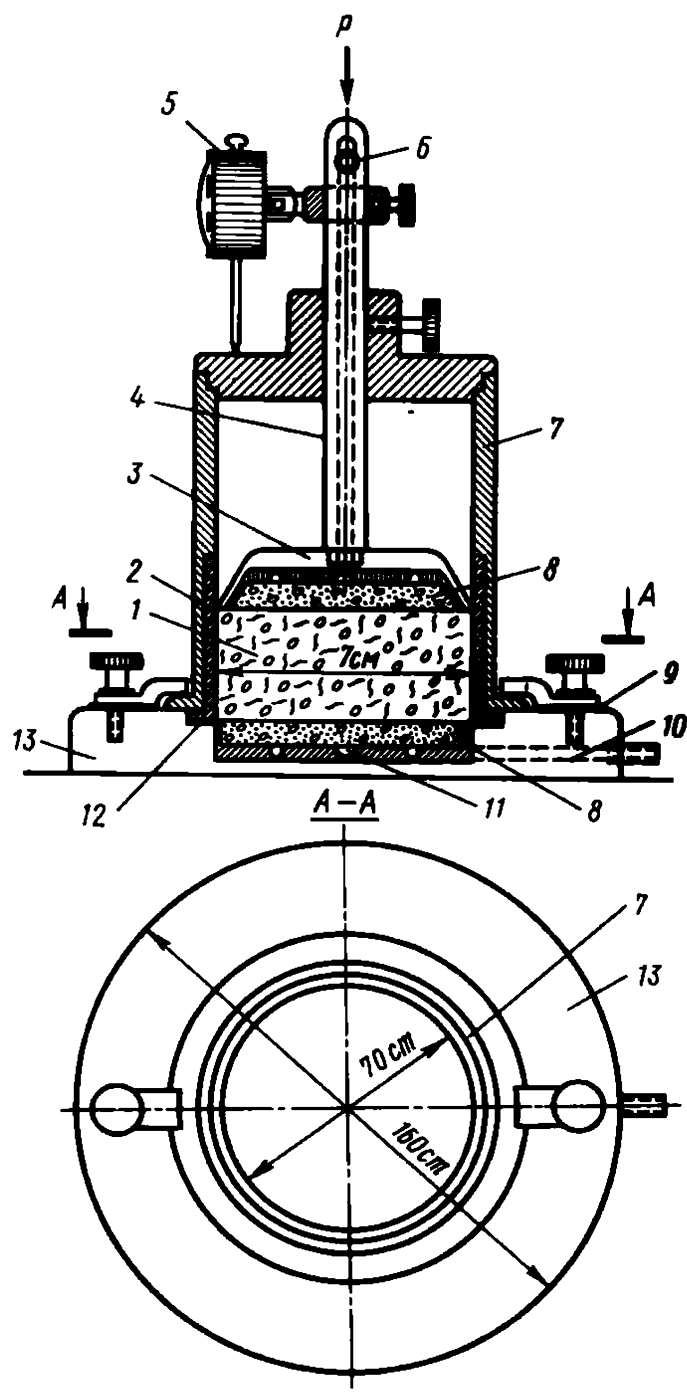


Fig. 14.7. Model MБC compression apparatus:

- 1—undisturbed rock sample; 2—perforated ring; 3—piston; 4—guiding rod; 5—micrometer dial gauge with adjusting ring and stop screw; 6—nipple; 7—cylinder; 8—porous stones; 9—rubber gasket; 10—conduit with nipple for drainage of water; 11—ring-shaped recesses; 12—rubber rings; 13—tray

The observation of the settlement of the sample induced by the load is performed using a special dial gauge accurate to the thousandth fractions of the millimetre. The testing device is generally filled with water to prevent dessication of the sample during the test. The test is, as a rule, conducted at several successively increased loads. The sample is maintained at each of these loads in the device until the onset of complete deformation stabilization (attenuation of settlement). Sometimes several weeks are needed until a soil is consolidated completely under one load or another.

Consolidation devices (oedometers) may very much differ in design but the principle remains the same. Figure 14.7 is a diagram of a consolidation device designed by Maslov and Baldysh.

A soil sample is commonly taken from the soil mass at a depth  $z$ . At this depth the soil sustains the weight of the overburden responsible for the magnitude of the natural (or normal in Terzaghi's terminology) load  $p_{nat}$ . Clearly,

$$p_{nat} = \rho_w z \quad (14.15)$$

where  $\rho_w$  is the bulk density of the overburden taking into account, when necessary, the buoyancy due to subsurface water.

The initial soil density should in principle correspond to the load  $p_{nat}$ . Consequently, at loads  $p < p_{nat}$  no compression must occur and it needn't be accounted for when determining the characteristics of soil compressibility. Hence the deformation of a soil sample acted on by a normal pressure should only be estimated if a load  $p = p_{nat}$  or above it (Figs. 14.8 and 14.9).

The removal of a soil sample from the soil mass almost invariably results in *initial decompression* of the soil accompanied by additional absorption of water and air and production of gas. The most important is the former factor (decompression due to additional permeability), especially when samples for consolidation tests are taken from appreciable depths, from beneath a body of water and sampling is time-consuming. Disregarding this factor may cause gross errors, often of the order of hundreds of per cent. To avoid the distortion of the observed results it is important that the first load in the test be higher than one corresponding to the natural soil density, or that at minor loads the test be performed in a wet medium without immersing the sample.

When studying the compressibility of dense clay samples the results of the test may prove to be in error (to several hundreds of per cent) because of the so-called plastic deformations. These deformations are due to dislocations of the soil sample inaccurately cut and poorly adjusted to the ring of the testing device. In such a case the directly obtained linear value

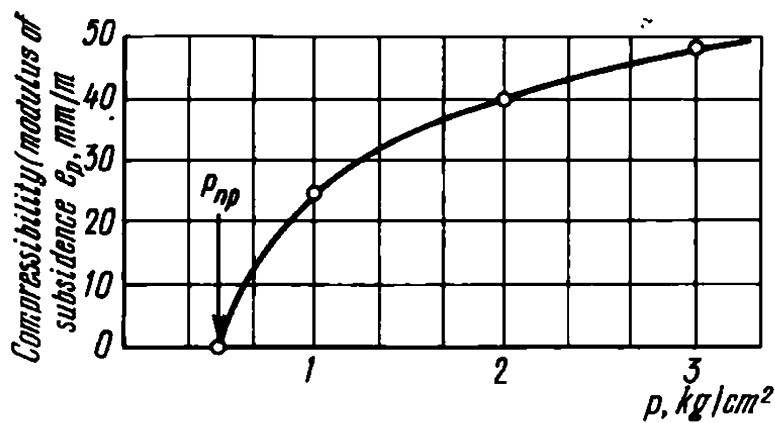


Fig. 14.8. Taking into account the weight of the overlying rock mass ( $p_{nat}$ ) when determining soil compressibility

of compression (settlement) of the sample  $\Delta h$  is checked by using alternative methods (referring to weight).

For a soil with a high degree of saturation ( $G = 1$ ) the voids ratio can be determined, whatever the state of the soil sustaining the load in terms of the moisture content, by using the familiar relationship  $\varepsilon_p = \rho_0 w_p$  [see Eq. (14.3)], where  $\rho_0$  is the soil's density (dimensionless).

To have a check on the value of the modulus of subsidence  $e_p$  for similar permeable soils the sample is weighed before and after the test. Then the following relationship is used:

$$e_p = 10\,000 \Delta Q / (h \omega)$$

(14.16)

where  $\Delta Q$  is the loss in the sample's weight due to the water squeezed out of it at a pressure  $p$ , in g;  $h$  is the original height of the sample, in cm;  $\omega$  is the cross sectional area, in  $\text{cm}^2$ .

For *soils containing air*, such methods of checking cannot be applied. The modulus of subsidence is then checked by referring to the change in the

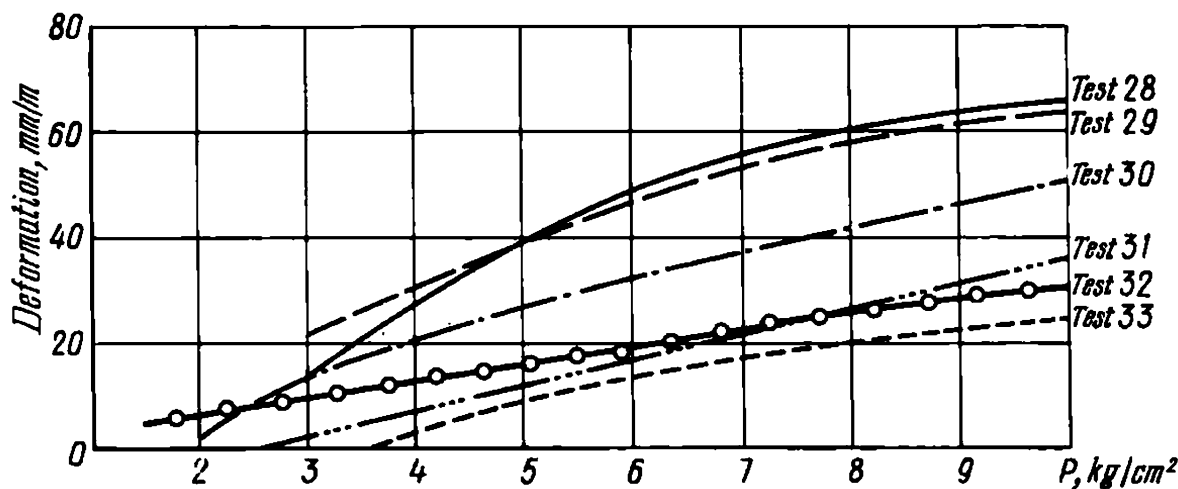


Fig. 14.9. Effect of the weight of the overburden on soil compressibility. Soft plastic Devonian clay

soil porosity,  $n$ , during the test using this relationship:

$$e_p = 10\,000 \frac{n_0 - n_1}{1 - n_1} \quad (14.17)$$

where  $n_0$  is the soil's porosity before the test;  $n_1$  is the soil's density at one or another degree of consolidation due to a load.

A very important element of a consolidation test is the study of the time rate of the load-induced compression of the soil. The functional dependence of the modulus of subsidence  $e_p$  on time is essential for predicting the settlement of a structure with time or for testing samples of different height to calculate stability of a structure's foundation if the underlying soil is poorly consolidated. The latter case calls for the determination of the coefficient of consolidation (see Sec. 22.2).

When evaluating the degree of stability of a soil mass at any stage of its consolidation pressure, we must establish, for the given load, the dependence of the moisture content on the duration of the sample's compression. If the test using a consolidation device employs a weight method, the moisture content  $w$  at a definite time moment  $T$  of the duration of the sample at pressure is found from the relationship

$$w_T = w_0 - \frac{Q_0 - Q_T}{Q_0} (1 + w_0) \quad (14.18)$$

where  $w_0$  is the soil's moisture content by the beginning of the test in fractions of unity;  $Q_0$  is the weight of the sample with the ring before the test;  $Q_T$  is that at a time moment  $T$  following some consolidation at a load  $p$ .

The results of the test are processed graphically as shown in Fig. 14.10.

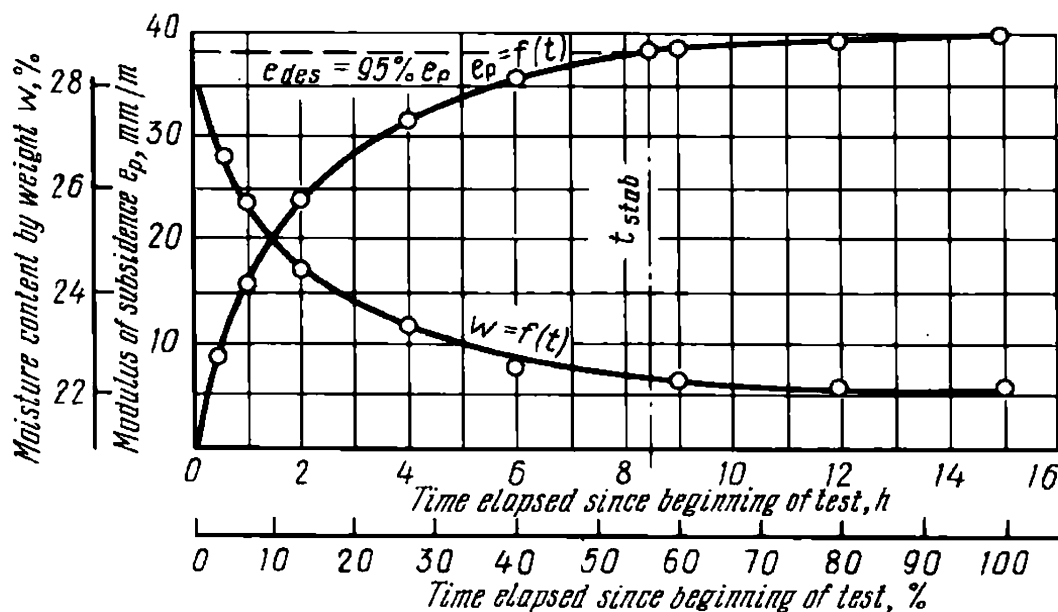


Fig. 14.10. Example of graphical treatment of time-dependent compression test

When conducting these operations it is generally difficult to determine the moment of the total compression of the samples  $t_{stab}$ .

Here are some data on the compressibility of clayey soils. As expected, the best in this respect are clayey soils belonging to the category of stiff, in particular, pre-Quaternary, varieties. These soils are generally characterized by a modulus of compression (deformation) which is on the average  $e_{2-2.5} = 5$  to  $8$  mm/m at the moisture content 8 to 15% or even 21%. Such are, e.g. Jurassic clays found in the Moscow Region referred to in Chapter 13.

In marly clays the modulus of compression or deformation often exceeds  $1\,000$  kg/cm<sup>2</sup>. Naturally, the deformability of weathered varieties increases, remaining, however, fairly great (modulus of deformation  $E_p = 250$  to  $400$  kg/cm<sup>2</sup>).

The deformability of bedrock clays with a softer consistency is accordingly higher. Such are, e.g. Cretaceous (Aptian) clays found in the vicinity of the town Gus'-Khrustal'ny. At a stiff plastic consistency ( $I_L = 0.50$ ) and average density ( $\varepsilon = 0.80$ ) they have a modulus of compression about  $e_2 = 30$  mm/m.

Of interest are deformability characteristics of Buchag and Kievan Tertiary clays widely distributed in the southern regions of the USSR. In particular, the modulus of compression (or deformation) of Buchag clays is  $e_5 = 25$  mm/m. Useful information is provided by tests of Kievan marly clays occurring in the same area with a semihard and hard consistency. At  $w = 34\%$ , the angle of friction  $\varphi = 20^\circ$  and cohesion  $c = 0.40$  kg/cm<sup>2</sup> they have a modulus of compression  $e_{3-5} = 20$  to  $30$  mm/m.

Gray Paleogene clays found in West Siberia also evoke much interest. They manifest an unusually low compressibility ( $e_{2-3} = 10$  to  $20$  mm/m) and a fairly high compressive strength, about  $6$  to  $11$  kg/cm<sup>2</sup>, at a very low density ( $\varepsilon = 1\,600$  to  $1\,700$  at  $\rho_w = 1.35$  to  $1.45$  t/m<sup>3</sup>). In addition, these materials are impervious. The above disagreement in their properties should be ascribed to the flask-like character of these materials (cementation by siliceous material at an early stage of formation, presence of agate and chalcedony).

We have mentioned the increased strength and lowered compressibility of layered clays. There are exceptions in the rules, however. One of classic examples is provided by soft plastic Devonian clays whose deposits serve as a support for structures of the Svir River Hydro-Electric Power Development that presented much trouble to the builders since the modulus of deformation of these soils is  $e_{3.5} = 10$  mm/m.

At this point we should warn against exaggerating indices of the compressibility of clays of a solid or semisolid consistency from the data of laboratory tests as a result of plastic deformation of the soil sample itself



(constant-volume deformation). Such types of deformation increase the soil compressibility by hundreds of per cent, deformations change in sign due to the swelling (heave) of the soil etc.

Quaternary clayey soils of weaker consistency typically possess an enhanced compressibility. The common and important feature of all these clay varieties is the dependence of the strength and deformation resistance on the moisture content and, consequently, consistency of the soil.

This feature is especially shared by Khvalynian clays in the Volga River Basin that very much differ in the moisture content. Their compressibility likewise very much fluctuates. The corresponding modulus of deformation also varies in a very wide range from 5 to 50 mm/m. Matters are complicated as to their tendency to swell.

Heavy loams with an increased porosity found in the area of the Penza watch-making factory resemble the above soil varieties. They have the voids ratio  $\varepsilon = 0.856$  to  $1.646$ , porosity  $n = 47$  to  $62\%$  at a moisture content  $w = 17.5$  to  $44.5$  ( $w_{aver} = 35\%$ ). The difference in the characteristics of these soils stems from the different backgrounds of their formation. Moreover, these soils exhibit definite subsidence (see Chapter 36). The modulus of sag in these soils is  $e_{sag} = 0$  to  $54$  mm/m.

Naturally, very permeable silty soils in a plastic liquid, to say nothing of a liquid, state may exhibit a very high compressibility. Typical in this respect are silts found in the Straight of Kerch with the moisture content above  $100\%$  which have a modulus of compression about  $e_1 = 250$  to  $300$  mm/m.

In our opinion, little purpose is served by studying the compressibility of sandy soils using consolidometers. The matter is that it is impossible, in experimental conditions, to simulate the natural occurrence of the sand mass and, accordingly, its behaviour *in situ*. The compressibility of sandy soils at a static load is generally inappreciable. Things stand differently with a dynamic load. This point is considered in Chapters 24 and 25. That is why the main requirement to be met when designing a structure supported by sandy soil under conditions of a static load is ensuring the stability of such a soil.

For fresh littoral sands with fractions of crushed shells found in the north eastern areas of the Black and Azov seas, generally silt-covered, the angle of internal friction is about  $30^\circ$ , the modulus of deformation  $300 \text{ kg/cm}^2$  ( $30 \text{ MPa}$ ). If relevant measures are taken, such sands may provide a reliable support for engineering structures.

Some remarks should be made concerning the compressibility of rock masses that are fissured due to normal stresses. The modulus of deformation of a massive rock is fairly high, generally of the order of hundreds of

thousands of  $\text{kg}/\text{cm}^2$ . Under conditions of weathering this characteristic decreases accordingly still amounting to tens of thousands of  $\text{kg}/\text{cm}^2$ .

Depending on similar conditions, the modulus of deformation of schists varies within a very wide range, from several thousand or hundred to hundreds of thousands of  $\text{kg}/\text{cm}^2$ . The modulus of deformation of gneissose granites found in the vicinity of the Dniester River for a fractured massive rock is not more than  $500 \text{ kg}/\text{cm}^2$ , for a sound rock mass it is up to  $500\,000 \text{ kg}/\text{cm}^2$ . The deformation of compaction of rock masses is mainly due to the closing of fissures after the rough surfaces of their walls have been smoothed and also to compaction of the fissure-filling material. This process takes time to occur.

Of considerable importance is the deformation of the massive rock under the aforementioned conditions acted on by lateral pressure, e.g. at the toe of a retaining wall and in the soil mass of a slope or hillside. Under certain conditions these deformations or dislocations which are time-dependent may take on a form of a pseudocreep and prove rather troublesome.

---

## Chapter 15

### Determination of Index Characteristics of Soils

---

#### Sec. 15.1. Basic Concepts

Index properties of definite soils occurring in a chosen horizon obtained by laboratory tests generally differ appreciably from job to job.

To be able to use certain characteristics for calculations the knowledge of definite quantities attesting to the physicommechanical properties of soils is needed. Thus we come to what are called *design values* of different index characteristics.

Proper care should be taken in determining these characteristics, especially ones of the strength of a soil, i.e. the angle of internal friction ( $\varphi_w$ ) and cohesion ( $c_w$ ). Exaggerated values of such characteristics in calculations may lead to the loss of stability and permanence of a structure. On the other hand, underestimation of soil properties often means excessive amounts of work, sophisticated protective measures, especially against landslides, and, as a result, unwarranted rise in costs in terms of money and time.

Hence a need in *reasonable averaging* of the experimentally obtained

data, generally with a certain margin of safety, depending on the number of experimental tests. It would be wrong to consider the arithmetic mean of one characteristic or another as a true one under conditions of a limited number of experimental determinations. The true value of, say, the angle of a soil's shearing resistance may theoretically be established only if an infinite number of experimental determinations,  $n$ , have been taken. If a limited number of tests have been made, e.g. to determine the shearing resistance,  $s_{pav}$ , its mean value may differ from its true value, the less is the number of shear tests.

Thus it becomes necessary to average design characteristics as definite *guaranteed* values to a certain degree of confidence governed by the number of the available experimental determinations,  $n$ . It is best to perform this operation by resorting to methods of *mathematical statistics*.

This method, however, may be used if an appreciable number  $n$  (at least 10 to 15) of experimental determinations, whose accuracy is not always known, have been made. At the same time the method requires much effort which is another constraint on its applications. This gave rise to approximate methods of the determination of various soil characteristics which will be considered in part in what follows.

### Sec. 15.2. Abridged Methods for Determining Design Characteristics

It is general practice to determine design characteristics from the average minimum or average maximum (for moisture content,  $w$ ) values of their experimental determinations, i.e. as the mean between the minimum (maximum) and the average values.

Despite its obvious simplicity, the method has a disadvantage: the number of trials is not taken into consideration. Moreover, the number of tests to determine the mechanical characteristics of soils (strength or compressibility indices) is generally small. Therefore, it is better to apply the same principle to determine design values of, say,  $\varphi_c$  and  $c_c$  from a diagram in Fig. 13.13 referring to the design value of  $w_c$  as an average maximum one.

What in this case facilitates the task is the availability of data on the soil's moisture content determined as a Class Two index from disturbed samples. It should be borne in mind that  $w_c$  must be greater than  $w_{av}$  since design values of  $\varphi_c$  and  $c_c$  decrease as the moisture content,  $w$ , increases. Yet even in this case the insufficient number of tests to determine design values of soil indices may cause accidents or unwarranted rise in costs.

An appreciable advantage coupled to great simplicity is offered by a method of guaranteed values of indices, e.g.  $\varphi_{w guar}$  and  $c_{w guar}$ . This

method, relying on principles of mathematical statistics, can be understood from a numerical example.

Suppose it is desired to determine the values of  $\varphi_{w guar}$  and  $c_{w guar}$  from a diagram of  $\varphi_w$  and  $e_w$  shown in Fig. 13.13, given 58 results of the soil's natural moisture content,  $w_{nat}$ , ranging from 24 to 43%. By dividing all moisture content values into 1% intervals we will obtain a number of values of experimental data falling in the particular interval. Let us define this number as a *frequency* and denote by  $m_i$ .

The values of frequencies corresponding to one interval or another are inserted in the respective columns in Table 15.1. For example, the frequency interval 32-33% corresponds to  $m = 6$ . Then calculate *the frequency rate*  $q_i$  in per cent. To find it from the frequency  $m_i$  divide the frequency in each interval by the total sum of trials,  $\Sigma n$ . In our case  $\Sigma n = 58$  determinations. Then the frequency rate  $q_i$  for the 32-38% interval will be  $q_i = 6/58 \times 100 = 10.3\%$ .

The frequency rate values are entered in the corresponding line of Table 15.1. Then calculate *the accumulated frequency rate*  $\Sigma q_i$  by successively adding together the frequency rates of individual moisture content intervals.

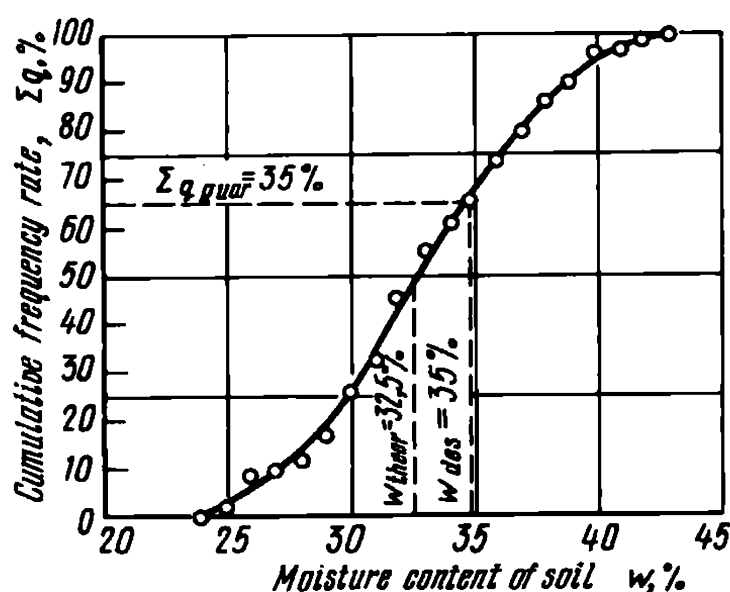
Table 15.1

Data for Plotting a Cumulative Curve to Illustrate Determination of Guaranteed Value of Moisture Content  $w_{quar}$  of Soil

Intervals of moisture content values, %	24-25	25-26	26-27	27-28	28-29	29-30	30-31	31-32	32-33	33-34
Frequency $m_i$	1	4	1	1	3	5	4	7	6	3
Frequency rate, $q_i$ , %	1.7	6.9	1.7	1.7	5.2	8.6	6.9	12.2	10.3	5.2
Cumulative frequency rate $\Sigma q$ , %	1.7	8.6	10.3	12.0	17.2	25.8	32.7	44.9	55.3	60.5

Intervals of moisture content values, %	34-35	35-36	36-37	37-38	38-39	39-40	40-41	41-42	42-43
Frequency $m_i$	3	5	3	4	2	3	1	1	1
Frequency rate, $q_i$ , %	8.5	5.2	6.9	3.4	5.2	1.7	1.7	1.7	1.7
Cumulative frequency rate $\Sigma q$ , %	65.7	74.2	79.4	86.3	89.7	94.9	96.6	98.3	100.0

Fig. 15.1. Determination of a guaranteed value of moisture content ( $w_{\text{guar}}$  of Neogene clays, the Ukraine) for assigning guaranteed values of the angle of internal friction  $\varphi_{\text{guar}}$  and cohesion  $c_{\text{guar}}$



For example, for the first interval the accumulated frequency rate is  $\Sigma q_1 = 1.7\%$ , for the second  $\Sigma q_i = \Sigma q_2 = 8.6$  etc.

The given calculations are also presented in Table 15.1. Clearly, the accumulated frequency rate for the last interval is  $\Sigma q_i = 100\%$ . From the data given in Table 15.1 plot a cumulative (integral) curve similar to a curve of granulometric analysis of sand in Fig. 15.1.

When establishing a guaranteed value of one characteristic of soils or another we must have what is known as a coefficient of confidence,  $a$ . In the given method, on theoretical premises, it is taken to be  $\alpha = 0.99$ . This condition guarantees the obtained value of an index which means that only in one case may the obtained value prove to be in excess of its true value. This is practically improbable.

Given a specified coefficient of confidence  $\alpha = 0.99$ , find from Table 15.2 the values of accumulated frequency rate  $\Sigma q_{\text{guar}}$  which is, naturally, increasing as the number of trials increases. In our case, after having 58 determinations of soil moisture content, according to the above table,  $\Sigma q_{\text{guar}} = 35\%$ , or, in view of the remark with respect to the guaranteed value,  $\Sigma q_{\text{guar}} = (100\% - 35\%) = 65\%$ .

Referring to Fig. 15.1, find the guaranteed value of the moisture content corresponding to  $\Sigma q_{\text{guar}} = 65\%$ ;  $w_{\text{guar}} = 35\%$ . Then, by referring to Fig. 13.13, it is possible to find the guaranteed values of  $\varphi_{\text{guar}} = 14^\circ$  and of cohesion,  $c_{\text{guar}} = 0.14 \text{ kg/cm}^2$ .

This method may be used to determine the guaranteed values of any characteristic of a soil's composition and state and to find a soil's shearing resistance or compressibility. As can be seen from Table 15.2, the method of average minimum and maximum values can only be applied if 25 to 35 determinations of one soil characteristic have been made.

Of a definite interest is a diagram in Fig. 15.2. As experimental data are

Table 15.2

Guaranteed Frequency Rate  $\Sigma q_{guar}$  Depending  
on the Number of Trials  $n$  at Degree  
of Confidence  $\alpha = 0.99$

Number of trials $n$	< 10	10-15	15-20	20-25	25-35	35-50	50-75	75
Guaranteed cumulative frequency rate $\Sigma q_{guar}, \%$	0	10	15	20	25	30	35	40

being made available, first determine the mean of the first two tests, then of three tests, four tests etc. of one and the same characteristic. Plot these values on the ordinate axis. Plot on the abscissa axis the definitions of the number of trials (tests) corresponding to definite mean values of index characteristics ( $n$ ).

As can be seen from Fig. 15.2, the intitally appreciable (with a small number of trials) spread of mean values of the shearing resistance at one or another load,  $p$ , drastically diminishes with increasing the number of trials. After only 25 trials the fluctuations of the mean values of a characteristic remain within reasonable limits sufficient for practical needs.

This indicates that we needn't continue the trials to determine the mean value of the index sought. If the number of trials is great it is helpful to use a logarithmic scale when plotting the abscissa axis for the given diagram.

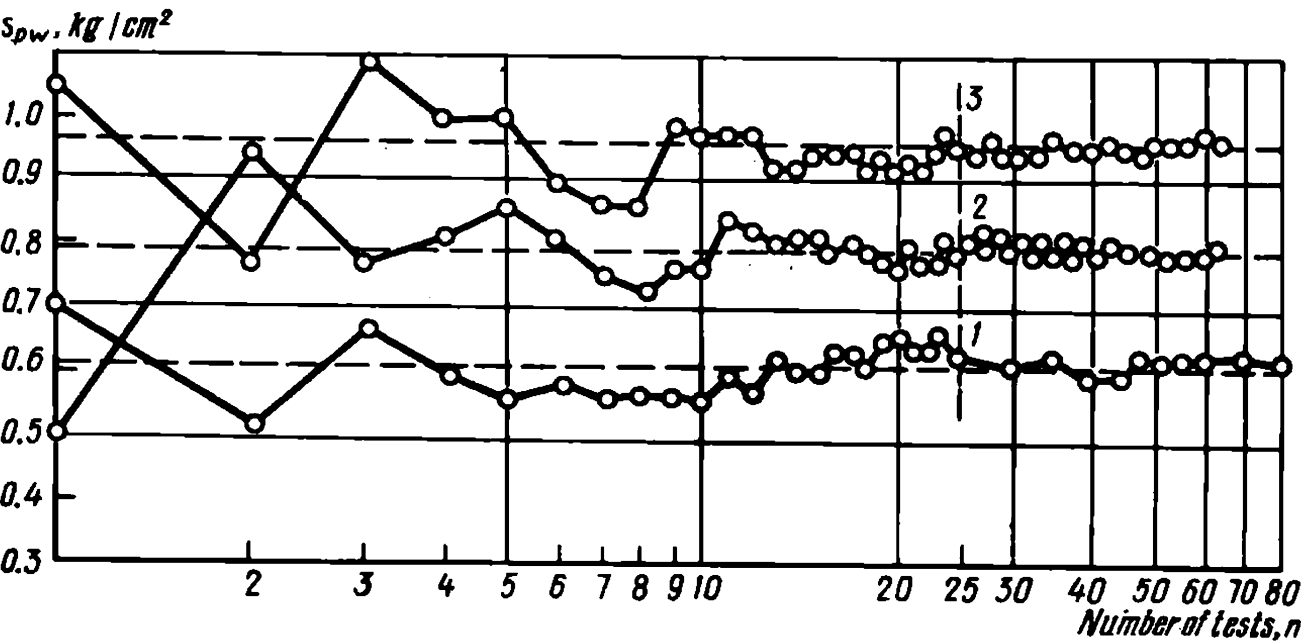


Fig. 15.2. Shearing stress of deluvial loams  $s_{pw}$  under loads  $p$ , equal to 1, 2, and 3  $\text{kg/cm}^2$  as the arithmetic mean of a series of trials depending on the number of trials  $n$

The above method of presenting the data of the tests is fairly efficient. It permits one to visualize the role and importance of the trials with the purpose, in the particular case, to study the shearing resistance of a clayey soil at different loads. This largely excludes gross errors in determining an averaged characteristic with a small number of trials.

In addition, this method makes it possible to establish the number of trials permitting averaging some definite characteristic relying on the data furnished by the trials at which no spread in mean values of the given index characteristic occurs any more. In the particular case this is achieved with 25 trials. Clearly, with a lesser number of trials the mean value of an index could not have been safely taken as the mean value determined by conventional methods.

## Part Three

### Basic Soil Mechanics

---

#### Chapter 16

#### The Behaviour of Soils in a Soil Mass in a State of Stress

---

##### Sec. 16.1. Fundamental Concepts

As has already been pointed out, it is the objective of engineering geology to study the geological features of the site of a proposed structure including soils and rocks that have specific traits and properties, geodynamic processes and events likely to present a hazard to the given structure and, finally, the regime of subsurface water at the particular job.

On the other hand, soil mechanics is the application of the principles of mechanics and geology during the construction and operation of engineering structures. These conditions are governed by the properties and composition of soils supporting the structure. Thus, soil mechanics is concerned with the evaluation of the strength and stability of soils supporting structure foundations and with a study of soil deformations induced by the applied forces, which are time-dependent processes.

Any loss in the strength and stability of the soil mass, and its deformations result from stresses. These latter include the own weight of the soil mass, the weight of the structure being built (dead load), and, in addition, external forces. Similar conditions may arise from environmental causes, such as seismic events, hydrodynamic forces etc.

To ensure the safe service of a structure it is necessary to control active stresses by using reactive forces of the resistance of the soil (earth pressure). Such conditions occur, in particular, in the foundation of a bridge pier imparting to the underlying soil the fraction of the weight of the bridge span (dead load) and of that of the traffic (live load).

Suppose that, owing to the joint action of the dead and live loads on the pier's base, the surface of the soil mass sustains a pressure along a band with a width  $B = 2b$  (Fig. 16.1). The magnitude and character of the pressure are not limited.

Let the origin of a coordinate system,  $O$ , be located at the centre of the loaded strip at a surface level of the soil mass (Fig. 16.1*a*). Draw the  $+Z$  axis vertically down, and the  $+X$  horizontally to the right of  $O$ . At a point  $A$  on the plane of the base of the loaded strip (under conditions of a plane



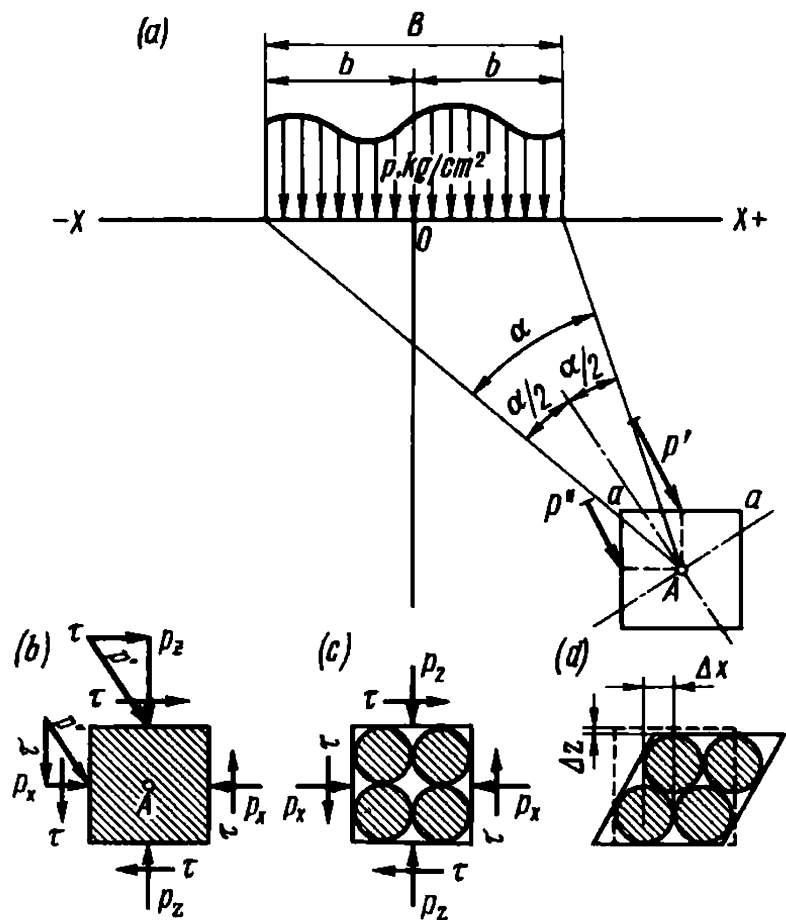


Fig. 16.1. State of stress and soil deformation at point A in a structure's subsoil

problem) choose an elementary square whose sides are  $aa$ ,  $ac$ , and  $cc$  arranged along the  $x$  and  $z$  axes, respectively.

Suppose that the stress from the load  $p_0$  along the strip  $B = 2b$  is distributed in the soil mass as *rays of force*. As it encounters the sides (faces) of the selected elementary square, each of the rays of force in contact with the element produces on these faces a definite effect in the form of total correspondingly directed stresses  $p'$  and  $p''$ .

In the general case the total stresses  $p'$  and  $p''$  will act on the sides of the element in question at an angle. Resolve  $p'$  and  $p''$  into components normal and tangential to the element's sides. Then the element will be found to be acted on by a system of active and reactive compressive normal stresses  $p_z'$  and  $p_x''$  and tangential (or shearing) stresses  $\tau$  (Fig. 16.1b). The orientation of the latter stresses,  $\tau$ , is governed by that of the total stresses  $p'$  and  $p''$  with respect to the sides of the elementary square.

Together with the reversibly directed reactive stresses on the opposite parallel faces the tangential stresses form two mutually balanced force couples.

The systems of normal  $p_z$  and  $p_x$  stresses (vertical and horizontal in the given case) exert an all-around pressure on the chosen element causing the consolidation of the soil and settlement of the structure. Viewed from this point, the normal stresses play a negative role. At the same time the system

of the shearing stresses causes a deformation in the aforementioned element.

Suppose further that the element includes several soil-forming grains (Fig. 16.1c). Assume these grains are spherical. According to the conditions of a plane problem we will have some circles in the element. The grains that are in close contact with the sides of the element respond to the slightest change in its shape. The distortion of the element, if the soil is insufficiently competent, is followed by a mutual displacement of the enclosed grains in the form of a *shear* (Fig. 16.1d). These grains move along some regular trajectories directed in the general case outward from the loaded strip and upward to the free surface of the soil mass.

If the process concerned is pronounced, the soil may squeeze out from beneath the foundation base which is likely to cause the total loss of stability by the structure's foundation. Thus we may state that the stability of the structure foundations is impaired by shearing (tangential) stresses. Under these conditions the tangential stresses that appear in the subsoil of a struc-

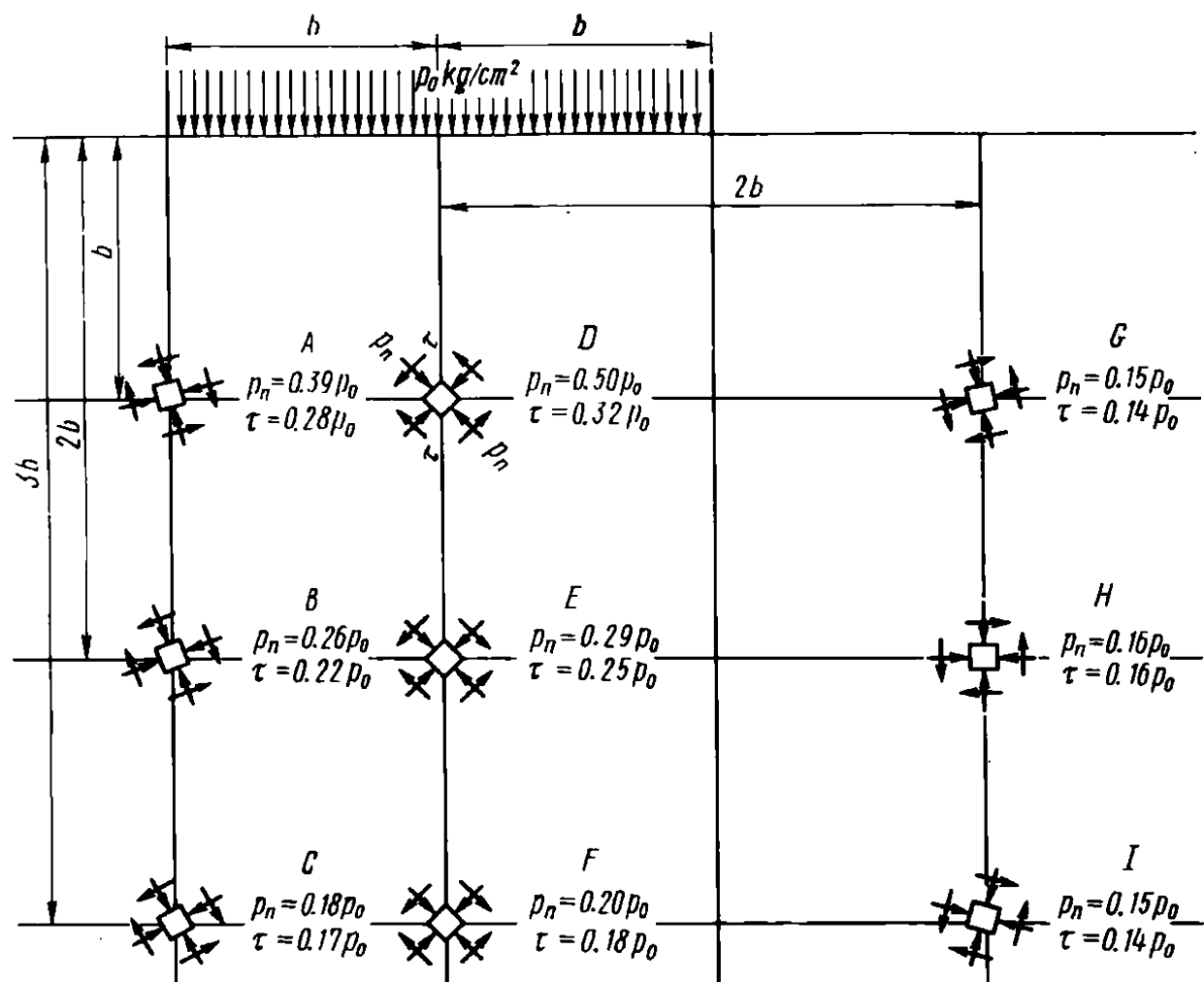


Fig. 16.2. Values of normal  $p_n$  and shearing  $\tau_{max}$  stresses for a given point depending on the location and orientation of the element

ture must be considered as an unfavourable factor which should be invariably taken into account when designing a structure.

The compressive normal stresses, in our case  $p_z$  and  $p_x$ , act in quite a different direction under the given conditions. The selected soil element is compressed under their effect, the soil particles come into close contact with each other thus enhancing friction between them. The soil's stability, its shearing resistance are thus enhanced which in the general case increases the bearing capacity and stability of the foundation. Viewed in this context, the normal stresses should be considered as an advantageous factor. Regretfully, the favourable effect of normal stresses appearing in the soil mass due to the application of an external load on the stability of a foundation soil is neither completely nor universally expressed.

Let us consider now conditions constraining the role of normal stresses. The magnitude of normal ( $p_n$ ) and shearing ( $\tau$ ) stresses that appear in the soil mass is, naturally, governed by the value and type of the applied load. However, what is by far the most important is the dependence of these values on the coordinates of a given point (under conditions of a plane problem  $x$  and  $z$ ) and necessarily on the orientation of the unit area passing through the point along which the normal  $p_n$  and tangential  $\tau$  stresses operate. This fact is illustrated in Fig. 16.2 by the variation of  $p_n$  and  $\tau$  depending on the above factors. The stresses are here evaluated by the corresponding vectors graphically represented in fractions of the load  $p_0$ .

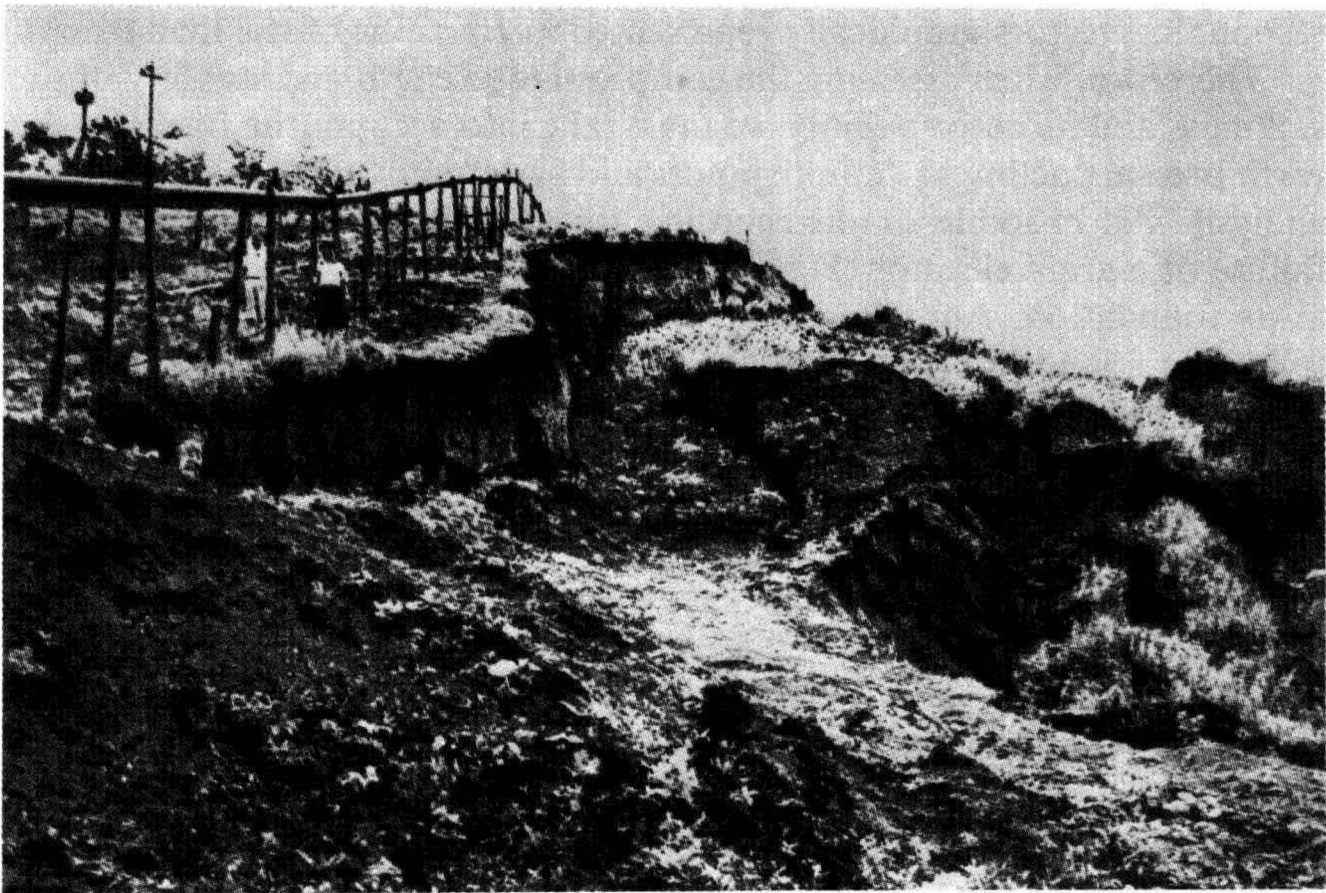
Therefore, when assessing the compressive strength and stability of the soil mass and its deformability we must take into account the forces of the earth pressure acting at definite points and at definite unit areas chosen for analysis. An example of disregarding this condition is provided by the failure of a grain elevator (Fig. 16.3) under conditions of excessive strains at its foundation. Another example is the loss of the stability of a slope following a landslide caused by the weight of the soil mass (Fig. 16.4).

Figure 16.5 is a graphic illustration of the hazard of a conspicuous settlement of a structure induced by an additional compression of the underlying soil due to the action of normal stresses. The failure to adequately account for the great compressibility of the soil, primarily, that of a layer of buried peat and the inexpedient use of pile foundations have led to a large and uneven or differential ( $\sim 2$  m) settlement of a bridge. This settlement has resulted in a very large damage to the span structure. The bridge in question represented a three-hinged arch, little sensitive to settlement. No doubt, had the design of the bridge been a two-hinged or hingeless type the settlement would have caused the total failure of the structure.

Pronounced differentiation in settlement and deformation of the foun-



**Fig. 16.3.** Failure of a grain elevator in the USA induced by excessive shearing stresses in its subsoil



**Fig. 16.4.** Landslide leading to loss in stability of a slope

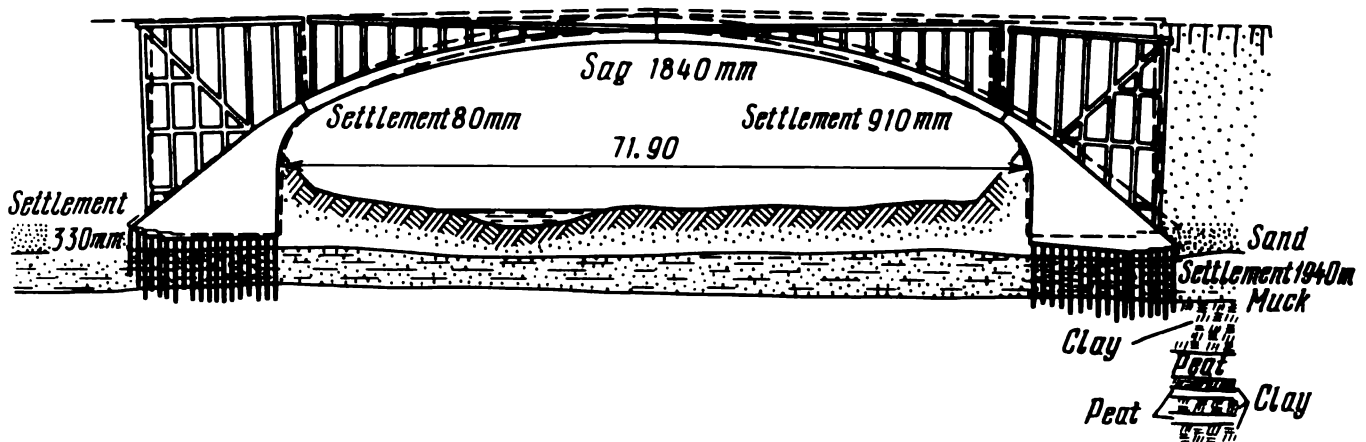


Fig. 16.5. Conspicuous settlement of a bridge's abutments resultant in its damage

dations of various industrial objects and industrial structures whose load-carrying elements belong to statically indeterminate systems may lead to similar results. These include multispans beams, multispans and multistore frames, hingeless and two-hinged arches etc. We will consider such cases elsewhere.

### Sec. 16.2. Forms of Expression of the State of Stress of the Soil Mass

It is the current aim of engineering geology and soil mechanics to reveal the state of stress in a soil mass acted on by some kind of load or another. The impressive body of evidence made available by the theory of elasticity especially facilitates this task. The concepts of this discipline, however, may be only applied to soil elastic bodies obeying Hooke's law and having a constant value of the modulus of elasticity ( $E = \text{const}$ ).

It should be pointed out from the start that the rock and soil masses typically fail to satisfy this condition. The fact is that the rock mass composed of hard and semihard varieties is invariably jointed. On the other hand, cohesionless soils like sand, gravel, shingles or broken rock are composed of individual grains that have no interconnection.

Clayey soils closer approach the idea of a solid elastic body although they represent an assortment of tiny crystals of clay minerals. Moreover, the mass of stiff or semistiff clayey soils is likewise typically fissured featuring a complex net of cracks.

At the same time, *residual deformations* are a common characteristic of all rocks and soils. Residual deformations in hard and semihard rocks are due to load-induced closure of the fissures whereas in grained and clayey soils these are caused by the irreversible consolidation accompanied by the decrease in the volume of voids.

Anyhow, the mass of rocks and soils taken together cannot be possibly considered as an elastic body with constant mechanical properties. This imposes a constraint on the unreserved use of the great bulk of information furnished by the theory of elasticity applicable to most diversified tasks.

Since a grained material, like sand or crushed rock, fails to satisfy Hooke's concept of an ideal solid, Professor I.I. Kandaurov has proposed a rigorous theory and calculation scheme to determine strains in discrete media. This scheme which underlies the method being considered relies on a concept of transferring the load sustained by an individual element of the medium onto two supporting elements. Under conditions of a plane problem the calculation uses a coefficient of distribution

$$\eta = 2\alpha/\beta^2$$

where  $\alpha = a/z$  and  $\beta = b/z$ ;  $a$  is the height,  $b$  is the width of the element.

The familiar equation given by Boussinesq for the determination of the vertical normal stress can be rewritten as follows:

$$\sigma_B = K_B P/z^2$$

where the coefficient  $K_B = 0.48$ .

According to M.N. Goldshtein, the stress  $\sigma_z$ , in conformity with the theory of a discrete medium, may be similarly represented as

$$\sigma_K = K_K P/z^2$$

Kandaurov's coefficient  $K_K$  is related with the value of the coefficient of distribution  $\eta$ . With  $K_B = K_K = 0.48$  the values  $\sigma_B = \sigma_K$  prove equal which means that the methods of the theory of elasticity and the theory of a discrete medium yield the same results in the determination of  $\sigma_z$ . With increasing the height  $a$  of an element of the medium and decreasing its width  $b$  the difference in the values of  $\sigma_B$  and  $\sigma_K$  becomes appreciable. So, with  $\eta = 4$  the value of  $K$  equals  $K_K = 1.27$  compared with  $K_B = 0.48$  due to which the difference between  $\sigma_B$  and  $\sigma_K$  is more than 2.5 times. However, determinations using this method have no practical value.

As has been shown by L.A. Uvarov, the values of vertical normal compressive  $p_z$  and tangential stresses  $\sigma_{zx} = \sigma_{xz}$  found by the method of elasticity and that of a discrete medium prove practically to be in agreement within the accuracy of solution of problems of soil mechanics. However, the body of mathematics involved in the theory of a discrete medium is too cumbersome.

It should be also noted that the Soviet scientists N.M. Gersevanov and V.A. Florin (1930-1940) have theoretically substantiated the concept of a pioneer of soil mechanics Professor Karl von Terzaghi (1923-1925) that it is possible to study strains in a soil mass in terms of the theory of elasticity

provided there is a load-deformation mechanical characteristic of a linear form. This concept has been repeatedly validated by practice during the construction of most important structures, and, primarily, of the Svir-Hydro-Electric Power Development (1929-1934). This, as it were, legalized the application of the data of the theory of elasticity to soil mechanics for the determination of strains in the soil mass as a medium featuring residual deformations with a load-dependent modulus  $E_p$ . Since the conclusions of the theory of elasticity could not be applied, special methods of soil mechanics had to be developed.

The last few decades have witnessed extensive use of a new method of solving problems of the theory of elasticity, a finite element method. The computer-aided use of this method has made it possible to deal with the most complicated problems of the theory of elasticity. Yet the application of the finite element method to even the simplest problems bearing on soil mechanics is at its initial stage.

The difficulty is due to the very principle of the method. The load-induced strains in the soil mass are here determined in terms of deformations by using the constant values of the modulus of elasticity and Poisson's ratio. This pathway seems to be in disagreement with the above conditions and needs to be adapted to problems posed by soil mechanics.

To keep the scope of the book within reasonable limits we have practically omitted numerical illustrations.\*

---

## Chapter 17

### Some Theoretical Facts Underlying Solutions of Problems Posed by Soil Mechanics

---

#### Sec. 17.1. The Strength of Soils

The problem is threefold: (1) the strength of the subsoil at a point in it; (2) the stability of the entire foundation of a structure; (3) the bearing capacity of a foundation.

The first aspect permits a possibility of a local loss in the soil's strength at a determined point in the structure's subsoil whose coordinates are  $x, z$ .

---

\* Such illustrations can be found in "Soil Mechanics with Numerical Examples" by Kotov, M.F. Vysshaya Shkola, 1968 (in Russian).

The second case is associated with a loss of soil stability in a more or less appreciable zone of the foundation likely to impair the stability of the whole foundation or the structure itself sometimes causing detrimental results if the stresses on the soil exceed a definite critical magnitude ( $p_{cr}$ ). Finally, the third aspect is in agreement with the complexity of the entire problem. It takes into account the bearing capacity of the structure's subsoil both from the standpoint of its strength and overall stability, and concurrently (which is most important) from that of deformations of a structure within reasonable limits  $p_{per}$ .

Methods for the evaluation of  $p_{cr}$  and  $p_{per}$  are dealt with in the following chapters. We must also necessarily bear in mind that in the most general case the degree of the soil strength is governed by the ratio of the shearing stress  $\tau$  (active pressure) acting on the soil to the effective shearing resistance of the soil ( $s_p$ ).

Let us introduce the concept of *a coefficient of operating conditions*

$$m = \tau/s_p \quad (17.1)$$

and of *a safety factor*

$$k_{saf} = s_p/\tau \quad (17.2)$$

As can be seen, the two concepts are inversely related and in both cases illustrate the behaviour of the soil in quantitative terms.

For reasons to be later understood, in what follows we will preferably choose the second constant,  $k_{saf}$ .

It will be recalled that in the general case the shearing resistance of soils,  $s_p$ , is described by this equation:

$$s_p = p_n \tan \varphi + c$$

Thus the value of the safety factor is in the general case dependent on those of the normal,  $p_n$ , and the tangential (shearing),  $\tau$ , stresses.

The magnitude of the factor of safety is directly related to the safety margin in the soil strength. These are three states of the soil strength:

- (1)  $k'_{saf} = s_p/\tau < 1.0$ , a state of unsafe strength (*supercritical state*) provided that  $\tau > s_p$ ;
- (2)  $k'_{saf} = s_p/\tau = 1$ , a state of limiting (critical) equivalent with  $s_p = \tau$ ;
- (3)  $k_{saf} = s_p/\tau > 1$ , a secured safety state with  $s_p > \tau$  (subcritical state).

When dealing with a task posed a need may arise: (1) to determine the safety factor from the soil's strength for the entire foundation, i.e.  $\Sigma k$ ; (2) to determine its minimum value for a given point,  $k_{saf.min}$ ; (3) the same, for the same point, yet for an oriented area (e.g. within a tilted seam  $k_{saf} \delta^\circ$ ).

*The first case* occurs if a preliminary investigation is to be made and the



soil mass is uniform in geological terms. Clearly, at this it is necessary to take into account the maximum tangential stress of all operating in the soil mass,  $\tau_{max\ max}$ .

*The second case* occurs if it is desired to determine  $k_{saf}$  for a point in the soil mass for a most disadvantageously oriented unit area, i.e. for the maximum value of the tangential stress at the given point,  $\tau_{max}$ .

*The third case* occurs when it is desired to determine and use for analysis a tangential stress  $\tau_\delta$ , i.e. one acting on an area oriented at an angle  $\delta^\circ$ .

Thus, complete analysis, apart from the corresponding normal stresses,  $p_n$ , calls for the determination, for various conditions of the loading of the soil mass, of the tangential stresses both for an individual point,  $\tau_\delta$ ,  $\tau_{max}$ , and for the entire foundation,  $\tau_{max\ max}$ .

### Sec. 17.2. The Determination of Normal and Shearing Stresses in a Soil Mass

The state of stress at any point of a plane field can be completely described if we know the values of the principal stresses ( $p_1$  and  $p_2$ , with  $p_1 \geq p_2$ ) and the orientation of *the principal directions* in which the principal stresses  $p_1$  and  $p_2$  are operating.

The orientation of the trace of a unit area  $I-I$  on a plane is determined from the value of the angle  $\delta^\circ$  formed between a normal to the area  $I-I$  and the principal direction in which the major principal stress  $p_1$  is acting (Fig. 17.1).

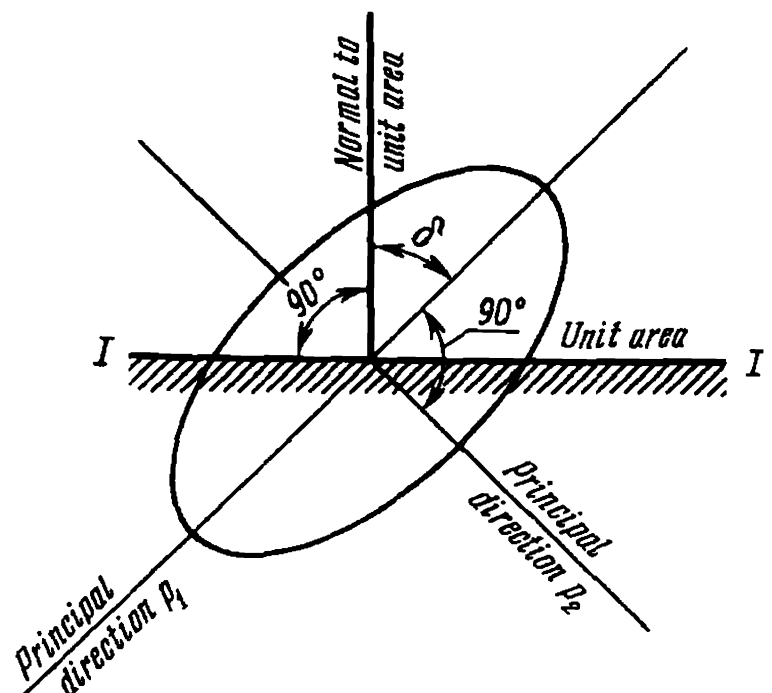


Fig. 17.1. Orientation of elementary area  $I-I$  with respect to principal directions  $p_1$  and  $p_2$

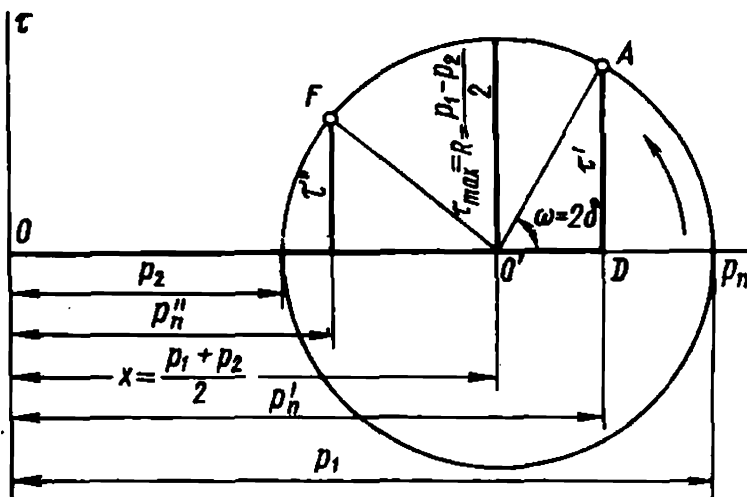


Fig. 17.2. Determination of shearing  $\tau_\delta$  and normal  $p_{n\delta}$  stresses by using Mohr's circle for differently orientated unit areas

With knowledge of  $p_1$  and  $p_2$  for a given point and of the angle  $\delta^\circ$  of orientation of the unit area to be analysed it is best to find values of  $p_{n\delta}$  and  $\tau_\delta$  for any conditions of loading the soil mass by using Mohr's circle of stress (Fig. 17.2).

The diagram is plotted as follows:

1. Suppose  $O$  is the origin of a rectangular coordinate system.
2. From the origin along the abscissa axis measure out segments representing, to an arbitrary scale, the values of the principal stresses  $p_1$  and  $p_2$ .
3. By using  $(p_1 - p_2)$  as a diameter, plot a circle whose radius is  $R = (p_1 - p_2)/2$  and whose centre is  $O'$  with the abscissa  $(p_1 + p_2)/2$ .

The values of normal and tangential (shearing) stresses,  $p_{n\delta}$  and  $\tau_\delta$ , acting on an elementary area inclined at an angle  $\delta^\circ$ , are found graphically from the location of the point  $A$  in Mohr's circle as shown in Fig. 17.2.

The above relationships permit a number of essential conclusions to be made:

1. The values of the principal stresses  $p_1$  and  $p_2$  are extreme for the normal stresses  $p_{n\delta}$  at the given point, i.e.  $p_2 \leq p_{n\delta} \leq p_1$ .
2. The maximum and the minimum values of a normal stress at a given point in the soil mass are thus limited by the values of the principal stresses  $p_1$  and  $p_2$  and occur on elementary areas connected with the principal stresses.
3. The normal stress acting on an area (always at a specified point  $D$ ) inclined at an angle  $\delta = 45^\circ$  to the principal directions, i.e. provided that  $\omega = 2 \times 45 = 90^\circ$ , equals

$$p_{n45^\circ} = \frac{p_1 + p_2}{2} \quad (17.3)$$

4. The value of the shearing stress  $\tau_\delta$  at a point  $A$  in the foundation is

within

$$0 \leq \tau_\delta \leq \tau_{max}; \quad \tau_\delta = 0 \quad (17.4)$$

5. The shearing stresses  $\tau_\delta = 0$  are operating along elementary areas connected with the principal directions, with  $\delta_1 = 0$  and  $\delta_2 = 90^\circ$ . At the same time the value of the shearing stress at a specified point attains its maximum value

$$\tau_{max} = (p_1 - p_2)/2 \quad (17.5)$$

acting on areas tilted at an angle  $\delta = 45^\circ$  to the principal directions, i.e. with the defining angle  $\omega = 2\delta = 2 \times 45^\circ = 90^\circ$ .

6. The values of  $p_{n\delta}$  and  $\tau_\delta$  for elementary areas inclined at angles  $0 \leq \delta \leq 45^\circ$  are found by solving the right-angled triangles whose hypotenuse is  $R = (p_1 - p_2)/2$ . In this case we obtain

$$p_{n\delta} = (p_1 + p_2)/2 + (p_1 - p_2) \cos 2\delta/2 \quad (17.6)$$

$$\tau_\delta = (p_1 - p_2)/\sin 2\delta/2 \quad (17.7)$$

One of the particular cases that occurs most commonly is that of the action in the soil mass of a uniformly loaded strip along the surface of an elastic semispace (Fig. 17.3).

In conformity with the theory of elasticity and structural mechanics in the particular case we have:

$$p_1 = (p_0/\pi)(\alpha + \sin \alpha); \quad (17.8)$$

$$p_2 = (p_0/\pi)(\alpha - \sin \alpha); \quad (17.9)$$

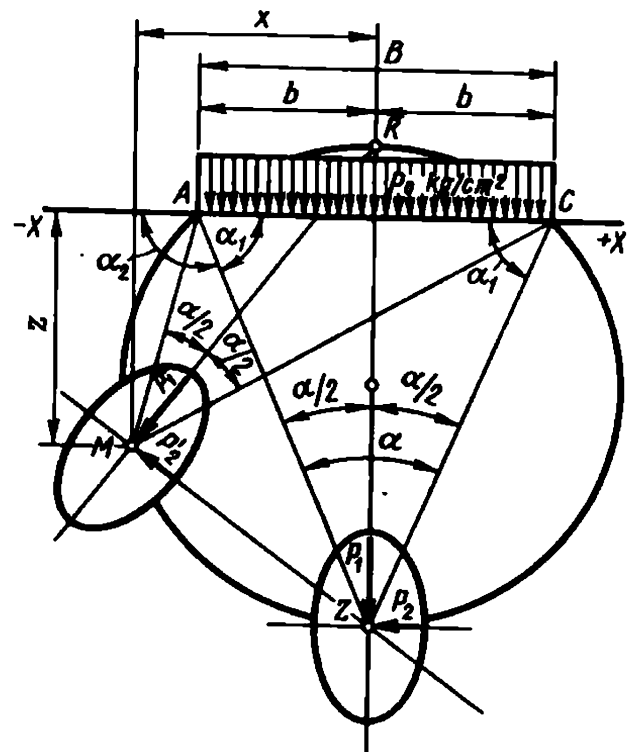


Fig. 17.3. Diagram for determining the angle of vision  $\alpha$  and principal stresses  $p_1$  and  $p_2$  for a uniformly loaded strip

7. The principal direction corresponding to the major principal direction of  $p_1$  coincides with *the bisector of the angle of vision*  $\alpha$ . A *bifocal coordinate system* is used in the given case as one leading to the simplest solutions.

In the above formulae  $p_0$  is the uniformly distributed strip load;  $\alpha$  is the angle of vision at which the strip load of a width  $B = 2b$  is seen from  $A$  in the underlying soil mass.

By using Mohr's circle we can easily find the stresses of interest to us, primarily the shearing stresses  $\tau_{max}$  and  $\tau_{max\ max}$ . According to Eq. (17.5), the stress  $\tau_{max}$  maximum for the particular point, corresponding to the most unfavourable orientation of the area at  $45^\circ$  to the principal directions, will be equal to

$$\tau_{max} = (p_1 - p_2)/2$$

By substituting into this equation the values of the principal stresses  $p_1$  and  $p_2$  from Eqs. (17.8) and (17.9) and by performing a few simplifications we get

$$\tau_{max} = (p_0/\pi) \sin \alpha \quad (17.10)$$

The maximum of possible values of  $\tau$  in the underlying soil mass is determined in the given conditions stemming from the fact that  $\sin \alpha_{max} = 1$ , which, in particular, corresponds to the angle of vision  $\alpha = 90^\circ$ . Then

$$\tau_{max\ max} = p_0/\pi \quad (17.11)$$

The above relationships are of much theoretical and practical value. In the first place, they attest to the direct dependence of the stresses  $p_1$ ,  $p_2$ ,  $\tau_{max}$  and  $\tau_{max\ max}$  on the magnitude of the uniformly distributed load  $p_0$ . Consequently, with a load  $p_0$  increased, say, 3 times, under the particular conditions the values of the principal stresses  $p_1$  and  $p_2$  and of the shearing stresses  $\tau_{max}$  and  $\tau_{max\ max}$  will increase accordingly. The values of  $p_1$  and  $p_2$  as well as of  $\tau_{max}$ , given  $p_0 = 1.0$ , are functions only of the angle of vision,  $\alpha$ .

Refer again to Fig. 17.3. As can be seen, the  $\alpha$  angles may be considered as being inscribed in the circle and subtended by a chord equal to the width of the loaded area,  $B = 2b$ . Hence, for any point in the soil underlying the loaded area located in this circle the angles of vision will be equal, i.e.  $\alpha = \text{const.}$

It also follows that at these points located on the entire circle corresponding to a definite angle of vision  $\alpha$  the values of  $p_1$  and  $p_2$  and those of  $\tau_{max}$  will similarly be equal. The given circles can thus be considered a locus (for the particular case) of  $p_1$  and  $p_2$ , of  $\tau_{max}$  and  $\alpha$ .

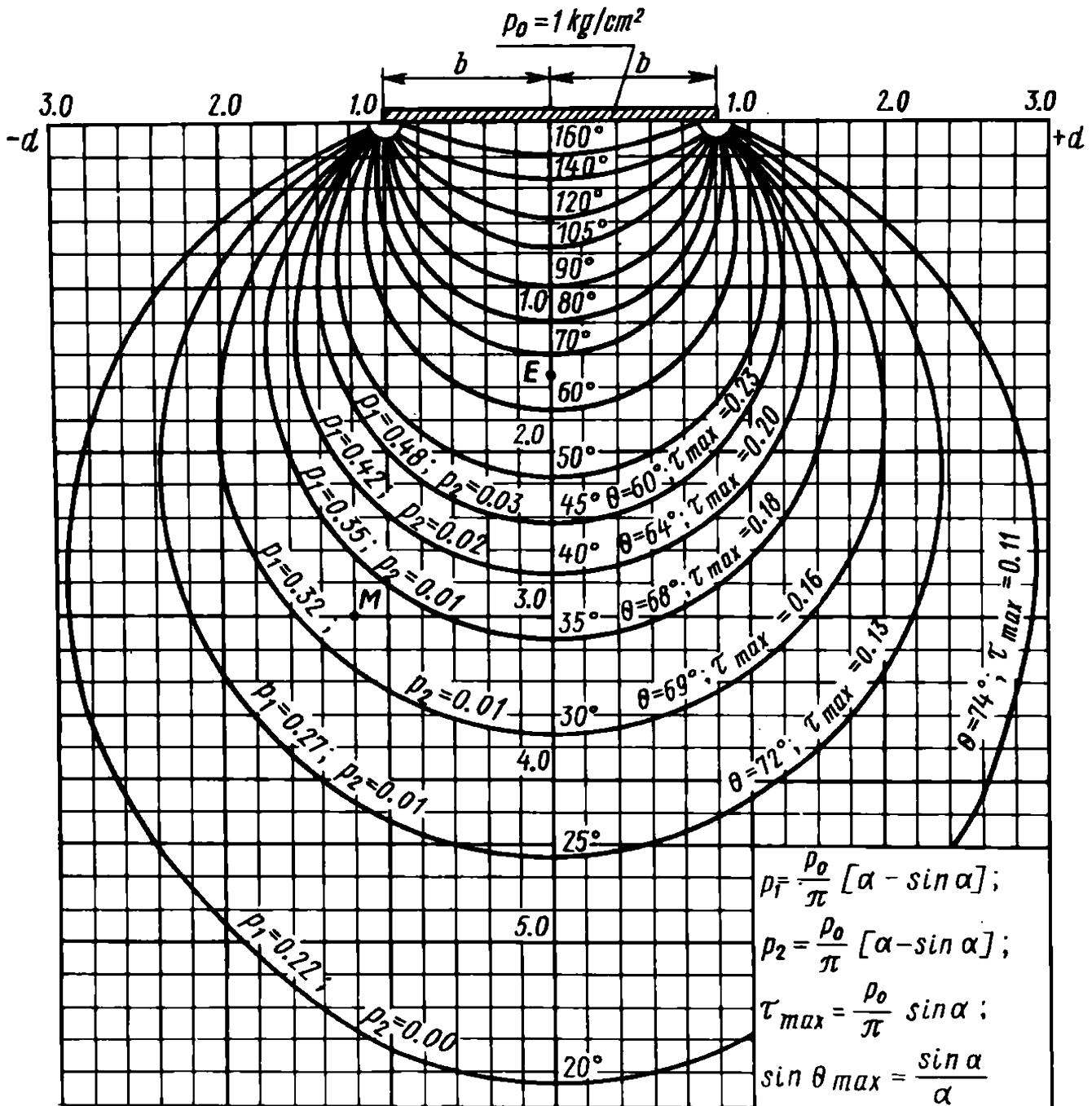


Fig. 17.4. Diagram of circles of stress in a relative,  $v$  and  $d$ , coordinate system for determining principal stresses  $p_1$ ,  $p_2$  and  $\tau_{\max}$  and angles of vision  $\alpha$  in fractions of the load  $p_0$

These concepts are used for plotting a diagram of circles of stress (Fig. 17.4) and compiling Table 17.1.

The diagram and table have been made in a relative coordinate system on the assumption that the abscissa  $d = x/b$  and the depth (ordinate)  $v = z/b$  are expressed in half widths,  $b$ , of the loaded strip. This permits easy use of the above materials for the determination of the sought values at any point in the underlying strata with the  $x$  and  $z$  coordinates for a case where  $p_0 = 1.0$  followed by calculations with  $p_0$ .

It is possible to determine the strength of a soil at a point whose coordinates are  $x$ ,  $z$ , acted on by shearing stresses  $\tau_{\max}$  and  $\tau_\delta$  operating, respec-

Table 17.1

Principal  $p_1$  and  $p_2$  and Shearing  $\tau_{max}$  Stresses  
in Fractions of a Uniformly Distributed Load  $p_0$  Depending  
on the Angles of Vision  $\alpha$

Angle of vision $\alpha$ , grad	$p_1$	$p_2$	$\tau_{max}$	Angle of vision $\alpha$ , grad	$p_1$	$p_2$	$\tau_{max}$
0	0.00	0.00	0.00	70	0.69	0.09	0.30
20	0.23	0.00	0.11	80	0.76	0.13	0.31
30	0.32	0.01	0.16	90	0.82	0.18	0.32
40	0.42	0.02	0.20	100	0.87	0.24	0.31
45	0.48	0.03	0.23	110	0.91	0.31	0.30
50	0.52	0.04	0.24	120	0.94	0.39	0.28
60	0.61	0.06	0.28				

tively, on unit areas with the orientation  $\delta = 45^\circ$  and  $\delta$ . This is possible to do with some reservation whose meaning will be further understood from the relationships

$$k_{saf.min} = S_{p\,45^\circ}/\tau_{max} \tag{17.12}$$

$$k_{saf\delta} = S_{p\delta}/\tau_\delta \tag{17.13}$$

Refer to Eqs. (17.3), (17.6), (17.7). Substitute here the values of  $p_1$  and  $p_2$  from Eqs. (17.8) and (17.9). After a few transformations we get

$$p_{n\,45^\circ} = (p_0/\pi)\alpha \tag{17.14}$$

$$p_{n\delta} = (p_0/\pi)(\alpha + \sin \alpha \cos 2\delta) \tag{17.15}$$

$$\tau_\delta = (p_0/\pi) \sin \alpha \sin 2\delta \tag{17.16}$$

Referring to Eq. (17.16), it is possible, in particular, for the given case, to find, at any point of interest to us, the values of the shearing (tangential) stresses  $\tau_{xz}$  and  $\tau_{zx}$  and plot the lines of equal  $\tau_{xz} = \tau_{zx}$  operating on horizontal and vertical unit areas. This plotting has been made in a relative coordinate system ( $d$  vs  $v$ ) in Fig. 17.5. This diagram may prove of much use to evaluate the degree of stability of a retaining structure referring to a thin layer in the underlying soil mass, e.g. plastic clay.

Similar solutions may be obtained for other loads as well. In particular, Fig. 17.6 presents a diagram to determine the principal stresses  $p_1$  and  $p_2$  in the case of a load on the surface of the soil mass obeying the law of a triangle. As usual, the graph is plotted in relative coordinates:  $d = x/b$

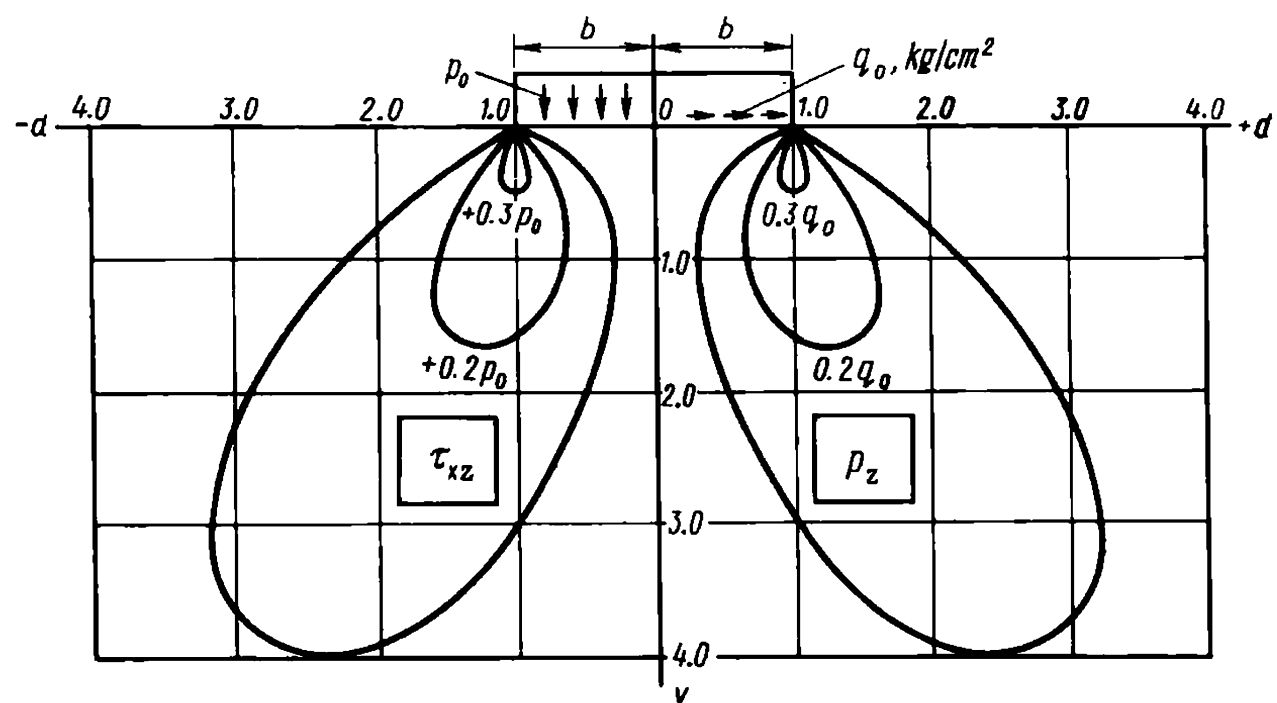


**Fig. 17.5.** Curves of equal shearing stresses  $\tau_{zx} = \tau_{xz}$  acting on horizontal and vertical unit areas sustaining a uniformly distributed load  $p_0$  (on the left) and vertical normal stresses  $p_z$  induced by a horizontal (shearing) uniformly distributed load  $q_{sh}$  (on the right). A plane problem

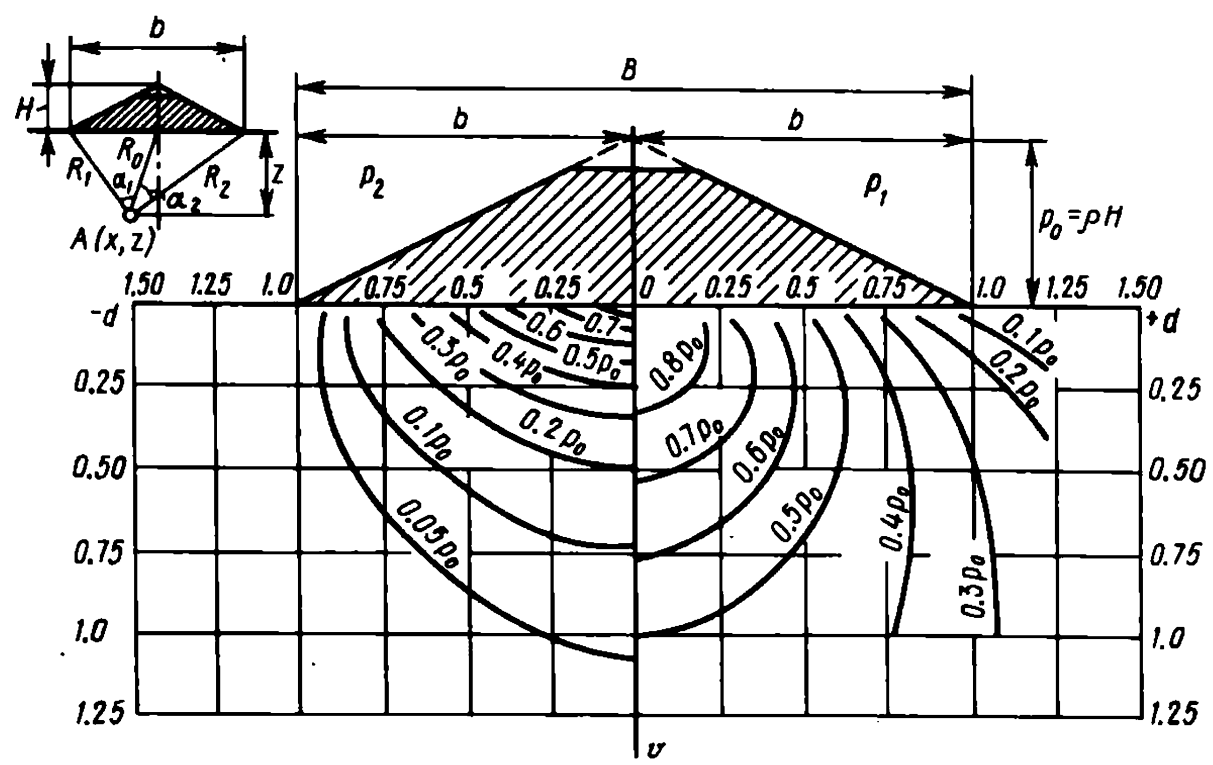


**Fig. 17.6.** Principal stresses  $p_1$  (right) and  $p_2$  (left) for a triangular load

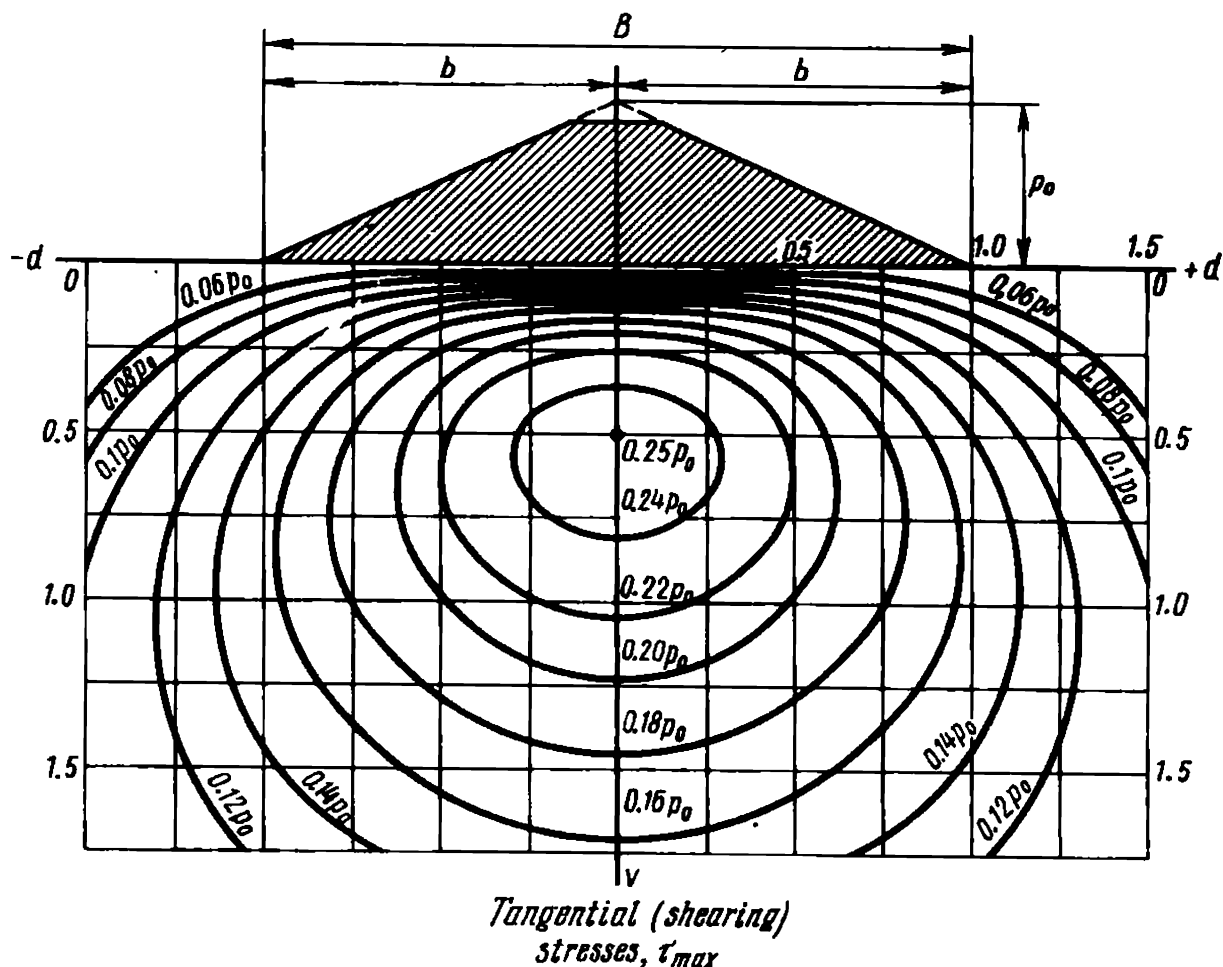


Fig. 17.7. Lines of equal shearing stresses  $\tau_{max}$  for a triangular load

and  $v = z/b$ , where  $b$  is half the width of the loaded strip. The values of  $p_1$  and  $p_2$  are given in fractions of the load:

$$p_0 = \rho H$$

where  $\rho$  is the bulk density of the soil in the embankment;  $H$  is its maximum height.

Figure 17.7 presents, for a similar case (triangular load), a diagram of lines equal to  $\tau_{max}$  ( $\tau_{max} = \text{const}$ ) determined accordingly from the principal stresses  $p_1$  and  $p_2$ .

It is good practice to use for road designing Eqs. (17.17) to find the values of principal stresses  $p_1$  and  $p_2$  under conditions of a trapezoidal load. These formulae can as well be used to evaluate the strain at the base of a railway embankment. The values of the quantities entering these formulae can be found by referring to Fig. 17.8.

It will be recalled, that according to the theory of elasticity, the major shearing stress

$$\tau_{max} = (p_1 - p_2)/2$$



and for the given case we have:

$$\left. \begin{aligned} p_1 &= \frac{p_0}{\pi a} \left[ a(\alpha_1 + \alpha_2 + \alpha_3) + b(\alpha_3 + \alpha_1) - y(\alpha_3 - \alpha_1) \right] \\ &\quad - z \ln \frac{R_1 R_4}{R_2 R_3} + z \sqrt{\ln^2 \frac{R_1 R_4}{R_2 R_3} + (a_3 - a_1)^2} \\ p_2 &= \frac{p_0}{\pi a} \left[ a(\alpha_1 + \alpha_2 + \alpha_3) + b(\alpha_3 + \alpha_1) - y(\alpha_3 - \alpha_1) \right] \\ &\quad - z \ln \frac{R_1 R_4}{R_2 R_3} - z \sqrt{\ln^2 \frac{R_1 R_4}{R_2 R_3} + (\alpha_3 - \alpha_1)^2} \end{aligned} \right\} \quad (17.17)$$

It is often required to evaluate the state of stress at the base of a railway embankment and to find the values of  $p_z$ ,  $p_x$  and  $\tau_{max}$ . The following equations are then used:

$$p_z = \frac{p}{\pi a} \left[ a(\beta_1 + \beta_2 + \beta_3) + b(\beta_1 + \beta_3) + x(\beta_1 - \beta_3) \right] \quad (17.18)$$

$$p_x = \frac{p}{\pi a} \left[ a(\beta_1 + \beta_2 + \beta_3) + b(\beta_1 + \beta_3) + x(\beta_1 - \beta_3) - 2z \ln \frac{R_1 R_4}{R_2 R_3} \right] \quad (17.19)$$

$$\tau_{max} = \frac{pz}{\pi a} \sqrt{\ln^2 \frac{R_1 R_4}{R_2 R_3} + (\beta_1 - \beta_2)^2} \quad (17.20)$$

The quantities entering these equations may be understood by referring to Fig. 17.9. Given the values of the normal stresses  $p_z$  and  $p_x$  and of the tangential stresses  $\tau_{zx} = \tau_{xz}$ , in all cases the value of the major tangential

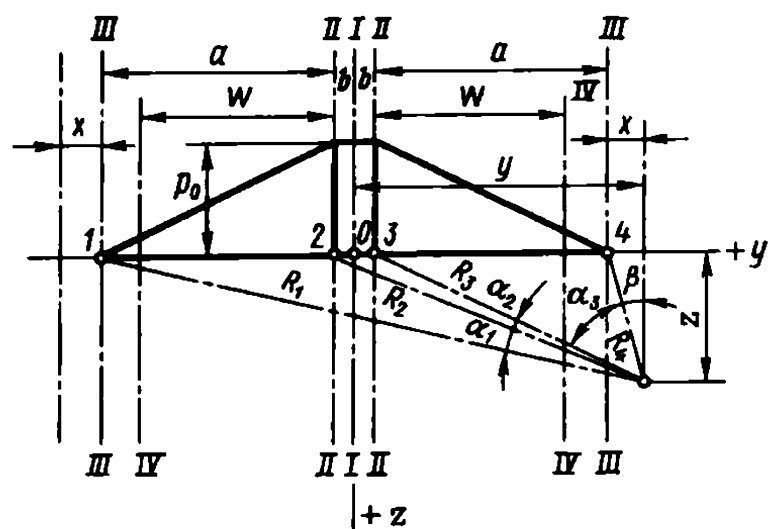


Fig. 17.8. Diagram for determining principal stresses  $p_1$  and  $p_2$  in a road embankment foundation. A trapezoidal load

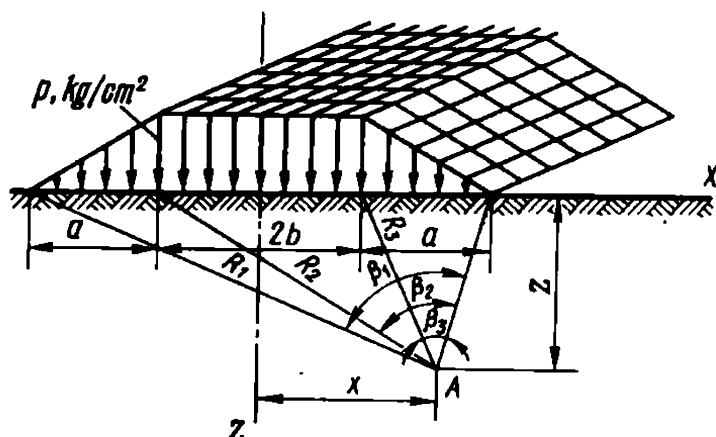


Fig. 17.9. Diagram for determining  $p_x$ ,  $p_z$  and  $\tau_{\max}$  in a road embankment foundation

(shearing) stress can be found from this relationship

$$\tau_{\max} = \frac{1}{2} \sqrt{(p_z - p_x)^2 + 4\tau_{zx}^2} \quad (17.21)$$

If we know the values of  $p_z$ ,  $p_x$  and  $\tau_{\max}$ , this relationship may be used to determine the value of the shearing stress  $\tau_{xz} = \tau_{zx}$  operating on horizontal and vertical unit areas.

Clearly, if we know the values of the normal stresses  $p_z$  and  $p_x$ , and of the shearing stresses  $\tau_{zx}$  and  $\tau_{xz}$ , operating on horizontal and vertical unit areas, we can, consequently, find the values of the principal stresses  $p_1$  and  $p_2$ . This may be done by using the familiar relationship

$$p_1, p_2 = \frac{p_z + p_x}{2} \pm \frac{1}{2} \sqrt{(p_z - p_x)^2 + 4\tau_{zx}^2} \quad (17.22)$$

### Sec. 17.3. Special Cases of the State of Stress of the Soil Mass

The above equations on which solutions of a number of problems to evaluate the state of stress of the soil mass rely, are dependent on formulae (A). These have been provided by the French scientist Boussinesq to determine the vertical,  $\sigma_z$ , and horizontal,  $\sigma_x$ , stresses, and the shearing stresses,  $\tau_{zx}$  and  $\tau_{xz}$ , acting on horizontal and vertical unit areas. The latter originate at a point located at a distance  $z$  in the soil mass from the concentrated vertical load  $P$  applied to the horizontal surface of the soil mass:

$$\begin{aligned} \sigma_z &= 3/2P/\pi z^2 \cos^3 \alpha \\ \sigma_x &= 3/2P/\pi z^2 \cos \alpha \sin^2 \alpha \\ \tau_{zx} &= \tau_{xz} = 3/2P/\pi z^2 \cos^2 \alpha \sin \alpha \end{aligned} \quad (A)$$

Here  $\alpha$  is the angle between the radius vector and the vertical passing through the point where the force  $P$  is applied.

O. Frölich (1933) later showed and G.K. Klein and M.V. Malyshev validated that from the theoretical viewpoint the derivation of these for-

mulae fully preserves its purity in this, more general, form:

$$\left. \begin{aligned} \sigma_z &= \nu/2 P/\pi z^2 \cos^\nu \alpha \\ \sigma_x &= \nu/2 P/\pi z^2 \cos^{\nu-2} \alpha \sin^2 \alpha \\ \tau_{zx} &= \nu/2 P/\pi z^2 \cos^{\nu-1} \alpha \sin \alpha \end{aligned} \right\} \quad (B)$$

The condition must be necessarily satisfied that the values of the characteristic  $\nu$  (coefficient of concentration of stresses) be within  $\nu = 1$  to 6.

Analysis shows that if  $\nu = 3$  we have a well known set of equations of Boussinesq, in particular, that reported above (A).

Apart from  $\nu = 3$  this characteristic has also the value  $\nu = 4$ . This case corresponds to a semispace whose modulus of deformation increases with depth. However, the analysis performed by the present writer together with the civil engineer D.V. Shnitkov (1936) has manifested that the set of equations (B) used for  $\nu = 4$  to predict settlement of even large structures does not lead to any significantly different result.

At the same time it has been indicated by Professor V.F. Babkov that the above solution with  $\nu = 6$  may well be used to evaluate the state of stress of soils with small cohesion that are in an immediate proximity to the loading area less than 1 m in size.

## Chapter 18

### Three Phases of the Behaviour of the Subsoils of a Structure

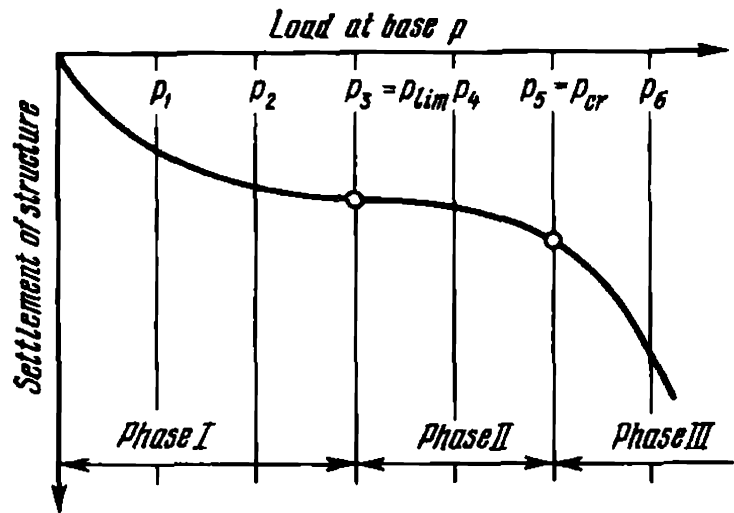
#### Sec. 18.1. General Considerations

It is possible to apply to the subsoil of a structure both a minor and a greater load ( $p_0$ , kg/cm<sup>2</sup> MPa). Naturally, with decreasing the permissible load on the soil,  $p_{perm}$ , other conditions being equal, it is necessary to increase the contact area of a foundation, use other, deeper foundation types or use piles, cofferdams and caissons. In so doing, it is most advantageous to have a minimum size of the footing so that it will ensure the stability and strength of the structure to be built allowing for likely settlement of the latter.

Refer to Figs. 18.1 and 18.2. A load (say,  $p_1$ ) applied to the surface of a soil almost immediately causes a complex state of stress in the soil mass. The normal stress  $p_n$  acting on the soil brings about the compression of the soil leading to the settlement of a structure (see phase I in Figs. 18.1 and 18.2).

**Fig. 18.1.** Three phases of loading and deformations of a structure's foundation:

phase *I*—soil compression in foundation (zone of principal influence  $p_n$ ); phase *II*—state of critical equilibrium (intermediate zone of influence of  $p_n$  and  $\tau_{max}$ ), local loss of stability by foundation soils; phase *III*—loss of total stability by foundation (phase of predominant role of  $\tau_{max}$ )



This process proceeding with time and varying in intensity has invariably an attenuated pattern. As the load on the soil increases to attain, say, the value  $p_2$ , under the same conditions there occurs further settlement. The rate of this process, however, drops due to the continued soil compression. The normal stresses,  $p_n$ , clearly prevail here. The action of the shearing stresses,  $\tau$ , is only of minor value, and they are invariably overcome by the shearing resistance of the soil ( $s_p > \tau$ ).

The conditions of loading and deformation of the underlying soil being considered correspond to *phase I* of the behaviour of the subsoil of the structure, i.e. *soil compression induced by the weight of the structure* under conditions of ensured soil strength and stability of the foundation.

An additional increase in the load ( $p_3$  in Fig. 18.1) leads to further settlement of the structure associated, apart from the added soil compression, with a certain amount of squeezing of the soil from beneath the base of the foundation around its periphery (*plastic regions*) where a local loss of the soil's strength occurs (*phase II* in Figs. 18.1 and 18.2). The effect of the  $p_n$

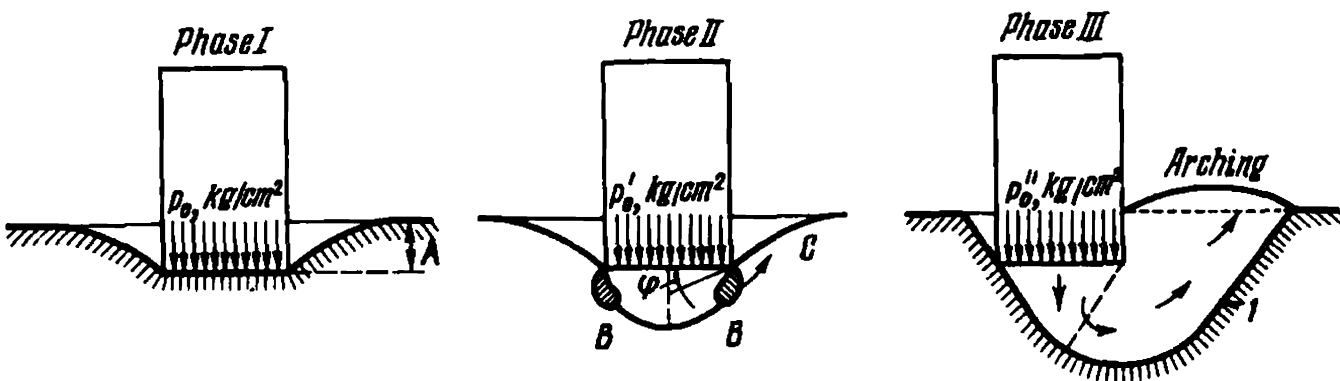


**Fig. 18.2.** Three phases in soil behaviour of structure foundations (compression, local dislocations phase, bulging):

A—settlement due to soil compression; B—zones of local displacements; C—squeezing out of soil; I—line of sliding

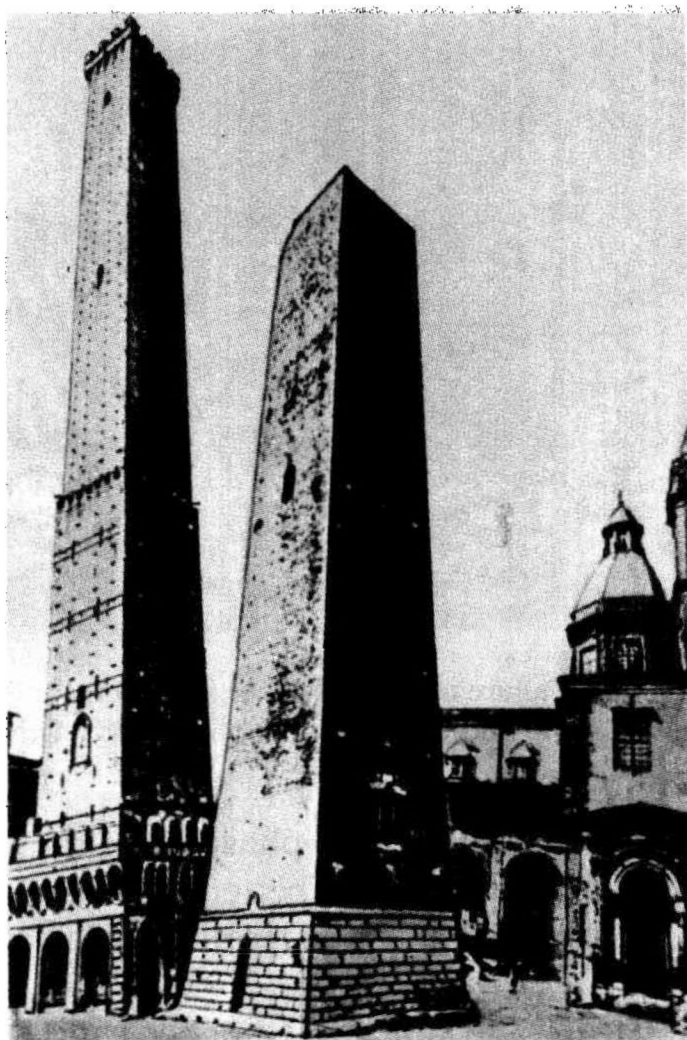


**Fig. 18.3.** Tipping of towers in Bologna in Italy induced by differential settlement due to excessive loading of the foundation soil (phase II of local displacements)

and  $\tau$  stresses is here expressed concurrently under conditions of the onset and continuation of the failure of the soil as the load increases with  $\tau > s_p$ . This phenomenon due to the shear in the soil is far from being always permissible, at least, within *strict limits*. In fact, at this stage of the soil's behaviour the structure's settlement proves often of great magnitude and cannot be taken into account when designing a structure, and is almost invariably very unequal (Fig. 18.3).

As a result of sliding of a clayey subsoil of the foundation this settlement is often of a non-damping pattern which may in isolated cases cause the loss of the overall stability by the structure.

The load corresponding to an early stage of the above phenomenon is termed *a limit load* ( $p_3 = p_{lim}$ ) and the behaviour of the soil in such conditions must be referred to phase II which should be more properly called a phase of *the loss of stability by the soil* or *a phase of local deformations*.

With further increasing the load  $p_{lim}$  the above phenomenon deteriorates and, as it attains the value  $p_5 = p_{crit}$ , there occurs a sudden and dramatic loss of the overall stability of the foundation induced by soil arching. It would be appropriate to describe this load as *a critical* one. This

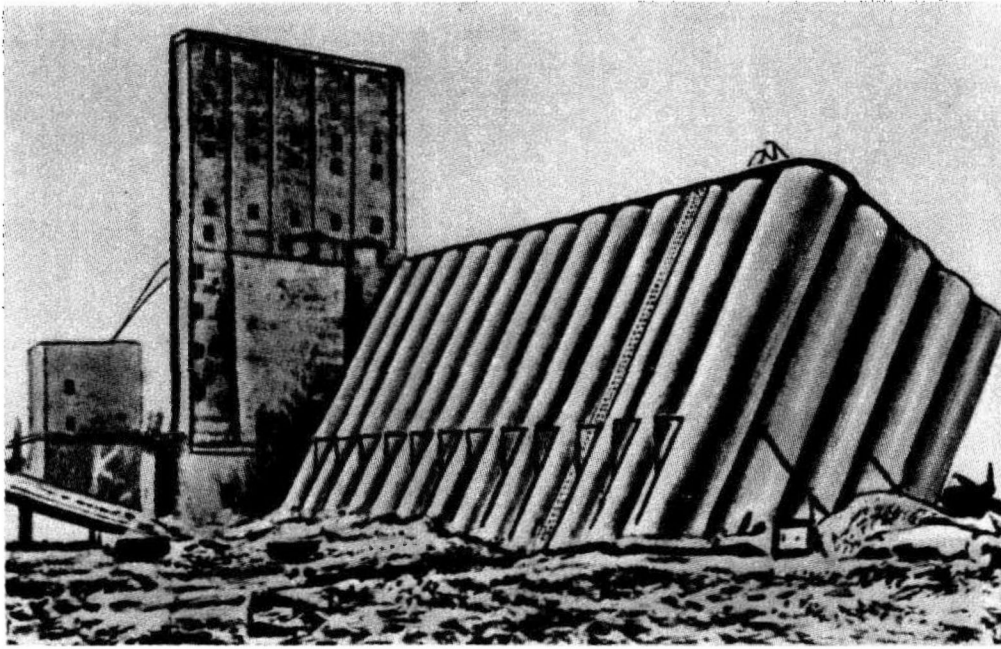


**Fig. 18.4.** Failure of a Transcona grain elevator (Canada) following unilateral settlement by 8.4 m and complete loss of stability of the foundation (phase III-soil heave)

process corresponds to phase *III* of the behaviour of the soil supporting the structure that could be better called a phase of the loss of the overall stability by the soil (phase of general shear and soil arching, see Figs. 18.1 and 18.2).

Clearly, in phase *III* the shearing stresses,  $\tau$ , prevail in the soil. This process associated with an increase in the adopted loading of the soil from  $p_0$  to  $p_{crit}$  which is critical for the particular case generally entails failure of the structure and cannot therefore be tolerated under any circumstances (Fig. 18.4).

It should be noted in this context that a greater depth of the foundation tends to inhibit soil arching. In the case of deep foundations generally supporting bridge piers and of extended structures such soil arching is practically excluded. The decisive role is here played by the behaviour of the soil in phase *II* (phase of loss of strength by the soil).

### **Sec. 18.2. The Loss of Strength and Stability by the Foundation**

As follows from what has been reported above, when evaluating the bearing capacity of the foundation of a structure two particular, although closely related, problems arise:

(1) evaluation of the condition of *loss of the stability* by the subsoil of the structure in phase *II* of the soil's behaviour followed, depending on one type of constraint or another, by the value of the limit load on the soil,

$p_{lim}$ . This first and foremost involves a possible and permissible deformation of the structure, necessarily taking into account the time factor;

(2) evaluation of the condition of the total *loss of the stability* by the foundation in phase *III* of the soil's behaviour and by the structure itself. Proceeding from these conditions, we determine the critical value of the load,  $p_{crit}$ , taking into consideration likely weakening of the subsoil with time.

## Chapter 19

### Evaluation of the Strength of the Subsoil of a Structure Disregarding Normal Stresses

#### Sec. 19.1. General Considerations

The effect of normal stresses on the strength (shearing resistance) of soils may be twofold: (a) an increase in the soil's density and a decrease in the moisture content of clayey soils (factor  $w$ ); (b) an increase in the value of the internal friction forces operative in the soil in conformity with the relationship

$$r = p_n \tan \varphi \quad (19.1)$$

as the first term of the familiar equation

$$s_p = p_n \tan \varphi + c \quad (19.2)$$

The effect of the normal stresses on the total value of the shearing resistance of soils is, naturally, limited by the magnitude of the angle of internal friction itself and drops to zero if it is equal to zero ( $\varphi = 0$ ).

Typical in this respect are plastic clays whose most important characteristic is  $\varphi_w = 0$ . However, on excessive wetting and with weak consistency the above rule is true of semiplastic clays as well, for which in the general case  $\varphi_w \neq 0$ . At high moisture contents the true angles of friction  $\varphi_w$  in these soils often prove to be close to zero, at any rate, below 5 to 7°. These angle values may be the upper level below which the action of the normal stresses on soil strength turns out to be inessential.

Undoubtedly, the values of angles of internal friction of pseudoplastic clays may increase following consolidation and drop in the moisture content [ $\varphi_w = f(w)$ ], e.g. induced by the weight of the structure being erected. Under this condition the shearing resistance of clayey soils will increase in

conformity with the familiar relationship

$$s_{pw} = p \tan \varphi_w + c_w$$

As is shown by practice and theory, as far as clayey soils are concerned, especially seems of marked depth, this process may take much time, years and decades. And, before the compression of at least part of the soil has largely terminated, the structure may prove helpless, as it were, in the face of excessive loads. This may cause instability, even collapse of the structure in hand.

As to *plastic varieties of clay*, and pseudoplastic clays with true angles of internal friction  $\varphi_w < 5$  to  $7^\circ$  (under conditions of unconfirmed possibility of their increase within permissible time periods) when evaluating the strength of the subsoil of a structure the advantageous effect of normal stresses should not be taken into account. Differently speaking, the following relationships should be used:

(a) for the general case

$$k_{saf} = c_w / \tau \quad (19.3)$$

(b) for plastic soils

$$k_{saf} = \Sigma_w / \tau \quad (19.4)$$

(c) for semiplastic soils

$$k_{saf} = (\Sigma_w + c_c) / \tau \quad (19.5)$$

The values of  $\tau$  in Eqs. (19.3) and (19.5) and similar equations must be substituted in conformity with the conditions of the problem in hand and by using Eqs. (17.10), (17.11) and (17.16). In such cases we will have:

(a) for a comparison and evaluation of the strength of the homogeneous subsoil (for the general case)

$$k'_{saf} = c_w / \tau_{max\ max} = \pi c_w / p_0 \quad (19.6)$$

(b) for the evaluation of the degree of the soil's strength at a point in the subsoil whose coordinates are  $x, z$ , for the most disadvantageously oriented unit area passing through this point

$$k''_{saf} = c_w / \tau_{max} = \pi c_w / (p_0 \sin \alpha) \quad (19.7)$$

(c) for the same point with the same  $x, z$ , coordinates, yet for a definitely oriented unit area (e.g. inclined through an angle  $\delta$ )

$$k'''_{saf} = c_w / \tau_\delta = \pi c_w / (p_0 \sin \alpha \sin 2\delta) \quad (19.8)$$

The last equation may be used, e.g. when evaluating the total shearing resistance of any retaining structure with respect to a weak horizontal



layer. For this case we have

$$\tau_{zx} = q_0/\pi[\alpha + \sin \alpha \cos (\alpha_1 + \alpha_2)] \quad (19.9)$$

where  $q_0$  is a horizontal shearing stress uniformly applied to the structure's subgrade;  $\alpha$  is the angle of vision, and  $\alpha_1$  and  $\alpha_2$  are the angles as plotted in Fig. 17.3.

The lines of equal  $\tau_{zx}$  for the particular case are given in Fig. 27.3 (see the next chapters); the same, as the function  $\tau_{zx} = f(p_0)$  in Fig. 17.5. Eqs. (19.4) and (19.7), like similar ones, may be adapted accordingly for the determination of a permissible load,  $p_{perm}$ , allowing for the conditions involved. In the particular case it is only necessary to equalize  $p_0 = p_{perm}$ . Then we will have

$$p'_{perm} = 1/k_{saf}\pi c_w \quad (19.10)$$

$$p''_{perm} = 1/k_{saf}\pi c_w/\sin \alpha \quad (19.11)$$

The overall cohesion  $c_w$  must be substituted into these equations in conformity with the soil variety: for plastic clays  $\Sigma_w$  and for pseudoplastic clays  $[\Sigma_w + c_c]$ . The determination of  $p'_{perm}$  from Eq. (19.10) has been derived for most rigorous conditions: there should not be a single point at the subgrade of the entire structure where the shearing stress  $\tau$  acting on the most disadvantageously oriented unit area would exceed the shearing resistance  $s$ , expressed in the given case by the cohesion  $\Sigma_w$  and  $(\Sigma_w + c_c)$ . It seems better to use in Eq. (19.10)  $k_{saf} = 1.0$  and consider  $p_{perm}$  as being not only a permissible but also as quite a safe load.

## Sec. 19.2. A Safe Load

$p_{saf}$  is a load determined with a large margin of safety and thus surely permissible for the structure in hand. The determination of  $p_{saf}$  proves very useful in many cases even for soils with  $\varphi > 5$  to  $7^\circ$  since under definite conditions this rules out more detailed calculations.

This may be the case when  $p_{saf}$  will exceed the load  $p_{str}$  needed for the particular structure and adopted from the designer's considerations. Thus Eq. (19.10) can, for practical purposes, take on this form:

$$p_{saf} = \pi c_w \quad (19.12)$$

It must be finally pointed out, referring to Eq. (17.11)  $\tau_{max\ max} = p_0/\pi$ , that for the case of a uniformly distributed load

$$p_{saf} \approx 3c_w \quad (19.13)$$

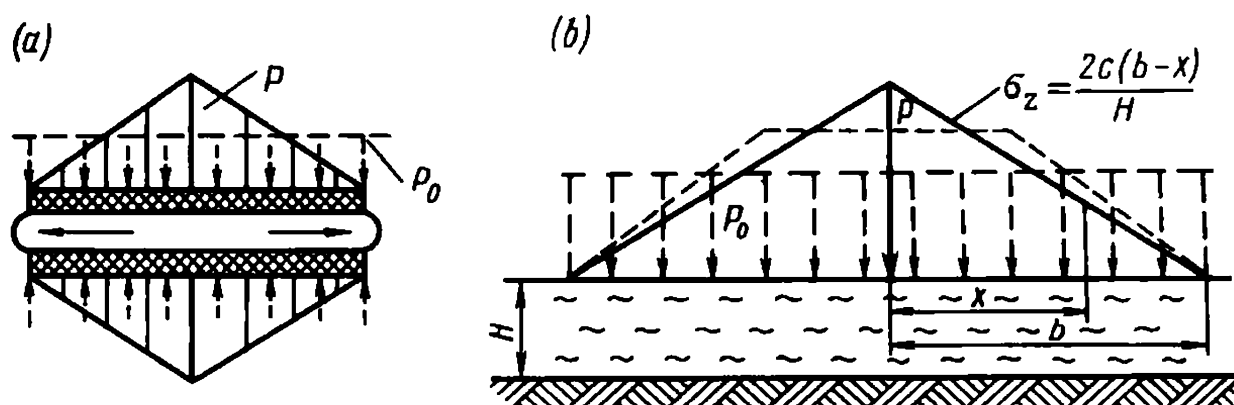


Fig. 19.1. Diagram for calculating stability of an embankment supported by a thin seam of plastic clay at  $\varphi_w = 0$ :

$a$ —compression of seam between two slabs;  $b$ —diagram of compressive pressures beneath the embankment

and to Fig. 17.7 for a triangular load

$$p_{saf} \approx 4c_w \quad (19.14)$$

Road designing practice often calls for evaluation of the stability and strength of layers of minor thickness of incompetent soils underlying an embankment. Such conditions may arise at flood plains, in bottomland and marshy areas and, which is especially important, at the subgrades of generally high bridge approach embankments.

Such conditions may frequently lead to the lateral yielding of the embankments subsoil followed by pronounced deformation and failure of the embankment.

This problem has been solved by Prof. L.K. Jürgenson of the Estonian SSR proceeding from the conditions of plastic deformations developing in this layer followed by squeezing of the material much like toothpaste out of a tube. According to his solution (Fig. 19.1) the average load ( $p_0$ ), limiting in this respect, can be found from this relationship

$$p_0 = 1/H cb$$

where  $H$  is the thickness of the thin layer,  $b$  is one-half of the width of the embankment,  $c$  is the cohesion of the soil (with the angle of internal friction tending to zero,  $\varphi \rightarrow 0$ ).

Note that with increasing the thickness of the layer the condition with respect to  $p_0$  is, naturally, aggravated. As follows from the above relationship, with the rate of slope of an embankment  $1/2$ , with  $h_{emb} = 10$  m the embankment will be already found in complicated conditions if the cohesion of the incompetent soil underlying the embankment, 2 m in thickness, is less than  $2 \text{ t/m}^2$ .

## Chapter 20

## Evaluation of the Strength of the Subsoil of a Structure Taking into Account Normal Stresses

## Sec. 20.1. Criterion of the Limit Strength of a Soil

The method outlined below relates to soils whose shearing resistance  $s_p$  or  $s_{pw}$ , apart from the density-moisture content, is also associated with the magnitude of the normal stress  $p_n$  or  $p$  acting on the soil. These soils include all varieties that strongly depend for their strength on friction, i.e. ones characterized by definite values of the angles of internal friction other than equal to zero ( $\varphi \neq 0$ ). These are first and foremost loose (cohesionless) as well as pseudoplastic and stiff clayey soils.

The problem is complicated by a need to solve it under conditions of a relatively unfavourable ratio of  $p_\delta$  to  $\tau_\delta$ . In the general case the safety factor of the soil at a point corresponds to  $\tau_{max}$  and refers to a unit area inclined through the angle  $\delta = 45^\circ$  with respect to the principal directions. This is not the case, however, in the soils being considered.

Let us introduce a concept of *an angle of inclination*  $\Theta$  (Fig. 20.1). In this figure the angle  $\Theta$  defines the value of deflection of the total stress  $p_{tot}$  acting on the particular unit area from the normal to this latter. On the other hand, it can be seen from this figure that

$$\tan \Theta = \tau/p_n \quad (20.1)$$

Let us consider this problem primarily with respect to loose cohesionless soils ( $c_n = 0$ ). As is known, for such soils  $s_p = p_n \tan \varphi$ . Assume that on a plane  $aa$  a weightless body lies with an identical lower surface. The total stress  $p_{tot}$  operates on a body at an angle to the vertical.

Resolve this stress into a normal,  $p_n$ , and a tangential,  $\tau$ , components

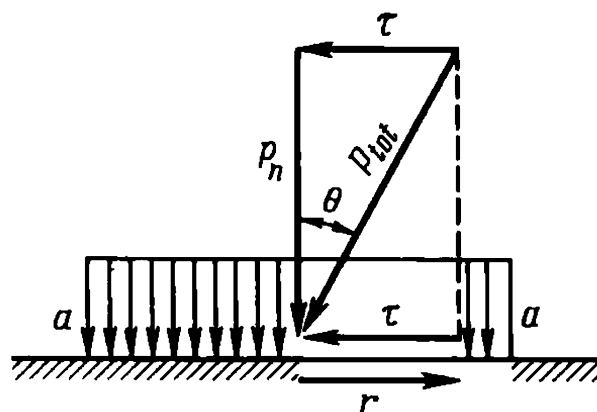


Fig. 20.1. Conditions of critical equilibrium of a given element on a definite plane unit area

obtaining

$$p_n = p_{tot} \cos \Theta \quad (20.2)$$

$$\tau = p_{tot} \sin \Theta \quad (20.3)$$

Under the effect of the shearing stress,  $\tau$ , the body in question may shear along the plane  $aa$ . This shear, however, is inhibited by the friction forces,  $r$ , that appear at the contact surface of the body's base and the above plane. The forces are equal to

$$r = p_n \tan \varphi_n \quad (20.4)$$

which, by virtue of Eqs. (20.2) and (20.3), yields

$$r = p_{tot} \cos \Theta \tan \varphi_n \quad (20.5)$$

At the state of complete equilibrium of the body

$$\tau = r \quad (20.6)$$

After substituting into this equation  $r$  and  $\tau$  from Eqs. (20.3) and (20.5) perform some simple transformations. This will yield

$$\sin \Theta / \cos \Theta = \tan \varphi_n \quad (20.7)$$

Consequently,

$$\tan \Theta = \tan \varphi_n \quad (20.8)$$

and, finally,

$$\Theta = \varphi_n \quad (20.9)$$

As is known, the angle of inclination at a point, much as the shearing stresses,  $\tau$ , varies depending on the orientation of the elementary area passing through the given point within

$$0 \leq \Theta \leq \Theta_{max}$$

Therefore the limit state (equilibrium) of the soil mass at a point is described by the equation

$$\Theta_{max} = \varphi \quad (20.10)$$

We arrive at a very important conclusion that under conditions of the given problem the stability of a grained (loose) soil is only determined by the ratio of the angle of maximum inclination,  $\Theta_{max}$ , to the angle of internal friction  $\varphi$ , characteristic for the given loose soil variety. The magnitude of the applied force and stress  $p_n$  and  $\tau$  is immaterial here. The strength of the soil, proceeding from this condition, may be lost at a minor pressure applied obliquely to the unit area, and vice versa.

Taking this into consideration we may formulate new strength criteria of strength for loose soils with  $c = 0$  at a point in the soil mass.

*The below limit* or subcritical stable state of a soil is with

$$\varphi > \Theta_{max}$$

*the limit or critical equilibrium* of a soil occurs with

$$\varphi = \Theta_{max}$$

the loss of stability (*above limit or super critical state*) by a soil occurs with

$$\varphi \leq \Theta_{max}$$

Note that the criterion  $\Theta_{max} = \varphi$  when studying the bearing capacity of the subsoil has been first proposed and applied by the Soviet scientists P.A. Minyaev and N.P. Puzyrevsky.

### Sec. 20.2. Determination of the Angle of Maximum Inclination $\Theta_{max}$ . Loose Cohesionless Soils

Figure 20.2 represents Mohr's circle constructed by using the principal stresses  $p_1$  and  $p_2$ . By connecting the representative point  $D$  with the origin of the coordinate system  $O$  we get a right-angled triangle  $OFD$ . The two sides,  $p_n$  and  $\tau$ , are known here, and, with the specified values of  $p_1$  and  $p_2$ , they are determined by the orientation of the elementary area (angle  $\omega = 2\delta^\circ$ ). Find the value of the angle  $\beta$  from this triangle:

$$\tan \beta = \tau/p_n \quad (20.11)$$

A comparison of this relationship with the equation  $\tan \Theta = \tau/p_n$  (see Eq. 20.1) already familiar to us makes it possible to write  $\beta = \Theta$ . We can thus find the angle  $\Theta_\delta$  from the specified values of the principal stresses  $p_1$  and  $p_2$  for elementary areas, whatever their orientation, by using Mohr's circle. At the same time it can be seen from the diagram that

$$\beta_{max} = \Theta_{max} \quad (20.12)$$

Differently speaking, the angle of maximum inclination  $\Theta_{max}$  in Mohr's diagram is determined by the value of the angle between the abscissa axis and a tangent to the circle (Mohr's envelope) drawn through the origin of the coordinate system (point  $C$  in Fig. 20.2).

As can be seen from the diagram, the angle of maximum inclination,  $\Theta_{max}$ , corresponds to the angle made by the abscissa axis and the tangent to the circle at the point  $C$ . We see that  $\Theta_{max}$  does not correspond to the elementary area along which  $\tau_{max}$  operates (angle  $\omega > 90^\circ$ ).

The radius vector  $EC$  forms an angle with the tangent at the point  $C$ . Consequently, the corresponding sides being perpendicular, the angle  $BEC = \Theta_{max}$ . Thus the angle of inclination  $\Theta$  at the given point, determined by the principal stresses  $p_1$  and  $p_2$ , attains its greatest value,  $\Theta_{max}$ , on an elementary area corresponding to the angle  $\delta$ :

$$\omega = 2\delta = 90^\circ + \Theta_{max} \quad (20.13)$$

$$\delta = (45^\circ + \Theta_{max}/2) \quad (20.14)$$

Let us define by  $\delta_{lim}$  the angle determining the orientation of the elementary area corresponding to the state of limit equilibrium at the given point. Then, by taking into account Eq. (20.10), we can write

$$\delta_{lim} = (45^\circ + \varphi_n/2) \quad (20.15)$$

or, considering this angle as being a complementary one,

$$\delta_{lim} = (45^\circ \pm \varphi_n/2) \quad (20.15')$$

It will be recalled that for a solid body  $\delta_{lim} = 45^\circ$  corresponds to the orientation of the elementary area with  $\tau_{max}$ . Express the value of the angle  $\Theta_{max}$  in terms of the principal stresses  $p_1$  and  $p_2$ . Refer again to Fig. 20.2. Find the value of  $\Theta_{max}$  from the right-angled triangle  $OCE$ . In this latter we know the hypotenuse  $OE$  which is the distance of the circle's centre from the origin of the coordinates. We also know the side  $EC$  equal to the radius of Mohr's circle. Thus we have

$$\frac{p_1 - p_2}{2} = \frac{p_1 + p_2}{2} \sin \Theta_{max} \quad (20.16)$$

whence

$$\sin \Theta_{max} = \frac{p_1 - p_2}{p_1 + p_2} \quad (20.17)$$

In the state of limit equilibrium  $\Theta_{max} = \varphi$ . In this case Eq. (20.17) takes on this form:

$$\sin \varphi_n = \frac{p_1 - p_2}{p_1 + p_2} \quad (20.18)$$

This relationship expresses the known *condition of plasticity of cohesionless loose bodies of soil* first established by the Scottish civil engineer Rankine (1856) and is therefore called after him.

The relationship (22.17) is of a general character and can be used whatever the form of the load for which there are formulae to determine the principal stresses  $p_1$  and  $p_2$ .

### Sec. 20.3. Evaluation of the Weight of the Soil Mass

The soil is acted on by the weight of the overburden overlying the particular horizon at any depth, including a distance  $z$  of a definite horizon  $AA$  from the soil's upper surface. The soil mass produces at the horizon  $AA$  a certain pressure determining the natural (gravitational) load  $p_{nat}$ . At this we assume

$$p_{nat} = \rho_{aver} z \quad (20.19)$$

where  $\rho_{aver}$  is the averaged mass density of the overburden.

It may be assumed that the action of the weight of the overburden on the entire soil mass obeys the hydrostatic law of stress distribution. For the particular case we adopt the coefficient of lateral pressure  $\xi = 1$  which is, certainly, an assumption. However, as has been shown by V.A. Florin (1959), this approximation does not invalidate any markedly the eventual computational results. In particular, with a twofold decrease of the coefficient of lateral pressure ( $\xi = 0.50$ ), the magnitude of the permissible load increases only by 10%.

Under this condition the principal stresses due to the weight of the soil mass  $p'_1$  and  $p'_2$  are mutually equal and equal to the natural load  $p_{nat}$ :

$$p'_1 = p'_2 = p_{nat} \quad (20.20)$$

which is verified by the familiar law of hydrostatic stress distribution at the contact surface between the soil surface and the load (principal stresses  $p_1 = p_2$ ).

At the same time any horizon from the upper surface of the soil mass

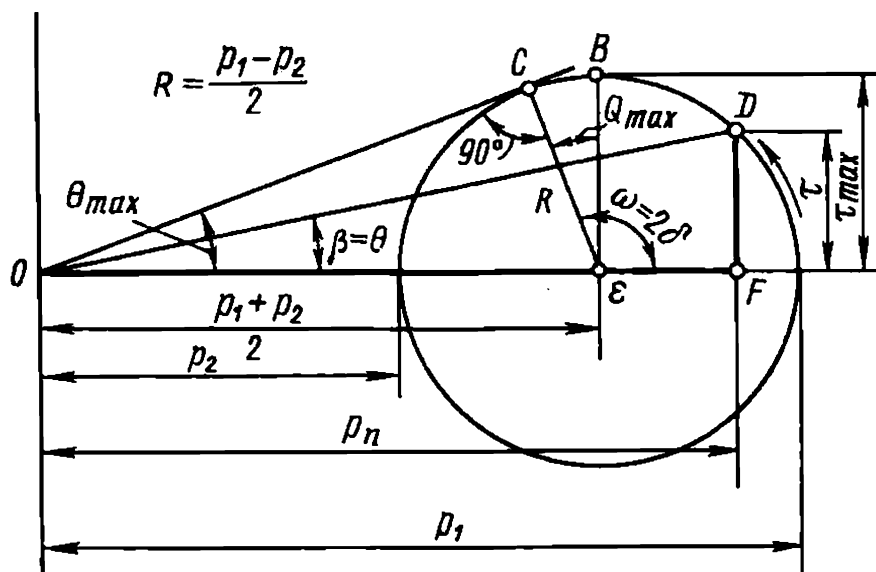


Fig. 20.2. Mohr's circle for determining angles of inclination  $\theta$  depending on the orientation of a unit area

may be considered as *a surface* one, bearing the weight of the overlying soil, as a uniformly distributed load with a load rate  $p_0$ , infinitely spreading in all directions. Under this condition any vertical axis will provide a symmetry axis and at any point of the imaginary surface the condition (20.20) will be satisfied.

According to the hydrostatic law of stress distribution these stresses at the given point prove equal in all directions. This makes it possible to use *the principle of superimposing the principal stresses* due to the external load  $p_1$  and  $p_2$  on strains  $p'_1 = p'_2 = p_{nat}$  caused by the overlying soil mass.

Viewed in the context of the above considerations the angle of maximum inclination  $\Theta_{max}$  for a definite point in the subsoil at a vertical distance  $z$  from the surface characterized by principal stresses induced by the external load  $p_1$  and  $p_2$  allowing for the soil's own weight can be determined by superimposing on the principal stresses in Eq. (20.17) of the stresses induced by the soil's own weight  $p_{nat}$ . After such a superimposition we obtain

$$\sin \Theta_{max} = \frac{(p_1 + p_{nat}) - (p_2 + p_{nat})}{(p_1 + p_{nat}) + (p_2 + p_{nat})} \quad (20.21)$$

Substitute into this relationship the value of  $p_{nat}$  from Eq. (20.19). Then Eq. (20.21) will finally take on this form:

$$\sin \Theta_{max} = \frac{p_1 - p_2}{p_1 + p_2 + 2\rho_{aver}z} \quad (20.21a)$$

The denominator in the right-hand side of this equation, compared with Eq. (20.17) increases continuously with increasing the depth  $z$  due to  $2\rho_{aver}z$ . This leads to decreasing the angle  $\Theta_{max}$  with depth and concurrently increases the stability of the soil mass.

It will be recalled that the bulk density of soils in the zone above the water table is generally close to  $2 \text{ t/m}^3$  but changes dramatically if the soil is found below the water table (i.e. when submerged). In this case the soil is acted on by the buoyant force of the groundwaters in conformity with the Archimedean principle.

Loose (grained) soils have pores filled with gravitational water. Each grain in the mineral skeleton is suspended separately. In this case for the determination of the bulk density  $\rho_{susp}$  of a grained soil in a suspended state we have

$$\rho_{susp} = (1 - n)(\rho_0 - 1) \quad (20.22)$$

As usual, here  $n$  is the porosity,  $(1 - n)$  is the volume of the solid



phase (skeleton particles) of the grained soil,  $\rho_0$  is the bulk density of the grains.

The voids in clayey soils are, as a rule, completely filled with bound water, and gravitational water is incapable of penetrating there. Under this condition a clayey soil, submerged, loses part of its weight (in volume). Hence for clayey soils  $\rho_{susp} = \rho_w - 1.0$ .

The bulk density of a submerged soil is generally close to  $1 \text{ t/m}^3$ . Thus a rise in the water table results in that the submerged soil mass loses in bulk density almost twofold. In conformity with Eq. (20.22), this reduces appreciably the bearing capacity of the subsoil of structures which may cause failure. We can thus see the great role in soil mass stability played by the level of the ground waters inundating the overburden.

**Evaluation of the depth of a structure's foundation.** Increasing the depth of the foundation of a structure is one of the simplest and efficient methods of enhancing the bearing capacity of the subsoil. Assume that a structure is erected on the upper surface of a soil mass, and use for calculations the weight of a soil layer,  $h_d$  in thickness. The design load on the soil,  $p_0$ , at the subgrade will then be found from the relationship

$$p_0 = p_s - \rho h_d \quad (20.23)$$

Thus the allowance for the depth of a structure's foundation reduces to the already familiar problem of taking into account the weight of the overlying strata when evaluating the bearing capacity of the soil mass. Then

$$p_{lim} = \rho_{aver} z' = \rho_{aver} (z + h_d)$$

where  $z$  is the depth of occurrence of the particular horizon below the level of actual application of the load  $p_s$  to the soil, i.e. below the base of the structure's foundation.

On this condition we can rewrite Eq. (20.22) to determine  $\Theta_{max}$  allowing not only for the weight of the soil but also for the depth of the foundation,  $h_d$ :

$$\sin \Theta_{max} = \frac{p_1 - p_2}{p_1 + p_2 + 2\rho_{aver}(z + h_d)} \quad (20.24)$$

The principal stresses  $p_1$  and  $p_2$  are in the given case established referring to the value of  $p_0$  given by Eq. (20.23). Hence it is in principle possible to ensure that for any point in the subsoil the condition  $\Theta_{max} > \varphi$  is satisfied by increasing accordingly the depth of the foundation even if the subsoil may have low bearing capacity. The use of this efficient measure, however, must be decided taking into account the economic and

technological advantages of all likely versions of construction of the foundation.

**Determination of  $\Theta_{max}$  taking into account soil's cohesion.** We have thus far dealt with the problem under conditions of loose soils having true or apparent cohesion ( $\Sigma_w = 0$  and  $c_c = 0$ ). In fact, however, soils do have a certain degree of cohesion which must be taken into consideration when evaluating the stability of the foundation of a structure. In order to account for a soil's cohesion in the evaluation of  $\Theta_{max}$  let us resort to an artificial technique, substituting the soil's cohesion by additional internal friction forces at a specified value of the angle of internal friction  $\varphi$  due to some additional increase in the depth of the structure's foundation  $h_s$ .

We will solve the problem if we find the value of  $h_s$  satisfying our condition and replace  $z$  in Eq. (20.24) by a new quantity,  $z'' = z + h_s$ .

The value of  $h_s$  can be determined if we carry out an equivalent substitution of the soil's cohesion,  $c$ , by forces of internal friction,  $r$ , caused by the weight of the soil's column whose bulk density is  $\rho_{aver}$  and height  $h_s$ . By taking this into account we can write:  $c = \rho_{aver} h_s \tan \varphi$ , where  $\tan \varphi$  is the coefficient of friction corresponding to the angle of internal friction  $\varphi$  adopted in the principal calculation. Hence

$$h_s = \frac{c}{\rho_{aver} \tan \varphi} \quad (20.25)$$

By virtue of Eq. (20.24), to determine the general form of  $\Theta_{max}$  allowing for the soil's own weight, the depth of the foundation and cohesion of the soil, we can write

$$\sin \Theta_{max} = \frac{p_1 - p_2}{p_1 + p_2 + 2\rho_{aver}(z + h_d + h_s)} \quad (20.26)$$

Clearly, the soil's cohesion increases the strength of the subsoil as does the increased depth of the foundation. We can at the same time see that the two factors may compensate each other. In particular, marked cohesion of the soil may ensure complete stability of a structure even on application of an appreciable load without increasing the depth of the foundation. This occurs when a structure is supported by a hard rock.

#### Sec. 20.4. Lines of Simultaneous Rupture and Regions of Limit State of Stress

Equations (20.22) to (20.26) make it possible to find the value of  $\Theta_{max}$  for any point in the subsoil under different initial conditions.

Having thus determined  $\Theta_{max}$  at a number of points in the subsoil of a structure and arranged these for convenience on an arbitrary grid, we can

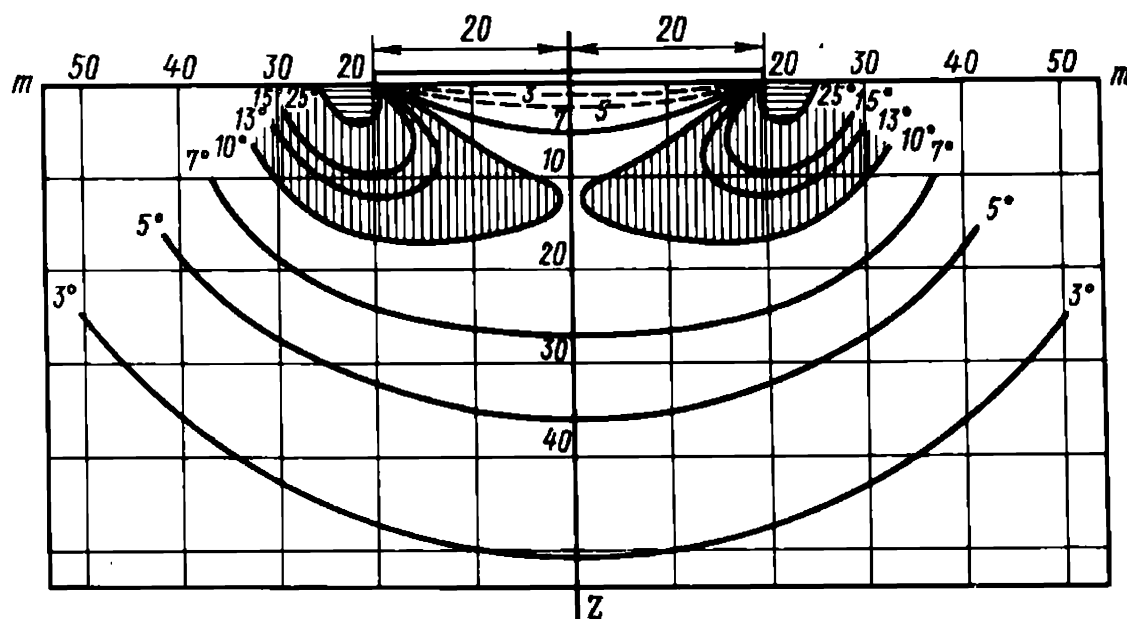


Fig. 20.3. Lines of equal angles of maximum inclination  $\theta_{max} = \text{const}$  and regions of loss of soil stability (plastic regions) at  $\varphi_1 = 10^\circ$  and  $\varphi_2 = 25^\circ$ . The particular case: width of loaded strip  $2b = 40$  m; load  $p_0 = 2.0$  kg/cm<sup>2</sup>; soil's bulk density  $\rho = 1.6$  t/m<sup>3</sup>; cohesion  $c = 0$

connect points of equal values of  $\Theta_{max}$  by smooth curves. The resultant curves of  $\Theta_{max} = \text{const}$  are called (as suggested by N.P. Puzyrevsky) lines of simultaneous rupture.

As has been made clear elsewhere, the criterion of the state of limit equilibrium for the particular case ( $\varphi_n \neq 0$ ,  $\varphi_w \neq 0$ ) is the observance of the equality  $\Theta_{max} = \varphi$  (see Eq. 20.10).

Having a pattern of the distribution of lines of  $\Theta_{max} = \text{const}$  for some particular case available, we can easily distinguish at the subsoil of the structure the regions of critical state of stress (regions of rupture). At this we proceed from the consideration that all points within these regions are characterized by  $\Theta_{max} > \varphi$ . Clearly, a line of simultaneous rupture corresponding to the condition  $\Theta_{max} = \varphi$  will be a contour (boundary) line of a region of rupture. An example of such a construction is provided by Fig. 20.3 showing the distribution of lines of simultaneous rupture for a particular case of loading the subsoil.

For determining the distribution of regions of the critical state of stress the angle of internal friction was originally adopted as being  $\varphi = 10^\circ$ . As can be seen, in the given case these regions are fairly conspicuous presenting a hazard to the structure's stability (vertically shaded). At increased values of the angle of internal friction (e.g. with  $\varphi = 25^\circ$ ) the regions of rupture dramatically decrease concentrating only at the edges of the structure (horizontally shaded).

It is self-evident that rupture zones in the subsoil are more developed in

soils with low bearing capacity (with small values of  $\varphi$ ,  $c$  and  $\rho_{aver}$ ) and at a high intensity of a load applied to the soil,  $p_0$ .

There are cases where, after constructing a pattern of distribution of lines of  $\Theta_{max}$  in the subsoil, it proves necessary to qualitatively evaluate soil strength at one point or another. The problem is generally solved referring to the factor of safety:

$$k_{saf\Theta} = s_{p\delta}/\tau_{\delta} \quad (20.26a)$$

where  $s_{p\delta}$  and  $\tau_{\delta}$  are, respectively, the shearing resistance  $s$  and the shearing stress  $\tau$ , acting on elementary areas appropriately orientated with respect to the principal stresses at a particular point  $\delta^\circ$ .

In the given problem, in particular, when solving it in terms of  $\Theta_{max}$ , the normal stress,  $p_n$ , cause the most hazardous critical state when acting on an elementary area in conformity with Eq. (20.14) at an angle

$$\delta = (45^\circ \pm \Theta_{max}/2)$$

Clearly, the shearing resistance  $s_{p\delta}$  acting on the area  $\delta$  can be found from the relation:

$$s_{p\delta} = p_{n\delta} \tan \varphi + c \quad (20.26b)$$

It will be recalled that normal stresses  $p_{n\delta}$  and, respectively, shearing stresses  $\tau_{\delta}$  acting on the elementary area  $\delta$  through principal stresses  $p_1$  and  $p_2$  are described by Eqs. (17.6) and (17.7):

$$p_{n,\delta} = \frac{p_1 + p_2}{2} + \frac{p_1 - p_2}{2} \cos 2\delta; \quad \tau_{\delta} = \frac{p_1 - p_2}{2} \sin 2\delta$$

Then, by virtue of Eqs. (20.26a) and (20.26b), for determining the factor safety  $k_{saf}$  we can write this formula for any point in the subsoil, whatever the pattern of loading:

$$k_{saf\Theta} = \frac{[(p_1 + p_2) + (p_1 - p_2) \cos 2(45^\circ \pm \Theta_{max}/2)] \tan \psi + 2c}{(p_1 - p_2) \sin 2(45^\circ \pm \Theta_{max}/2)} \quad (20.26c)$$

As is known, the limit state  $\Theta_{max}$  corresponds to the angle of internal friction of the soil  $\varphi$ . Then Eq. (20.26c) for this state can be rewritten as:

$$k_{saf\Theta} = \frac{[(p_1 + p_2) + (p_1 - p_2) \cos 2(45^\circ \pm \varphi/2)] \tan \varphi + 2c}{(p_1 - p_2) \sin 2(45^\circ \pm \varphi)} \quad (20.26d)$$

Clearly, when applying this relationship, the principal stresses  $p_{1c}$  and  $p_{2c}$  at a point in the subsoil whose coordinates are  $(x, z)$  must be determined taking into account the external load,  $p_0$ , the soil's bulk density  $\rho$

allowing for, when necessary, its submersion in the groundwater, the depth of the foundation  $h_d$ , and, finally, cohesion of the soil  $c$ .

By virtue of Eqs. (20.22), (20.24), (20.25) and (20.26)

$$p_{1c} = p_1 + \rho(z + h_d + h_s); \quad p_{2c} = p_2 + \rho(z + h_d + h_s)$$

where  $p_1$  and  $p_2$  are the principal stresses corresponding to the external load. Then the principal equation (20.26d) for determining the factor of safety  $k_{saf\theta}$  can be finally presented as follows:

$$k_{saf\theta} = \frac{[(p_1 + p_2) + 2\rho(z + h_d + h_s) + (p_1 - p_2) \cos 2(45^\circ \pm \varphi/2)] \tan \varphi + 2c}{(p_1 - p_2) \sin 2(45^\circ \pm \varphi/2)} \quad (20.26e)$$

To determine the value of the angle of maximum inclination  $\Theta_{max}$  for a case of a compound load Eq. (20.26) and others stemming from this cannot be applied since it is impossible to sum up the principal stresses induced by particular loads since the orientations of principal directions do not agree. In this case the angle  $\Theta_{max}$  is determined in terms of the sum of stresses  $p_z$ ,  $p_x$ , and  $\tau_{zx}$  acting on horizontal and vertical elementary areas from these particular loads by using this relationship:

$$\sin^2 \Theta_{max} = \frac{(p_z + p_x)^2 + 4\tau_{zx}^2}{[p_z + p_x + 2\rho_{aver}(z + h_d + h_s)]^2} \quad (20.26f)$$

We distinguish two forms of regions of critical state of stress: an open and a closed one. In an *open form* lines of simultaneous rupture do not close and come to the surface of the soil mass (right-hand side of Fig. 20.4). This form occurs in the case of a shallow footing and a loose cohesionless soil ( $c = 0$ ). In a *closed form* lines of  $\Theta_{max} = \text{const}$  close on themselves in the soil mass (left-hand side of Fig. 20.4).

This form is typical of deep foundations and soils that have a certain degree of apparent cohesion  $\Sigma_w$  or true cohesion  $c_s$ , i.e.  $c_w \neq 0$ .

The role of cohesion in the surface zones bordering on the structure becomes fairly appreciable since the absolute value of the shearing stress  $\tau_{max}$  tends here to zero. For this reason it is not uncommon that even minor cohesion may be sufficient to deal with hazardous shearing stresses likely to appear here and ensure adequate stability of the subsoil of the structure.

The particular method of plotting lines of simultaneous rupture of the soil from points of rupture is especially advantageous when it is required to analyse a complex geological structure of the supporting soil mass. The subsoil may often be composed by layers of different soils with different strength characteristics ( $\varphi$ ,  $c$  and  $\rho$ ). Therefore, when determining  $\Theta_{max}$  for points within each layer, we must take into account its index characteristics.

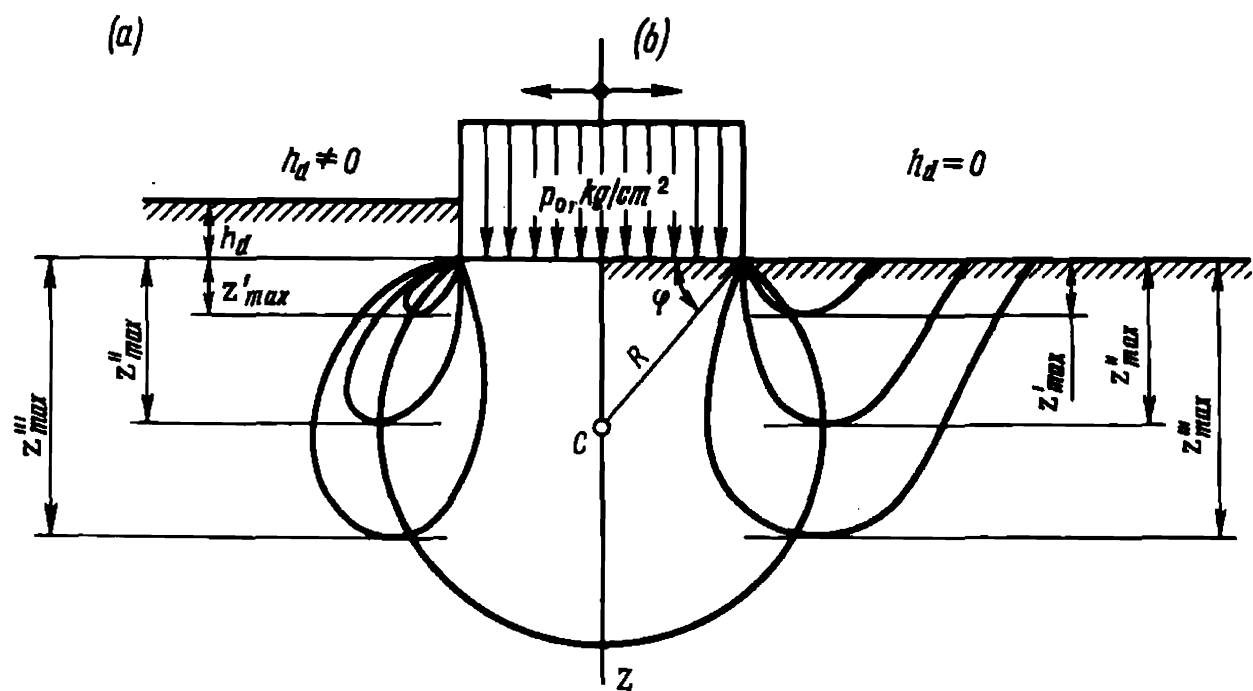


Fig. 20.4. Lines of equal angles of maximum inclination  $\theta_{max} = \text{const}$  under increasing loading  $p'_0, p''_0$ , and  $p'''_0$ :  
a—for a deep footing (left); b—for a shallow footing

To conclude, all the above constructions of lines of simultaneous rupture ( $\Theta_{max} = \text{const}$ ) and of regions of critical state of stress of a soil are of more or less arbitrary character. Nevertheless the given method of analysis of the behaviour of the subsoil, especially when evaluating the geotechnical conditions of erecting a proposed structure and assessing various versions may often prove most useful. This is due to the fact that the method of plotting lines of simultaneous rupture and determination of regions of critical state of a soil provides us with an approximate but a very vivid picture of the behaviour of a soil acted on by a load under specified conditions.

Sec. 20.5. Critical Safe  $p_{saf}$  and Permissible Load

The case of a uniformly distributed load. Refer to the principal equation (20.26) for determining  $\Theta_{max}$

$$\sin \Theta_{max} = \frac{p_1 - p_2}{p_1 + p_2 + 2\rho_{aver}(z + h_d + h_s)}$$

The principal stresses  $p_1$  and  $p_2$  at a uniformly loaded surface of the subsoil, as has been shown, are found from Eqs. (17.8) and (17.9).

Substitute the values of  $p_1$  and  $p_2$  for a uniformly distributed load into Eq. (20.26). Referring to Fig. 20.4, find the value of  $z_{max}$  corresponding to

the largest value of  $z' - z'''$  of a line of simultaneous rupture  $\Theta_{max} = \varphi$  at the subsoil of the structure at one load or another,  $p_0$ :

$$z_{max} = \frac{p_0}{\pi \rho_{aver}} (\cot \varphi + \varphi - \pi/2) - (h_d + h_s) \quad (20.27)$$

This relationship shows that points of  $z_{max}$  corresponding to various loads,  $p_0$ , lie on the same circle from which the subgrade of the structure is visible at an angle

$$\alpha = (\pi/2 - \varphi)$$

The radius  $R$  of the circle on which  $z_{max}$  points lie for a definite constant angle of vision  $\alpha$ , is found from the relation

$$R_{z_{max}} = b / \cos \varphi \quad (20.28)$$

where  $b$  is half the width of the loaded area.

As follows from Eq. (20.27), the depth of occurrence of the regions, and, consequently, of load relief, other conditions being equal, the expansion of regions of rupture increases with increasing the value of the load  $p_0$ . As  $p_0$  increases, the lowest point of the curve of  $\Theta_{max} = \varphi$  with the ordinate  $z_{max}$ , i.e. one corresponding to the lower boundary of expansion of the region of the soil's rupture, slides on the circle plotted by the previously described method. Thus we can call this circle a *guiding* one.

Clearly, on this condition the region of soil rupture with increasing  $p_0$  falls deeper under the loaded area. What has been said above is illustrated by Fig. 20.4 for cases of a shallow and a deep foundation.

Let us solve Eq. (20.27) with respect to  $p_0$ :

$$p_0 = \frac{\pi \rho_{aver} (z_{max} + h_d + h_s)}{\cot \varphi + \varphi - \pi/2} \quad (20.29)$$

where  $p_0$  is the load at which under the particular values of  $h_d$ ,  $\rho_{aver}$ ,  $\varphi$  and  $c$  the region of soil rupture penetrates into the subsoil of a structure to a depth  $z_{max}$ .

Find the safe load  $p'_{saf}$  which rules out completely regions of critical state of stress (rupture regions) in the subsoil. This should prevent the structure's settlement induced by plastic deformations in the supporting soil mass. To solve problem we safely use conclusions of the theory of elasticity. Clearly, this condition will be observed at  $z_{max} = 0$ .

A substitution into Eq. (20.29) of the values of  $p'_{saf}$ ,  $z_{max} = 0$  and  $h_s$  from Eq. (20.25) yields

$$p'_{saf} = \frac{\pi \rho_{aver} [h_d + c / \rho_{aver} \tan \varphi]}{\cot \varphi + \varphi - \pi/2} \quad (20.30)$$

For grained (cohesionless) soils with  $c = 0$ , Eq. (20.30) takes on a simpler form:

$$p'_{saf} = \frac{\pi \rho_{aver} h_d}{\cos \varphi + \varphi - \pi/2} \quad (20.31)$$

This form of equation has been first proposed by the Soviet scientist N.P. Puzyrevsky and later validated by the Austrian O.Frölich.

It will be recalled that the relationship followed from the state of stress due to a load  $p_0$  is found from the formula  $p_0 = p_s - \rho h_d$  (see Eq. 20.23).

Hence the ultimate value of the safe load  $p_{saf}$  is

$$p_{saf} = p'_{saf} + \rho h_d \quad (20.32)$$

Note that in this equation  $p'_{saf}$  is a load found from Eqs. (20.30) and (20.31), and  $\rho$  is the bulk density of the soil layer removed when excavating the foundation's trench with a depth  $h_d$ .

Analysis shows that the deep penetration of rupture areas under the base of a structure, to say nothing of their closure there renders the operation of the structure especially disadvantageous. This includes primarily a likelihood of a sudden and dramatic settlement followed by tilting of individual elements of the structure. Such settlement is generally very differential and cannot be predicted or calculated.

Equations (20.30) and (20.31) would be more justified to apply since they rely on a condition of a total absence of rupture (yield) regions in the subsoil of the structure. Then we may well use equations of an elastic semispace for the present analysis.

The safe loads  $p'_{saf}$  and  $p_{saf}$  found from the above equations are thus concurrently *perfectly permissible* ones,  $p_{perm}$ . However, as indicated by building practice, the requirement of the total absence of regions of a critical state of stress at the subsoil of a structure turns out to be too rigorous, especially with wide foundations.

Thus, it became feasible to assume loads  $p_{saf}$  found from these formulae as quite permissible and safe ones and, at the same time, ones that may be increased for practical purposes. This means that it was actually permissible to have regions of critical state of stress in the subsoil of a structure.

Building practice indicates that regions of rupture are permitted beyond the contour of a structure's foundation. In this case regions of rupture affect only external soil masses, the structure itself being supported by a stable soil mass. The load applied to the soil corresponding to this condition may be assumed to be permissible,  $p_{perm}$ .

To consider this case, refer to Fig. 20.5. The maximum depth of the



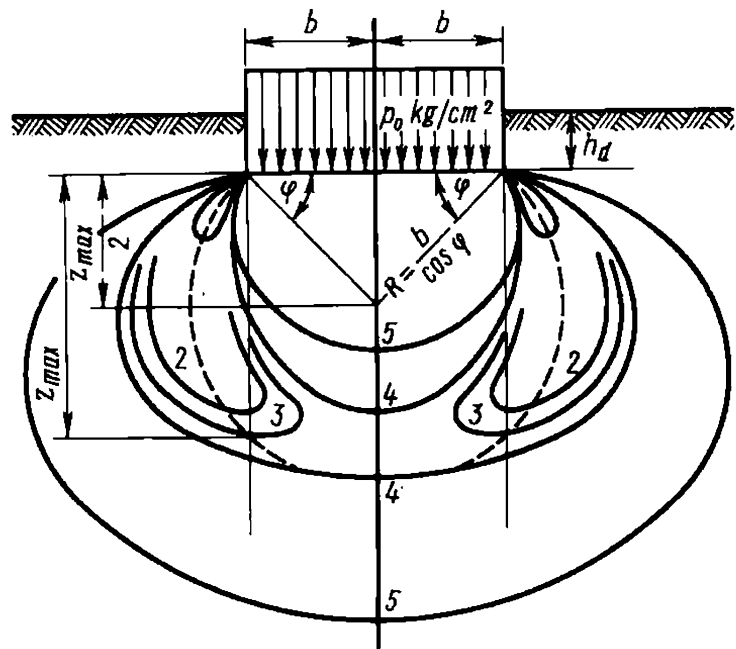


Fig. 20.5. Diagram for determining allowable load proceeding from strength of soil (phase II)

region of rupture,  $z_{max}$ , is determined from Eq. (20.27):

$$z_{max} = \frac{p_0}{\pi \rho_{aver}} (\cot \varphi + \varphi - \pi/2) - (h_d + h_s)$$

Moreover, we know that all points of  $z_{max}$  with increasing  $p_0$  slide along the guiding circle of a radius found from Eq. (20.28):

$$R_{z_{max}} = b / \cos \varphi$$

Hence it follows that

$$z_{max}/2 = R \sin \varphi \quad (20.33)$$

or

$$z_{max} = 2b (\sin \varphi / \cos \varphi)$$

which means

$$z_{max} = 2b \tan \varphi \quad (20.34)$$

A substitution of  $z_{max}$  from this relationship into Eq. (20.27) yields

$$2b \tan \varphi = p_0 / \pi \rho_{aver} (\cot \varphi + \varphi - \pi/2) - (h_d - h_s) \quad (20.35)$$

Let us solve this equation with respect to  $p_0$  and substitute  $p_0$  by a new quantity,  $p'_{saf}$  (permissible load). As usual, define the value of  $h_s$  as

$$h_s = \frac{c}{\rho_{aver} \tan \varphi}$$

Having completed these operations, by referring to Eq. (20.35), we will get a new relationship for determining  $p'_{perm}$ , this time under conditions of

partial expansion in the subsoil of a structure of regions of critical state of stress:

$$p'_{perm} = \frac{\pi \rho_{aver} [2b \tan \varphi + h_d + c/(\rho_{aver} \tan \varphi)]}{\cot \varphi + \varphi - \pi/2} \tag{20.36}$$

As can be seen, this equation suggests the dependence of  $p'_{perm}$ , apart from other factors, on the width of the foundation, increasing, naturally, as the latter increases. It should be noted, however, that if we exclude from this equation the width of the loaded area for  $c = 0$ , this relationship fully agrees with the familiar equation (20.31) which is a particular case of the formula proposed by this writer. Determine finally the value of  $p_{perm}$  similarly to Eq. (20.32) from the relationship

$$p_{perm} = p'_{perm} + \rho h_d \tag{20.37}$$

To facilitate the use of Eqs. (20.36) and (20.37), Fig. 20.6 presents a graph for calculations. This graph gives several coefficients of the bearing capacity ( $M_b$ ,  $M_h$ , and  $M_c$ ) governed by the soil's angle of internal friction  $\varphi$  and, consequently, connected with the width of the loaded strip  $2b$ , depth of the foundation  $h_d$ , and cohesion  $c$ . The values of these coeffi-

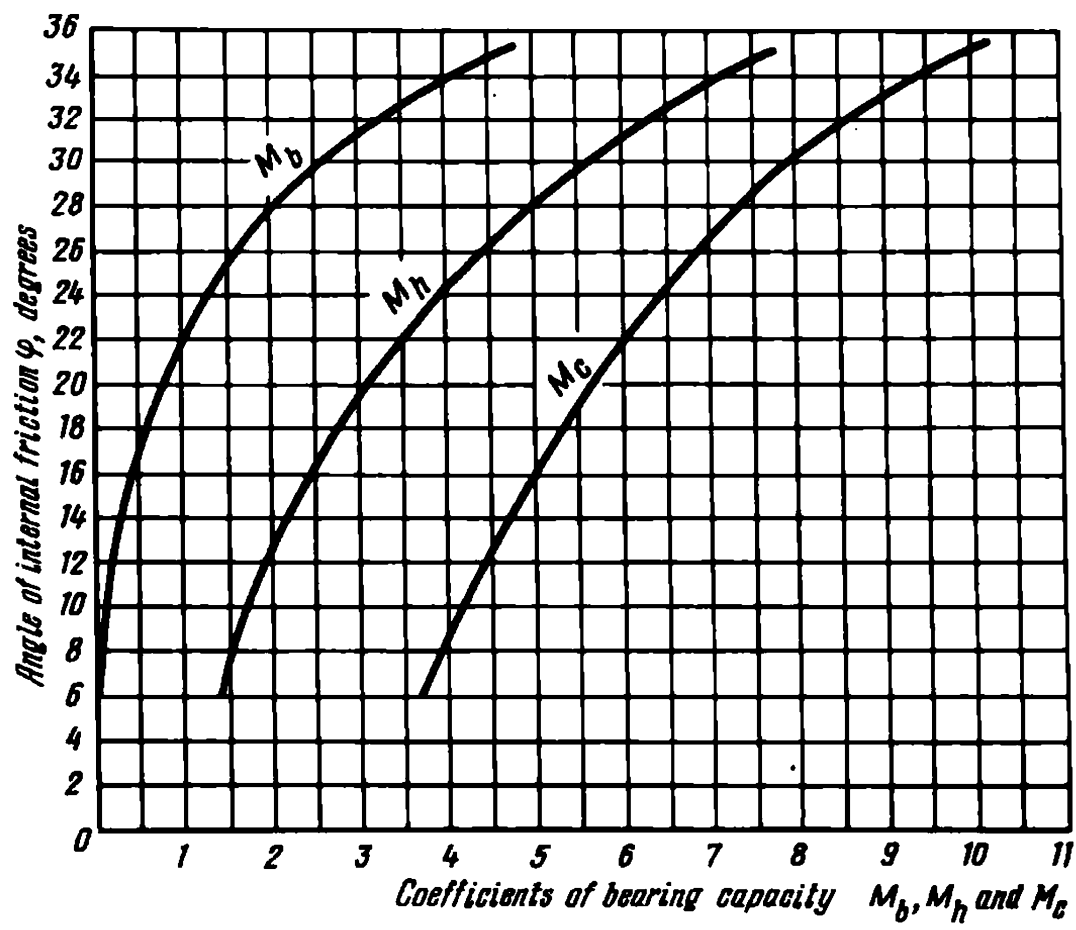


Fig. 20.6. Diagram for determining coefficients of the bearing capacity  $M_b$ ,  $M_h$ , and  $M_c$  in N.N. Maslov's formula

cients are found from these relationships:

$$\begin{aligned} M_b &= \frac{\pi \tan \varphi}{\cot \varphi - \pi/2 + \varphi}; \\ M_h &= (M_b / \tan \varphi) + 1; \\ M_c &= M_b / \tan^2 \varphi \end{aligned}$$

So that this graph may be used, Eqs. (20.36) and (20.37) have been thus unified:

$$p_{perm} = [M_b \times 2b + M_h h] \rho_{aver} + M_c c \quad (20.38)$$

Equation (20.38) takes into account the weight of material removed from the excavation from Eq. (20.37). Thus the results obtained are final ones.

The following example illustrates the use of this diagram. Suppose it is required to determine the permissible load from Maslov's equation, given that the width of the base of the structure's foundation is  $2b = 12$  m; its depth is  $h_d = 2.0$  m; the bulk density of the soil, when submerged, is  $\rho_s = 0.98$  t/m<sup>3</sup>; the angle of internal friction is  $\varphi = 22^\circ$ ; cohesion is 0.2 kg/cm<sup>2</sup> or  $c = 2$  t/m<sup>2</sup>.

Take from the diagram the values of  $M_b$ ,  $M_h$  and  $M_c$  for  $\varphi = 22^\circ$ . Then substitute these into Eq. (20.38) obtaining  $p_{perm} = (0.985 \times 12 + 3.44 \times 2)0.98 + 6.04 \times 2 = 30.4$  t/m<sup>2</sup> or  $\approx 3$  kg/cm<sup>2</sup>.

Equations (20.36) and (20.38) can be used for analysis of the subsoil composed of a cohesive soil ( $c > 0$ ) only on the condition that the angle of internal friction in it is  $\varphi > 5$  to  $7^\circ$ . Otherwise, as has been shown by practice, better results can be obtained by applying the given formulae for the calculations. In these we assume  $c = 0$  (at minor values of soil cohesion) or carry out soil computations by using the relationships without taking into account normal stresses (see Chapter 19) and ignoring the inappreciable internal friction of the soil which little contributes to the soil stability.

As has been pointed out elsewhere, Eq. (20.36) has been derived on the condition that a loss of soil stability immediately under a structure's foundation contour is impermissible. As demonstrated by construction practice, this ensures permissible conditions of the structure's operation. This condition is, however, not a single one.

Alternatively, Eq. (20.30) is modified following from conditions of penetration of plastic regions under the edges of the loaded strip to a depth equal to one-fourth of the foundation's width. This is how the building code SNiP II-15-74 determines the permissible load on the soil  $R$  proceeding from a second critical state and likely conditions of the structure deformations (phase II of the soil behaviour). For calculating the founda-

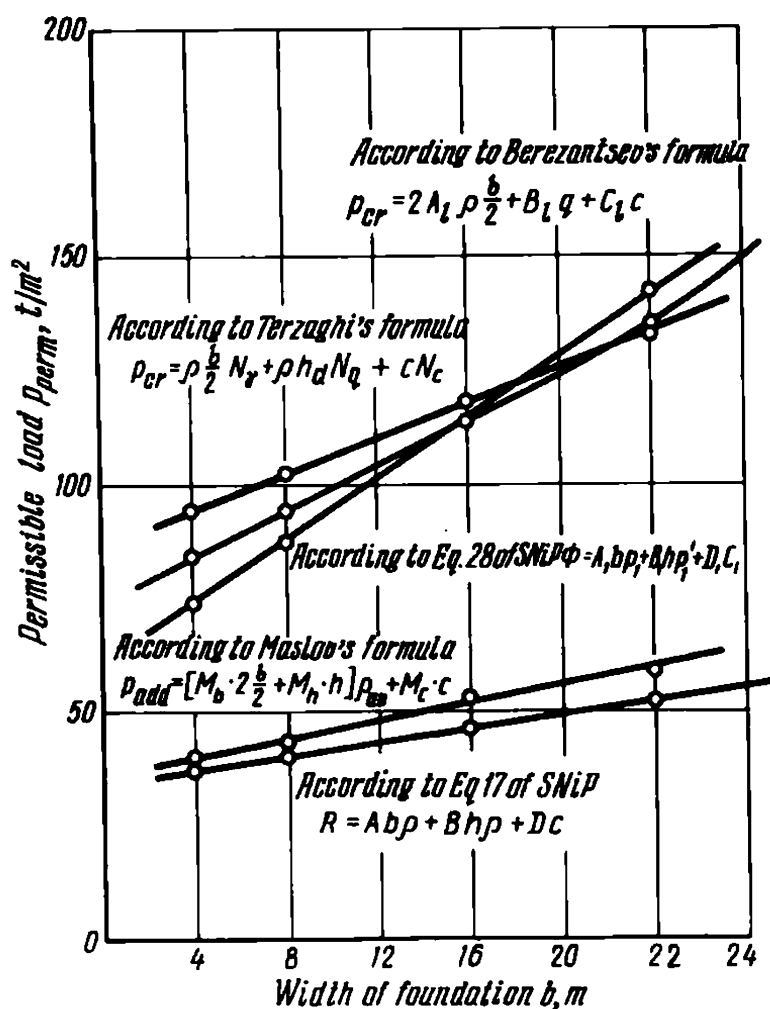


Fig. 20.7. Graph showing relationships between the allowable, limiting and critical loads on a structure's subsoil and the total width of footing  $b$  when determining these by using different formulae. A plane problem for  $\varphi = 16^\circ$ ,  $c = 4 \text{ t/m}^2$ ,  $h_d = 3.0 \text{ m}$

tion of an engineering or other structure without a basement the coefficient of operation conditions  $m_1$  and  $m_2$  and the factor of safety  $k_n$  are assumed equal to unity in this formula in the case of a critical state of stress. According to SNiP, the permissible load is

$$R = A b \rho + B h \rho + D c$$

where  $A$ ,  $B$ , and  $D$  are parameters of the bearing capacity governed by the angle of internal friction  $\varphi$ ;  $b$ , what is most important, is the total smaller side (width) of the base of the foundation;  $h$  is its depth.

Figure 20.7 is a diagram permitting some comparisons to be made. The diagram gives the value of  $p_{perm} = f(b)$  for definite general initial conditions:  $\varphi = 16^\circ$ ,  $c = 4 \text{ t/m}^2$ ,  $h = 3.0 \text{ m}$ ,  $\rho_{aver} = 2.0 \text{ t/m}^2$ .

As can be seen, the values of  $p_{perm}$  and  $R$  found from Eq. (20.38) and Eq. 17 from SNiP almost agree, especially when the foundation width ( $b$ ) is small which is usually the case.

It appears to us, however, that Eq. (20.36) and Eq. (20.38) following from this are of more practical value compared with Eq. 17 suggested by SNiP.

It should be finally pointed out that the conditions of performance of a

more or less wide foundation vary if the structure of the supporting soil mass is different. In particular, if the upper layers are composed of more stable soils underlain by less competent ones, then a structure with a spread foundation will operate in more disadvantageous conditions. This is due to the fact that regions of detrimental deformation may develop in less competent layers of the supporting soil mass.

## Chapter 21

### Critical Load when the Total Stability of the Subsoil of a Structure Must Be Ensured (Arching Phase)

#### Sec. 21.1. Theoretical Solutions

A theoretical solution of the problem of the critical load  $p_{crit}$  on the soil in the general case needs solutions of complex differential equations of a limiting (plastic) equilibrium together with a condition of plasticity.

An example of one of such simplified solutions proposed by V.G. Berezantsev in 1952 is provided by the following relationships for the determination of the boundary coordinates of a critical load  $p_b'$  and  $p_b''$ :

$$p_b' = \{2\rho b [ae^{(\pi/2 - 2\varphi)\tan\varphi} + B] + qCe^{(\pi/2 - 2\varphi)\tan\varphi}\} \left(1 + \frac{1}{2}\sin 2\varphi\right) \quad (21.1)$$

$$p_b'' = qDe^{\pi \tan\varphi} \quad (21.2)$$

where  $\rho$  is the soil's bulk density;  $b$  is half the foundation width;  $A$ ,  $B$ ,  $C$  and  $D$  are coefficients representing complex functions of the angle of inner friction found from special tables.

Note that, complex as it is, Eq. (21.1) corresponds to a particular case of solving the problem (soils with  $c = 0$ ) and a form of the curve of sliding specified in advance.

Even if approximate methods are used and assumptions made, these solutions prove to be too sophisticated which largely decreases their usefulness and poses a constraint on their practical applications. In addition, such solutions have not been duly approved by building practice.

For a soil exhibiting only cohesion, solutions in a simple closed form are easily obtained in many particular cases. In our approach these solutions are applicable to subsoils composed of plastic clays which depend for their shearing resistance solely on apparent cohesion,  $\Sigma_w$ .

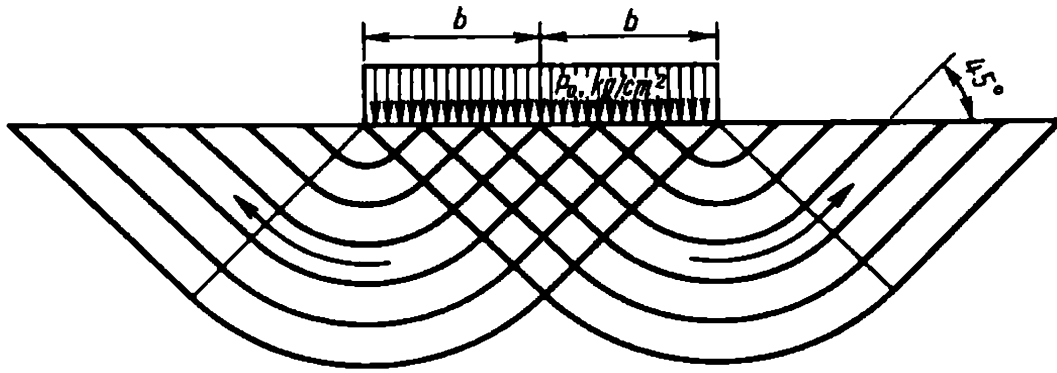


**Fig. 21.1.** Lines of sliding (at an angle  $45^\circ$  to principal directions) in a medium manifesting cohesion only

The problem of a critical load on such a soil has been considered by the German scientist Ludwig Prandtl. Assuming that a medium has only cohesion and ignoring the weight of the soil, he expressed the critical load in conditions of a two-dimensional problem by the following straightforward formula:

$$p_{cr} = (\pi + 2.0)c = 5.14c \quad (21.3)$$

Here  $c$  is the medium's cohesion, corresponding in our case to apparent cohesion  $\Sigma_w$  for plastic clayey soils.

The pattern of the distribution of lines of sliding in a medium acted on by an outer strip load as applied to the given case is shown in Fig. 21.1.

Allowing for the roughness of the base of the footing, Terzaghi gives the following equation for a two-dimensional problem:

$$p_{crit} = 5.7c \quad (21.4)$$

According to Ishlinsky, for square base footings

$$p_{crit} = 5.71c \quad (21.5)$$

Having considered the critical load induced by a circular rigid plant, Hanks has obtained the following solution for this case:

$$p_{crit} = 5.64c \quad (21.6)$$

For a rectangular footing, according to Shield, we have, after generalizing the methods considered by him:

$$p_{crit} = (5.14 + b/l)c \quad (21.7)$$

where  $b$  is one-half of the loaded area;  $l$  is its length.

The above formulae indicate that loading the surface along some restricted area somewhat increases the bearing capacity of  $p_{crit}$ . With  $l = \infty$ , i.e. under conditions of a flat problem, Eq. (21.7) becomes identical to the relationship (21.3).

Equations (21.3) and (21.7) are similar in form. Thus it is possible to unify all these equations relating to the direct loading of the surface ( $h_d = 0$ ), to simplify matters, by the following relationship:

$$p_{crit} = (\pi + 2.5)c \quad (21.8)$$

or

$$p_{crit} = 5.64c \quad (21.9)$$

It will be recalled that in the case of a direct load on the surface ( $h_d = 0$ ) the safe load (or bearing capacity)  $p_{saf}$ , taking into account local deformations for the case of a uniformly distributed load is found from these equations:

$$\begin{aligned} p_{saf} &= \pi c = 3.14c \\ p_{saf} &= \pi \Sigma_w = 3.14 \Sigma_w \end{aligned}$$

When elaborating a theory of critical equilibrium, L. Prandtl emphasized a rapid increase in the bearing capacity if the medium has internal friction ( $\varphi \neq 0$ ). In particular, for conditions corresponding to Eq. (21.3) Prandtl has shown that at  $\varphi = 10^\circ$  the value of  $p_{crit} = 6.98c$ , and at  $\varphi = 20^\circ$  it becomes  $p_{crit} = 10.33c$ .

It should be also noted that with a sufficient area of the foundation supported by a soil manifesting internal friction ( $\varphi \neq 0$ ) it would be erroneous to omit the soil's own weight.

### Sec. 21.2. Semiempirical Relationships

The very complexity of the problem posed, all necessary factors being taken into account ( $\varphi \neq 0$ ,  $c \neq 0$  and  $\rho \neq 0$ ), is the reason why soil scientists are looking for alternative solutions in determining the bearing capacity of the soil, such that are simpler in form and are in better agreement with the actual behaviour of the subsoil of a structure and, even if semiempirical, are more convincing from the viewpoint of civil engineering.

**Initial concepts.** Basing on his mathematical analysis, Prandtl proposed a calculation scheme in 1921 to determine the critical load (bearing capacity) on loose soils with  $\varphi \neq 0$ . This scheme represented with some modifications in Fig. 21.2 provided a basis for all hypotheses and studies that followed.

Most semiempirical relationships to be considered involve a number of assumptions. It is assumed that subsoil stability at loads in excess of critical ones starts to be lost as a result of displacement along a certain surface of sliding and arching of entire soil blocks as if these were solid monolith

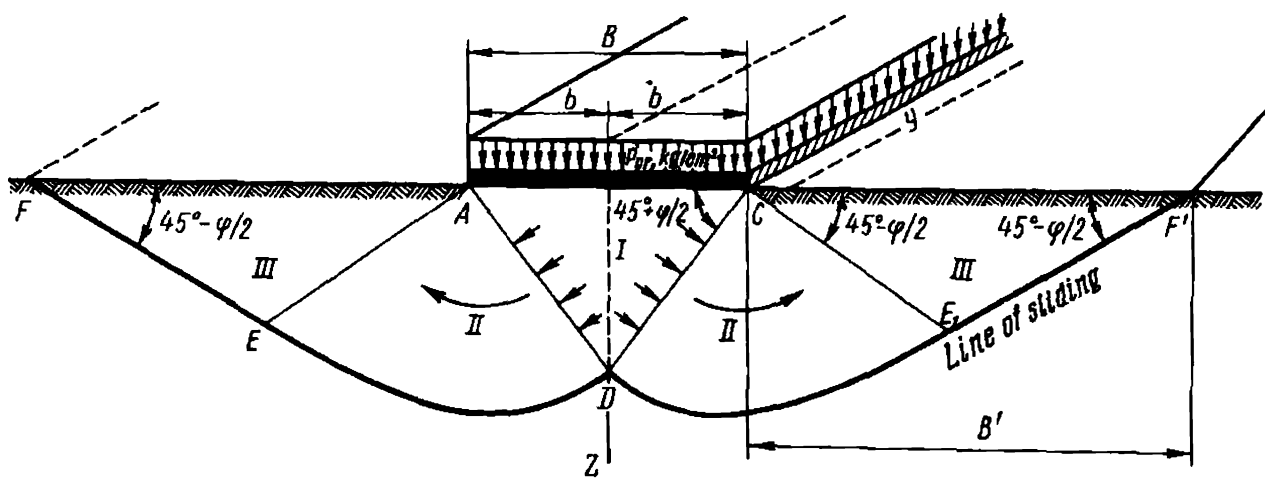


Fig. 21.2. Diagram (after L. Prandtl, 1921) for determining a critical load  $p_{cr}$  for soils with  $\varphi \neq 0$

bodies. The surfaces of sliding in a two-dimensional problem are projected on the plane of the drawing as lines (trajectories) of sliding.

If arching occurs, the lines of sliding in the soil mass coincide:

for soils with  $\varphi = 0$  (soft plastic clays) with directions that are at  $45^\circ$  relative to the principal directions (unit areas on which  $\tau_{max}$  operate);

for soils with  $\varphi \neq 0$  (grained soils, stiff and semiplastic clays) with elementary areas of critical equilibrium, i.e. at angles relative to the principal directions (Eqs. 20.15 and 20.15a):

$$\delta_{crit} = (45^\circ + \varphi_n/2); \quad \delta'_{crit} = (45^\circ - \varphi_n/2)$$

Lines of action of the major principal stress, i.e. the corresponding principal direction at the side of the loaded area coincides in its boundary with the surface of the soil mass (the angle of vision  $\alpha$  decreases here to zero). Under this condition the emergence of lines of sliding to the soil surface at  $F$  and  $F'$  is measured: (a) in soils with  $\varphi = 0$  in terms of the angle  $\beta = 45^\circ$ ; (b) in soils with  $\varphi \neq 0$  in terms of the angle  $\beta' = (45^\circ - \varphi/2)$ .

In Prandtl's scheme (Fig. 21.2) the line of sliding of a complicated shape includes three symmetric segments: (1)  $AD$  or  $DC$  — straight ones; (2)  $DE$  or  $DE'$  — curved ones (e.g. obeying the law of logarithmic spiral); (3)  $EF$  or  $E'F'$  — straight ones.

According to Prandtl's scheme, a partially surface-loaded medium develops three zones that are symmetrical about the  $Z$  axis. Zone I appears as a wedge formed by the load-compressed soil. This wedge is closely linked with the structure and shifts together with it as if it were a solid body, mostly vertically downward. As it moves, the wedge pushes aside the soil mass layers that are adjacent to it in zone II. The excessive load causes these layers to lose stability and pass to a plastic state (deformations phase in a supercritical state) and, in turn, stress the soil in zone III. As a result



the latter shifts laterally along the surface of sliding and upward. This is how soil heaving (or arching) occurs in the zone adjacent to the structure.

According to Fig. 21.2, soil upheaval may theoretically occur in one or two lateral directions. Yet in actual practice, by virtue of general differentiation in loading and non-uniformity of the soil a loss in subsoil stability invariably follows from a unilateral soil upheaval. This leads to unilateral sliding of the wedge of soil along one of its lateral surfaces, e.g. along  $AD$ . Clearly, this causes, apart from the settlement of the structure, some bending momentum and lateral displacement. Such deformations occurring at the final stage of deformations of a structure's subsoil are very characteristic. It should be additionally noted that deformations in a structure occur abruptly and take very short time, generally of the order of several minutes.

It is not uncommon that soil upheaval from beneath the base of a structure is followed by excessive settlement in terms of metres. Such excessive settlement is generally associated with the loss of stability of the supporting soil layers, and is called, in Terzaghi's terminology, *sinking* of the footing.

Figure 20.4 illustrates the failure of a structure induced by soil heaving. The Transcona grain elevator that rested on a soft clay settled by 8.8 m and tilted through  $27^\circ$ .

These factors that are intricately connected defy rigorous mathematical analysis. The difficulties posed by the problem are primarily due to the indefinite shape of the line of sliding in different conditions. So most semiempirical formulae proposed for the evaluation of the bearing capacity of the subsoil likely to arch rely on approximating schemes relating mainly to the shape of lines of sliding.

**Pauker's formula.** The Russian engineer and scientist G.E. Pauker first made in 1856 an attempt to deal with the problem. His approach is of interest since it was proposed at a time when theoretical and practical soil study was at an embryonal stage. Pauker's method literally revolutionized the outlook at construction on incompetent soils. It did so since most civil engineers, Pauker's contemporaries, had believed that a structure could reliably rest only on solid rock, hard clay or similar materials having true cohesion. Pauker has proved that any soil including a saturated one may safely support any load provided the foundation is sufficiently deep.

Pauker's formula has been deduced on the assumption that the subsoil tends to be squeezed from beneath the edge of the foundation meeting at this a resistance to deformation owing to friction forces in the backfill.

For a case where the soil has no cohesion, i.e. with  $c = 0$  and  $h_c = 0$ , Pauker's formula takes on this form:

$$p_{crit} = \rho h_d \tan^4 (45^\circ + \varphi/2) \quad (21.10)$$

If we take into account cohesion of the soil the above equation assumes the following form:

$$p_{crit} = \rho(h_d + h_s) \tan^4 (45^\circ + \varphi/2) \quad (21.11)$$

where, as always,  $h_s = c/\rho \tan \varphi$ .

As follows from Pauker's formula, the critical load (bearing capacity, according to K. Terzaghi) at  $c = 0$  is in a direct linear relationship to the depth of the foundation  $h_d$  and, which is noteworthy, to the soil's bulk density  $\rho_w$ . This soil characteristic, when submerged, is twice as small compared with the bulk density of the soil above the water table. This implies that under such conditions the bearing capacity of a submerged soil decreases almost twofold.

Pauker's formula was extensively used by the civil engineers in pre-revolutionary Russia, especially, when it was desired to determine the necessary depth of a foundation at a specified load on the subsoil. Notwithstanding some limitations, this formula is still valid, in particular, in preliminary soil exploration. The matter is that, unlike other formulae, Pauker's equation calls for no subsidiary graphs or tables. However, the results obtained by using Pauker's and other popular formulae prove to be in a fairly close agreement\*.

Experiments staged by different workers suggest that with a deeper foundation *lines of sliding* in *in situ* conditions have a complex pattern due to formation of a triangular wedge made up of a consolidated soil under the loaded strip. This wedge pushes aside the surrounding soil mass and, under definite conditions, may cause the total loss of stability by the subsoil following soil heaving from beneath the structure\*\*.

It is difficult to obtain an exact solution of the problem under such conditions as the shape of this wedge has been insufficiently investigated in various conditions and due to a need to allow for the own weight of the soil as a certain volumetric force.

V.G. Berezantsev has proposed an approximate solution of a two-dimensional case for small continuous footings resting on sand. He assumed that the consolidated soil wedge is an isosceles triangle in shape

---

\* The derivation of Pauker's formula can be found in N.N. Maslov. *Basic Soil Mechanics and Engineering Geology*. Moscow, 1968, pp. 346-351 (in Russian).

\*\* A concept of a wedge of soil, of much value in current theory, was first applied in 1914 for the evaluation of the bearing capacity of the soil supporting the structures by Professor Belzetsky of the Petersburg Polytechnical Institute. This problem was approached again by M.Kh. Pigulevsky who pointed to the presence of such a wedge under a rigid loaded plate.

whose hypotenuse equals  $2b$  of the footing. In this case

$$p_{crit} = 2A_1\rho b + B_1q + C_1c \quad (21.12)$$

Note that the bearing capacity of the sandy subsoil generally determined experimentally in a number of instances can much (1.5 to 2 times) exceed that found from calculation formulae. The bearing capacity of square footings proves at this to be 1.20 to 1.25 times greater than that of continuous footings. This is, incidentally, substantiated by reports presented to the Fourth, Fifth and Sixth International Conferences on Soil Mechanics and Foundation Engineering held in London in 1957, in Paris in 1961, in Montreal in 1965. This fact is to a certain degree a proof to Berezzantsev's formulae.

Attention should be also drawn to the results of a theoretical study conducted by M.I. Gorbunov-Posadov. He has established that a consolidated wedge in the mass of a sandy subsoil of a rigid foundation appears as an isosceles triangle with the base coincident with the width of the foundation and angles at the base of the foundation equal to the angle of internal friction of the soil. This conclusion, to a certain degree contradicting the assumptions underlying a number of semiempirical formulae, is another proof of the fact that we have not as yet completely understood stability of foundation soils. It also shows that solutions suggested so far are only approximate.

According to the Soviet construction rules SNiP 11-15-74, the bearing capacity of the subsoil  $\Phi$  for the vertical component of the load is allowable to determine with some reservations by using the relationship

$$\Phi = bl(A_1b\rho_1 + B_1h\rho_1 + D_1) \quad (21.13)$$

$A$ ,  $B$ , and  $D$  are dimensionless quantities governed by the angles of friction of the supporting soils,  $\varphi_1$ , at a vertical load. They are equal, respectively, to  $\lambda_\gamma$ ,  $\lambda_q$ , and  $\lambda_c$ . These quantities are established from a diagram in Fig. 21.3 contained in Appendix 5 of SNiP. Here  $b$  is as usual the total width of the footing,  $l$  is its length.

Equation (21.13) follows from conclusions made by V.G. Berezzantsev and in both cases yields close results as indicated by a particular case in Fig. 20.7.

Foreign civil engineers commonly use Terzaghi's formula to determine the critical load,  $p_{crit}$ . Unlike other formulae, Terzaghi's formula allows for the rigidity of the foundation and roughness of its base. This formula relies for its derivation on the familiar calculation scheme proposed by Prandtl (see Fig. 21.2), also with some assumptions made, however. These

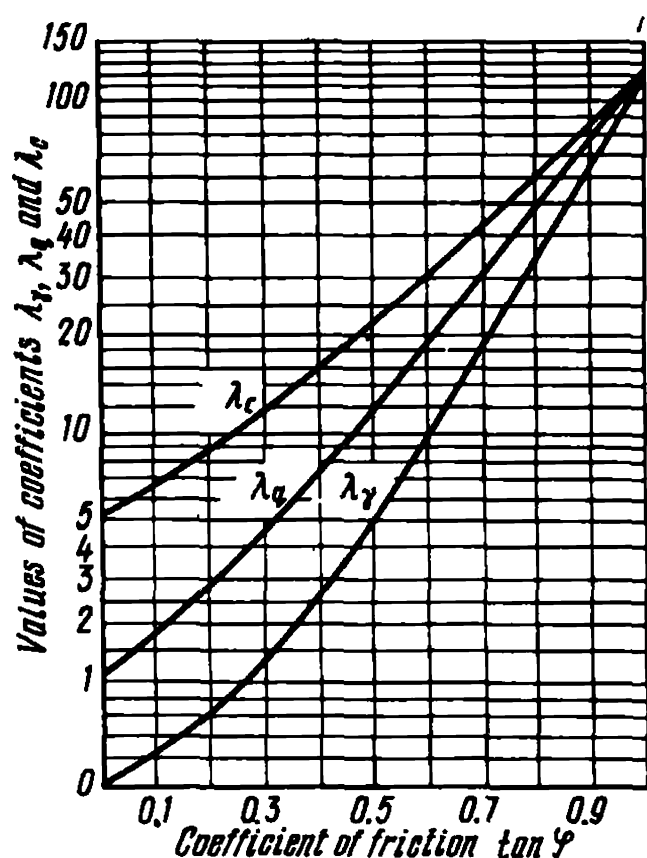


Fig. 21.3. Coefficients  $\lambda_\gamma$ ,  $\lambda_q$  and  $\lambda_c$  for determining  $A_1$ ,  $B_1$ , and  $D_1$  by using SNIIP's Formula 28

latter, however, concern primarily different treatment of various supporting soils.

Terzaghi has proposed two versions of his formula. *The first version* is valid for footings supported by stiff and consolidated soils as well as loose soils that generally cause, following excessive loading, abrupt and marked structure settlement and deformation induced by soil heave.

*The second version* applies for designing foundations resting on soft plastic and semiplastic clays that at an early stage of deformation induced by excessive loading result in pronounced structure settlement due to local dislocations and soil heaving from beneath the foundation. It is only at the final stage that they cause conspicuous subsidence of soil as a result of arching.

When using the second version (for soft clays) it is a good plan to introduce the values of  $\varphi'$  and  $c'$  as fractions of  $\varphi$  and  $c$  determined by using Coulomb's equation, viz.

$$\tan \varphi' = (2/3) \tan \varphi \quad (21.14)$$

$$c' = (2/3)c \quad (21.15)$$

K. Terzaghi presents formulae for continuous footings (plane problem) and square and circular footings. Both versions are similar differing only in numerical values of the coefficients prefixing the bearing-capacity factors

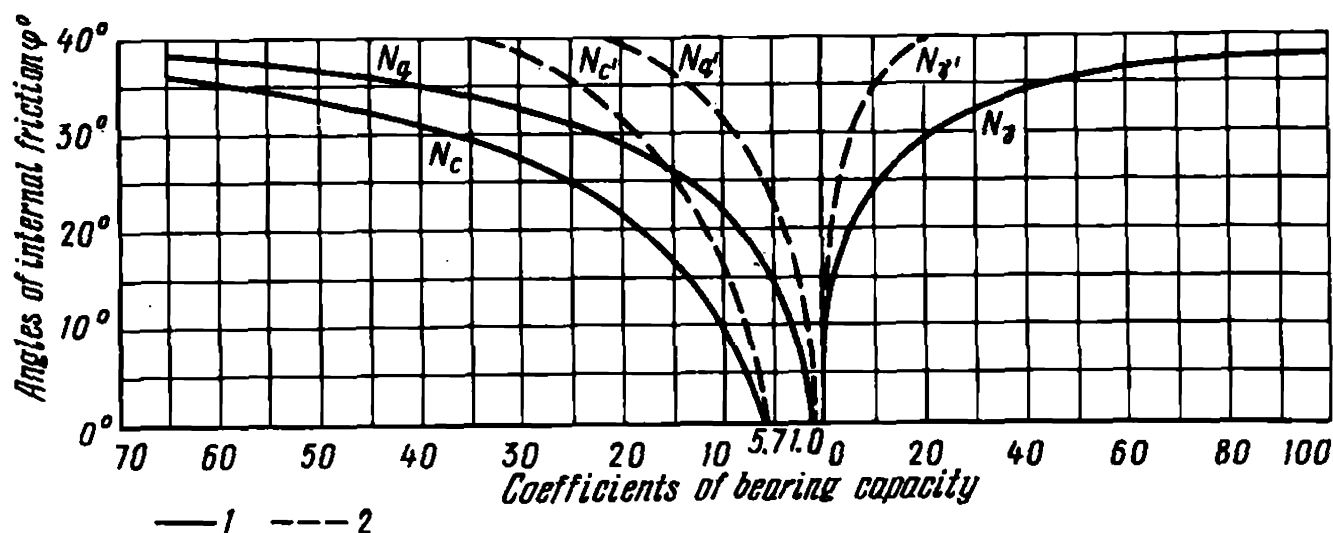


Fig. 21.4. Values of the coefficients of the bearing capacity in Terzaghi's formula  $N_\gamma$ ,  $N_q$ , and  $N_c$  depending on the angle  $\varphi$  of the soil:

1—for relatively competent soils; 2—for incompetent soils

$N_\rho$  and  $N_c$ . Thus for continuous footings

$$p_{crit} = \rho b N_\rho + \rho h_d N_q + c N_c \quad (21.16)$$

and for square footings

$$p_{crit} = 0.8 \rho b N_\rho + \rho h_d N_q + 1.3 c N_c \quad (21.17)$$

The values of the bearing-capacity factors  $N_\gamma$ ,  $N_q$ , and  $N_c$  for stiff consolidated clays and grained soils in either version are taken from a graph (Fig. 21.4). The different values of these factors as shown in the latter figure point to a decrease in the design value of the angle of friction and cohesion in conformity with Eqs. (21.14) and (21.15) for soft plastic and semiplastic clays.

As follows from Fig. 20.7, in a particular case, when the foundation is relatively small in area, Terzaghi's formula gives values that are somewhat higher than ones obtained by using formulae proposed by Berezantsev and SNIIP, remaining, however, fairly close to these.

The above solutions, far from being exhaustive, relate only to formulae especially popular in this country and elsewhere. Now we come to the question as to where these solutions may be used.

The problem under consideration involves the evaluation of the magnitude of the critical load  $p_{crit}$  which brings about failure of the supporting soil mass accompanied by dislocations of the underlying strata along a curved line of sliding in a lateral direction and upward. This takes place only at pronounced loading, especially when a structure is supported by a raft foundation at a marked depth. In the latter case very huge soil masses are involved with a large surface of sliding.

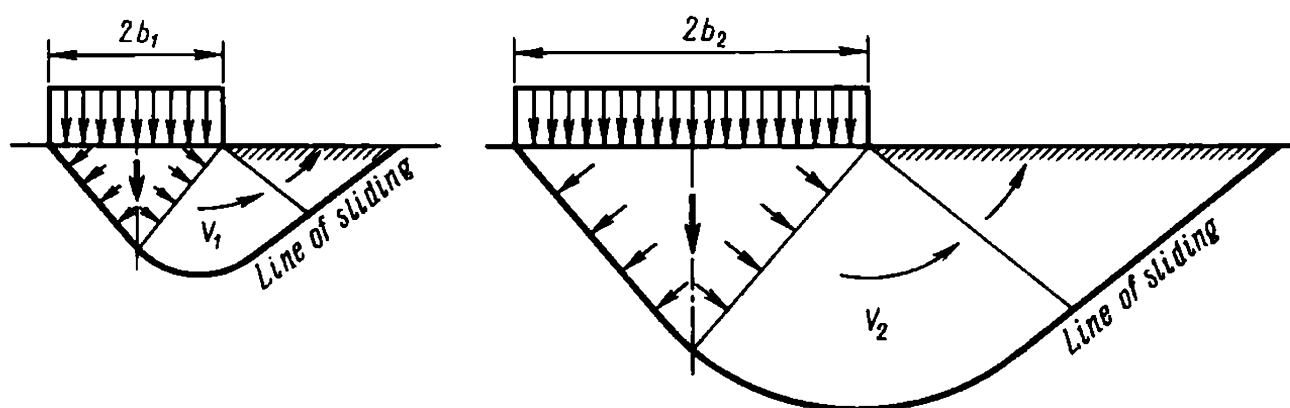


Fig. 21.5. Increase in volumes of heaving soil masses  $V$  following an increase in the width  $2b$  of the loaded strip  $2b$  at  $h_d = \text{const}$

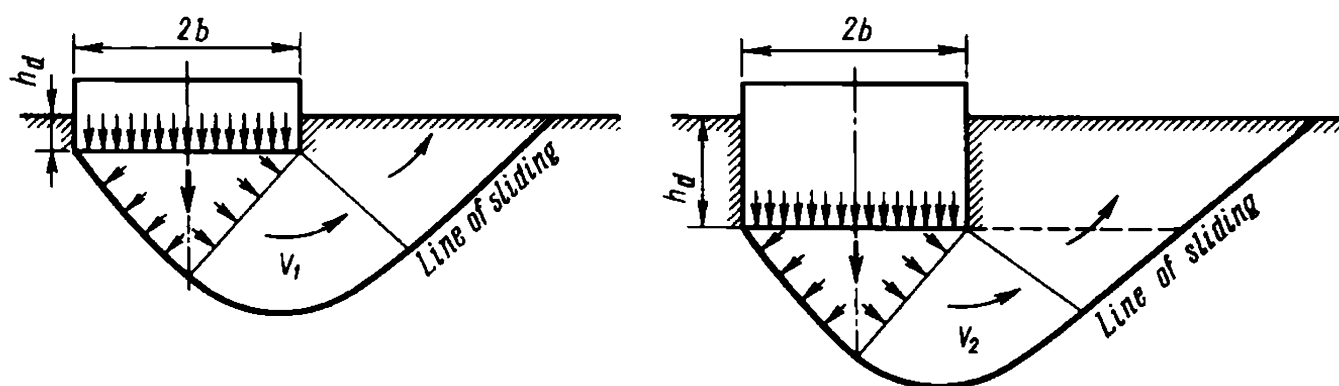


Fig. 21.6. Increase in volumes of heaving soil masses  $V$  following an increase in the depth of the foundation  $h_d$  at a constant width of the loaded strip ( $2b = \text{const}$ )

Failure and dislocations of these soil masses can occur only after the dead load (the weight of the structure) overcomes the passive pressure of the soil resisting this deformation. Hence an idea of the critical load of soil arching.

The passive pressure of the subsoil (subgrade reaction) results from a necessity to withstand forces of friction and cohesion appearing and acting along the surface of sliding. Naturally, friction forces increase with increasing the weight or, differently speaking, volume of the dislocated soil mass, the bulk density of the soil remaining unchanged. At the same time, the longer is the line of sliding, the greater will be the total sum of friction forces operating over the surface of sliding.

The volume of the dislocated and arched soil is determined by the width of the loaded strip and depth of the foundation which can be seen in Figs. 21.5 and 21.6 and calls for no comment.

It may prove then that even at limit loads,  $p_{lim}$ , that are much less than critical loads,  $p_{crit}$ , the regions of local shears will be impermissibly developed viewed in terms of the likely deformation of the structure in hand.

This can be visualized by referring to Fig. 20.7. Given that  $b = B = 8 \text{ m}$ ,  $\varphi = 16^\circ$ ,  $c = 4 \text{ t/m}^2$ ,  $\rho = 2.0 \text{ t/m}^3$  and  $h = 3 \text{ m}$ , the limit load  $p_{lim}$  as determined by using Maslov's formulae, Eq. (20.38), and Eq. 17 in SNiP are in the range of  $40 \text{ t/m}^2 = 4 \text{ kg/cm}^2$ . On the other hand, in phase *III* of the soil's behaviour, given the identical initial data, the critical load ( $p_{crit}$ ) determined from Eq. 28 in SNiP, Terzaghi's and Berezantsev's vary in the range 87 to  $102 \text{ t/m}^2$  or, 8.7 to  $10.2 \text{ kg/cm}^2$ .

Under such circumstances, when it is desired to establish permissible loads on the soil,  $p_{perm}$ , it is better to rely on solutions relating to phase *II* (using  $p_{lim}$ ). Alternatively, when determining  $p_{perm}$  through the value of the critical load,  $p_{crit}$ , corresponding to phase *III* of soil heaving it is well to use a definite factor of safety,  $k_{saf}$ .

It may be considered to be an established fact that the value of  $k_{saf}$  is governed by a number of factors, primarily the size of the structure and the properties of the supporting soil layers. Thus the value of  $k_{saf}$  cannot remain the same and must be determined for each particular job.

Foreign practice, when finding the permissible load  $p_{perm}$  by using Terzaghi's formulae, uses a coefficient of safety  $k_{saf} = 2$  to 3 compared with 1.25 to 1.50 commonly used in the USSR. This, as it were, implies a definite uncertainty toward the design scheme underlying this solution. Hence general practice of determining the permissible load with respect to phase *II* of local deformations, e.g. by using Eq. (20.38), precluding soil arching, especially, when large footings are involved.

## Chapter 22

### Increasing Strength of Clayey Soils Induced by Consolidation with Time Under the Own Weight of a Structure

#### Sec. 22.1. Pore Pressure and Filtrational or Primary Consolidation of Soils

The shearing resistance of a clayey soil in its natural state,  $s_{pw_{nat}}$ , is described by this relationship:

$$s_{pw_{nat}} = p_n \tan \varphi_{w_{nat}} + c_{w_{nat}} \quad (22.1)$$

where  $\varphi_{w_{nat}}$  and  $c_{w_{nat}}$  are, respectively, the true angle of friction and total cohesion corresponding to the natural density-moisture content of the soil.

In addition, the weight of a structure being erected generally provides a surcharge compressing the subsoil by its weight and thus increasing its bearing capacity. Unlike the effect of the factor  $p_n$ , soil consolidation by the weight of the structure does not immediately increase soil stability and generally takes lengthy time periods. When preparing a design, it is often necessary to rely on the initial values of constants of the shearing resistance of a clayey soil in its natural state ( $\varphi_{w_{nat}}$ ,  $c_{w_{nat}}$ ). In such a case the initial shearing resistance,  $s_{pw_{nat}}$ , will often fail to be in agreement with the conditions of the design.

Thus we come to a problem of *consolidation* of clayey soils, i.e. compression proceeding with time under a vertical load.

Depending to the particular conditions,  $s_{pt}$  can be established by two alternative methods allowing for: (1) the so-called *pore pressure* or, more correctly, pore water pressure  $u_t$ , appearing in the soil as a result of a surcharge; (2) the load-induced change in the density-moisture content of soil  $w_t$  and, as a result, an increase with time of  $\varphi_{wt}$  and  $c_{wt}$ .

In conformity with the theory of pore pressure the shearing resistance of soil with time,  $t$ , i.e.  $s_{pt}$ , can be in principle found from this relationship:

$$s_{pt} = (p - u_t) \tan \varphi' + c' \quad (22.2)$$

where  $\varphi'$  is the angle of internal friction and  $c'$  is cohesion of the soil determined by the open shear method from the density-moisture content  $w_p$ , equivalent to loads  $p$  corresponding to total consolidation under this load;  $u_t$  is the pore (in excess of hydrostatic) pressure in the time period  $t$  appearing in the moisture filling the voids and sustaining to some degree the load applied to the soil (neutral pressure). According to the theory of pore pressure and Eq. (22.2), the shearing resistance of soil  $s_{pt}$  varies with time as the soil is being consolidated in the range from  $s_{p \lim}$  to  $s_{pt}$  only due to the change with time of a normal stress acting on the soil  $p_t = (p - u_t)$ . Clearly, this change is in turn associated with the change with time of the pore pressure,  $u_t$ , itself.

As follows from the theory of pore pressure, if a surcharge  $\Delta p$  is applied to a completely saturated soil ( $G \approx 1$ ), this surcharge is at the first moment imparted to the moisture in the voids, i.e.  $u_0 = p$ , which gives rise to the pore pressure. Note that the load  $p_{zsk}$  is not at all transferred to the skeletal (hard) particles of the soil. This means that  $p_{zsk} = p - u_0 = 0$ .

As the soil is further being consolidated and the moisture contained in it squeezed out of the pores, the pore pressure gradually decreases. At the moment the density-moisture content  $w_p$  becomes equivalent to the load, the pore pressure drops to zero ( $u_t = 0$ ). The load applied to the soil will be then totally sustained by the soil's skeletal particles ( $p_{sk} = p$ ), compression of the soil will stop.



At the initial moment of the application of the load the shearing resistance of the soil at  $u$ , will remain equal to the initial value, e.g. the natural one ( $s_0 = s_{pw \text{ nat}}$ ). Later, as the pore pressure  $u$ , decreases, according to the given theory, the shearing resistance continues to grow, in conformity with Eq. (22.1), until it finally attains a value of  $s_p$  equivalent to the load.

Thus, according to the theory of pore pressure, the surcharge  $\Delta p$  on the soil at a depth  $z$  causes a complex state of stress which can be approximated by using the relationship

$$p_{zt} = p_{zsk} + u_{zt} \quad (22.3)$$

Here for time  $t$ :  $p_{zt}$  is the total pressure;  $p_{zsk}$  is the effective pressure on the soil's skeletal particles;  $u_{zt}$  is the pore (neutral) pressure.

Then the principal equation of the theory of pore pressure (22.2) will take on this form:

$$s_{pzt} = p_{zskt} \tan \varphi' + c' \quad (22.4)$$

The determination of  $p_{zskt}$  is one of the principal tasks in the theory of soil consolidation as applied to completely saturated clays of weak consistency (flowing and flowing plastic).

So that this problem can be solved it is essential to establish the infiltration regime of soil under conditions of load-induced squeezing of the water out of the soil. For this reason the particular division of the theory in question is termed *a theory of filtrational consolidation*. For a one-dimensional case this theory bases on the principle of equality of the volume (or discharge)  $q_z$  to the water squeezed out of the soil at a depth  $z$  under a load  $p_z$  to the value of the decreasing voids ratio of the soil as the latter is being compressed, i.e.

$$dq_z = \frac{dn}{dt} dz \quad (22.5)$$

Dr. Karl von Terzaghi, basing on the above relationship, has proposed this, now classical, solution of the problem:

$$c_v \frac{d^2 p_{zsk}}{dz^2} = \frac{dp_{zsk}}{dt} \quad (22.6)$$

An essential term of this differential equation is  $c_v$ , which represents *the coefficient of consolidation* characterizing the initial conditions of the consolidating soil and the consolidation process proper. This coefficient is

equal to

$$c_v = \frac{K_p(1 + \varepsilon_{av})}{a\rho_w} \quad (22.7)$$

where  $K_p$  is the coefficient of permeability;  $\varepsilon_{av}$  is the average value of the voids ratio of the consolidating soil over the range from its initial to the ultimate (equivalent) state;  $\rho_w$  is the density of the water (expressed in kg and cm,  $\rho_w = 0.001 \text{ kg/cm}^3$ );  $a$  is the coefficient of compressibility,  $\text{cm}^2/\text{kg}$ , indicative of the effect of the load factor on the rate of soil consolidation in conformity with the known equation of the compression ratio

$$a = \frac{\varepsilon_0 - \varepsilon_1}{p_1 - p_0}.$$

The use of the differential equation (22.6) leads to a relatively fast converging series.

In view of the approximate nature of these calculations, when evaluating the degree of soil consolidation at a depth  $z$  at a normal pressure  $p_z$  acting here it is sufficient for practical purposes to apply only the first term of this series:

$$p_{zskt} = p_z \left( 1 - \frac{4}{\pi} \sin \frac{\pi z}{2H} e^{-N} \right) \quad (22.8)$$

where  $p_z$  is the load (pressure) at a depth  $z$ ;  $H$  is half of the thickness of the consolidating layer at a *bilateral drainage*;  $N$  is a definite dimensionless quantity:

$$N = (\pi^2/4)c_v(t/H^2) \quad (22.9)$$

where  $t$  is the current time coordinate.

It is often necessary, especially because of long time periods taken by construction work, to estimate the time  $T_{stab}$  needed for complete consolidation of the subsoil under the effect of one load or another. Taking into account the asymptotic nature of the relation  $p_{zskt} = f(t)$ , it seems plausible to consider  $T_{stab}$  to be 95% of the total consolidation of the soil, i.e. with the degree of consolidation alternatively called per cent consolidation  $U_t = 0.95$  taken from Table 22.1.

For this value of  $U_t$  the value of the coefficient  $N$  is given by the above table to be  $N = 2.8$ . Then, instead of Eq. (22.9) for  $T_{stab}$  we will have

$$N = (\pi^2/4)(c_v/H^2)T_{stab} = 2.8 \quad (22.10)$$

or

$$T_{stab} = 1.13H^2/c_v \quad (22.11)$$

Table 22.1

The Values of  $N$  at Constant Pressure with Depth  
at Different Values of Degree of Consolidation  $U_t$

$U_t$	$N$	$U_t$	$N$	$U_t$	$N$	$U_t$	$N$
0.05	0.005	0.30	0.17	0.55	0.59	0.80	1.40
0.10	0.02	0.35	0.24	0.60	0.71	0.85	1.69
0.15	0.04	0.40	0.31	0.65	0.84	0.90	2.09
0.20	0.08	0.45	0.39	0.70	1.00	0.95	2.80
0.25	0.12	0.50	0.49	0.75	1.18		

Let us introduce a new constant, a *generalized coefficient of consolidation*  $\zeta$  measured in  $t^{-1}$ :

$$\zeta_{cons} = c_v/H^2 \quad (22.12)$$

By using (22.10) and referring to Eq. (22.12) we can write

$$\zeta_{cons} = \frac{K_p(1 + \varepsilon_{av})}{a\rho_w H^2} \quad (22.13)$$

Then, by virtue of Eqs. (22.10) and (22.12):

$$T_{stab} = 1.13/\zeta_{cons} \quad (22.14)$$

or roughly

$$T_{stab} \approx 1/\zeta_{cons} \quad (22.14')$$

It should be noted that the use of Eq. (22.14) jointly with (22.13) makes it possible to find for clays the value of the coefficient of permeability of the given clayey soil from the results of a laboratory compression test. The value of  $H$  will correspond to half the height of the soil sample.

Alternatively, by compressing a soil sample of a height  $h_s$  under laboratory conditions it is possible to determine the value of  $K_p$  that would ensure this course of the process. By referring to a consolidation curve ( $\varepsilon = f(t)$ ), we can establish the time period (in s) taken for the soil sample to attain 50% of the compression. This will speed up the testing procedure and yield an accuracy sufficient for this approximate method. According to V.F. Babkov's findings and in conformity with the above data, when considering the filtrational (permeability) consolidation, this 50% corresponds to the time factor  $T_t \approx 0.2$ . Then, by virtue of Eqs. (22.12) and (22.13)

$$T_t = \frac{c_v t_{0.5}}{h^2} = \frac{K_p(1 + \varepsilon_{av})}{a\rho_w} \frac{1}{h^2} t_{0.5} = 0.2$$

Hence the coefficient of permeability

$$K_p = \frac{0.2a\rho_w h^2}{(1 + \varepsilon_{av})t_{0.5}} \quad (22.15)$$

There are a number of factors that act to invalidate this determination, especially for fairly dense clays.

It will be recalled that the above equations are valid only at a constant value of  $p_z$  acting vertically on the soil mass of the foundation. There are numerous solutions also for other conditions, e.g. for the case where there occurs attenuation of the dependence  $p_z = f(z)$  when approximating the depth of the soil mass according to the law of the triangle. The ultimate solutions of all these problems prove quantitatively fairly close to one another. Since they are of an approximating character, these solutions may be reduced to the above relationship (22.15).

It is possible to predict the magnitude of the stress on the soil skeletal particles,  $p_{zskt}$ , during the time period  $t$  in conformity with the theory of pore pressure by referring to Eq. (22.8). At this we rely on the values of  $N$  determined for different time periods  $t$  using Eq. (22.9) or, still better, by applying the generalized coefficient of consolidation  $\zeta_{cons}$  found from this relationship:

$$N = (\pi^2/4)\zeta_{cons}t \quad (22.16)$$

This relationship has been obtained by substituting into Eq. (22.9) the value of  $\zeta$  in conformity with Eq. (22.12). Clearly, on this condition the values of  $c_v$  or  $\zeta_{cons}$  may be calculated by using Eqs. (22.7) and (22.13) followed by determinations by laboratory tests of a number of particular constants entering these equations.

A simpler and more reliable way to find the value of  $N$  would be to determine it directly by observing the time  $T_{stab}$  of a specimen in a compression test. The value of the generalized coefficient of consolidation for laboratory conditions,  $\zeta_{cons.exp}$ , can then be found from the relationship

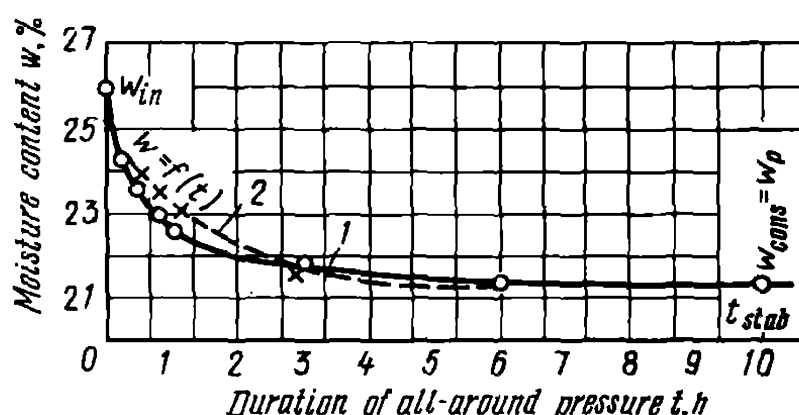
$$\zeta_{cons.exp} = 1.13/T_{stab.exp} \quad (22.17)$$

Eq. (22.12) should be used to determine the value of the coefficient  $\zeta_{cons.nat}$  characterizing the actual natural conditions of a soil. In conformity with this relationship, at the same value of the coefficient of consolidation ( $c_v = \text{const}$ ) for the same soil the value of the generalized coefficient is inversely proportional to the squared half of the height of a sample ( $h_s$ ) and half of the thickness of the naturally occurring soil layer ( $H_{nat}$ ):

$$\zeta_{cons.nat} = \zeta_{cons} \left( \frac{h_{exp}}{H_{nat}} \right)^2 \quad (22.18)$$

Fig. 22.1. Soil consolidation (light loam of a liquid plastic consistency) in laboratory conditions. Load  $p = 3.0 \text{ kg/cm}^2 \approx 0.3 \text{ MPa}$ :

1—curve for determining soil moisture content at repeated weighing; 2—calculation curve plotted from Eq. (22.19)



For further calculations refer to Eqs. (22.16) and (22.8).

The easiest way to determine the shearing resistance of a soil in an unconsolidated state ( $s_{pt}$ ) is through the moisture content as a function of time  $w = f(t)$  followed by the determination of constants of the shearing resistance,  $\varphi_{wt}$  and  $c_{wt}$ , versus time,  $t$ , using a graph in Fig. 13.13.

The solution of a particular problem of filtrational consolidation thus becomes a complex task where conclusions of the theories of pore pressure and density-moisture content combine.

The solution using the method in question calls for: (1) results of a compression test to determine the relationship  $w_t = f(t)$  at a load  $p = \text{const}$  (Fig. 22.1); (2) values of  $U_t$ , the degree of consolidation or percent consolidation as a function of the values of the already familiar dimensionless quantity  $N$ , i.e.  $U_t = f(N)$ .

The method in question mainly relies on the relationship

$$w_t = w_{in} - (w_{in} - w_{fin})U_t \quad (22.19)$$

where  $U_t$  is the degree of consolidation or percent consolidation;  $w_t$  is the moisture content varying under a load acting for a time period  $t$ ;  $w_{in}$  and  $w_{fin}$  are, respectively, the initial and the final moisture content. Note that  $w_{fin} = w_p$ , where  $w_p$  is the moisture content at a load  $p$ .

Clearly,  $U_t$  is in the range of  $0 \leq U_t \leq 1$ .

The value of  $U_t = 0$  (initial period, moment of application of load at  $t = 0$ ), in conformity with Eq. (22.19), corresponds to the initial moisture content of the soil, i.e.  $w_{t=0} = w_{in}$ . On the other hand,  $U_t = 1.0$  corresponds to the time the soil has completely consolidated under a load, i.e. to the time period  $t_{stab}$  and moisture content

$$w_{t_{stab}} = w_{cons} = w_p$$

For the determination of intermediate values of the degree of consolidation,  $U_t$ , for one time period or another,  $t$ , the following relationship

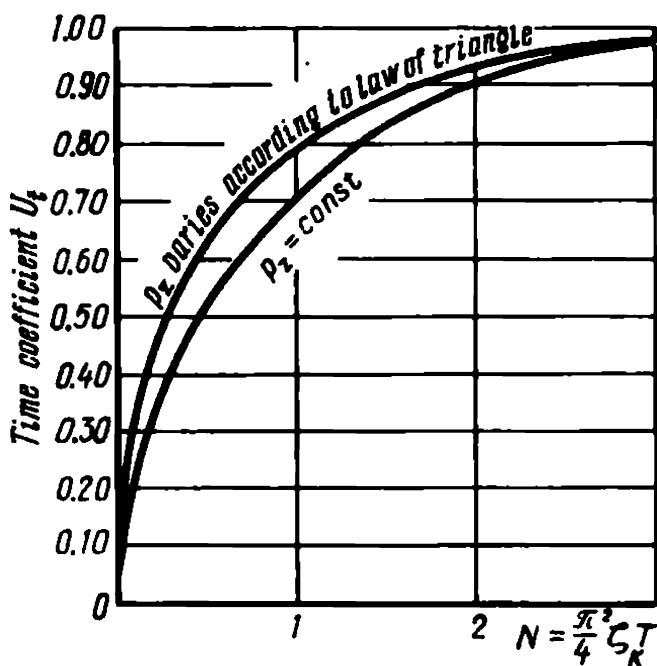


Fig. 22.2. Change in the degree of consolidation  $U_t = f(N)$  with maintaining normal stress  $p_z$  in the depth of the soil mass constant or decreasing obeying the straight line law

can be used

$$U_t = 1 - \frac{8}{\pi^2} \left[ e^{-N} + \frac{1}{9} e^{-9N} + \frac{1}{25} e^{-25N} + \dots \right] \tag{22.20}$$

This relationship also refers to a one-dimensional case of soil consolidation where the compressive stress remains constant throughout the depth  $z$  of the soil mass, i.e.  $p_z = p = \text{const.}$

For practical purposes the first term of the series (22.20) will suffice, i.e.

$$U_t = 1 - \frac{8}{\pi^2} e^{-N} \tag{22.21}$$

The quantity  $N$  in the given case is also found by using Eq. (22.9) or (22.16).

A number of graphs and tables are available to determine  $N$  as a function of the degree of consolidation,  $U_t$ , or vice versa various conditions of attenuation of the pressure  $p_z$  with increasing the vertical distance  $z$ . Table 22.1 and Fig. 22.2 present the data for a case where  $p_z = f(z) = \text{const.}$

As has been already noted, the above relationships and data listed in Table 22.1 are valid for a plane case. Figure 22.2 demonstrates the character of the variation of  $U_t = f(N)$  with change in the normal stress in the soil mass, say, in conformity with the law of a triangle. The difference in the values of  $N$  is here insignificant for different laws of attenuation of normal stresses in the soil mass.

The solutions of a plane and a three-dimensional problem proposed by different workers are too complicated to be of practical value. It will be

recalled that the above solutions, in view of the findings of construction practice, may only be used for a study of the behaviour of saturated soils of weak consistency acted on by a load during a definite time period. Even when applied in this narrow field, the theory of pore pressure has a number of obvious and not immediately visible disadvantages.

Let us recall the principal equation of the theory of pore pressure, Eq. (22.2):

$$s_{pt} = (p - u_t) \tan \varphi' + c'$$

In conformity with this relationship, if an added load is being applied to the soil, the pore pressure can only increase when skeletal particles come together, i.e. when the soil is consolidating or, alternatively, when the load is imparted to the liquefied soil mass as a whole.

In this case the surcharge on the soil is first sustained by at least part of its skeletal particles and is only later imparted to the soil moisture causing pore pressure. This pressure will never attain the value of  $u_{t=0} = p$ . Thus the basic concept of the theory of pore pressure is invalidated.

The latter theory further maintains that the shearing resistance of a soil  $s_{pt}$  in accord with Eq. (22.2) increases with time only due to internal friction when the pore pressure in the soil gradually diminishes. Pseudoplastic, to say nothing of plastic, clayey soils demonstrate that  $\varphi_n \rightarrow 0$ . Consequently, consolidation in such soils only insignificantly increases their shearing resistance.

Such a conclusion radically contradicts actual construction practice. It appears that an essential role in the observed disagreement between theoretical prediction of consolidation and the evidence furnished by *in situ* investigations of clays of dense consistency should be attributed to specific properties of the bound pore water. Under such conditions Darcy's law underlying deductions from the theory of permeability consolidation is no longer valid for the percolation regime due to the enhanced viscosity of the pore water.

The theory of pore pressure has some more, less important limitations. These include the difficulty to predict the value of  $u_t$  and measure it which calls for sophisticated apparatus both for laboratory and *in situ* tests.

Efforts have been recently made to improve this theory, e.g. by taking into account rheological properties of soils. An important contribution to this search is due to Soviet soil scientists. The process, however, is on the whole so involved and is governed by so many factors that it is practically impossible or at least very hard to take them into consideration in a mathematical model.

The above circumstances impose a serious constraint on the practical

use of the theory of pore pressure and data on permeability consolidation for the general case. Notwithstanding what has been said, the theories of pore pressure and permeability consolidation may be used for predicting  $s_{pt} = f(t)$  in remolded clays of flowing and flowing-plastic consistency.

### Sec. 22.2. Consolidation Index $n$ and Its Significance

The important difference of the method relying on a theory of density-moisture content and taking into account the consolidation index  $n$  from the method of permeability consolidation is that the process of clay consolidation with time is studied as a whole. It does not take into account the effect of individual governing factors. On the other hand the method in question has no limitations to its use either in terms of soil consistency or degree of saturation.

We can predict increased stability of a clay at a load with time by applying this relationship

$$s_{pt} = p \tan \varphi_t + c_t \quad (22.22)$$

where  $s_{pt}$  is the shearing resistance of the soil at a load  $p$  during a time period  $t$ ;  $\varphi_t$  and  $c_t$  are, respectively, the angle of internal friction  $\varphi_w$  and total cohesion  $c_w$  as applied to the density-moisture content of the soil acted on by a load  $p$  during time  $t$ . In Eq. (22.2) which is basic for the theory of pore pressure the constants  $\varphi'$  and  $c'$  remain unchanged throughout the process which is unlikely. According to these index characteristics the shearing resistance of a soil varies only due to the effective pressure on the soil with time which is little convincing.

At the same time consolidation of a clay under a load with time is of a different nature, as follows from Eq. (22.2). The load applied here to the soil during the entire consolidation period is uniform throughout the time of its application.

In the given case, as the density-moisture content of a soil  $w$  varies, so do the indices  $\varphi_w$  and  $c_w$ . This is a quite obvious and convincing statement. Analysis relies on determining the values of  $\varphi_{w(t)}$  and  $c_{w(t)}$  with respect to the density-moisture content attained by the time  $t$  by using graphs of a type shown in Fig. 13.13 and similar ones. These very indices are used in eventual analysis and calculations.

The essence of the method can be understood if we conduct consolidation tests of the same soil under identical conditions yet involving soil layers of different thickness ( $H$  and  $h$ ). We should refer to this relation-



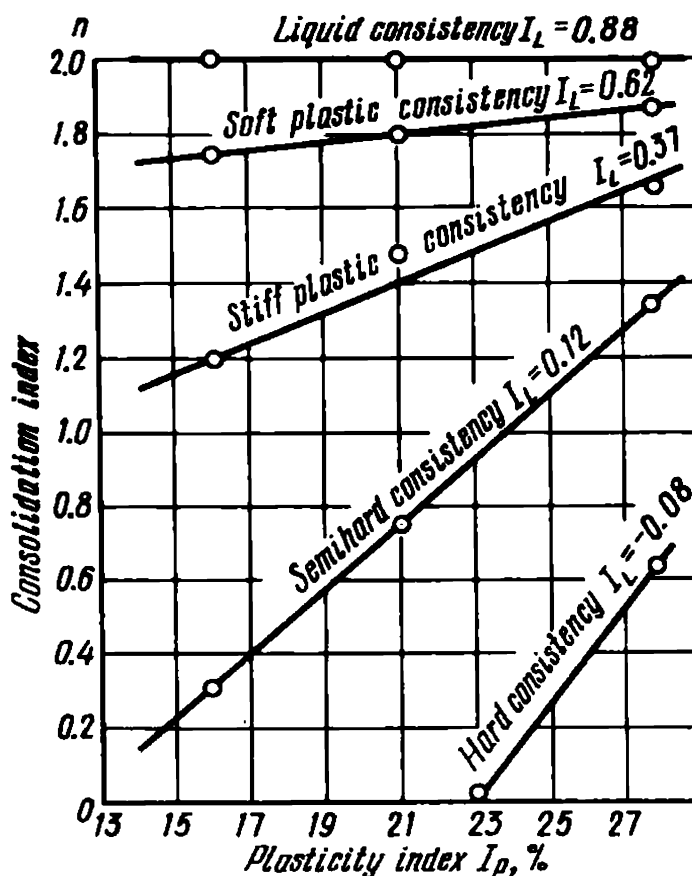


Fig. 22.3. Relationship between the consolidation index  $n$  and the plasticity index  $I_p$  and consistency  $I_L$

ship:

$$T_w = t_w \left( \frac{H}{h} \right)^n \quad (22.23)$$

where  $T_w$  and  $t_w$  are times needed for consolidation of a clay at a specified load  $p$  to attain the same density-moisture content ratio  $w$  yet in soil layers that are  $H$  and  $h$  in thickness, respectively;  $n$  is the consolidation index characterizing the specific conditions of consolidation of the given soil and the properties of the soil proper, such as composition, state etc.

The value of the consolidation index  $n$  lies in the range  $0 \leq n \leq 2$ . As shown by experience, this value is linked with the consistency index ( $I_L$ ) and composition of soil through the plasticity index ( $I_p$ ) and moisture content ( $w$ ). Figure 22.3 demonstrates these relationships. It follows from the diagram, in particular, that  $n = 2$  corresponds only to a liquefied soil.

It will be recalled that in conformity with the permeability theory of consolidation the rate of consolidation of a clay layer is quadratically related with the thickness of the consolidating layer ( $H^2$ ). This provides proof to the restriction of safe use of permeability consolidation to soils of liquid consistency or one close to it.

The consolidation index  $n = 1.5$  is generally typical of hard plastic soils, whereas  $n = 0$  is valid for hard soils. As follows from the analysis and Eq. (22.23), the rate of consolidation of hard and partly semihard

clays is practically independent of the thickness of the consolidating layer. In view of the fact that the state of a hard or even semihard clay is very much that of a solid rock, such a conclusion is quite plausible.

The aforementioned dependence of the consolidation index on the plasticity of soil in terms of the plasticity index  $I_p$  and consistency index  $I_L$  to a definite degree substantiates a hypothesis that these are governed by the amount of the water contained in the soil's pores, i.e. free (gravitational), semibound and bound water.

The data in Fig. 22.3 may undoubtedly prove useful for rough estimates. A more accurate determination of  $n$  calls for staging the requisite laboratory tests at a specified load. The purpose of these compression tests is to determine the time needed for consolidation of soil samples of different height to a definite density.

The value of  $n$  is then found from the relationship

$$n = \frac{\ln (t_2/t_1)}{\ln (h_2/h_1)} \quad (22.24)$$

where  $t_1$  and  $t_2$  are times taken by soil samples of respective heights  $h_1$  and  $h_2$  to attain the specified density.

When using the above relationships following both from the theory of pore pressure and from that of density-moisture content ratio, since they are only approximate ones, it is invariably of crucial importance to have field control of the degree of soil consolidation achieved in *in situ* conditions. Such control requires that the pore water pressure in the soil be followed by using fairly sophisticated apparatus, in the first case; or by determining by conventional means the moisture content that will have changed by a definite moment, say, due to the increased weight of a structure being erected, in the second case. Clearly, the second method of solving the problem is much easier.

The above method of increasing the bearing capacity of clayey, to say nothing of silty, soils with marked moisture content due to their compression by the weight of a structure being erected is often the only way out.

A most convincing proof in favour of such a solution is provided by faultless performance of massive buildings from reinforced concrete of the Hanoi Polytechnical Institute resting on silt deposits of the bottomland of the Red River characterized by a very low bearing capacity. On a fill of sand a raft foundation was placed in the form of a slab of reinforced concrete from which columns for the ground floor protruded. The entire ground floor of the structure was filled by a 7 m high layer of wet sand acting as a surcharge. There was no interruption in the construction work. As the weight of the structure increased the sand was gradually removed and

spread nearby. Construction presented no difficulty and the structure has been in operation for over 20 years without failure.

Another example is provided by the construction, using the same principle, of bridge piers in the Lake of Onega supported by a 7 m thick layer of very incompetent deposits of silty clay. The load on the subsoil supporting the piers was  $1.5 \text{ kg/cm}^2$ . The soil was artificially compressed by placing on a 0.5 to 1.0 m high layer of sand a five-metre high layer of riprap that later provided the foundation for the pier cribwork. The voids in the riprap layer were for the first time in engineering practice sand-washed to enhance stability of the rock dump.

If incompetent clay layers alternate with sand lenses, in order to speed up compression of the subsoil by the weight of the structure a system of sand draining wells or boreholes of increased diameter can well be used. This method was first used during the construction of the buildings of the Lower Svir Hydro-Electric Power Development.

## Chapter 23

### The Initial Pressure Gradient. Its Role in Limiting Consolidation of Clayey Soils

#### Sec. 23.1. Introduction

That the initial gradient could be a limiting factor in load-induced consolidation of a clay has been already noted. As has been demonstrated by Soviet soil scientists, water infiltration (percolation) in clayey soils is only possible to occur at a hydraulic head greater than its original value  $j_{in}$  (S.A. Roza, 1947). At gradients less than  $j_{in}$  clay is practically impervious.

Consolidation of clay involves removal of an amount of water from the soil which is excessive for the new state of the latter. This squeezing occurs due to a definite *hydraulic pressure gradient*  $j_{pr}$ . This gradient is conditioned by the value of the load applied to the soil and the distance travelled by the water. The gradient  $j_{pr}$  attains its maximum value in a clay layer at surfaces of contact with the draining layers. With increasing the distance from the draining layer the value of  $j_{pr}$  drops. If a clay layer lies between two draining layers  $j_{pr}$  proves to be the least in the middle of the layer.

This results from a gradational increase of the total amount of the water to be removed, the lesser the distance to the draining layer. It may prove then that in some zones of the clay layer  $j_{pr}$  is less than  $j_{in}$ . Water will

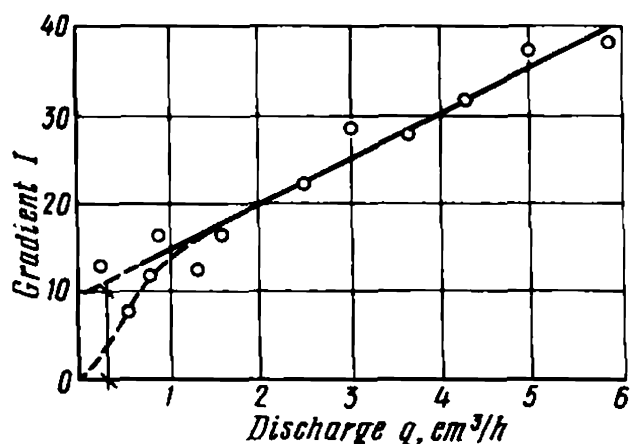


Fig. 23.1. Initial gradient  $I_{in}$  as a factor much inhibiting seepage in clayey soils at small gradients  $I$  (points indicate data of different tests of the same soil)

not be removed from such zones. The density-moisture content ratio will not then change. At least, it will remain for indefinitely long time periods equal to the initial  $w_{nat}$ . As to consolidation of the soil, it will be restricted by fairly narrow zones adjoining horizons of contact where  $j_{pr} > j_{in}$ .

An example can be provided by Fig. 23.1 illustrating results of a test involving water seepage through a soil at different gradients with concurrent determination of the discharge  $q$  of the percolating water. We could expect that the discharge  $q_i$  at a gradient  $j_i$  will vary according to Darcy's law:

$$q_i = \omega K_p j_i \quad (23.1)$$

where  $K_p$  is the coefficient of permeability;  $\omega$  is the cross-section of the passage through which percolation occurs.

In conformity with Eq. (23.1), the discharge rate is connected to the gradient through a linear relationship and is zero at  $j = 0$ . However, as can be seen from Fig. 23.1, at small gradients the above relationship is invalidated which is characteristic of most clayey soils.

In fact, the zero discharge ( $q_i = 0$ ) practically establishes at a value of the gradient other than zero called *the initial gradient* ( $j_{in}$ ). The linear character of the relationship  $q = f(j)$  at gradients  $j_i < j_{in}$  is apparently violated. With decreasing values of  $j_i < j_{in}$  the intensity of infiltration dramatically drops with time.

In view of low permeability of clayey soils it is commonly assumed that at gradients  $j_i < j_{in}$  percolation discontinues altogether, i.e. under such conditions  $v = 0$  and  $q = 0$ .

The pressure gradient  $j_{pr}$  of the pore water in the soil mass under the surcharge  $\Delta p$  can under definite conditions be less than the initial gradient, i.e.  $j_{pr} < j_{in}$ . Clearly, the initial gradient may frequently be very large in value ( $j_{in} = 5$  to 20 or even  $j_{in} = 40$  to 50).

The character of the initial gradient is apparently conditioned by small porosity, i.e. the smallness of the pores in clayey soils. This porosity decreases even more as the soil is being compressed by a load. An impor-

tant factor contributing to this phenomenon is the nature of the bound and semifree pore water enveloping the soil's solid constituents filling to an extent the soil's voids. Apparently, in order that resistance to transport of this water under given conditions be overcome, substantial effort may be required, i.e. pressure associated with the already increased values of the hydraulic head and gradient.

When estimating the importance of  $j_{in}$  we must take into account the fact that conditions of a compression test very much differ from *in situ* conditions. With a small height of the soil sample (short infiltration path factor) the compression of the soil in a compression test generally proceeds at marked gradients  $j_{pr}$ , often measured in thousands of units. Under experimental conditions this causes soil consolidation even at minor loads.

On the other hand, in actual conditions where clay strata may be of appreciable thickness at identical loads, the pressure gradient in the soil mass may prove to be negligible, of a few units only. Clearly, on this condition and at the above values of  $j_{in}$  the clay layer will consolidate only in zones of inappreciable thickness adjoining the draining layers. This specific feature of clays has been substantiated by field observations made both in this country and elsewhere.

To be able to solve the problem of the likely effect of  $j_{in}$  soil consolidation due to the weight of the structure being erected (it should be noted in advance, also that of the zone determining structure settlement induced by normal stresses) we must know how to evaluate the thickness of the active zone  $D_j$  in the middle of the clay layer. The active zone  $D_j$  in the particular case is the part of the soil stratum which is in contact with the draining layers where  $j_{pr} > j_{in}$  and where the soil is likely to consolidate under the effect of the added load.

### Sec. 23.2. Theoretical Premises

Let us refer to Fig. 23.2. Suppose that at a certain depth in the moisture-free soil mass a clay layer occurs which is  $H$  in thickness and has a definite moisture content (under conditions of complete saturation). The clay layer is acted on by a surcharge (added load)  $\Delta p$ . The clay layer is being drained only upward.

At this load the clay layer must be compressed throughout its thickness. From the viewpoint of the theory of the initial gradient, however, the problem becomes complicated. Assume the initial soil's porosity is  $n$ , and the initial gradient found from tests is  $j_{in}$ . The soil's moisture content, the soil being saturated ( $G = 1$ ), can be determined by using this relationship:

$$w = \frac{n}{(1 - n)\rho_0}$$

where  $\rho$  is the soil's bulk density.

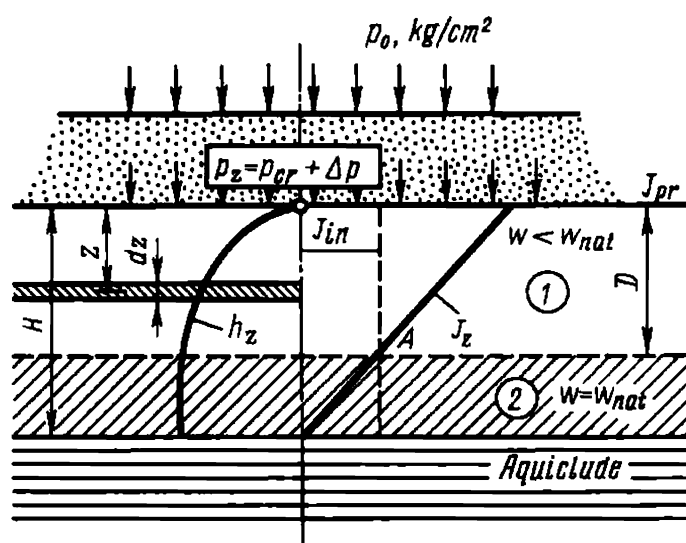


Fig. 23.2. Diagram of rough evaluation of a likely effect of the initial gradient  $I_{in}$  on soil consolidation

Assume further (the assumption is valid only for some period of time of soil consolidation) that the rate of soil consolidation remains unchanged throughout the process. Denote this rate by a loss in  $n$  of the soil with time as  $t$ . Define the quantity obtained by  $\mu$  and call it *a coefficient of static consolidation*. It is equal to

$$\mu = \frac{dn}{dt} (t^{-1}) \quad (23.2)$$

where  $t^{-1}$  is a measurement unit reverse to time (1/s, 1/yr).

Clearly, under the particular conditions (at  $G = 1.0$ ) the rate of soil consolidation will concurrently indicate the discharge velocity of the water squeezed out of the soil in unit time from unit volume of the soil due to the load acting on it. Let us select an elementary layer which is  $dz$  in thickness in the particular soil layer at a vertical distance from its top. As the soil is being compressed all the moisture squeezed out of the lower soil layer which is  $(H - z)$  in thickness must penetrate through this horizon with the area  $\omega$  per unit time. This discharge  $q_z$  at a depth  $z$  will be equal to

$$q_z = \omega \mu (H - z) \quad (23.3)$$

On the other hand, this discharge may occur only if in the elementary layer  $dz$  there is a hydraulic *pressure gradient*

$$j_{pr} = \frac{dh_{zpr}}{dz} \quad (23.4)$$

where  $h_{zpr}$  is the moisture removing pressure head.

Then in conformity with Darcy's law

$$q_z = K_p \omega \frac{dh_{zpr}}{dz} \quad (23.5)$$

By comparing Eqs. (23.4) and (23.5) we will obtain

$$dh_z = \frac{\mu}{K_p} [H - z] dz \quad (23.6)$$

Let us integrate this equation following from the fact that at  $z = 0$ , i.e. on the contact surface between the consolidating and the draining layer,  $h_z = 0$ :

$$h_z = \frac{\mu}{K_p} \int [H - z] dz \quad (23.7)$$

or

$$h_z = \frac{\mu}{K_p} \left[ Hz - \frac{z^2}{2} \right] \quad (23.8)$$

As can be seen, the relationship of the pressure head of the layer  $h_z = f(z)$  has the shape of a parabola (see the left-hand side of Fig. 23.2). Clearly, with  $z = 0$  and  $z = H$  we will have, respectively,

$$h_z = 0; \quad h_z = \frac{\mu}{K_p} \frac{H^2}{2} \quad (23.9)$$

To determine the pressure gradient  $j_{pr}$  from Eq. (23.4) we must differentiate Eq. (23.8) with respect to  $z$ . Then

$$j_{zpr} = \frac{dh_z}{dz} = \frac{\mu}{K_p} (H - z) \quad (23.10)$$

This relationship is already of a linear character (see the right-hand side of Fig. 23.2:  $j_{pr \min} = 0$  for the foot of the layer at  $z = H$ );

$$j_{pr. \max} = \frac{\mu}{K_p} H$$

(at  $z = 0$ , i.e. at the roof of the layer).

Thus the pressure gradient increases with increasing the soil's compressibility (weak consistency, low density, increased load — factor  $\mu$ ), the thickness of the layer being compressed (factor  $H$ ), and with decreasing its permeability (factor  $K_p$ ). Such a conclusion seems to be fairly logical.

Let us cut off from the seam's top a horizon at a depth  $D$  determining the location of  $A$  for which the equality  $j_{zpr} = j_{in}$  is valid. Thus the layer in question which is  $H$  in thickness consists of two zones.

*In the first zone* which is  $D$  in thickness (active zone) soil consolidation will occur in conformity with filtrational (percolation) consolidation laws (with the gradient  $j_{pr}$  decreasing in proportion to the depth of the active

zone). The soil here will ultimately consolidate attaining the moisture content  $w_p$ , i.e. one that corresponds to the load  $p$ .

*In the second zone* the soil's initial (natural) moisture content will remain practically unchanged. Accordingly the initial shearing resistance of the soil will not change. At the same time the moisture in the soil's voids in the second zone will be at a definite head  $h_z$  which more often than not will be a factor decreasing the normal stress and, consequently, the shearing resistance of the soil at the given horizon:

$$s_{pw} = (p_{nat} - \rho_w h_z) \tan \varphi_w + c_w$$

where  $\rho_w$  is the density of the moisture.

An essential argument in favour of the theory of the initial gradient is provided by the commonly observed excess (pore) pressure in the mass of silty deposits which serves a proof of the fact that the process of compression of the deposit is still in progress.

## Chapter 24

### The Hydrostatic and Hydrodynamic Effect

#### Sec. 24.1. The Essence of the Phenomenon

The practice of construction and operation of structures supported by or built on sand has witnessed a number of cases when the structures lost stability and underwent substantial deformations due to the action of ground and subsurface waters. In such circumstances the saturated sands completely lost stability and passed to a liquid state. Banks composed of sandy soils likewise frequently lose stability due to dynamic stresses. Cases have been recorded of slides and total failures of sand dams and levees as well as of catastrophic failures of approach embankments of bridges due to the weight of railway trains. Sometimes these failures led to massive losses of human lives (accident in 1928 in Weesp, Holland). We know the instances of complete destruction of port facilities and even buildings in urban areas as a result of the dynamic action of passing traffic. Some of the Munich streets had to be closed to traffic because of excessive settlement and damage to buildings.

As has been pointed out in Chapter 18, stability of saturated soils is of especial importance for foundations of structures in seismic areas.

We have repeatedly emphasized the effect of the uplift pressure in the



soil mass on the degree of the stability of the foundation as well as in the mass of slopes and faces. Of not lesser significance is the hydrodynamic regime of subsurface waters.

As has been demonstrated by practice of tunnel driving, as the alignment of a tunnel traverses a tectonic zone, especially, and old buried depression filled by fresh deposits, liquefied soil masses, notably fine- and small-grained sands or quicksands may rush into the tunnel from the overburden. A well-known example is quicksands outbreak in the tunnel of Medon (France). A passage was being driven there in 1939 in the mass of marl close to the roof of the layer, the stratum of marl being overlain by a thick layer of aquiferous fine-grained sands. The thin roof of marl failed and a substantial section of the excavated passage was filled by liquid sand material. Construction had to be suspended for a lengthy time period.

An even more serious accident occurred during the construction of the Lötschberg Tunnel, from Kandersteg to Gopperstein (Switzerland) between October 1906 and September 1911. About two miles in from one portal the drilling broke into an ancient glacial gorge, and in an instant 8,000 cu. yd. of material rushed in, and 25 men lost their lives. The heading had to be bulkheaded off, and the alignment changed. The tunnel was eventually completed, being 870 m longer than had been anticipated.

A serious hazard to a diversion tunnel driven during the construction of the Khram Hydro Power Station in Georgia (USSR) in 1954 was presented by the inrush of a quicksand material from the overburden composed of ancient lacustrine deposits. The overburden overlain by a thick basalt mass was entered by the tunnel. Similar problems have been encountered during the construction of the underground in Leningrad.

### Sec. 24.2. The Hydraulic Gradient as a Means of Hydrodynamic Action

As has been shown by experience, the likelihood of sand transport from the soil mass by seepage pressure is conditioned by the hydraulic gradient  $I$  in the subsurface water flow and primarily by the value of the so-called output gradient  $I_{out}$  in the vicinity of the free surface of the layer.

Let us select an element of a cross section  $\omega$  and length  $l$  in the mass of the soil where seepage flow operates (Fig. 24.1). Water flow (seepage or percolation) in the given element occurs due to the difference between the hydrostatic pressure  $H_1$  and  $H_2$  operating along cross sections 1-1 and 2-2 at the ends of the element. The specific pressure in these cross sections will be

$$p_1 = \rho_w H_1; \quad p_2 = \rho_w H_2$$

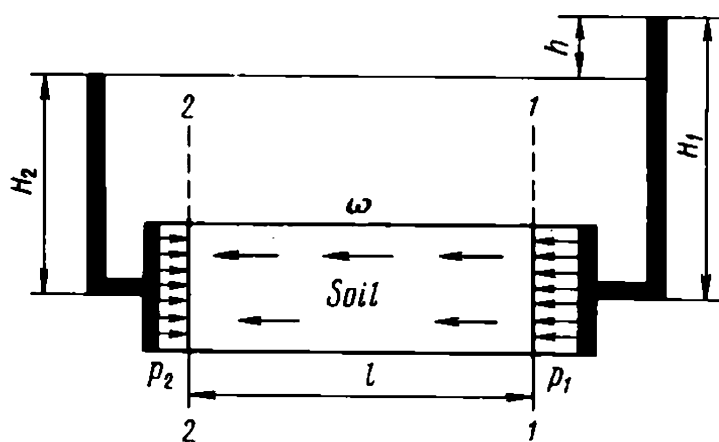


Fig. 24.1. Diagram showing seepage acting on a soil

The piezometric heads  $P_1$  and  $P_2$  acting at the right and left extremities of the element will equal

$$P_1 = \rho_w H_1 \omega; \quad P_2 = \rho_w H_2 \omega$$

Apparently, seepage pressure  $W_p$  as a driving force directed to the left and imparted to the entire soil element whose volume is  $V = \omega l$  will be

$$W_p = P_1 - P_2 = \rho_w h \omega \quad (24.1)$$

where  $h = H_1 - H_2$ .

Then the seepage pressure  $W_p$  acting on the soil's unit volume will be found from the relationship

$$W_p = w_p / V$$

which, by virtue of Eq. (24.1), yields

$$W_p = \rho_w h \omega / (\omega l) \quad (24.2)$$

Cancelling  $\omega$  and denoting the hydraulic gradient as  $I = h/l$  yields

$$W_p = \rho_w I \quad (24.3)$$

This equation is of much value for our analysis. If the flow of water is directed upward, it will decrease the weight of the soil mass in proportion to the magnitude of the gradient responsible for this flow (uplift pressure). Given that the bulk density of soil, when submerged, is  $\rho'_w$ , equilibrium will be observed on condition that

$$\rho'_w = w_p$$

or

$$\rho'_w = \rho_w I_{cr}$$

Assuming  $\rho' = 1.0 \text{ t/m}^3$  and  $\rho_w = 1.0 \text{ t/m}^3$ , the critical value of the gradient equivalent to total uplift pressure will approach  $I_{cr} = 1.0$ , or,

more precisely, the quantity

$$I_{cr} = \frac{\rho'_w}{\rho_w} = \rho'_w \quad (24.4)$$

or, differently speaking, the bulk density  $\rho'_w$  of the soil in a submerged state, expressed in  $\text{t/m}^3$ .

According to Darcy's law the discharge velocity is  $v = K_p I$ . Hence  $v_{cr}$  as the critical velocity of the flow of water through the soil will be equal to  $v_{cr} = K_p I_{cr}$ . By virtue of Eq. (24.4) we obtain for this velocity the following value

$$v_{cr} = K_p \quad (24.5)$$

This equation makes it possible to determine the value of the critical velocity for one soil or another depending on its coefficient of permeability.

Theoretical analysis and actual observations suggest that the excess hydrostatic pressure  $h_z$  and, consequently, the pressure gradient  $I$  responsible for the behaviour of the soil may appear in a submerged sand mass owing to a number of factors. Of these, the most important are: (1) upward seepage pressure acting on the toe of a dam or dike; (2) wave making pattern in the water reservoir overlying the soil mass; (3) upward flows of water induced by dynamic effects (vibrations).

The problem of soil resistance to seepage pressure has been considered in sufficient detail in many aspects and from different viewpoints in various reports, preeminently submitted by the VNIIG Institute (Russian abbreviation for the All-Union Research Institute for Hydraulic Engineering). This was reflected in the relevant codes and regulations.

### Sec. 24.3. Conditions Resulting in Loss of Stability of Soils in Open Cuts

As has been demonstrated by practice of civil engineering, unlift pressure must be taken into account when excavating a pit and, especially, when draining it. If the soil mass includes water-bearing layers (aquifers) (sand, gravel, jointed sandstone or limestone) alternating with impervious clay layers (aquicludes), precautions must be taken against outbreak of subsoil pressure waters to the excavated pit which would entail inundation of the pit and detrimental deformations of the foundation of the structure designed.

Ripping soil mass of conspicuous thickness composed of granular, to say nothing of fine-grained, sands, unless adequate drainage work has been performed, almost invariably brings about the liquefaction of such sands.

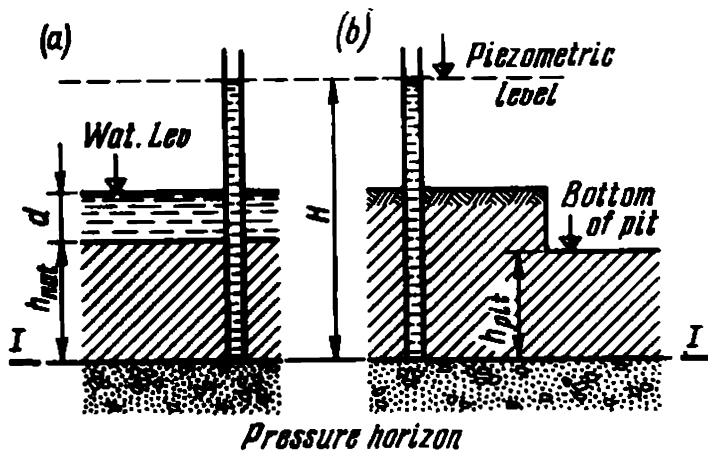


Fig. 24.2. Diagram showing the uplift pressure of water head under conditions of:

*a*—natural regime; *b*—excavating and draining a pit

This occurs due to the uplift pressure of the subsurface water flowing to open pits. The relatively low permeability of such soils inhibits drainage by pumping from the surface whereas the magnitudes of the gradient (discharge gradient) become especially appreciable in horizons adjacent to the bottom of an open pit.

The soil here generally sustains a minor fraction of the weight of the overburden of the given horizon or may even sustain no weight at all. So it is not uncommon that the soil at the bottom of a pit totally loses its stability and passes to the plastic and liquid state and acquires the properties of quicksand. As a result conditions of construction work become prohibiting. Matters are particularly bad when a sand layer directly overlies the massive pervious solid rock showing pronounced jointing and containing much moisture.

It is very often quite a problem to deal with liquefaction of soils in open pits, e.g. using pile foundations. It is especially so if soil liquefaction affects the subsoil to a considerable depth. Sandy slopes of open pits passing to the liquid state and quicksand outbreak from out the soil mass result in failures of the pit flanks and present a hazard to equipment located at the crest of the bench, e.g. cranes.

Soil stability at the bottom of a pit may be lost during drainage due to *outbreak of pressure waters* or because of the direct action on the soil of *upward flow of water*. Let us consider the first problem. As can be seen in Fig. 24.2, the soil mass composed of impervious materials is underlain by an aquiferous layer  $h_{nat}$  in thickness with a pressure head  $H$ . The soil mass is overlain by a surface water layer  $d$  in depth. The natural pressure at the top of the aquiferous layer *I-I* will be found from the relationship

$$p_{nat} = [\rho_w d + \rho_v h_{nat}] - \rho_w H \quad (24.6)$$

It will be recalled that  $\rho_w$  and  $\rho_v$  define, respectively, the bulk density of the water and of the soil whose voids are water-clogged. For an open and drained pit, if the aquiferous layer preserves its piezometric level, at the

level 1-1 we will have

$$p_{pit} = p_v h_{pit} - \rho_w H \quad (24.7)$$

Naturally, in the given case the soil mass loses in weight. Decompression of the soil is then likely to occur coupled to added saturation, drop in stability and swelling of the pit's bottom, often in terms of tens of centimetres. The onset of equilibrium at the level 1-1 will take place at  $\rho_v h_{pit} = \rho_w H$ .

The bulk density of the soil is generally  $\rho_v = 2.0 \text{ t/m}^3$ . Hence the critical value of the soil layer,  $h_{cr}$ , underlying the pit's bottom and overlying the roof of the aquiferous level will be found as

$$h_{cr} = H/2 \quad (24.8)$$

At all values of  $h_{pit}$  approximating  $h_{cr}$  the soil at the bottom of the pit will be found in detrimental conditions sometimes leading to catastrophic failures due to inrush of pressure waters into the pit. If such conditions are likely to arise it is usual to limit the depth of the excavation or employ drainage sumps the water out of which is pumped automatically\*.

Let us now consider failure of the sand mass induced by upward seepage pressure (*hydrodynamic effect*).

Stability of any soil variety at a definite specified point in the foundation of a structure is found from the magnitude of the safety factor  $K_s$  by using the relationship

$$K_s = s_p / \tau_{max}$$

The shearing resistance  $s_{pn}$  of a sandy or any other loose cohesionless soil in static conditions is determined from the familiar equation  $s_{pn} = p \tan \varphi_n + c_n$ .

The hydrodynamic effect reveals itself by the pressure exerted on the soil mass by the flow of water. This pressure is directly associated with the magnitude of the hydrodynamic or simply dynamic head  $h_z$  that determines the hydraulic regime of the seepage flow. The pressure  $p_h$  induced by the head  $h_z$  is governed by the bulk density of the seepage water  $\rho_v$  and is found from the equation

$$p_h = \rho_w h_z \quad (24.9)$$

Analysis shows that in the particular case it is only *the upward seepage flow* which is able to produce the uplift pressure on the soil mass that is of importance. Thus the shearing resistance of a sand mass,  $s_{dyn}$ , under

---

\* This technique was originally applied in 1927 during the construction of a dam for the Svir Hydro-electric Power Development.

hydrodynamic conditions is found (for a one-dimensional problem) from the relationship

$$s_{dyn} = (p - \rho_w h_z) \tan \varphi_n + c_n \quad (24.10)$$

where  $h_z$  is the hydraulic head at the level  $z$ .

As demonstrated by practice, the shearing strength especially decreases in the case of loose sands with almost no cohesion. The above equation will then take on this form:

$$s_{dyn} = (p - \rho_w h_z) \tan \varphi \quad (24.11)$$

Clearly, at any dynamic head  $h_z$  other than equal to zero, the shearing resistance of sand somewhat lessens which may impair soil mass stability and the stability of surface structures.

The first term in the right-hand side of Eq. (24.10) vanishes at

$$p = \rho_w h_z \quad (24.12)$$

whence

$$h_z = p / \rho_w$$

The shearing resistance of the sand is then zero. Clearly, under such conditions the sand passes to the liquid state completely losing its stability and bearing power.

## Chapter 25

### Settlement of Structures and Their Stability

#### Sec. 25.1. Introduction

As has been already emphasized, in order that catastrophic failures be avoided it is of crucial importance to ensure the stability of the foundation of any engineering structure. Construction practice indicates, however, that satisfaction of this condition alone does not always guarantee structure stability and adequate conditions of performance.

Proper conditions of operation are often violated by structure settlement induced by deformations of incompetent soils at load. This is often the case when the foundation of a structure is underlain by layers of peat, silt, watered loess and loessian-type soils with marked porosity as well as by poorly consolidated clay.

The settlement of structures is invariably differential due to a number of causes such as nonuniform foundation conditions, unequal loading and stress distribution in the soil mass etc. In many instances the value of settlement attains tens of centimetres and exceeds 1 m if the subsoil includes strata of silt deposits or weak soils.

Building practice has witnessed cases of major settlement. An interesting example is provided by settlement of an old fountain built in 1810 in Istanbul that settled more than 180 cm or by that of several buildings in Shanghai that attained the magnitude 150 to 200 cm. A record was established by buildings in Mexico City that have settled 7 m due to the drop in the water table (cf. Sec. 30.1).

Pronounced sensitivity of lacustrine bentonite clays whose moisture content often exceeds 300% calls for deep pile foundations if an important structure is to be erected (see Fig. 25.5).

Such foundation conditions may lead to: (a) major settlement, tilting and deformation of individual members of a structure or of the latter itself; (b) loss in the strength of the structure due to cracks and ruptures resulting from excessive strains.

Excessive tilting should be avoided when such structures are involved as

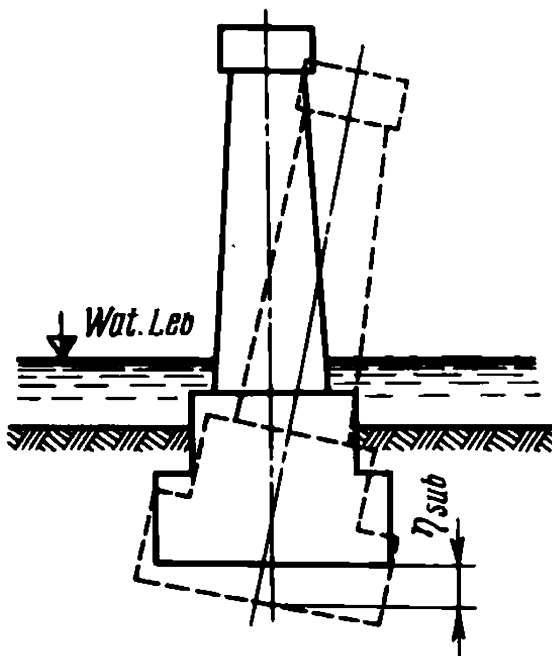


Fig. 25.1. Settlement and tipping of an individual bridge pier

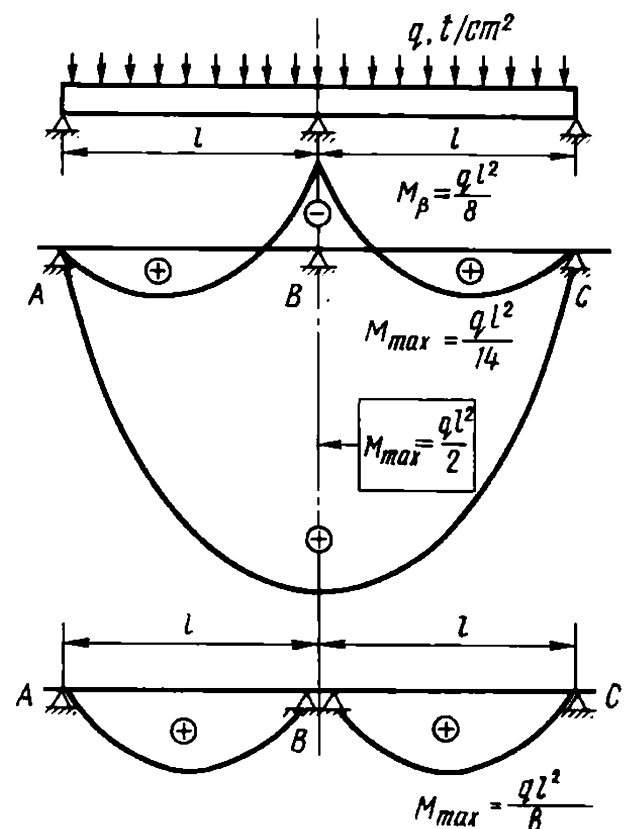


Fig. 25.2. Effect of a settlement of an intermediate abutment of a two-span continuous beam on the magnitude and sign of the bending moment

tall bridge piers, lighthouses, range markers, various towers, stacks etc. (see Fig. 18.3).

Of a definite interest is the settlement of a bridge across the Mosyr River (1922). This bridge had three spans 107 m each, supported by high masonry piers, and a wooden approach structure about 970 m long and 21 m high.

The intermediate piers, having penetrated a thick layer of silt deposits, rested on caissons put to a depth of 20 to 22 m. These measures, however, proved to be insufficient. Immediately on completion (1907) continuous settlement and tilting of the piers had been detected. Differential and conspicuous settlement of the bridge piers that had attained by 1922 1 m coupled to the tilting of the top by 1.25 m led ultimately to failure of the bridge which had to be rebuilt.

Major settlement and tilting of high bridge piers (Fig. 25.1) may result from deterioration of foundation conditions of bridge trusses. Unequal settlement, deformation and tilt of bridge piers rigidly connected with the span structure (frame, hingeless arch etc.) will invariably enhance bending moments and transverse forces acting on the structure and sometimes causing excess stresses. Especially detrimental effect is brought about by differential settlement of piers and abutments of a multispan continuous structure as one, e.g. represented in Fig. 25.2.

### Sec. 25.2. Differential Settlement and Its Results

The sag of a beam whose span is  $L$  resting on two abutments, as is known, is found from the relationship

$$f = \frac{5}{384} \frac{qL^4}{EI}$$

where  $EI$  is rigidity.

In conformity with this equation the sag of a reinforced concrete beam 60 by 75 cm in cross section and with the span  $L = 2l = 14.0$  m at a load 3 t/m attains  $f = 3.3$  cm. At a relative settlement of the intermediate pier  $B$  by more than 3.3 cm the particular two-span continuous beam with the span length  $l = 7$  m proves to be a conventional two-piece beam supported by two abutments whose span is  $L = 2l = 14$  m. Then the moment  $M_B''$  will operate along the axis of  $B$  whose value is

$$M_B'' = + qL^2/8 = ql^2/2 = + 74 \text{ t} \cdot \text{m}$$

rather than the previous moment

$$M_B' = - ql^2/8 = - 18.3 \text{ t} \cdot \text{m}$$



Thus at the settlement of  $B$  with respect to  $A$  and  $C$  more than 3.3 cm the normal stresses induced by bending will not only increase fourfold in the beam but at  $B$  will change in sign. The latter circumstance may prove especially detrimental for the performance of a reinforced concrete beam.

It must also be noted that very often the cause of major settlement and tilting of bridge abutments in the direction of the banks is earth pressure of the foundation of high approach embankments. This factor was in part responsible for the failure of the bridge illustrated in Fig. 16.5.

Disregarding the conspicuous compressibility of the subsoil, and first of all a layer of buried peat coupled to underpinning of the bridge by piles resulted in marked settlement of the bridge (about 2 m). This caused substantial damage to the span structure.

The bridge in question was a three-hinged arch type, very little susceptible to settlement. No doubt, had this bridge been built as a two-hinged or hingeless arch, such settlement would have brought about total destruction.

When deciding on the erection of a long-span bridge of a hingeless arch type on bedrock clay strata, always take care of the possibility of differential settlement. It is of interest to mention the settlement of an arch-type, 120 m long span bridge across a lock of the Moscow Canal. Out of precaution a three-hinged version (statically definite design) of the bridge was decided upon with pile foundations resting on Jurassic clays. As has been expected, the bridge abutments settled 5 to 6 cm, half of the settlement like that of the abutment, across the Kazanka River (see Fig. 16.5) being due to the pressure of the 25 m high embankment on the latter's toe. This resulted in the tilting of the abutments toward the embankment.

Marked nonuniformity of settlement and tilting of the abutments have resulted in similarly disadvantageous conditions for various industrial objects and other engineering structures incorporating continuous members (multispan girders, multispan and multistorey trusses, hingeless and two-hinged arches etc.). The expected settlement of, say, bridge piers, places definite constraints on the design of span structures. Thus use of continuous girders must be avoided out if very nonuniform pier settlement is likely to occur. Alternatively, jacking mechanisms should be provided to compensate for the observed settlement. We can recall the old bridge near Kursk carrying the Moscow-Kharkov highway across the Seim River that existed until World War II.

During the construction of the Matsesta viaduct near the town of Sochi, a settlement of one of the pile-underpinned piers was detected at the moment the load on the subsoil attained half the design value. Because of this a wooden framework was built on the top of the uncompleted pier filled with rock and sand whose total weight was about 5 000 t, somewhat higher

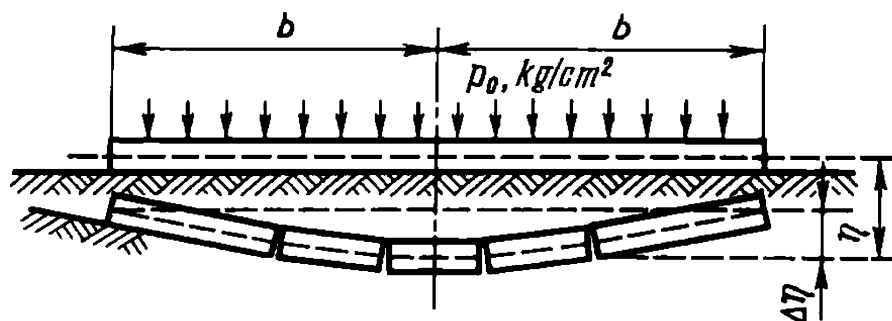


Fig. 25.3. Deformation of a foundation raft at a uniformly distributed load

than the design value. The surcharge first led to an abrupt settlement of the pier which then began to decrease gradually. The design of the span structure was altered: two-hinged arches were substituted by three-hinged ones, permitting differential, up to 15 cm, settlement. Since the settlement had subsided, systematic observations of the piers were stopped several years ago.

Monolith structures, such as masonry buildings, may also undergo nonuniform settlement. It should be mentioned at this point that the settlement of structures even resting on a perfectly uniform foundation will always be differential because of specific conditions of the distribution of strains in the soil mass considered in what follows. The peak of the subsidence of a surface-loaded strip typically occurs at the central area of the loaded strip. In this case even a perfectly uniform load causes a sag of the structure (Fig. 25.3), and if the monolith structure is insufficiently strong, it will develop cracks.

In actual practice, due to general nonuniformity of subsoil strata, unequal loading and differential strength of the structure, the latter develops a complex pattern of cracks (Fig. 25.4).

Construction practice has detected another important fact, the unequal rate of structure settlement. Let us define it as  $\Delta\eta_{sub}$ . Its value is

$$\Delta\eta_{sub} = (\eta_{sub\ max} - \eta_{sub\ min}) \quad (25.1)$$

where  $\eta_{sub\ max}$  and  $\eta_{sub\ min}$  are, respectively, maximum and minimum settlement of the particular structure.

As has been demonstrated by practice, the nonuniformity of structure settlement increases in proportion to the magnitude of the structure settlement. It may attain as much as 50% of the value of the average settlement  $\eta_{sub\ av}$ :

$$\Delta\eta_{sub} = 0.5\eta_{sub\ av} = 0.5 \left( \frac{\eta_{sub\ max} + \eta_{sub\ min}}{2} \right) \quad (25.2)$$

Thus at the average structure settlement  $\eta_{sub\ av} = 5$  cm its nonuniformity is  $\Delta\eta_{sub} = 2.5$  cm. At the average settlement  $\eta_{sub\ av} = 40$  cm,  $\Delta\eta_{sub}$  equals 20 cm. Clearly, in the latter case the structure in hand will operate under more complicated conditions.

As can be seen, any structure resting on clayey or sandy subsoils is liable to settlement. What is needed is to predict the value of the expected settlement of the object being designed and the permissible settlement of the structure in hand.



Fig. 25.4. Cracks in a building following an unequal settlement of one of its corners

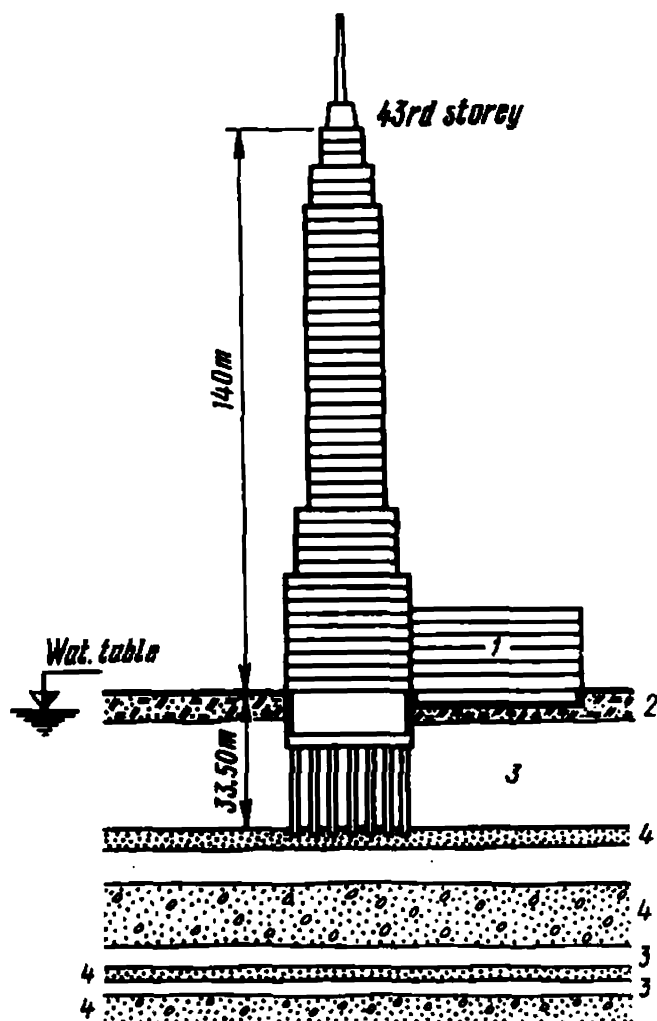


Fig. 25.5. Skyscraper in Mexico City supported by a pile foundation of conspicuous depth to avoid excess settlement and tipping:

1—five-storey building resting on a shallow footing; 2—backfill and sand deposits; 3—volcanic silt; 4—sand strata

Bridge construction uses the following recommended values:  
the limit permissible uniform settlement of a pier (in cm)

$$\eta_{sub\ lim} = 1.5 \sqrt{l}$$

the difference in settlement of the adjacent piers (cm)

$$\Delta\eta_{sub} = 0.75 \sqrt{l}$$

the limit horizontal displacement of the top of a pier along and across the bridge, cm

$$u_{lim} = 0.5 \sqrt{l}$$

In the above formulae  $l$  is the length of the shorter span adjoining the given pier in m. The minimum value of  $l$  is assumed as being equal to 25 m.

It is of interest that in conformity with the regulations acting in Great Britain the settlement of a structure that can be tolerated is 7 cm for clays, 4 cm for nonuniform settlement conditions, and 5 and 3 cm, respectively, if a sag is not more than 1 in 150.

For conditions prevailing in this country the critical values of deformation and average settlement for various buildings and structures are envisaged by the Soviet Civil Engineering Code of Practice, SNiP II-15-74,

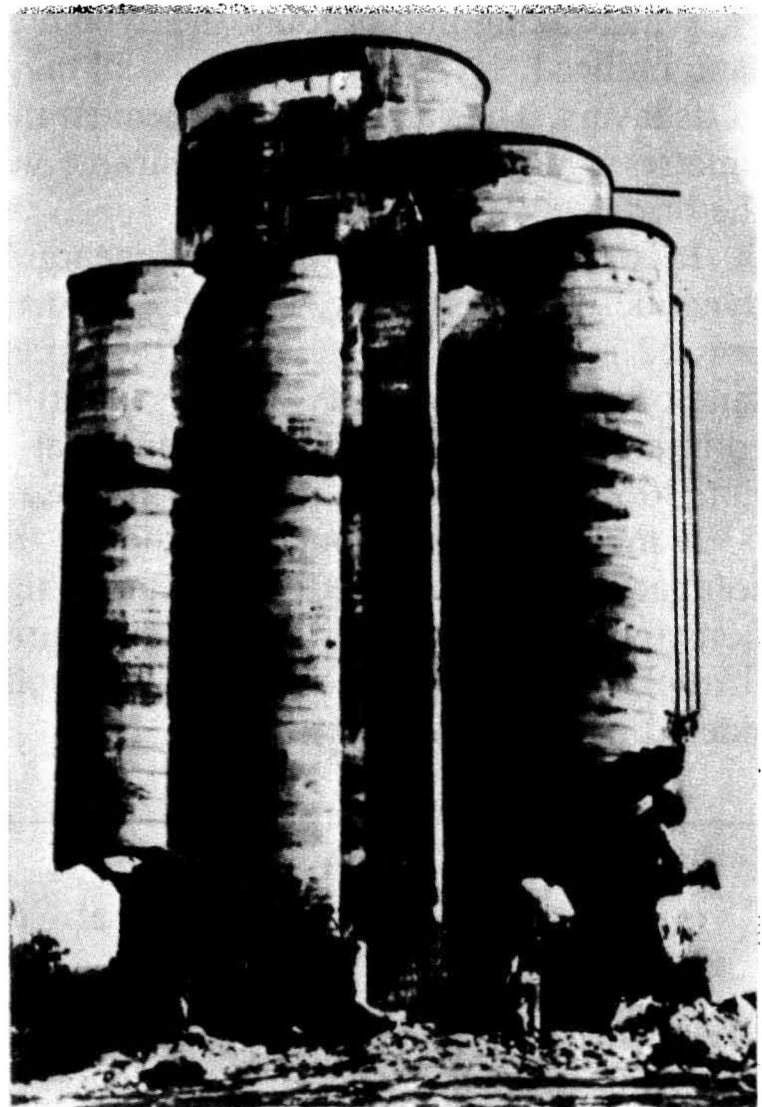


**Fig. 25.6.** Failure of a grain elevator in Siracuse (USA) due to conspicuous and differential settlement of its elements

Table 10.8. Depending on the design features and structure type these limit values are in the range from 8 to 40 cm.

The civil engineer must be aware of the fact that the highest structure settlement generally occurs as the structure is being erected when it is easy to correct all the detected defects. The builder should be able in due time to predict changes likely to appear in the foundation because of the action of the weight of the structure itself. This alone can prevent the detrimental effect of such changes. One of the steps to control settlement is underpinning by using piles (Fig. 25.5).

Repair, reinforcement and reconstruction of a structure damaged by deformations in the foundation generally require much effort and are very costly.

A typical failure of such type is illustrated in Fig. 25.6. This is a grain elevator in Siracuse, USA, seriously damaged as a result of conspicuous nonuniform settlement of the central and principal elements supported by clays of various compressibility (soft plastic clays with organic inclusions and gravelly sands).

When taking into account the dynamic stresses on loose masses of dry sand induced, say, by vibrations, sand may subside owing to consolidation of its layers. The value of the settlement may sometimes attain tens of centimetres which is especially undesirable where the embankment passes to the bridge.

It is easy to predict this phenomenon by determining the modulus of dynamic compressibility,  $e_{dyn}$ , by means of a simple dynamic test, expressed in mm/m. The test must be carried out with consolidation of the sand of a definite porosity value by vibrating it in a vessel at a predetermined intensity of the dynamic action and at a specified external load  $p$ . Section 30.2 deals with this problem in more detail.

It must be finally concluded that in the general case, apart from soil compaction, structure settlement can be significantly affected by deformations induced by irreversible soil dislocations associated with plastic and rheological (creep) phenomena in silty soils. These problems will be considered in later chapters.

---

## Chapter 26

### Principal Theoretic Premises to Predict Structure Settlement

---

#### Sec. 26.1. Introduction

To predict the settlement and deformation of a structure means to solve the problem in forecasting the surface subsidence and deformation of the underlying strata due to the stresses applied to these.

Under particular conditions we have to determine the possible deformation of the soil mass owing to compression of individual soil layers under normal stresses  $p_z$ ,  $p_x$  and  $p_y$ , appearing in the overburden on the application of a load to it. Clearly, the values of  $p_z$ ,  $p_x$  and  $p_y$ , will vary as the  $z$ ,  $x$ ,  $y$ -coordinates of the particular point change.

Leaving aside the nonuniformity of the soil mass with depth governed by genetic and lithologic mechanisms, we must recognize the generally occurring increase of the modulus  $E_p$  of compression of the soil with increasing the depth. This can be ascribed to the increasing soil density resulting from the greater weight of the soil layers,  $p_{lim}$ , overlying the given horizon. This will inevitably affect the final value of the surface subsidence, as in the particular case the deep horizons do not contribute essentially to the total compression of the soil mass due to the weight of the structure in hand.



known in mechanics at a constant value of the modulus of elasticity  $E$  independent of the load  $p$ , i.e.  $e = p/E$ .

Apart from the dependence on the load  $p$  the modulus of deformation  $E_p$  differs from the modulus of elasticity  $E$ , by the presence, in the compression zone, of irreversible (plastic) deformation which is almost its inevitable part. For an elementary layer,  $z$  in thickness, we have

$$e_{pz} = \frac{d\eta_{sub}}{dz} \quad (26.2)$$

A substitution into Eq. (26.1) of the value of  $e_{pz}$  from Eq. (26.2) yields

$$d\eta_{sub} = \frac{p_z}{E_{pz}} dz \quad (26.3)$$

Consequently, the total subsidence of the loaded strip of the overburden  $\eta_{sub}$  will be found from the relationship

$$\eta_{sub} = \int_0^{\infty} \frac{p_z}{E_{pz}} dz \quad (26.4)$$

where  $p_z$  and  $E_{pz}$  are the variables which are a function of the depth  $z$ .

Thus the solution of the problem of deformation of the soil mass, the subsidence of its surface and settlement of the structure itself under the particular conditions calls for the determination of the functional relationships  $p_z = f_1(z)$  and  $E_{pz} = f_2(z)$ .

Even in the simplest, one-dimensional case we are faced with almost unsurmountable mathematical difficulties. In addition, the relationship between  $E_{pz}$  and  $z$  under actual conditions proves to be very much involved. This renders it impossible to be represented in a simple mathematical form. This is due to the commonly observed occurrence in the foundation of a structure of various soil layers with different characteristics (bulk density and unit density) and compressibility.

This picture is being made even more complex by conditions of watering in the soil mass and its effect on the magnitude of the natural load  $p_{nat}$ . Under such conditions we have to avoid the solution in the general form by integrating Eq. (26.4) and solve the problem by algebraic summation. The total subsidence of the soil's surface is found from the relationship

$$\eta_{sub} = \sum_0^D \eta_{sub\ i} \quad (26.5)$$



where

$$\eta_{sub\ i} = \frac{p_z}{E_{pz}} h_i \quad (26.6)$$

In the last two equations  $\eta_{sub\ i}$  is compression subsidence of a definite design layer  $h_i$  thick selected in the foundation soil mass on the condition that the variations of  $p_z$  and  $E_{pz}$  are so small that can be considered constants for this layer.

The limit of summation  $D$  in the particular case (with a small thickness of the layer being compressed) coincides with the thickness of the layer. In a more general case (conspicuous thickness of the layer) the limit  $D$  is governed by a depth  $z$  whose increase in soil computation does not practically lead to increased structure settlement due to the low compressibility of the deep soil layers and small values of normal stresses operating here.

A substitution of  $\eta_{sub\ i}$  from Eq. (26.6) into (26.5) yields a relationship for determining the structure settlement  $\eta_{sub}$  for a one-dimensional problem:

$$\eta_{sub} = \sum_0^D \frac{p_z}{E_{pz}} h_i \quad (26.7)$$

This relationship, fairly simple in itself, makes it rather difficult to determine the design values of the modulus of compression  $E_{pz}$  allowing for the soil density increasing with depth and the value of the normal stress  $p_z$  itself.

Moreover, construction practice generally calls for solutions both of two-dimensional and three-dimensional problems. Besides, it may sometimes be necessary to allow for the anisotropy of the soil mass. Such a need arises whenever stiff materials composing the subsoil are alternated by layers of incompetent soils demonstrating high compressibility.

All these facts point to the indisputable advantages and practical usefulness of the method of the prediction of the settlement of a structure by referring to the modulus of compressibility  $e_p$  compared with the modulus of deformation  $E_p$ .

The following method of the evaluation of consolidation deformation of an elementary layer satisfies these general requirements.

### Sec. 26.2. Useful Formulae

The basis of the method outlined is the determination of the relative deformation  $e_z$  along the  $Z$  axis induced by the application of normal stresses in a triaxial compression state equal to the relative soil deformation along the same axis by a stress  $p_z$  minus the expansion induced by strains

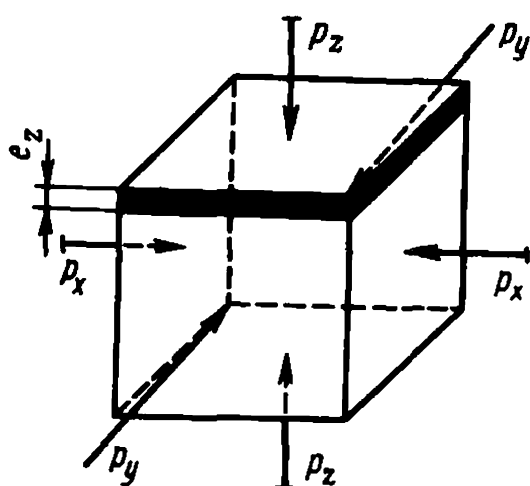


Fig. 26.2. Diagram for forecasting soil mass subsidence for a three-dimensional case

along the  $X$  and  $Y$  axes. The relative deformation  $e_z$  is in this case found from relationships of the type of Eq. (26.1) through strains  $p_z$ ,  $p_x$  and  $p_y$ .

In the more general method being described  $E_p$  is considered as being a variable and the particular subsidence  $\eta_i$  is determined only in terms of the relative deformations  $e_{pz}$ ,  $e_{px}$  and  $e_{py}$ , appearing along the  $Z$  axis due to the normal strains  $p_z$ ,  $p_x$ ,  $p_y$ . The relative deformation values are obtained directly from the data of the triaxial compression test, a soil compressibility is expressed through the modulus of compressibility. The magnitude of the relative deformation of an elementary layer is determined for the particular load from the compression curve rather than by calculations by using the  $e = p/E$  type relationships. Thus calculations automatically take into account the curvilinear nature of the relationship between soil deformation and the load as one of its most important properties.

As postulated by laws of mechanics, the relative compressive deformation  $e_z'''$  of a definite body of soil along the  $Z$  axis for a three-dimensional problem under the combined effect of a system of compressive normal strains  $p_z$ ,  $p_x$  and  $p_y$  acting along the respective coordinate axes can be found from the relationship

$$e_z''' = [e_{pz} - \nu(e_{px} + e_{py})] \quad (26.8)$$

where  $e_{pz}$ ,  $e_{px}$ ,  $e_{py}$  are relative deformations of a definite body of soil along the  $Z$ ,  $X$ ,  $Y$  axes under the direct and isolated action of the respectively directed normal stresses  $p_z$ ,  $p_x$  and  $p_y$  (Fig. 26.2).

If we define the coefficient of the lateral strain by  $\nu$  we will have a pseudoanalogue of Poisson's ratio  $\mu$  which in our case is assumed to be constant, viz. independent either of the magnitudes of  $p_z$ ,  $p_x$  and  $p_y$  or the direction in which they act\*.

---

\* The symbol  $\mu$  is used for Poisson's ratio. We employ the symbol  $\nu$  for this coefficient to emphasize its different use for soils as distinct from solids.

For further reasoning let us assume the modulus of the "free" (unconfined) compression  $E$  (analogue of the modulus of elasticity or Young's modulus) likewise independent of the value or direction in which the load is operating. Then, in conformity with Hooke's law,

$$e_{pz} = p_z/E; \quad e_{px} = p_x/E; \quad e_{py} = p_y/E \quad (26.9)$$

By substituting the values of  $e_{pz}$ ,  $e_{px}$  and  $e_{py}$  into Eq. (26.8) we will get

$$e_z''' = [p_z/E - \nu(p_x/E + p_y/E)] \quad (26.10)$$

Factoring out the modulus of compression  $E$  yields a relationship which is well known in mechanics

$$e_z''' = 1/E [p_z - \nu(p_x + p_y)] \quad (26.11)$$

The direct use of this relationship for predicting structure settlements or deformations induced by settlement cannot be made. This is because the modulus of compression entering this equation, independent of either normal stresses  $p_z$ ,  $p_x$ , and  $p_y$  or their direction fails to characterize the actual properties of soils. Although in the isotropic soil mass the value of  $E$  along all coordinate axes under the same loads may be assumed to be constant, we cannot disregard its dependence on the magnitudes of the loads proper. It would mean disregarding one of the most essential properties of soils, viz. the presence of a residual fraction there. It will be recalled that the compression characteristic of soils is invariably of a curvilinear form which can be seen from its very name, the compression curve.

When we consider the modulus of compression of soil is invariably constant even for a definite selected layer of a definite density, we incur, in principle, an error which may sometimes be of appreciable magnitude. When trying to predict structure settlement and deformations we have therefore to regard  $E$  for the general case to be dependent both on the values of  $p_z$ ,  $p_x$ ,  $p_y$  and on the direction in which they act.

Let us denote the moduli of compression  $E$  corresponding to the values and directions of  $p_z$ ,  $p_x$  and  $p_y$  by the symbols  $E_{pz}$ ,  $E_{px}$ ,  $E_{py}$ . Equation (26.10) will then take on this form:

$$e_z''' = \left[ \frac{p_z}{E_{pz}} - \nu \left( \frac{p_x}{E_{px}} + \frac{p_y}{E_{py}} \right) \right] \quad (26.12)$$

Clearly, it proves now impossible to factor out the modulus of compression  $E_p$ . Assume  $E_{pz}$ ,  $E_{px}$  and  $E_{py}$  constant in conformity with Eq. (26.1)

$$e_{pz} = p_z/E_{pz}; \quad e_{px} = p_x/E_{px}; \quad e_{py} = p_y/E_{py} \quad (26.13)$$

and substitute these into Eq. (26.12) thus obtaining again Eq. (26.8):

$$e_z''' = [e_{pz} - \nu(e_{px} + e_{py})]$$

When using this relationship for purposes to be considered further we must bear in mind that it is valid for varying values of  $E_{pz}$ ,  $E_{px}$  and  $E_{py}$ .

The present method of predicting the settlement and deformation of a structure relies on Eq. (26.8) and direct use of the compression curve for the given soil variety expressed as a relationship between the relative deformation  $e_{pz}$ ,  $e_{px}$  and  $e_{py}$  (for the anisotropic structure of the soil mass) and the normal strains  $p_z$ ,  $p_x$  and  $p_y$ .

This automatically takes into account the modulus of compression  $E_p$  depending on the load  $p$  operating at the given horizon which, as has been pointed out above, is of much importance.

Apart from this, there is no need in converting the values of deformation of loaded samples obtained from compression tests to the values of the voids ratio  $\varepsilon$  or, at least, to the values of the moduli of compression  $E_p$ .

The subsidence  $\eta_{sub\ z}$ , resulting from soil consolidation within the given layer  $h_i$  in thickness can be determined from the following relationship

$$\eta_{sub\ z} = e_z h_i \quad (26.14)$$

By taking into account this equation we can rewrite Eq. (26.8) as follows:

$$\eta_{sub\ z}''' = h_i [e_{pz} - \nu(e_{px} + e_{py})] \quad (26.15)$$

A substitution into this equation of  $e_{pz}$ ,  $e_{px}$  and  $e_{py}$  directly obtained from a triaxial compression test leads to some error. This is due to the fact that to calculate the deformation of the soil mass we use the data of a compression test where it is impossible to simulate the lateral strain of the soil sample. On the other hand, in actual conditions there is a likelihood of the selected layer of the subsoil demonstrating a definite amount of lateral expansion although this is restricted by the weight of the overlying soil strata and horizontal stresses  $p_x$  and  $p_y$  appearing in the subsoil due to the action of the weight of the structure itself.

The error due to disregarding the conditions of the compression test by Eq. (26.15) is generally within the accuracy of the total possible estimation settlement of the structure. When needed, however, these test conditions may be easily taken into consideration in the given case as well which is explained in what follows.

Refer again to Eq. (26.15) to predict settlement under conditions of a triaxial state of stress

$$\eta_{sub\ z}''' = h_i [e_{pz} - \nu(e_{px} + e_{py})]$$

As is known, Poisson's ratio  $\mu$  must always be less than 0.5 or at least approximating this value (for liquids). For soils, the value of  $\nu$ , the pseudoanalogue of  $\mu$ , with rare exceptions (very incompetent clays) is less than 0.3.

It is known, at the same time, that the horizontal strains  $p_x$  and  $p_y$  in the subsoil of a structure rapidly drop with depth. At any rate, they decrease much faster than the normal vertical stresses  $p_z$ . This is especially evident when we refer to the axis of the loaded strip where the load generally attains its peak value.

The relatively small magnitudes of  $\nu$  and of  $p_x$  and  $p_y$  result in that the second, bracketed term of Eq. (26.15) affects insignificantly the value of the settlement,  $\eta'_{sub\ z}$ . Moreover, if we omit the term including  $\nu$ ,  $p_x$  and  $p_y$  from Eq. (26.15) the design value of the settlement  $\eta'_{sub\ z}$  is somewhat increased which, to a certain degree, compensates our disregarding the conditions of the compression test.

Thus, when predicting the settlement of a structure, it is often well to assume the value of the coefficient of the lateral strain  $\nu = 0$  in Eq. (26.15). The latter relationship takes on then this form

$$\eta'_{sub\ z} = h_i e_{pz} \quad (26.16)$$

Note that the last relationship with the above reservation is in full agreement with the case of a uniaxial state of stress.

Let us return to a correction to Eq. (26.15) to allow for the conditions of a triaxial compression test. As shown by analysis, the relationship between the stress and deformation expressed through the modulus of compression  $E_p$ , in the case of unconfined expansion takes on this form:

$$e_z = \frac{1}{E_p} \frac{(1 + \nu)(1 - 2\nu)}{(1 - \nu)} p_z \quad (26.17)$$

It follows that if we want to express the relative deformation  $e_z$  for unconfined soil expansion through the modulus of soil compression  $E_0$  found directly from a compression test (0 is a symbol for a ring), then it would be more correct to write

$$e_z = \frac{1}{E_{exp}} \frac{(1 - \nu)}{(1 + \nu)(1 - 2\nu)} p_z \quad (26.18)$$

The modulus of compression  $E_0$  is found from the relationship

$$E_{exp} = p_z / e_{z\ exp} \quad (26.19)$$

where  $p_z$  is the test pressure,  $e_{z\ exp}$  is the relative compression deformation of the soil sample during the test at a load  $p_z$ .

Let us denote by  $M$  the term

$$M = \frac{(1 - \nu)}{(1 + \nu)(1 - 2\nu)} \quad (26.20)$$

Let us describe  $M$  as a conversion factor (operator).  $M$  is invariably greater than, or, at least (for Poisson's ratio  $\nu = 0$ ) equal to unity.  $M$  makes it possible to relate the values of the moduli of compression of unconfined  $E_p$  and triaxial  $E_0$  as follows:

$$E_{exp} = ME_p \quad (26.21)$$

or, by substituting into the latter equation the value of  $M$  from (26.20), we have

$$E_{exp} = \frac{(1 - \nu)}{(1 + \nu)(1 - 2\nu)} E_p$$

Clearly, the modulus of deformation obtained by a compression test  $E_0$ , showing a definite degree of resistance to the compression of the sample due to the presence of a ring, must be greater than the modulus of soil deformation under field conditions, i.e.  $E_0 \geq E_p$ . Equation (26.15) then takes on its final form:

$$\eta'''_{sub\ z} = Mh_i[e_{pz} - \nu(e_{px} + e_{py})] \quad (26.22)$$

At  $\nu = 0$  the coefficient  $M$ , in conformity with Eq. (26.20), becomes equal to unity. Then Eq. (26.15) becomes identical to Eq. (26.16), i.e.

$$\eta'_{sub\ z} = h_i e_{pz}$$

Let us proceed now to the derivation of a formula to predict structure settlement for a two-dimensional problem. The relative deformation along the  $Y$  axis is then

$$e_y = 0 \quad (26.23)$$

By allowing for this condition and taking into consideration a restraint on the lateral expansion of the sample in the compression test we get

$$e''_z = (1 - \nu^2) \left[ e_{pz} - \frac{\nu}{1 - \nu} e_{px} \right] \quad (26.24)$$

and, accordingly,

$$\eta''_{sub\ z} = (1 - \nu^2) \left[ e_{pz} - \frac{\nu}{1 - \nu} e_{px} \right] h_i \quad (26.25)$$

By introducing into the last relationship the operator  $M$  to allow for the

conditions of the compression test and including in the latter the values of  $e_{pz}$  and  $e_{px}$  obtained directly from the test data, we ultimately get

$$\eta''_{sub\ z} = Mh_i(1 - \nu^2) \left[ e_{pz} - \frac{\nu}{1 - \nu} e_{px} \right] \tag{26.26}$$

It is apparent that with  $\nu = 0$  this equation will also be identical to Eq. (26.16), i.e.  $\eta'_{sub\ z} = h_i e_{pz}$ .

In order to be able to use the above equations for predicting the subsidence  $\eta'''_{sub\ z}$  and  $\eta''_{sub\ z}$  of a selected soil layer for a two- and a three-dimensional problem we must know the values of the operator  $M$  and of the coefficient of the lateral expansion of the soil  $\nu$ . The conversion factor  $M$  is functionally connected with  $\nu$ , i.e. it can be easily found from Eq. (26.20), if we know the coefficient  $\nu$ .

The value of  $\nu$  for soils is hard to determine directly. An easier way is to find it through the coefficient of the lateral pressure  $\xi$  which is related with  $\nu$  through this equation:

$$\nu = \frac{\xi}{1 + \xi} \tag{26.27}$$

The easiest method of determining *the coefficient of lateral pressure*  $\xi$  is by using the apparatus for a triaxial test, called a stabilometer. The value of this coefficient is then found from the relationship

$$\xi = \frac{\Delta p_2}{\Delta p_1}$$

where  $\Delta p_1$  is the vertical surcharge, and  $\Delta p_2$  is the horizontal pressure induced by it.

At the same time the coefficient of lateral pressure  $\xi$  at critical equilibrium may be related with the angle of internal friction of the soil  $\varphi$

Table 26.1

The Coefficients of Lateral Pressure  $\xi$ ,  
Lateral Expansion  $\nu$  and Transition  $M$  for Different Clayey Soils

Soil type	$\xi$	$\nu$	$M$
Hard clays .....	0.11-0.25	0.10-0.20	1.02-1.11
Dense clays .....	0.33-0.45	0.25-0.30	1.20-1.25
Medium-density clays .....	0.49-0.59	0.33-0.37	1.46-1.76
Plastic clays .....	0.61-0.82	0.38-0.45	1.86-3.80

through the familiar equation

$$\xi = \tan^2 (45^\circ - \varphi/2) \quad (26.28)$$

This formula is valid only for loose cohesionless soils ( $c = 0$ ). The value of  $\xi$  for clayey soils can be determined roughly from the relationship

$$\xi = \tan^2 (45^\circ - \psi_p/2) \quad (26.29)$$

where  $\psi_p$  is the angle of the shearing resistance at a load  $p$ , found from the relationship

$$F_p = \tan \psi_p = \tan \varphi + c/p$$

To conclude, Table 26.1 lists the values of the coefficients  $\xi$ ,  $\nu$  and  $M$  for several clayey soils determined as the means of a series of tests.

It will be recalled that for a liquid obeying the hydrostatic law the coefficient of lateral pressure  $\xi = 1$  which corresponds to the coefficient  $\nu = \mu = 0.5$ .

## Chapter 27

### Normal Stresses in the Subsoil of a Structure and Methods of Their Determination

#### Sec. 27.1. Determination of Normal Stresses Under Conditions of a Plane Problem

The prediction of the settlement and deformations of structures calls for determining the values of normal stresses  $p_z$ ,  $p_x$  and  $p_y$  for a three-dimensional case, and  $p_z$  and  $p_x$  for a two-dimensional case.

Let us first consider the latter problem as a simpler one. The stresses  $p_z$  and  $p_x$  are expressed in the least complicated form through the angle of vision  $\alpha$ .

A theoretical solution for the case of a uniformly distributed load  $p_0$  yields the following relationships:

(a) for vertical normal compressive stresses

$$p_z = \frac{p_0}{\pi} [\alpha - \sin \alpha \cos (\alpha_1 + \alpha_2)] \quad (27.1)$$





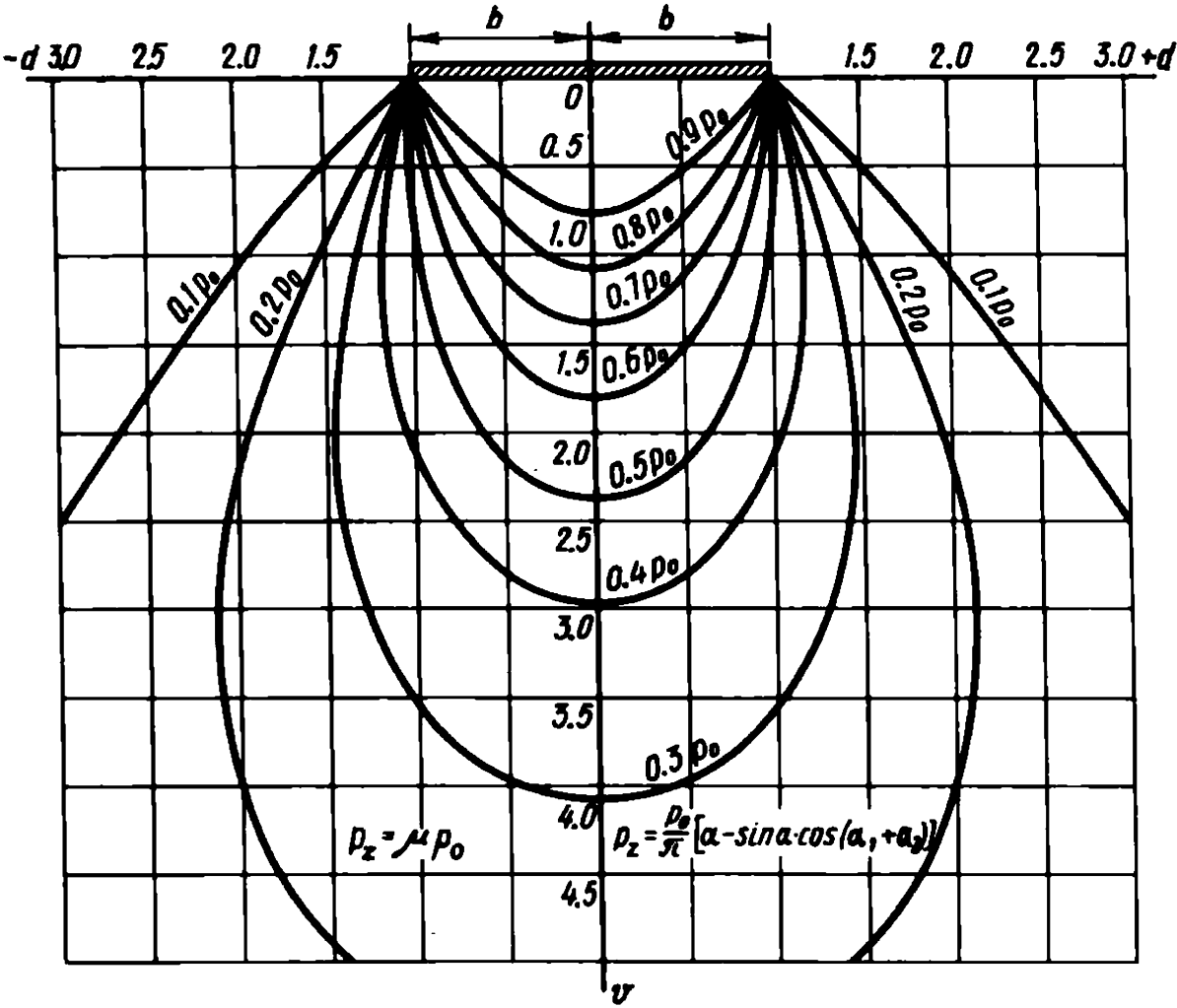


Fig. 27.2. Equal vertical compressive stresses  $p_z$  in a relative coordinate system at a uniformly distributed load  $p_0$

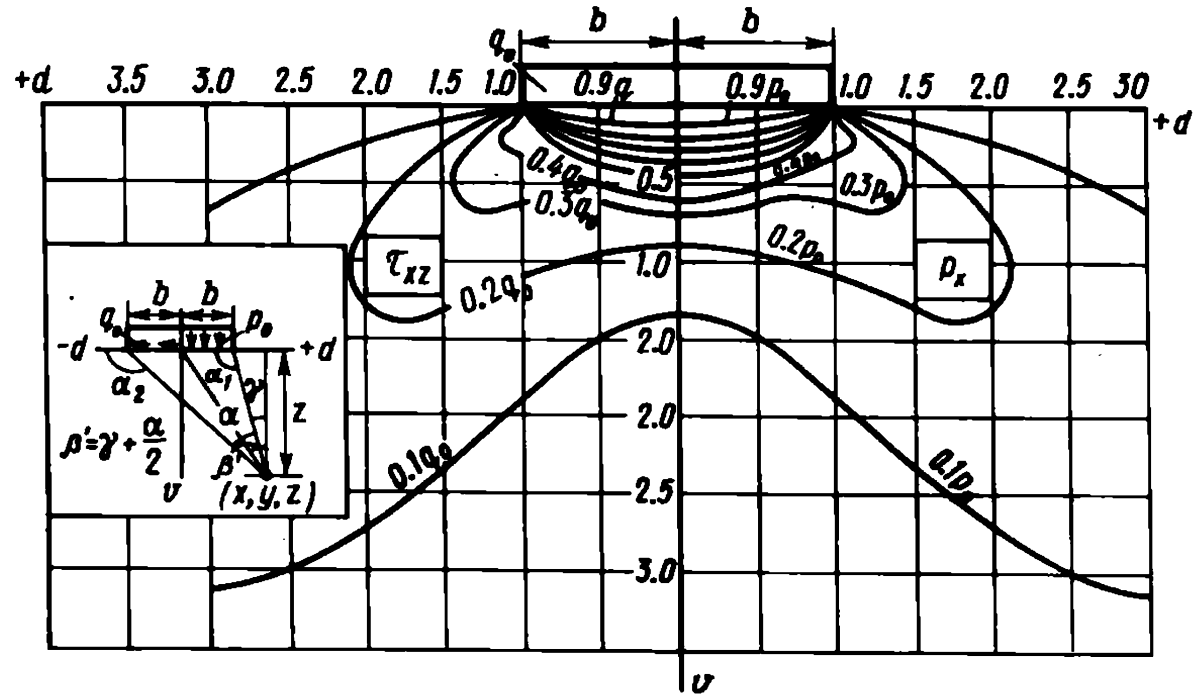


Fig. 27.3. Equal horizontal normal stresses  $p_x$  induced by a vertical uniformly distributed load  $p_0$  and of shearing stresses  $\tau_{xz}$  due to a horizontal uniformly distributed tangential load  $q_0$

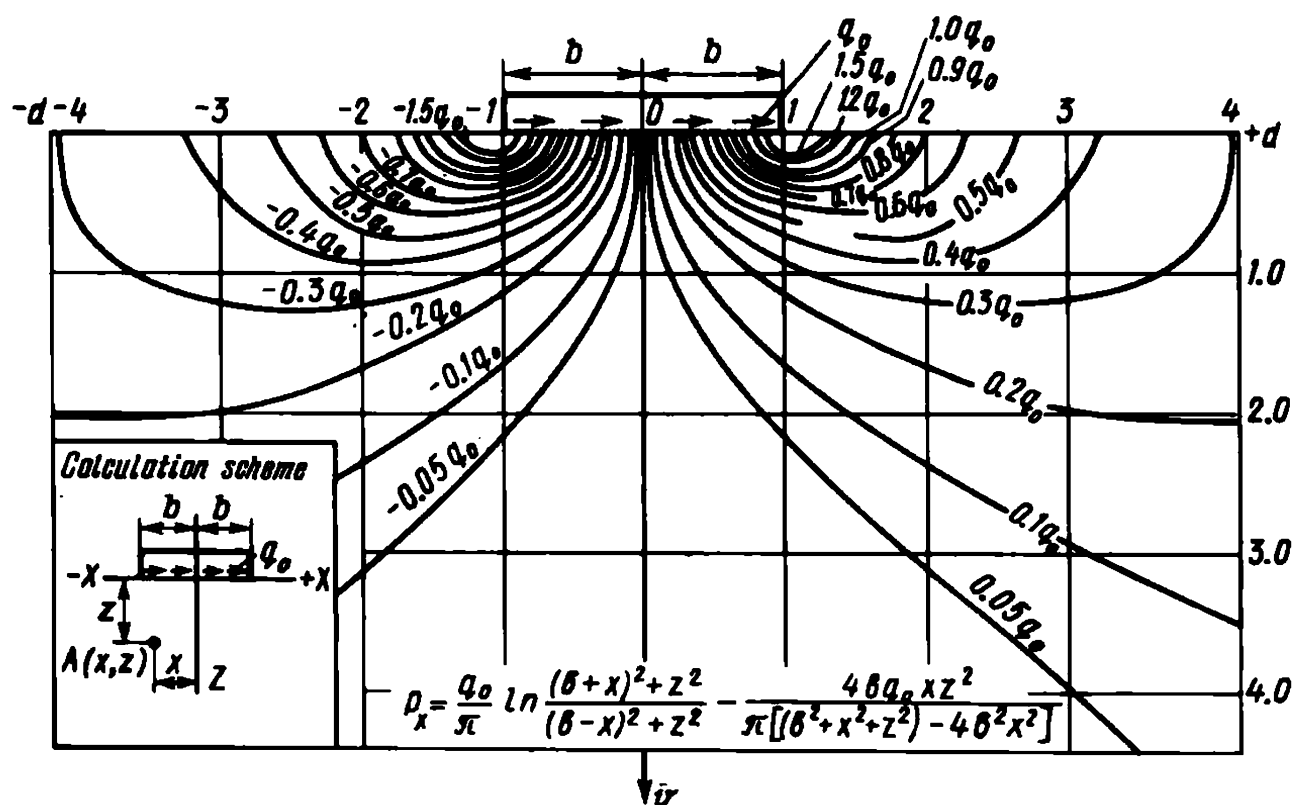


Fig. 27.4. Curves of equal horizontal stresses  $p_x$  induced by a uniformly distributed tangential load  $q_0$

pearing in the soil mass due to the effect of a load  $q_0$  tangential to the surface.

These curves have been plotted by referring to points obtained by calculations using Eqs. (27.1) and (27.2). Some of the calculated results are presented in Tables 27.1 and 27.2. As usual, the position of a point is determined by the  $v$  and  $d$  relative coordinates expressed in fractions of half the loaded strip  $b$ . Recall that  $v = z/b$  and  $d = x/b$ .

The stresses are also shown on the curves as fractions of the intensity of the load on the surface, i.e. in fractions of  $p_0$  (as the respective coefficients  $\mu$  and  $\nu$ ).

The diagrams very graphically show the picture of variation of the normal stresses  $p_z$  and  $p_x$  in the subsoil of a structure. Of much interest to us is the very intensive decrease in the horizontal normal stress  $p_x$  with depth  $v$  in the range of a contour of the width  $B = 2b$  of the loaded strip and, especially, along the symmetry axis.

It should be emphasized once more that  $p_z$  attains its peak value along the symmetry axis ( $x = 0$ ;  $d = 0$ ) on the surface of the subsoil ( $z = 0$ ,  $v = 0$ ), dropping to a more or less degree with depth and distance from the  $Z$  axis obeying a definite curvilinear regularity governed by Eq. (27.1). The way  $p_z$  is varying as a function of  $z(v)$  and  $x(d)$  can be seen from Figs. 27.5 and 27.6.

Table 27.1

The Values of Horizontal Normal Stresses  $p_z/p_0 = \mu_z$  for a Plane Problem  
and a Vertical Uniformly Distributed Load  $p_0$

$\nu$	$d$											
	0.0	0.1	0.2	0.3	0.5	0.7	1.0	1.5	2.0	3.0	4.0	5.0
$\mu$												
0.0	1.000	1.000	1.000	1.000	1.000	1.000	?	0.000	0.000	0.000	0.000	0.000
0.1	1.000	1.000	1.000	1.000	1.000	1.000	0.500	0.002	0.000	0.000	0.000	0.000
0.2	0.998	0.996	0.996	0.996	0.989	0.961	0.499	0.010	0.005	0.000	0.000	0.000
0.3	0.993	0.998	0.987	0.985	0.966	0.910	0.498	0.030	0.005	0.001	0.000	0.000
0.5	0.960	0.960	0.954	0.942	0.907	0.808	0.496	0.090	0.019	0.002	0.001	0.000
0.7	0.906	0.905	0.900	0.887	0.830	0.732	0.489	0.148	0.042	0.005	0.004	0.001
1.0	0.822	0.820	0.815	0.807	0.728	0.651	0.479	0.218	0.084	0.017	0.005	0.003
1.5	0.670	0.666	0.661	0.647	0.607	0.552	0.449	0.262	0.145	0.050	0.015	0.007
2.0	0.540	0.540	0.543	0.535	0.511	0.475	0.409	0.288	0.185	0.071	0.029	0.013
3.0	0.397	0.395	0.395	0.389	0.379	0.354	0.334	0.273	0.211	0.114	0.059	0.032
4.0	0.306	0.305	0.304	0.303	0.292	0.291	0.275	0.243	0.205	0.134	0.083	0.561
5.0	0.242	0.242	0.242	0.241	0.239	0.237	0.231	0.215	0.188	0.140	0.094	0.065

Table 27.2

The Values of Horizontal Normal Stresses  $p_x/p_0 = \nu_x$  for a Plane Problem  
and a Vertical Uniformly Distributed Load  $p_0$

$\nu$	$d$											
	0.0	0.1	0.2	0.3	0.5	0.7	1.0	1.5	2.0	3.0	4.0	5.0
$\mu$												
0.0	1.000	1.000	1.000	1.000	1.000	1.000	?	0.000	0.000	0.000	0.000	0.000
0.1	0.972	0.872	0.871	0.861	0.885	0.774	0.468	0.123	0.042	0.015	0.009	0.006
0.2	0.754	0.750	0.742	0.736	0.685	0.593	0.437	0.190	0.079	0.030	0.016	0.016
0.3	0.643	0.643	0.618	0.615	0.564	0.482	0.405	0.238	0.117	0.047	0.027	0.015
0.5	0.450	0.448	0.440	0.462	0.399	0.356	0.348	0.286	0.171	0.074	0.041	0.026
0.7	0.314	0.309	0.305	0.301	0.286	0.276	0.291	0.284	0.200	0.096	0.054	0.034
1.0	0.134	0.186	0.191	0.199	0.178	0.195	0.225	0.224	0.211	0.122	0.074	0.049
1.5	0.080	0.081	0.081	0.087	0.097	0.114	0.143	0.180	0.185	0.145	0.097	0.068
2.0	0.042	0.042	0.043	0.045	0.055	0.067	0.089	0.123	0.145	0.135	0.103	0.077
3.0	0.015	0.013	0.013	0.017	0.021	0.028	0.040	0.063	0.084	0.102	0.097	0.083
4.0	0.006	0.006	0.006	0.007	0.010	0.013	0.021	0.033	0.049	0.071	0.078	0.075
5.0	0.000	0.000	0.000	0.000	0.002	0.004	0.011	0.020	0.030	0.048	0.062	0.053

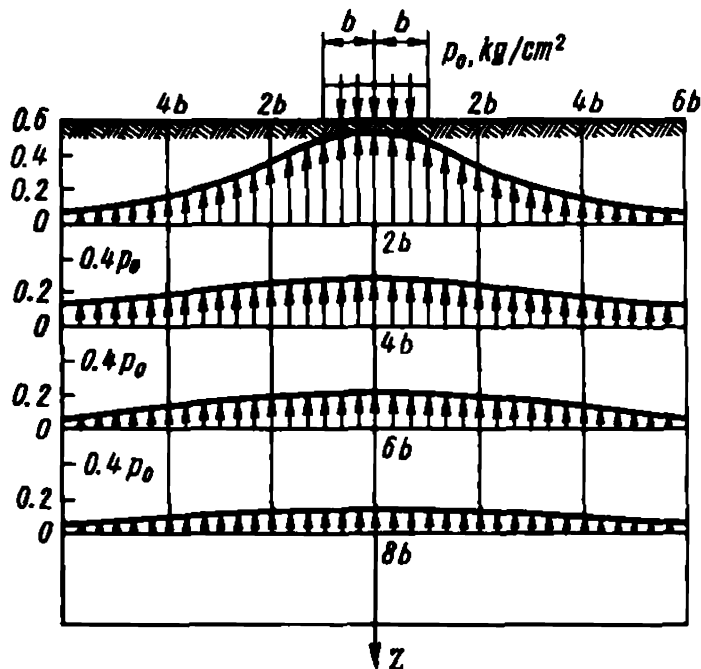


Fig. 27.5. Distribution of vertical normal stresses  $p_z$  at various depths  $z$  from ground surface (after V.F. Babkov)

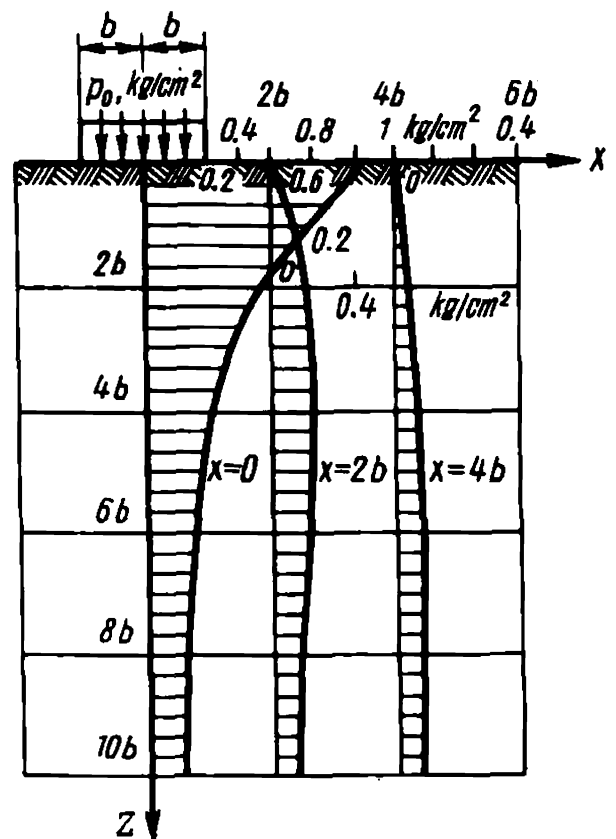


Fig. 27.6. Distribution of vertical normal stresses  $p_z$  in vertical directions (after V.F. Babkov)

It should be borne in mind that the values of the vertical normal  $p_z$  and horizontal normal  $p_x$  stresses along the symmetry ( $Z$ ) axis are exactly identical to the principal stresses  $p_1$  and  $p_2$  acting here. To better understand this, let us again refer to Fig. 27.1.

Let us apply Eqs. (27.1) and (27.2) to determine  $p_z$  and  $p_x$ . The construction in Fig. 27.1 indicates that the angle  $\beta = \alpha_1$ . Then (see the angles at  $C$ )

$$\text{Then} \quad \alpha_1 + \alpha_2 = 180^\circ$$

$$\cos(\alpha_1 + \alpha_2) = \cos 180^\circ = -1.0$$

A substitution of the value obtained into Eqs. (27.1) and (27.2) yields the relationships to determine  $p_z$  and  $p_x$  along the symmetry ( $Z$ ) axis:

$$p_z = (p_0/\pi)(\alpha + \sin \alpha); \quad p_x = (p_0/\pi)(\alpha - \sin \alpha)$$

which means that these stresses exactly correspond to the principal stresses  $p_1$  and  $p_2$  determined from the same equations. This makes it possible to find  $p_z$  and  $p_x$  for the axis of a loaded strip from the values of the principal stresses  $p_1$  and  $p_2$ .

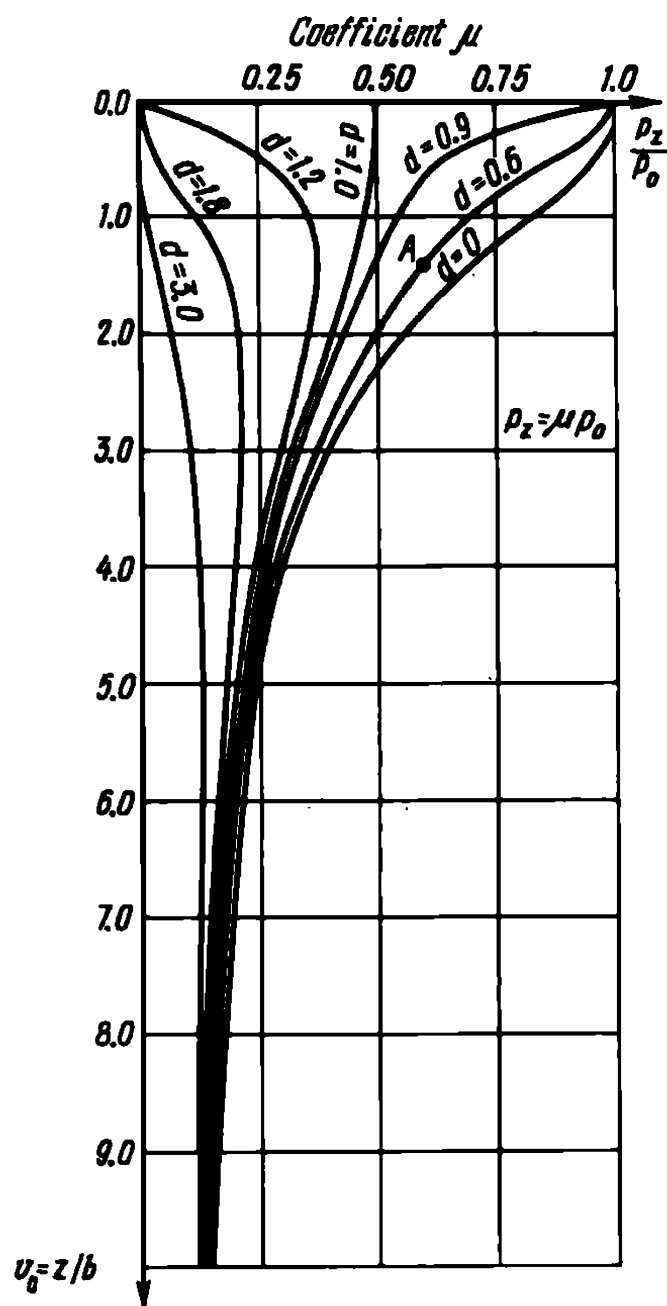


Fig. 27.7 Chart for estimating vertical normal stresses  $p_z$  through coefficient  $\mu$  from the formula  $p_z = \mu p_0$  as a function of the relative depth  $v = z/b$  for different vertical directions  $d = x/b$ . Uniformly distributed load. Plane problem

At the same time it is often necessary to determine  $p_z$  and  $p_x$  for various depths  $z$  along other directions with  $x$  and  $d$  coordinates other than zero. Graphs of the type shown in Fig. 27.7, known in civil engineering as lily-shaped curves, are very useful for such cases.

Along the abscissa axis in these diagrams the values of  $\mu_z$  and  $\nu_x$  determining the values of  $p_z$  and  $p_x$  induced by a load on the surface are plotted.

The relative depths expressed in fractions of half the width of the loaded strip, i.e.  $v = z/b$  are plotted along the ordinate axis. The family of the curves plotted in the graphs shows the values of the vertical and horizontal stresses  $p_z$  and  $p_x$  at one depth or another along a definite direction at a relative distance  $d = x/b$  from the symmetry axis of the loaded strip.

As the width of the loaded strip is decreased, so are, accordingly, the values of  $p_z$  and concurrently  $p_x$  for the same depth decreased. This

regularity follows from a more intensive dissipation of the state of stress in the soil mass with a lesser width of the loaded strip. We have repeatedly stressed this regularity as one of the most important mechanisms in soil mechanics.

B. Hansen has proposed the following abridged formulae to determine the normal stresses  $p_z$  and  $p_x$  where errors remain within reasonable limits.

1. *A plane problem* (a flexible band) or continuous footing:

$$p_z = \frac{P}{B + z}; \quad p_x = \frac{PB^2}{(B + z)^2} \quad (27.4)$$

where  $P = p_0 B$ , and  $B = 2b$  is the entire width of the loaded strip.

Until the depth  $z < b$  we may assume the normal stresses as being constant and equal to

$$p_z = p_0 \quad \text{and} \quad p_x = 0.6p_0$$

2. *A square footing* (centre):

$$p_z = \frac{P}{(B + z)^2}; \quad p_x = \frac{PB^2}{(B + z)^4} \quad (27.5)$$

where  $P = p_0 B^2$ .

3. *A rectangular footing* (centre):

$$p_z = \frac{P}{(B + z)(L + z)}; \quad p_x = \frac{PB^2}{(B + z)^3(L + z)} \quad (27.6)$$

where  $B = 2b$  and  $L = 2a$  is the total width and length of footing.

We have so far dealt with determinations of normal stresses  $p_z$  and  $p_x$  for a given point whose  $z$  and  $x$  coordinates are known in the soil mass where a strip (plane case) is acted on by a uniformly distributed load with an intensity  $p_0$ , kg/cm<sup>2</sup>.

Texts on soil mechanics present formulae and graphs for determining  $p_z$  and  $p_x$  similar to ones considered above for different surface loading conditions (triangular, trapezoidal, parabolic shearing load  $q_0$  uniformly distributed over the surface etc.).

We will present only two calculation graphs (Figs. 27.8 and 27.9) to determine the values of the vertical and horizontal normal stresses  $p_z$  and  $p_x$  induced by a load uniformly distributed over the surface of the subsoil following the law of an isosceles triangle.

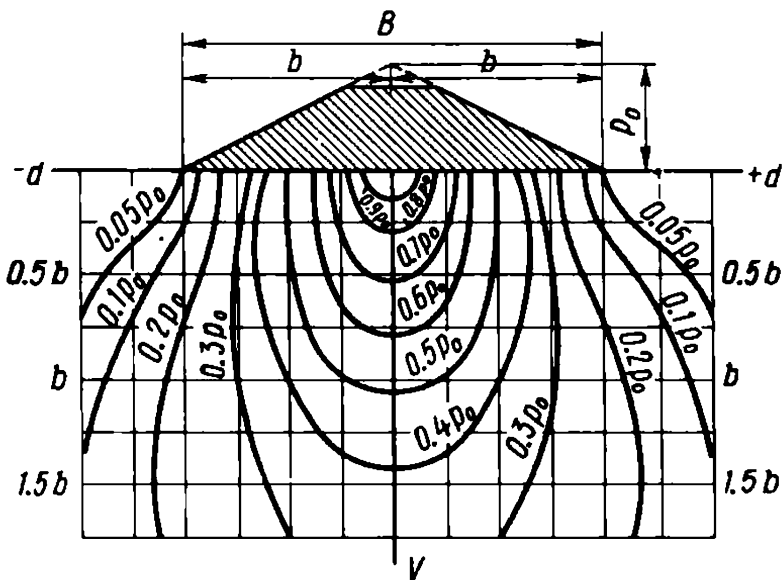


Fig. 27.8. Vertical normal compressive stresses  $p_z$  induced by loading obeying the law of an isosceles triangle in a relative  $v = z/b$  and  $d = x/b$  coordinate system

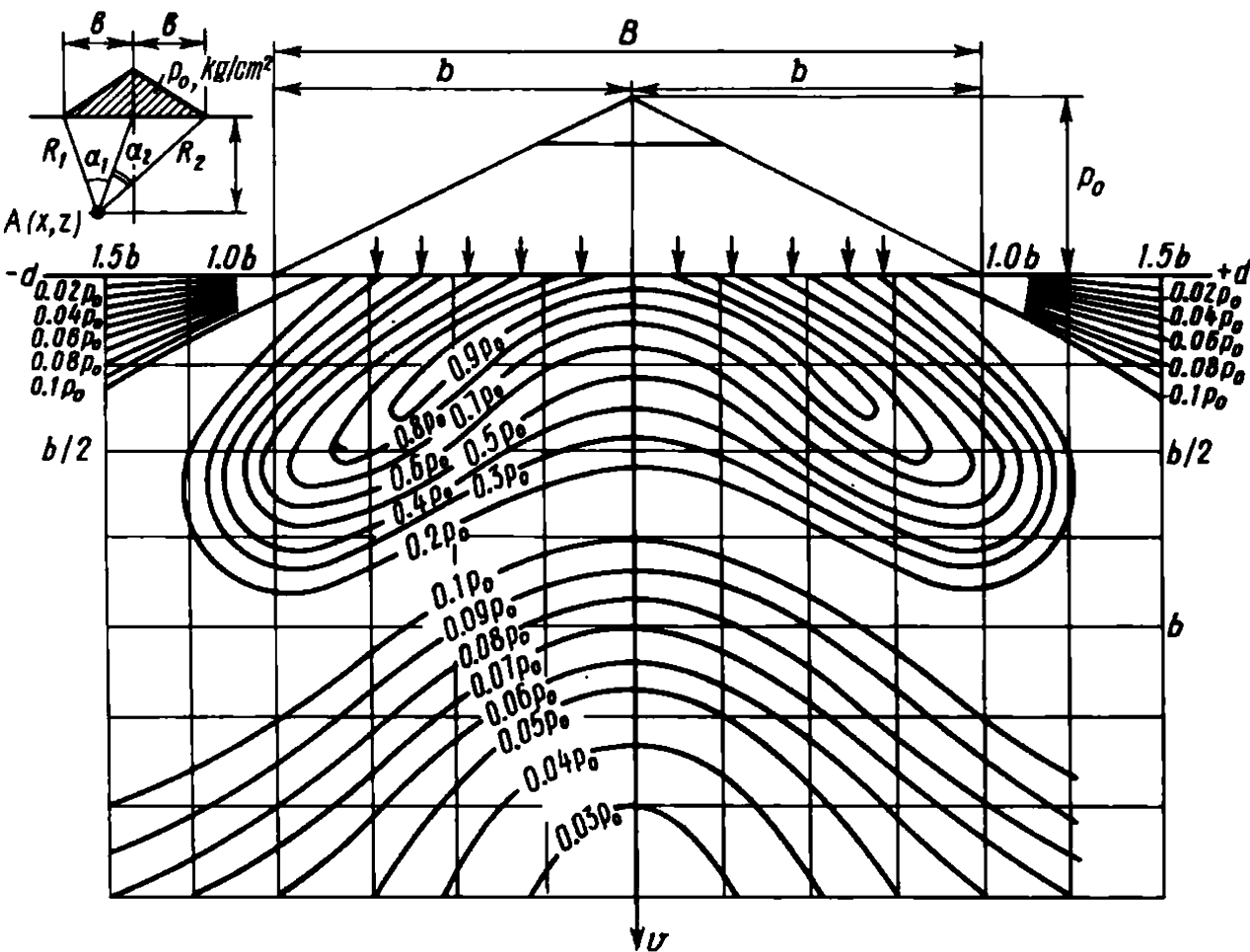


Fig. 27.9. Horizontal normal compressive stresses under identical conditions (see Fig. 27.8)



These graphs are plotted by using the following relationships:

$$p_z = \frac{p_0}{\pi b} [b(\alpha_1 + \alpha_2) + \chi(\alpha_1 - \alpha_2)] \quad (27.7)$$

$$p_x = \frac{p_0}{\pi b} \left[ b(\alpha_1 + \alpha_2) + \chi(\alpha_1 - \alpha_2) - 2z \ln \frac{R_1 R_2}{R_0^2} \right] \quad (27.8)$$

The values of  $\alpha_1$  and  $\alpha_2$  entering these formulae are given in Fig. 27.9. This case commonly occurs when it is desired to determine  $p_z$  and  $p_x$  at one point of a high embankment or another.

The construction of this graph relies on the previous principle. It is plotted in a relative  $v$  and  $d$  coordinate system in fractions of half the width of the loaded strip  $b$ . The values of  $p_z$  are expressed here in fractions of the load  $p_0$  determining the pressure on the underlying soil due to the weight of the embankment along the symmetry ( $Z$ ) axis. Apparently,

$$p_0 = \rho_w H \quad (27.9)$$

where  $H$  is the height of the fill in m;  $\rho_w$  is the bulk density of the soil in the fill.

The method of using the graphs is conventional.

In order to evaluate the state of stress in the foundation of a highway embankment (trapezoidal load) the available formulae and graphs can be used.

However, it is often simpler and better to determine the state of stress at a point in the foundation of an embankment (fill) from the difference of stresses arising here for a load obeying the law of an isosceles triangle. This is twofold: I — a larger triangle with the base equal to that of the embankment; II — a smaller triangle whose base is equal to the width of the roadway of the embankment (crown) and sides coincident with the slopes of the embankment in shape.

The stresses under the base of a fill extending in one direction are equal to the stresses induced by the weight of the fill as if expanding indefinitely from the base in both directions (plane case).

Practice suggests that it is better to start the construction of a bridge by first erecting the abutments and filling the approach embankments. This ensures a more uniform settlement of the entire bridge structure and better conditions of its service. In actual work, however, these recommendations are only rarely followed.

Sec. 27.2. Determination of Normal Stresses in a Three-Dimensional Case

Solving this problem by using the formulae is a very complicated and time-consuming task. Therefore in design work it is usual to apply “lily-shaped” curves or special tables permitting normal stresses to be determined by the easiest way.

Figures 27.10 to 27.12 present the data for finding the vertical,  $p_z$ , and horizontal,  $p_x$  and  $p_y$ , stresses for a surface area, rectangular in shape,

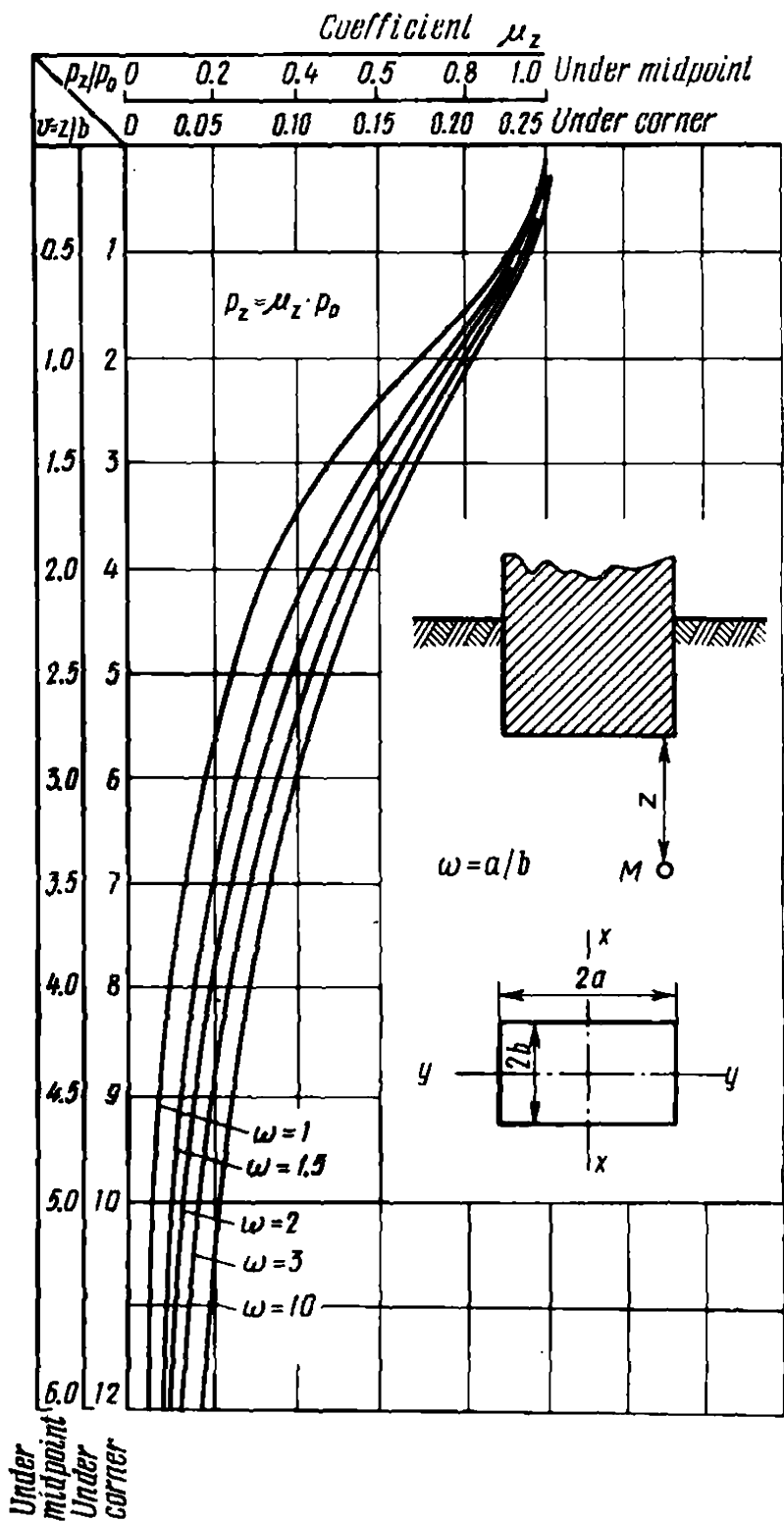


Fig. 27.10. Chart for estimating  $p_z = \mu_z p_0$  due to a uniformly distributed load  $p_0$ . Three-dimensional problem

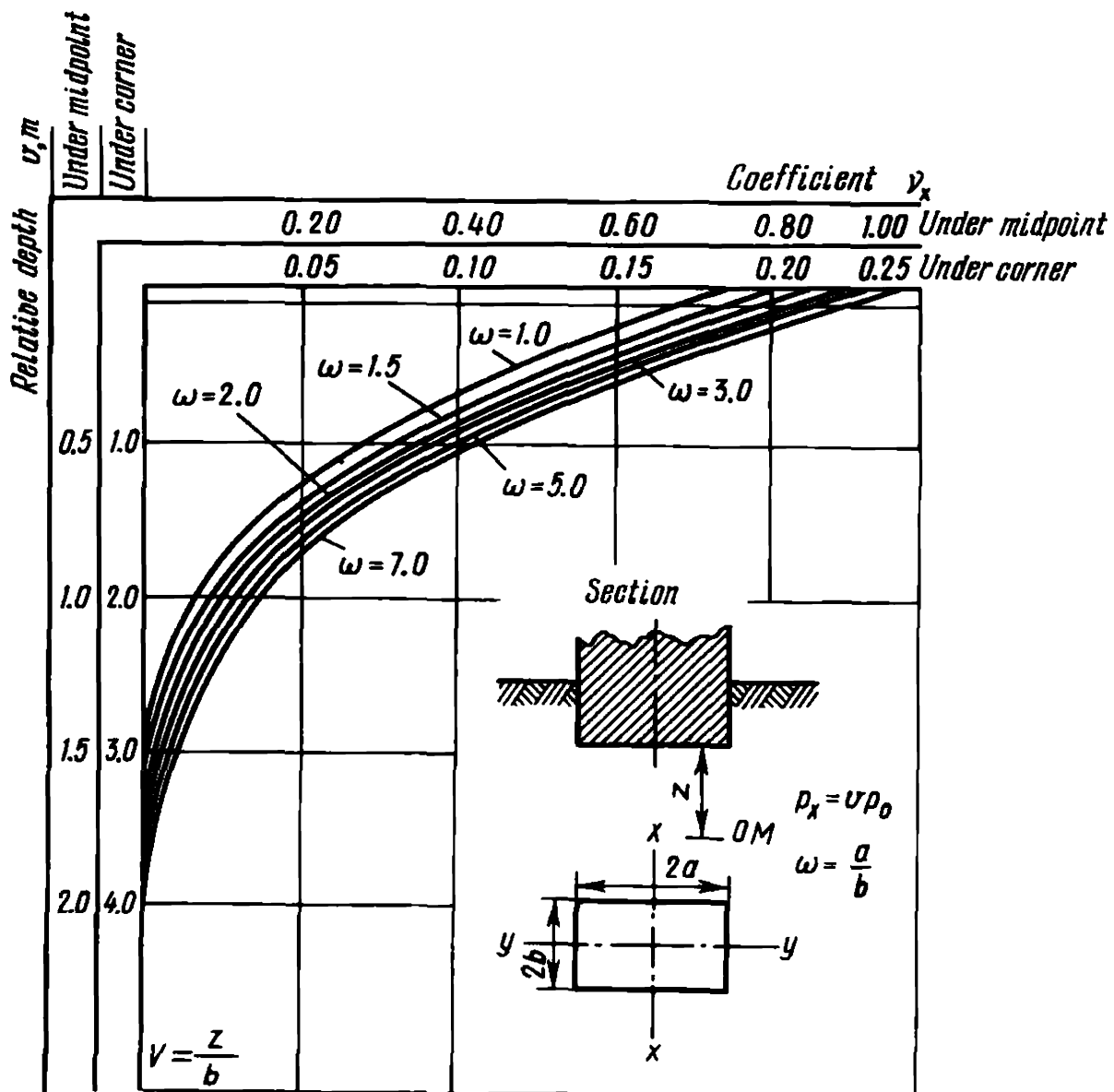


Fig. 27.11. Chart for estimating  $p_x = \nu_x p_0$  for a three-dimensional problem. Poisson's ratio is  $\mu = 0.25$

whose width is  $2b$  and length  $2a$ , and which sustains a uniformly distributed load with the intensity  $p_0$ . Each of the graphs is provided with two scales permitting us to establish the values of the conversion factors  $\mu_z$ ,  $\nu_x$  and  $\varepsilon_y$  for determining the corresponding normal stresses  $p_z$ ,  $p_x$  and  $p_y$  both under the midpoint of the loaded strip and under its corners. The graphs are plotted in an arbitrary reference frame.

The values of the coefficients  $\mu_z$ ,  $\nu_x$  and  $\varepsilon_y$  for the case of a three-dimensional load are determined, taking into account the degree of elongation of the loaded strip  $\omega$  which is equal to

$$\omega = 2a/2b = a/b$$

For a square  $\omega = 1$ ;  $\omega = 10$  practically corresponds to a load on a strip of an infinite length (plane problem).

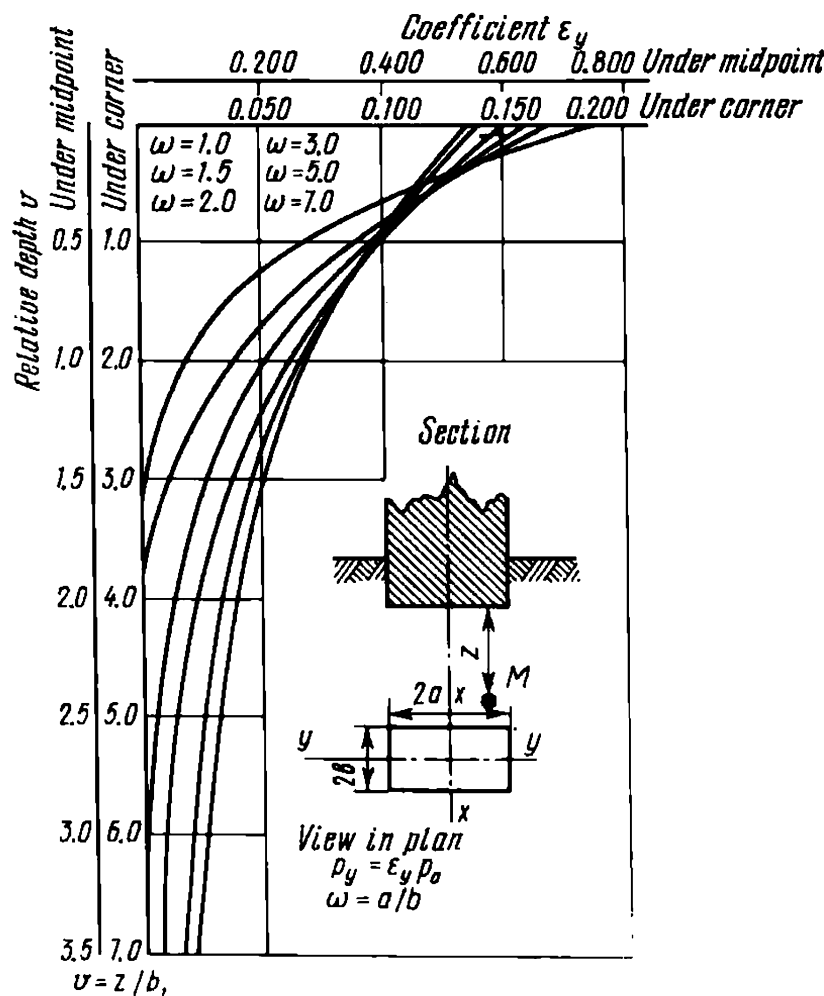


Fig. 27.12. Chart for estimating a second horizontal stress  $p_y = \epsilon_y p_0$  for a three-dimensional problem. Poisson's ratio  $\mu = 0.25$  ( $\omega = 1.0$ -upper curve)

Figure 27.10 and Table 27.3 related to it are applied for determining the vertical normal stress  $p_z$ . Note that the magnitude of  $p_z$  both in a three-dimensional and plane problem is independent of the value of the coefficient of the lateral strain  $\nu$ . Consequently, Fig. 27.10 and the data listed in Table 27.3 are valid for determinations of strains in soils of any consistency and, thus, with different values of Poisson's ratio.

Graphs for determinations of  $p_x$  and  $p_y$  in a three-dimensional case are plotted for a particular problem where  $\nu = 0.25$ . It should be remembered, however, that excepting the soils of very low bearing power the case in question can be considered universal within the accuracy limits imposed by practice.

The appropriate scales in the graphs permit one to find the values of the relative normal stresses under the midpoint and the corners of the loaded strip simultaneously.

The vertical stress in the semispace at a definite depth under the corner of a loaded rectangular strip equals one-fourth of the stress under the centre of the strip at half the depth. Note also that the stress in any point of the

Table 27.3

The Values of a Conversion Factor  $\mu_z$  to Determine  $p_z$  Below the Centre of the Loaded Area. The Case of a Three-Dimensional Plane and a Uniformly Distributed Load

$\nu$	$\omega$								
	1.0	1.5	2.0	3.0	4.0	5.0	6.0	7.0	8.0-10.0
	$\mu_z$								
0.5	0.94	0.95	0.95	0.95	0.95	0.95	0.96	0.96	0.96
1.0	0.71	0.77	0.78	0.80	0.81	0.82	0.82	0.82	0.82
1.5	0.49	0.58	0.63	0.66	0.66	0.66	0.67	0.67	0.67
2.0	0.34	0.43	0.48	0.52	0.54	0.54	0.55	0.55	0.55
3.0	0.18	0.26	0.30	0.35	0.35	0.38	0.39	0.40	0.40
4.0	0.10	0.16	0.19	0.24	0.27	0.28	0.29	0.30	0.30
5.0	0.07	0.11	0.13	0.16	0.20	0.21	0.23	0.23	0.24
7.0	0.04	0.06	0.07	0.10	0.12	0.14	0.15	0.16	0.17
10.0	0.01	0.03	0.04	0.05	0.07	0.08	0.09	0.11	0.11
15.0	0.002	0.01	0.02	0.02	0.03	0.04	0.05	0.05	0.06

foundation, whatever its coordinates, equals the sum of the angular stresses for rectangles converging at the given point and having there their common corner.

When it is necessary to allow for the rigidity of the foundation or structure of one shape in plan or another (e.g. for determining the vertical stress  $p_z$  under an absolutely rigid circular footing) we can refer to the relevant formulae or design graphs presented in special texts.

Chapter 28

Methods of Predicting Settlement of Structures with a Consolidating Foundation Soil

Sec. 28.1. Method of Summation

It will be recalled in the first place that prediction of settlement and deformation of the foundations should be made after the previous site exploration has established safety and stability of the underlying soil under a possible effect of various geodynamic mechanisms and forces applied to the subgrade.

As has been already pointed out, the settlement of the surface of the soil mass under the live load (weight of the structure) and settlement of the structure are in practice determined by summing up the subsidences of individual design layers constituting the soil mass of the foundation through the use of Eq. (26.5).

If the geomechanical characteristics of the soil are described by the coefficient of its relative deformation  $e$  or modulus of soil compressibility  $e_p$  expressed in per mil, Eq. (26.5) for the general case takes on this form:

$$\eta_{sub} = \sum_0^D e_{pz} h_i \quad (28.1)$$

where  $\eta_{sub}$  is the total settlement of the structure;  $D$  is the active zone, i.e. the thickness of the soil mass to be taken into account when determining the settlement (summation limit);  $e_{pz}$  is the relative subsidence along the  $Z$  axis caused in such cases by the surcharge acting on the given design soil layer and induced by all the three components of the added normal stresses  $p_z$ ,  $p_x$  and  $p_y$ ;  $h_i$  is the design load.

By virtue of Eq. (28.1) the final formulae for determining the ultimate settlement of the structure  $\eta_{sub}$  in conformity with Eqs. (26.22), (26.26) and (26.16) can be represented as follows:

(a) for a three-dimensional case

$$\eta_{sub}''' = \sum_0^D M h_i [e_{pz} - \nu(e_{px} + e_{py})] \quad (28.2)$$

(b) for a two-dimensional case (plane problem)

$$\eta_{sub}'' = \sum_0^D M h_i (1 - \nu^2) \left[ e_{pz} - \frac{\nu}{1 - \nu} e_{px} \right] \quad (28.3)$$

(c) for a one-dimensional case

$$\eta_{sub}' = \sum_0^D h_i e_{pz} \quad (28.4)$$

In the above equations  $e_{pz}$ ,  $e_{px}$  and  $e_{py}$  are the relative deformations induced by the respective added stresses  $p_z$ ,  $p_x$  and  $p_y$ .

It should be remembered that the conversion factor  $M$  permitting transition from conditions of a compression test using a ring with the established values of  $e_{pz}$ ,  $e_{px}$  and  $e_{py}$  without lateral expansion of the soil sample

(confined test) to conditions of unconfined soil deformation is related to the coefficient of lateral deformation  $\nu$  through Eq. (26.20).

Depending on the type of problem (three-, two- or one-dimensional), accurate analysis requires the use of Eq. (28.2), (28.3) or (28.4), respectively. However, as manifested by a study of these equations, sufficiently accurate results are very often obtained by referring to the simplest of the above relationships, (28.4), derived for a one-dimensional case.

This is due to the inappreciable effect on the calculated results of the value of  $\nu$  when in the range  $\nu < 0.25$  to  $0.30$ . It is seen from Eq. (26.20) for determining  $M$  and from Eqs. (28.2) and (28.3) for evaluating settlement of a structure,  $\eta_{sub}$ . Note that the values of  $\nu \approx 0.20$  to  $0.25$  correspond to most common soil conditions.

A substitution into Eqs. (28.2) and (28.3) of the value of  $\nu = 0$  makes them identical to Eq. (28.4), i.e. in this case

$$\eta_{sub}''' = \eta_{sub}'' = \eta_{sub}' \quad (28.5)$$

It will be recalled that the values of the horizontal stresses  $p_x$  and  $p_y$  are generally less than that of the vertical normal stress  $p_z$ . In addition soils typically possess a certain degree of anisotropy. Owing to this fact the magnitude of their deformation due to horizontal stresses  $p_x$  and  $p_y$  is also often very much less than that of the deformation induced by the vertical normal stress  $p_z$ . All this, taken together, permits the use of Eq. (28.4) to predict settlement of structures under general conditions.

If a need arises to take into account the weight of a neighbouring structure adding to the settlement of the structure in hand, Eqs. (28.2) and (28.3) are useful.

This may be the case when we consider the effect of the weight of a high approach embankment on the settlement of a bridge abutment. The horizontal stresses must also be allowed for when determining normal stresses by superposing them under similar conditions.

We must also refer to Eqs. (28.2) and (28.3) when the structure foundation soil is composed by layers of low bearing power, say, marshy soils that have the coefficient of transverse deformation  $\nu \geq 0.3$ . This is conditioned by a dramatic rise of the role played by horizontal normal stresses (shears)  $p_x$  and  $p_y$  outside the contour of the structure (see, e.g. Fig. 27.3).

When using Eq. (28.4), it is better to determine the values of  $p_z$  from the graph  $p_z = f(z)$  in Fig. 27.10 plotted for a three-dimensional case allowing for the elongation of the structure  $\omega$ . As pointed out above, at values of  $\omega > 6$  this condition is of no practical value. Therefore it is very often quite allowable to use for calculations a graph in Fig. 27.7, constructed for a plane problem, notwithstanding the smallness of the loaded strip in plan.

The latter graph greatly facilitates calculations for predicting the sub-

sidence of the surface of the supporting soil in any direction at any values of their  $x$  and  $d$  abscissas which accounts for their extensive use in engineering practice in this country.

The next task relating to predicting structure settlement from Eqs. (28.2), (28.3) and (28.4) is how to split the subsoil into design layers. The first step is to establish the summation limit  $D$ . This limit determines the thickness of what is known as *an active (or thrust) zone* or active Rankine zone.

The thickness of the latter zone can be determined from the relative value of the stress  $p_z$  compared with the natural load  $p_{nat}$  or expected settlement of the structure. The thickness of the active zone  $D$  for a structure with dimensions limited in plan is governed by the depth at which the normal pressure  $p_z$ , accurate to  $\pm 0.05 \text{ kg/cm}^2$ , equals 0.2 of the natural load  $p_{nat}$  due to the weight of the overlying soil layers, i.e.

$$p_{zD} = (0.2_{nat} D \pm 0.05) \quad (28.6)$$

As is known, soil compressibility may differ very much from one soil variety to another. Therefore, when estimating the thickness of the active zone  $D$ , it is better to proceed from a requirement that the error in the determination of the settlement  $\eta_{sub}$  due to disregarding the compression of the underlying soil horizons should not exceed 5%. Clearly, the determining factor will be the curvature rate of the compression curve  $e_p = f(p)$ .

The design thickness of the active zone  $D$  has been reconsidered in recent time taking into account the initial gradient. Thus  $D$  may prove much less than expected in conformity with the rules presented above (refer to Chapter 23 and Fig. 23.2). This fact may enable the common overestimation of design values of settlements of structures compared with the actual values to be accounted for.

Splitting the subsoil into more layers increases the accuracy of the calculations yet concurrently makes them more bulky. The existence in the subsoil of individual strata possessing different properties and compressibility values predetermines a need of considering them as separate design soil layers.

The design value of the initial load  $p_0$  is conditioned both by the type, purpose and size of the structure in hand and by the depth of its foundation  $h_d$ . The value of  $p_0$  is found from the relationship

$$p_0 = p_s - \rho h_d \quad (28.7)$$

where  $\rho$  is the bulk density of the soil at the horizon of the foundation allowing, whenever necessary, for the uplift pressure induced by the water in the soil;  $\rho h_d$  is the stress induced by the weight of the soil removed from the excavation for the foundation.



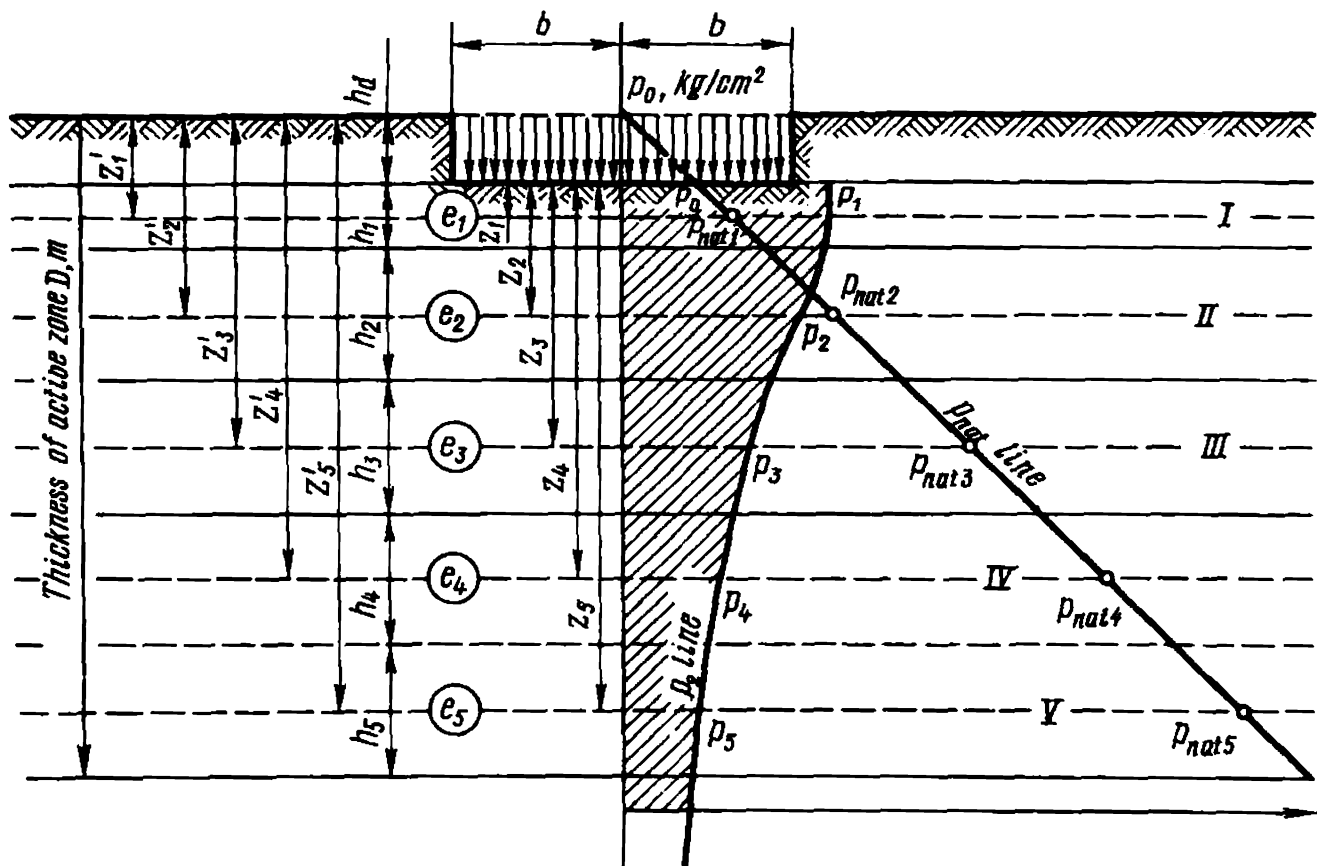


Fig. 28.1. Diagram showing method for forecasting the settlement of a structure by a method of layer by layer summation

We may thus conclude that, other conditions being equal, the settlement of a structure,  $\eta_{sub}$ , decreases with increasing the depth of the foundation. Clearly, at the depth of the foundation  $\eta_d = p_s/\rho$  the design value of the load  $p_0$  will be zero. Then, disregarding a likelihood of heaving of the bottom of the excavation, the structure will not undergo any settlement ( $\eta_{sub} = 0$ ).

The following steps in predicting the settlement of a structure are these. First, suppose that the subsoil within the active zone  $D$  is homogeneous and isotropic.

Figure 28.1 presents a calculation diagram for predicting the settlement of a structure, and Fig. 28.2 a compression curve in the form of a relation-

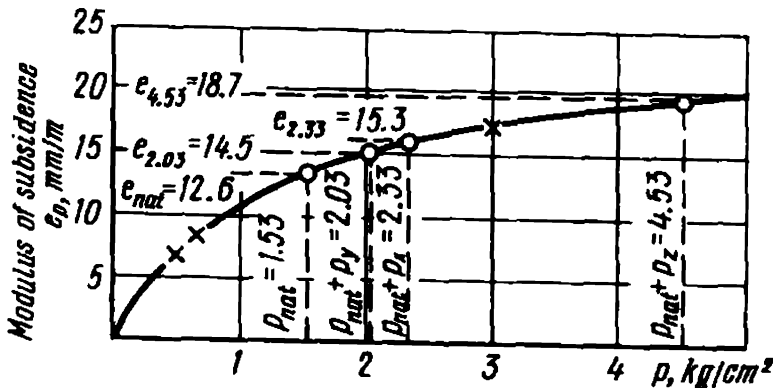


Fig. 28.2. Compression curve illustrating an example of forecasting the settlement of a structure

ship between the modulus of compressibility  $e_p$  and the load  $p$ , i.e. as an equation  $e_p = f(p)$ .

The satisfaction of the condition of uniformity and isotropy of the underlying soil testifies to the same physicommechanical characteristics of the soil mass within the entire depth of the active zone  $D$ . The compressibility of soil decreases with depth  $z$  following a definite regularity in proportion to the increase in its density owing to the greater weight of the overlying layers, i.e. the dead load or natural load  $p_{nat}$ .

The isotropy of soil points to the uniform compressibility of the soil along the three,  $Z$ ,  $X$  and  $Y$ , axes. This makes it possible to use the same compression curve (e.g. one in Fig. 28.2) to predict deformations throughout the depth of the subsoil  $D$  and to calculate the moduli of compressibility  $e_{pz}$ ,  $e_{px}$  and  $e_{py}$  corresponding to the effect of  $p_z$ ,  $p_x$  and  $p_y$ .

For further reasoning let us refer to Fig. 28.1. To calculate the settlement the whole active zone is divided by the method outlined above into a number of design layers I-V and the thickness of each of these,  $h_i$ , is measured. For each of the design layer a midline is drawn, by referring to which all calculations for determining  $p_z$ ,  $p_x$ ,  $p_y$  and the respective compressibility moduli  $e_{pz}$ ,  $e_{px}$  and  $e_{py}$  are made. The ordinates  $z_i'$  of these midlines relative to the surface of the foundation and  $z_i$  relative to the base of the footing are determined. Apparently,

$$z_i = z_i' - h_d \quad (28.8)$$

The next step is to determine the values of  $p_z$ ,  $p_x$  and  $p_y$  for depths  $z_i$  by applying one method or another governed by the conditions of the problem (three-, two- or one-dimensional). The stresses  $p_z$ ,  $p_x$  and  $p_y$  are invariably found with respect to the design load  $p_0$  calculated by using Eq. (28.7).

The curves  $p_z = f_1(z)$ ;  $p_x = f_2(z)$ ;  $p_y = f_3(y)$  are plotted on the calculation graph (Fig. 28.1) from the obtained values of these stresses. By way of illustration Fig. 28.1 presents a curve for a vertical normal stress  $p_z$ . A line of the natural load  $p_{nat}$  due to the own weight of the soil is shown. This line is plotted from the surface of the soil, allowing for the natural density of soil, by referring to the relationship

$$p_{nat\ i} = \rho_{av} z_i'$$

where  $p_{nat\ i}$  is the natural load in  $\text{kg/cm}^2$  or  $\text{ts/m}^2$  for each of the design layers referred to the midline:  $\rho_{av}$  is the average bulk density for the overburden of the given horizon allowing, wherever necessary, for the buoyancy effect.

Naturally, in each of the design layers I-V, before the erection of the structure began, the soil had been acted upon by the natural load  $p_{nat\ i}$ . As the structure was being built the soil conditions in each layer changed due

to the stresses emerging there,  $p_z$ ,  $p_x$ ,  $p_y$ . These added stresses cause compression of each soil layer giving rise to subsidence  $\eta_{sub\ i}$ . The value of this latter for each design layer is found from one of the equations: (26.22), (26.26) or (26.16).

The values of the relative deformations  $e_{pz}$ ,  $e_{px}$ ,  $e_{py}$  entering the above relationships emerge in the given version of the problem due to the added action on the particular soil layer of  $p_z$ ,  $p_x$  and  $p_y$  in excess of  $p_{nat}$  induced by the weight of the overlying soil mass. The total subsidence of the entire soil mass is found from Eq. (26.5) as a sum of all individual subsidences

$$\eta_{sub} = \sum_0^D \eta_{sub\ i}$$

or from Eqs. (28.2), (28.3) and (28.4). This terminates calculations for determining the expected value of the eventual settlement of the structure  $\eta_{sub}$ .

One of the principal operations of the arithmetic in question is the establishment of the moduli of compressibility  $e_{pz}$ ,  $e_{px}$  and  $e_{py}$  as applied to the conditions of the particular problem. Let us consider an example to understand this operation.

Suppose it is desired to determine the subsidence  $\eta_i'''$  under conditions of a three-dimensional problem for the design layer at which horizon the natural load  $p_{nat} = 1.53 \text{ kg/cm}^2$  (0.15 MPa) and  $p_z = 3.0 \text{ kg/cm}^2$ ;  $p_x = 0.80 \text{ kg/cm}^2$  and  $p_y = 0.50 \text{ kg/cm}^2$ . The thickness of the layer is  $h_i = 2.5 \text{ m}$ ; the coefficient of lateral strain is  $\nu = 0.25$ .

The value of  $M$  found from Eq. (26.20) is

$$M = \frac{1 - \nu}{(1 + \nu)(1 - 2\nu)} = \frac{1 - 0.25}{(1 + 0.25)(1 - 0.5)} = 1.2$$

Let us find the value of the modulus of compressibility  $e_{p\ nat}$  corresponding to the value of  $p_{nat} = 1.53 \text{ kg/cm}^2$  from the compression curve in Fig. 28.2. This gives  $e_{p\ nat} = 12.6 \text{ mm/m}$ . Then we find the values of  $(p_{nat} + p_z)$ ,  $(p_{nat} + p_x)$  and  $(p_{nat} + p_y)$  and the respective moduli of compressibility  $e$  from the compression curve. Finally we determine the values of  $e_{pz}$ ,  $e_{px}$  and  $e_{py}$  by using the relationships

$$\begin{aligned} e_{pz} &= e_{(p_{nat} + p_z)} - e_{p_{nat}}; \\ e_{px} &= e_{(p_{nat} + p_x)} - e_{p_{nat}}; \quad e_{py} = e_{(p_{nat} + p_y)} - e_{p_{nat}} \end{aligned}$$

Thus we establish the values of  $e_{pz}$ ,  $e_{px}$  and  $e_{py}$  corresponding to the added consolidation of the soil in excess of its natural state under the effect of the load  $p_0$  again imparted to the soil mass.

The values of the design moduli of compressibility  $e_{pz}$ ,  $e_{px}$  and  $e_{py}$  are listed in Table 28.1. The values of  $e_{z, x, y}$  in the last column of the table correspond to the values of  $e_{pz}$ ,  $e_{px}$  and  $e_{py}$  found from the differences in the above equations. By substituting into the relevant equation the specified

Table 28.1

Data on Calculating Subsidence to Illustrate the Example

Axis	$p_{nat}$ , kg/cm <sup>2</sup>	$p_{z,x,y}$ , kg/cm <sup>2</sup>	$p_{nat} +$ $p_{z+x+y}$ , kg/cm <sup>2</sup>	$e_{p_{nat} +}$ $p_{z,x,y}$ , mm/m	$e_{p_{nat}}$ , mm/m	$e_{z,x,y}$ , mm/m
Z	1.53	3.0	4.53	18.7	12.6	6.1
X	1.53	0.80	2.33	15.3	12.6	2.7
Y	1.53	0.50	2.03	14.5	12.6	1.9

and obtained values we get

$$\eta'''_{sub\ i} = 1.20 \times 2.5[6.1 - 0.25(2.7 + 1.9)] = 14.9\text{ mm}$$

Then we determine the settlement by applying Eq. (26.22)

$$\eta'''_{sub\ i} = Mh_i[e_{px} - \nu(e_{px} + e_{py})]$$

Let us find the settlement  $\eta'_{sub\ i}$  for the same case by referring to the abridged formula (28.16) derived for a one-dimensional problem

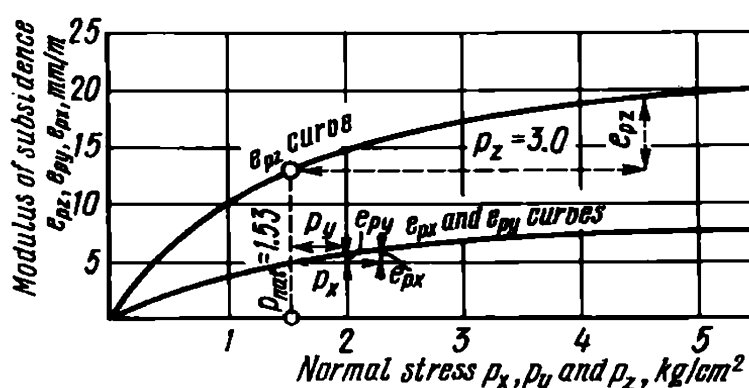
$$\eta'_{sub\ i} = h_i e_{pz}$$

A substitution into this relationship of the corresponding values of  $h_i = 2.5\text{ m}$  and  $e_{pz} = (18.7 - 12.6) = 6.1\text{ mm}$  yields  $\eta'_{sub\ i} = 2.5 \times 6.1 = 15.3\text{ mm}$ .

The values of  $\eta'''_{sub}$  and  $\eta'_{sub}$  found for a three- and a one-dimensional problem prove to be generally close, the discrepancy being permissible for practical purposes.

We have so far been concerned with the isotropic (in terms of compressibility) foundations. The soil compressibility of a foundation in a vertical direction is generally greater than in a horizontal direction. This is accounted for by the presence of stiffer layers, e.g. consolidated sand, in the stratified clayey soil mass. The compression curve alone is not sufficient for determining the relative deformations or moduli of subsidence  $e_{pz}$ ,  $e_{px}$  and  $e_{py}$  along the Z, X and Y axes.

Use has then be made of two compression curves: one for the vertical stresses  $p_z$ , another for the horizontal stresses (shears)  $p_x$  and  $p_y$  (Fig. 28.3). In so doing the values of  $e_{px}$  and  $e_{py}$  should be determined according to the



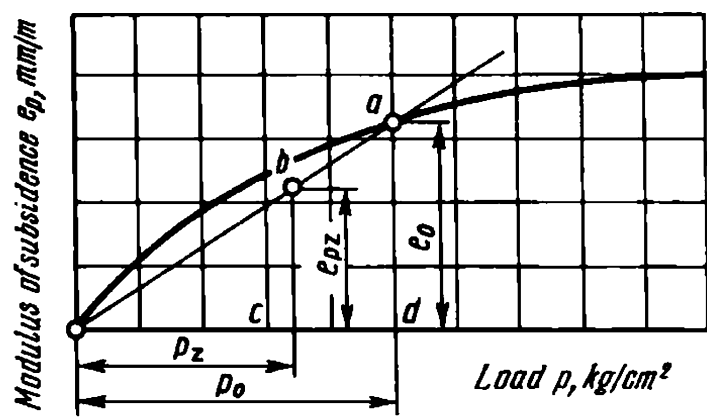


Fig. 28.4. Compression curve simplified

The above method of evaluation of the likely settlement of a structure through relative deformations or moduli of compressibility  $e_{pz}$ ,  $e_{px}$  and  $e_{py}$  is, naturally, one of possible solutions. The Soviet building code SNiP II-15-74 recommends, in particular, that the ultimate settlement of a structure should be determined by referring to the modulus of deformation  $E_i$ . The following equation to find the value of the ultimate settlement  $S$  is suggested:

$$S = \beta \sum_{i=1}^n \frac{p_i h_i}{E_i}$$

where  $n$  is the number of the layers in the consolidating soil;  $p_i$  is half the sum of vertical normal pressures in  $\text{kg/cm}^2$  transmitted to the upper and the lower boundary of a layer  $i$  from the pressure by the foundation of the structure;  $h_i$  is the thickness of a layer  $i$  in  $\text{cm}$ ;  $E_i$  is the modulus of deformation of a layer  $i$  determined by field testing (loading by a testing plate) in  $\text{kg/cm}^2$ ;  $\beta$  is a dimensionless quantity correcting the abridged calculation scheme and taken as being equal to 0.8 for all soil varieties.

The coefficient  $\beta$  is, in fact, a reciprocal of the conversion factor  $M$ , i.e.  $\beta = 1/M$  and can be found from Eq. (26.20) in conformity with the data in Table 26.1.

The formula proposed by SNiP is valid for one-dimensional state of stress. Moreover, it does not allow for the dependence of  $E_i$  on  $p_i$  and is assumed to be constant for some soil variety. When determining the conversion parameter  $\beta$  the dependence of the coefficient of lateral strain on the degree of density and moisture content of clayey soils is not taken into account. From this viewpoint the SNiP 5 formula is much simpler than the previously presented equations (26.22) and (26.26) although it is more complex than Eq. (26.16).

Given identical initial data, in particular, assuming that the modulus of deformation  $E_i$  is independent of the stresses  $p_z$ ,  $p_x$  and  $p_y$ , all these formulae yield practically analogous results.

It should be finally pointed out that the predicted values of structure settlement prove mostly to be *larger* than the actual magnitudes. This results from the inevitable weakening of soils when taking samples from the intact soil mass and from plastic deformations caused by all-round pressure on the soil specimen and smoothing the lateral and upper and lower surface of the sample during the test. Such deformations are especially pronounced in dense clays manifesting low compressibility. Errors incurred in the experiment may many times exceed the value of, say, the modulus of compressibility  $e_p$  as a characteristic of the actual soil compression induced by loading. Therefore the coefficient of soil compressibility, e.g.  $e_p$  must be determined by allowing for the variation of the density-moisture of the soil during the test at a load.

As already reported, the discrepancy between the calculated and actual settlement can be very much affected by the initial hydraulic gradient in the soil  $J_{in}$ . This latter prevents load-induced consolidation of the soil when the appearing pressure gradient  $J_{pr}$  responsible for removal of the moisture from the soil proves to be less than  $J_{in}$ . Then the thickness of the active zone is characterized only by the boundary layers of a clay mass that are in contact with the draining layers where  $J_{pr} > J_{in}$ . This may appreciably decrease the thickness of the design active zone  $D$  and, consequently, the settlement of the structure.

We feel that if adequate progress in theoretical aspects of the above problems is made we will dispense with empirical corrections and formulae little suited for general soil conditions.

### Sec. 28.2. Approximate Methods of Predicting Settlement of Structures

Despite its apparent simplicity, the summation method of estimating settlement is very often too labour-consuming. This is especially important when designing a relatively small and elementary structure. The inappreciable size of the footing and of the structure itself have as a result that the vertical stresses  $p_z$  are rapidly dampened by the underlying soil layers. Thus it becomes possible to ignore the effect of the natural load on the settlement of the structure without incurring an error of any importance.

We may also assume that the modulus of deformation  $E$  is independent of the normal stresses induced by the weight of the structure itself in the soil mass, i.e. we may consider  $E = \text{const}$ . Then we will deal with a linear relationship between the relative deformation or modulus of compressibility  $e_p$  and the load  $p$ .

To understand it better, let us refer to Fig. 28.4. Let us find in the compression curve a point  $a$  corresponding to the design load transmitted to the

soil by the base of the foundation  $p_0$  and connect it with the origin of the coordinates by a straight line. This line will further serve as a compression curve.

Let us obtain a relationship for determining the modulus of compressibility  $e_{pz}$  corresponding to the stress  $p_z$ . Clearly,  $p_z \leq p_0$ . Let us find  $e_{pz}$  from the congruent triangles  $boc$  and  $aod$ . Thus we have

$$e_{pz}/e_0 = p_z/p_0 \quad (28.9)$$

where  $e_0$  is the modulus of compressibility corresponding to the load transmitted to the soil,  $p_0$ .

Hence

$$e_{pz} = \frac{e_0}{p_0} p_z \quad (28.10)$$

At the same time the subsidence of an elementary soil layer  $dz$  in thickness may be expressed as

$$d\eta_{sub} = e_{pz} dz$$

Then the total settlement of a structure equals

$$\eta_{sub} = \int_0^{\infty} e_{pz} dz \quad (28.11)$$

A substitution of the value of  $e_{pz}$  from Eq. (28.10) into Eq. (28.11) yields

$$\eta_{sub} = \int_0^{\infty} \frac{e_0}{p_0} p_z dz \quad (28.12)$$

Let us refer to Fig. 28.5 representing the lines 1, 2 and 3 of the values of  $p_z$  as functions of the depth  $z$  for a three-dimensional problem, given rectangular areas of the soil surface of various lengths sustaining a load:

$$\omega = a/b$$

where  $b$  is half the width;  $a$  is half the length of the loaded rectangle.

The integral in Eq. (28.12) stands for the area  $F$  of the epure bounded on two sides by the coordinate axes and on a third side by the curve  $p_z = f(z)$ . Differently speaking,

$$F = \int_0^{\infty} p_z dz \quad (28.13)$$



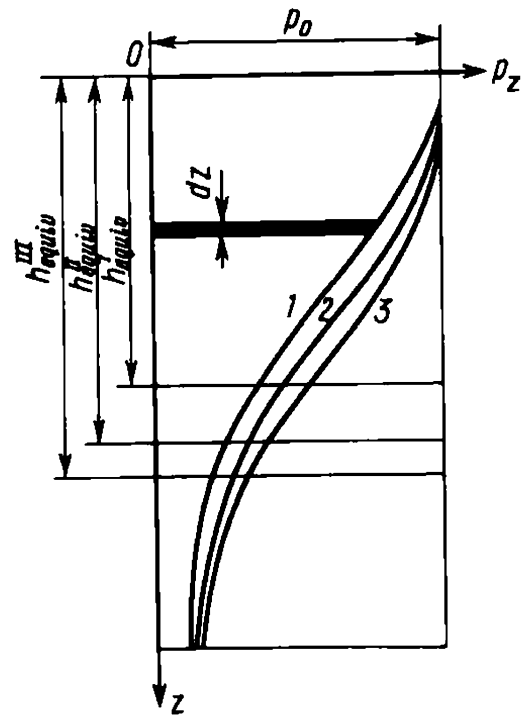


**Fig. 28.5.** Value of  $h_{eq}$  depending on the shape of  $p_z = f(z)$  curves determined by the ratio between the sides of the loaded strip (three-dimensional problem). Figures on the curves indicate numerical values of the ratio of the length to the width of the loaded strip  $\omega = a/b$

Consequently, Eq. (28.12) will take on this form:

$$\eta_{sub} = \frac{e_0}{p_0} F \quad (28.14)$$

The area of the epure  $p_z = f(z)$  can be represented as an equivalent area of a rectangle with sides  $p_0$  (design load) and reduced equivalent depth  $h_{equiv}$  (see Fig. 28.5). Then, by virtue of Eqs. (28.13) and (28.14),  $F = p_0 h_{equiv}$  and, finally,

$$\eta_{sub} = e_0 h_{equiv} \quad (28.15)$$

Thus the settlement of a structure  $\eta_{sub}$  is found as a product of the reduced depth  $h_{equiv}$  of a definite soil layer with the modulus of compressibility  $e_0$  induced by the load of the structure  $p_0$ .

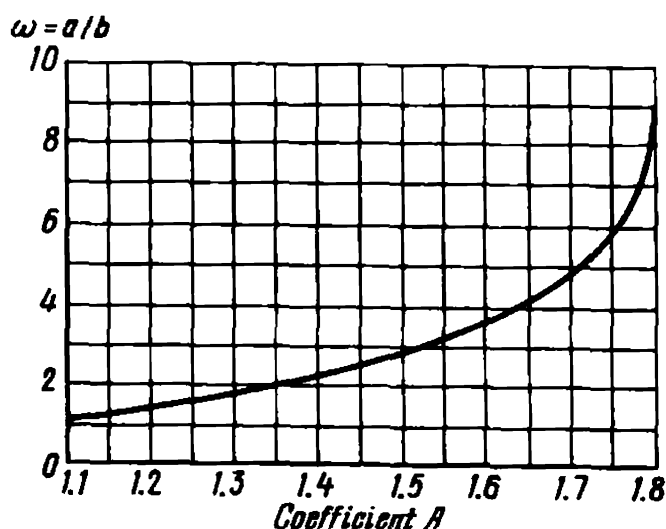
Equation (28.15) is very simple but requires knowledge of  $h_{equiv}$ . Since the character of the  $p_z = f(z)$  epure is governed by the size and shape of the structure in hand, so will, clearly, the value of  $h_{equiv}$  be conditioned by the same factors. The equivalent depth may be represented as a function of  $b$  (half the width of the footing) and  $\omega$  (the ratio of the sides of the loaded strip):

$$h_{equiv} = 2Ab \quad (28.16)$$

where  $A$  is a quantity governed by  $\omega$  and characteristic of the elongation of the loaded strip.

Figure 28.6 demonstrates the relationship between  $A$  and  $\omega$ , allowing for stresses to a vertical distance equal to  $10b$ . So, for an infinite length of

Fig. 28.6. Chart for determining  $A$  in Eq. (28.17) to forecast settlements of small size footings



a loaded strip (continuous footing)  $A_{\infty} = 1.8$ ; for a square foundation  $A_{sq} = 1.1$ . Other cases can be interpolated.

In conformity with this, Eq. (28.15) can be rewritten as

$$\eta_{sub} = 2Abe_0 \quad (28.17)$$

or, by defining the total width of the footing as  $B$ , for the general case

$$\eta_{sub} = AB e_0 \quad (28.18)$$

For a continuous footing

$$\eta_{\infty} = 1.8Be_0 \quad (28.19)$$

for a square foundation

$$\eta_{sq} = 1.1Be_0 \quad (28.20)$$

**Example.** The foundation is 2 by 3 m in size. The design load is  $p_{des} = 2.5 \text{ kg/cm}^2$ . The compression curve is shown in Fig. 28.2. The sides ratio is  $\omega = 3/2 = 1.5$ . It is required to find the settlement of the foundation.

Referring to Fig. 28.6, for  $\omega = 1.5$ , we find that  $A = 1.25$ . From the compression curve we find  $e_{2.5} = 15.5 \text{ mm/m}$ . Then  $\eta_{sub} = 1.25 \times 2.0 \times 15.5 = 38.7 \text{ mm}$ , or roughly 4 cm.

This formula is also convenient for estimating settlements of larger structures. It must be remembered, however, that in this case the values of settlement will be exaggerated. Practice suggests that a correction factor, always less than unity, should be applied here.

The vast assortment of formulae available in soil mechanics includes a number of relationships for determinations of the total subsidence  $\eta_{sub}$  using various loaded plates. Most of these relationships have been derived by assuming the constant values of moduli of total deformation throughout

the depth of the subsoil  $z$ , i.e. by assuming  $E = \text{const.}$  For example, the subsidence of the foundation soil surface at the centre of a circular loaded area is found from this relationship:

$$s_c = p_0 d / C \quad (28.21)$$

where  $d$  is the diameter of the loaded circle;  $C$  is what is called *a coefficient of elastic semispace* determined from the formula

$$C = \frac{E}{1 - \nu^2} \quad (28.22)$$

where  $\nu$  is a coefficient of lateral strain.

The subsidence of a stiff circular specimen can be established from the relationship

$$\eta_{sub} = 0.785 p_0 d / C \quad (28.23)$$

and of a square specimen,  $B$  on the side from

$$\eta_{sub} = 0.88 p_0 B / C \quad (28.24)$$

### Sec. 28.3. Some General Conclusions from the Theory of Settlement of Structures

Analysis of the distribution of stresses and strains in *the homogeneous* soil mass coupled to that of the nature of the settlement and deformations of actual structures permits some practical conclusions of practical value to be made. The most important of these, sometimes out of line with commonly accepted ideas, are as follows.

1. Other conditions being equal, the settlement of a structure with increasing the load  $p_s$  applied by the base to the supporting soil grows following a definite attenuating curvilinear dependence mirroring the shape of the compression curve.

2. As the dimensions and the width of the loaded strip increase due to the less intensive attenuation of the stresses in the soil mass the thickness of the active zone increases.

3. The settlement of a structure with a spread foundation, other conditions being equal, due to a greater depth of the active zone, is invariably of a smaller magnitude compared with a smaller structure. This regularity is, however, valid only for the thickness of the underlying soil being compressed greater than the depth of the active zone. At a relatively small thickness of the consolidating subsoil the settlement is independent of the size of the structure in hand.

4. An incompetent soil layer found at a certain depth enhances the settlement greater, if the area of the footing is large. This is due to the rapid attenuation of the stresses in the case of minor structure which may not affect the sensitive layer.

5. When definite soil varieties are involved, the settlement of a structure is much affected by loading of the adjacent area which may cause added deformation or tilting of the structure outside. This conclusion, following from the law of the distribution of the stresses in the soil mass under conditions when zones of stress are superposed under the adjacent parts of a structure, is true only if the consolidating layer is of marked thickness.

6. All kind of unequal loading becomes uniform at a definite horizon in conformity with the law of the distribution of stresses in the subsoil. This is, however, valid only when the thickness of the consolidating soil is much greater than the width of the loaded strip.

7. Under the above conditions and at a fairly large thickness of the compressing soil compared with the width of the footing the settlement of a structure is governed by its total weight  $P$  and not only by the unit load  $p_0$  transmitted by the base of the footing on the foundation soil.

8. In conformity with the law of the distribution of vertical normal stresses along a horizontal line a uniformly loaded foundation beam tends to sag, its bulge downward. The maximum settlement coincides with the midpoint of the beam, the minimum with its ends, being, however, other than zero. Therefore, if the stiffness of the beam is not zero, contact pressure at the subgrade is distributed nonuniformly.

9. If the underlying soil is insufficiently stable and competent, especially at the edges of the foundation which may be largely due to its insufficient depth and poor cohesion of the soil, the epure loses its saddle-like shape. In such case the performance conditions somewhat improve.

10. The magnitude of the expected settlement is often overestimated. As actual practice shows, the differential settlement of a structure proves to be the most detrimental if it increases rapidly. A gradational increase in the load transmitted to the soil may sometimes enable the structure, as it were, to adapt to the settlement pattern. The resultant deformations do not cause then any appreciable damage. Rheological events, largely, creep, play here the crucial role. At the present time, when the structures are erected with an unheard rate of construction, the problems concerned with settlement of structures and nonuniformity are of great practical significance.

Notwithstanding the rudimentary character of the proposed method of forecasting the settlement of a structure, when intelligently used, it may yield quite satisfactory results even if important projects are involved. The

history of a dam across the Svir River may serve as an example. The preliminary settlement computations indicated that filling the reservoir of the Svir 3 Hydro-electric Power Development would cause the powerhouse to tilt upstream about  $1^\circ$ . This computed tilt was in excess of the admissible value, and it was decided to install the turbine shafts out of plumb. When the reservoir was filled, the shafts were practically vertical\*.

---

## Chapter 29

### Forecasts of Time-Dependent Settlements of Engineering Structures

---

#### Sec. 29.1. Consolidation of a Uniform Soil Mass

As has already been reported, if the supporting soil of a structure is stable, it is the consolidation of the soil due to the weight of the structure that is the crucial factor in its settlement.

Load-induced time-dependent soil consolidation has been considered in Chapter 24. The conclusions made there hold good for analysis of the settlement of a structure as well. In particular, remarks concerning the role of fluidity and permeability deformation in consolidation of clayey soils characterized by the value of the coefficient of consolidation  $n$  are fully valid. The same is true of the determining role in the consolidation rate and, hence, the rate of subsidence, played by the coefficient of permeability  $K_p$  of the consolidating soils (direct relationship) and by the thickness of the consolidating layer (inverse quadratic relationship) coupled to drainage conditions.

Use can well be made of all the above formulae for determining computational coefficients and consolidation parameters together with theoretical argumentation bearing on forecasts of conditions of consolidation, in particular, the role played in the forecast by the degree of consolidation  $U_t$ .

By knowing the degree of consolidation  $U_t$  and its relation to the time factor  $T_t$ , the settlement of a structure  $\eta_{sub\ T}$  within a time period can be found from the relationship

$$\eta_{sub\ T} = \eta_{sub\ fin} U_t \quad (29.1)$$

---

\* Reported by H. Graftio and quoted by K. Terzaghi and R.B. Peck (op. cit., pp. 494-496).

where  $\eta_{sub\ fin}$  is the ultimate settlement of the structure corresponding to the total consolidation of the foundation.

How to forecast the time-dependent settlement of a structure by using the above equation can be best understood if we refer to a numerical illustration.

**Example.** The subsoil of a proposed large structure is composed of well draining medium-grained sands with an intermittent seam of soft plastic clay  $2H = 2.5$  m in thickness occurring below the water table. The average bulk density of the subsoil partly acted on by uplift pressure is  $\rho = 1.35$  t/m<sup>3</sup>, the natural moisture content of soil is  $w_{nat} = 30\%$ ; its bulk density is  $\rho_0 = 2.7$  t/m<sup>3</sup>. The coefficient of clay permeability is  $K_p = 5 \times 10^{-9}$  cm/s. The vertical normal stress at the horizon of occurrence of the seam in question is  $p_z = 1.25$  kg/cm<sup>2</sup>. At  $p_z = 1.25$  kg/cm<sup>2</sup> the modulus of compressibility is  $e_{1.25} = 22$  mm/m. It is required to plot, for a one-dimensional problem, a curve of the subsidence rate  $\eta_{sub\ T}$  with time, induced by percolation (filtrational) consolidation of the particular clay seam.

The first step is to determine the final settlement of the structure  $\eta_{sub\ fin}$  due to the consolidation of the clay seam  $2H = 2.5$  m in thickness. Let us find  $\eta_{sub\ fin}$  by using this elementary relationship:

$$\eta_{sub\ fin} = e_p h_i$$

In our example  $e_p = 22$  mm/m and  $h_i = 2H = 2.5$  m. Then  $\eta_{sub\ fin} = 22 \times 2.5 = 55$  mm.

In order to solve the time-dependent version of the problem, by using Eq. (22.7) determine the coefficient of consolidation  $c_v$ :

$$c_v = \frac{K_p(1 + \varepsilon_{av})}{a\rho_v}$$

The voids ratio  $\varepsilon_{nat}$  corresponding to the initial (natural) density will be found from Eq. (14.3):  $\varepsilon_{nat} = \rho_0 w_{nat} = 2.7 \times 0.3 = 0.81$ .

Find the voids ratio  $\varepsilon_p$  corresponding to the load sustained by the clay seam  $p_z = 1.25$  kg/cm<sup>2</sup>:

$$\varepsilon_p = \varepsilon_{nat} - \frac{ep(1 + \varepsilon_{nat})}{1\ 000} = 0.81 - \frac{22(1 + 0.81)}{1\ 000} = 0.77$$

Now determine the average voids ratio  $\varepsilon_{av}$ :

$$\varepsilon_{av} = - \frac{\varepsilon_{nat} + \varepsilon_p}{2} = \frac{0.81 + 0.77}{2} = 0.79$$

Find the coefficient of compressibility  $a$  by using Eq. (14.5):

$$a = \frac{\varepsilon_1 - \varepsilon_2}{p_2 - p_1}$$

In the particular case  $\varepsilon_1 = \varepsilon_{nat} = 0.81$ ;  $\varepsilon_2 = \varepsilon_p = 0.77$ ;  $p_1 = p_{nat}$  (natural load of the overlying strata);  $p = p_{nat} + p_z$ .

At the same time

$$(p_2 - p_1) = [(p_{nat} + p_z) - p_{nat}] = p_z \quad (29.2)$$

Then  $a$  will be obtained from the relationship:

$$a = \frac{\varepsilon_{nat} - \varepsilon_p}{p_z} \quad (29.3)$$

which in our case equals

$$a = \frac{0.81 - 0.77}{1.25} = 0.032 \text{ cm}^2/\text{kg}$$

The coefficient of permeability of the soil is given to be  $K_p = 5 \times 10^{-9} \text{ cm/s}$ . By converting it to cm/yr we have

$$K_p = 5 \times 10^{-9} \times 86\,400 \times 365 = 0.16 \text{ cm/yr}$$

Now we have all the data for determining the coefficient of consolidation  $c_v$  by referring to Eq. (22.7):

$$c_v = \frac{0.16(1 + 0.79)}{0.032 \times 0.001} = 9460 \text{ cm}^2/\text{yr}$$

Let us recall Eq. (22.12) to calculate the generalized coefficient of consolidation  $\zeta_K = c_v/H^2$ .

According to the conditions of the problem, drainage of the consolidating layer occurs in the upward and downward direction. Thus the design value of  $H$  in our case equals half the thickness of the layer, i.e.  $H = 1.25 \text{ m}$  or  $125 \text{ cm}$ . Then, by using Eq. (22.12), we obtain  $\zeta_K$

$$\zeta_K = \frac{9460}{125^2} = 0.606 \text{ yr}^{-1}, \quad \text{or} \quad 0.05 \text{ mo}^{-1}$$

Determine the time period for stabilization of the settlement from Eq. (25.14):

$$T_{st} = 1.13/\zeta_K = 1.13/0.05 = 22.6 \text{ mos}$$

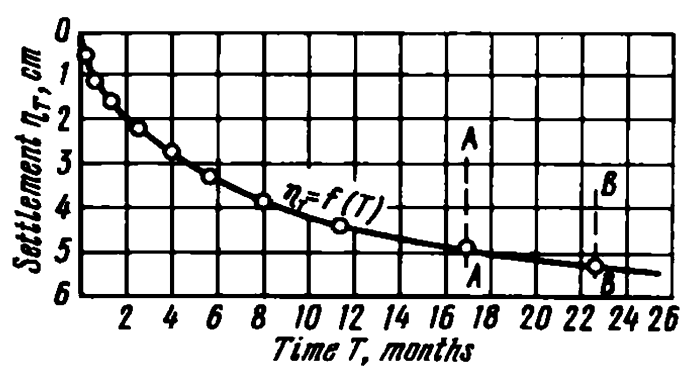


Fig. 29.1. Time-settlement curve (object No. 1):  
A-A—time of rough completion of structure;  
B-B—time of total completion of structure

Refer now to Table 22.1. By using Eq. (22.9), find  $N$  for different  $T$ :

$$N = \frac{\pi^2}{4} \frac{c_v}{H^2} T, \quad \text{or} \quad N = \frac{\pi^2}{4} \zeta_K T$$

For our particular case

$$N = \frac{\pi^2}{4} 0.05 T = 0.125 T \tag{29.4}$$

Then, given a series of values of  $T$  beginning from 0 to  $T = T_{st} = 22.6$  mos, by applying Eq. (29.4), find the values of the degree of consolidation  $U_t$  corresponding to these time intervals. For our example we find the value of  $U_t$  for  $T = 2.5$  mos. In our case  $N = 0.125 \times 2.5 = 0.31$ . By referring to Table 22.1, for  $N = 0.31$  we find that  $U_t = 0.40$ . Then, in conformity with Eq. (29.1), the settlement of the structure for  $T = 2.5$  mos will amount to  $\eta_{sub T} = 0.40 \times 5.5 = 2.2$  cm.

A diagram of the time-dependent increase of the settlement has been plotted to illustrate the above example (Fig. 29.1). The character of the  $\eta_{sub T} = f(T)$  curve shown in this diagram is very typical.

It should be remembered that soil mechanics has at its disposal an array of relationships for predicting the settlement of structures at variable values of  $p_z$  within the layer of interest. The principle of application of these formulae is as usual.

In addition, there are several methods of forecasting consolidation of the foundation and of evaluating the settlement of structures with time for a two- and a three-dimensional problem. But, since they are too bulky and involve a number of assumptions, they do not find universal use in design practice.

**Sec. 29.2. Consolidation of a Stratified Soil Mass**

The easiest way to forecast the settlement of a structure with time if this is supported by the soil mass composed by layers of materials with dif-



ferent characteristics is by using the relation:

$$T_{lay} = t_{exp} \left( \frac{H_{lay}}{h_{exp}} \right)^n \quad (29.5)$$

where  $T_{lay}$  and  $t_{exp}$  are, respectively, the time periods taken by consolidation of the soil layer  $H_{lay}$  in thickness and of the soil specimen  $h_{exp}$  in height;  $n$  is the consolidation index determined by laboratory tests of soil samples of different heights from Eq. (29.5) in the range of values  $0 \leq n \leq 2$ .

The solution is started by identifying in the soil mass the sand strata likely to provide draining for removal of the water squeezed out of the clay layers as these are consolidating under loading. Then all the clay layers are labelled by I, II, III etc., the thickness of each,  $H_1, H_2, H_3$  etc. is determined and the depth of occurrence established. It is by referring to these layers that we will mainly calculate the settlement of the structure and the time of its stabilization.

By conventional means we find the particular ultimate subsidence  $\eta_{sub i}$  of each of the identified layers considering each layer as a design one. Then the total ultimate settlement of the structure will be found from summing up the particular subsidence values:

$$\eta_{sub fin} = \sum \eta_{sub i} \quad (29.6)$$

By referring to consolidation curves for the representative samples taken from all clay layers we find the time  $t_i$  for consolidation of each sample within the loading range  $p_{nat}$  to  $p_{nat}$  plus  $p_z$ . The step that follows is to calculate the time taken by the ultimate settlement of the structure induced by the subsidence of each layer by comparing the thickness  $H_i$  with the heights of the samples  $h_i$  tested in the laboratory. This is done by using Eq. (29.5). Suppose, for example, that by determining the times of consolidation of samples of different heights we have found from Eq. (22.24) that  $n = 1.5$  which is really very often the case. Then Eq. (22.23) takes on this form:

$$T_i = t_i \left( \frac{H_i}{h_i} \right)^{1.5} \quad (29.7)$$

where  $T_i$  is the time period of total stabilization of the settlement of the structure due to the subsidence of the given layer;  $H_i$  and  $h_i$  is the thickness of the soil layers and the height of the representative soil samples in cm or m;  $t_i$  is the time taken for stabilization of the subsidence of the sample tested in the laboratory.

The total duration of the settlement of the entire structure will equal to  $T_{i\max}$ , i.e. the time taken by the displacement of the layer where the rate of consolidation is the lowest:

$$T_{i\max} = \max t_i \left( \frac{H_i}{h_i} \right)^{1.5} \quad (29.8)$$

Let us then determine the settlement of the structure by referring to a time interval of interest to us,  $T$ , less than  $T_{i\max}$ . We calculate what fraction of the total time taken by the ultimate displacement of each layer  $T_i$  is contributed by  $T$ . Then, by using the diagrams showing consolidation curves for soil specimens sampled from each layer and by referring to  $T_i$ , we ascertain the settlement of the structure  $s_i$  owing to displacement of each layer in  $T$  as part of the total settlement  $\eta_{sub\,fin}$ . Then the total settlement of the structure during the time period  $T$  will be found as the sum of the individual displacements:

$$\eta_{sub\,T} = s_1 + s_2 + s_3 + \dots + s_n \quad (29.9)$$

## Chapter 30

### Particular Cases of Forecasting Deformations of Foundations and Settlement of Structures

#### Sec. 30.1. The Effect of the Lowering of the Water Table

Lowering the water table may cause large settlement of buildings supported by incompetent soils. The settlement increases due to the greater weight of the overlying layers conditioned by removal of the uplift pressure.

This is illustrated by a number of buildings in Mexico City, where the subsoil consists of soft bentonitic clays with horizontal layers of water-bearing sand, the moisture content amounting to 200-250%. This fact is responsible for their marked compressibility. The withdrawal of water by pumping from sand layers has led to settlement, sometimes in terms of metres (Fig. 30.1).

To control major settlement, all important structures in Mexico City are being underpinned by piles that may penetrate into the subsoil up to 30 m (see Fig. 25.6). In the USSR major settlement occurs if buildings are underlain by peat layers of substantial thickness. If a peat deposit is drained



**Fig. 30.1.** Building in Mexico City that has settled 7 m due to a drop in the water table

and dries up, its own weight may cause appreciable settlement. An example can be provided by the excessive settlement of some buildings in the town of Archangel. The structures settled 3 to 4 m after the peat deposit underlying them had been drained. The unit load on the subsoil was about  $0.5 \text{ kg/cm}^2$ .

### **Sec. 30.2. The Effect of Vibrations on a Sandy Subsoil**

All varieties of grained loose soils have a specific structure skeleton. When clean, i.e. free of earth, organic or other admixtures, these soils are composed of individual hard grains of quartz, feldspar etc.

In the particular case the grains are in direct contact. Therefore the angle of internal friction for loose soils is as large as  $\varphi = 30^\circ$  and more, and cohesion is small ( $c = 0.10 \text{ kg/cm}^2$  and less). If the footing of a structure is sufficiently deep, this typically ensures a fairly high bearing power of the sandy foundation. Chapter 20 has presented a number of examples illustrating this. Because of the presence of hard skeletal particles grained soils have fairly low compressibility. These advantageous properties are demonstrated by loose soils that only sustain a static load.

Dry grained soils acted on by relatively weak vibrational loads (acceleration rate is  $\alpha < 2\,000\text{ mm/s}^2$ ) are little sensitive to a dynamic load. The coefficient of internal friction  $\tan \varphi_{dyn}$  drops then by 10 to 15%.

As has been established, a loose mass of sand acted on by a shock gradually compresses which leads to the subsidence of the entire surface. When a roadway is involved, the hard pavement becomes deformed which fact entails different consequences. Thus there arose a theory of vibrational compression and of vibrational curves plotted as a function, e.g.  $\varepsilon_j = f(\eta)$ , where  $\eta$  is a relative acceleration in fractions of the acceleration due to gravity, i.e.  $\eta = a/g$ , where  $g$  is gravitational acceleration (Fig. 30.2).

D.D. Barkan has proposed the following empirical formula to describe a vibrocompression curve:

$$\varepsilon_j = \varepsilon_\infty + (\varepsilon_0 - \varepsilon_\infty)e^{-\beta\eta}$$

where  $\varepsilon_\infty$  is the voids ratio at the maximum possible density of the sand;  $\varepsilon_0$  is that of a sand in an extremely loose state;  $1/\beta\eta$  is the acceleration of the vibration causing compression until the voids ratio  $\varepsilon_\infty$  is reached.

By knowing the initial (static) voids ratio ( $\varepsilon_{in}$ ) of the subsoil of the road pavement and the voids ratio  $\varepsilon_j$  the sand may attain following a prolonged dynamic action at a relative acceleration  $\eta$  it is possible to find the modulus of vibrational compression of the sand in mm/m:

$$e_{p\,dyn} = 1\,000 \frac{\varepsilon_{in} - \varepsilon_j}{1 + \varepsilon_{in}}$$

We may assume  $e_{p\,dyn}$  is functionally related to loading although the mechanism of it has not yet been understood.

Given the value of  $e_{p\,dyn}$  indicative of the amount of the subsidence of the soil surface expressed in mm for a layer 1 m thick induced by a load  $p$ , it is easy to determine the subsidence of a 0.5 m thick layer as  $s_{dyn\,sub} = 1/2 e_{p\,dyn}$ . For example, for  $e_{p\,dyn} = 20\text{ mm/m}$  the displacement is  $s_{dyn\,sub} = 10\text{ mm}$ .

For more important structures the method of forecasting the vibration-

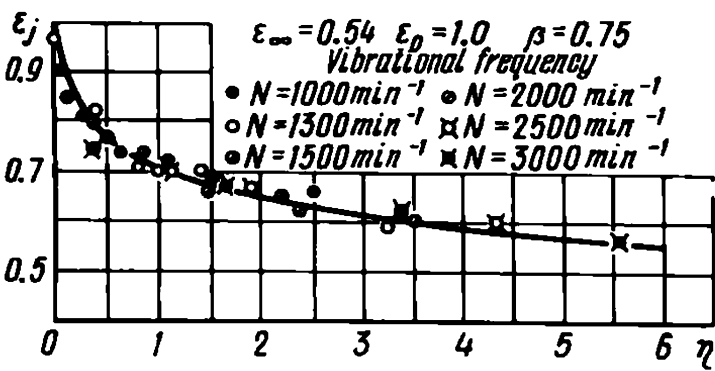


Fig. 30.2. Vibrocompression curve showing a relationship between the voids ratio  $\varepsilon_j$  and relative vibrational acceleration acting on sand  $\eta$  (after D.D. Barkan)

Table 30.1

Data Showing the Effect of Continuous Vibrations of the Soil on Settlement of Building Foundations

Acceleration of vibrations of soil surface near foundations, cm/s <sup>2</sup>	Characteristics of dynamic settlements of foundations	
	in saturated silty sands, liquid plastic clays and other incompetent soils	in sands (excepting ones listed in the left-hand column) and plastic clayey soils
Up to 5	Minor attenuating settlement	No settlement
From 5 to 15	Minor unattenuating settlement (2-3 mm/yr)	Inappreciable unattenuating or feebly attenuating settlement (1-2 mm/yr)
From 15 to 30	Unattenuating settlement (3-5 mm/yr)	Unattenuating settlement (2-3 mm/yr)
From 30 to 50	Major unattenuating settlement (more than 5 mm/yr)	Unattenuating settlement (3-5 mm/yr)

induced settlement is identical to one used for predicting a settlement at a static load (Chapter 28). Some conclusions may be made from this.

According to D.D. Barkan, the process of vibrational compression with time *t* proceeds obeying the relationship

$$\epsilon_t = \epsilon_j + (\epsilon_0 - \epsilon_j)e^{-\beta_t t}$$

If the sand layer is sufficiently thick, the process of the vibration-induced compression may last very long and attain very large magnitudes.

Shocks affecting the subsoil of a structure, whatever the type of soil material, when sufficiently intensive, may cause added settlement. Viewed in this context, the findings of Prof. O.A. Savinov obtained by lengthy observations deserve much attention (Table 30.1).

Attention should be drawn to the results of tests of dynamic compression of sands in a dry and a saturated state at one intensity of vibrations or another referring to the relative acceleration measured in fractions of acceleration due to gravity (Fig. 30.3). As follows from these curves, a loaded sand mass (*p* ≠ 0) decreases compression of the sand strata.

An apparatus shown in Fig. 30.4 has proved very useful for studies of the dynamic regime of sand. When tests are to be run, this apparatus is mounted on a shaking table. The pressure is imparted to the soil sample through a spring. This rules out the effect of inertia which is enevitable in gravitational apparatuses and which impairs the accuracy of the experimental results.

Of course, the dynamic impact of the passing vehicles on the roadbed is generally much less than that of heavy road building machinery. However,

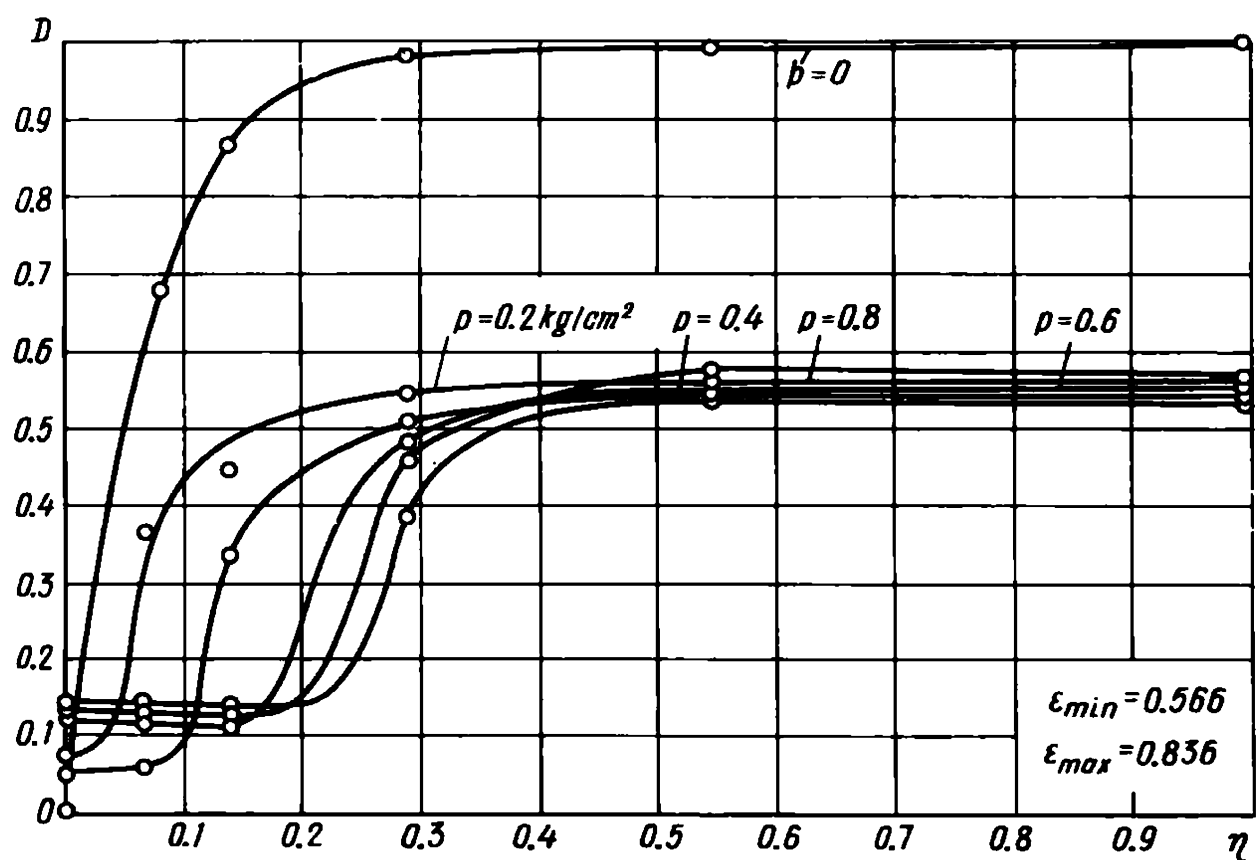


Fig. 30.3. Chart showing the relationship between (1) compression of dry (medium-grained) sand and relative density  $D$  and (2) the relative vibrational intensity  $j$  at different loads  $p$

the vibrations we feel sitting in our homes as trucks are passing by demonstrate how essential it is to take into account the dynamic action of such vibrations on the sandy subsoil, whenever an important structure is to be designed. Proof can be provided by cracks in buildings underlain by sand strata erected along busy streets (e.g. in Riga).

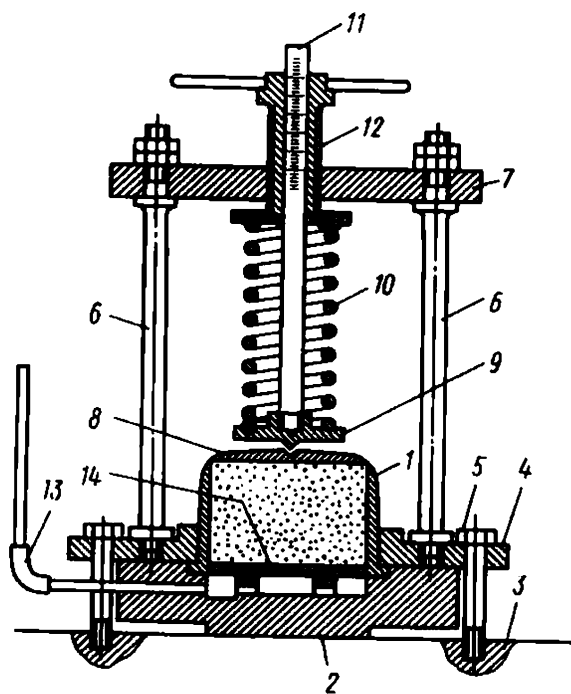


Fig. 30.4. Diagram of apparatus for testing vibration-induced compression of sands (after O.A. Savinov):

- 1—mould for soil sample; 2—tray; 3—seal; 4—fixing plate;
- 5—fixing bolt; 6—bolt; 7—upper retaining plate;
- 8—loading weight on soil sample; 9—loading device;
- 10—helical spring; 11—bar; 12—sleeve; 13—rubber hose;
- 14—porous disk

The present writer's findings suggest that trucks and trams travelling at high speeds cause vibrations with accelerations between 100 to 200 mm/s<sup>2</sup>. These values may sometimes dramatically increase.

As especially adverse effect is produced by meeting or overtaking traffic. Under unfavourable conditions (large weights and high speeds) the amplitude of vibrations of the roadbed may attain 0.10 mm or more at a vibrational frequency  $f = 10$  to 15 Hz which corresponds to the acceleration of up to 1 000 mm/s<sup>2</sup>.

Naturally, the aforementioned processes and phenomena greatly contribute to the deformations of the roadbed, especially when high and nonuniform speeds of vehicles are involved.

In order to preclude harmful effects of these events it is a good plan, before placing a hard pavement, to compact the underlying sand until it attains the voids ratio  $\varepsilon_j$  likely to be achieved during the operation of the road. This may eliminate additional vibration-induced settlement altogether.

Attention is being currently drawn to deformations and strength of a hard pavement placed on an insufficiently compacted sand roadbed (subgrade) which will inevitably sustain vibrations.

### Sec. 30.3. Taking Into Account the Anisotropy of the Subsoil

Anisotropy occurs if the subsoil is composed of thin alternating layers of different materials resulting from specific facies of soil accumulation. If the soil mass has different deformability in a horizontal direction (modulus of deformation is  $E_1$ ) and in a vertical direction (modulus of deformation is  $E_2$ ), to determine  $p_z$  and  $p_x$  for a linear load we may use K. Wolf's formulae:

$$p_z = \frac{2qz^3}{\pi R^2 R_1^2} K \quad p_x = \frac{2qzx^2}{\pi R^2 R_1^2} K \quad \tau_{xz} = \frac{2qxz^2}{\pi R^2 R_1^2} K$$

In these equations  $q$  is a load per unit length of the loaded strip;  $R$  is a distance from the loaded strip to the particular point and

$$R_1 = \sqrt{K^2 x^2 + z^2}$$

In its turn,

$$K = \sqrt{E_2/E_1}$$

The coefficient of the lateral strain  $\nu$  is assumed as being the same in either direction.

The anisotropy of the subsoil tells on the stress concentration along the

axial line. At  $K = 1$  the above formulae take on a form typical of a homogeneous soil mass.

In the general case the anisotropy affects the patterns of the soil's state of stress induced by an external load. As is shown by analysis, however, it is difficult to determine this factor since it calls for labour-consuming computations. On the other hand, field observations conducted by the present writer, in particular, during the construction of the Svir Hydro-electrical Development in 1931 to 1934, disclosed what small effect the pattern of lamination by thin sand and sandstone layers of the clay mass produces on the stress distribution throughout the subsoil.

M.A. Bio has substantiated this conclusion theoretically. He has found that the clay mass that contains thin seams of sand only insignificantly (by about 6%) increases attenuation of stresses in the soil mass.

Due to the above reasons the anisotropy of the soil mass is not generally taken into account in forecasts of deformations and settlements of structures. At the same time, when dealing with a three- or two-dimensional problem the subsoil's compressibility in a vertical and a horizontal direction can be easily determined through constants  $e_{px}$  and  $e_{py}$  as already outlined (cf. Chapter 28).

#### Sec. 30.4. Taking into Account the Stratified Pattern of the Soil Mass

In many jobs, especially when the structure in hand is of large area, the subsoil is composed of layers of different compressibility. This influences the magnitude of the eventual settlement and must be taken into account under definite conditions. The simplest example is the distribution of stresses in a two-layered foundation.

Road building extensively uses an approximate *equivalent layer method* proposed by Prof. G.I. Pokrovsky. It is basically this. Settlements of two beams supported by the ground and sustaining identical loads will be equal only if they are of the same rigidity, i.e.

$$E_1 J_1 = E_2 J_2 \quad (30.1)$$

Only if this condition is satisfied the pressures on the soil at points of application of loads will be equal. As is known, the moment of inertia for a rectangular cross-section beam is

$$J = BH^3/12 \quad (30.2)$$

A substitution of the value of  $J$  from this equation into Eq. (30.1) after



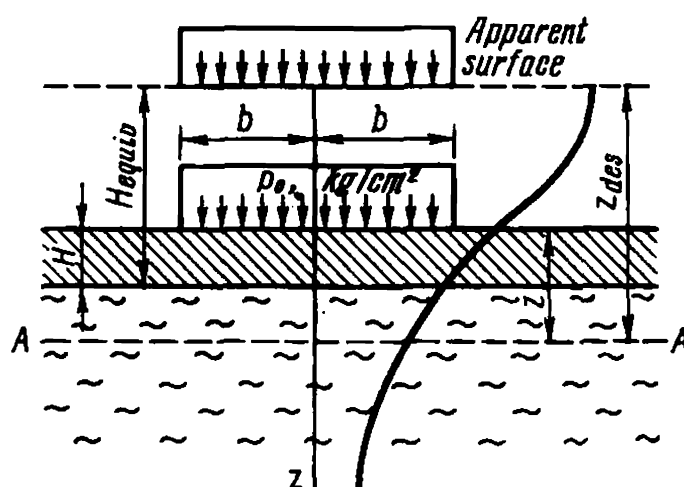


Fig. 30.5. Chart for calculating a two-layer system (method of equivalent layer)

the requisite transformations yields

$$H_1 = H_2 \sqrt[3]{E_2/E_1} \quad (30.3)$$

where  $H_1$ ,  $H_2$  and  $E_1$  and  $E_2$  are, respectively, the thicknesses and moduli of deformation of the two layers (1 and 2).

Thus the stress distribution in a two-layered subsoil is determined by replacing the thickness of the topsoil by an *equivalent thickness*  $H_{equiv}$  found from Eq. (30.3) which for the particular case will take on this form:

$$H_{equiv} = H_1 \sqrt[3]{E_1/E_2} \quad (30.4)$$

This is illustrated by Fig. 30.5. In the particular case it is assumed that the topsoil has a lesser compressibility.

The next step is to determine the vertical normal stresses at one depth or another,  $z$ , of the underlying layer at the level  $AA$  by using the conventional method assuming

$$z_{des} = z + (H_{equiv} - H_1) \quad (30.5)$$

Based on experimental data, Prof. N.N. Ivanov has proposed a modified formula for pavements:

$$h_{equiv} = H \sqrt[2.5]{E_{pav}/E_{subgr}} \quad (30.6)$$

where  $E_{pav}$  and  $E_{subgr}$  are the moduli of deformation of the pavement and of the subgrade, respectively;  $H$  is the thickness of the pavement. A solution has been suggested by Prof. B.I. Kogan for a case where the modulus of deformation  $E_z$  decreases in the soil mass exponentially:

$$E_z = E_0 e^{-\beta(z/H)}$$

where  $E_0$  is the modulus of deformation induced directly by the load;  $z$  is the ordinate of the particular point;  $\beta$  is a coefficient indicative of the intensity of the modulus's variation.

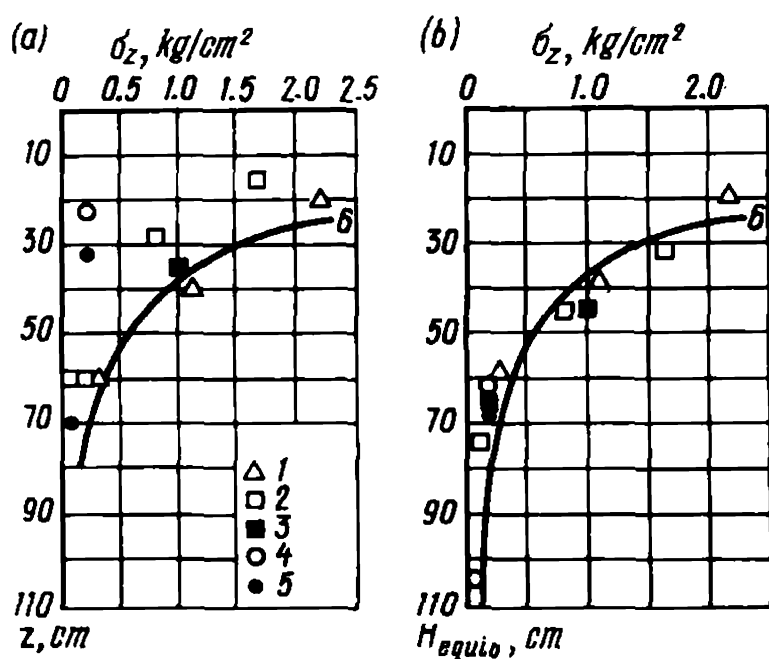


Fig. 30.6. Distribution of stresses in a highway foundation soil:

*a*—actually measured; *b*—when substituting a roadbed by an equivalent soil layer; 1—dirt road pavement; 2—cobble-stone pavement; 3—crushed rock surface course; 4—asphalt-concrete coat on pavement; 5—asphalt-concrete coat on crushed rock foundation; 6—theoretical stress distribution

This relationship is applied in road building to calculate the thickness of a road pavement.

It is worth mentioning the findings of Prof. V.F. Babkov who has determined stresses in various types of pavement (Fig. 30.6). His findings attest to the practical usefulness of the equivalent layer method.

Clearly, the above solutions are only rudimentary and need further development and elaboration. The problem is much more involved than can be judged from the aforementioned solutions. In particular, we have not touched upon the variation in the pressure imparted to the soil's skeletal particles by the instantaneous application of a load of rapidly rotating vehicle's wheels. It appears that in this case an important role is played by the pore water pressure which, incidentally, is demonstrated by works of G.S. Kanayan of the Moscow Highway Engineering Institute.

### Sec. 30.5. Taking Into Account the Geological Features of the Subsoil

Analysis of the stress distribution in the stratified soil mass shows that if the dip of the layers is equal to  $45^\circ$  it is possible to determine the stresses by conventional means. At greater angles of the dip the values of  $p_z$  are greater with depth compared with a homogeneous soil mass. This case may be considered as similar to a concentrated transmission of the pressure exerted by the foundation base to deeper horizons by means of friction piles.

If the angle of the dip is less than  $45^\circ$ , the reverse is true: stresses will attenuate more rapidly with depth and  $p_z$  with increasing the depth will be smaller compared with the homogeneous soil mass, the harder layers playing the part of distribution plates.

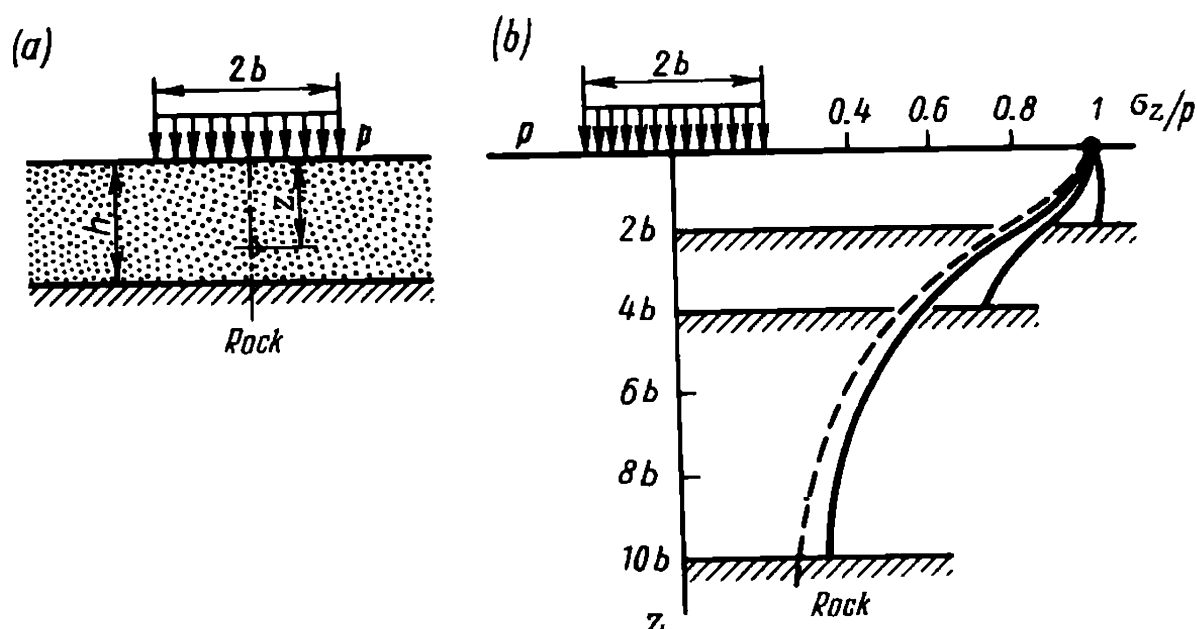


Fig. 30.7. Distribution of stresses with depth at shallow occurrence of competent bedrock:

*a*—general scheme; *b*—stress curves

The disturbance of occurrence of the layers in the subsoil invariably renders the matters more complicated. This is due to the fact that the structure may be supported by different rocks whose layers may possess different compressibility. It may cause differential settlement of the structure.

It should also be noted that the inclined occurrence of the layers is generally conditioned by the stratified structure of the soil mass where soil strata may often have undergone metamorphism to one degree or another. Under such conditions rocks generally manifest increased density and stability which decreases the effect of the above adverse factors.

If the soil layer  $h_{gr}$  with a considerably smaller thickness of the active zone  $D$  and a hard layer underlying the soil whose compressibility is much less are present, then the pattern of stress distribution is changed. In this case the stresses are concentrated with the depth of the layer which is illustrated by Fig. 30.7 plotted by referring to the data presented by K.E. Egorov. This problem becomes of practical importance if the thickness of the compressing layer is quite commensurable with the width  $2b$  of the loaded strip.

### Sec. 30.6. Forecast of the Tipping of a Monolith Tower Type Structure

A need may sometimes arise to forecast a likely tipping of structures, such as bridge piers and abutments, various towers, lighthouses, tall stacks etc. The tipping of a tower may be due to two causes: the heterogeneous subsoil where one side of the foundation is underlain by a soil of lower

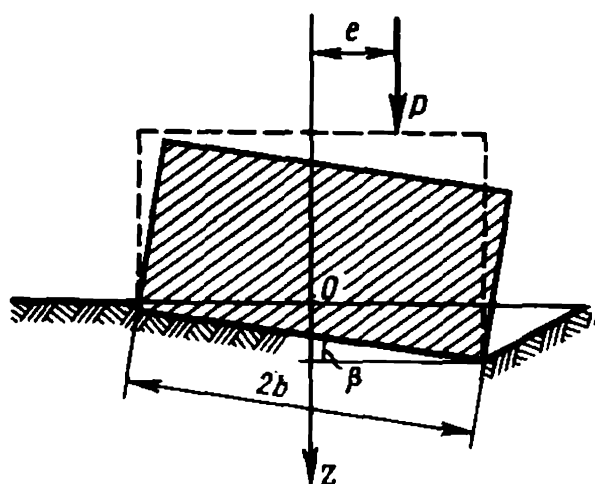


Fig. 30.8. Chart for predicting the tipping of a structure

bearing capacity; the eccentrical application of a load on the subsoil which results in a bending moment (Fig. 30.8).

In order to evaluate the possible tipping of the structure in the first case (nonuniformity of the subsoil) as described above we must determine the subsidence of the subsoil within the boundary of the footing of the structure by referring to at least three vertical lines I, II and III (two at the edges of the footing, one at its centre). Naturally, calculations should be made, concurrently taking into account the geological features and compressibility of the materials occurring here. From the values obtained of the subsidences  $\eta_I$ ,  $\eta_{II}$ ,  $\eta_{III}$  a subsidence curve is plotted. Having taken into account the pronounced degree of rigidity of such structures, the subsidence curve is averaged by smoothing it out. The inclination of the line obtained is measured and compared with the height of the structure.

In the second case (eccentric loading of the subsoil following the law of a trapezoid) the tipping  $\omega$  as tangent of the angle of the inclination of the foundation base of the structure to the horizontal  $\theta$  with the width of the footing  $b$  can be determined from the difference in the settlements of the edges of the footing found for the stresses acting here in the soil mass, i.e.

$$\omega = \tan \theta = \frac{\eta_{sub\ 1} - \eta_{sub\ 2}}{b}$$

The tipping of the top of a structure (say, a bridge pier) can be then determined from the relationship  $u_b = \omega h_0$ , where  $h_0$  is the distance from the foundation base to the top of the pier.

If the planimetric size of the structure is small, the subsoil's compressibility may be assumed constant with depth,  $E = \text{const}$ . Then, according to Paragraph 11 of Appendix 3 of the Soviet Building Code SNIIP II-15-74 the tipping of the structure can be determined by using these formulae:

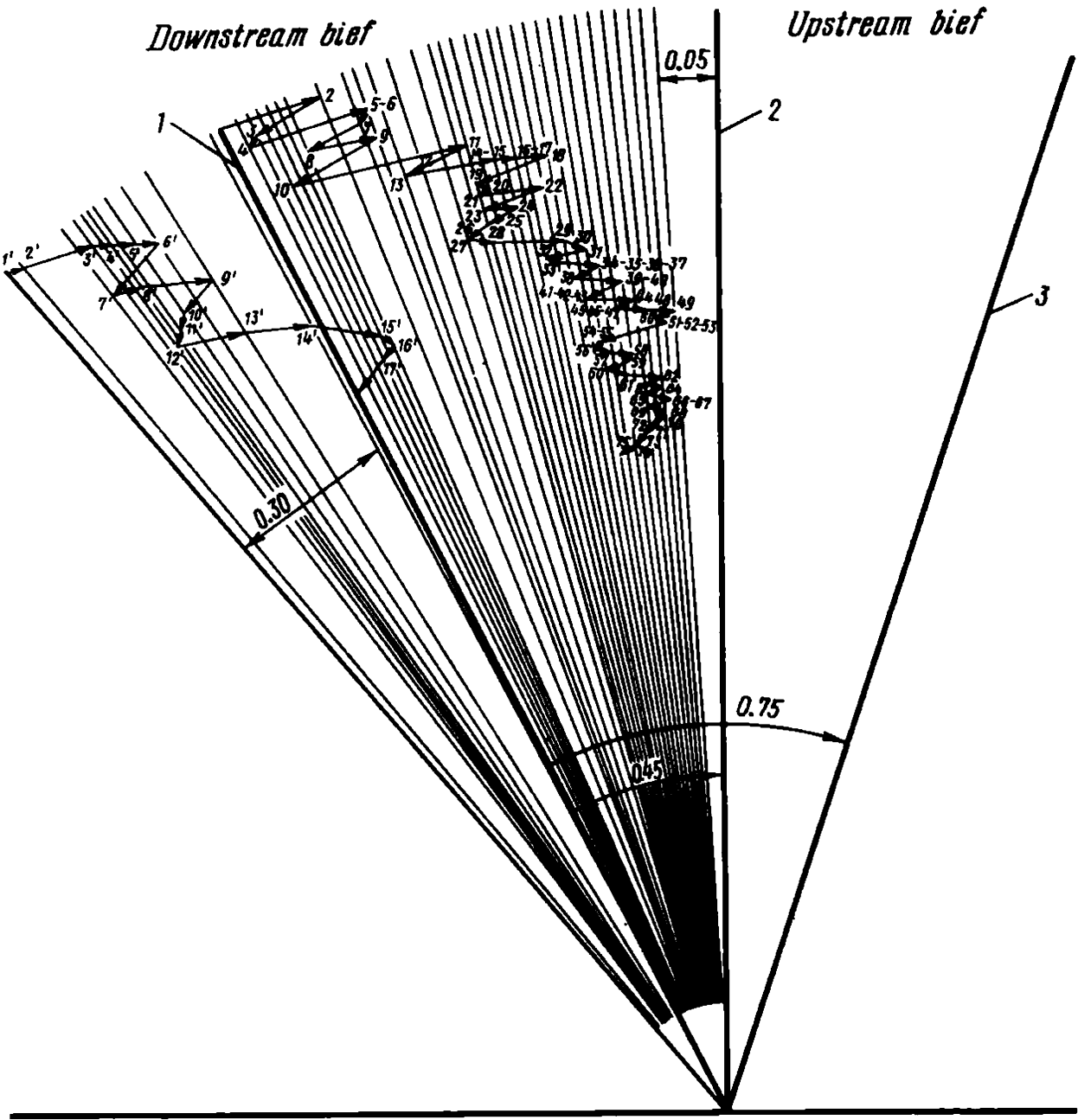


Fig. 30.9. Chart showing eventual correction of the deliberate tilt of the shaft of Turbine IV of the Svir Hydroelectrical Power Development. The initial tilt was  $0.45 \times 10^{-3}$ :  
1—start of installation operations; 2—vertical axis of the project; 3—axis of the turbine shaft at the moment the lower ring of the nozzle is installed

(a) for a rectangular footing along its shorter side (transverse axis)

$$\tan \beta_b = i_b = \frac{1 - \mu^2}{E} k_b \frac{Pe_b}{b^3} \tag{30.7}$$

(b) for a circular footing with a radius  $r$

$$\tan \beta_r = i_r = \frac{3}{4} \frac{1 - \mu^2}{E} \frac{Pe_r}{r^3} \tag{30.8}$$

where  $P$  is the concentrated force in kg;  $e_b$ ,  $e_r$  are eccentricities in cm;  $b$  is

half the width of the footing;  $E$  is the modulus of deformation in  $\text{kg/cm}^2$ ;  $\mu$  is the coefficient of the lateral strain;  $k_b$  is a coefficient governed by the ratio of the sides of the footing (for a square it is 0.50, for a 1/3 ratio it is 0.33).

Hence the deviation  $s$  of the top of a structure which is  $H$  in height from the plumb line is found by using the relationship

$$s = H \tan \beta \quad (30.9)$$

A practical example of the eventual correction of the deliberate tilt of the shaft of Turbine IV of the Svir Hydro-electrical Power Development due to the expected tilting upstream of the powerhouse upon filling the reservoir is provided by a large-scale diagram (Fig. 30.9). The design tilt was  $0.45 \times 10^{-3}$ . The turbine shaft was practically vertical when the reservoir was filled.

### Sec. 30.7. The Behaviour of the Soil Under the Impact of a Rolling Wheel

This concerns mainly dirt and temporary roads. As such roads are built and operated it is desired to ensure the maximum trafficability and minimum deformation of the roadbed so that ruts are not formed. This calls for evaluation of the soil's bearing power as a foundation of a rolling wheel. Differently speaking, we must determine the state of stress of the soil and its resistance to normal and shearing stresses.

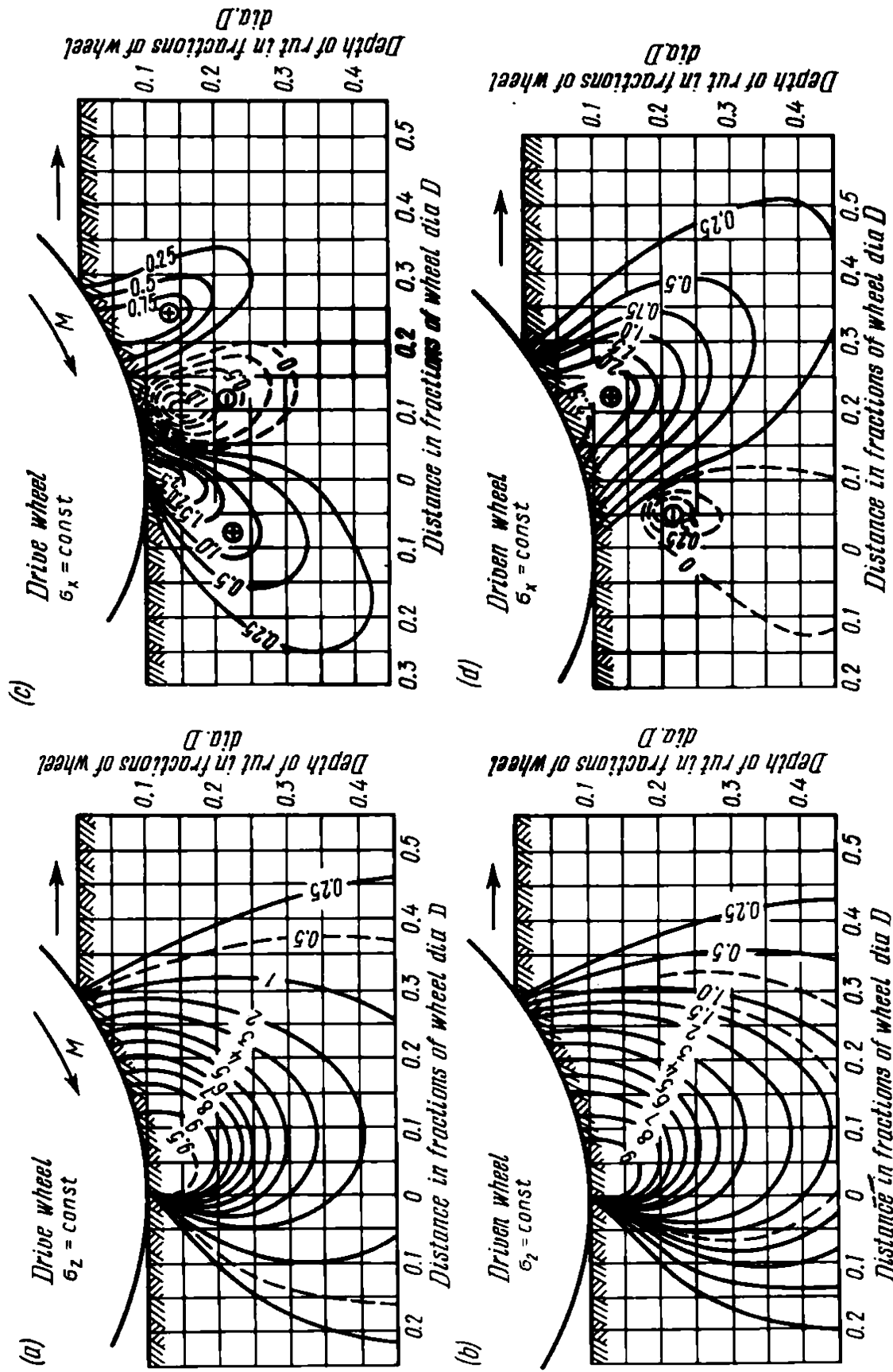
The task is made more complicated by the specific behaviour of the soil in the particular case (dynamic and short-term load, its nonuniformity under wheels and with time etc.). This prevents us from providing at present time a reliable solution and makes us treat the problem from a semiempirical viewpoint.

Figure 30.10 presents vertical and horizontal stress fields under a driving and a driven wheel. These data can be to a certain degree relied upon in evaluating conditions of rutting as the soil is being compacted by numerous vehicles.

In practical work use is mainly made of the following empirical formula proposed by Bernstein-Letoshchiev:

$$q_z = C \left( \frac{z}{z_0} \right)^\mu \quad (30.10)$$

where  $q_z$  is the bearing stress resistance of soil at a depth  $z$  in  $\text{kg/cm}^2$ ;  $C$  is the resistance of soil at a depth  $z_0 = 1 \text{ cm}$  (generally omitted);  $\mu$  is a parameter characterizing the increase of the resistance of soil with depth on increasing the depth of the rut.



**Fig. 30.10** Contour lines of equal stresses in a soil under a rolling wheel (rut being 10 cm deep);  $\mu = 1$  and  $C = 100 \text{ kg/cm}^2$ ; coefficient of cohesion of tyre to soil is  $\varphi = 0.30$ :

a, b—vertical normal stresses; c, d—horizontal normal stresses

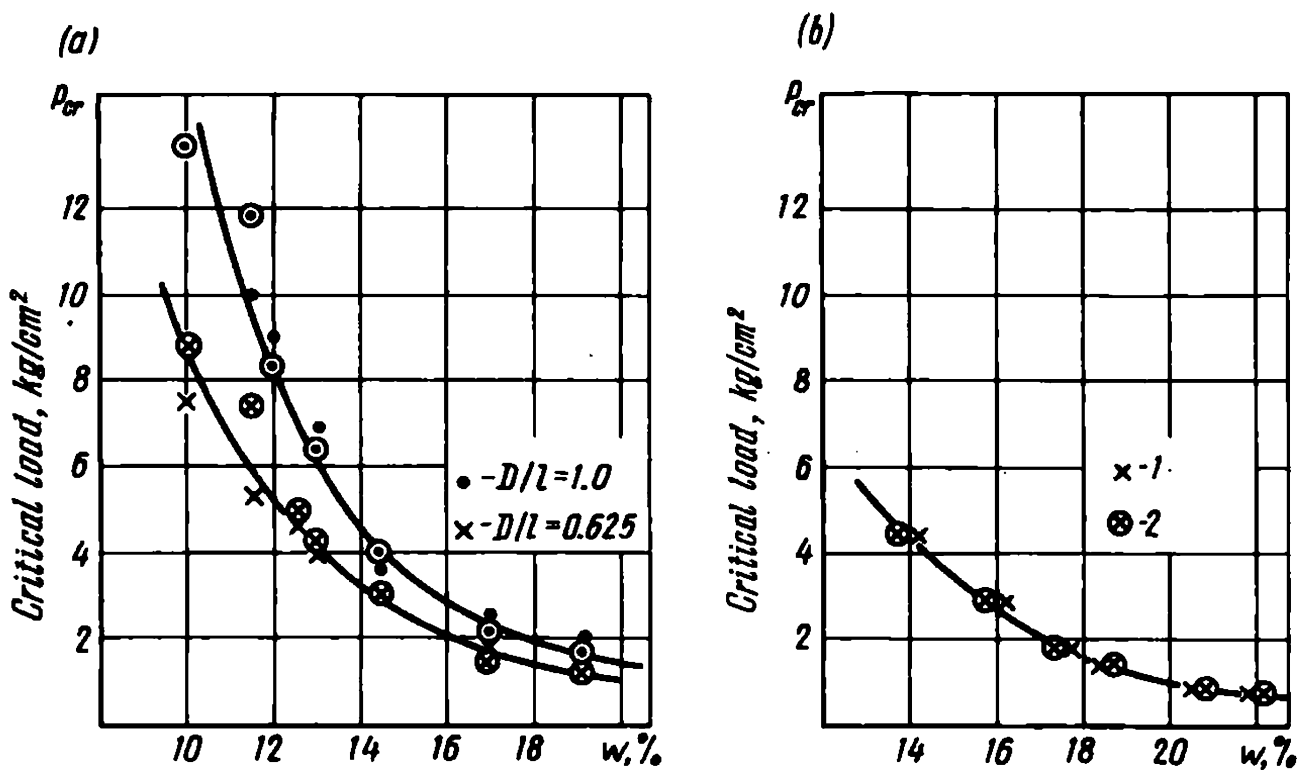


Fig. 30.11. Chart showing the relationship between a critical load  $p_{cr}$  and the moisture content  $w$ :

$a$ —smooth-wheel roller;  $b$ —pneumatic-type roller; soil is loam with the original density  $\rho_l^{in} = 0.90 \rho_{max}$ ;  $1$ —results of pressure of the loading plate and of the pneumatic-tyred wheel;  $2$ —as calculated through  $\varphi_w$  and  $c_w$

Of much interest are efforts of A.D. Kayumov to evaluate the strength of soil (acted on by a critical pressing load  $p_{cr}$ ) as it is being compacted by smooth-wheel and pneumatic tyred rollers.

He has derived his formulae following from approximate solutions by the method of critical equilibrium (two-dimensional case). The equation for determining a critical load on the soil when using a smooth wheel roller has this form:

$$p_{cr}^{sm} = KN_{\varphi}^c c_w, \tag{30.11}$$

where  $N_{\varphi}^c$  is a function of the angle of internal friction;  $c_w$  is cohesion in  $\text{kg/cm}^2$ ;  $K$  is a correction coefficient found experimentally taking into account the effect of the faces of the loading plate and the relative depth of its penetration into the soil.

When the road bed is being compacted by pneumatic tyred rollers the following relationship is useful:

$$p_{cr}^{pn} = N_{\varphi}^{pl} c_w (1 + a_{\varphi}/n) \tag{30.12}$$

where  $N_{\varphi}^{pl}$  is a function of the angle of internal friction (two-dimensional case);  $a_{\varphi}$  is a coefficient governed by the angle of internal friction;



$n = l/2b$  is a coefficient allowing for the length to width ratio of the area of load transmission;  $l$  and  $b$  are the length and width of the loading plate in cm;  $c_w$  is cohesion in  $\text{kg/cm}^2$ .

Graphs presented in Fig. 30.11 point to a good agreement between the above formulae and the experimental results obtained by the workers of the Hidgway Engineering Research Institute.

Sec. 30.8. Cyclic Loads

Experiments conducted by G.S. Kanayan aimed at gaining an insight into the nature of the processes occurring in a completely saturated precompressed clayey soil due to cyclic loads have demonstrated that in the particular case seepage consolidation occurs even if the loads act during very short (0.2, 0.5 and 1.0 s) time intervals (Fig. 30.12). The water squeezed out of a soil sample on its being loaded in a cyclic mode attests to

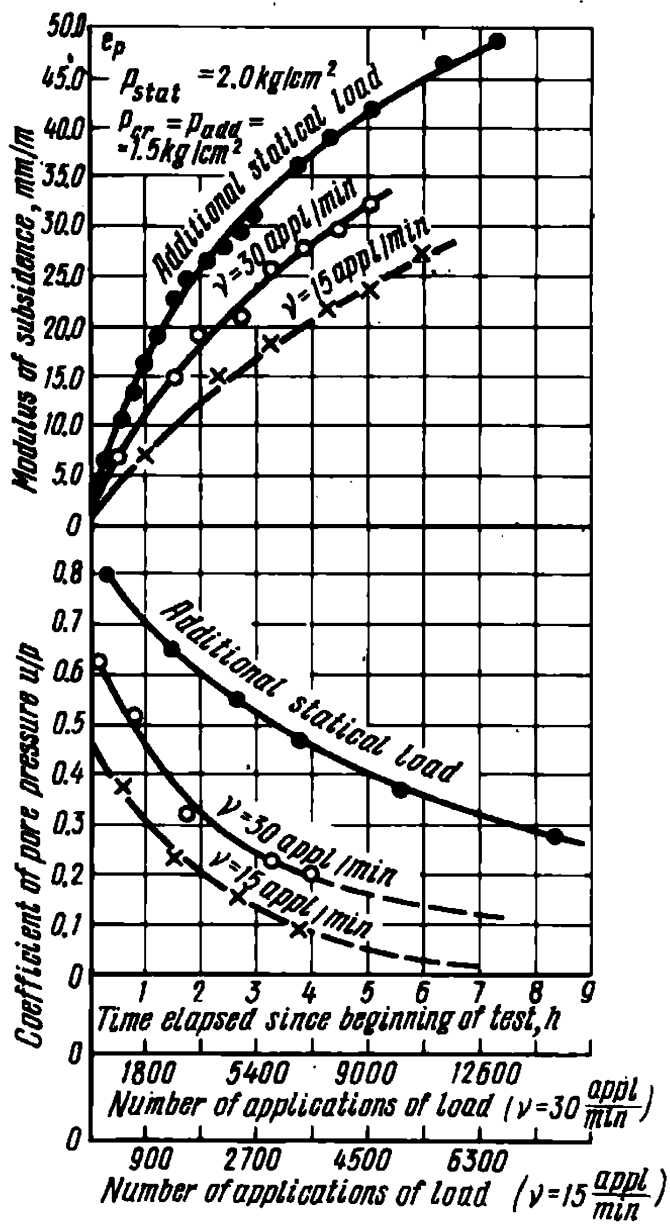


Fig. 30.12. Change of the coefficient of pore water pressure  $\alpha_p$  and of the modulus of compressibility  $e_p$  with time upon action of a cyclic load on semihard Kudinov clay. The coefficient of saturation is  $G = 1, 0$ . Duration of load is  $t = 1.0 \text{ s}$

a process of seepage consolidation. As a clayey soil which has low permeability is being compacted, pore water pressure,  $u$ , appears there.

G.S. Kanayan has established that in soils of different granulometric composition being compressed by the same static load and sustaining a cyclic load there appears pore water pressure  $u$  of various magnitudes. It is the larger, the greater is the clay content of the soil and the frequency of the load being applied. The pore water pressure attains its maximum value ( $u_{max}$ ) not immediately but after a definite lapse of time. After it has attained its maximum, the pore pressure starts gradually to decrease notwithstanding the enhanced number of cycles. The pore pressure  $u_t$  induced in such soils by a load  $p_0$  causes the normal stresses  $p_z$  and  $p_x$  to decrease whereas the magnitude of the shearing stresses  $\tau$  immediately attains its peak value. Therefore, by any time moment  $t$  the magnitude of the operating normal and shearing stresses, as established by V.A. Florin, will have been equal to

$$p_{z_t} = p_z - u_t; \quad p_{x_t} = p_x - u_t; \quad \tau_t = \tau_{con}$$

As has been pointed out above, the pore pressure  $u_t$  diminishes with time. As a result, the stresses  $p_{z_t}$  and  $p_{x_t}$  will increase and tend to  $p_z$  and  $p_x$ . This fact revealed by G.S. Kanayan (1973) should be taken into consideration since it is likely to cause soil building beneath the wheels of a rapidly moving vehicle due to the drop in the compressive stresses and, accordingly, decreased shearing resistance of the soil.

If the voids of a clayey soil contain air or some other gas, the above process occurs more rapidly because of the pronounced compressibility of gases. It is only the viscosity of the soil that inhibits this process. In the particular case the compressive deformation gradually transforms to elastic deformation.

Weakly compressed dry sands are the first to compact under the conditions involved since they sustain a dynamic load. An essential role is also played here by the forced introduction of hard particles into the voids of soil. Clearly, in order to forecast the settlement of a structure in such conditions we need compression curves showing the modulus of compressibility of the soil  $e_p$  at one load or another depending on the number of the repeated short-time cycles of loading and removal of load from soil samples. Such tests call for special periodic-action loading devices.

It follows from the above that compaction of a roadbed composed of clay materials by rolling may be primarily achieved due to the reduction of the voids in the embankment, say, due to the presence of soil lumps formed during the construction of the fill by using one type of machinery or another. The strength of the soil conditioned by its moisture content in the lumps thus becomes important.

---

## Chapter 31

### **Rheological Phenomena. Their Role in the Bearing Capacity and Time-Dependent Deformation of Clays**

---

#### **Sec. 31.1. General Considerations**

Most physical bodies are liable to slowly attenuating or continuous deformation induced by time-dependent load. This type of deformation is termed *creep*.

Most clayey soils are subject to creep movement in a pure form under the action of the shearing stresses leading to rearrangement of the skeletal particles of the soil.

Cohesionless soils, e.g. sands are subject to continuous deformation under the effect of vibrations. This type of deformation conditioned by mutual displacement of sand grains in a dynamic mode may be described as *pseudocreep*.

This latter may account for the commonly observed deformation of rock masses with joints. This deformation occurs as the fissures gradually close under the effect of load and the rough walls of the fissures are smoothed down by a shear. Creep is especially typical of clayey soils of soft consistency.

If a clayey soil, as a definite physical body, is acted on by shearing stresses, then the mechanical equilibrium of the system is generally apparent even if the shear may seem to be stabilized. If a soil is being acted on by a sustained load a *true* equilibrium is absent. This is revealed depending on the intensity of the acting force, the properties and state of soil as it is being subjected to a time-dependent continuous strain. Then the soil's skeletal particles rearrange, and the free energy accumulated during the shearing deformation is released and decreased. This leads to creep or fluidity of the soil depending on definite conditions to be considered in part in what follows.

*Relaxation* (relief of stress) is especially revealed if a soil is sustaining a constant load in confined conditions. Then, as the free energy gradually decreases, the skeleton of the soil gradually resumes its original form, the deformations are attenuated and the shearing stresses dissipate. Thus, rheological phenomena, primarily creep, in soils are directly associated with shears.

A shear failure often causes tipping and irregular settlement. A classical example of tipping is the Leaning Tower of Pisa (Figs 31.1 and 31.2) that has been tipping and settling for centuries.



Fig. 31.1. Tipping of the Leaning Tower of Pisa during 8 centuries

Figure 31.1 is a general view of the Tower of Pisa. Tipping of the Tower’s top is now about 5 m and the vertical settlement of its southern part is 3.2 m. Figure 31.2 illustrates its settlement during more than 800 years. It also presents data on changes in the weight of the structure as it was gradually constructed between 1174 and 1350. Other relevant data are given in Fig. 31.3.

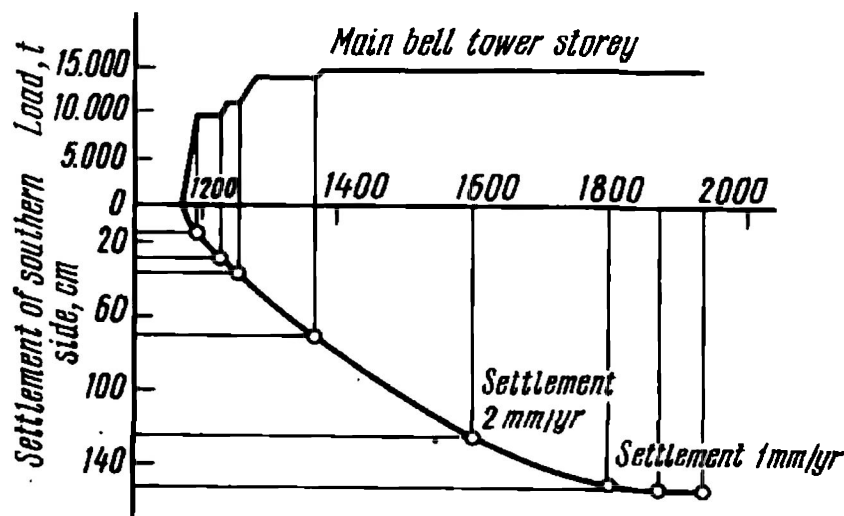


Fig. 31.2. Chart showing the settlement of the northern (higher) side of the tower since its construction and an increase in weight in the course of its lengthy construction period

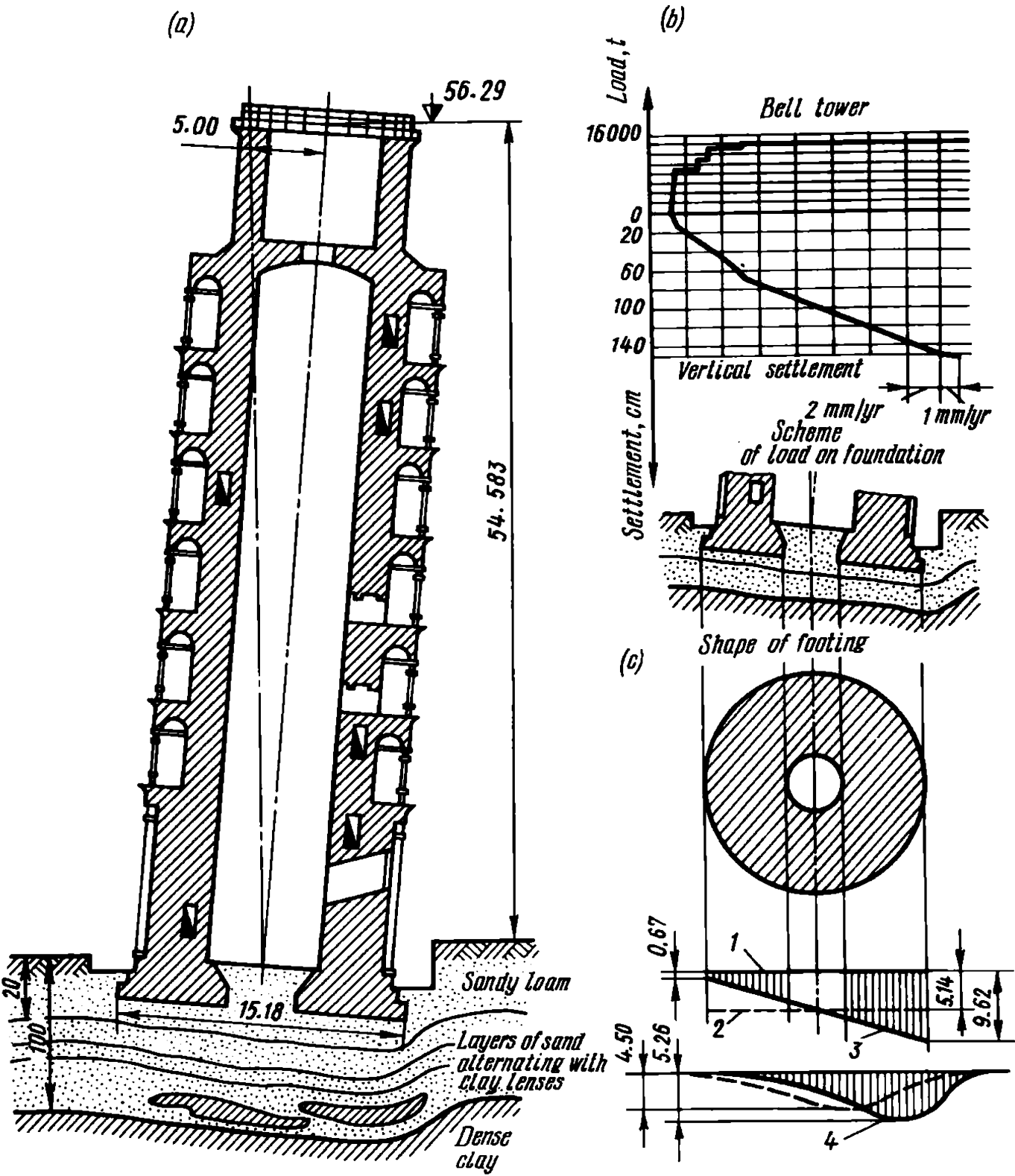


Fig. 31.3. Cross sections, probable soil conditions and pressure on the subgrade and at a depth 8 m:  
a—vertical section of the tower; b—settlement curve; c—shape of footing and load on the subgrade and at a depth 8 m

The following chapters consider in more detail the methods for taking into account rheological phenomena in construction practice. Creep types and magnitudes may differ much. In particular, the value, intensity and duration of the soil mass are its characteristics. This phenomenon, in addi-

tion, may involve the relief of the state of stress during relaxation and load-induced drop in the bearing power of clayey soils.

Sustained deformations of the foundation soil are always undesirable, especially when they are of marked magnitude and intensity. Structures we build should operate for many decades. Therefore soil creep even at a negligible rate (e.g. 5 mm/yr) may in the long run attain several tens of cm which is impermissible and may lead to failure. A typical example may be provided by the deformation of the headwork of the Dzora Hydro Power Station (Armenian SSR) which lead to its failure.

Particularly susceptible to creep are soil strata underlying statically indeterminate engineering structures. These may mainly include two-hinged bridge arches, hingeless vaults, especially multi-span structures. Such phenomena may cause disadvantageous conditions of the service of multi-storey and multi-span monolith and prefabricated constructions etc. Such deformations, if large in magnitude and differential, inevitably lead to excessive stresses in the members of such constructions, often detrimental.

Clearly, when designing a structure to be supported by a clayey soil, the likelihood of creep should be primarily considered. If such a possibility exists it is necessary to predict the pattern of the expected deformation of the subsoil and of the structure itself, i.e. its probable duration, intensity and magnitude. Finally, it is imperative that we find out if such a deformation can be tolerated or *protective* measures are needed.

The problem of the bearing capacity of clayey soils and time-dependent loss in their stability is of paramount importance whenever a clay foundation soil is involved. This is especially important if we recall examples when slopes that had for decades been stable began to creep without any visible cause.

The common cause of such soil movements was deterioration with time of clays composing the soil mass of the slopes. This factor should always be borne in mind, and knowledge is needed what the strength of soil will be with passage of time.

**Main principles of predicting soil movements.** In order to forecast creep it is invariably necessary to determine the magnitude of the time-dependent deformation  $u$ . Two versions are possible: (1) creep-induced deformation of the slope, retaining wall etc. is determined. Then it becomes necessary to forecast the magnitude of the soil creep under the particular conditions at a definite time period  $T$  of the structure's service; (2) we must determine the likelihood of creep-induced deformation of the structure being designed and the magnitude of its expected deformation by a definite time period  $T$  of its service in future.

Problems of the first type can be best solved by referring to what is known as a *phenomenological theory*. This theory calls for determinations,

by means of observations, of the value of one kind of time-dependent deformation or another of a structure (e.g. of the displacement of a retaining wall), i.e.  $u(t) = f(t)$ .

Thus, what must be done in this case is to extrapolate the experimentally determined relationship into the future. This relationship is often easy to establish, then the solution is simple. Suppose we know the rate of the displacement of the wall,  $v$ , which remains constant in time,  $v_t = \text{const.}$  The displacement of the wall  $u_T$  in the time period  $T$  will then be found from this relationship:

$$u_T = vT$$

This type of *established creep* is rare and is invariably undesirable since it is most likely to change into progressive creep. In the latter case soil failure occurs at one moment or another entailing catastrophic results.

In other more complex and more general cases deformation associated with creep has an attenuated pattern. The velocity of creep,  $v_t$ , is then nonuniform, but time-dependent, i.e.  $v = f_1(t)$ . The deformation proper also becomes time-dependent  $u_z = f_2(t)$ .

At low creep velocities it is rather difficult to experimentally determine the above relationships. The form of these relationships is frequently governed by a number of factors which makes matters more complicated.

To give an example, let us refer to the most elementary relationship proposed by Buissmann:

$$u_t = [a + b \ln t]$$

where  $a$  and  $b$  are experimentally determined parameters of the magnitude of the deformations of the structure  $u_{t_1}$  and  $u_{t_2}$  at two moments of time  $t_1$  and  $t_2$ .

As can be seen, the first problem in forecasting for a future moment  $T$ , a creep deformation whose starting moment has been established by observations, is in principle simple. An empirical formula must, however, be found to describe the creep deformation with time or its velocity.

This method of creep forecast can be applied if the foundation conditions of the structure (loading and soil properties) remain unchanged throughout the period of interest to us. Otherwise the problem becomes complicated and can be solved by referring to specified preliminary data. This version is used to forecast creep-induced deformation of a proposed structure yet to be built.

Viewed in the context of the phenomenological theory, this problem relies for its solution on experimental identification of the type of creep deformation (e.g. degree of sensitivity) allowing for the change in the intensity of loading, hereditary characteristics, aging etc. Based on these in-

vestigations, it will be finally possible to set up an empirical relationship mirroring the time-dependent character of creep deformation which enters the Boltzmann-Volterra equation as a subintegral function. To set up the above relationship, we need a number (as many as 8) of experimentally determined parameters. This is unfeasible since requisite tests involve undisturbed soil samples. Moreover, there is no unambiguous way of transferring the forecast data obtained phenomenologically from laboratory tests to the actual structure being designed.

By contrast, some advantageous features of the second of the rheological methods, physico-technical forecast of creep, become particularly apparent. This method was proposed by the author as far back as the 1930ies and has since been developed by his disciples, notably Z.M. Karaulova, basing on findings obtained in practical work.

### Sec. 31.2. Main Features of the Physico-Technical Theory of Creep Properties

This theory relies on a hypothesis of viscous soil deformation due to shearing (tangential) stresses  $\tau$ . Viscosity of clays is conditioned by their apparent cohesion  $\Sigma_w$ . As is known, cohesion is especially pronounced in soft clays. For this reason such clays are especially prone to earth movement.

From this viewpoint load-induced forces of internal friction operating on soil  $p_n \tan \varphi_w$  and of true cohesion  $c_s$  are inhibitory factors. If the shearing stresses  $\tau$  acting on the soil are of minor magnitude, the above forces may stop sliding altogether. Thus the two factors, when jointly operating and affecting the rheological properties, can be considered as a constraint on the expression of strain-induced soil yield, i.e. as a *yield point*  $\tau_{lim}$ .

The yield point which is not associated with relaxation can be described in terms of the given theory as follows:

$$\tau_{lim} = p_n \tan \varphi_w + c_s$$

The possibility and intensity of soil displacement in the particular case is governed and characterized by *the unattenuated part of the shearing stress*  $\Delta\tau$

$$\Delta\tau = \tau - \tau_{lim} = \tau - (p_n \tan \varphi_w + c_s)$$

Hence it can be seen that for forecasting the intensity of soil displacement the theory under consideration relies on general concepts familiar to the civil engineer.

*The coefficient of viscosity and the yield point mirroring the natural*



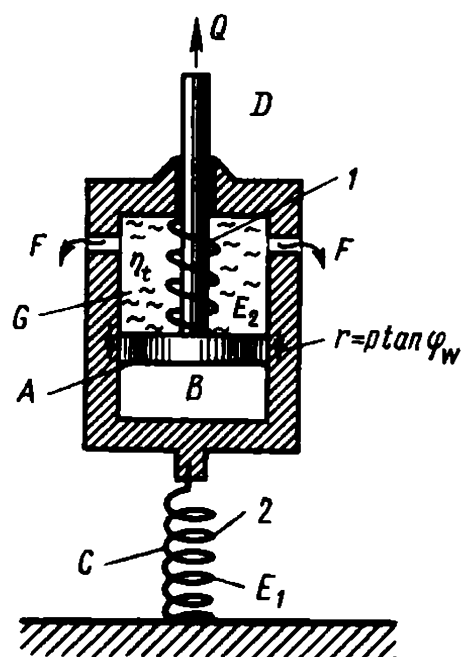


Fig. 31.4. Rheological model for testing clayey soils (proposed by N.N. Maslov in 1964):

1—spring from glass; 2—spring from soft iron

properties and state of clays in the soil mass are assumed as being characteristics of their rheological properties.

The creep property of clays is conditioned by the unique nature of pellicular water enveloping the tiniest particles that compose such soils. The pellicular water contained in the layer closest to the surface of the particle behaves as if it were a plastic solid; if it is located some distance away from that surface, as sort of pseudoplastic liquid. This pellicular water possesses a certain degree of viscosity conditioned by the origin and concentration of electrolytes saturating the pore water in such soils. The creep property is a function of the apparent cohesion  $\Sigma_w$  typical of clayey soils. It reveals itself in cumulative stresses in the soil acting on one particle group or another composing the soil which leads to rupture of tiniest bonds and to small-scale displacements in the soil mass.

The author has proposed a model (Fig. 31.4) to consider the fashion the creep property of clays and the factors of the time-dependent decrease in their strength is expressed from the viewpoint of the physico-technical theory. The model relies on those proposed earlier for Newtonian (N-liquid), Maxwellian (M-liquid) and Bingham-Schwedoff (B-Schw-liquid) viscous bodies. It bases on the familiar relationship describing the shearing strength of clays:

$$s_{pw} = p \tan \varphi_w + \Sigma_w + c_s$$

Suppose we have a cylinder *A* where a piston *B* is moved due to some causes. The cylinder is attached to the floor by means of a helical spring  $E_1$  from soft iron. The rod *D* of the piston *B* has a helical spring  $E_2$  from glass. Two small diameter apertures *F* are provided in the cylinder walls. The cylinder's upper chamber *G* is filled with a viscous liquid, e.g. heavy

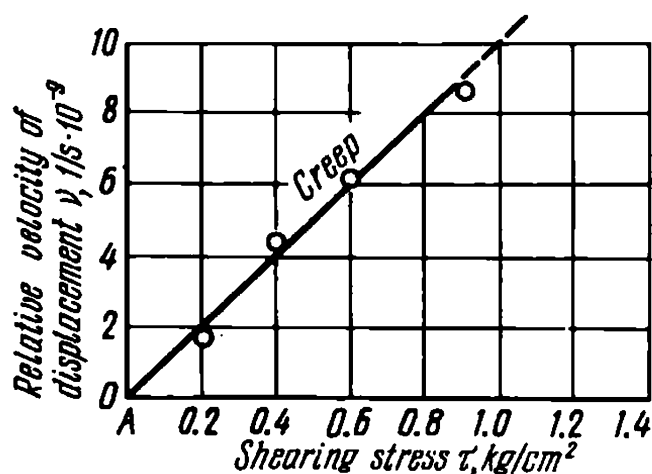


Fig. 31.5. Chart showing a relationship between the relative velocity of creep  $\nu = v_0/d$  and the shearing stress  $\tau$ :

$v_0$ —apparent velocity of displacement (cm/s);  
 $d$ —free height of sample 2.3 cm high. Moisture content is  $w = 30.3\%$ ; vertical load is  $p = 3.0 \text{ kg/cm}^2$

mineral oil. A definite pulling force  $Q$  is being applied to the entire system through the rod  $D$ . Clearly, after the force has been applied, it is immediately followed by a certain amount of deformation of the system which is primarily due to the expansion of  $E_1$  from soft iron. Depending on the magnitude of  $Q$ , this deformation may be elastic (reversible) or plastic (residual or irreversible).

Note that the piston can move in the cylinder only after  $Q$  has overcome the friction forces  $r \cdot p \tan \varphi_w$  appearing at the piston's lateral sides that are in contact with the cylinder walls as well as the resistance of  $E_2$ . Once the two resistance forces are overcome, the piston will meet with a different kind of resistance, that of the oil filling  $G$ . Clearly, other conditions being equal, the velocity of this movement will be governed by the oil's viscosity  $\eta$ , and the size of  $F$ . If the trajectory of  $B$  is appreciable, the fragile helical spring may be crushed. The initial and subsequent resistance to the movement of the piston may dramatically drop thus enhancing the pressure of the piston on the oil and more intensively squeezing it out of  $G$ . The velocity of  $B$  will naturally increase, too.

As has been shown by investigations, the forces of internal friction  $p \tan \varphi_w$  and irreversible cohesion  $c_s$  do not change with time from the mechanical viewpoint. On the other hand, the apparent cohesion  $\Sigma_w$  responsible for plasticity and viscosity of clayey soils may be regarded as some temporal fact fully revealing itself on instantaneous loading and vanishing if the soil is acted on by a sustained pressure.

Analysis of the soil's behaviour in the model in Fig. 31.5 permits the following analogies to be made:

1. The system's initial deformation due to the extension of  $E_1$  may be likened to the initial deformation of a soil, partly elastic and partly inelastic, depending on the magnitude and pattern of the load imparted to the soil (assumed instantaneous deformation).

2. The friction force  $r$  acting on the lateral surface of  $A$  may be likened

to the internal friction in a clayey soil that can change with time primarily due to fluctuations of the soil moisture content.

3. The shear viscosity of the liquid in  $G$  whose coefficient of viscosity is  $\eta_l$  can be assumed to correspond to the resistance of a clayey soil governed by the latter's apparent cohesion  $\Sigma_w$ . Clearly, both the viscosity of the soil and apparent cohesion fluctuate with alterations of the moisture content  $w$  during long periods of time due to structural changes in the soil.

4. The resistance offered by  $E_2$  may be taken as corresponding to the irreversible cohesion of the soil  $c_s$ . The soil's cohesion due to rigid and irreversible bonds may be disturbed by a definite amount of deformation of the soil. At the same time  $c_s$  may increase with time due to thixotropy and structural changes and secular degeneration of the apparent cohesion of clay to rigid bonds of true cohesion.

The above analogies and the model of behaviour of a clay acted on by time-dependent shearing stresses enabled the author as far back as 1949 to formulate the following criteria of creep properties:

(a) instantaneous failure of soil

$$\tau > p \tan \varphi_w + \Sigma_w + c_s \quad (31.1)$$

(b) creep deformation is absent

$$\tau < p \tan \varphi_w + c_s \quad (31.2)$$

(c) the soil maintains its stability throughout the service period of the structure

$$\begin{aligned} \tau &> p \tan \varphi_w + c_s \\ \tau &< p \tan \varphi_w + \Sigma_w + c_s \end{aligned} \quad (31.3)$$

concurrently satisfying the conditions of manifesting the creep properties.

The soil preserves its stability for an indefinite period, yet, due to earth movement, the irreversible time dependent cohesion  $c_s$  will be lost owing to the total drop in the soil's strength.

Thus the creep properties of clays are a function of their apparent cohesion  $\Sigma_w$  and appear only if this latter reveals itself in the behaviour of the given soil. It also seems that clays can slide under the above conditions only if the shearing stress  $\tau$  acting on it exceeds a definite value called by us a *yield point* or flow limit  $\tau_{lim}$  and determined from the relationship

$$\tau_{lim} = p \tan \varphi_w + c_s \quad (31.4)$$

The true (structural) cohesion is being treated in this particular case in somewhat broader terms as one demonstrating an irreversible character independent of its origin.

Hence a subdivision of the total cohesion  $c_w$  typical of clays into apparent and true cohesion. As has been pointed out in Chapter 13,  $c_w$  can be

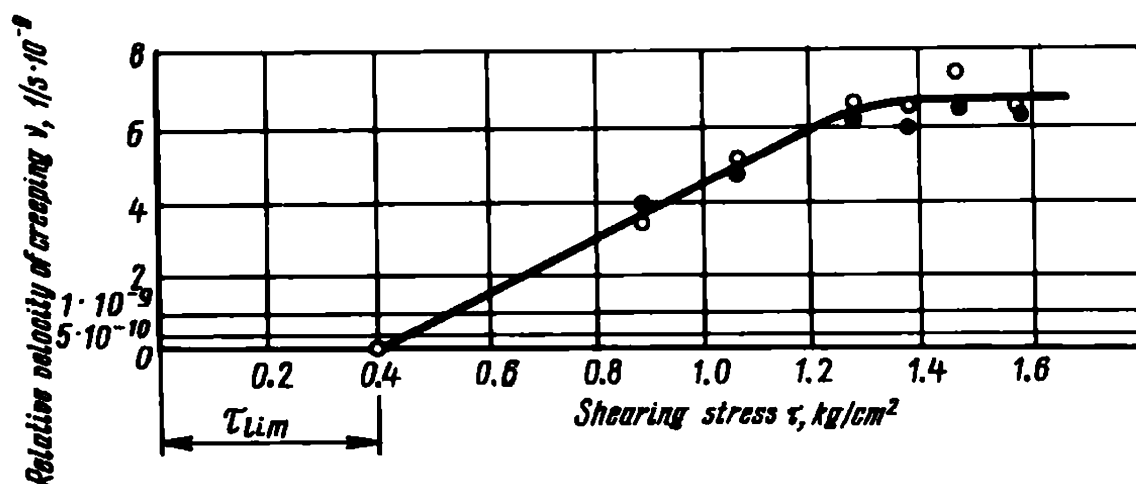


Fig. 31.6. Relative creep velocity  $\nu$  as related to the value of the shearing stress  $\tau$ . Remolded clay occurring in the Saratov region (after S.N. Sotnikov):

load is  $p = 3.0 \text{ kg/cm}^2$ ; shearing resistance is  $s_p = 2.76 \text{ kg/cm}^2$ ; height of sample is  $h = 2.5 \text{ cm}$ ; moisture content is  $w = 33\%$

subdivided by different methods including the halved sample technique.

All clays conveniently fall into three principal groups:

- (a) stiff clays ( $\varphi_w \neq 0, \Sigma_w = 0, c_s \neq 0$ );
- (b) pseudoplastic clays ( $\varphi_w = 0, \Sigma_w \neq 0, c_s \neq 0$ , or  $c_s = 0$ );
- (c) plastic clays (viscous liquid) ( $\varphi_w = 0, \Sigma_w \neq 0; c_s = 0$ ).

*Stiff clays* which mainly include cemented clay varieties of ancient origin (argillites, siliceous and marly clays etc.) manifest marked hardness and strength. A shear is a deformation typical of such soils. As to creep properties, in conformity with Eq. (31.4), such clays present no interest which fact is validated by practice.

*Plastic clays* possess quite different properties. Their strength and shearing resistance are conditioned only by  $\Sigma_w$ . These clays have water colloidal properties which are responsible for their pronounced instability.

As follows from Eq. (33.4), the yield point of plastic clays is  $\tau_{lim} = 0$ . Thus these soils may slide at slightest provocation. The pattern of deformation due to creep properties of plastic clays is shown by Fig. 31.5 illustrating the relationship between the relative creep velocity  $\nu$  (i.e. velocity referred to a unit of the free height of a sample  $d$ ) and the shearing stress for a Kinel clay sample,  $\tau$ .

The properties of *pseudoplastic clays* are intermediate between plastic and stiff varieties. Due to the internal friction ( $\varphi_w \neq 0$ ) and, sometimes, true cohesion ( $c_s \neq 0$ ) they have a definite yield point  $\tau_{lim} > 0$  in the case of earth movement. Therefore such soils can demonstrate creep properties only if the shearing stress  $\tau$  can overcome a definite resistance governed by the value of the yield point  $\tau_{lim}$ , i.e.  $\tau > \tau_{lim}$ . This shear deformation is illustrated by a diagram (Fig. 31.6) using the same coordinate system as in Fig. 31.5. Here  $\tau_{lim} \approx 0.4 \text{ kg/cm}^2$ .

At the same time, as follows from Eq. (31.4), the yield point  $\tau_{lim}$  for pseudoplastic clays is governed by the magnitude of the normal stress  $p$  being applied to the soil increasing in proportion with it. In addition, it always remains related to the angle of internal friction of the soil  $\varphi_w$ . The value of  $\tau_{lim}$  also changes with fluctuations of the soil's moisture content  $w$ . By virtue of what has been established, the yield point may be presented as follows:

$$\tau_{lim} = f(p, w \text{ and } t) \quad (31.5)$$

Clearly, the creep deformation itself can be induced by the active, unattenuated part of the shearing stress:

$$\Delta\tau = \tau - \tau_{lim} \quad (31.6)$$

or

$$\Delta\tau = \tau - (p \tan \varphi_w + c_s) \quad (31.7)$$

**Main principles of forecasting earth movement.** According to Newton, the velocity of viscous flow  $v_z$  at some depth from the surface of the deforming layer,  $D$  in thickness, in the simplest case at a constant value of the shearing stress applied to its surface and unchanged with depth and at a coefficient of soil viscosity  $\eta$  is found from this relationship:

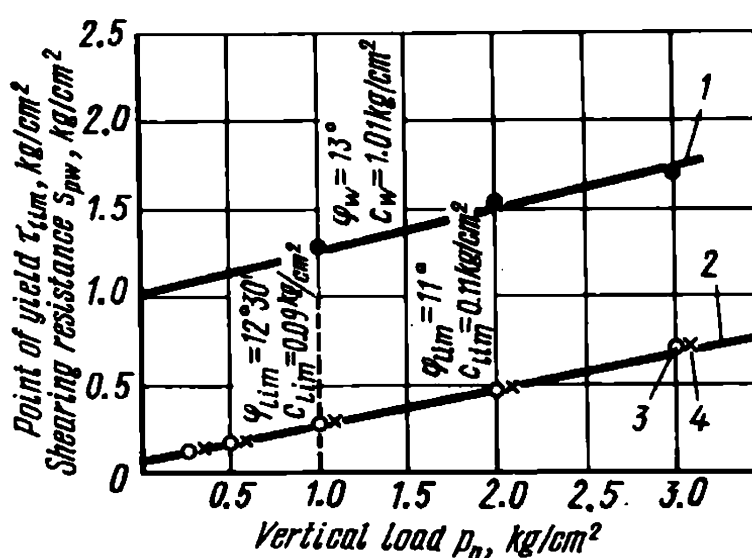
$$v_z = \frac{\tau}{\eta} (D - z) \quad (31.8)$$

It can be seen that  $v = f(\tau)$  is a linear relationship which is to a certain degree reflected in Figs. 31.6 and 31.7. Thus the velocity of the viscous flow  $v_0$  at the surface of the material with  $z = 0$  will be

$$v_0 = \frac{\tau}{\eta} D \quad (31.9)$$

Fig. 31.7. Experimental determination of the yield point  $\tau_{lim}$ . Neogene clay found in the Ukraine. The original moisture content is  $w_{orig} = 31.1$ ; the final moisture content is  $w_{fin} = 28.3\%$ :

1—tests to evaluate the shearing resistance  $s_{pw}$ ; 2—tests to find the yield point  $\tau_{lim}$ ; 3—test 4, apparatus 1; 4—test 5, apparatus 2



Under similar conditions, yet for a medium with an initial shearing resistance ( $\tau_{lim} \neq 0$ ), according to Bingham-Schwedoff, we have

$$v_z = \frac{\Delta\tau_z}{\eta} (D - z) \quad (31.10)$$

whence, by using Eqs. (31.6) and (31.7), we can write for the given case

$$v_z = \frac{\tau - (p \tan \varphi_w + c_s)}{\eta} (D - z) \quad (31.11)$$

and at the surface of the layer at  $z = 0$

$$v_0 = \frac{\tau - (p \tan \varphi_w + c_s)}{\eta} D \quad (31.12)$$

At the same time, it has been rigorously established that the coefficient of viscosity does not remain constant with time. It varies, e.g. with time-dependent density-moisture of a soil and due to colloidal processes (thixotropy and syneresis). Thus, by virtue of the relationship  $\eta_t = f(t)$ , according to N.N. Maslov, we will have

$$v_z = \frac{\tau}{\eta_t} (D - z) \quad (31.13)$$

$$v_z = \frac{\tau - \tau_{lim}}{\eta_t} (D - z) \quad (31.14)$$

By differentiating the above equations with respect to  $z$  we will have:

(a) for plastic clays ( $\tau_{lim} = 0$ )

$$dv = - \frac{\tau}{\eta_t} dz \quad (31.15)$$

(b) for pseudoplastic clays ( $\tau_{lim} \neq 0$ )

$$dv = - \frac{\tau - \tau_{lim}}{\eta_t} dz \quad (31.16)$$

These two differential equations are the principal ones in the physico-technical theory of earth movement. The yield point in all of the above equations is

$$\tau_{lim} = p \tan \varphi_w + c_s$$

The  $\tau_{lim}$  is one of the most important rheological characteristics of clays. Given the true angle of internal friction  $\varphi_w$ , true cohesion  $c_s$  of a soil, we can determine its yield point from the above relationship.

It is not uncommon that  $\eta_{lim}$  has to be established experimentally. The most convincing method for this determination is to decrease the velocity of a sample's shear to one approaching the zero value, say  $v = a \times 10^{-8}$  to  $a \times 10^{-9}$  cm/s by gradually decreasing the shearing stress applied to it at  $p = \text{const}$ . This shearing stress,  $\tau$ , is assumed as being  $\tau_{lim}$ .

Tests are conducted at several specified values of normal stresses  $p_i = \text{const}$  followed by plotting a graph (Fig. 31.7). It contains data on the test to determine  $\tau_{lim}$  of one of clay varieties as described above. The same diagram presents the results of a standard shear test of the same soil.

It is worthwhile noting that in perfect conformity to the physico-technical theory of earth movement the angles  $\varphi_w$  and  $\varphi_{lim}$  practically agree. On the other hand, the cohesion  $c_{lim}$ , in accordance with the above theory, represents only a small fraction of the total cohesion  $c_w$ . This method is especially expedient to use for testing hard and semihard clays when subdivision of  $c_w$  into  $\Sigma_{lim}$  and  $c_i$  generally yields results that are not very much reliable.

### Sec. 31.3. The Coefficient of Viscosity of Clays and Methods for Its Determination

As follows from the physico-technical theory of earth movement, apart from shearing resistance characteristics of soil ( $\varphi_w$ ,  $\Sigma_w$ ,  $c_s$ ), we must also know the coefficient of viscosity  $\eta$ .

The easiest way to determine its value is by a *method of controlled deformation* or by a heavy ball method.

The former method is this. We determine the value of the shearing stress,  $\tau_{cr}$  at which a soil sample placed in a shear test apparatus at a specified normal stress  $p$  and deformation velocity  $v_{sh} = a(10^{-5}$  to  $a \times 10^{-8})$  cm/s moves practically at constant  $\tau$ , i.e. exhibits creep properties.

With knowledge of  $\tau_{cr}$  or  $\Delta\tau_{cr}$ ,  $p$ ,  $v$  and  $d$  (free height of tested sample) we can find the value of  $\eta$  for any moment of time  $t_{exp}$  passed since the beginning of the test by using Eq. (31.9) or (31.12).

When applying the heavy ball technique proposed by Z.M. Karaulova of the Moscow Highway Engineering Institute, we establish the velocity at which a steel ball 0.5-1.5 cm in diameter,  $d$ , already half submerged, settles into the soil being tested. The velocity is artificially enhanced by applying an excess load  $P_i$  to the ball. The apparatus is mounted on a stand, a dial gauge is used for observations (Fig. 31.8).

The determination of the coefficient of viscosity is based on Stokes' law

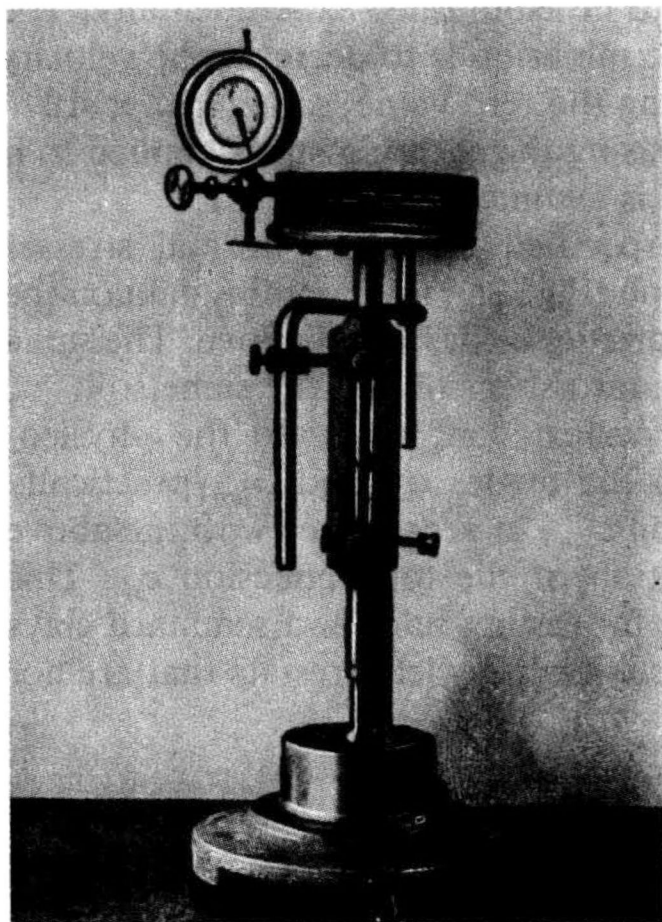


Fig. 31.8. General view of apparatus for determining the coefficient of viscosity of clayey soil by the heavy ball method (after Z.M. Karaulova)

by using the relationship

$$\eta_{St} = \frac{\rho_b - \rho_s}{18\nu} d^3 \quad (31.17)$$

where  $\rho_b$  is the apparent density of the ball;  $\rho_s$  is the soil's density;  $\nu$  is the velocity at which the ball settles into the soil.

In the given case we rely on Stokes' law which determines the velocity at which a spherical particle of a given diameter and density settles in a quiet liquid of a definite density and viscosity ( $\eta$ ).

The apparent density of the ball  $\rho_b$  is found from the formula

$$\rho_b = (P_{syst} + P_{load})/V_b \quad (31.18)$$

where  $P_{syst}$  is the weight of the entire fluid and the ball;  $P_{load}$  is the weight of the excess load (surcharge);  $V_b$  is the volume of the ball.

The quantities entering these formulae are expressed in g, cm and s. The coefficient of viscosity is expressed either as  $\eta_{St} = a \times c \times \text{g/cm}^2$  or in poises,  $\eta_p = 10^3 \eta_{St}$ .

Determinations of  $\eta$  by the method of controlled shearing deformation and by the heavy ball technique give fairly comparable results. The obtained value of  $\eta_p$  are referred to one value of moisture content or another. The



value of  $\eta_p$ , depending on the moisture content and consistency of the soil is generally found in the range  $\eta_p = a \times (10^{12} \text{ to } 10^{14})P$  increasing for hard soils to  $\eta = a \times 10^{15-16}$  or decreasing for soft soils to  $\eta = a \times 10^{11}P$  and lower.

In civil engineering the coefficient of viscosity is generally expressed in  $s \times \text{kg/cm}^2$ . This unit of viscosity is roughly  $10^6$  times greater than the physical unit of viscosity known as a poise (P) and measured in  $s \times \text{dyn/cm}^2$ .

It should be borne in mind that for converting the value of  $\eta$ , if expressed in P, the former must be increased tenfold, i.e.

$$\eta_s \times \text{kg/cm}^2 \times 10^6 = \eta_p \quad (31.19)$$

The change of the coefficient of viscosity with time  $\eta_t$  is well described by a relationship proposed by Maslov and Perzots

$$\eta_t = \eta_f - (\eta_f - \eta_{in})e^{-\mu t} \quad (31.20)$$

where  $\eta_{in}$  and  $\eta_f$  are, respectively, the initial and the final values of  $\eta$ ;  $\mu$  is a parameter characterizing the properties of the soil.

The final value of  $\eta_{fin}$  may be assumed for the time of service of the structure  $t_s$ , say, during 100 years. By using Buissmann's formula we get

$$\eta_t = (a + b \ln t) \quad (31.21)$$

which in the particular case yields

$$\eta_{fin} = (a + b \ln t_s) \quad (31.22)$$

where  $a$  and  $b$  are parameters determined for the times  $t_1$  and  $t_2$  from the curve illustrating Eq. (31.21)

$$\eta_t = f(t)$$

Knowing the values of  $\eta_{in}$  and  $\eta_f$  and allowing for  $t_1$  and  $t_2$ , we can easily find the parameter  $\mu$  by taking the log of Eq. (31.20):

$$\mu = 1/t \ln \frac{(\eta_f - \eta_{in})}{(\eta_f - \eta_t)} \quad (31.23)$$

where  $\eta_t$  is the coefficient of viscosity for the time  $t$  which is of interest to us.

#### Sec. 31.4. Long-Term Stability of Clay Slopes

Quite a number of cases have been recorded when slopes and hillsides composed of clayey soils that had been stable for decades started to slide without any apparent provocation and failed. Literature reports on

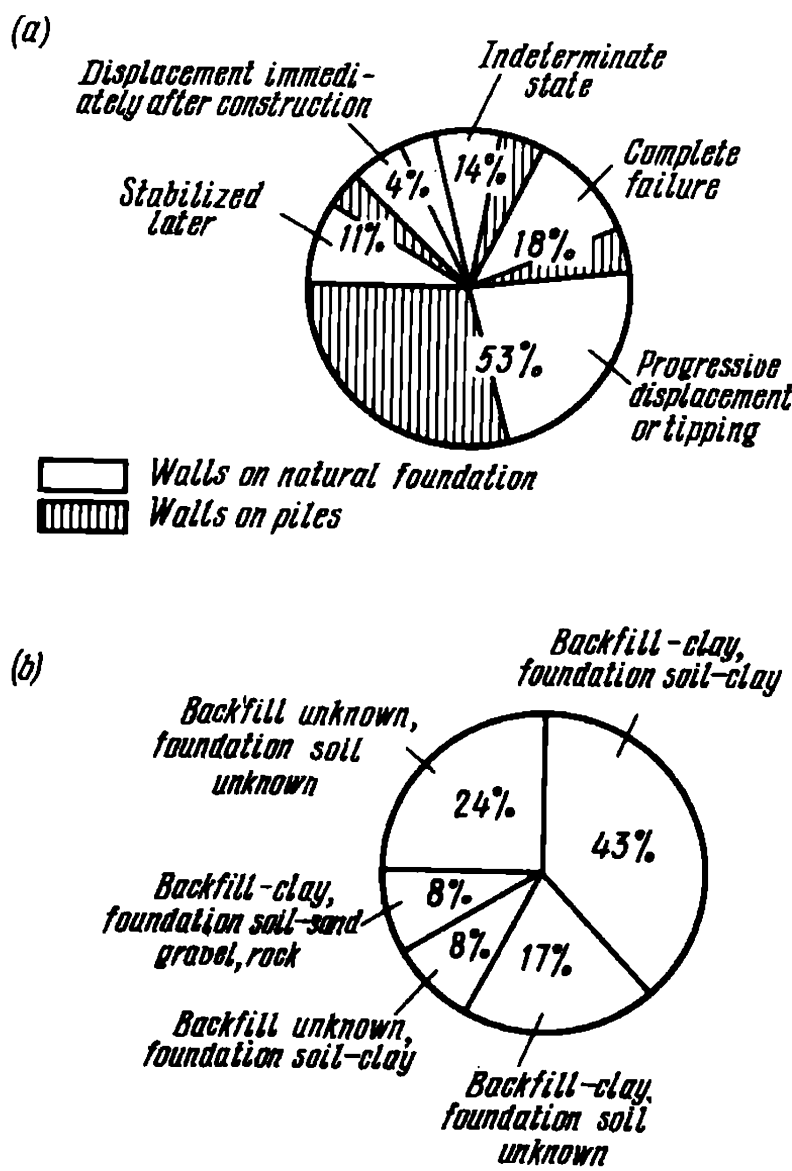


**Fig. 31.9.** Diagram illustrating soil conditions of a retaining wall (after E. Peck, USA):  
*a*—pattern of deformation; *b*—soil in foundation and in backfill of a wall which is in progressive displacement and tilting

numerous structures resting on clays which after a passage of time underwent detrimental changes leading to loss of stability. Retaining walls are of especial interest to transport facilities engineering. A number of British and American soil scientists have given detailed descriptions of these structures, including D.J. Henkel, A.W. Skempton, R.B. Peck. Failures of old retaining walls that have occurred in recent years in London deserve special attention. These walls deteriorated several decades following their construction having served fairly adequately.

In his account of the deformation and failure of one of such walls in 1941 A.W. Skempton has pointed out that during the twenty nine years of its service the bearing capacity of the clays supporting it dropped by 61%. The structure experienced continuous displacement that had been within 6 mm/yr before the failure. Immediately prior to the failure the displacement amounted to 45 cm.

Figure 31.9 illustrates very interesting facts on the mode of operation of retaining walls investigated and reported on by R.B. Peck to the Second In-

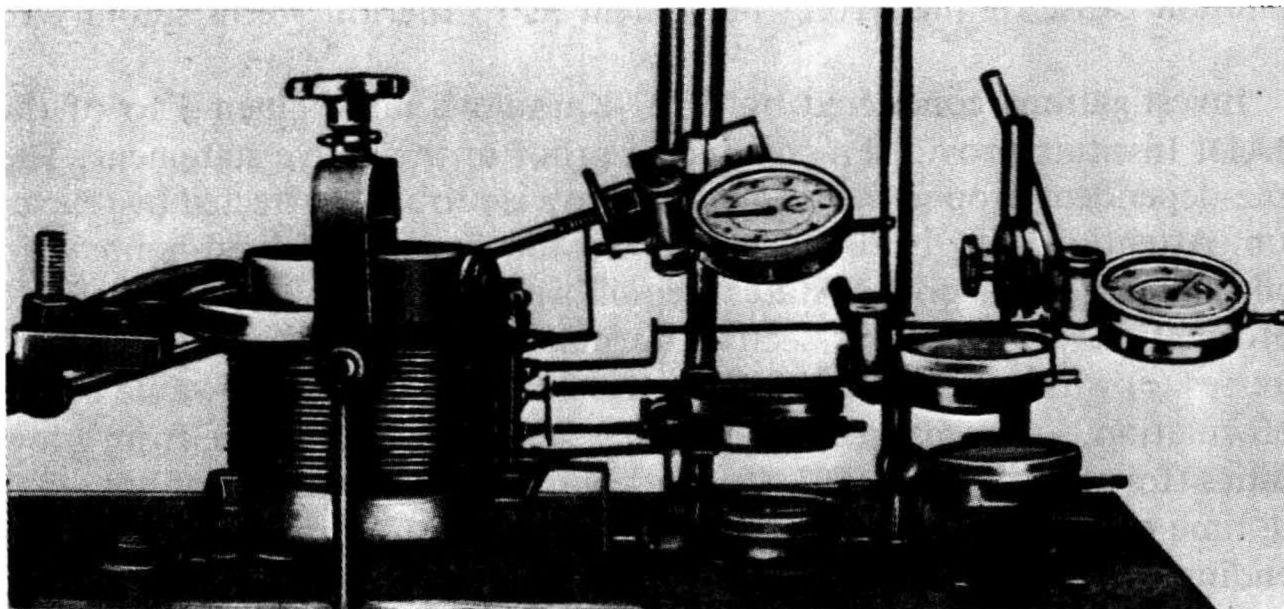


**Fig. 31.10.** General view of apparatus for slow shear tests of clayey soil samples

ternational Conference on Soil Mechanics. The role of deformation of clays in the foundations and fills of retaining walls was here especially evident. Analysis of such case histories has led to realization of the fact that the causative agents of the deformation and instability of these structures are the rheological properties of clays due to their creep properties and time-dependent loss of the bearing capacity.

Part of these structures were underpinned by piles. Practically all of them exhibited one kind of deformation or another. 18% were completely destroyed, 53% were in a state of progressive movement. A number of instances are known where bridge abutments have continuously advanced and tilted which is especially dangerous for arch-type bridges and anchor supports of suspension bridges (a bridge across the Danube in Budapest etc.).

Viewed in the context of fundamental concepts of the physico-technical theory of earth movement and its rheological criteria, the loss of the bearing capacity of clays with time is due to the disturbance of rigid irreversible bonds of true cohesion  $c$ , typical of such soils as these manifest creep properties. Special hazard is presented with time by stiff and pseudoplastic clays whose bearing capacity is largely conditioned by this irreversible part of cohesion.

At the same time the bearing capacity of plastic, to say nothing of liquid clays that do not manifest rigid irreversible bonds, on increasing their density and decreasing moisture content and due to expression of definite colloidal processes may increase in the course of soil alteration. This is especially true of remolded clays. Disregarding the above factors is the

common cause of the wrong judgement as to the long-term stability of clays.

Investigations conducted by Z.M. Karaulova and Nguen Tho of the MADI Institute provided a convincing proof of the above statement. The time-dependent drop in the stability of clays is probably affected by relaxation. Attention must be drawn to the fact that rupture of rigid bonds  $c_s$  in soil as it passes to a critical state of equilibrium occurs following a definite deformation  $\gamma$  of its cross section normal to the direction of tangential stresses ( $\tau$ ) within the depth of the active zone  $D$ . The critical value of the deformation,  $\gamma_{cr}$ , measured in per cent, is generally in the range from a few unities (for stiff clays) to 20% (for soft plastic clays). It is also of note that the time of yield is determined only by the value of  $\gamma_{cr}$  and may vary depending on the rate of the deformation  $\nu$ .

To conclude, Fig. 31.10 presents the general view of an apparatus for slow shear tests of clay samples of increased height. The sample is placed in a rubber sleeve to prevent it from dessication during lengthy tests and is protected from being crushed by a set of metal rings.

---

## Chapter 32

### Rheological Phenomena. Their Role in Performance of Retaining Structures

---

#### Sec. 32.1. Classification Schemes

The structures that are acted on by great lateral pressures include retaining walls supporting soil masses, back-filled bridge abutments, arch-type bridge piers and anchor supports of suspension bridges. Bridge piers may sometimes sustain appreciable horizontal pressure (up to 100 t) due to the action of drifting ice fields and impacts of vessels. The urgency of the problem as applied to bridge piers is substantiated by numerous examples of horizontal movement, say, of some of bridges in Moscow and Kineshma.

When evaluating the degree of stability of a structure acted on both by vertical and horizontal (shearing) pressures we must always take into account a likely loss of stability of a structure due to lateral displacement or sinking into the soil (Fig. 32.1).

A *horizontal shear* (translational or shallow slide), generally occurs as advance over a more or less plane surface of sliding often coincident with the contact of the subgrade and the foundation base (Fig. 32.1a).

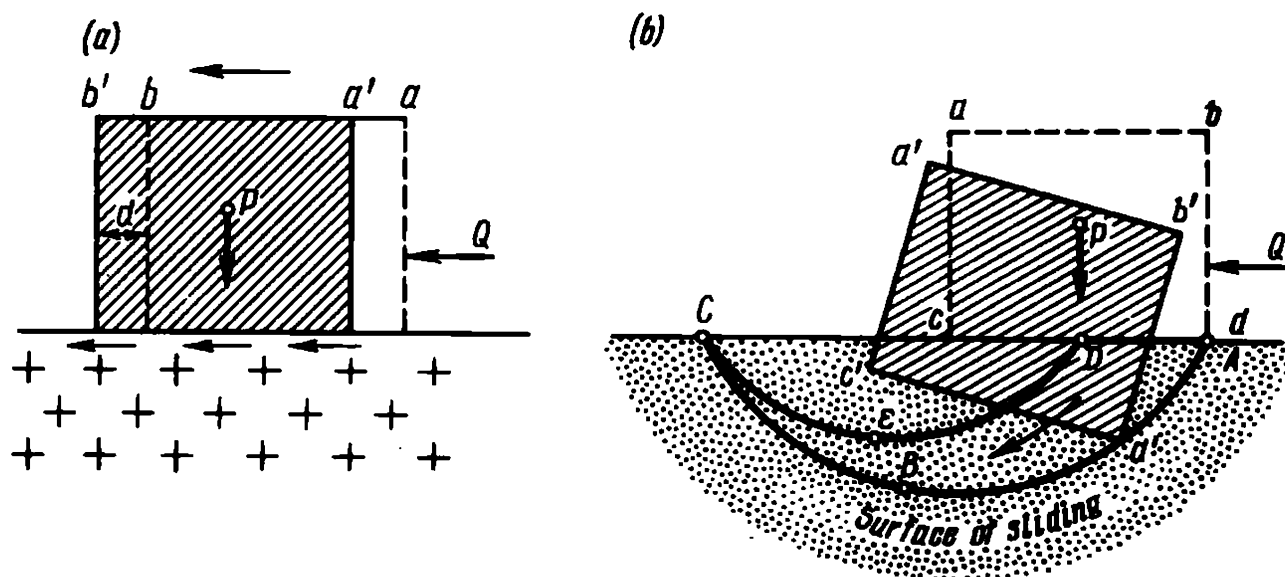


Fig. 32.1. Diagram illustrating displacement of a retaining structure:

$a$ —shallow slide;  $b$ —deep slide

This type of displacement typically takes place at fairly low vertical loading and relatively great shear pressure applied to a structure which has a rather large footing (factor  $2b$  — the effect of the width of a foundation or structure).

A rotational or deep slide. In the case of *sinking into the ground*, as the term suggests, the structure sinks into the ground, tilts and slides along a curvilinear or more complex surface of sliding, say,  $ABC$  or  $ADEC$  (Fig. 32.1*b*). The structure foundation slides and the structure deforms conspicuously. The surfaces of sliding penetrate into the soil mass, therefore earth pressure comes into play. As a result, earth movement occurs along a lubricated soil surface ("earth slides along earth"). The decisive role is here played by the total shearing resistance of the soil both due to friction forces and cohesion (apparent and true) of the soil. The shape of the surface of sliding is conditioned by the size and weight of the structure, by the foundation conditions and bearing capacity as well as the character of the load being applied.

Unlike the translational slide the rotational slide generally occurs if the foundation soil has low bearing capacity and sustains an excess dead load (weight of the structure). The following conditions are responsible for the deep slide and the fashion in which it takes place. A vertical force  $P$  applied to the subsoil of the structure produces shearing stresses  $\tau_p$  in the foundation soil. Shearing stresses  $\tau_Q$  induced by a shearing force  $Q$  are superposed on  $\tau_p$ . This decreases the shearing resistance of soil which is responsible for a curvilinear relationship  $\tau_{curv} = f(p)$ . All these processes lead under given conditions to a deep slide.

Where the structure is being acted on by  $Q$ , the shearing strains  $\tau_p$  and  $\tau_Q$  are differently directed. Since they attenuate each other, the stability of soil increases. Under definite conditions this results in a complicated pattern of the curve of sliding (line  $ADEC$  in Fig. 32.1 *b*), and the slide occurs in part along the plane of the structure foundation. It appears that we are witnessing here an intermediate form between a translational and a deep slide.

If  $P$ , and, consequently,  $p$ , are appreciable, the stresses  $\tau_p$  may prove so conspicuous as to rule out the shearing resistance of the soil. As a result the structure will not be able to sustain a horizontal force  $Q$  of any magnitude without marked deformation.

Both the translational and deep slide are generally followed by catastrophic events, so care must be taken to avoid the possibility of such deformation from the very start.

There may be two forms of a translational slide:

(1) *a contact slide* generally occurring along the subgrade of a structure if the subsoil is composed of sufficiently hard and dense rocks with relatively high bearing capacity;

(2) *a slab slide*, earth movement of generally minor thickness of a soil with low stability (e.g. soft plastic clay) incorporated in a mass of more stable soils.

All structures with shallow footings and acted on by horizontal loads must necessarily be tested for translational slide. The test is easy and at the same time very instructive.

Let us consider the general case of such a test (Fig. 32.2). A structure the area of the footing of which is  $\omega = 2b \times 2a$  transmits a vertical load  $P$  to the foundation soil. Concurrently it is acted on from above and from beneath by the shearing forces  $Q_{up}$  and  $Q_{down}$ . These forces may be induced by the water pressure upstream or downstream, earth pressure, outward thrust of arch span structures, pull by ropes of massive anchor supports of suspension bridges, braking forces etc.

Suppose that  $Q_{up} > Q_{down}$ . Thus there exists a possibility of a translational slide of the structure along its subgrade  $AA$  to the left as viewed in Fig. 32.2 when part of the structure is below the soil water level and the water table. This results in uplift pressure acting on the base of the structure with a resultant  $U$ . The depth of the foundation of the structure on the upper and lower sides is, respectively,  $h_{up}$  and  $h_{down}$ . Hence it follows that the shearing forces acting on the upstream side are augmented by the active earth pressure  $E_{a, up}$  transmitted to the upstream face of the foundation of the structure. Earth pressure imparted to the downstream face of the foundation prevents displacement of the structure and is in the given case passive earth pressure ( $E_{p, down}$ ).

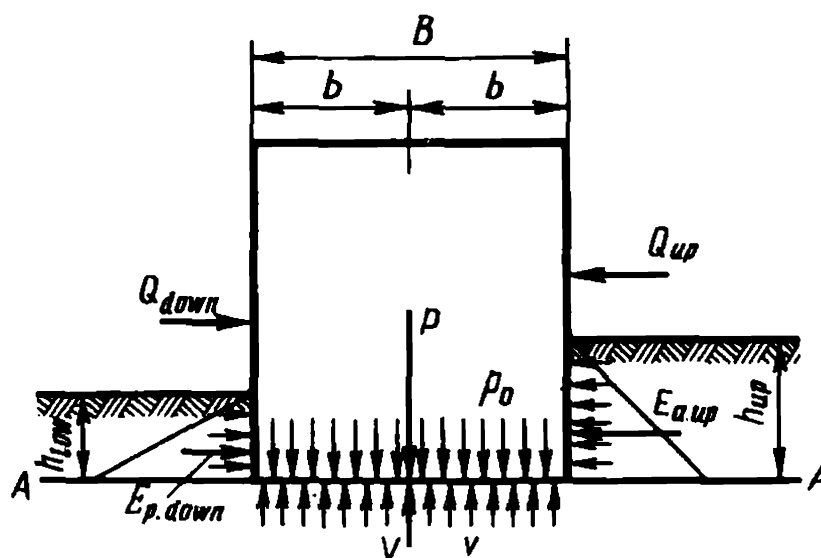


Fig. 32.2. Diagram for checking stability of a retaining structure to a shallow slide

The evaluation of the shearing strength of the structure involving a likely shallow slide along  $AA$  consists in the determination of the value of the safety factor  $k_{sl}$  found from the relationship

$$k_{sl} = R/S \quad (32.1)$$

where  $S$  are active shearing forces acting on the structure;  $R$  are passive forces.

In the particular case we have

$$S = (Q_{up} - Q_{down}) + (E_{a,up} - E_{p,down})$$

$R$  is composed of:

(a) friction forces  $T$  appearing beneath the structure taking into account, wherever necessary, uplift pressure:

$$T = (P - U) \tan \varphi$$

(b) cohesion forces  $C$  of the soil over the contact area  $\omega$  at the structure base or footing or, when testing for a slab slide, cohesion in the sliding slab:

$$C = \omega c$$

Thus the total shearing resistance of the structure will be

$$R = T + C = (P - U) \tan \varphi + \omega c$$

A substitution of the values of  $S$  and  $R$  into Eq. (32.1) finally yields

$$k_{sl} = \frac{(P - U) \tan \varphi + \omega c}{[Q_{up} - Q_{down}] + [E_{a,up} - E_{p,down}]} \quad (32.2)$$

When testing a structure for resistance against a translational slide along a relatively deeply occurring intercalation, the normal stress cor-

responding to the dead load  $P$  in Eq. (32.2) must be corrected for the weight of the soil mass between the structure base and the intercalation, i.e.  $P_p$ :

$$P_p = P + \omega h_{int} \rho_w$$

where  $\omega$  is the area of the base of the structure;  $h_{int}$  is the depth of occurrence of the design intercalation below the base of the structure;  $\rho_w$  is the bulk density of the soil.

The backpressure  $U$  in Eq. (32.2) must be taken in this computation at the foot of the incompetent layer.

If the latter is overlain by a fairly thick overburden, the magnitudes of passive and active earth pressure  $E_{a.up}$ ,  $E_{p.down}$ ,  $E_{a.down}$  are determined from a graph in Fig. 32.2 and Eq. (32.2) taking into account the design depths:

$$\begin{aligned} h_{up.des} &= h_{up} + h_{int} \\ h_{d.des} &= h_{down} + h_{int} \end{aligned}$$

Differently speaking, the computation is referred to the level of the roof of the incompetent layer.

If it is desired to consider the possible role of rheological factors in the operation of retaining structures in more detail, it will be recalled that for the simplest case (vertical back face, horizontal backfill, absence of load, absence of friction along the contact surface  $AA$  back wall — backfill material) the diagram of active earth pressure with the height of the wall appears as a triangle  $bcd$  (Fig. 32.3a). For cohesionless soils ( $c = 0$ ) this pressure at a depth  $z$  from the surface of the backfill will be found from the relationship

$$p_x = p_z \xi$$

or

$$p = \rho z \tan^2 (45 - \varphi/2) \quad (32.3)$$

where  $\xi$  is the coefficient of lateral or active earth pressure designated as  $E_a$ .

The coefficient  $\xi$  corresponds to a state of limiting equilibrium. For this state, generally called a state of plastic equilibrium, between the principal stresses  $p_1$  and  $p_2$  Rankine's equation (20.18) is valid

$$\sin \varphi = \frac{p_1 - p_2}{p_1 + p_2}$$



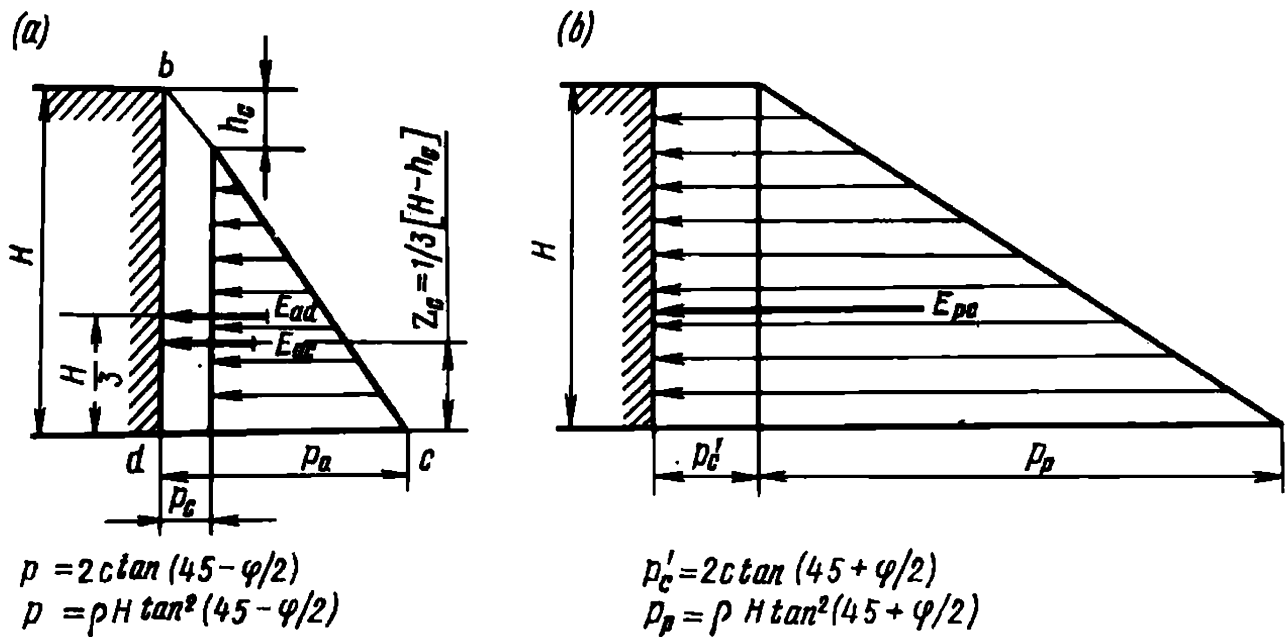


Fig. 32.3. Diagram showing active ( $E_a$ ) and passive ( $E_p$ ) earth pressure on a retaining wall for cohesionless ( $c = 0$ ) and cohesive ( $c \neq 0$ ) soils:

$a$ —active pressure;  $b$ —passive pressure

A solution of this relationship with respect to  $p_2$  yields

$$p_2 = p_1 \frac{(1 - \sin \varphi)}{(1 + \sin \varphi)}$$

or

$$p_2 = p_1 \frac{(\sin 90^\circ - \sin \varphi)}{(\sin 90^\circ + \sin \varphi)}$$

Following elementary trigonometric transformations, by using relationships for the difference and sum of sin angles, we get

$$p_2 = p_1 \cot(45^\circ + \varphi/2) \tan(45^\circ - \varphi/2)$$

or

$$\xi = \frac{p_2}{p_1} = \tan^2(45^\circ - \varphi/2)$$

The stresses at the foot of a wall  $H$ , in height, i.e. with  $z = H$ , are equal to

$$p_x = p_a = \rho H \tan^2(45^\circ - \varphi/2) \quad (32.4)$$

At the same time the resultant of this pressure  $E_a$  for the whole of the wall applied at  $1/3$  of the height from the foot, being the area of the

triangle  $bcd$ , will be found as

$$E_a = (\rho H^2/2) \tan^2 (45^\circ - \varphi/2) \quad (32.5)$$

The magnitude of the back pressure or total passive pressure  $E_p$  for the same conditions will be

$$E_p = (\rho H^2/2) \tan^2 (45^\circ + \varphi/2) \quad (32.6)$$

The cohesion of the soil acts to decrease the unit active earth pressure  $p_a$  on the wall at any point of its height by the value  $p_c$  equal to

$$p_c = 2c \tan (45^\circ - \varphi/2) \quad (32.7)$$

After a few transforms we can obtain the following formulae for determining the total active  $E_{a.c}$  and total passive pressure  $E_{p.c}$  on a wall,  $H$  in height, taking into account soil cohesion:

$$E_{a.c} = \frac{1}{2} \rho H^2 \tan^2 (45^\circ - \varphi/2) - 2c \left[ H \tan (45^\circ - \varphi/2) - \frac{c}{\rho} \right] \quad (32.8)$$

$$E_{p.c} = \frac{1}{2} \rho H^2 \tan^2 (45^\circ + \varphi/2) + 2cH \tan (45^\circ + \varphi/2) \quad (32.9)$$

After comparing these two equations with Eqs. (32.5) and (32.6) let us rewrite these as follows:

$$E_{a.c} = E_a - 2c [H \tan (45^\circ - \varphi/2) - c/\rho] \quad (32.10)$$

$$E_{p.c} = E_p + 2cH \tan (45^\circ + \varphi/2) \quad (32.11)$$

As is known, the values of  $E_a$  and  $E_p$  are determined from the areas of the corresponding diagrams of triangles of earth pressure acting on the wall. As follows from Eqs. (32.10) and (32.11), the total pressures  $E_{a.c}$  and  $E_{p.c}$  are obtained by subtraction from or addition to the triangles of pressure  $E_a$  and  $E_p$  of rectangles whose areas are determined by the second terms of these relationships (Fig. 32.3).

The operation conditions on the back face of a retaining structure become involved if the structure is underlain by cohesionless and insufficiently dense soils, especially when they are submerged and if the structure in hand is likely to be acted on by dynamic loads, say, induced by seismic events. As has been demonstrated, sandy soils may then liquefy, losing all internal friction forces between particles. If such conditions obtain, the backpressure of earth found from Eq. (32.6) will drastically decrease attaining the limiting value of the active pressure of a heavy fluid with a unit density  $\rho$ , i.e.

$$E_p = E_a = \rho \frac{H^2}{2}$$

The operation of a retaining wall becomes especially complex if it rests on clay and supports a clay slope.

Analysis of structures under investigation has demonstrated that earth backpressure  $E_{p.down}$  acting on the back face can take place only if the back face of the structure foundation exerts pressure on the soil. Therefore, for the total backpressure  $E_{p.down}$  to come into play, the structure may move horizontally. Moreover, whenever soils composing the foundation demonstrate marked compressibility, a load acting on the soil within the zone of  $E_{p.down}$  compresses the soil, thus decreasing the shearing effect of the structure and, accordingly, the magnitude of backpressure. To sum up, a definite, sometimes conspicuous displacement of the structure is needed so that the total magnitude of  $E_{p.down}$  may be exhibited. The possibility of such displacement is generally avoided.

It should also be kept in mind that in contradistinction to formulae determining active earth pressure, when referring to formulae of passive earth pressure assuming a plane surface of sliding the results are often very much exaggerated compared with real values. The error is greater the larger is the angle of internal friction of the soil. So, for  $\varphi = 16^\circ$  the error is only 15-20%, whereas for  $\varphi = 30^\circ$  it amounts to 100% etc.

This is why it is customary to use for calculations not  $E_{p.down}$  but active earth pressure operating on the back face of the structure  $E_{a.down}$  with all reservations presented in what follows.

### Sec. 32.2. Rheological Properties of the Foundation Soil of Retaining Walls

When designing a retaining wall supported by clay the first step is to determine its long-term stability taking into account the long-term stability of the material in contact with the wall. Then determine under what conditions the soil will demonstrate its creep properties.

It will be recalled that the total cohesion of clays ( $c_w$ ) is determined by the relationship

$$c_w = \Sigma_w + c_s$$

where  $\Sigma_w$  is cohesion of a water colloidal character involving irreversible bonds;  $c_s$  is rigid structural cohesion with irreversible bonds.

It would be expedient to introduce into analysis that follows a coefficient of sliding  $F_p$  found in the general case from the relationship

$$F_p = \tan \varphi + c/p \quad (32.12)$$

By taking into account the generally assumed subdivision of the total

cohesion  $c_w$  we will have

$$k_{sl} = \frac{PF_p}{[E_{a.up} - E_{p.down}]} \quad (32.13)$$

where  $P$  is the weight of the retaining wall. Then we can write

$$F_p = \tan \varphi_w + \frac{\Sigma_w + c_s}{p_n} \quad (32.14)$$

The normal pressure for a plane case for 1 m of the length of the footing of a retaining wall with the width  $B$  is found from the relationship

$$p_n = \frac{P}{B \times 1}$$

A substitution into Eqs. (32.13) and (32.14) yields

$$k_{sl} = \frac{P \left[ \tan \varphi_{wf} + \frac{\Sigma_{wf} + c_{sf}}{p_n} \right]}{E_{a.up} - E_{p.down}} \quad (32.15)$$

The letter  $f$  in the subscripts of  $\varphi_{wf}$ ,  $\Sigma_{wf}$  and  $c_{sf}$  indicates that these constants characterize soils in the foundation of the retaining wall and are needed for evaluation of the total stability of the structure. Since soils in the foundation of the retaining wall and in the backfill differ, let us denote the constants of the latter by a letter "b" (for backfill).

Viewed from the standpoint of the physico-technical theory of earth movement, the rheological soil conditions, in conformity with the aforementioned creep criteria, are governed by the conditions of implementation of the total cohesion of the soil ( $c_w$ ) including the apparent cohesion ( $\Sigma_w$ ) and true (structural) cohesion ( $c_s$ ). In addition, the true angle of internal friction is invariably taken into account ( $\varphi_w$ ).

If the problem is approached in this fashion and Eq. (32.15) operates with one kind of soil characteristic or another, always including  $\varphi_w$ , it is convenient to handle the following values of the factor of safety against sliding of the retaining wall:

1.  $k_{\varphi c_w}$  — to denote the degree of the total stability of the structure without allowing for the time factor, i.e. concurrently using the total cohesion for calculations  $c_w = \Sigma_w + c_s$ .

2.  $k_{\varphi \Sigma_w}$  — to evaluate the conditions of stability of the structure with

forces of apparent cohesion  $\Sigma_w$  of the soil coming into play excluding the true cohesion  $c_s$  disturbed during soil deformation.

3.  $k_{\varphi c_s}$  — same, taking into account the true cohesion  $c_s$ , yet excluding forces of  $\Sigma_w$ .

4.  $k_{\varphi}$  — same, excluding from calculations cohesion forces ( $c_w = 0$ ) and taking into account internal friction forces only ( $\varphi_w$ ).

When using these characteristics for analysis viewed in terms of fundamentals of the physico-technical theory of earth movement and with invariable in time earth pressure from the side of backfill ( $E_a = \text{const}$ ) the conditions of operation of the retaining wall will be as follows:

at  $k_{\varphi c_w} \geq 1.0$  the wall will possess a definite and, possibly, excessive (viewed from the economical standpoint) margin of safety;

at  $k_{\varphi c_w} < 1.0$  the wall will not have sufficient margin of safety and will collapse during operation; remedial measures are needed;

at  $k_{\varphi c_s} > 1.0$  the wall has an appreciable margin of safety which eliminates a possibility of earth movement ( $\tau < \tau_{lim}$ );

with  $k_{\varphi c_w} > 1.0$  but concurrently with  $k_{\varphi c_s} < 1.0$ , i.e. under conditions of mobilization of cohesion forces, the wall has a definite margin of safety but will operate in conditions of likely earth movement;

at  $k_{\varphi \Sigma_w} > 1.0$  and concurrently with  $k_{\varphi} < 1.0$  the stability of the wall is guaranteed but with inevitable earth movement;

at  $k_{\varphi} > 1.0$  stability of the wall is guaranteed in all cases without creep deformation.

If creep deformation is not excluded, soil stability may decrease with time due to disturbance of rigid bonds of true cohesion  $c_s$ . Under such circumstances it may drop to zero. Clearly, stability of the structure will not then be guaranteed. In such cases and whenever displacement of a wall is undesirable, remedial measures must be taken. These may include increasing the width of the base or replacing the backfill material by another, more competent one.

If the backfill is a soil likely to lose its stability with time under conditions of continuous displacement of the wall due to rupture of rigid bonds of true cohesion, the magnitude of  $E_a$  should be determined differently. If the backfill includes excessively compressed soils, continuous displacement of a wall causes decompression of the soil which loses its strength both due to decreased total cohesion  $c_w$  and decreased angle of internal friction. Things are different when we deal with a change in pressure on the wall acted on by the sand backfill. Excessive compression of the backfill sand leads to excessive pressure on the wall which decreases as it is displaced to a definite limit.

### Sec. 32.3. Forecasting a Translational Slide of a Retaining Wall with Time

Under definite conditions it is allowable to have a retaining wall displaced within definite limits of its attenuation or duration magnitude.

Our investigations have demonstrated (1958) that for approximate forecast of the phenomena under consideration involving generally occurring problems of translational slides one may well use the equations proposed by Newton (for plastic clays) and by Bingham and Schwedoff (for pseudoplastic clays) as ones fairly adequately describing earth movement in actual conditions. According to Bingham and Schwedoff, we have Eq. (31.10)

$$v_z = \frac{\Delta\tau_{zx}}{\eta} (D - z)$$

where  $\Delta\tau_{zx}$  is the active (unattenuated) part of the shearing stress appearing on a horizontal unit area at a depth  $z$  beneath the base of the foundation of a structure induced by a uniformly distributed tangential load  $q$ ;  $\eta$  is the coefficient of viscosity of the clay;  $D$  is the thickness of the active zone of the soil subjected to shear and taking part in earth movement;  $v_z$  is the velocity of the movement at a depth  $z$ .

As follows from Chap. 31,

$$\Delta\tau_{zx} = \tau_{zx} - \tau_{z\lim} \quad (32.16)$$

where  $\tau_{zx}$  is the shearing stress on a horizontal unit area at a depth  $z$ ;  $\tau_{z\lim}$  is the yield point at a depth  $z$ .

The value of  $\tau_{zx}$  can be found from a relationship proposed by us in 1934:

$$\tau_{zx} = \frac{2q}{\pi} \left( \arctan \frac{b}{z} - \frac{bz}{z^2 + b^2} \right) \quad (32.17)$$

where  $b$  is half of the structure's width imparting to the soil a uniformly distributed shearing stress.

At the same time, by virtue of Eq. (32.4), for a horizon at  $z$  we can write

$$\tau_{z\lim} = (p_0 + \rho_b z) \tan \varphi_b + c_s \quad (32.18)$$

where  $p_0$  is the vertical pressure on the subgrade;  $\rho_b$  is the bulk density of the soil taking into account its buoyancy. The stress  $p_z$  in Eq. (32.18) is assumed to be constant and equal to  $p_0$  owing to a generally limited thickness of the active zone  $D$ .

The thickness of  $D$  is found assuming  $\Delta\tau_{zx} = 0$  since then  $v_z = 0$  (see Eq. 31.10) and at a depth  $z$  no creep deformation of soil occurs. By virtue



By integrating this relationship we obtain a formula for determining the velocity of the displacement of the structure supported by pseudoplastic clays:

$$v_0 = \frac{D}{\eta} \left\{ \left[ \frac{2q}{\pi} \arctan \frac{b}{D} \right] - \left[ \left( p_0 + \frac{\rho_b}{2} D \right) \tan \varphi_w + c_s \right] \right\} \quad (32.22)$$

It can be seen from this example that, other conditions being equal, the velocity of the displacement dramatically increases with increasing the size of the structure ( $2b$ ).

The velocity of the displacement of a structure resting on plastic clays is found from the relationship

$$v_0 = \frac{1}{\eta} \frac{2qD}{\pi} \arctan \frac{b}{D} \quad (32.23)$$

This formula is a particular case of Eq. (34.22). It is obtained by substituting here of values of  $\varphi_w = 0$  and  $c_s = 0$  which is characteristic of plastic clays.

Eqs. (32.22) and (32.23) for forecasting the velocity of displacement of a retaining structure are valid for a relatively rare case where the soil's viscosity remains constant with time. Gradual attenuation of the structure's displacement occurs much more commonly. It appears that this process is due to the compression of the soil acted on by the weight of the structure (settlement) as well as to essentially important events typical of colloidal systems (thixotropy, syneresis, colloidal aging etc.).

If such conditions obtain, the civil engineer needs knowledge of the velocity and magnitude of a possible displacement of the structure during a number of years with varying values of  $\eta$  of clays with time, i.e. with  $\eta_t = f(t)$ , where  $t$  is time. As is known, the velocity of earth movement,  $v$ , for a definite moment of time,  $t$ , is measured by a quantity which is a time-dependent derivative of the path travelled. In the given case

$$v = \frac{d\lambda}{dt} \quad (32.24)$$

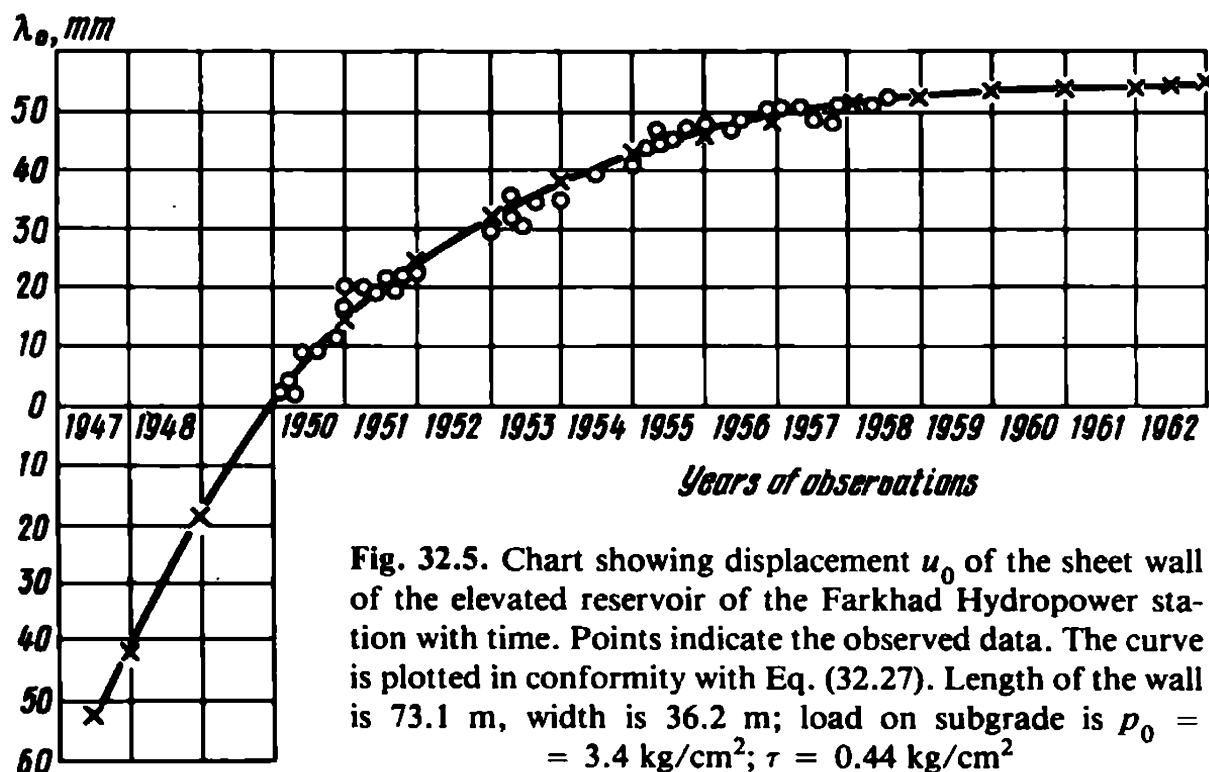
where  $\lambda$  is displacement (sliding) of the structure.

Consequently,

$$\lambda = \int v dt \quad (32.25)$$

After substituting into this equation the value of  $v_0$  from Eq. (32.22) and inserting here, in turn, the values of  $\eta_t$  in conformity with Eq. (31.20)





we can write

$$\lambda = \int D \left\{ \left[ \frac{2q}{\pi} \arctan \frac{b}{D} \right] - \left[ \left( p_0 + \frac{\rho_b}{2} D \right) \tan \varphi_w + c_s \right] \right\} \frac{dt}{\eta_f - (\eta_f - \eta_{in})e^{-\mu t}} \quad (32.26)$$

After evaluating the integral and finding a constant of integration following from the condition that at  $t = 0$  the value of displacement is also zero, we finally obtain this relationship for determining the possible displacement of the structure being acted on by a horizontal pressure in time  $t$ :

$$\lambda = D \left\{ \left[ \frac{2q}{\pi} \arctan \frac{b}{D} - \left( p_0 + \frac{\rho_b}{2} D \right) \tan \varphi_w + c_s \right] \right\} \times \left\{ \frac{t}{\eta_f} + \frac{1}{\mu \eta_f} \ln \frac{\eta_f - (\eta_f - \eta_{in})e^{-\mu t}}{\eta_{in}} \right\} \quad (32.27)$$

The problems considered above are essential for bridge construction whenever the horizontal pressures transmitted to a structure must be attenuated in the soil or rock mass. Such structures primarily include backfilled bridge abutments.

Figure 32.5 demonstrates the pattern of increased displacement of a retaining structure with a time-dependent increase in the coefficient of



$\varphi$ , angle of internal friction. A triangle of forces is constructed for each slip prism, the direction of the reaction of wall remaining unchanged ( $E_{a.up}$  is directed at an angle  $\varphi_0$  to the normal of the back face of the wall). As to the reaction of the stable part of the soil  $R_i$  acting at an angle  $\varphi$  to the normal of the trace of the surface of sliding, it varies depending on the value of  $\alpha$ . It is best to arrange all plotting as shown in Figure 32.6, measuring out forces  $Q_1$  from one common point.

Such a diagram enables the maximum  $E_{a.up}$  to be easily found. In fact, the sides of the triangles of forces  $S_1V_1$ ,  $S_2V_2$  represent the values of active earth pressure  $E_{a.up}$  transmitted to the retaining wall that correspond to different angles of inclination of the surface of sliding. By connecting points  $V_1, V_2, V_3 \dots$  by a smooth line we obtain a curve of change in earth pressure  $E_{a.up}$ ;  $E_{max}$  will be found by drawing a tangent line to the curve obtained parallel to  $Q$  and by measuring, to the scale of forces, a segment  $SV$  drawn through the point of tangency parallel to force  $E$ .

Certainly, the above methods are far from reflecting the multitude of problems concerned with the operation and calculation of retaining walls. Some of the reported data only suggest pathways to applications of rheological analysis of retaining structures when designing them.

**A deep slide.** Based on theoretical premises and assumptions of one kind or another, soil scientists have proposed different methods for determining stability of structures acted on by a horizontal (shearing) load  $H$  that may lead to a deep slide.

*A method of circular-cylindrical surface of sliding* (Fig. 32.7) has become the most popular in construction for the given purposes.

As can be seen, a circular-cylindrical surface of sliding  $ABDE$  occurs at some depth in the subsoil of the structure. Due to the action of forces imparted to the foundation of the structure, this latter, together with part of its subsoil moves to the left rotating in a clockwise direction about a central point  $O$ . This is accompanied by rotation of a certain amount of the foun-

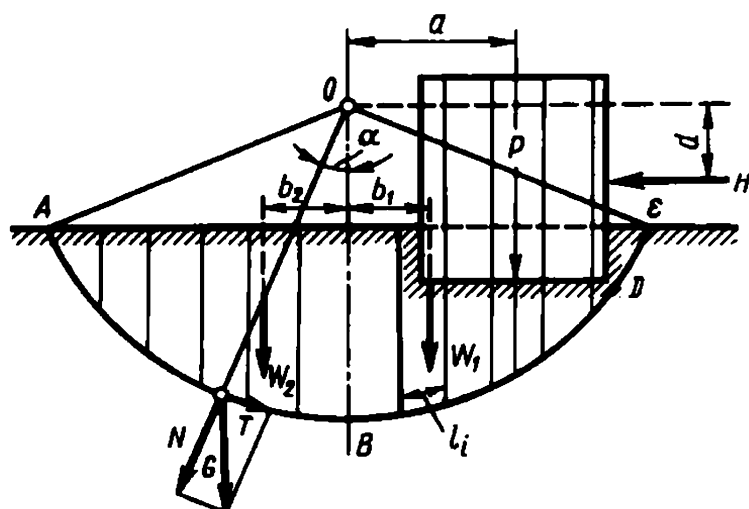


Fig. 32.7. Diagram for evaluation of stability of a retaining structure by the method of circular cylindrical surface of sliding

dation soil assumed as being one solid body together with the structure. It is further assumed that none of the elements composing this volume of soil mutually shift. Then the line of sliding will be determined by an arc of a circle of radius  $R$  and centre  $O$  invariably passing through a point  $D$  in the base of the structure.

The method basically is to determine the minimum value of the factor of safety margin  $k_t$  corresponding to the specified conditions and loads. The factor of safety against sliding is then found by dividing the sum of moments  $M_{res}$  of all forces of passive or active earth pressure by the sum of moments of all shearing forces acting on the slip prism ( $M_{sh}$ ):

$$k_t = M_{res}/M_{sh} \quad (32.28)$$

As has been already noted, resisting and shearing moments are referred to the central point  $O$  of the arc of sliding. When determining *the active forces* one must take into account the dead load  $P$ , horizontal pressure  $H$ , sustained by the structure and transmitted to its foundation, and, in the general case, the weight of the soil mass  $W_1$  and  $W_2$  in the slip prism allowing, whenever needed, for uplift pressure.

*The passive forces* that must be taken into account when determining  $M_{res}$  include friction forces  $T$  appearing at the surface of sliding under the action of the dead load and weight of the soil, and also cohesion forces  $C$  acting at the surface of sliding. These latter are determined by the value of cohesion  $c$  inherent to the particular soil and the length of the segment of the surface of sliding,  $l_i$ , intercepting the given layer.

To determine the values, points of application and lines of operation of active earth pressure poses no problem. The frictional forces  $T$  preventing displacement of the rebound prism and acting along the surface of sliding at the interface between the displacing body and the soil mass remaining stable are found for each of the individual blocks into which the rebound prism is deliberately separated. This condition follows from the curved shape of the surface of sliding.

The frictional force  $T_i$  for each of such blocks is found from the relationship

$$T_i = N_i \tan \varphi_i = G_i \cos \alpha_i \tan \varphi_i \quad (32.29)$$

where  $G_i$  is the weight of the particular block of soil;  $N_i$  is a normal component of the weight of the soil;  $\alpha_i$  is the angle of inclination of the surface of sliding to the horizontal referred to a tangent at the centre of the base of the block; the angle  $\alpha$  is numerically equal to that between a vertical through the centre of the curve of sliding and the radius vector  $R$  of the arc of sliding dropped to the point of tangency;  $\varphi_i$  is the angle of internal friction of soil at the particular segment of the surface of sliding.

In the general case a surface or line of sliding may intersect several layers demonstrating different shearing resistance. This fact is taken into consideration by introducing the requisite values of  $\varphi$  and  $c$  when determining  $T_i$  in different blocks.

In conformity with what has been said above the cohesion forces  $C$  developing at the arc of sliding are composed of individual forces acting along the surface of sliding within the segment intercepted by this latter with cohesion  $c_i$ . If we define the length of sliding within the given block as  $l_i$ , we can find the total resistance due to cohesion for the entire arc of sliding:

$$C = \Sigma c_i l_i \quad (32.30)$$

If the soil mass is homogeneous,  $C$  can be found from a simpler relationship

$$C = cL \quad (32.31)$$

where  $L$  is the total length of the arc of sliding being a sum  $\Sigma l_i$ .

Thus the moment of resistance can be represented as follows:

$$M_{res} = \Sigma G_i \cos \alpha_i \tan \varphi_i R + \Sigma c_i l_i R \quad (32.32)$$

The right-hand side of this equation includes the radius of the surface of sliding  $R$  being an arm of action of friction  $T_i$  and cohesion  $C_i$  forces applied to the surface of sliding relative to the centre of sliding,  $O$ .

The moment of the active forces,  $M_{sh}$ , is found from this relationship:

$$M_{sh} = Pa + Hd + \rho V_1 - \rho V_2$$

where  $a$  and  $d$  are arms;  $\rho V_1$  is the weight of the prism  $W_1$ ,  $W_2$ .

It is often the case that the ground surface is assumed true level when dealing with such problems. Then the gravitational forces of the soil prism  $W_1$  and  $W_2$  are equal and symmetrical about a vertical through  $O$ . Therefore their moments with respect to  $O$  are mutually balanced. Then for  $M_{sh}$  we have a simpler relationship

$$M_{sh} = Pa + Hd \quad (32.33)$$

Then the relationship for determining the factor of safety against sliding takes on this form:

$$k_t = \frac{\Sigma G_i \cos \alpha_i \tan \varphi_i R + \Sigma c_i l_i R}{Pa + Hd} \quad (32.34)$$

In this and above equations the quantities  $a$ ,  $d$  and  $R$  are arms of forces of one type or another with respect to the centre of the arc of sliding,  $O$ . The location of  $O$ , and, consequently, position and curvature rate of the

arc of sliding are determined by repeated calculations proceeding from the least value of the factor of safety, that is, from conditions in which their position is the least advantageous.

When using Eq. (32.34), we have to take into account the dead load minus the weight of the soil removed from the excavation pit in accord with the principle: "any structure penetrating into the soil loses in weight as much as the soil removed". This permits complete symmetry needed. A structure's stability is considered as being ensured if the factor of safety against sliding is  $k_f = 1.25$  to  $1.50$  (depending on the kind of the structure in hand).

In this computation rheological properties of clays must be allowed for as outlined in Chap. 31. For example, if slides must be prevented, we must disregard apparent cohesion of clays  $\Sigma_w$  when evaluating the total cohesion  $c_w$  since we must ensure that  $k_{c_s} > 1$ . Methods for forecasting a time-dependent displacement of structures for the case of a deep slide have not as yet been elaborated.

As can be seen, the proposed technique is simple in principle and convincing which has been validated by experimental results and extensive use in actual construction work. This technique proves especially efficient when the structure of the subsoil is erratic involving layers of different index properties. At the same time it is not free from some limitations conditioned by assumptions made in the initial calculation scheme.

---

## Chapter 33

### Rheological Events. Their Effect on Settlement of Structures

---

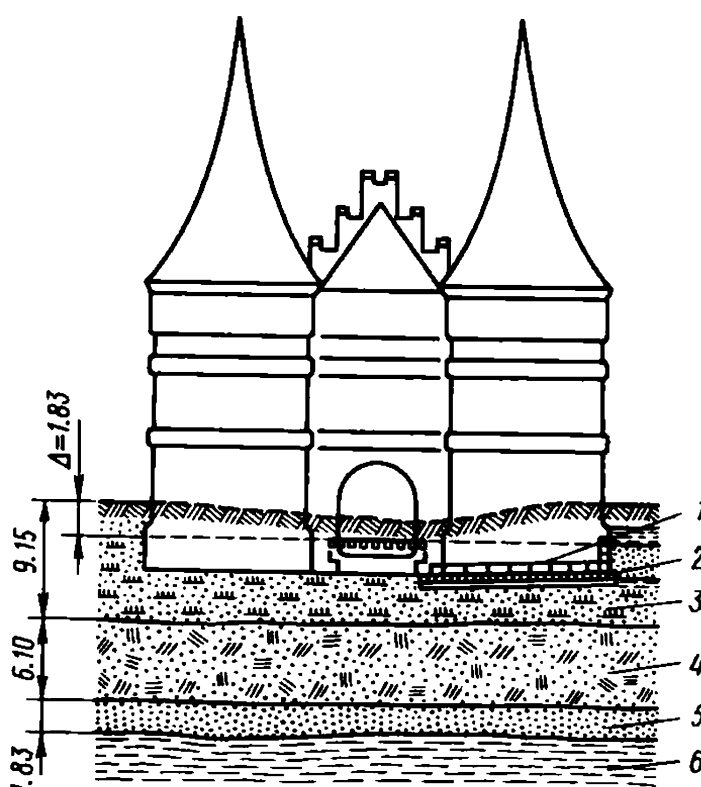
#### Sec. 33.1. Introduction

In fairly recent past the settlement of structures in a two-dimensional case was considered to be due only to the compression of the underlying soil strata induced by the joint action of compressive normal stresses ( $p_z$  and  $p_x$ ). Generally long periods taken by settlement were generally ascribed to the slow rate of consolidation of clays that have very small values of the coefficient of permeability.

Analysis of the settlement of structures is at present extended. It is believed that important factors of the ultimate settlement under definite

**Fig. 33.1.** Diagram illustrating settlement of the Holstentor in Lübeck

1—granite blocks; 2—wooden raft foundation;  
3—swamp soil; 4—peat deposit; 5—alluvial  
sand deposit; 6—competent marl bed



conditions are tangential or shearing stresses and deformations they cause. Viewed from this standpoint, continuous settlements, taking sometimes decades or even centuries (let us recall the Leaning Tower of Pisa) thus become understandable.

The settlement of the Holstentor, a monument of architecture in Lübeck (Fig. 33.1) is of interest. This monument, 500 years old, has settled 180 cm and is still continuing to settle. Other examples can be cited.

It is not uncommon that such continuous and marked settlements lead to catastrophic failures. The failure of a grain elevator (see Fig. 16.3) is a typical illustration. This structure exerting a load  $p_0 = 2.5 \text{ kg/cm}^2$  on the foundation soil (plastic clays with moisture content 34 to 46%) was supported by a thick reinforced concrete raft foundation located 3.25 m below the surface. The settlement had been in progress for a long period of time, yet failure was instantaneous.

The possible role played by rheological events in settlement of each particular structure can in principle be determined by successive calculations by referring only to the total cohesion ( $c_w$ ), only to the true cohesion  $c_s$ , apparent cohesion ( $\Sigma_w$ ), only to the angle of internal friction  $\varphi_w$ , by establishing when necessary the factors of safety  $k_{c_w}$ ,  $k_{c_s}$ ,  $k_{\Sigma_w}$ , and, finally,  $k_{\varphi}$ . These coefficients are found by using one formula or another determining the critical load  $p_{cr}$ . For example, use can be made of Eq. 28 proposed by the SNiP Civil Engineering Code of Practice (cf. Eq. 21.13) depending on the load on the soil and design of the structure ( $p_s$ ).

Thus for the general case we have  $k_{\varphi c_w} = p_{cr}/p_s$ . Calculations are then made as usual. In particular,  $k_{\varphi c_s} > 1.0$  ensures long-term stability of a structure ruling out earth movement. If  $k_{\varphi c_s} < 1.0$  and  $k_{\varphi c_w} > 1.0$ , that is, if the soil has an apparent cohesion,  $\Sigma_w$ , displacement occurs that may be followed by rupture of rigid bonds of true cohesion. Finally, if  $k_{\varphi \Sigma_w} > 1.0$  and concurrently  $k_{\varphi} < 1$  the total stability of a structure ensured within definite limits may be followed by continuous settlement.

It should be pointed out that these problems, especially concerning forecasts of time-dependent settlement under conditions of earth movement proposed at present for particular cases need further elaboration.

### Sec. 33.2. A Particular Case of Forecasting Settlement of a Structure on Unsaturated Soil\*

Let us assume that the subsoil of a structure composed of clays rules out a forecast of settlement when the coefficient of permeability is much less than unity (say,  $G < 0.60$ ). To evaluate the likely settlement of a structure experimental data must be available obtained by a slow soil test, that is,  $e_{p_0} = f(t)$ .

In the given case  $e_{p(t)}$  is the modulus of compressibility, that is, the relative compressive soil deformation under load  $p$  expressed in per mil ( $\text{‰}$ ) determined in time  $t$  by laboratory tests and field experiments using loaded plates via the modulus of deformation  $E_{p(t)}$  from the following relationships:

under laboratory conditions

$$e_{p(t)} = 1\,000 \frac{\Delta h(t)}{h_{\text{sample}}} \quad (33.1)$$

for field tests

$$e_{p(t)} = 1\,000 \frac{p}{E_{p(t)}} \quad (33.2)$$

$$s_{pl} = \frac{\omega p_0 B}{E_{p(t)}} (1 - \mu^2) \quad (33.3)$$

where  $s_{pl}$  is the settlement of the loaded plate;  $\omega$  is the coefficient of the shape generally taken equal to 0.75;  $p_0$  is a load on the plate;  $B$  is the side of the loaded plate;  $\mu$  is the coefficient of lateral deformation (strain), pseudoequivalent of Poisson's ratio. In most cases  $\mu = 0.25$  to  $0.30$ .

---

\* After N.N. Maslov and K.T. Kajamanov.



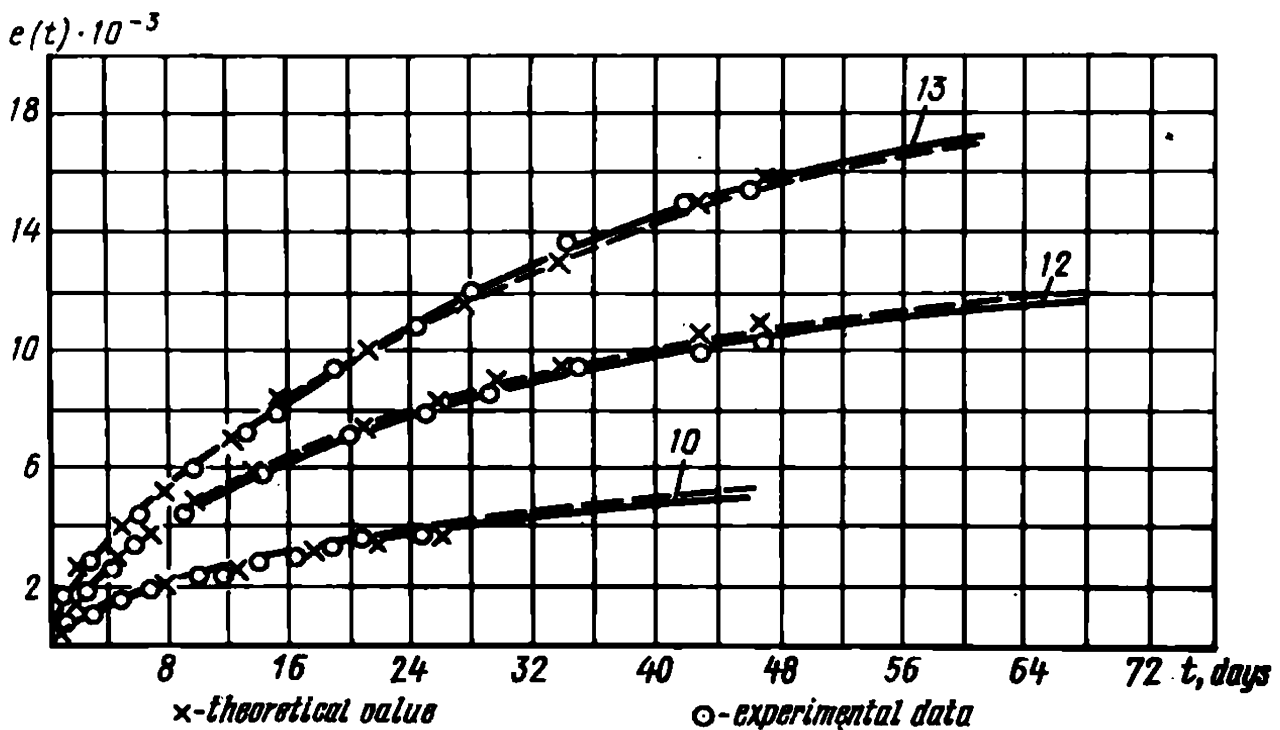


Fig. 33.2. Chart showing experimentally obtained (solid lines) and theoretical (dashed lines) curves of relative creep deformation  $e_t$  with time  $t$ :  
10, 12, 13—sequence numbers of tests

Figure 33.2 is a chart showing the  $e_{p(t)} = f(t)$  relationship representing curves plotted from the experimental data and empirical relationships of the exponential function type

$$e_{p(t)} = Mt^m \quad (33.4)$$

By differentiating this equation with respect to time  $t$ , we obtain a new formula for describing the relative soil compression rate induced by the dead load

$$\dot{e}_{p(t)} = \frac{de_{p(t)}}{dt} = Mmt^{(m-1)} \quad (33.5)$$

It is also known that

$$\dot{e}_p = p/\eta_t \quad (33.6)$$

or

$$\eta_t = \frac{p}{Mmt^{(m-1)}} \quad (33.7)$$

The last formula makes it possible to determine, through the function of  $e_{p(t)} = f(t)$ , the coefficient of soil viscosity for any period of time  $t$  including that for the initial time moment ( $t = 0$ ), that is,  $\eta_{in}$ .

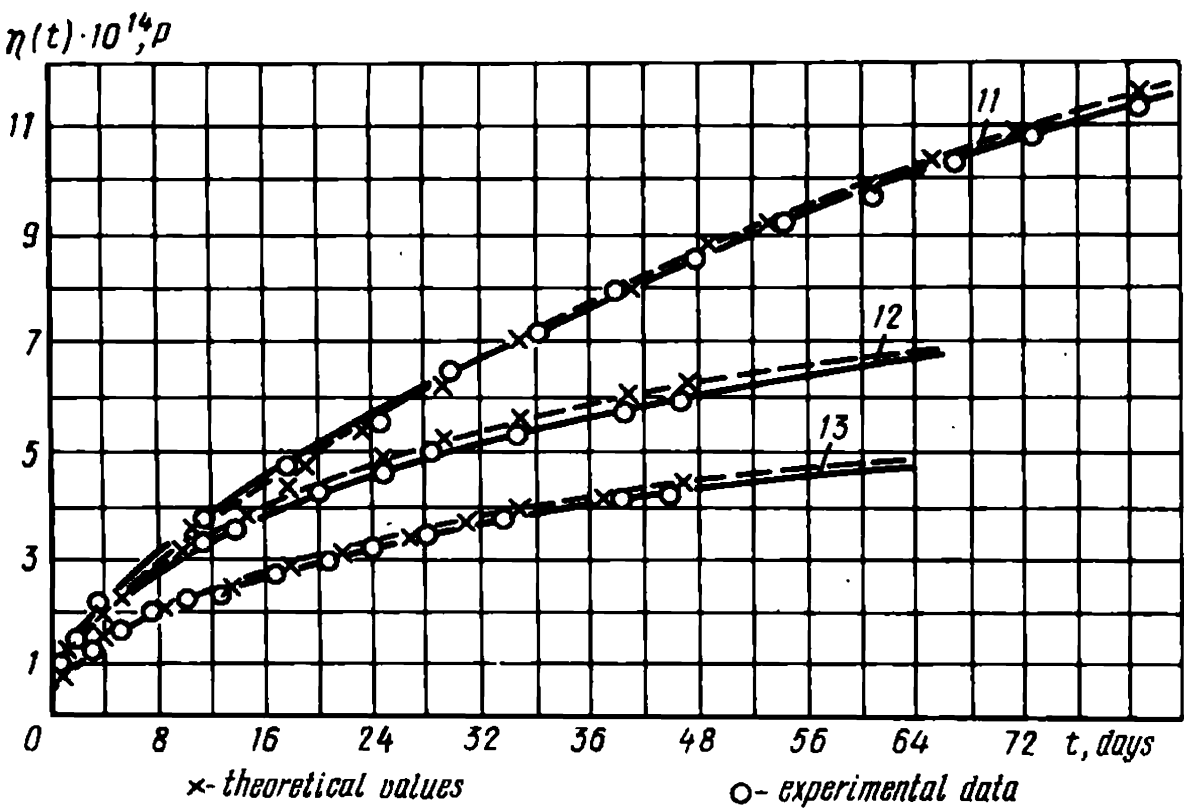


Fig. 33.3. Chart illustrating approximation of alteration of the coefficient of viscosity  $\eta_t$  with time  $t$  by using Eq. (33.7):  
11, 12, 13—sequence numbers of tests

Further analysis for describing the time-dependent change of the coefficient of viscosity, that is,  $\eta_t = f(t)$ , uses the familiar relationship

$$\eta_t = \eta_{fin} - (\eta_{fin} - \eta_{in})e^{-\mu t} \tag{33.8}$$

This relationship for a particular case is diagrammatically shown in Fig. 33.3.

By virtue of Eqs. (33.6) and (33.8) we can write

$$\frac{de(t)}{dt} = e_p = \frac{p_{des}}{\eta_{fin} - (\eta_{fin} - \eta_{in})e^{-\mu t}} \tag{33.9}$$

By integrating this relationship over an interval from 0 to  $t$  we obtain Eq. (33.10) to describe the  $e_{p(t)}$  relationship as a time-dependent function in this form:

$$e_{p(t)} = p_p \left\{ \frac{t}{\eta_{fin}} + \frac{1}{\mu_{fin}} \ln \left[ \frac{\eta_{fin} - (\eta_{fin} - \eta_{in})e^{-\mu t}}{\eta_{in}} \right] \right\} \tag{33.10}$$

This relationship can be used to determine the value of the modulus of compressibility of soil (subsidence)  $e_p$  with time  $t$  if the coefficient of viscosity varies,  $\eta_t = f(t)$ .

Under such conditions the time-dependent structure settlement will be

described by a relationship known from the general theory of forecasting settlement of structures:

$$s(t) = \int_0^D e_{p_z}(t) dz \quad (33.11)$$

The variation of the modulus of compressibility is taken here into account not only as a function of time  $t$  but also as that of the change of the normal stress  $p_z$  with depth  $z$  according to the law of distribution. Clearly, for this we must have as the integrand element under the integral sign to be solved over an interval from 0 to  $D$  (active zone) the value of the vertical normal stress  $p_{z\ des}$  as a function of the thickness of the soil mass, that is,  $p_{z\ des} = f(z)$ , in conformity with Eq. (33.10).

There are several methods of solving this problem. To simplify matters and extend its use can be made of the method of Brinch-Hasen (cf. Chap. 27) which permits this relationship to be expressed in a simple form for definite three-dimensional cases. To illustrate, let us use the Brinch-Hasen solution for a square loaded area of the surface of the soil mass:

$$p_z = p_{des} \frac{B^2}{(B + z)^2}$$

Then we can write this integral relationship to determine the time-dependent settlement of a structure, that is,  $s(t) = f(t)$ :

$$s(t) = \int_0^D \frac{B^2}{(B + z)^2} p_{des} \left\{ \frac{t}{\eta_{fin}} + \frac{1}{\mu \eta_{fin}} \times \right. \\ \left. \times \ln \left[ \frac{\eta_{fin} - (\eta_{fin} - \eta_{in}) e^{-\mu t}}{\eta_{in}} \right] \right\} dz \quad (33.12)$$

By integrating it over the above interval we finally obtain

$$s(t) = p_{des} \frac{BD}{B + D} \left\{ \frac{t}{\eta_{fin}} + \frac{1}{\mu \eta_{fin}} \ln \left[ \frac{\eta_{fin} - (\eta_{fin} - \eta_{in}) e^{-\mu t}}{\eta_{in}} \right] \right\} \quad (33.13)$$

Clearly, the pattern of increasing and attenuating of the settlement  $s(t)$  will be mainly conditioned by an increase with time of the coefficient of viscosity  $\eta_t$ .

### Sec. 33.3. The General Case

The Soviet scientists N.A. Tsytovich, S.S. Vyalov, S.R. Meschan, Yu.K. Zaretsky, Z.G. Ter-Martirosyan et al. have proposed special methods and formulae to forecast the qualitative and quantitative

magnitudes of rheological events and, in particular, creep deformations in the settlement of structures. These methods are based on the familiar concept of the nature of what is called the secondary branch of a compression curve. Thus only one of the aspects of the problem is being considered here, that of earth movement due to normal stresses on *the sine qua non* condition of time-dependent attenuation of settlement.

The author believes this phenomenon is of paramount importance in deformations of structures induced by shearing stresses invariably appearing in the subsoil under the action of the dead load. In this, the soil shearing resistance is taken into account. Such analysis does not rule out detrimental development of the phenomenon with time. This is what makes the present approach distinctly different from those proposed by the aforementioned scientists.

Since the role of rheological phenomena in settlements of structures is poorly understood use has currently to be made of approximate methods. One of these relies on the following principles.

1. Rheological events may affect the settlement of a structure increasing it with time if the subsoil is composed of clays with creep properties and due to the drop in the compressive resistance of the subsoil to the normal stresses as a result of disturbance of the soil structure and slow squeezing out of the soil from beneath the structure induced by tangential stresses.

2. The above events may occur in the subsoil of a structure only in regions of creep deformation, that is, only if the shearing stresses at any points in such regions exceed the yield point, viz.,  $\tau > \tau_{lim}$ .

3. The value of the yield point must be established experimentally or by referring to Eq. (31.4):

$$\tau_{lim} = p_n \tan \varphi_w + c_s$$

4. The velocity of creep deformation at any point in the subsoil of the structure is ascertained from the value of the factor of safety against sliding by referring to the relationships:

$$k'_{sl} = \frac{\tau_{lim}}{\tau} \quad (33.14)$$

or

$$k_{sl} = \frac{p_n \tan \varphi_w + c_s}{\tau} \quad (33.15)$$

Clearly, if  $k_{sl} > 1.0$  creep deformation (earth movement) at the given point is unlikely, and vice versa.

5. The most unfavourable ratio between the normal and shearing stresses at a point in the subsoil is established, depending on the strength of the soil, allowing for the angle of inclination  $\Theta$ . As reported in Chap. 20,

the most disadvantageous orientation of an elementary area passing through a point in a strained medium is determined by the relationship

$$\delta = (45^\circ \pm \Theta_{max}/2)$$

or, in the limiting state,

$$\delta = (45^\circ + \varphi/2) \quad (33.16)$$

where  $\delta$  is the angle between a normal to the elementary area and the principal stress as the line of action of the major principal stress  $p_1$ . Following from the above conditions, Eq. (33.15) will take on this form:

$$k_{ssl} = \frac{p_{n\delta} \tan \varphi_w + c_s}{\tau_\delta} \quad (33.17)$$

where  $p_{n\delta}$  and  $\tau_\delta$  are normal and shearing stresses appearing in the subsoil in a state of stress in an elementary area through the particular point and oriented as described above.

The easiest way to determine  $p_{n\delta}$  and  $\tau_\delta$  for elementary areas with the angle of orientation  $\delta = (45^\circ + \varphi/2)$  is via the principal stresses  $p_1$  and  $p_2$  appearing in the loaded soil mass (see Eqs. 17.6, 17.7, and also 20.26c and 20.26d).

By taking into account the weight of the soil mass (bulk density  $\rho$ ), true cohesion  $c_s$  as the respective apparent depth of the foundation  $h_s = c_s/(\rho \tan \varphi_w)$  and possible foundation depth  $h_d$  in conformity with Eq. (20.26e) for determining the coefficient of creep deformation we can finally write

$$k_{ssl} = \frac{[(p_1 + p_2) + 2\rho(z + h_d + h_s) + (p_1 - p_2)\cos^2(45^\circ + \varphi/2)]\tan\varphi_w + 2c_s}{(p_1 - p_2)\sin 2(45^\circ + \varphi/2)} \quad (33.18)$$

It should be kept in mind that the above analysis takes into account only true cohesion  $c_s$  entering Eq. (31.4) for determining the yield point  $\tau_{lim}$ . At the same time the angle of internal friction of soil,  $\varphi_w$ , in density-moisture of soil,  $w$ , corresponds to the particular period of its behaviour.

It will also be pointed out that the possibility of progressing regions of creep deformation of the subsoil of a structure being designed should be excluded as uncontrolled settlement (refer to the Leaning Tower of Pisa). During construction creep deformations, that is, regions where  $k_{ssl} < 1.0$  may be tolerated yet within allowable limits governed by the design of the structure being erected and on the all-important condition that this deformation terminates by the time the structure will be put into operation.

The development of regions of creep deformation by the end of one period or another can be determined from the density-moisture of the soil that appears at that time due to the dead load and the value of  $\varphi_{T\ constr}$  followed by calculating the new factor of safety against sliding  $k_{s\ sl}$ .

Forecasts of increased soil density-moisture for one period of time or another are made by filtrational consolidation methods for liquid plastic and liquid soils and by referring to the coefficient of consolidation  $n$  for denser soils.

For rough evaluation of this phenomenon it is allowable to determine the value of  $n$  taking into account the geological features of the subsoil of a structure depending on plasticity and consistency of clayey soils by referring to a chart proposed by Maslov and Le Ba Lhiong (see Fig. 22.2).

The above solutions involve the values of principal stresses  $p_1$  and  $p_2$  appearing in the soil mass due to the dead load and forces applied to it. These quantities should be determined depending on the type of structure by using formulae and diagrams, including ones given above for a uniformly distributed load, for triangular and trapezoidal loads (see Eqs. (17.8), (17.9) and (19.10) and also Figs. 17.4 and 17.6).

Certainly, all calculations for rheological forecast of the subsoil of a structure should be made only on the condition that total stability of the subsoil, allowing for the overall cohesion  $c_w = \Sigma_w + c_s$ , is fully guaranteed ( $k_{s\ sl} > 1$ ).

# Part Four

## Basic Engineering Geology

---

### Chapter 34

#### Classification of Rocks and Soils

---

##### Sec. 34.1. The Principle of Classification

There is a vast assortment of rocks: the number of the most important rock varieties is well over several thousand. At the same time, viewed from the standpoint of engineering geology, different rocks often demonstrate fairly similar or common properties. Indeed, for the civil engineer there is no essential difference between granite and diorite. When sound and unweathered, the two rocks can safely support the heaviest structures. This enables us to forgo detailed consideration of the multitude of rocks and soils.

The above features permit categorization of rocks and soils according to their main engineering geological characteristics. When solving problems encountered by the civil engineer, this fact appreciably cuts on the number of design schemes in soil mechanics. Moreover, the limits of rational applications of conclusions from soil mechanics extend conspicuously.

Even visual inspection of rocks discloses that these materials generally differ in strength conditioned by the pattern and rigidity of bonds between minerals and particles composing them. Loose (cohesionless) soils are devoid of such internal bonds which makes it possible to refer them to an individual class of granular rocks (sand, gravel, crushed rock etc.).

Rocks demonstrating inner bonds between mineral particles can differ very much in their origin and behaviour. So, hard rocks possess irreversible rigid bonds of true cohesion  $c$ , which makes these materials similar to solids and imparts them pronounced strength. Unlike hard rocks, clayey soils depend for their strength on water-colloidal molecular bonds. The intensity of these bonds is largely governed by the density and moisture content of soil. These are reversible bonds. As is known, this type of strength is of frictional character and is called apparent cohesion. It is denoted as  $\Sigma_w$ . Quite a number of materials are characterized by other specific properties.

##### Sec. 34.2. Classification of Rocks and Soils

By virtue of the above considerations we can refer rocks and soils to four principal classes: Class One—*hard rocks* where rigid structural bonds

prevail; Class Two—*argillaceous soils* exhibiting water-colloidal bonds; Class Three—*loose or granular soils* without internal bonds; Class Four—*specific rocks* which have specific bonds.

Class One rocks are divided according to their relation to water. Thus we have *impervious and pervious rocks*.

Perviousness of hard rocks is determined by their stability to being dissolved (leaching). The degree of water resistance of clayey soils is governed by their greater or smaller sensitivity to water.

The two categories of Class One, Two and Three soils and rocks fall into corresponding groups.

**Class One (hard) rocks** are divided into groups according to their genesis responsible for specific forms of weathering of impervious rocks and leaching of pervious rocks. The fact that clay materials such as argillites and aleurolites, indeed, semihard rocks, are referred to *argillaceous rocks* is due to their clay origin, their compressibility under load leading to increased shearing resistance, partial sensitivity to water etc.

The expedience of division of *loose (granular) soils* of Class Three is ex-

Engineering Geological Classification

Class One. Hard rocks					
Category One—impervious (non-leaching)			Category Two—pervious (leaching)		
Group One—magmatic rocks	Group Two—metamorphic slates	Group Three—sedimentary cemented	Group One—organo-geneous	Group Two—products of chemical decomposition	Group Three—cemented by pervious material
Granite, diabase, porphyry, basalt, syenite, andesite	Gneisses, quartzite, marble, siliceous slates, micous slates, schiste	Siliceeous conglomerates, sili-ceous, breccia, siliceous sand-stones, siliceous lime-stones, opoka	Lime-stones, shell rock, dol-omite lime-stones	Rock salt, gypsum, anhyd-ride, dol-omites	Calcareous sandstones and con-glomerates, gypsum-bearing con-glomerates



plained by their different permeability and different stability of such soils, when saturated, to hydrodynamic and dynamic effects.

Class Four (*specific*) rocks demonstrate characteristic properties to be considered for each rock variety taking into account specific conditions of the behaviour of the particular rock or soil as well as the purpose and type of the structure being designed. Chapters that follow consider in more detail some of the most important materials of this class.

That a definite rock or soil is referred to one class or another makes it possible to approximately understand its properties in engineering geological terms. Classification of rocks and soils permits more ample presentation of regularities of the most important *geodynamic processes and phenomena*.

Geotechnical classification scheme of rocks and soils is presented in Table 34.1. The list of the rock and soil names is far from being exhaustive and is given as typical examples.

Further subdivision of rocks which in principle has no limits can be made according to the purpose in mind. For example, if it is desired to have

Table 34.1

of Rocks (After N.N. Maslov)

Class Two. Clayey Soils			Class Three. Loose (granular) soils		Class Four. Specific Soils
Category One—per- vious, slightly softening in water (cemented)	Category Two (pervious, softening in water)			Category One—pervious (insoluble)	
	Group One—hard and semihard	Group Two— plastic	Group Three— liquid	Group One— detrital, or clastic	Group Two—sands
Argillites, aleu- rolites, schists, opoka clays	Various clay varieties of dif- ferent consistency, various loams and sandy loams of varying consistency			Shingle, crushed rock, gruss and gravel from ig- neous and me- tamor- phic rocks	Derived from quartz, feld- spar, arkose, olivine  Marshy dep- osits: muck, peat, loess, glacial till, per- mafrost and backfill soils, cultured stratum

a detailed classification of argillaceous soils according to their shearing resistance we will have to categorize them as stiff clays, pseudoplastic clays and plastic clays. Yet such detailed scheme aimed at unified classification covering all cases of our analysis would be too bulky and thus not expedient.

---

## Chapter 35

### Swamp and Silty Deposits. Peat

---

#### Sec. 35.1. Swamp and Silty Deposits (Muskeg Materials)

These include primarily various silts and peat, soils exhibiting as a rule low bearing capacity and often described as organic terrain.

It is not uncommon that overwetted clay materials at an early stage of formation of clayey soils involving microbiological processes are referred to silts. Even if the total stability of a roadbed is ensured, this circumstance leads to deformation of the subsoil and roadbed proper when Phase Three of the soil behaviour occurs (arching).

Organic terrain can be found almost in all climatic zones, but they are especially abundant in the central and northern regions of the Soviet Union covering huge areas. Suffice it to say that in West Siberia alone marshes occupy more than 300 000 km<sup>2</sup>.

Conditions that lead to origination of marshy areas are: humid climate (precipitation exceeds evaporation); the presence of depressions or lowlands; impervious soils occurring close to the earth's surface.

Road and bridge builders often meet with organic and similar terrains in the flood plains of large rivers (Fig. 35.1).

Abandoned river channels gradually turn into closed boggy depressions. During high floods these are filled with silt and clay materials forming *cut-offs*. Very often peat deposits are produced there in which case silt and clay deposits are added to by decayed plant remnants.

Cut-offs provide specific conditions for deposit accumulation. This gives rise to *muck*.

Deposits accumulated in abandoned river channels are of soft plastic or liquid consistency and are absolutely unsuitable as foundation material. It is therefore customary to construct embankments for cut-off crossings such that they rest on a hard floor of a cut-off.

The moisture content of muck often exceeds 100%. The voids ratio in



Fig. 35.1. Marshy terrain in a river floodplain

such materials ( $\epsilon$ ) is generally 1-2 and sometimes greater. They exhibit exceptional compressibility, up to 100 and 150 mm per 1 m. The angle of internal friction only rarely attains  $10-11^\circ$  with apparent cohesion merely  $0.05-0.01 \text{ kg/cm}^2$ .

V.V. Shugaev has studied in particularly great detail geotechnical properties of muck deposits. According to their genesis and properties, this worker has subdivided these materials into those of ancient origin (often of semihard consistency), of young origin (of plastic consistency) and modern deposits of liquid consistency. Clearly, modern muck deposits have the least bearing capacity.

Muck deposits of ancient origin manifest increased strength and deformation-resisting characteristics. With the moisture content  $w = 30\%$  they have the angle of internal friction about  $20^\circ$  and apparent cohesion up to  $0.7 \text{ kg/cm}^2$ . The angle of internal friction in muck deposits of young origin drops to  $10^\circ$  and apparent cohesion to  $0.10 \text{ kg/cm}^2$ . As to modern muck deposits, their angle of internal friction is not greater than  $6-9^\circ$  and apparent cohesion is only  $0.10 \text{ kg/cm}^2$ .

In like manner the deformation-resisting properties of muck deposits vary. The modulus of compressibility of muck deposits of ancient origin at a load  $p = 2 \text{ kg/cm}^2$  may be roughly estimated as about 40 mm/m, for those of young origin (high flood plain)—40-100 and for modern deposits (low flood plain)—150 to 275 mm/m.

If the hydrological regime of a river changes, the muck deposits may be overlain by alluvial deposits of sand and clay. This gives rise to buried lens-

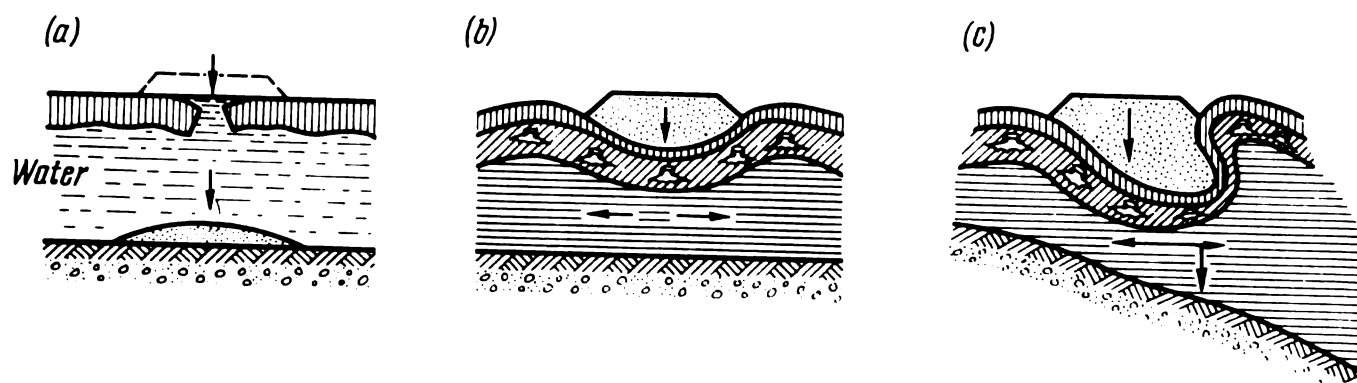


**Fig. 35.2.** Possible patterns of deformations of embankments on marshes (after N.P. Kuznetsova):

*a*—rupture of the peat deposit; *b*—squeezing out of incompetent silt deposits from the edges of an embankment; *c*—sliding of embankment

shaped deposits of peat and silt. To detect such deposits is a necessary and concurrently very difficult task of exploratory work of the geotechnician.

Plastic deformations of the foundation material of structures erected in such conditions induced by shearing stresses are very often the causative agents of their settlement and deformations. Local shears and associated squeezing out of soil from beneath the edges of the foundation or structure are generally hard to avoid. This inevitably results in conspicuous and differential settlement of the structure. Clearly, such phenomena are especially pronounced if the foundation material includes incompetent muck layers.

Embankments often have to be built over waterlogged areas or even swamps. This is often the case in river flood plains where high embankments must be erected for river crossings. When designing these under such conditions it is imperative that sudden subsidence and deformation of the embankment be taken into account (Fig. 35.2).

If a structure being designed will be supported by a foundation that includes silt layers we shall have to allow for their marked compressibility, slow load-induced consolidation, rheological properties and their capacity to liquefy under a dynamic effect.

The bearing capacity of silt deposits with time can very often be increased by placing a structure on a mat of sand that will compress, together with the weight of the structure, the foundation (cf. Chap. 27)\*.

### Sec. 35.2. Peat and Peat Deposits

Muskeg materials are mainly composed of accumulations of plant remnants, largely of mosses of different origin (of the sphagnum type, meadow

\* Other methods may be proposed for this (cf. Krynine, op. cit., p. 600 ff.) —  
*Translator's note.*

peat, woody peat etc.) at various stages of decomposition and, in part, of clays and fine sands.

Peat is a fibrous very weak soil, dark brown in colour which is able to absorb great amounts of water. The distribution of peat deposits is limited by the area of the marches (organic terrains). Most marches are filled with peat to the hard floor.

The upper peat layers filling a bog may be underlain by liquefied oozes of organic origin (sapropel) and even rise to the surface of the water reservoir. The former is typical of peat bogs that form from vegetation growth over shallow water areas or waterlogged lowlands. The thickness of peat deposits is then rather small. The two latter forms are characteristic of deeper reaches of a water reservoir at early or late stages of overgrowth. The peat deposits may then be of conspicuous thickness, 10 to 12 m or more.

Muskeg materials in the European regions of the USSR generally demonstrate a greater degree of humification compared with those occurring in Siberia and are less compressible. This difference is due to environmental conditions, vegetation cover and hydrogeological factors of peat production. Peat deposits are commonly uniformly saturated. There are, however, dry peat deposits that are watered only periodically.

Minor density and high moisture content are specific properties of peat. According to G.G. Trishin, the moisture content of peats occurring in West Siberia, depending on their origin and degree of humification, varies over the range from 700 to 1000% and more.

Since peat exhibits marked compressibility, the calculation of settlement referring to the modulus of deformation varying with depth, for example, from  $E_p = 8 \text{ kg/cm}^2$  at a depth of 1-2 m to  $17 \text{ kg/cm}^2$  at a depth 5 m is valid for this material to a greater extent than to other soils.

The compressibility of peat, other conditions being equal, is very much dependent on the degree of its humification. According to *in situ* tests, the modulus of compressibility of caked buried peats is within 40 to 80 mm/m. For other peat varieties the modulus of compressibility is much greater, attaining as much as 200-300 mm/m.

As to the bearing capacity of peats that are completely consolidated, depending on their type (meadow peat, woody-sphagnum peat), it is rather high:  $\varphi = 25-35^\circ$  and  $c = 0.10-0.20 \text{ kg/cm}^2$ .

On the other hand, unconsolidated sufficiently decayed peat has a high moisture content (320-440%), according to the data presented by Prof. N.N. Morareskul, the angle of internal friction is 3 to  $13^\circ$  and  $c = 0.15-0.35 \text{ kg/cm}^2$ .

Thus peat in a road foundation deteriorates its operating conditions, primarily due to low strength and bearing capacity of peat when it is decayed considerably.

Particular difficulties are met with when building structures on organic terrain because of the low bearing capacity and stability of silt deposits or presence of sapropels in the peat deposits coupled to marked compressibility of peats.

Silt deposits generally have very low values of the angle of internal friction ( $\varphi_w = 2-4^\circ$  and less) and apparent cohesion only  $\Sigma_w = 0.95 \text{ kg/cm}^2$ . For this reason road embankment foundations often lose strength and stability even if the height of the embankment is small (see Fig. 35.2).

The pronounced compressibility of exposed peats follows from their conspicuous moisture content ( $w$  is 800% and more and inappreciable density  $\rho \approx 1.0 \text{ t/m}^3$ ). With  $p = 0.50-0.75 \text{ kg/cm}^2$  the modulus of compressibility may frequently amount to several hundred mm per 1 m ( $e_p = 100-300 \text{ mm/m}$  and more).

If exposed peat layers are 5 m and more in thickness, the settlement of an embankment can be several metres which is impermissible, unless remedial measures are taken. This must be borne in mind, especially when designing roads, to say nothing of river crossings. This problem is particularly important in view of the fact that peat deposits are compressed at ever slower rates and may take centuries to be completely consolidated. The best way out is, when expedient, to drain as fast as possible the water from the peat deposit as it is being compressed under load. One of the possible techniques is use of filter wells. Of certain interest is the safe service for over a hundred years of a bridge in Germany erected on a 8-10 m thick peat deposit compressed by sand piers.

Sand filter wells were first advantageously used in California in 1934-1935 when carrying a road over a marsh 7.5 to 15.0 m in depth.

The possibility of building highways over marshy areas is of especial interest for this country, now that gas and oil deposits have been discovered in the tundra belt of the northern regions of the USSR. Improved roads are being built there over terrain previously impassable.

Credit is due to the Soviet scientists V.D. Kazarnovsky and I.E. Evgen'ev who have elaborated a complex method of construction of roads in such forbidding conditions, now advantageously put to practice. The method relies on precompression of embankment foundation by a temporary surcharge, increased height of embankment by placing material which will be then hauled to other sections of the road as the given section is being constructed.

The step-by-step use of prefabricated rigid pavement accompanied by compacting the base course after the most dangerous deformation of the roadbed proves very efficient. Sand piers (or caissons) find ever increasing applications for consolidation of peat deposits and marshy soils jointly with sand filter wells.

Buildings construction on organic terrain employs special techniques. Very insignificant deformations of buildings constructed on peat bogs with settlement up to 1.5 m and even more have been recorded in this country (for example, in Archangel) and elsewhere (Hannover). Most of these structures are supported by wooden raft foundations.

Four to five storey masonry houses are currently being built on peaty soils by using modern techniques, including ones reported above. These are storey-by-storey reinforced concrete rigidity belts proposed at his time by Prof. B.D. Vasilyev and developed by B.I. Dalmatov (Leningrad, Okhta district) where building settlement up to 40-60 cm is tolerable. However, we must take into account the possible subsidence of the building site on a peat deposit of substantial thickness following a drop in the water table (see Sec. 30.1).

Civil engineers must be warned against excessive reluctance to construct if a mineral subsoil includes fairly thin layers of buried peat to say nothing of peaty soils (up to 20%) and on reclaimed lands.

Attention, however, should be called to the failure of a bridge across the Kazanka River. Inadequate preliminary site exploration was the cause of that concentrated load of a bridge pier was transmitted through a pile foundation to a deposit of buried peat. As a result of differential settlement of the pier almost by 1 m the bridge was damaged.

The settlement of a road embankment built over marshy areas composed of silt and peaty soils is generally retarded. It has been established that the surface course can be laid on the base if the foundation settlement has attained 90% of its final magnitude. As has been pointed above, this case corresponds to the coefficient of consolidation  $c_v = 0.80$  and  $e_{p90}$ . The settlement will be equal to

$$\eta_{sub} = \sum_0^D e_{p90} h_i$$

The settlement may then last several years. It will take as much time before improved pavement can be laid and the road can be built.

To remedy this situation, several methods have been proposed. One of these consists in the following. A road is built within the specified amount of earth work as the narrowest possible strip which increases the height of the fill and, consequently, the consolidating pressure on the embankment foundation. Clearly, this enhances the consolidation rate. The required modulus of compressibility under such conditions  $e_{p90}$  at a greater load can be achieved in a shorter period of time yielding thus positive results. Then the roadway is levelled. The advantageous effect of such technique is that the weakest topsoil layers are squeezed out from beneath the road embankment which in the general case decreases the total settlement of the fill.

The second method is to remove part of the weakest peat layers in conformity with the law of filtrational consolidation stating that the duration of consolidation  $t_1$  and  $t_2$  in seams of the same soil of different thickness  $h_1$  and  $h_2$  is directly proportional to their square, that is, for  $h_2 > h_1$

$$t_2 = t_1(h_2/h_1)^2$$

Regretfully, this method is often hard to use. Moreover, this is valid only for very weak clayey soils.

As has been pointed out above, it has become popular to enhance the rate of consolidation of incompetent clayey and even peaty soils by means of vertical drainage wells. For this, boreholes are drilled under the embankment of possibly large diameter. These are filled with sand which provides good filtering material. This facilitates withdrawal of water from the soil mass as it is being compressed by the weight of the fill. Depending on the local conditions this measure may give different results. A successful example of this method is shown in Fig. 35.3.

For rough estimates of *high-moor peats* the following index characteristics can be used: the volume weight (bulk density) is  $\rho = 0.95-1.05 \text{ t/m}^3$ ; the density is  $\rho_0 = 1.5-1.8$ ; the moisture content is 500-1500%; the ash content is 3-20%; the coefficient of compressibility is  $a = 3-14 \text{ cm}^2/\text{kg}$ ; the angle of internal friction is  $\varphi = 10-30^\circ$ .

The index characteristics of *buried peat* are:  $\rho = 1.2-1.4 \text{ t/m}^3$ ;  $\rho_0 = 1.9-2.2 \text{ t/m}^3$ ;  $w = 100-300\%$ ; the ash content is 30-70%;  $a = 0.2-0.4 \text{ cm}^2/\text{kg}$ ;  $\varphi = 27-30^\circ$ .

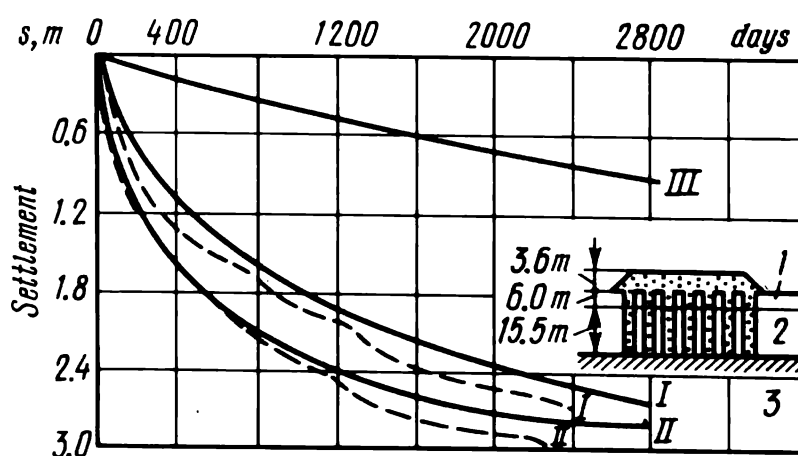


Fig. 35.3. Chart showing the effect of vertical drains on the velocity of settlement of an embankment of muck foundation following completion of construction (solid lines indicate calculated settlement; dashed lines—observed settlement):

I—drains spaced at intervals of 4.2 m; II—same, at 3.3 m; III—design settlement without drains; 1—washed up soil; 2—muck; 3—sand



---

Chapter 36**Loess and Loessian Soils.  
Seasonal Changes in Bearing Capacity**

---

**Sec. 36.1. General Characteristics**

Loessian soils include aeolian, or wind-blown materials, such as loess, loess-like loams and sandy loams formed during deluvial, proluvial and alluvial sedimentation. Despite the different conditions of formation, loess, loess-like loams and sandy loams demonstrate properties that are common: light brown colour; marked porosity, sometimes visible to the unaided eye; farinaceous texture; slight cementation generally induced by calcium carbonate. In addition, if a loess deposit is wetted, it rapidly consolidates and the structure built on it settles. This property is termed hydroconsolidation.

Loessian soils are distributed in dry areas (the Middle Asia, the Ukraine, Transcaucasian regions, the North Caucasus, South Siberia (Fig. 36.1). They can range from several metres to several tens of metres in thickness (for example, loess deposits in the vicinity of Tashkent are 40-50 metres thick). The thickness of aeolian loesses changes from place to place, even within the same area it may be conditioned by the character of the relief buried under the loess deposit.

Wind-blown loess generally forms during the lengthy accumulation of the atmospheric dust on the earth's surface. The rate of this deposition is very slow, a few millimetres a year. With passage of time this wind-deposited material is partly cemented by the salts in the soil mass. This gives rise to a loess deposit. It is commonly called *primary loess*.

*Secondary loess* is a loessian-type soil transported over short distances by water and somewhat differs from primary loess. Sometimes these soils are layered, contain inclusions of sand or shingles and are often alternated by seams of sand or gravel. Such soils are generally called *loess loams*.

Loessian-type soil is a weakly moist (the maximum moisture content is 10%), somewhat cohesive clay material, light yellow, grayish yellow or straw-coloured, easily rubbed between the fingers and, what is the most important, porous.

Loessian soils, especially aeolian, demonstrate a relatively high calcium carbonate content.

The porosity values of dry or slightly wetted loessian soils are generally in the range 40-47% but may sometimes attain 55-60%. Long vertical tubes penetrating the entire soil mass are probably casts of plant roots.

According to their granulometric composition loesses belong to

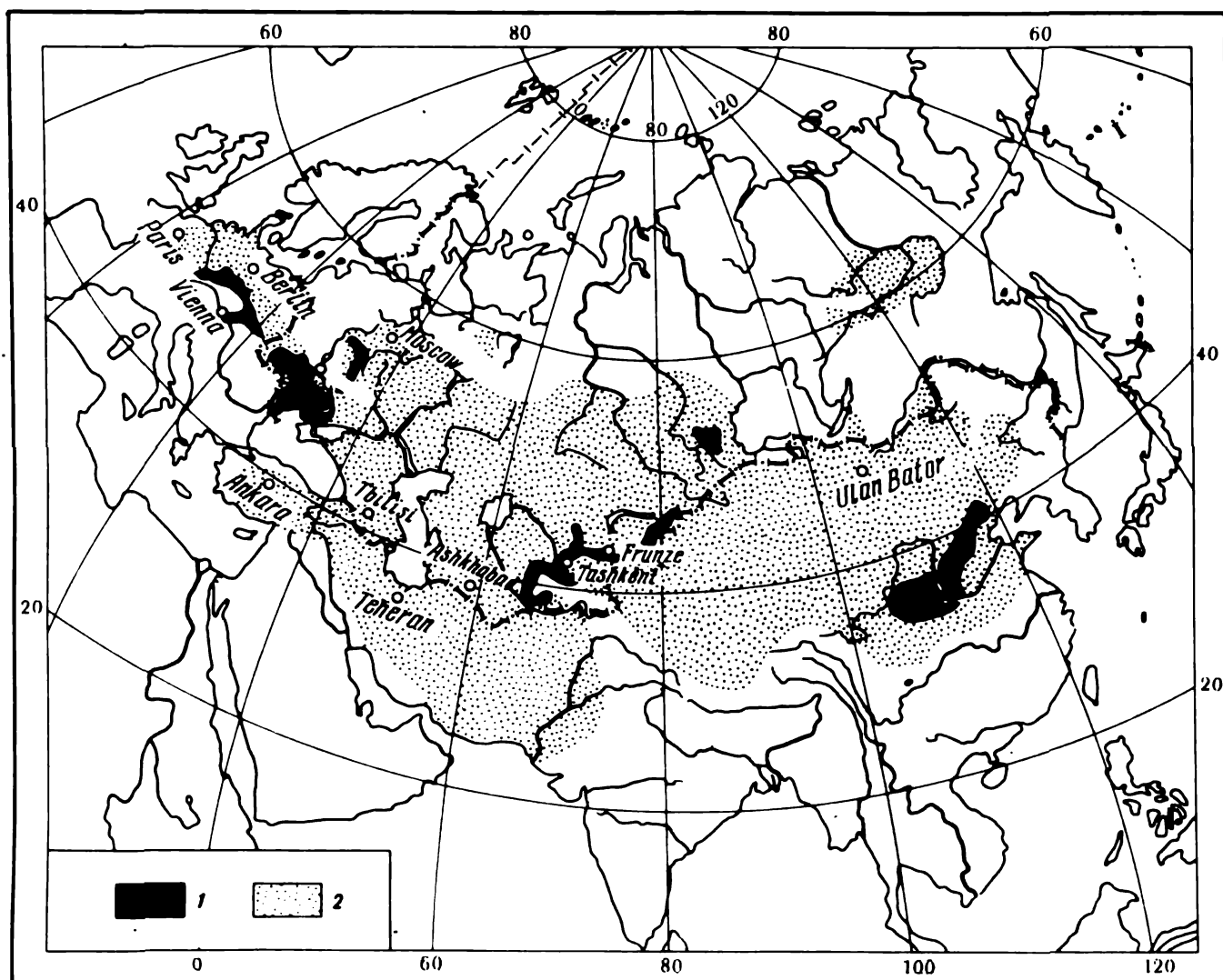


**Fig. 36.1.** Map showing distribution of loess and loessian-type soils:

1—typical loesses; 2—loessian-type soils

powdered soils: the fines content (0.05-0.005 mm in diameter) is almost always exceeding 60-70%, sometimes being as much as 85 or even 90%.

What makes loesses specific is their marked difference in behaviour conditioned by the moisture content. If the latter is 6-9% or less, loess exhibits a relatively high bearing capacity, substantial strength and stability on slopes. The temporary crushing strength of such loesses often exceeds  $4-5 \text{ kg/cm}^3$ . Even heavy structures imparting a load about  $4 \text{ kg/cm}^3$  on a loess foundation settle inappreciably. Loess slopes in such a state can stand practically vertically (Fig. 36.2). If wetted, loess dramatically loses its stability and strength, slopes collapse. If the toe of a loess slope is submerged, this causes major slides followed by spalling and settlement. Submerged loess is subject to scour which, under given conditions, triggers erosion. Upon wetting, loess demonstrates pronounced compressibility and structures constructed on it conspicuously settle. Due to inevitable differential settlement, structures, even transmitting minor loads on the loess foundation soil, are



**Fig. 36.2.** Loess slopes flanking a river valley



**Fig. 36.3.** Deformations in a building due to differential settlement (initial stage)

cracked, tilt and show other deformations (Fig. 36.3). Structures on loess may sometimes settle 1 m which leads to detrimental deformations.

Wetting of the foundation soil composed of loess and loessian materials can be induced by various causes: poor withdrawal of meteoric and in-



Fig. 36.4. Failure of flanks of a canal excavated in a loess deposit induced by soil movement

dustrial waters, damaged water pipes and sewage pipelines, rise in the water table following the construction of a dam, seepage from canals etc.

When a canal in a loess mass is filled with water, canal flanks exhibit pronounced deformations: cracks appear (Fig. 36.4), flanks settle frequently. The settlement may sometimes be in terms of metres.

### Sec. 36.2. Subsidence of Loess

The property of loessian soils to deform is termed *subsidence*, and soils exhibiting this property are called *subsiding* ones.

As has been already mentioned, loessian soils are widely distributed in this country, so construction on subsiding, incompetent soils is of much importance. Compared with soils of the identical granulometric composition, loesses are generally extremely porous which does not agree with the mode of their occurrence. Hence a concept of *excessive porosity* of incompetent soils with respect to the overlying soil strata.

To characterize the relative natural density of a soil, that is, its porosity, one may well use *the coefficient of natural density*

$$\beta = \frac{n_{nat} - n_{equiv}}{n_{equiv}} \quad (36.1)$$

where  $n_{nat}$  is the natural porosity;  $n_{equiv}$  is the porosity value of the given soil corresponding to the natural load.

In  $n_{nat} = n_{equiv}$ , the coefficient  $\beta = 0$ , and the soil is in an equilibrium state. At  $\beta > 0$  the soil is incompetent, and it is more so, the larger is the value of  $\beta$ . At  $\beta < 0$  the soil has insufficient porosity and under definite circumstances it is liable, when wetted, to decompression and swelling.

According to the SNiP, the Soviet Civil Engineering Code of Practice, incompetent subsiding soils include such soil varieties, whose coefficient  $S$  (for subsidence), found from Eq. (36.2), if the moisture content is  $G < 0.8$ , is less than the values governed by the plasticity index of soil,  $I_p$ , and lying in the range from 0.1 to 0.24 (Sec. 2.13 of SNiP):

$$S = \frac{\varepsilon_L - \varepsilon}{1 + \varepsilon} \quad (36.2)$$

where  $\varepsilon$  is the voids ratio of the soil sample of original moisture content and porosity;  $\varepsilon_L$  is that for the moisture content approaching the liquid limit  $W_L$ . The following formula is used to find  $\varepsilon_L$ :

$$\varepsilon_L = W_L(\rho_s/\rho_w) \quad (36.3)$$

where  $\rho_s$  and  $\rho_w$  are densities of soil and water, respectively.

Because of the small clay content of loessian soils and high dust particle content the water colloidal bonds active there and responsible for apparent cohesion of clayey soils are relatively weak. They reveal themselves only if the moisture content of soil is small. Cohesiveness of dry loess with the moisture content 4-9% ensures interlocking of soil particles and, consequently, relatively high strength.

Wetting of the soil results not only in that the previously dry voids are filled with water, but, primarily, in thicker water pellicules on soil-composing particles.

As the soil swells, the rigid bonds cementing it are ruptured; cohesion drops to zero. The cohesiveness of the soil and friction forces acting in it dramatically decrease. When excessively wetted, the angle of internal friction of loess appreciably drops (to 10-12°). Accordingly, the shearing resistance and, consequently, bearing capacity of soil decrease. When acted on by load, loess is markedly compressed, its porosity decreases attaining its equivalent value  $n_{equiv}$ , and the structure resting on it settles conspicuously.

Figure 36.5 is a chart showing various possible cases of settlement of structures supported by loessian soils with the same original porosity value. Time since the start of construction is plotted on the abscissa axis, structure settlement on the ordinate axis.

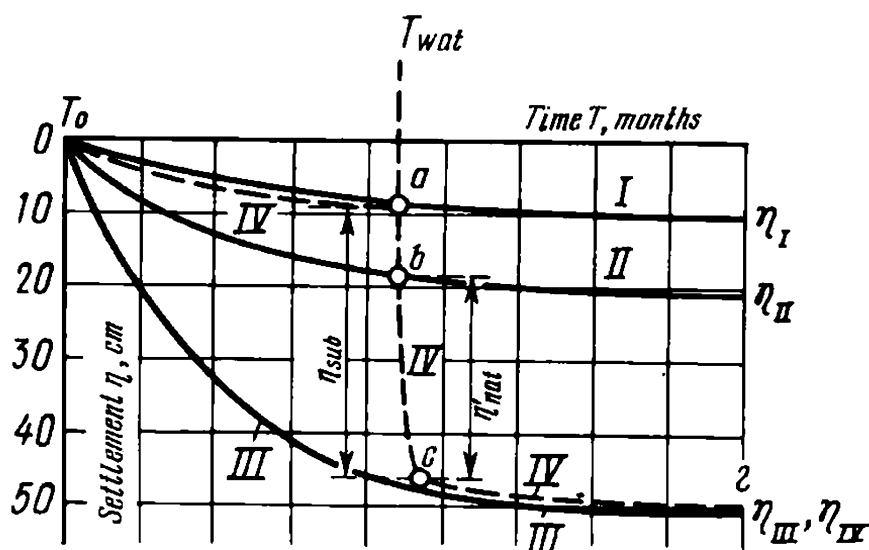


**Fig. 36.5.** Typical curves of settlement of a structure on loess under different conditions

Curve *I* corresponds to a structure on a dry loess mass with the moisture content 4-9%. The moisture regime of the loess deposit is preserved throughout the observation period. The shearing resistance of the soil in this condition is conspicuous, since it demonstrates pronounced strength and negligible compressibility, and the settlement of a structure on it is inappreciable.

Curve *II* represents the behaviour of a structure of an increased (18-23%) moisture content loess deposit. The degree of wetting remains constant in this case, too. Due to the greater moisture content the total shearing resistance of soil drops increasing its compressibility. The settlement of the structure  $\eta_2$  increases which often leads to cracks in buildings.

Curve *III* shows the behaviour of a loess deposit submerged at the very start of construction work. The moisture content then attains its peak value, its strength is minimum, and compressibility is dramatically enhanced. Clearly, the settlement is much greater than in the two previous cases.

Curve *IV* demonstrates conditions that are common for loessian soils. In its natural state loess is dry preserving this condition for a period of time from  $T_0$  to  $T_{wat}$ . At  $T_{wat}$  the loess deposit is watered which deteriorates its conditions. The process of structure settlement will then be characterized by three different branches: *Oa*, *ab* and *cd*. At the early stage (branch *Oa*) curve *IV* coincides with curve *I* (dry loess). At the third stage (branch *cd*) curve *IV* agrees with curve *III* (wetted loess). At the second, intermediate, stage (branch *ab*) at first coincident with the starting period of loess wetting,  $T_{wat}$ , the settlement suddenly rises. This rise is responsible for the magnitude of the settlement.

To sum up, the settlement of the structure occurs in the given case due to loess watering and is followed by a rapid transition of stage *I* to stage *III*. Sudden settlement generally causes cracks and deformations of struc-

tures, sometimes total failure. Clearly, under such conditions it is possible to ensure the normal performance of a structure only if we select the adequate design and construction methods. At the same time, as has been already reported, a number of structures built on loess deposits are still functioning adequately.

The above analysis shows that the most unstable are loess deposits that may be wetted during the service period of the structure. On the other hand, loess deposits naturally occurring below the water table are more reliable in this respect. It follows, then, that during the exploration of the building site the location of the water table and the subsurface hydrological regime must be determined.

Other conditions being equal, the value of soil subsidence  $\eta_{sub}$  is governed by the thickness of the loess deposit occurring above the water table. This value increases almost in direct proportion to the thickness of such a deposit. Naturally,  $\eta_{sub}$  is also governed by the degree of compressibility of materials composing the given soil mass.

The degree of subsidence of loessian soils similarly to compressibility of other soil varieties, can be best represented in terms of the relative deformation  $e_p$ .

We will express this value in per mille and operate with a *modulus of compressibility*  $e_{p\ sub}$  which corresponds to subsidence in mm of a 1 m thick soil layer as it is being wetted at a surcharge  $p$  in kg/cm<sup>2</sup>.

The degree of subsidence of different loess varieties and loessian soils similarly to clayey soils is conditioned by their composition and state.

According to the SNiP Civil Engineering Code of Practice, the measure of subsidence of a soil is the relative subsidence  $\delta_{sub}$ , which represents its relative compression induced by wetting and is found from this relationship:

$$\delta_{sub} = \frac{h' - h_{sub}}{h_0}$$

(36.4)

Table 36.1

Relationship Between the Degree of Subsidence  
in Dry Loess and Its Porosity

Subsidence property of soil	Porosity $n$ , %	Modulus of compressibility, mm/m
Non-subsiding	40	0
Slightly subsiding	40-45	10
Subsiding	45-50	50
Strongly subsiding	50-55	100
Extremely subsiding	> 55	≥ 100



where  $h'$  is the height of the soil sample in a confined test at a load  $p$  in  $\text{kg}/\text{cm}^2$ ;  $h_{sub}$  is the height of the same sample at the identical pressure following wetting;  $h_0$  is the height of the same soil sample with the original moisture content at a natural pressure in a confined test.

A very important characteristic of the degree of subsidence of loessian soils is thier porosity. The relationship between the degree of subsidence of dry loess and porosity is given in Table 36.1.

The moisture content of a loessian soil is an important factor for evaluating its degree of subsidence. The lower the original moisture content value, the greater compressibility of soil on watering and, consequently, the larger the settlement of the structure supported by it.

### Sec. 36.3. The Principle of Forecasting Subsidence

The modulus of compressibility of loessian soils is generally found by testing.

Laboratory tests determine the compressibility of soil under different loads, and compression curves are plotted (Fig. 36.6). However, unlike common compression tests, these tests for the initial stage of loading are conducted without submerging the soil samples. This stage generally is typified by the low compressibility of soil (branch A). The step that follows is to supply water to the testing machine at a definite load which is of interest to us (say, at  $p = 3 \text{ kg}/\text{cm}^2$ ). The soil sample sustaining the same load suddenly settles (branch B). Then the submerged sample is compressed. As can be seen from the figure, the test, as it were, simulates the settlement of a structure shown in Fig. 36.5. The modulus of compressibility is found from the length of the segment  $ab$ . In the given case  $e_{wat sub} = 52 \text{ mm}/\text{m}$ .

To have more reliable data on the degree of subsidence (compressibility) of loess, field tests are often made. In so doing, the additional settlement of soil under a loaded plate is observed, the soil being wetted. The loaded plate 50 by 50 or 70 by 70 cm (better 1 by 1 m) is installed on a layer of

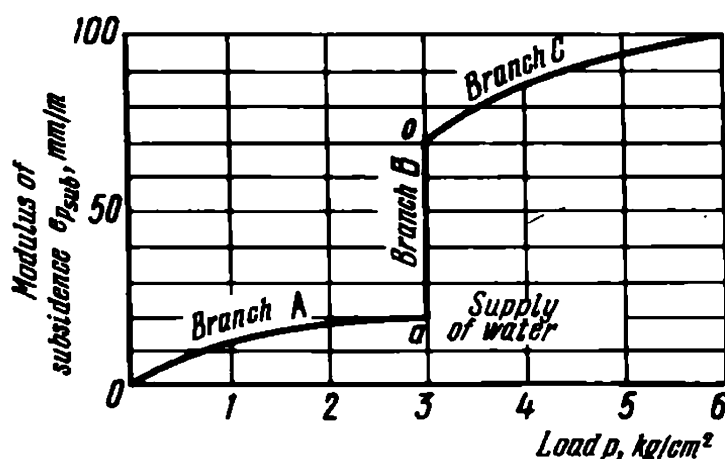


Fig. 36.6. Example of processing a laboratory test to determine the modulus  $e_{p sub}$  in loess



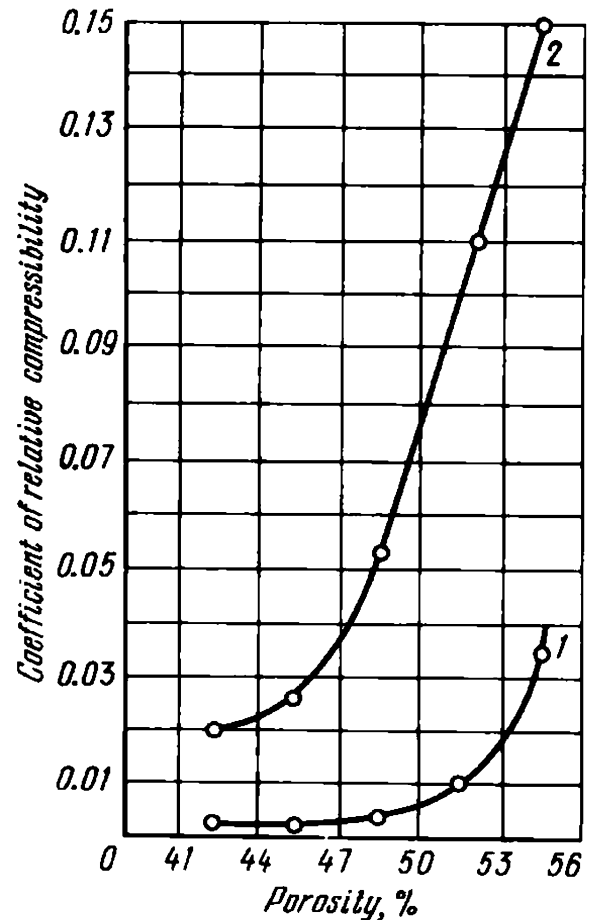


Fig. 36.7. Change in subsidence of loess depending on its density and load:

1— $p = 0.45 \text{ kg/cm}^2$ ; 2— $p = 4.0 \text{ kg/cm}^2$

sand in a test pit. To eliminate bulging of soil from beneath the plate, the test pit is filled with sand to some depth. Then a load is applied to the plate and its settlement observed. After the settlement has stopped, water is supplied in tubes to the sand layer to water the loess mass. If the soil being tested is subsiding or troublesome, the loaded plate settles dramatically.

For control, before and after the test soil samples are taken from beneath the plate, and the initial and final porosity  $n_0$  and  $n_1$  are determined. The modulus of compressibility is found from the relationship

$$e_{p \text{ sub}} = \lambda / 1.1D \quad (36.5)$$

where  $\lambda$  is the settlement of the loaded plate in mm that occurred after submergence of soil in the test pit;  $D$  is the side of the square plate in m.

To have a check, the following formula is used:

$$e_p = 1000 \frac{n_0 - n_1}{1 - n_1} \quad (36.6)$$

where  $e_p$  is the compressibility or modulus of compressibility of soil in mm per metre of the thickness of the soil mass.

A very important element of the test is determining the limiting subsidence  $p_{lim}$  (Fig. 36.7), that is the load value below which the soil does not subside. If  $p_{str} < p_{lim}$  then the foundation is most likely to be stable.

The angle of internal friction in loess, depending on its composition (clay particle content) and moisture content can vary in a wide range from 10 to 27°. The value of cohesion is likewise governed by these conditions and fluctuates from 0.1 to 1 kg/cm<sup>2</sup>.

Loessian soils occurring in the vicinity of Dneprodzerzhinsk whose porosity up to the depth 6 m is  $n_1 = 47-51\%$ , and to the depth 6-10 m is  $n_2 = 40-43\%$ , and 10-14 m below the surface is  $n_3 = 35-41\%$  having the respective bulk densities and moisture contents:  $\rho_1 = 1.30-1.40 \text{ t/m}^3$  and  $w_1 = 3.7-13\%$ ;  $\rho_2 = 1.55-1.60 \text{ t/m}^3$  and  $w_2 = 10-15\%$ ;  $\rho_3 = 1.57-1.64 \text{ t/m}^3$  and  $w_3 = 10-13\%$  are typical of the Ukraine.

As can be seen, loessian soils occurring in the uppermost level (up to 5-6 m in thickness) demonstrate the smallest density. Their porosity is over 45% and moisture content is inappreciable (5-8% on the average). Therefore such soils are most liable to subsidence. This has been validated by *in situ* and laboratory tests. Stable soils occur at lower horizons (at depth below 6 m).

The thickness of loess deposits in the neighbourhood of Tsymlyansk Hydro Power Station is in the range from 8 to 15 m. The thickness of loessian soil deposits found on terraces of more ancient origin in the Don River basin attains 25-40 m. The dust particle content is 50-60%, moisture content is 13-18%. The modulus of compressibility of these soils for porosity  $n \approx 39-48\%$  is  $e_{3 \text{ sub}} = 26-120 \text{ mm/m}$ .

Of much importance are stability characteristics of the loessian soils being considered after being wetted during subsidence (without previous compression). Then, at a load  $p = 3.0 \text{ kg/cm}^2$  the angle of internal friction is 11-19° and cohesion is  $c = 0.05$  to  $0.20-0.50 \text{ kg/cm}^2$ . Even smaller values have been reported in literature.

Apart from remedial measures taken for compressing loess deposits (machine compacting, sand caissons, preliminary wetting etc.) use is made of *the principle of initial pressure* (limiting subsidence). This means that load  $p_{\text{sub lim}}$  below which submerged loess does not subside. This value generally increases with depth from 0.5 to 1.5 kg/cm<sup>2</sup>.

Permeability of loess is due to its fine granular structure and marked porosity with more or less vertical root holes. For this reason undisturbed loess has very great permeability in a vertical direction. The surface water easily reaches the lower layers of loess deposits often forming aquifers of minor thickness. At the same time horizontal permeability of loess is insufficient because of the fine granular structure of this material. Loess yields water very reluctantly.

More often than not loess and loessian-type soils have high salt and gypsum contents. As water seeps down, continuous (secondary) subsidence oc-

curs. According to findings of S.V. Dan and L.N. Lomidze, the content of easily dissolved salts in loess in excess of 0.7% causes added subsidence of 5% and more. The leaching effect may give rise to subsidence of loessian soils with pronounced gypsum content in excess of 15%.

---

## Chapter 37

### Glacial Deposits

---

#### Sec. 37.1. The Composition of Glacial Deposits

These are of special interest, being widely distributed in this country. Such deposits are of conspicuous thickness (sometimes tens of metres) and present often the uppermost and appreciable crustal layer. Therefore glacial soils and deposits frequently provide immediate foundation for structures being erected.

As has been pointed out in Chap. 3, the last glaciation period in this country included three stages: *Likhvin*, *Dnieper* and, the most recent, *Valdai* glaciation (see Fig. 3.5). There is a more detailed classification of these stages (see Fig. 37.1).

*Boulder clay*, or moraine demonstrates the most advantageous properties.

This material, found in the mass of deposits of more recent origin frequently provides the most reliable foundation for a designed structure.

*Moraine* is generally a deposit of dense boulder clay, loam or sandy loam containing gravel, shingle and detritus of different degree of smoothness (boulders). The composition of the moraine is governed by that of the underlying soils and the distance to the feeding area. Covering the pre-glaciation relief by a cover of varying thickness, moraine is found at different heights above sea level and on different land forms (Fig. 37.2).

Several moraine horizons can be distinguished, separated by deposits of interglacial stages.

Moraine is an unstratified deposit, generally brown, gray or brownish red in colour. Boulders, gravel, crushed rock and other detrital materials are erratically distributed in moraine, yet their content in the lower strata is conspicuous.

Moraine deposits may include lenses and seams of sand, gravel and shingles. If these inclusions contain pressure water, cuts in such materials often cause landslides.

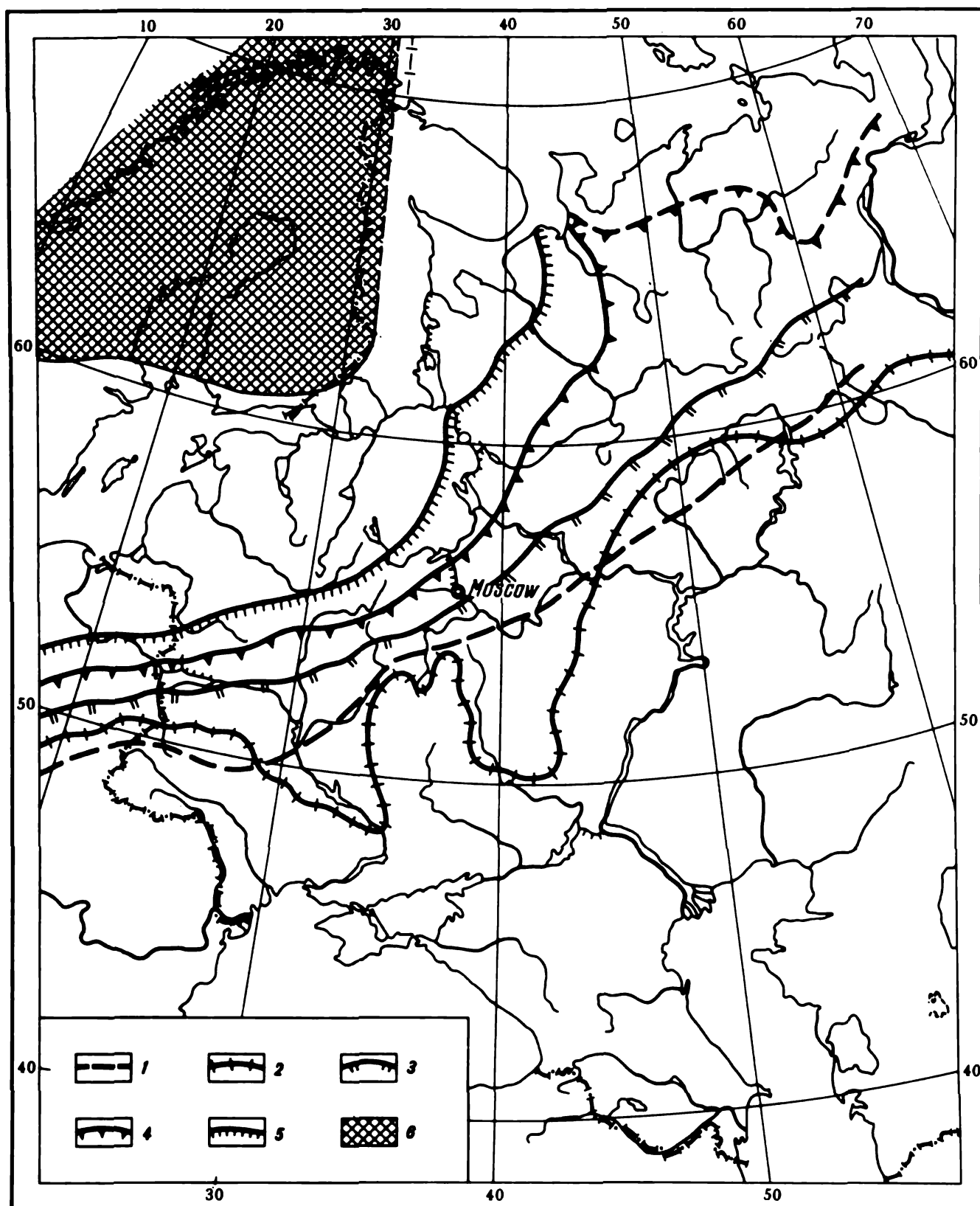


**Fig. 37.1.** Map showing the distribution of particular stages of glaciation in the Quaternary period on the territory of the European USSR (after G.P. Gorshkov and A.F. Yakushova)

1—assumed expansion of Oka glaciation; 2—assumed expansion of Dnieper glaciation; 3—expansion of Moscow glaciation; 4—that of Kalinin glaciation; 5—that of Ostashkovo glaciation; 6—ice sheet of Europe 10-11 thousand years ago



Fig. 37.2. Boulders on a moraine deposit of ancient origin



Fig. 37.3. Fluvio-glacial deposit in the flank of an open cast (Svir River region)

Moraine lacks cementation materials and, consequently, has no cohesion. For this reason its construction properties are mainly conditioned by the greater or smaller content of clay minerals and density.

Moraine soils found in the northern regions of the USSR have a specific feature. These are often very fine sand and rock flour. Seepage flow and hydrodynamical pressure often render these soils rather unstable. This property can generally be ascribed to the marked content of powdered particles

that demonstrate low compressibility and marked shearing resistance under load (coefficient of internal friction being 0.4-0.5) and, at the same time, very small cohesion. The absence of cohesion, the small permeability and density of these soils lead to sloughing of slopes composed of such materials. At conspicuous gradients resultant from excavating deep open casts and due to the effect of vibrations such soils easily liquefy forming *quicksands*.

When operating in such open casts excavators may sink in the upper layer of such troublesome soil.

*Fluvioglacial deposits* are made by the streams carrying the outwash from the melting glaciers. These materials have different granulometric composition and demonstrate different engineering properties, even ones of quicksands (Fig. 37.3).

### Sec. 37.2. Glacial Deposits from the Viewpoint of Geotechnics

Sand varieties of fluvioglacial deposits demonstrate inappreciable compressibility at a static load. At the same time, due to generally marked porosity they easily consolidate under the effect of vibrations thus causing conspicuous settlement of structures acted on by dynamic load. It is good practice to use pile foundations in such soils since pile driving compresses the foundation soil enhancing its bearing capacity. Moraine does not contain readily dissolved soils, yet may have carbonate content as much as 25%.

In the state of natural moisture content moraine is very dense and can support almost vertical slopes in excavation pits. The original moisture content of moraine does not usually exceed 12-14%. Its compressibility is inappreciable (about 5-25 mm per one metre of the soil mass). Compared with other continental Quaternary deposits moraines are more competent and often provide structure foundations. The angle of internal friction of moraines is at least 23-26°. Cohesion often is of relatively high value, about 0.4-0.6 kg/cm<sup>2</sup>.

Moraine deposits of the Valdai glaciation including, in particular, loams are widely distributed in the north west of the European USSR. These materials are, as a rule, of hard and semihard consistency. With the moisture content  $w = 15-20\%$  they have a high bulk density of skeletal particles (about 1.85-2.0 t/m<sup>3</sup>), the coefficient of internal friction is 0.40-0.55 and cohesion is 0.3-1.0 kg/cm<sup>2</sup>.

When estimating the bearing capacity of glacial deposits we must keep in mind that they differ very much both in composition and mode of occurrence. This circumstance may prove crucial in differential settlement of structures.

Permeability and moisture bearing capacity of moraine deposits are governed by composition and density. Moraine clays have a very small value of the coefficient of permeability and a relatively high initial gradient (the coefficient of permeability is about  $a \times 10^{-8}$  cm/s and initial gradient is 4-9).

For areas of earlier ice coverage (mainly in the Leningrad Region) *varved clays* formed in lakes of the later glaciation period are typical. These clays are known also as varves consisting of intermittent uniform laminae of silt and clay. This structure of varved clays is due to that they were laid down by melt water feeding the lakes during the glacial epoch and to the seasonal pattern of this deposition.

Varved clays found in the Leningrad Region and on the territory occupied by Leningrad occur as deposits 10-15 m in thickness and are underlain by deposits of an earlier glacial period. When intact, such clays have a sufficiently high strength, but if disturbed, they demonstrate liquid plastic or even liquid consistency, drastically decreasing their strength and deformation resistance.

Being of relatively young origin, varved clays possess low density and often high moisture content approaching 35% and sometimes even 45%. The compressibility of these clays practically always is more than 40 mm per one metre of the soil mass, in separate cases attaining 60-80 mm per one metre.

---

## Chapter 38

### Permafrost. Soils in Permafrost

---

#### Sec. 38.1. Introduction

*Permafrost*, or *permanently frozen ground* is a deposit of soil and rock in which subfreezing or freezing temperatures exist throughout the year.

Such temperatures probably have existed continuously for an indefinitely long time (presumably for tens of thousand years). The average temperatures of the permafrost are in the range from 0 to  $-7^{\circ}\text{C}$ . As a rule, they do not drop below  $-8^{\circ}\text{C}$ .

Permafrost soils cover vast territories in the north and north-east of this

---

\* According to Krynine and Judd (op. cit., p. 390), the permafrost terminology contains many terms borrowed from Russian.





cur as tiny crystals and capillaries to major lenses or even layers up to 20 m thick. Such ice layers of substantial depth are found in the areas of the most inclement climatic conditions. This ice, known as fossil ice, appears as a rock and covers vast areas.

The perennially frozen layer may be tens of metres in thickness and may occasionally attain several hundred metres. So, in Yakutsk the thickness of the ice layer (not entirely penetrated by boring) is 116 m, in Spitzbergen more than 240 m. The greatest thickness of ice deposits found in Northern Yakutia, near the coast of the Laptev sea, is about 600 m. Permafrost is absent or occurs at deeper horizons beneath great river valleys. An example is the valley of the Lena River whose waters contain large amounts of heat.

According to one theory, the origin of permafrost can be traced to the last glaciation period that has been in progress until now. Another theory holds that it results from modern environmental conditions.

Permafrost generally prevents flow of groundwater and provides an aquiclude. Yet fine capillaries may contain fluid water, and groundwater does circulate in veins of melted ground.

The hydrostatic pressure may cause groundwater to force its way to the upper surface. The ice fields or icings thus form (the Russian term *nahledee* is often used instead). They may cover substantial areas (Fig. 38.2).

Soils in permafrost are generally silts, sandy loams, loams etc. When frozen, these soils attain properties of hard rocks with marked cohesion and



Fig. 38.2. Icing encroaching on a road (photograph by A. Tursumbaev)

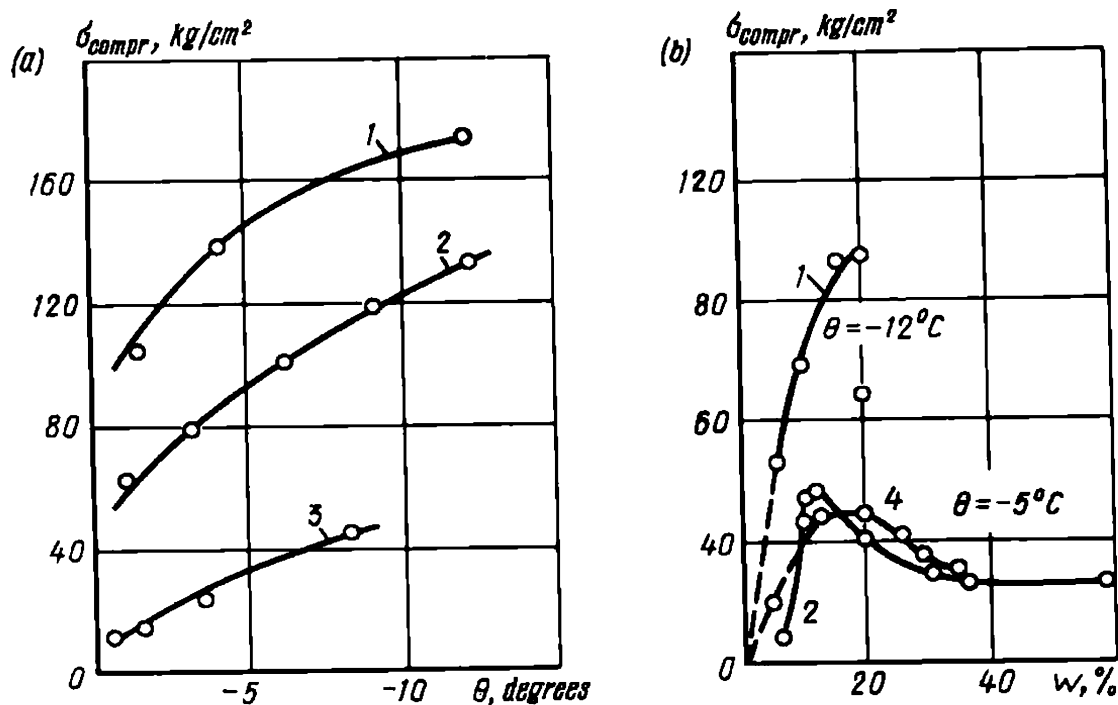


Fig. 38.3. Charts illustrating the relationship between the shearing resistance of frozen soils and temperature (a) and moisture content (b) (after N.A. Tsitovitch):

1—sand; 2—sandy loam; 3—clay (fraction content less than 0.005 is 51%); 4—silty clay (fraction content less than 0.005 is 63%)

rigidity. Powdered sands freeze below  $-0.3^\circ\text{C}$ ; sandy loams at  $-0.6^\circ\text{C}$ ; loams at  $-1.0^\circ\text{C}$ , plastic clays at  $-1.5^\circ\text{C}$ . The compressive strength of frozen clayey soils increases with lowering the temperatures, being on the average in the range from 5 to 20 kg/cm<sup>2</sup> and more. The shearing strength of these soils follows the same regularity and typically varies from 5 to 15 kg/cm<sup>2</sup>.

Water-containing varieties of clayey soils (clays, loams, sandy loams) and sands, when frozen, drastically increase their compressive and shearing strength. The soil particles are then tightly cemented by ice. It can thus be seen that the strength of such soils is conditioned by the temperatures, lowering as these increase (Fig. 38.3).

An essential role in strength of frozen soils is played by optimum moisture content. In the range of temperatures typical of the soil under consideration ( $-2$  to  $-8^\circ\text{C}$ ) the modulus of deformation is several thousand kg/cm<sup>2</sup> and more. The strength of a frozen soil is mainly due to cohesion (60 to 95%).

Viscous plastic deformation is an important feature of soils in permafrost areas. Their resistance may be conspicuous at the initial moment of application of load. With time, however, their shearing strength may drop appreciably.

Charts in Fig. 38.4 illustrate this phenomenon associated with *long-term stability* of soils in permafrost. At the initial moment of load application (curve 1) the soil demonstrated  $\varphi = 14^\circ \text{C}$  and  $c = 4.2 \text{ kg/cm}^2$ . After continuous application of the load (curve 2) the angle  $\varphi$  dropped to  $4^\circ \text{C}$ , and cohesion (Fig. 38.4b) to  $0.9 \text{ kg/cm}^2$ . Clearly, disregarding this important factor may, under definite conditions, lead to detrimental results.

It is worthwhile mentioning studies of Prof. S.S. Vyalov suggesting an inevitable reduction of stability of permafrost soils (with respect to cohesion) induced by time-dependent loading even if the thermal regime of soil remains constant. For example, heavy powdered sandy loam at  $-1.2^\circ \text{C}$  one minute after loading exhibited 62% of the initial strength. An hour later it dropped to 36%, the limiting load being 25%. The initial compressive strength was  $7.3 \text{ kg/cm}^2$ , the final— $1.6 \text{ kg/cm}^2$ .

When thawed, silty and clayey solid liquefy, manifesting excessive moisture content and negligible bearing capacity. The weight of water in thawed soil may sometimes exceed that of soils particles. The shearing resistance of such soils is also very small.

Clearly, under similar circumstances the dead load perfectly allowable for solid permafrost soil may prove excessive for a liquefied material. Soil from beneath the foundation starts to bulge which results in differential settlement of the structure. Therefore, when building structures on permafrost, care must be taken to prevent them from changes in the thermal regime of the structure foundation.

This is how things stand when constructing on frozen soils that liquefy on thawing. Different conditions obtain when competent soils are involved. The best foundations are provided by coarse-grained sands, gravels,

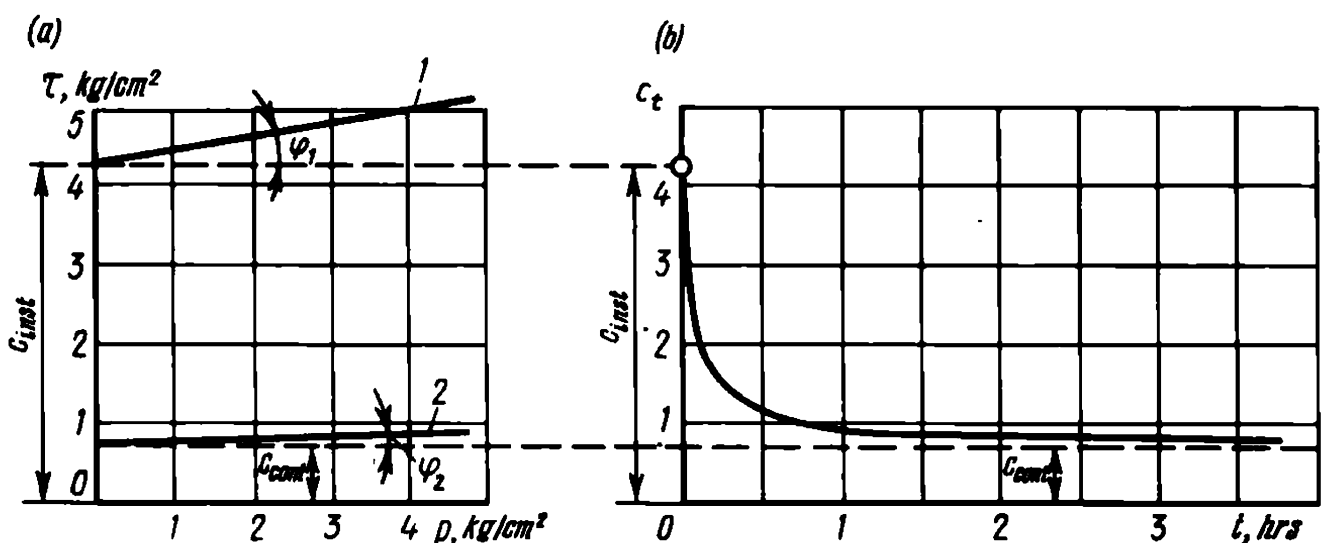


Fig. 38.4. Charts illustrating the relationship between the parameters of shearing resistance of a frozen clayey soil ( $w = 33\%$ ,  $T = -1^\circ \text{C}$ ) as shown by experiments of N.A. Tsitovitch

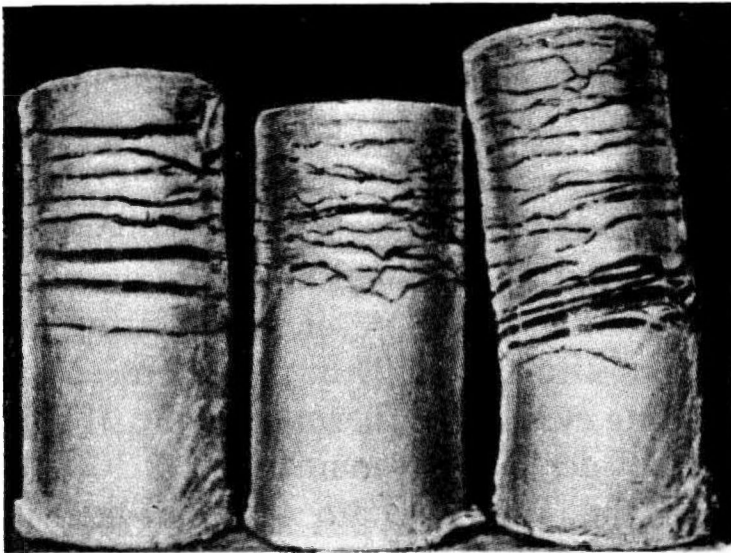


Fig. 38.5. Ice seams in soil samples

deposits of crushed rock etc. located above the water table and, consequently, composed of loose unfrozen materials (*dry permafrost*).

As demonstrated by practice, soil heaving in permafrost is particularly detrimental for pile foundations of bridges, especially, wooden. Heaving occurs as the frost zone (or *the active layer*) which freezes in winter and thaws in summer increases in volume. Another essential factor contributing to heaving of structural members is frost-induced adhesion (termed *adfreezing*) of soil in contact with the lateral surfaces of supports.

Adfreezing of permafrost soil to wood varies from 3 to 25 kg/cm<sup>2</sup>, depending on the physical properties of soil, its moisture content, thermal regime, and on whether the surface of contact is smooth or rough.

The active layer expands, and, hence, heaves mainly due to formation of interlayers of ice in the soil as water migrates (Fig. 38.5). This process consists in vertical pumping of water from lower strata. Clearly, this can occur only if the water table is at a small depth. Added saturation of soil causes ice formation, soil heave (this may appear as soil blisters or “*hydrolaccoliths*” as oversize heaves are called) and dramatic drop in bearing capacity upon thawing, especially, when the structure of soil is disturbed.

Water migration in permafrost soils first discovered and investigated by Russian and Soviet scientists is mainly conditioned by osmotic pressure at temperature gradients and also by internal stresses appearing in the soil freezing nonuniformly.

The most intensive water migration occurs when light loams and powdered sandy loams are involved. The inappreciable permeability of clayey soils generally prevents intensive water migration. Ice interlayers forming in a soil mass as this is being frozen may be from fraction of the millimetre to tens of centimetres and more. This process is responsible for *the amount of the ice* in the given permafrost deposit.

Permafrost soils containing numerous ice interlayers responsible for the ice content expressed in per cent stand aside. When thawed, such soils yield conspicuously which leads to settlement of structures on them.

The depth to which thawing penetrates is generally differential, this process is often continuous which causes unfavourable soil conditions. Charts in Fig. 38.6 demonstrate specific features of consolidation of soils under study at an initial load  $p = 1.0 \text{ kg/cm}^2$ . N.A. Tsitovitch and his disciples have studied in detail the thawing of permafrost soils.

Frost heaving, that is, expansion of saturated soil upon freezing is one of essential physical properties of permafrost soils used in construction of roads.

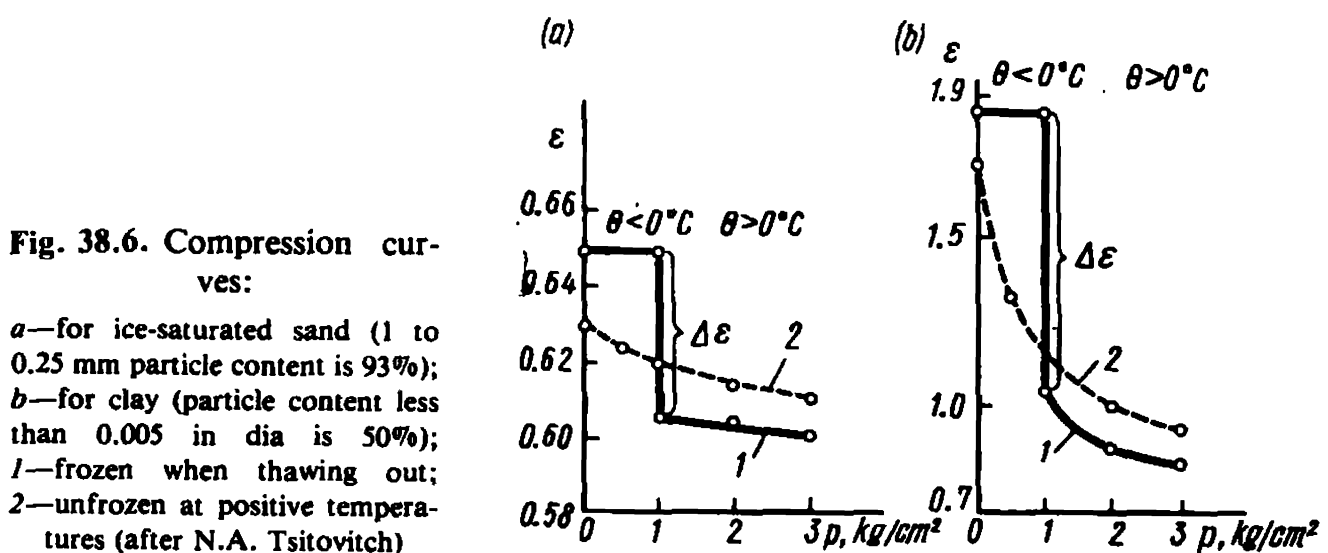
The degree of frost heaving is determined by referring to the coefficient of frost heaving  $K_{heav}$ . It is established by testing a soil sample using a special apparatus. The soil sample placed in a metal ring 50 mm in diameter and height is subjected to one-sided freezing in a freezing chamber at  $-5^\circ\text{C}$ . As the test is being conducted, provisions are being made to permit vertical capillary and pellicular water flow to the freezing zone. The increase in the height of the specimen is then determined. The coefficient of frost heaving is found as the ratio of the maximum increment of the height of the specimen  $\Delta h$  to the original height  $h$  and is expressed in per cent:

$$K_{heav} = (\Delta h/h) 100$$

Depending on the value of  $K_{heav}$ , we distinguish between non-heaving ( $< 1\%$ ), slightly heaving (1-4%), heaving (4-7%), appreciably heaving (7-10%), and extremely heaving ( $> 10\%$ ) soils.

The degree of frost heaving of soils in permafrost must be studied when constructing roads on them.

Lifting of bridge foundations is a variety of heaving deformation increasing with time. It can often attain 1.5-2 m and sometimes exceeds 3 m.



Deformations of bridges induced by ice-fields (nahledee) are of a different nature.

There are three types of ice-fields, or icings: *river*, *confined-water pressure*, and *common* ice fields.

River ice-fields form as river waters penetrate to the ice-covered river surface producing conspicuous ice layers. These may be 4 m and more in thickness. Adfreezing to bridge supports and rising jointly with the ice cover during spring and summer high floods, icings may sometimes pull out piles, deform supports and even cause bridge failures. This actually has occurred on several rivers in Siberia.

With the onset of winter the groundwater is confined between the permafrost table and the frost table providing the boundary of the increasingly thickening active zone. At low points of relief pressurized water will try to seek points of weakness, that is, where the frozen active zone is the thinnest or absent altogether. As a result, the water will rush upwards, flood the free space, and, upon freezing, form icings of unusual shapes.

Ice-fields also interfere with proper service of bridges. We know instances of total destruction of wooden bridges by icings. This, for example, occurred in 1928 on the Onona River where a bridge was cut off by an ice-field.

The most advantageous foundations for construction in permafrost areas are provided by competent bedrock or loose frozen soils (sand, gravel, crushed rock) coupled to a low location of the water table.

### Sec. 38.2. Construction in Permafrost Areas

We can conclude that permafrost clayey soils, when thawed, generally turn into liquid mud with almost zero bearing capacity. On the other hand, when frozen, they demonstrate high bearing properties.

Practice of construction in Norilsk has shown that permafrost soil foundations are fairly stable and even in the absence of competent bedrock foundations, provided that temperatures  $-2$  to  $-3$  °C are maintained, buildings as ones with ventilated basements have been adequately functioning for decades.

Construction in Vorkuta at first disregarded permafrost ( $-0.2$  to  $-0.7$  °C) conditions of the permafrost soils. Then resort had to be made to the above method of using ventilated basements. Buildings in the two towns are in proper conditions.

Isolation of engineering structures from permafrost soils by employing pile foundations frozen into the permafrost previously defrosted by steam pipes with points or by electroheating is a most promising method.

Criteria of subsurface investigations and designing of structures in per-

mafrost areas are presented in the Code of Practice SNIIP-II-18-76. This manual proposes these variants of construction: I—disregarding the permafrost conditions of the foundation material (competent bedrock and semihard rocks without conspicuous ice-filled fissures and coarse detrital soils without ice interlayers; II—preserving the permafrost conditions of the structure foundations (bridges and unheated buildings where measures are provided to maintain permafrost); III—tolerating the possible thawing of the permafrost foundation material during construction and operation of structures (with minor structure settlement and steps taken to avoid differential settlement); IV—with preliminary defrosting of the foundation material before the foundation is built (under conditions where permafrost materials are inevitably thawed (which cannot be tolerated) during operation of, say, a dam supported by bedrock with ice-filled fissures).

When deciding of the version of construction, we must take into consideration the type and eventual service of the structure and the particular permafrost conditions. Construction using variant II involves reinforced concrete piles frozen into the permafrost and provision of basements ventilated in winter.

Construction of roads in permafrost areas employs embankments using variant II (preservation of permafrost conditions). The height of the embankment,  $H$ , is calculated proceeding from the standard depth of freezing and thawing of the soils in the fill,  $H_f$ , allowing for the heating effect of slopes and colour of the pavement ( $m_1$  and  $m_2$ , respectively), by referring to this relationship:

$$H = m_1 m_2 H_f$$

where  $H$  is the requisite height of the fill in  $m$ .

The coefficient  $m_1$  allowing for the added heat influx via embankment slopes is

$$m_1 = \sqrt{F_1/F_2}$$

where  $F$  is the area of the roadbed;  $F_1$  is the area of the embankment foundation. In particular with 1/1.5 slopes and given the width of the roadbed equal to 7.5 m, the value of  $m_1$ , depending on the height of the embankment, is within 1.08 to 1.07, that is, varies insignificantly.

The value of  $m_2$  for black pavements is assumed to be 1.12-1.50 depending on the environmental conditions. To conclude, it must be noted that Soviet soil scientists led by Prof. N.A. Tsitovitch, Corresponding member of the USSR Academy of Sciences are in the forefront of the world's permafrost studies.

---

Chapter 39

---

**Rock Weathering. Its Importance in Geotechnics**

---

**Sec. 39.1. The Processes of Weathering.  
Eluvium and Its Geotechnical Characteristics**

Weathering is disintegration and alteration of the composition and state of rocks in sites of their natural occurrence due to physical processes, chemical and biological agents.

Products of modern weathering of rocks remaining *in situ* and overlying original rocks gradually passing to the former are called *eluvium* or *eluvial deposits*.

There are these types of weathering: (a) disintegration (by physical agents); (b) decomposition (produced by chemical agents); (c) decomposition and disintegration (by biological agents and effects of vegetation).

Rocks are generally acted on by all the three types of weathering. These, however, reveal themselves with different intensity conditioned by the climatic and other environmental factors. Weathering by physical agents generally enhances joints typical of rock masses. An important role is played in this process by conspicuous diurnal temperature gradients and water. Water penetrating into fissures and freezing there exerts tremendous lateral pressures, the rock fails in tension which leads to further widening of the fissures and joints.

Due to the continuous action of the above factors the hard rocks are more and more separated into more or less regular blocks typical of the particular variety of igneous rocks governed by conditions of formation (Fig. 39.1). Due to weathering the hard rock mass becomes flaggy or mattress-shaped in structure especially characteristic of granites (Fig. 39.2). With passage of time these blocks are further separated forming accumulations of crushed rock and gruss.

Weathered blocks, more or less large *fragments*, crushed rock and gruss remain *in situ* burying parental rock or move downslope. This results in rock falls and rock slides.

Physical disintegration of rocks typically occurs in areas where inclement continental conditions prevail, notably high mountainous regions.

*Chemical weathering* of rocks is their decomposition induced by atmospheric gases and water containing dissolved salts and gases (mainly oxygen and carbon dioxide) coupled to products of decomposition of organic matter.

The least stable of plutonic rocks pushed to the upper layers by one process or another are granites, diorites etc.



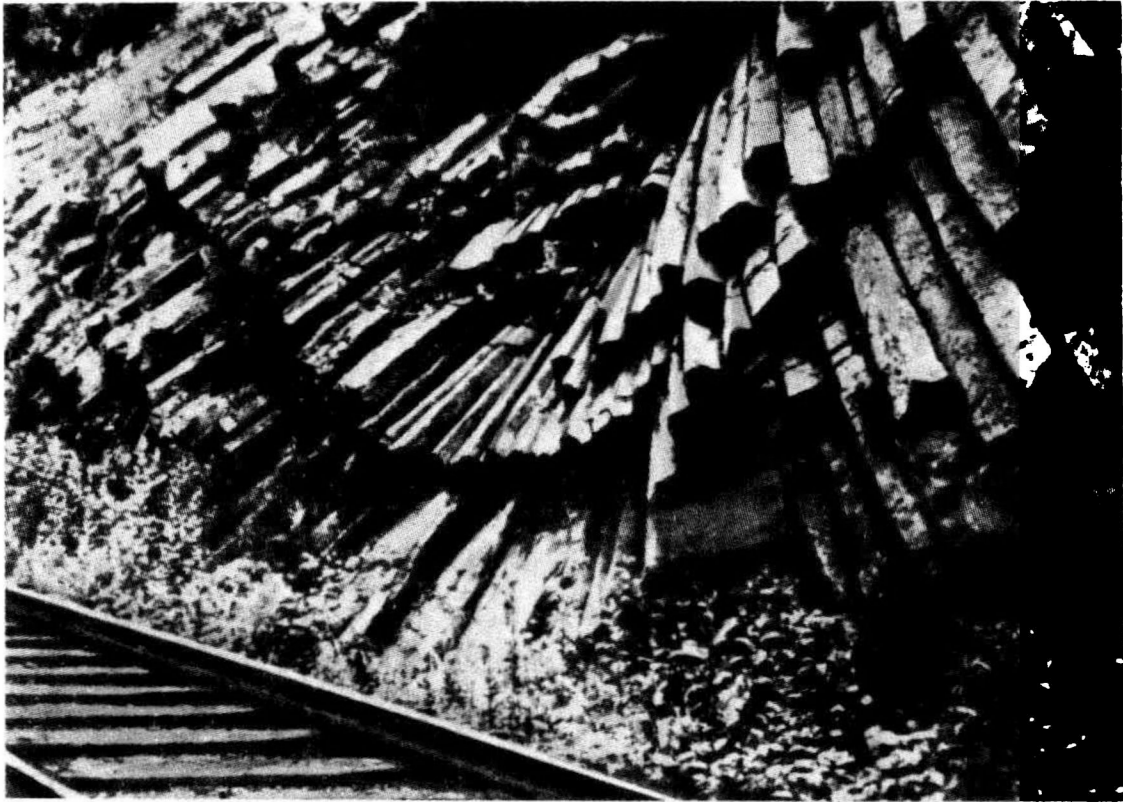


**Fig. 39.1.** Basalt columns in a zone of active weathering (photograph by Z.P. Potapova)

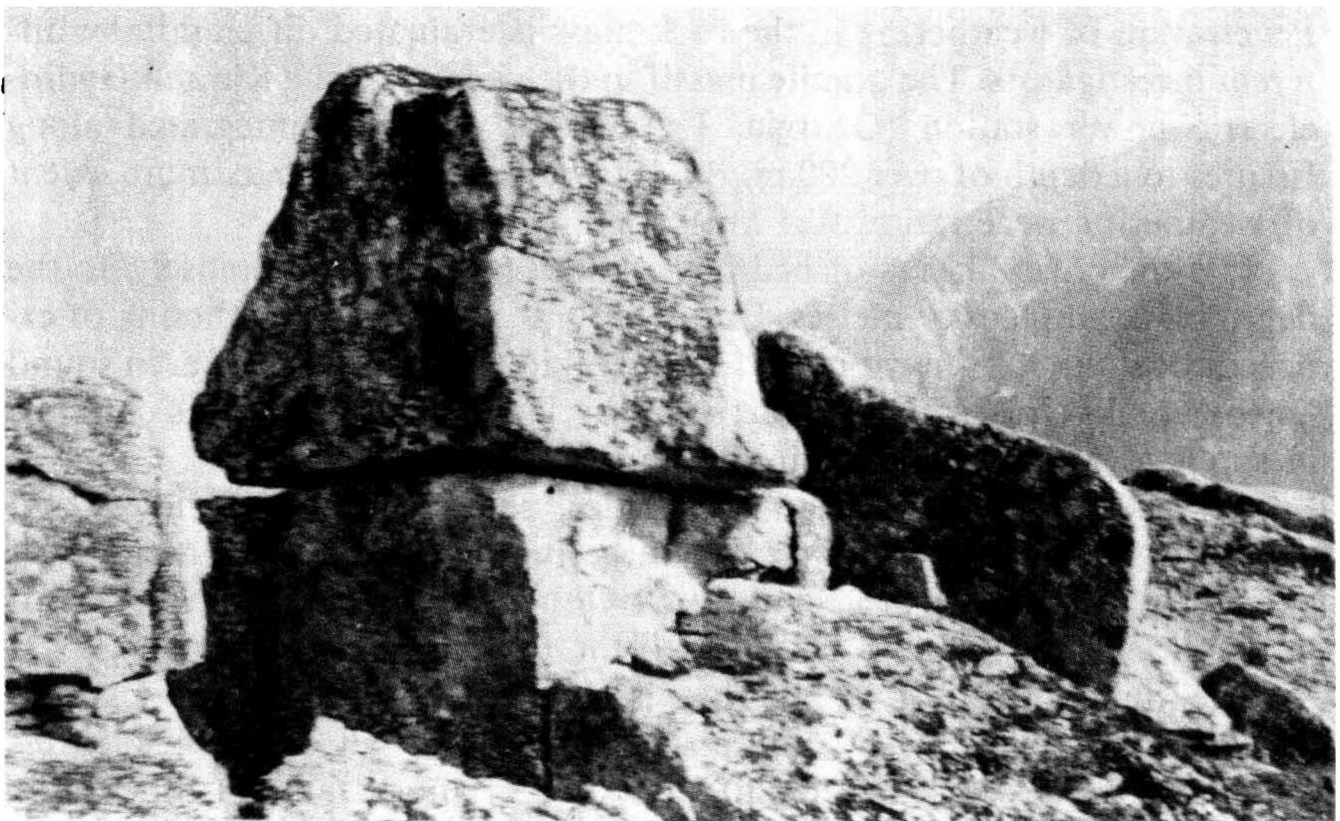


**Fig. 39.2.** “Nature’s architecture”. Unusual form of granite weathering in the Kolyma River basin (photograph by Lengydroproekt Institute)

Chemical decomposition of feldspars is an important causative agent of weathering of igneous rocks, primarily granites. This process induced by reaction of water and carbon dioxide produces kaoline  $\text{Al}_2\text{O} \cdot 2\text{SiO}_2 \times \times 2\text{H}_2\text{O}$ . The rate of chemical decomposition is especially conspicuous in humid and warm areas.

*Weathering of rocks by biological agents* may take on different forms. Various microorganisms and vegetation play an essential role in these processes.

Vegetation acts on rocks both as a physical factor (wedging effect of growing roots, rocking of tall trees by wind) and as a chemical agent (acids liberated by roots). Mosses and lichen of all types able to decompose even the hardest materials are especially detrimental.

Fissures in weathered rocks are generally filled with clayey products of decomposition of the same rock. As it further decomposes, more and more clayey material is produced. The final products of weathering of most rocks generally represent clays or loams with more or less amount of detrital material.

Weathering of fairly impervious rocks involves only rock masses located above the level of surface and subsurface waters, that is, in the zone of intensive disintegration. It can thus be concluded that the depth of penetration of weathering is the greatest in areas where the rock mass was for a lengthy period of time in continental conditions and was not submerged. Penetration of weathering in the rock mass is evaluated differently by different investigators. The granite massif in the vicinity of the Khrami Hydroelectric power station (Georgia, USSR) was found disintegrated along fissures to a depth of over 200 m. B.B. Polynov reports the maximum extent of weathering penetration (0.5 km).

It is the crustal layers of bedrocks that decay the most intensely, to the depth of several tens of metres. Under definite conditions weathering of exposed rock outcrops may proceed rather rapidly. So, surfaces of even sound igneous rocks (for example, quartz porphyries) within 15-20 years can turn in spoils to a plastic clay with quartz crystals.

As has been pointed out, clay shales, shaking shales, argillites and aleurolites are especially subject to weathering (Fig. 39.3). Such rocks must be rapidly worked and protected from weathering, say by preserving a protective layer which should be removed the last.

The main effect of weathering is weakening of disintegrating and decomposing rocks. The compressive strength of all hard rocks after weathering proves to be lowered to one extent or another, mainly due to the drop in the true cohesion. This reveals itself primarily in increased jointing of the rock mass. As a result of commonly observed kaolinization

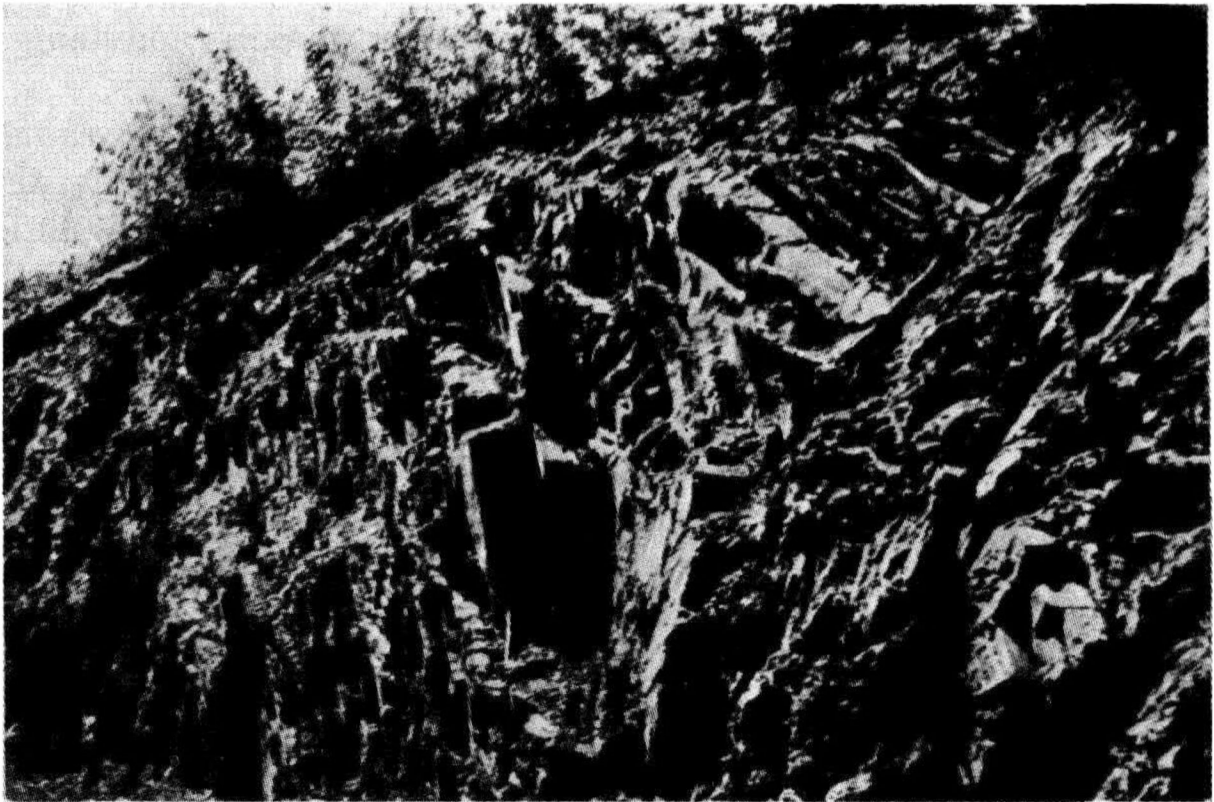


Fig. 39.3. Weathering form typical of schists

weathered rocks often demonstrate a marked clay content. This process, naturally, occurs at a faster rate if the rock is wetted, in particular, if river banks are submerged during high floods. It must be also noted that weathering of the rock mass generally occurs nonuniformly, the rate of the process being faster at zones of weakness which causes marked differentiation of the weathered rock both in terms of composition and extent.

Clearly, the conditions described above impair the bearing capacity of structure foundations (in particular, bridge abutments) composed of weathered rocks. They also increase rock pressure in tunnels driven in weathered rock beds. Rock pressure in tunnels generally increases some distance in from the portals where weathering usually reveals itself the most conspicuously (surface zone of slopes). This occurred when driving the Adjaris-Tskhali (Transcaucasia) tunnel where ground composed of strongly decomposed argillaceous sandstone caved in.

It should be borne in mind that in zones of tectonic fracture, raptures, folding, chipping of rocks, particularly, in cores of squeezed folds the extent of active weathering may be of the order of many tens of metres (so called pockets).

Thus decomposed ground may be encountered in a tunnel not only near portals but also in some localities of the alignment, demonstrating, on the whole, sound and competent material. These events, naturally, complicate

matters when a tunnel is being driven and stronger supports and lining are needed.

The drop in the bearing capacity of foundations composed of weathered rocks requires that pressure on the subgrade be reduced or that the depth of the foundations be increased to ensure total stability of, say, bridge abutments and to lower settlement. Particularly small bearing properties are exhibited by weathered metamorphic shales, such as micaceous phyllites, to say nothing of chlorite and talc varieties.

The total stability of bridge abutments, especially when at a small distance from the edge of the bank, may often prove insufficient. It is a good plan, then, to place bridge piers and abutments as well as supports for other structures on sound bedrock, having previously removed the decayed material.

Weathering processes able to cause sudden and dramatic drop in the strength and bearing capacity of clayey soils may occasionally occur at an exceptionally rapid rate attaining as much as several centimetres per day.

Untimely cuts are made rather frequently. In these conditions, especially, when clayey soils are involved, frost weathering coupled to wetting of soil by accumulated meteoric and ground water is especially detrimental.

It should be concluded that the simplest solution is to erect structures on sound weathered rock. This calls for removal of the decayed upper material. Moreover, the alignment of a river or valley crossing and tunnel is located by the site where decomposed rock masses are the least and the extent of the active weathering zone is the smallest.

If decayed material is impossible to remove, special engineering measures must be provided to ensure the strength and stability of the structure proposed under unfavourable conditions.

### **Sec. 39.2. Debris Formation. Talus Deposits and Their Role in Landslides**

*Talus* or *talus deposits* are spalled material fallen from decomposed rock outcrops and transported to the toe of a slope by gravity or the action of meteoric water.

Talus deposits (colluvial soils) are accumulations of nonuniform loose angular and nonfoliated material. Very often talus is clay or loam mass containing angular rock fragments differing in size and shape.

Talus deposits make up in many instances substantial sections of slopes. This is, for example, the case of the Black Sea coast of the Caucasus and Crimea when talus deposits encircle practically the toe of the mountains (Fig. 39.4). Talus deposits shifting downslope toward the sea cause numerous landslides presenting a danger to land uses and villages.



Fig. 39.4. Talus deposit at the southern coast of the Crimea

Talus is generally the thickest at the toe of a slope, and the thinnest at steeper sections of the slope. Substantial talus deposits are accumulated at depressions on slopes, such as buried lateral valleys. Then the thickness of talus may attain as much as several tens or even hundreds of metres.

In contradistinction to eluvium, talus deposits, excepting the upper sections of slopes, often overlie alien rocks and soils. At the same time talus deposits, whatever their location, *except for the lowest* (say, at the toe of a slope), are in a state of unstable equilibrium. This fact is very important, being responsible for stability of talus on mountain slopes when earthwork is to be done (excavating a power canal, construction of a road, making a cut etc.).

By virtue of the process of talus formation, this spalled material is moving downslope, but the rate of this movement may be so small as to be hardly noticeable.

It is often quite a problem to remove the entire deposit of talus so that a structure may be supported by a competent bedrock since talus is generally very thick and is widely distributed.

Retaining walls are used to control talus slides. If the talus deposit is small in thickness, has a low moisture content and the retaining wall will rest on sound bedrock, this structure will be efficient, otherwise it will be of no service.

Added wetting of talus is the main factor contributing to instability of such deposits. Talus on slopes may be wetted by various agents. These include meteoric water, a rise in the level of water reservoir, water seepage from a power canal, vegetable garden irrigation, sewage water leakage etc.

Stability of talus deposits on slopes can also be impaired by ground-water seeping at the contact with bedrocks. Water seepage occurs when a talus deposit, being a shifting mass of clay material, acts as bedding of all aquifers of bedrock on the slope. The water, devoid of escape, saturates the talus deposit, making it heavier and eliminating apparent cohesion of the clayey mass. The uplift pressure of the seeping water causes talus slide even on very gentle slopes with the angle of dip only  $4^\circ$  or less.

The coarser the grains in the talus deposit, the less likely it is to creep. However, excessive precipitation may trigger mudflows in mountain valleys entraining even detrital material composed of large fragments.

The shearing strength of talus can vary over a wide range depending on its composition and water content. Thus, clayey talus deposits can have the angle of internal friction varying from  $4-5$  to  $45^\circ$ , and apparent cohesion from  $0.05$  to  $0.5 \text{ kg/cm}^2$ . Thus from the engineering point of view talus may prove a troublesome ground. Therefore special care must be taken when exploring a building site.

The low stability of talus deposits can be inferred from the character and relief of the slope and also the presence of landslide cirques as evidence of previous talus creeps, of various fissures. Other symptoms include deformed, tilted trees (drunken forest), inclined telegraph posts and structures, waterlogged sections on slopes, warped pavements, paths etc.

If the talus deposit is thin it is best to remove it and place a roadbed or other structure on sound bedrock thus saving time and labour.

### Sec. 39.3. Wind Action

Wind is a very important weathering agent. *Deflation* or removal of decomposed rock materials by the wind coupled to corrasion and abrasion causes erosion of intact, unweathered rocks.

Fine rock materials are transported from one place to another by the wind currents. Thus the wind plays the part of a *transporting agent*.

Fine material may sometimes be carried away to places thousands of kilometres from their parental rock deposits. Coarser particles, as sand, are transported several metres, rarely hundreds of metres away. Sand, as it were, is *winnowed*.

The material transported by the wind eventually settles on the earth's surface and is fixed in place by one agent or another. Vegetation (grass, undergrowth, trees) are an important factor in this process.



Accumulation of material carried by the wind sometimes takes long periods of time, and the depth of deposited material is gradually increased. Thus *aeolian deposits* form. These include *aeolian sands* (sand dunes and barchanes) and *aeolian loess* which demonstrates very specific properties. Loess deposits often attain several tens of metres in thickness (see Fig. 36.2).

Aeolian loess appears as somewhat cohesive silty nonfoliated soil light yellow or greyish yellow in colour that can be easily rubbed between the fingers and, which is essential, very porous. Porosity coupled to high content of dust particles make loess and loessian loams rather a pervious soil (see Chap. 36).

*Sand dunes* and *barchanes* are mounds or drifts of wind-blown sand material. Dunes typically occur along sea and lake coasts and large river banks (the Dnieper, Volga, Don and others). Sand dunes are very often found on the coast of the Baltic sea and its gulfs. They are 20 m and more in height there. Barchanes may be found in arid and semiarid plains. In the Soviet Middle Asian republics barchanes cover an area of about 1 million km<sup>2</sup>. Their height is often tens of metres and sometimes more.

Barchanes are generally composed of rather angular sand grains which makes them more stable compared with sand dunes composed of fairly smooth grains. This property is due to the origin of sand in dunes transported and deposited in water reservoirs and streams where it is continuously rolled and washed. Therefore sands in dunes are cleaner which is responsible for lowered dynamical stability of this material. This property of sands in dunes has brought about a number of major accidents.

Sand dunes and barchanes are movable soils transported by prevailing winds. Depending on such factors as, primarily, the force of the wind and aridity, the velocity of movement of sand dunes and barchanes may vary from 2-4 to 10-20 m a year. In rare instances, if the dunes and barchanes are low and wind is strong, this velocity may attain several metres a day.

The moving sand dunes and barchanes may be detrimental for villages and engineering structures. Advancing sands bury cultivated lands, houses and settlements, irrigation networks etc. It is in this fashion that certain states perished in the past. In the recent years Soviet archeologists have discovered numerous remarkable historical monuments in desert areas of the Middle Asia: fortresses, palaces, mausoleums (Khoresm) that remained buried by sands for centuries. Ancient temples and structures (for example, in Egypt) that laid under sands for millennia are currently being found by archeologists. Road cuts and canals are traps for the sands which are moving or wind-blown. Case histories are known when highway cuts 2-3 m deep were buried under sand within a year.

As great a hazard is presented by the reverse process when the dune sand

is blown away. Then the road foundations may be eroded by wind, especially in bridge approaches. The foundations of bridge abutments, viaducts and other structures can be left completely exposed.

Apart from moving sands, there are *stabilized* dunes. These can be found in northern forested areas of the USSR.

The principal method of stabilizing dunes and, to some extent, barchanes is by seeding the dunes with vegetation. Planting grass and undergrowth is an efficient method extensively used for stabilization of movable sands. Depending on the particular climatic conditions bushes or grass varieties may be planted. Planting young mountain pines stabilizes dunes in northern areas. *Aristida pennata*, *A. plumosa* and leafless bush variety, *Haloxylon aphyllum* are extensively used in desert areas in the Middle Asia.

Southern regions use *Ammodendron*, oats thriving on sand, *Amphiphila arenaria*, ryegrass and coast wheat for the same purposes. The same cereals are very advantageous for stabilizing sand fills. Apart from planting vegetation various shields may be employed. This forms sort of burial places for barchanes devoid of mobility. However, if the vegetable cover is disturbed (say, by earthwork), sand dunes and barchanes may again start to drift.

Successful but still costly efforts have been made in this country to stabilize moving sands by coating them with binding materials, such as crude road oil, road asphalt emulsion and paraffin-fuel oil mixtures.

As has been established by practice, such stabilization is quite feasible but labour-consuming.

#### Sec. 39.4. Soils. Formation of Soils

Under definite conditions products of weathering may form a topsoil layer of the earth's crust. The topsoil is understood to include the uppermost crustal strata changed by the joint effect of weathering and soil formation. Biological processes prevail in the latter process.

Soils are a function of the physiogeographic conditions of the climate, parent materials, vegetation, animal kingdom, relief, terrain and its age. The main role in formation of soils is played by the climate. The other factors are subsidiary and are not responsible for production of the soil type, contributing only to formation of varieties within one soil type group. Since climate is of a zonal character, principal soil types are distributed in conformity with the climatic zones on the globe.

If we proceed from the north southwards, we can distinguish the following zonal types of soil in this country: tundra soils, podzols and turf-podzol soils, grey forested-steppe soils, Chernozem soils (a group of neutral soils rich in humus), brown soils of dry steppes, grey-coloured soils occurring in arid steppes and deserts, red soils.



Apart from the above zonal soil types, there are intrazonal groups of soils within individual soil zones. The most typical of them in the northern and forested (temperate) areas are swamp soils (organic terrain), and in the southern regions saline soils (solonetz and solonchak soils).

Soil layers generally demonstrate a very complex and erratic structure. Yet definite generalizations can be made. It is customary to divide the upper crustal layers into the *A*-horizon (zone of leaching) and *B*-horizon. The *B*-horizon is underlain by the *C*-horizon (the bedrock, or substratum).

The *A*-horizon has generally three subdivisions: litter, leaf mold (designation  $A_0$ ); humus soil ( $A_1$ ); leached grey soil from which chemical substances are washed out to the *B*-horizon. This is the secondary layer of leaching and is sometimes called an illuvial horizon. A brief characteristic of soil types is given below.

*Tundra soils* are generally waterlogged due to marked air humidity and low evaporation rate typical of high latitudes. The swampy character of such soils results also from the shallow depth of the permafrost table in tundra areas.

Because of the low temperatures organic matter in tundra regions decay exceptionally slowly, so tundra soils demonstrate a very inappreciable humus content. These soils are extremely loose, have much poorly decomposed vegetable remnants, are rapidly soaked on wetting and shrink on drying. All this, taken together, makes tundra soils very inadequate construction materials or material for roadbeds.

*Podzol and turf-podzol soils* are found in forest regions. The  $A_2$ -horizon is composed of grey soils resembling ash by colour, hence this name. Much precipitation in this zone washes out soluble chemicals from this subdivision. The lower strata of the *B*-horizon are enriched by salts removed from the topsoil. These salts somewhat cement the low horizon soil which appears as small sharp-edged nut-shaped clods or columns.

Engineering properties of soils of this group are governed by the composition of the parent material. Generally they provide fairly satisfactory construction material which is especially true of sandy and sandy loam varieties.

*Grey forest soils* are intermediate between chernozem and podzol soils. They are typically found in areas where forest belts are alternated by steppe areas. Such regions are known as forest-steppes. Construction properties of this soil group differ from one variety to another. Part of them can resemble turf-podzols, another part chernozem soils.

*Chernozem soils* occur in the steppes where the climate is warm and the rate of decay of vegetable and animal remnants is very intensive. This makes the soil rich in humus and black in colour. The thickness of chernozem rocks may be 1 m and sometimes more.

These rocks are the best for agriculture but provide very poor material for construction due to high moisture capacity, stickiness and sensitivity to water. When dry, they are dusty, in rain they turn into liquid mud, and dirt roads become impassable.

*Chestnut-coloured soils* are found south and south-east of the Chernozem soil belt. They are typical of regions where relatively little precipitation falls and evaporation rate is intensive. They form in areas characterized by a long and hot summer and a short severe winter.

They demonstrate low moisture content. They owe their name to their colour. The shade of colouration is conditioned by the humus content. Thus there may be many varieties of chestnut-shaded soils, from light to dark brown. Chestnut-coloured soils occurring in semiarid steppes in the southern regions of this country are fairly satisfactory construction material. Their principal defect is their softening on being wetted. However, in warm southern areas they dry up rapidly.

*Brown soils* are typically found southeast of the area of light chestnut-coloured soils, where there is still less precipitation. The climate is more continental in character which is responsible for the marked salinity of the soils. Notwithstanding low humus content, when adequately watered, these soils are rather fertile. The marked salinity, however, very much lowers their construction properties.

*Desert soils* differ appreciably in composition. Due to environmental conditions characteristic of desert regions these soils are poor in humus and concurrently rich in various salts including calcium carbonate, sodium chloride and sulphite, magnesium and even soda. Desert soils are often

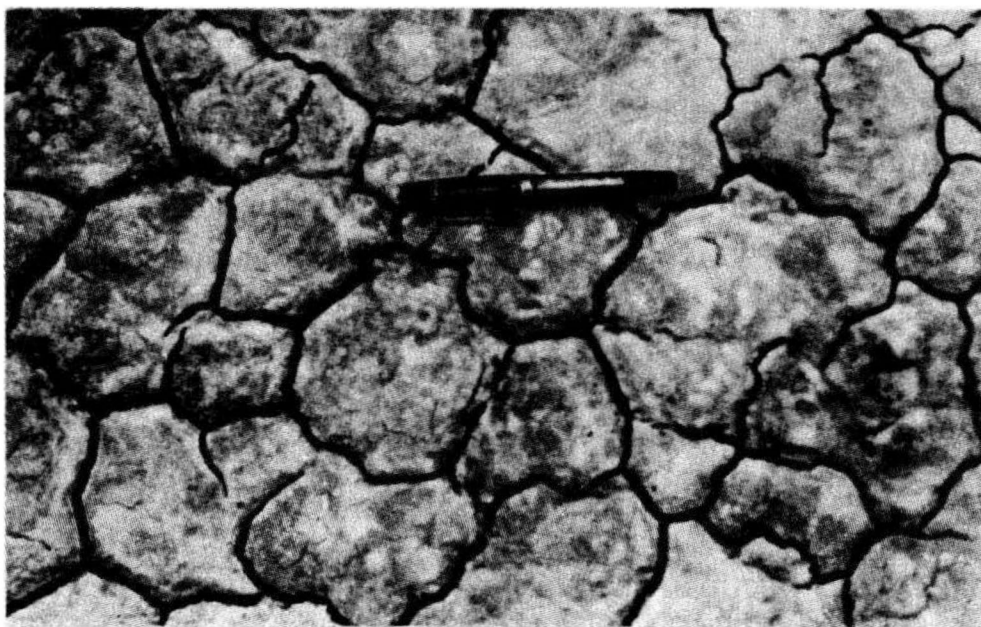


Fig. 39.5. Takyr in a dry season

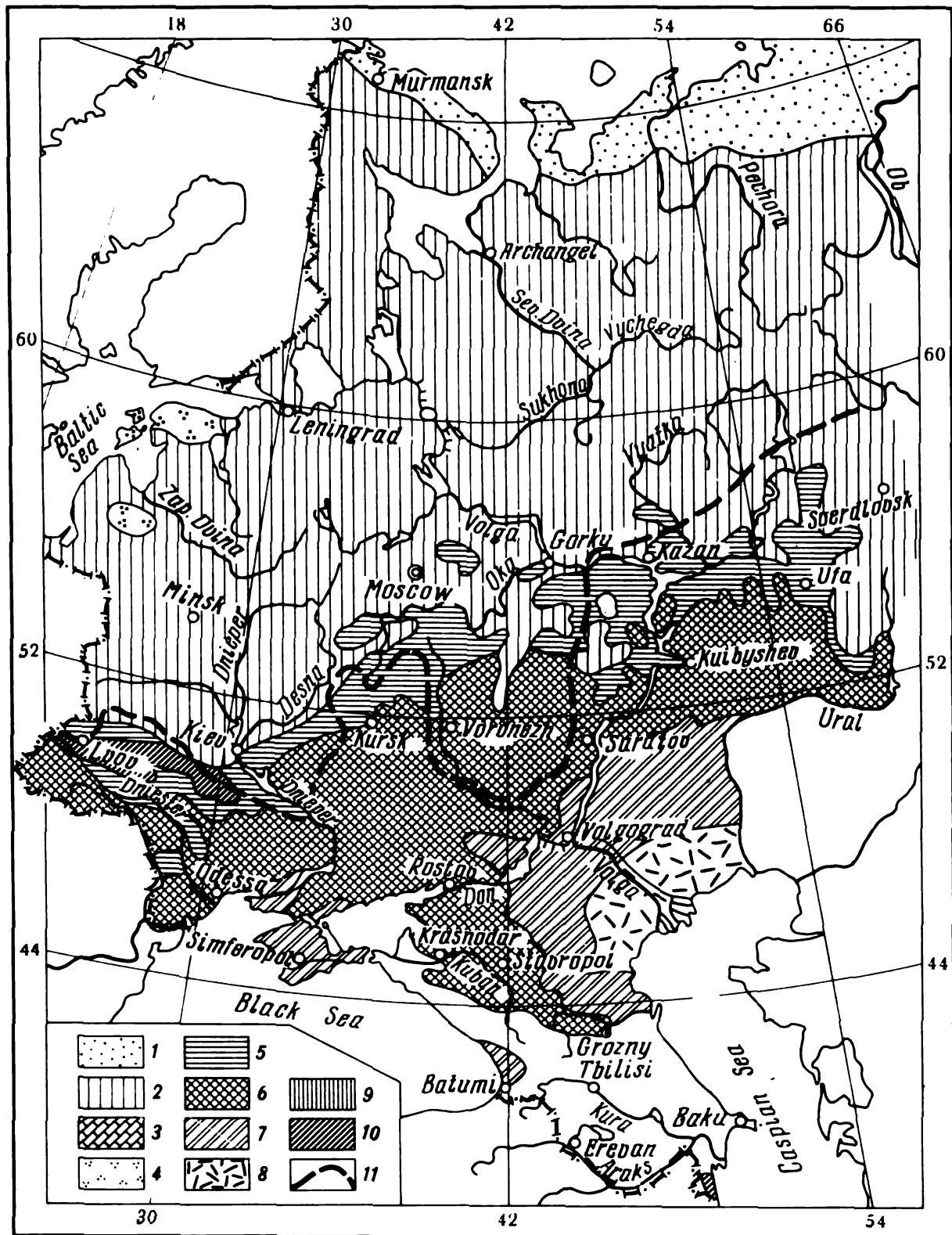


Fig. 39.6. Schematic soil map of the European USSR (after N.A. Kachinsky):

1—tundra soils; 2—podzol (partially waterlogged at places) soils; 3—mountain-forest podzol soils; 4—turf humus-carbonate soils alternated by podzol soils; 5—gray forest soils and other soils of the forest-steppe; 6—Chernozem soils; 7—chestnut-coloured soils with scattered Solonetz soils; 8—brown Solonetz soils occasionally wind-blown; 9—brown-red soils of Crimean and Caucasian deciduous forests; 10—red, yellow and subtropical podzol soils; 11—expansion of drift boulders

called grey or light-coloured soils. They occur on a vast territory lying south of the brown soils. Their construction properties are very poor. Due to the marked salt contents they are very dusty and rapidly soften on wetting.

*Red earth* (or red loam) are rocks commonly found in warm areas with much or excessive precipitation and abundant forest vegetation (the Black Sea coast of the Caucasus and of the Crimea). Their distribution in this country is very limited.

*Solonchak* (light-coloured soil rich in soluble salts) and *solonetz* (black alkali soil with a columnar structure) soils are mainly found in hot arid regions. Groundwater circulating close to the earth's surface rises to the uppermost soil layers and, upon evaporation, causes salts to accumulate on the ground. In dry weather the surface layer in such areas is covered by salt deposits, and the ground appears white or whitish. After rains the solonchak soils turn into viscous impassable salty swamps. Meteoric water, dissolving the salt in the topsoil, percolates to deeper horizons, and solonchak soils gradually become solonetz soils less rich in salts.

These soils are not, as a rule, used for roadbeds. Construction manuals, however, envisage use of these soils as material for roadbed foundation and subbase.

The so-called *takyr*s constitute a specific relief feature in the Middle Asia. These are argillaceous aggregations containing gypsum and carbonates with a smooth surface. In dry seasons they are very hard and are broken by fissures into more or less regular figures (Fig. 39.5). In rainy periods they transform to a clay soil mass with excessive water content and are impassable.

Figure 39.6 is a schematic soil map of the European part in the USSR.

---

## Chapter 40

### Mud Rock Flows

---

#### Sec. 40.1. General Considerations

Landslides, known as *mud spates* or *mud rock flows* may occur in mountainous areas under definite conditions. These are saturated material accumulating in ravines, on steep mountain slopes and sometimes in the mountain river valleys rushing downslope. They transport rock fragments of the detritus covering the slopes.

Mud rock flows originate as follows. During heavy rainstorms in moun-

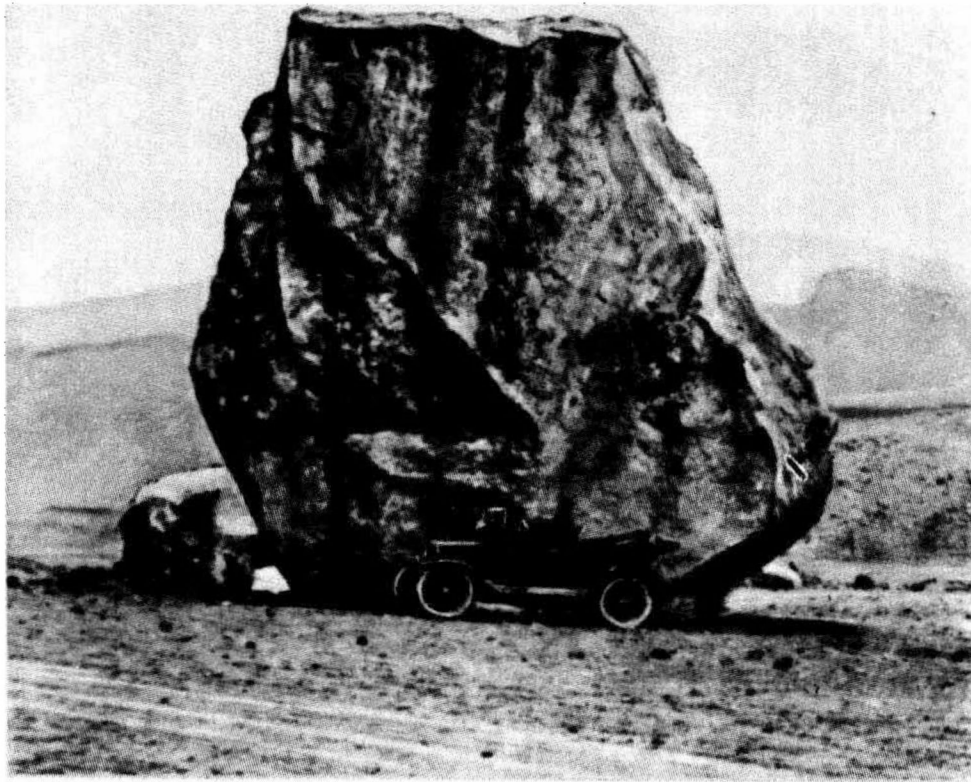


Fig. 40.1. Rock displaced by a mud rock flow. Tajikistan

tainous areas and upon sudden melting of snow on steep slopes of mountain valleys slides and creeps occur. Talus deposits generally representing loamy material with inclusions of crushed rock and larger rock fragments whose position on the slopes is relatively unstable are the first to slide. Excessive wetting drastically decreases cohesiveness of talus deposits and lowers their shearing resistance. This material rushes in a swift torrent downslope at velocities 4 to 6 and sometimes 10 m/s. Rains enhance this process.

As they are moving, semifluid talus deposits rush down a ravine or valley, transporting collapsed bank material and, which is important, that of tributary *debris cones*. This huge mass of liquid mud and debris brushes aside almost all natural obstacles in its path.

The debris transported by the mud rock flows often produce dams 5 and even 10-15 m in height. When these dams are broken, even more detrimental conditions arise. Special danger is presented by large rock fragments carried by the mud rock flow.

Cases have been reported when a mud rock flow transported rock blocks up to 1 500 cubic metres in size (Fig. 40.1). Rock fragments in a mud rock flow may often constitute half of the total mass or more. The density of the mud rock flow material is up to 1.4-1.5 t/m<sup>3</sup>. All structures, buildings, bridges etc. encountered by a mud rock flow may prove to be in very dangerous conditions and even collapse.



**Fig. 40.2.** Road covered by debris brought by a mud rock flow

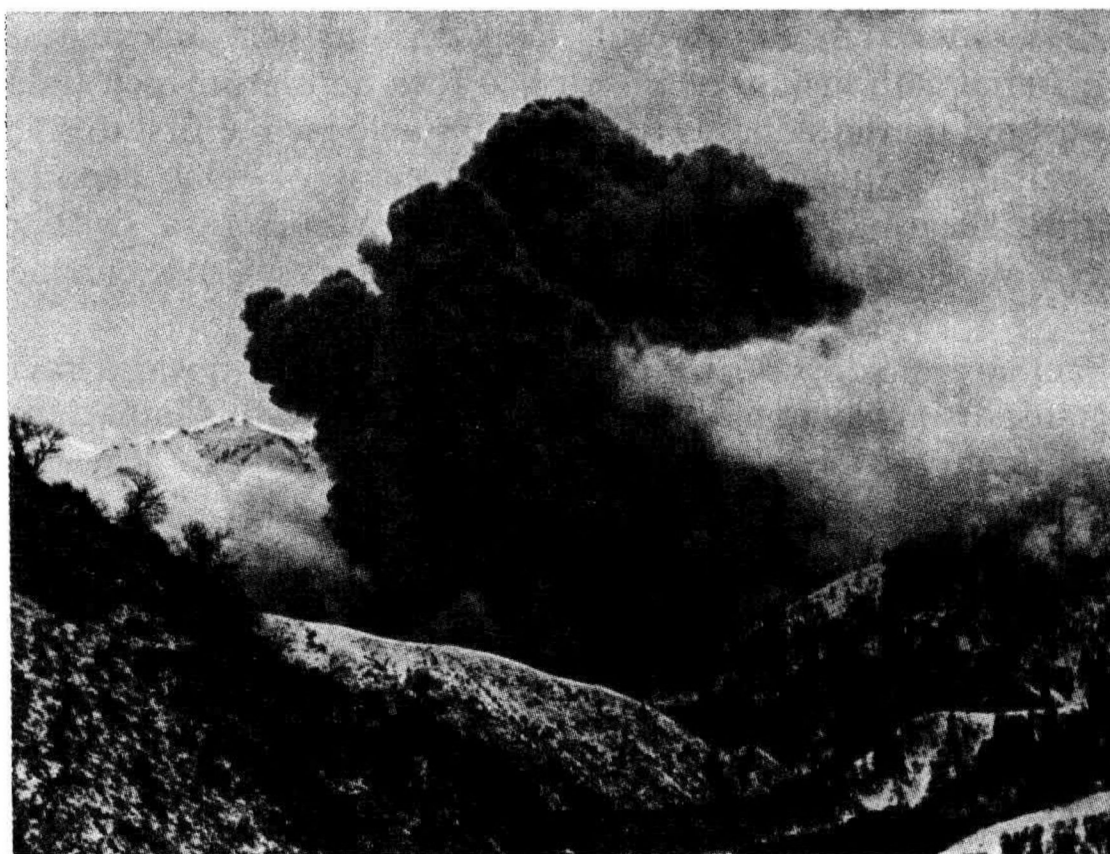


**Fig. 40.3.** Directed blast for construction a 100 m high dam to control mud rock flows in the Almaatinka River valley





**Fig. 40.4.** View of the dam after the directed blast

Mud rock flows are common occurrence in the Caucasus and Transcaucasia, at the Black Sea coast and particularly in the Middle Asia.

A great disaster induced by a mud rock flow occurred in Alma-Ata in 1921. The flow carried away 182 houses with their inhabitants. Some 400 people lost their lives. The weight of the material transported to this city was about 1.5 million tons.

After the flood decline the valley is covered by a layer of liquid mud (1 m and more in thickness) and numerous rock fragments. Cultivated land then has to be rehabilitated, streets and roads in valleys must be cleared of the mud flow material (Fig. 40.2).

A 100-m high dam constructed by directed blastings on the two rocky banks of the river Almaatinka is currently protecting Alma-Ata from mud rock flows (Figs. 40.3 and 40.4). The structure proved efficient in 1973 when a large-scale mud rock flow attacked again this city. The dam retained over 4.5 million cubic metres of the mud rock flow material that would have rushed to the city if this retaining structure had not been built.

A 5 291 tons of explosives was necessary to build this dam (Fig. 40.5). This amount, however, sets no record.

So, during the construction of the Amu-Bukhara canal a 9 352 tons of explosives was simultaneously used. The unique feature of a blast in Medeo



**Fig. 40.5.** View of the dam after construction

was that one of the five charges exploded simultaneously contained 3 604 tons of explosives. This is a world record still unbeaten.

Clearly, construction in a mountain river valley requires previous site investigations to determine the mud rock flow hazard of the particular locality. Especially often landslides leading to mud rock flow occur in mountain valley ravines with a steep angle of dip ( $15^\circ$  and more), composed of clayey schists.

### **Sec. 40.2. Protective Measures**

Mud rock flow control is a difficult problem. Stabilization of talus and debris likely to trigger a mud rock flow may prove an efficient method of control. If the talus deposit is insignificant, any retaining structure would do. It is sometimes convenient, especially when a dry ravine is involved, to construct a masonry retaining wall. Large-mesh wire fences installed in the upper reaches of rivers have been used advantageously.

Planting trees on mountain slopes may be an efficient method of flow control. Destruction of vegetation, primarily deforestation, and cattle grazing are strictly prohibited in areas subject to landslides.



If the stream of a mud rock flow is of marked depth, control becomes complicated even on roads. Under such conditions it is a good plan to carry the road over the likely channel of flow, locating bridge abutments at safe level or, at least, with spans not less than 4 m apart. Moreover, it is necessary to increase the distance between the lower part of the span structure with respect to the design water level by 1 m compared with a general 0.5 m. This, for example, has been done with a bridge carrying the Military Georgian Road across the Khandes-Khevi stream and elsewhere.

The alignments of important roads across areas where mud rock flows occur must be sited at a higher level than usual. It may prove useful to build flumes over a road so that a mud rock flow could cross it overhead.

---

## Chapter 41

### Karst Phenomena

---

#### Sec. 41.1. General Considerations

The karst phenomena is a specific form of chemical weathering. Limestones and gypsum are particularly subject to this phenomenon. Under definite conditions voids, caverns, underground passages and even large caves form in masses composed of these materials. The Kungur cave (Perm Region) in a gypsum deposit with labyrinths totalling 46 km in length and the great cave in a limestone deposit of Novyi Afon (New Athos) are the best known in this country.

As various rock species are being leached passages and cavities tend to be interconnected. Thus continuous passages of marked length (solution channels) originate. Karst events occur very often on valley slopes.

The cave-in of the roof of a karst void results in a sinkhole (Fig. 41.1). A sinkhole over 100 m in diameter and 20 m in depth formed in 1937 in the Ivanovo Region. Solution channels sometimes cover vast areas producing karst topography. Recent sinkholes and caves present special danger suggesting that the chemical decomposition of rocks is intense in the given area. The age of the sinkholes can be determined from the amount of vegetation and smoothness of their edges.

Solution channels have often originated at the ground surface. Most of them result from karst events occurring at the contact with a soil layer releasing carbonic acid.

In karst areas rivers may sometimes be lost underground forming



Fig. 41.1. Sinkhole in the Sulak River basin

subterranean streams. An example is provided by the Shaora River (West Georgia) that emerges again at the surface 2 km away, this time under the name of the Sharauli River.

Apart from the above type of caves and sinkholes there are buried solution channels overlain by materials deposited after the karst phenomena occurred. If a karst area is overlain by clay deposits, all voids are generally filled by this material (as, for example, karst caverns in Pontian limestones in the southern Ukraine).

The intensity of karst phenomena associated with leaching of carbonate and sulphate rocks is conditioned by the solubility of their salt components. So, gypsum solubility in distilled water may attain 2.6 g/l, of calcium dioxide 0.013 g/l. If the water contains free carbon dioxide  $\text{CO}_2$ , solubility of limestones and dolomites (calcium and magnesium dioxides) increases by a factor of manifold. In particular, if total free carbon dioxide content in the subsurface water is 15-40 mg/l, calcium solubility increases up to 150 mg/l.

The dissolving action of free carbon dioxide on limestones and dolomites consists in that  $\text{CO}_2$  transforms practically insoluble calcium and magnesium carbonates to soluble bicarbonates. The reaction proceeds as

follows:



On the other hand, the free  $\text{CO}_2$  content in the water does not affect solubility of gypsums or anhydrides (calcium sulphate salts), whereas sodium chloride increases gypsum solubility almost fourfold. The magnesium sulphate present in the solution causes gypsum to be almost insoluble in such water.

The solubility of salts is governed by the concentration of the particular solution. As the solution is being saturated, its solution power drops, becoming zero upon complete saturation. Viewed in terms of karst events, the most detrimental effect is produced by meteoric water percolating, say, through fissures, to the mass of soluble rock. As the water infiltrates, it is being saturated more and more, the concentration of the solution increasing, the solution power dropping. Thus at the initial stage the somewhat lengthy path of water percolation imposes a constraint on the leaching process.

As is shown by studies of V.G. Naumenko, the intensity of gypsum leaching is entirely governed by the velocity of subsurface flow and is independent of the extent of the opening of fissures. If the fissures continue to develop, the velocities of flow of water circulating there dramatically increase, being in direct proportion to the square of the fissure opening.

Karst phenomena are particularly pronounced in the corresponding rock mass in the vicinity of draining valleys where subsurface water flow velocities are the greatest. Karst events are gradually attenuated below the draining horizon. Therefore at deeper horizons karst produces caverns in the rock mass (Fig. 41.2).

Under definite conditions even such relatively hardly soluble rocks as limestones may be leached to a great extent. Especially pronounced are karst phenomena where rocks are jointed (limestone pavement). Viewed in this content, especially hazardous are all kinds of tectonic lines (displacements, faults, splittings etc.).

Note, however, that the water-induced leaching of carbonate rocks (limestones and dolomites) proceeds at rather a low rate and at low intensity. Therefore, when evaluating properties of such rocks, we must mainly take into account karst which is present in these rocks. Compared with the actual service time of engineering structures, the likelihood of deterioration of karst phenomena in such conditions is ruled out.

Things are different when such rocks as gypsum and rock salt are involved. Due to their great solubility, beds composed of such rocks underly-

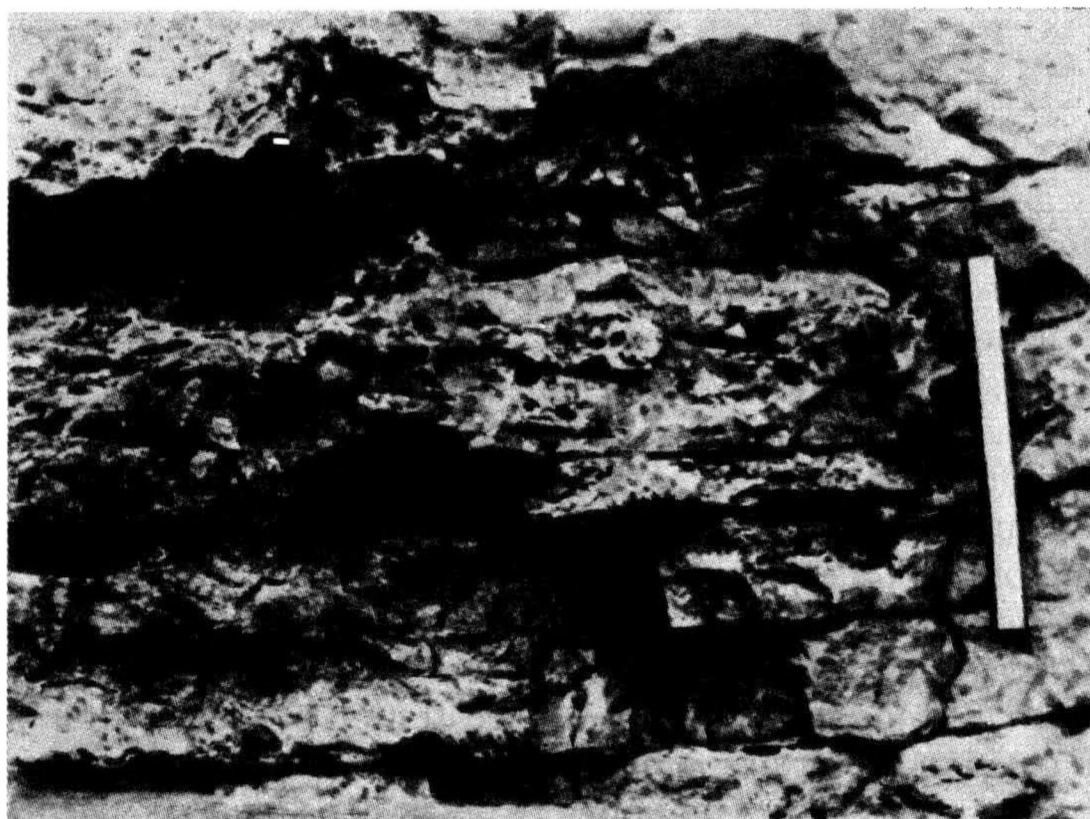


**Fig. 41.2.** Plates of weakly cavernous dolomites. Caverns are oriented along bedding layers

ing structures are very likely to be leached. In definite conditions karst phenomena in gypsum deposits can dramatically develop causing detrimental results. It should be noted that karst develops in sulphate rocks at a much greater velocity and new solution channels and caverns may be formed each year.

### **Sec. 41.2. Conditions of Construction**

Construction of engineering structures in karst areas generally poses major problems. For example, if a tunnel will pierce a rock mass composed of carbonate rocks (limestones, dolomites), it may contain solution channels, especially dangerous of which are caverns (such are, for example, tunnels found at the 527th kilometre of the Tbilisi-Julfa railway).

Particularly difficult conditions arise if the floor of a karst cavern is located below the road bed since it proves then a problem to ensure design elevations of intratunnel trestles, bridges, embankments etc. So, an arch bridge with the aperture 4.5 m had to be built in a tunnel driven through a karst-affected rock mass.

Cases may occur when a tunnel section has to be abandoned and its alignment changed. This is what took place when a tunnel taking the Rome-Naples highway penetrated a 50 m high cavern near its roof.

Tunnels where rock blocks may fall from the top of karst caverns must be lined. When deciding on the design of a lining we must take into account a possibility of intense blows and that the lining may be damaged by falling blocks of large size. Driving a tunnel in a karst area poses the greatest difficulty and may sometimes lead to detrimental consequences if the tunnel meets with an underground stream and the heading is flooded at a discharge rate up to  $10 \text{ m}^3/\text{s}$ .

Karst caverns found close to the ground surface may present a real danger to massive engineering structures. So, solution channels appeared beneath railway embankments built on gypsum deposits (Ufa Region, 1927). Sinkholes sometimes occurred as the water from railway embankment side ditches percolated downwards.

If a bridge abutment has to be erected in a karst area, there is always a danger of its settlement or even collapse due to failure of karst caverns found under the structure (Fig. 41.3). The easiest way out is to locate the structure proposed outside the danger area. If this is impossible, it is allowable to site structures where karst events reveal themselves the least. One should avoid tectonic zones where karst is the most likely to develop.

If a structure cannot be located in a more convenient site, the required strength of the foundation may be attained by injections at pressure: of lean mixtures enriched by small-grain or fine-grain sand at an early stage, and of cement-clay mixture at the next stage. In the latter case only such caverns are filled whose size may present a danger to the structure in hand, rather than wasting grout on small fissures.

It must be noted, however, that sometimes there are no grounds for ex-



Fig. 41.3. Failure of a bridge induced by collapsed caverns. The foundation soil included limestone filled with caverns

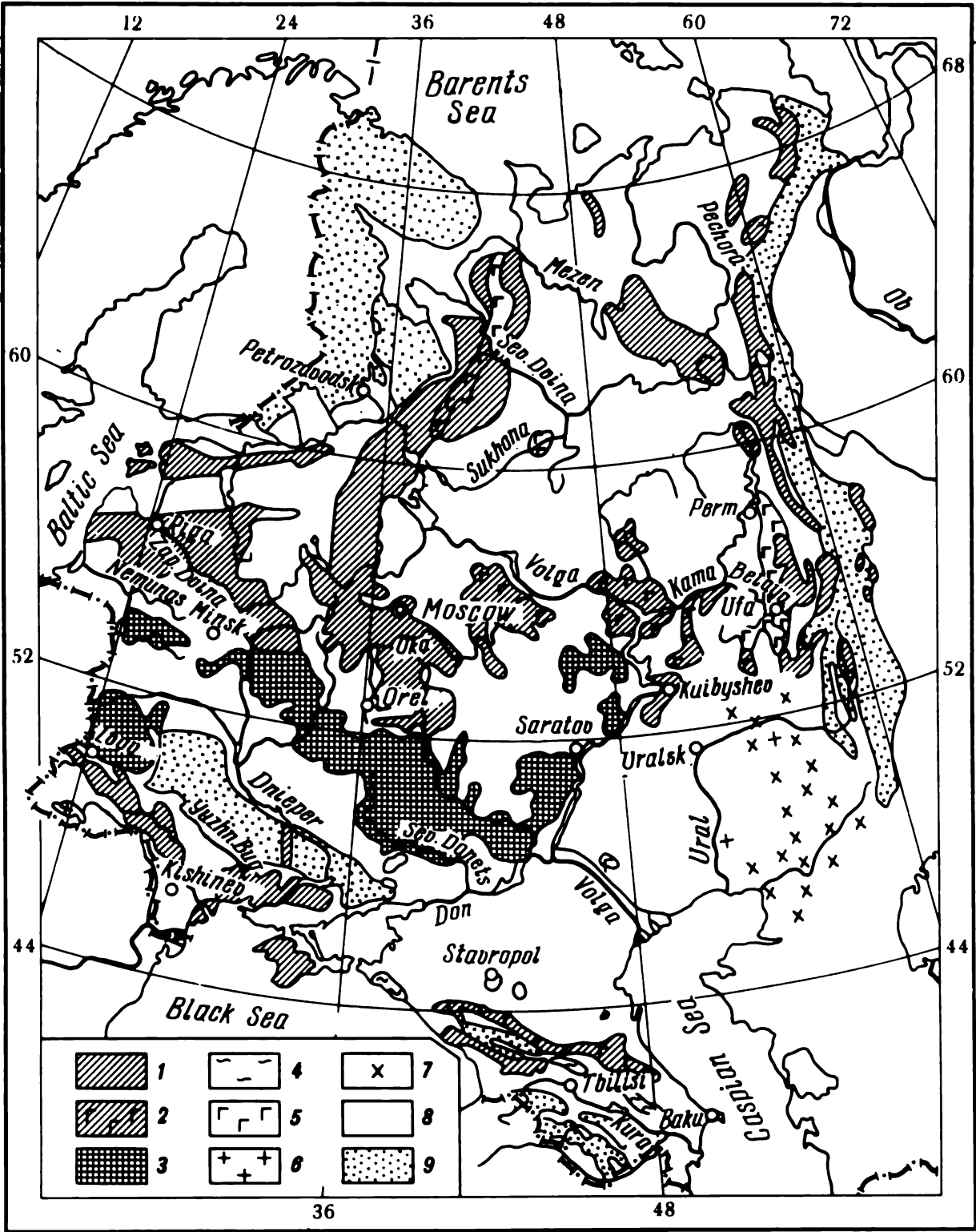
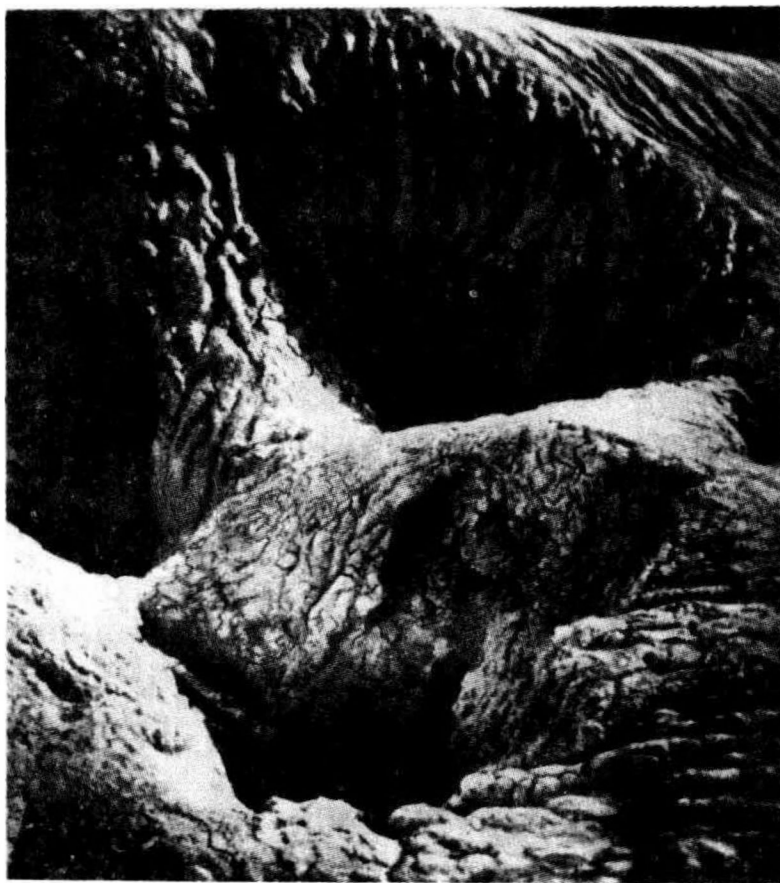


Fig. 41.4. Map showing distribution of karst areas in the European part of the USSR, Urals and Caucasus (after N.V. Rodionov). Karst rocks:

1—limestones, marmors and dolomites; 2—sulphate carbonate rocks; 3—chalk, marl chalk mass; 4—carbonate flysh; 5—gypsums and anhydrides; 6—salt, salt cupolas; 7—non-karst rocks; 8—sedimented rocks; 9—plutonic, metamorphic and volcanic rocks

cessive fear of karst events. This is shown by the faultless service of a number of bridges, for example, the Sviyaga bridge across the Volga River supported by karst rocks. The right bank embankment rests there on a rock



**Fig. 41.5.** Clayey karst topography in saline soil

mass containing gypsum-bearing marls and dolomites of the Permian period. Sinkholes are found nearby. A bridge across the Oka River is found in similar conditions. Gypsum-bearing rocks occur there beneath alluvial deposits supporting the bridge piers. The latter operate quite satisfactorily. By contrast, the right-bank abutment resting on a rock mass free from karst hazard, proved to be deformed by a landslide.

In the USSR karst occurs in the Baltic states, Moscow Region, Donets Coal Basin, Urals, Ufa Plateau and elsewhere. Karst phenomena are also common in the Crimea, Middle Asia, many areas of the Caucasus and the Far East. A sketch map in Fig. 41.4 shows the distribution of karst phenomena in the European regions of the USSR.

Mild and specific forms of karst occur in deposits of writing chalk on the Russian plain. Chalk, being a fairly incompetent material, is not only easily dissolved but also washed out by the water circulating in the fissures. Karst caverns are generally filled with sand and clay material which largely inhibits further development of karst and even totally stops karst events.

Still another, most peculiar form of karst should be mentioned. This is clay karst, particularly typical of saline and, notably, gypsum-bearing clay deposits. Under definite circumstances caverns, sinkholes and other solution channels are formed (Fig. 41.5). Clay karst occurs due to pronounced solubility of saline powdered clayey soils which they demonstrate under certain conditions following alternating wetting and dessication.



---

## Chapter 42

---

### Erosion. Its Effect of Road and Bridge Construction

---

#### Sec. 42.1. Gully Erosion, or Gullying

Landscape features are generally influenced by the action of running water on rocks and soils composing the earth's upper layers. This process is known as erosion. Erosion may be induced both by permanent streams of water and by occasional ones, resulting from meteoric water and melting of the snow.

Gully erosion is directly associated with what is called subsurface or bottom erosion and reveals itself as continuous washing out of the bottom of a gully. As the vertex of a gully is being washed out, the gully extends backstream, against the direction of the water flow. This is known as *head* or *retrogressive erosion*.

Formation of new gullies and extension of existing gullies present a danger to cultivated lands and to roads and other engineering ventures. As gully erosion proceeds, ravine flanks increase in height and width at the top. Moreover, as follows from the theory of stability of slopes, in soils manifesting some cohesion a steeper slope will be flat at its lower part. As a result, as a gully is being deepened, its width at the top increases.

The velocity of erosion progress, sometimes exceptionally great, is dangerous for structures, populated areas and land use features (Fig. 42.1). Cases have been recorded when the annual rate of gully erosion attained several tens of metres. This was due to retreat of gully vertices. These factors, coupled to increased width and depth, may, with time, cause structures located near gullies to be underscoured and lose stability. This may happen to approach embankments and, in particular, bridge abutments. The situation becomes even more dangerous since the velocity of gully erosion is often quite conspicuous when large gradients are involved.

Care must be taken when designing drains for road side ditches and chutes so as to prevent them from turning into new sites of erosion. Drained water may easily trigger erosion if the alignment of a road is sited on erodible terrain and side ditches are not lined.

A gully may attain several tens of metres in depth and its length may vary appreciably, sometimes increasing to 5-10 or even 20 km. Factors enhancing gullying include: the presence of incompetent, easily eroded soils in the upper crustal layers; intensive rainfall; low base level of the river network and, consequently, low groundwater drainage base level; insufficient degree of forestation.



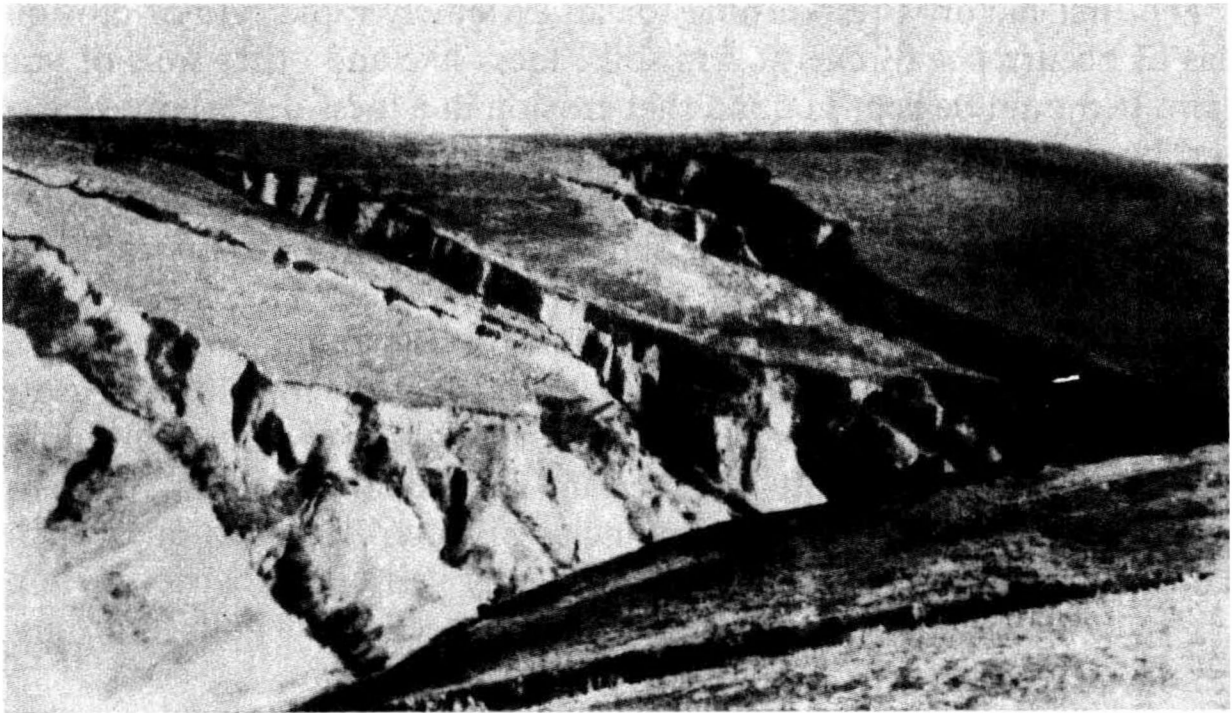


**Fig. 42.1.** Ravines in a steppe area



**Fig. 42.2.** Deep soil erosion and formation of a ravine in a loess deposit

The first factor is responsible for an extremely rapid rate of erosion in areas of occurrence of chernozem soils, loess-like and other soils of young origin. It should be kept in mind that erosion in a loess deposit may be triggered by the wrong design of a road side ditch or chute (Fig. 42.2) or by such minor, at the first glance, factor as shrew burrows. High-velocity runoff (frequent torrential rains, sudden melting of an appreciable snow layer) will increase erosion.

The location of the base level imposes a constraint on the depth of gullies and, as a result, on their maximum width at the top. To decrease gully formation some prophylactic measures can be taken, such as prohibition of slope deforestation, cattle grazing and land cultivation etc.

Active measures of gully erosion include primarily regulation of surface runoff by banking of ravines, especially gully vertices; provision of a network of draining ditches and chutes etc.; protection of gully bottoms by specially designed structures; planting trees and bushes.

Steps sometimes have to be taken to decrease lateral or sideways erosion. The easiest method is to arrange, at the foot of a gully, longitudinal brush woven fences with intervals backfilled by earth, or to plant vegetation on the slopes.

### **Sec. 42.2. Erosion in River Valleys**

As has been already noted, erosion induced by the action of running water is an exceptionally important factor shaping the earth's surface. Erosion produced by a stream may take on the form of a deepened river bed (bottom, or deep erosion) or of a widened river valley (lateral erosion). The intensity of erosion is conditioned by the strength of the materials being eroded and by the velocities of the water flow. Clearly, incompetent rocks with little or no cohesion are the most liable to erosion.

In addition, the intensity of erosion is governed by the character and amount of material being transported by the stream and its abrasive properties. Especially conspicuous abrasive effect is produced on a river bed by clastic rocks, such as cobbles, pebbles, gravel and quartz sand. Note that hard rocks are eroded by the sediment, the eroding action of clean water being inappreciable. Clearly, the degree of erosion is governed by the velocity of the stream.

The duration and capacity of a stream are important factors conducive to erosion. However small the rates of the above processes may be, their prolonged action will bring conspicuous alterations. Even the erosion-resistant rocks cannot withstand the action of running water, river valleys are gradually deepened and widened; elevations separating river valleys are gradually worn down and lowered, the slopes flattened. In the long run, ero-



Fig. 42.3. Youthful stage of a river valley. Region of Garm (Tajikistan)

sion and erosion-induced sedimentation causes mountainous relief to be milder. Numerous examples can be provided by deep canyons with rocky slopes. These include, in particular, canyons of the Angren plateau in Fergana with walls up to 1 000 m in height; the Daryal gorge in the Caucasus, deep river valleys flanked by almost vertical basalt banks in Armenia.

The early, or *youthful* stage of landscape formation in any country is accompanied by increased erosion with river valleys cutting deep into rock massifs (Fig. 42.3).

With the passage of time, as a result of erosion the landscape becomes smoother, resembling a plain, as it were. This is a *mature* stage of the landscape (Fig. 42.4). The river valleys are relatively shallow increasing in width. The action of erosion markedly decreases. This stage is followed by an *old age* (Fig. 42.5). The country appears as a *base-level plain* known alternatively as a *penplain*. Relief being flat, the action of erosion practically terminates at this stage. This stage, however, may either remain unattained or demonstrate a relatively temporal character being disturbed by tectonic events.

The degree of erosion is particularly great during periods of tectonic activity associated with land uplifts and mountain building. Conversely, in periods of tectonic quiescence the intensity of erosion is gradually decreased due to the general smoothing down of the terrain due to erosion. A tectonic uplift of the terrain leads to revival of erosion activity followed by rejuvenation of relief, and the geologic cycle may begin again.

The velocity of water in a stream and, consequently, intensity of erosion are governed by the river gradients. For this reason the action of erosion is especially pronounced in mountainous country with large gradients where stream erosion prevails. In flat country the intensity of stream erosion drops appreciably and is often followed by lateral erosion.

The natural channel of a stream is particularly subject to erosion. The depth of water over flood-plain areas during high-flood periods (freshets) is generally much less than in the main stream. Moreover, flood-plain areas are generally covered by vegetation (meadow grass, bushes etc.). Both these factors decrease the water velocities at these sections due to which erosion only rarely reveals itself in flood-plain areas.

The elevation of the mouth of a stream is typically conditioned by the mean level of the body of water (sea, lake) into which the stream flows. Consequently, the degree of erosion is limited by this level, known, as has already been mentioned, as base level.

The base level of rivers flowing into a sea or an ocean is provided by sea level. In the general case this level is fairly constant (mean sea level). Yet in definite conditions it may fluctuate. Such fluctuations are known as eustacy and may, for example, be associated with glaciation periods, i.e. with times of major ice coverage of vast areas of land. This may cause disturbance of the hydrologic cycle. There is belief that during the last glaciation period that included several stages and lasted 10-500 000 years B.C. sea level dropped 50 m and even more.



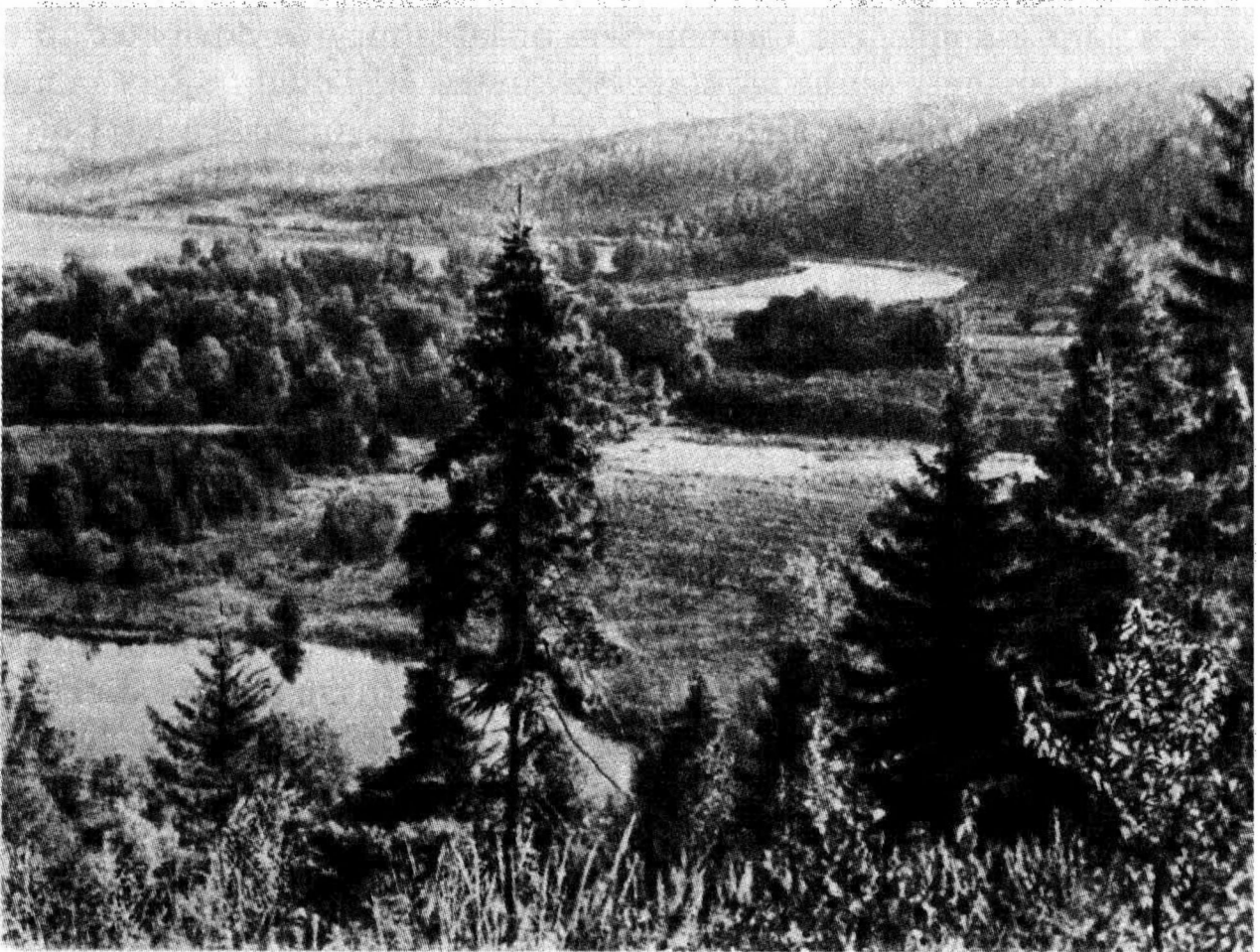


**Fig. 42.4.** Mature stage of a river valley



**Fig. 42.5.** Old age of a river valley. Lower reaches of a large river

Unlike open water basins, fluctuations of sea level in closed bodies of water as, for example, the Caspian Sea, or lakes may be attributed to environmental changes as the most general causes. It should be kept in mind that the recorded historic period has witnessed a drop in sea level of the Caspian by about 12 m which fact is evidenced by relics that were submerged on the western coast of this sea including ruins of fortresses and ancient burial mounds.

Clearly, base level of river tributaries will be provided by the water level of the main stream. It is of interest to note that the right bank of the Volga River is dissected by very deep gullies.

Apart from the aforementioned general causes, base level of a tributary running across mountainous country may be raised, should the stream valley be dammed by fallen material. The base level will then be the crest of the obstacle. If a river is closed by a dam, the level of the reservoir becomes base level. Naturally, under such conditions the scale of erosion will be appreciably decreased. On the other hand, stream erosion at one section of the stream or another may be conspicuously enhanced due to a hydroengineering venture, such as clearing of the river channel, byway, wasteway etc.

As has been pointed out above, erosion played an extremely important role in the formation of river valleys and landscape features in the geologic past. However, even nowadays erosion may appreciably affect highway engineering structures, notably, bridges.

Allowance for channel degradation must be made by the civil engineer; whenever bridge piers have to be erected in the river channel or in the adjoining flood-plain area submerged during high floods. The fact that the cross section of a stream is confined by the bridge piers thus increasing flow velocities causes intensive degradation of the river channel. The degree of erosion will be the greater, the less cohesive are the materials of the channel. Viewed from this standpoint, alluvial deposits, primarily sand deposits, completely devoid of cohesion, manifest the least stability. By contrast, bedrock (pre-Quaternary) hard and argillaceous materials are more erosion-resistant.

At the same time, all rock and soil varieties, excepting sound unweathered igneous rocks and some particularly stiff and hard crystalline metamorphic schists, may be completely underscoured from between bridge spans within the period of the service of a bridge.

Construction practice has witnessed many accidents caused by underscouring of bridge piers induced by channel degradation since inadequate protection measures were taken. The principal step to be made here is to increase the depth of penetration of bridge pier foundation such as to

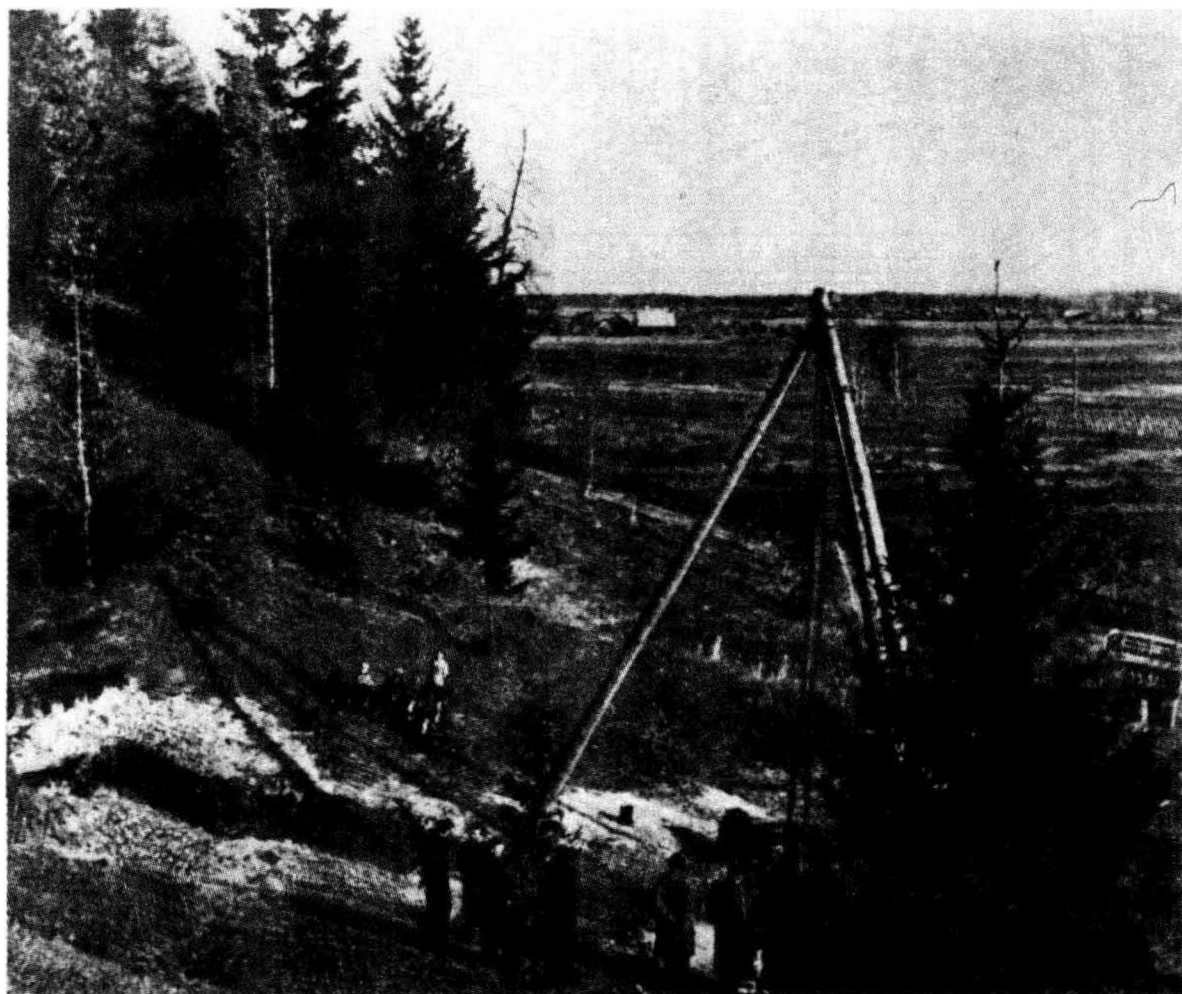


Fig. 42.6. Elevated right bank of the Volga River. The flood can be seen in the background. In the foreground is a drilling rig

avoid underscoring by stream erosion. The requisite depth of penetration is established from the likely channel degradation so as to ensure the river cross section and water flow velocities. Such auxiliary measures as placing riprap, heavy brush rolls, driving sheet pile fenders etc. may also be useful.

It must be borne in mind that river channel degradation may be often conducive to landslides and bank failures. *Lateral erosion* may sometimes present not lesser danger to a bridge or road by undercutting river banks. So, river sections aligned with a meridian scour their right banks particularly severely (Baer's rule generally known as Coriolis Effect).

Lateral erosion may cause the stream channel to shift intensively towards the right river bank. This is the reason why the right river banks are elevated, the left banks generally representing vast flood-plain areas degraded by erosion (Fig. 42.6). The low-lying left banks often feature sharply bending loops (see Fig. 42.4) known as *meanders* (from the Greek Maiandros, a twisting river in Phrygia flowing into the Aegean Sea).

Transverse displacement of a stream occurs within the boundaries of its valley. The river is then said to be meandering in its valley (meander plain).

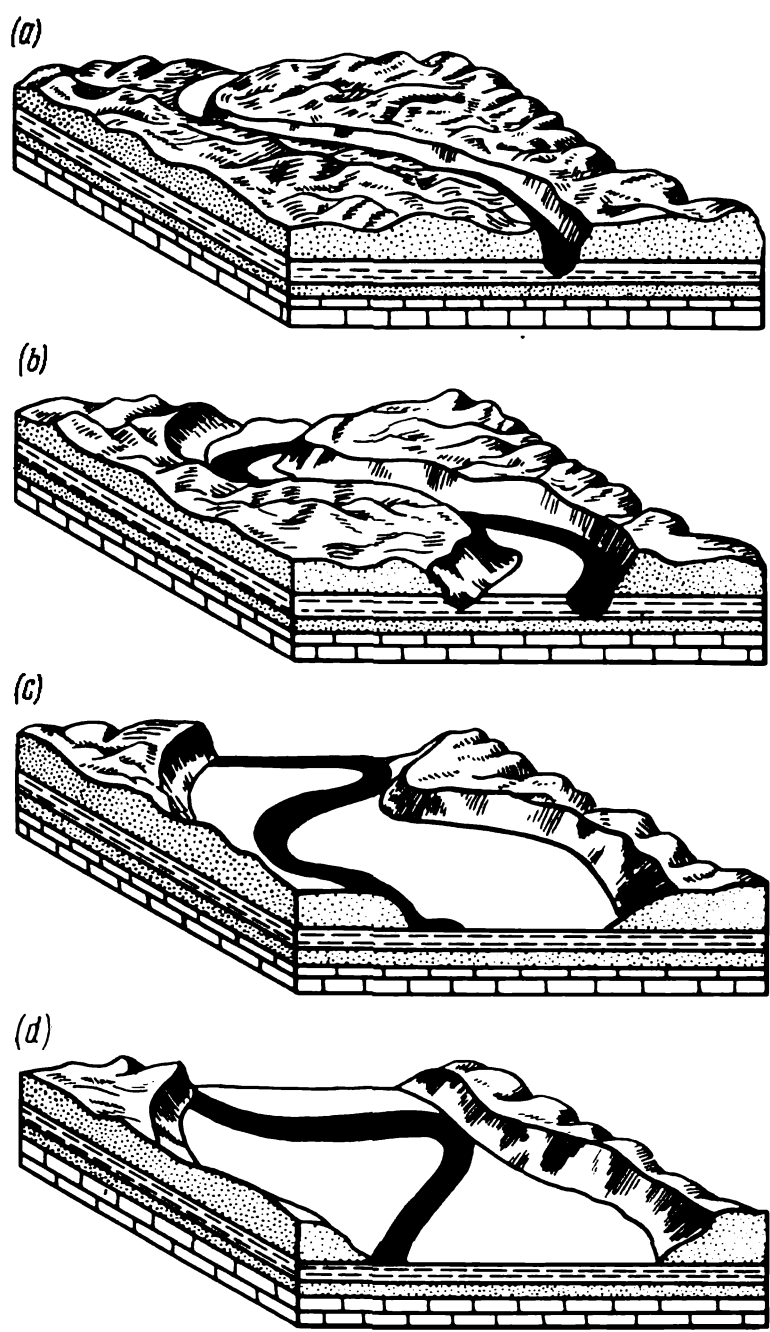


**Fig. 42.7.** Expansion of a river valley induced by lateral erosion:  
*a—c* are consecutive stages of valley erosion

The action of lateral erosion causes the river valley to expand gradually (Fig. 42.7), the expansion being the larger, the less competent are the rocks composing the valley flanks. As meanders are being by-passed during the straightening of the natural channel they form what are known as oxbow lakes. During high floods the oxbow lakes are often flooded, providing, as it were, pockets for silt deposition. The by-passed meanders on lacustrine flood-plain areas frequently form water-logged areas and peat swamps.

Increased lateral erosion may endanger engineering structures including highways and bridge abutments if these are located too close to the bank crest or if requisite protective measures have not been taken. The rate of this process, however, is very slow, since lateral valley erosion generally affects



bedrocks. Moreover, this process follows definite regularities and can be easily predicted since the most dangerous bank sections where the degree of erosion is particularly great can be visually detected. Landslides and screes occurring along the bank strip provide an important indication of the process at work. Concave sections of river channels immediately acted on by the stream are especially liable to this process.

Protection measures for landslides control and bank consolidation often help control lateral erosion. When siting a structure it is sometimes best to locate it where the river banks are less likely to slide.

On the other hand, if this is unfeasible, it is good practice to site the designed structure, say, a bridge abutment or road alignment some distance from the river bank crest. Thus a kind of right-of-way is provided, such that landslides would occur during a more or less lengthy period of time without affecting the structure in hand.

Clearly, the width of the right-of-way is governed by local conditions and results of site investigations. Site investigations may often be aided by calculations of slope stability and determinations of a safe slope profile as applied to the particular job.

It is worthwhile noting that the town Cherny Yar on the Volga riverside some 300 years ago was threatened by the advancing river and had to be moved an appreciable distance from the river bank. Despite this, the town quarters adjacent to the riverside are being again encroached on by the river.

Previously built structures may often be found in danger zone. Remedial measures must then be taken. It is the objective of civil engineering to deal with these technical problems. It should be pointed out here that the lateral shifting of a river channel is an involved geological phenomenon which is often hard to control. Therefore it is often best to move the structure being endangered to a safer site.

By contrast, control of river meandering within its valley is much more complicated. The thing is that this process occurs in a meander plain previously degraded by the stream. Erosion in this case takes on the form of washing out of water-borne silt, loose incompetent soils that are easily eroded (Fig. 42.8). Unless proper remedial measures are taken and allowance is made for the likely underscoursing of bridge abutments by lateral erosion when siting these latter, detrimental results that will be hard to correct may follow.

Meandering of a river within its valley may sometimes lead to catastrophic consequences. An example is to be found in the scouring by the Amu Darya River of the area occupied by the town Turtkul, capital of the Karakalpak Autonomous Soviet Socialist Republic. As a result, the town

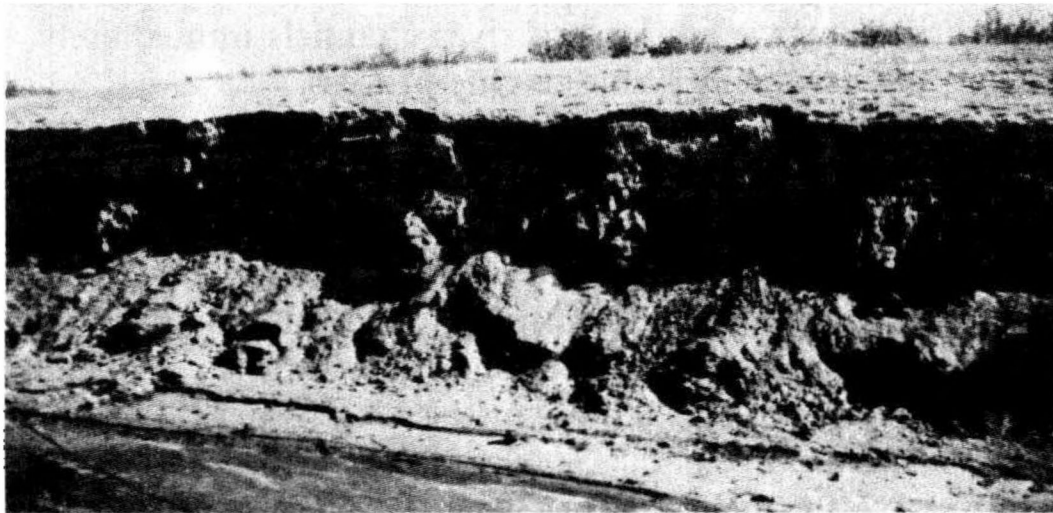


**Fig. 42.8.** High-flood scouring of a river bank composed of incompetent soils

had to be transferred to a new locality where the garden city Nukus was built.

Whenever it is desired to construct a bridge, the problem of the requisite depth of penetration of bridge abutments into the foundation soil must be studied so as to avoid detrimental effects of lateral erosion. If feasible, bridge abutments should rest on erosion-resistant rocks.

### **Sec. 42.3. Formation of River Valleys**

The general directions of rivers and, consequently, river valleys, agree with the relief features. Upper reaches of a river are commonly found in a divide. The direction of the stream is often conditioned by the geological features of the particular area, and the planimetric position of its valley is governed by tectonic disturbances that facilitate their scouring by stream erosion. The orientation of a river valley may be alternatively due to tectonic lines of fractures and faults, as, for example, the Samarskaya Luka (Samara Bend) of the Volga River.

The present hydrologic features were formed gradually and, in so doing, did not remain unaltered. That the regime of a river changed in the course of time is evidenced by *stream (or river) terraces*, a series of level surfaces along a river valley with more or less abrupt slopes above the stream level.

The terrace closest to the water level is called a *flood-plain terrace* and is submerged during the high flood periods.

Terraces at higher levels are known as *benches*. A flood-plain terrace may differ in width from several tens of metres to as many kilometres. For example, the Volga Aktyubinsk flood-plain area is 30 to 60 km in width. River bank terraces (benches) are often of definite extent and generally located at several levels (Fig. 42.9).

Terraces may be sometimes formed by rejuvenation of a river when stream erosion becomes more severe and the river cuts into its own bed. The resultant valley is generally narrower and water level lower. All terrace benches correspond to the location of the river bed at one stage of the river valley or another.

Depending on their origin, there are *erosion* and *accumulation* terraces. Erosion terraces formed by the wearing action of running water appear in valley slopes composed of bedrocks (Fig. 42.10). By contrast, accumulation terraces are made up of various alluvial deposits whose composition mirrors one period of the stream's cycle or another (Fig. 42.11).

Erosion terraces appear at sections of the stream where stream erosion is continuous. Such sections correspond to scour areas. At the same time erosion terraces are an indication of several stages of deep erosion when base level is suddenly lowered.

Accumulation terraces are formed under a complex river regime conditions with several alternating erosion cycles. For better understanding of this statement, let us refer to Fig. 42.12. *Stage a* appears if base level is low. Erosion causes the river valley to deepen and widen giving rise to erosion terraces. *Stage b* corresponds to an abrupt rise of base level. Deep erosion discontinues. The valley is filled by alluvial sediments to a level corresponding to that of the stream bottom at this erosion stage. *Stage c* is induced by conditions that obtain after the subsequent drop in base level. This stage witnesses increased erosion. The river valley is deepened again, the stream cutting into previously deposited sediments.

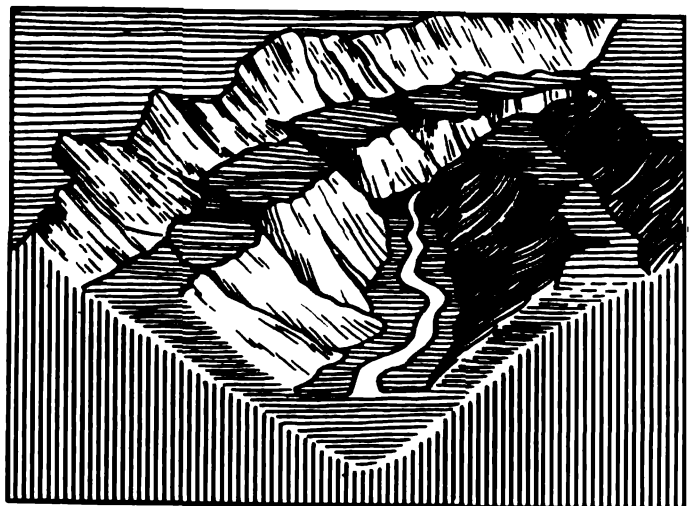


Fig. 42.9. Terrace forms

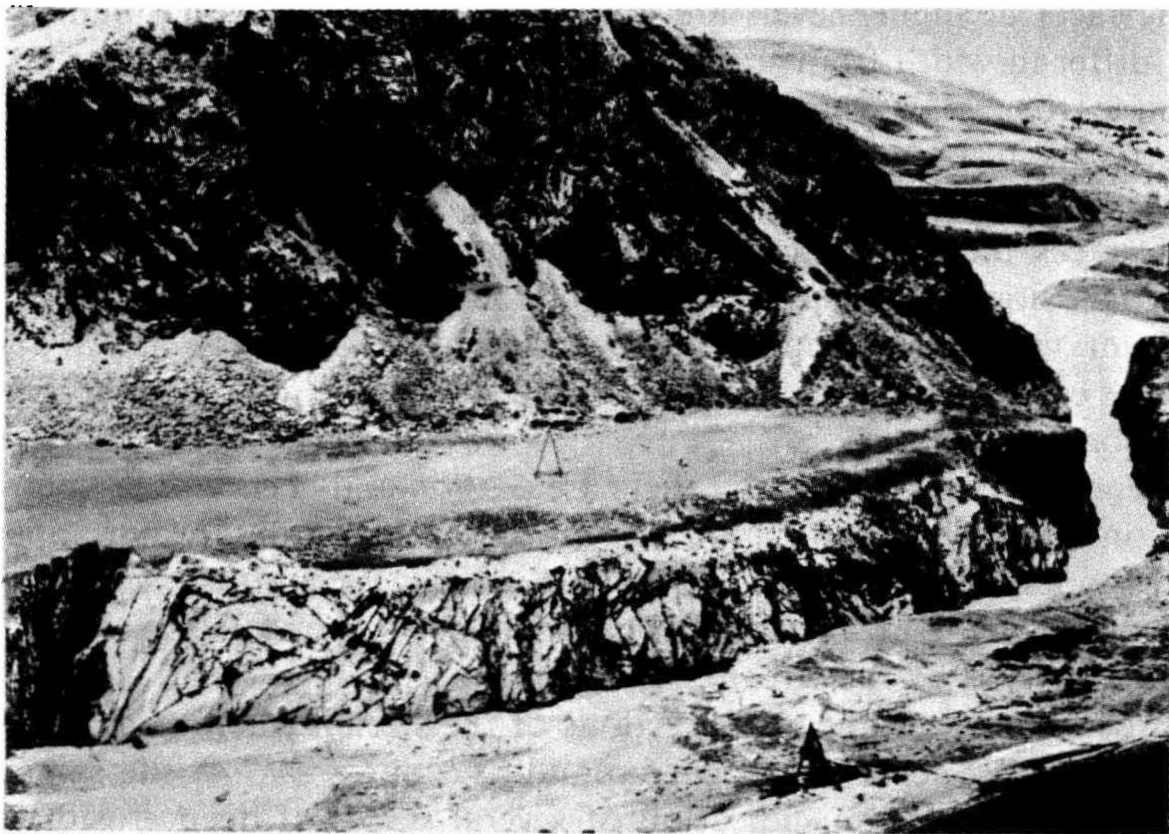


Fig. 42.10. View of erosion-induced terrace (Chervak River valley, Uzbekistan)



Fig. 42.11. View of an alluvial terrace

Thus accumulation terraces are formed being composed of alluvial materials (Fig. 42.13). Attention must be called to the character of such terraces for adequately locating a river or valley crossing.

Fig. 42.12. Stages of formation of an alluvial terrace:

*a*—low base level; *b*—abrupt increase in base level; *c*—subsequent lowering of base level

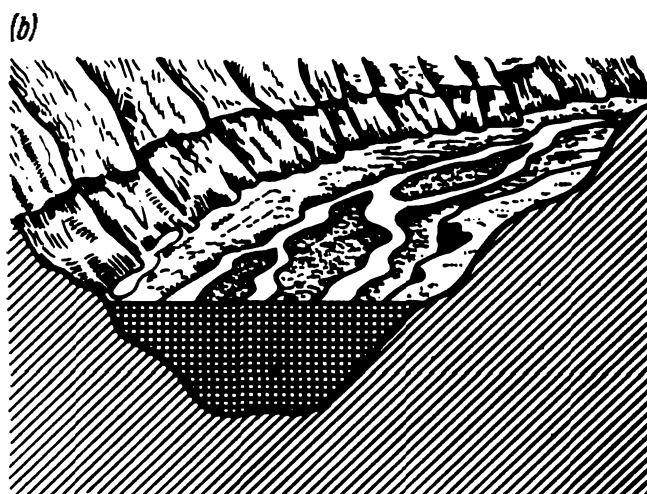
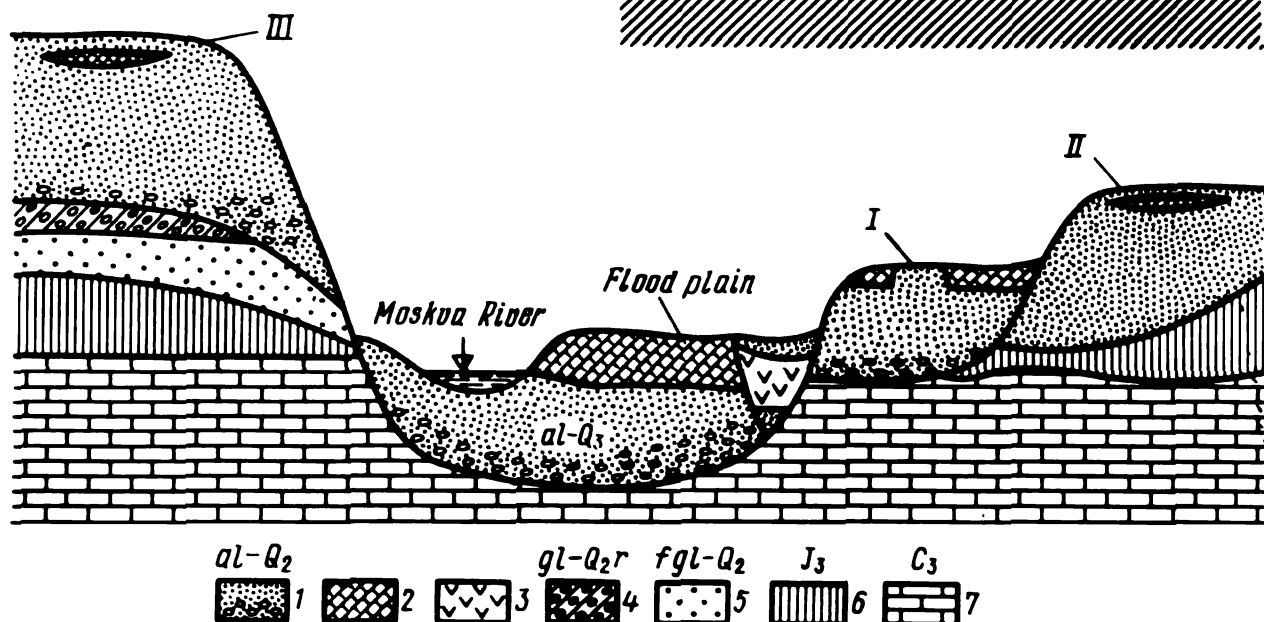


Fig. 42.13. Diagram showing the geologic section of the Moskva River valley and facies classification (after F.V. Kotlov):

*I, II, III*—sequence numbers of terraces;  
*1*—river bed facies (sands generally with inclusions of gravel, crushed rock and boulders);  
*2*—floodplain facies (sandy loams, loams and clays); *3*—buried abandoned river channel facies (clays, silts and peat); *4*—glacial deposits; *5*—fluvioglacial deposits; *6*—bedrock (upper Jurassic horizons); *7*—upper Jurassic horizons; *7*—upper Carboniferous deposits



**Sec. 42.4. Alluvial Deposits**

Stream deposits, generally termed alluvial deposits or simply alluvium, are mainly made up of granular soils. Stream alluvium occurs at the edge of the floodplain and in the river bed. Its composition is governed by the tractive force (TF) of the flowing water that does not remain constant in the course of time which fact affects the character of alluvium. The tractive force of a stream drops with reduction of water velocities. Naturally, it is coarser products, such as boulders and gravel that are first deposited to be then followed by sand material.

**Boulders** are generally found in the mass of stream deposits when mountainous rivers with large gradients are involved (Fig. 42.14). Appreciable deposits of boulders may also occur in the stream bed of a lowland river or its tributaries in the mass of alluvium both of recent and ancient origin. Such materials are commonly due to glacial drift which is known to frequently contain boulders.

**Gravel**, as a rule, constitutes the major fraction of alluvium in mountainous country (Fig. 42.15). The different petrographic composition of these deposits is conditioned by the type of parent rocks (igneous, metamorphic, sedimentary etc.). Sand conglomerates and sand and clay materials are characteristic of alluvial deposits.

In the middle and lower reaches of a lowland river gravel deposits found



**Fig. 42.14.** Boulder deposits in a scoured section of a river





Fig. 42.15. Mountainous river bank composed of gravel

in alluvium of modern origin occur as lens-like seams. These gravel lenses are usually alternated by sand layers. Irregularity of occurrence and appreciable thickness are peculiar features of these deposits.

Some river valleys in glaciated areas may contain conspicuous amounts of gravel that often attain tens of metres in thickness. These detrital deposits representing products of moraine erosion, typically encountered in northern regions, are found as thin seams in ancient valleys and their branches, being often buried under alluvium of younger origin.

Unlike coarser detrital materials, *sands* (especially small- and fine-grained) can be transported by the river many hundreds of kilometres downstream. For this reason, sand alluvial materials can be found in large river valleys appreciable distances from locations where they were deposited.

River sand deposits generally consist of quartz particles with some admixture of more stable materials, such as magnetite, hornblende, mica and feldspars originating from Plutonic and metamorphic rocks. Alluvial sands are generally well rounded and nonuniform. Their grains may differ in diameter.

Stream bed sand deposits at sections of relatively large gradients generally occur as lenses in gravel deposits, and are rapidly scoured. At lowland reaches they are often alternated by gravel layers and lenses. Clay

seams may also be encountered in which case sand particles are very much contaminated by clay admixtures. Sands invariably demonstrate laminar structure which points to a variable direction of the water flow in the stream during the sedimentation period.

Sand deposits sedimented at lower reaches of a large river demonstrate regular stratified structure, fine grain and much greater uniformity indicative of better sorting. They occur in layers sometimes attaining tens of metres in thickness. Deltaic deposits of a large river may occasionally be several hundred metres thick.

Meandering of a river in its own valley influences very much the distribution of different lithologic varieties in alluvial deposits.

An alluvium mass may contain lacustrine, swamp deposits, as well as talus and even aeolian soils. Floodplain area alluvium sometimes overlies layers of buried peat, heaps of tree trunks etc. So, the excavation of an open pit in the course of the construction of the Gorky Hydro Power Station revealed at a depth of some 8 m quite a number of half-decayed oak trunks which points to a change in the river regime that occurred in the past.

In general, a mass of alluvium represents erratic layers of sands of various grain size, gravel, loam, peat etc. Yet at the same time the geologic section of an alluvium mass demonstrates gradual (with likely deviations) transition from coarser- to finer-grained materials if we follow from bottom to top. Gravel deposits are often encountered when alluvium deposits are ripped (Fig. 42.16).

One of important aspects of the geotechnical study of alluvium is evaluation of its thickness under various conditions.

The thickness of alluvium within one reach of a river or another is conditioned by many factors, the most important one being base level and its fluctuations. Alluvial deposits attain the greatest thickness if base level rises after remaining low for a lengthy period of time. Indeed, if base level has been low for a long time, the stream bed is being intensively worn as the river valley cuts into the massif of surrounding rocks. If base level rises, say, during the sinking of land, the river valley proves to be lying much lower than the new base level which is advantageous for filling the resultant valley by alluvial deposits. Such conditions arose, for example, in the valley of the Volga River and its tributaries.

Continuous and lengthy lowering of base level (for example, when the area is being uplifted) increases stream bottom erosion. Alluvium accumulates then in such small amounts that the thickness of stream deposits is negligible. An example can be found in the Kura River near the town Mingechaur. As a result of continuous, still in progress, upheaval of the Bozdag ridge dissected by the Kura River, alluvium in this river is only a few metres in thickness or is absent altogether.





**Fig. 42.16.** Strata of alluvial deposits in a steep river bank. It can be seen that the size of fractions decreases with decreasing the depth of strata

The thickness of alluvium may be determined by methods of geologic reconnaissance, for example, by sample bore holes. However, when a large job is involved, it should be borne in mind that alluvium deposits may overlie buried relief of ancient origin very much degraded by erosion. Alluvial materials may fill deep gullies, river tributaries, and, finally, ancient stream channels. Clearly, the thickness of such deposits is con-

spicuous. Special care must be taken when exploring cutoffs and materials filling these latter. Logging bore holes must then be spaced at close intervals.

General geologic analysis of the region including river terraces and base level of the river at different stages of river development may prove of much service.

When dry, alluvial gravel and sand deposits are loose-textured, cohesionless, or in the presence of clay admixtures, represent materials demonstrating a little cohesion. The degree of apparent cohesion of clayey sand is conditioned by clay content as well as density and moisture content and must be taken into account.

The angle of internal friction  $\varphi$  is fairly high in pebble, gravel and sand varieties. It is in fact independent of the moisture content of soil, but may drop appreciably with decreasing density. The angle  $\varphi$  generally varies in the range from 30 to 36° depending on the size of fractions. The value of the angle  $\varphi$  is greater, the larger is the diameter of grains. With decreasing density the angle of internal friction of sand often drops to 20-22°.

Accumulation conditions of alluvial sands may be such, that they demonstrate high porosity (generally it is close to 40%, but may occasionally attain 50% or more).

Dynamic stability of such saturated sands is almost nil. The slightest vibrations, induced, for example, by passing vehicles, or operation or travelling of earth-excavating machinery, may cause such sands to liquefy and completely lose stability. This presents a danger both to structures and to submerged sand slopes.

Alluvial sands deposited at locations below bars and narrow river sections are especially loose and, consequently, hazardous. That is why, whenever a building site to be explored, the means must be found to determine the natural density, dynamic stability and compressibility of sand (cf. Sec. 30.2).

Water-laid coarse and fine gravel deposits are poorly compressible under load. Structures resting on loose or weakly compressed small- or fine-grained sands will settle the most. However, even when such soils are concerned, settlement of a structure acted on by a relatively high static load is generally within a few centimetres. It is primarily due to the compression of the uppermost crustal layer inevitably disturbed by excavating operations. In this respect it is noteworthy to refer to the data on monitoring of settlement of piers of the Mississippi River Bridge at New Orleans, Louisiana. The settlement of the piers transmitting a load of the foundation base equal to 6.25 kg/cm<sup>2</sup> was within 8.5 cm, the average settlement being 5 cm. Stabilization of the settlement of all bridge piers occurred during three years.

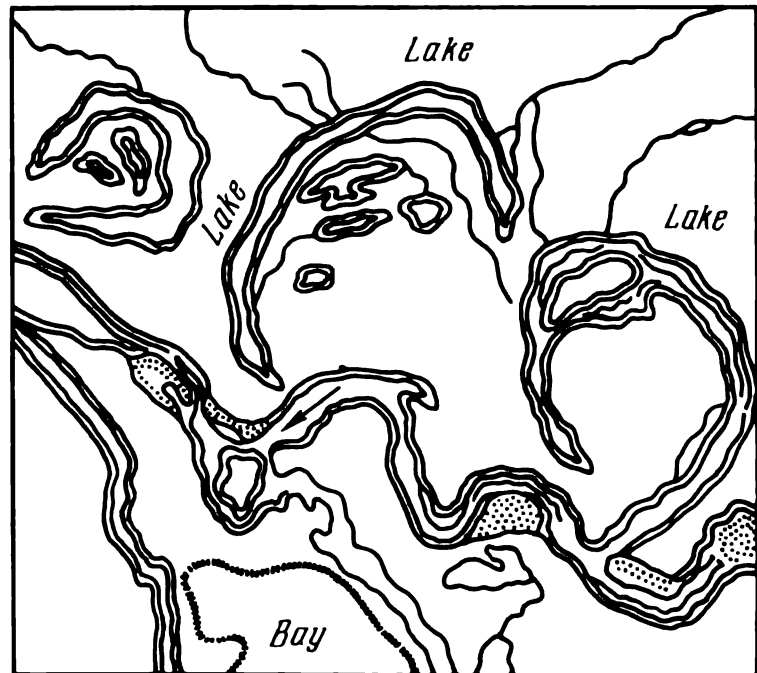


Fig. 42.17. Cutoffs and oxbow lakes

By contrast, things are different when a structure is being erected under similar conditions but is acted on by a dynamic load. Even if total dynamic stability of the structure is ensured, its settlement may attain an appreciable magnitude, up to several decimetres. Therefore, when designing a structure to be acted on by dynamic loads, site investigation is needed to be able to predict the pattern of the likely settlement.

Slope stability of alluvial deposits may be easily disturbed by seepage action generally due to removal of sand from sand seams occurring in the mass of soil of a slope.

*Permeability* (or perviousness) of alluvial deposits is governed by their composition and, in part, density. Coarse gravel deposits manifest the largest permeability and, consequently, under definite conditions the greatest water bearing capacity. Permeability of sands is conditioned by the size of grains. Clearly, apart from other factors, an essential role is played here by small fractions content. So, gravel whose pores are completely filled by sand, manifests a lower filtrational capacity than sand. Clay material likewise is an inhibiting agent.

Gravel and sands of alluvial deposits are commonly used as materials of construction. The most advantageous conditions for quarrying such materials are commonly provided when working accumulation benches at elevated levels free from the action of groundwater.

Sand and gravel materials deposited along a river are generally abundant but are nonuniformly distributed. For example, mountain river alluvium may have sufficient amounts of gravel and little sand. Yet, when prospecting for construction materials, one must keep in mind that the

location and regime of a stream may have undergone major changes. Therefore prospecting operations must necessarily rely on general analysis of geological features of the given area.

Alluvial *clayey soils* are mainly formed in lowland river valleys. They compose typically the upper parts of flood-land areas and river terraces (see Fig. 42.13) and *cutoffs* (abandoned river channels, Fig. 42.17).

Floodplain clayey soils are formed during high flood periods when the water flows quietly and slowly over floodplain areas. The load of the freshet water contains suspended fine sand and clay material, which after being deposited on the floodplain bottom covers the latter by clayey sediment of variable thickness. This process, repeating annually, in the long run causes clayey soils to be formed on the floodplain area.

The thickness of floodplain clayey soils is inappreciable attaining only 3-5 m. These soils contain a large proportion of sand and pulverized particles. These are poorly sorted out, often include organic matter or may involve buried soil horizons, that is, have stratified structure.

Variable lithological composition is typical of alluvial clay deposits that may consist of sandy loams, loams and clays. Moreover, no definite regularity in vertical or horizontal structure can be traced. Lack of cementation is another feature of clay deposits due to which clayey alluvial soils easily lose stability and strength with increasing moisture content. The parameters of the shearing resistance governed by the degree of looseness and moisture content are, on the average, as follows: the angle of internal friction is  $16-22^\circ$ , cohesion is  $0.15-0.4 \text{ kg/cm}^2$ .

Being loose-texture, clayey alluvial soils cause settlement which is mainly conditioned by their consistency, that is, density-moisture. Alluvial clays demonstrate conspicuous compressibility. Even dense clay varieties have compressibility some 10-20 mm per metre of the thickness of the soil mass. It is the nonuniform lithologic composition of these soils which is responsible for differential settlement of structures resting on them.

Sections of the river channel bypassed by the river (cutoffs and oxbow lakes) gradually transform into waterlogged depressions (see Fig. 42.17) which are filled to ever greater degree by silt and clay during the high flood periods. Peat is often deposited in cutoffs and oxbow lakes in which case silt and clay materials are added to by products of decay of vegetable remnants (cf. Chap. 35).

The moisture content of muck found in cutoffs often exceeds 100%, the compressibility of such materials is pronounced, up to 100 and 150 mm per metre of the thickness of the mass. The angle of internal friction seldom attains  $8-10^\circ$  and apparent cohesion is about  $0.05-0.1 \text{ kg/cm}^3$ .

As the river regime changes, sediments deposited in cutoffs may be overlain by sand and clay alluvial deposits. This gives rise to buried peat

and muck deposits. To detect these latter in the course of geotechnical studies is a necessary but very difficult problem.

Clayey alluvial soils are practically impervious.

As can be seen, the composition and properties of materials composing alluvium may sometimes prove fairly involved which is most important when planning a structure, notably, a bridge.

---

## Chapter 43

### Abrasion and Its Effect in Modern Conditions

---

#### Sec. 43.1. Shaping of Shores of Seas and Lakes

The destruction of a sea or lake shore line by waves and currents must be studied to prevent or stop it by protective works to be built in a port. Similar problems have to be dealt with by the road builders when the alignment of a highway or railroad is located in close proximity to the shore line. Such conditions obtain, for example, in mountainous country with a narrow shore line, such as the Black Sea shore of the Caucasus.

What concerns us now is the destruction of the shore front by heavy seas. This geological activity of the sea causes all prominent elements of land to be eroded and degraded, thus forming vast lowland areas. This process is known as *abrasion* (from Latin *abradere*, scrape off) (Fig. 43.1).

The shaping of geological features of the particular area is of paramount importance in view of exceptional scale the phenomena in hand may take. In the early geologic periods sea practically covered all modern land, and, as a result, its destructive activity affected all land areas at one period of time or another. During marine transgressions that occurred in all geologic epochs abrasive processes were associated with tectonic events (sinking of land).

The destruction of a sea shore line is induced by the impact of the waves coupled to uplift pressure on the rock mass as well as due to compression of the air trapped in the voids of rocks and vacuum events. The impact of waves may sometimes be very conspicuous. An example is to be found in a case when heavy seas moved a rock block weighing 1370 t more than 10 m away during a storm in the bay of Week (Scotland).

The intensity of abrasion is conditioned by an assortment of factors. The most important of these are: the degree to which the water basin is open; the depth of the littoral zone responsible for attenuating the impact

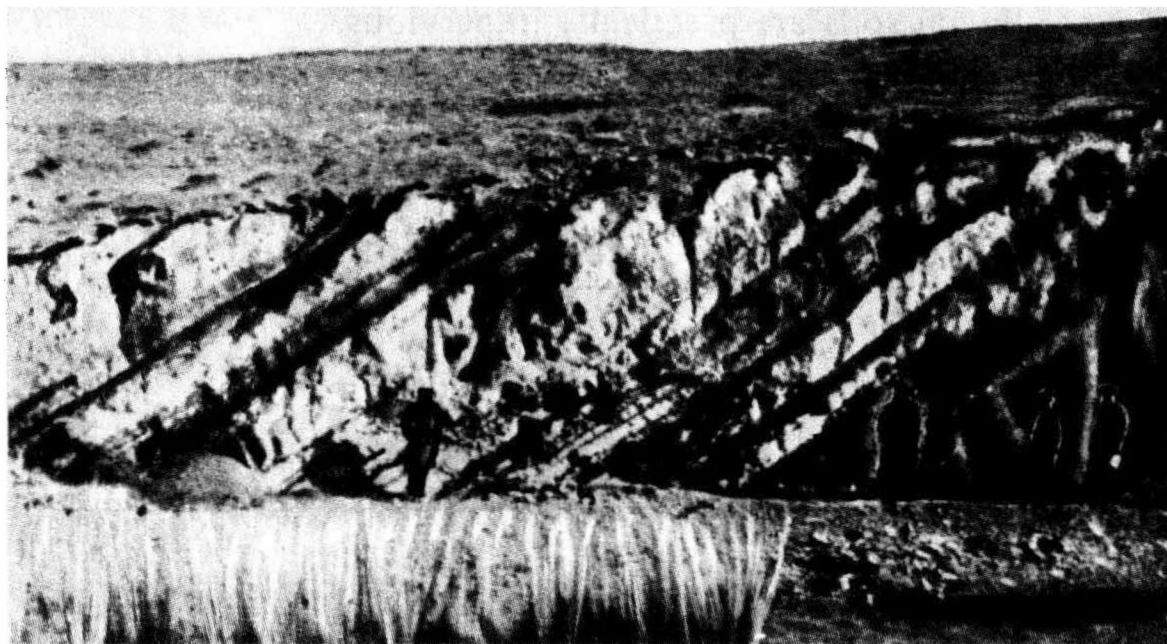


**Fig. 43.1.** Effects of abrasion. Smoothed surface of steeply dipping strata of marine deposits (sandstones, aleurites, argillaceous slates)

of waves; the direction of prevailing winds; tidal events; climatic features of the area, and, which is generally most essential, strength and stability of rocks being influenced by wave action. Particularly disadvantageous conditions obtain when soil strata occur horizontally or, which is even worse, when rock (soil) strata are inclined in a direction opposite to the sea. If the shore is sloping, the intensity of abrasion is decreased.

Depending on the particular conditions, the intensity of shore front disintegration may fluctuate in the range of several centimetres to several metres per annum.

The rate of abrasion of a shore composed by hard rocks within short periods of time may seem negligible. However, similarly to other geological processes at work, the results of abrasion should be considered in terms of lengthy geological periods.

Viewing abrasion from this standpoint, we have every ground to assert that in the course of time any seashore massif, even composed of hardest rocks, under definite conditions may be totally eroded or even destroyed. This is evidenced by remnants of previously impressive mountain structures destroyed by erosion and abrasion (for example, in the Donets Coal Basin).

If there is a longshore current acting along a shore line, products of shore erosion may be transported to conspicuous distances. Sea currents are generally caused by winds and tides. They carry small- and fine-grained sands, products of erosion of sea shores. These deposits are replenished by

large quantities of detrital material transported by large rivers to the seas. Under definite conditions sand is redeposited, forming shoals, bars, sand spits, and sand beaches. Then a need arises to protect port approaches from silt and sand wash. Dredging must often be undertaken so that depth of navigation channels be maintained permitting the passage of vessels.

Defense works, however, to protect shore line areas and structures found there, especially, at locations where land is retreating and sea advancing are much more important.

In former times sea shores were generally protected by massive retaining walls. These barriers, however, often collapsed in the course of time which points to a need of using such structures more cautiously. Construction of groins and jetties facilitating accretion of material to increase man-made sand beaches (for example, in Sochi) presents a better means of shore-line protection.

It should always be borne in mind that abrasion of a shoreline may often trigger landslides and rock falls.

### Sec. 43.2. Transformation of Margins of Water Reservoirs

This is transformation of shores of artificial water reservoirs under new conditions (relatively rapid submergence of land areas). Such reservoirs may often be very large in area. For example, the area of the Shcherbakov reservoir is close to that of Onega Lake.

Formation of a reservoir commonly causes the water level to rise by several tens of metres. The water floods such sediment layers which were never submerged even during the highest floods in the historical past. Moreover, the conspicuous length of such a reservoir facilitates *wave making*. In stormy weather the newly formed shore front is attacked by waves which may attain several metres in height.

The shores, if composed of relatively incompetent soils, start rapidly to collapse (Fig. 43.2). This process, associated with abrasion in man-made conditions may sometimes proceed at a rapid rate. A shore line area, sometimes several metres in width, may be washed away in the course of a few years. This may endanger urban areas, industrial objects and transport routes which will have to be relocated. If it is more economical, defense works may be built. As to new construction objects, these should be sited at a safe distance from the margins of the reservoir.

Clearly, this problem should be approached taking into account the long-term action of waves eroding the shore line. As is known, the service period of special engineering structures is fairly limited. For structures we are concerned with, the process of marginal degradation must be predicted for the nearest 20-100 years. Note that marginal degradation may be also





Fig. 43.2. Illustration of marginal degradation

due to the shallowing of the reservoir, especially at the coastal strip, owing to deposition of products of shore erosion.

Observations demonstrate that shores of reservoirs are washed out particularly severely at concave sections of the shore and at promontories, and also if the waves attack the shore line at an angle. In the latter case the wave velocities are 2-3 times greater than when the direction of waves is perpendicular to the shore line.

A rise in the level of the reservoir causes parts of the slopes that previously were above the water table to be saturated. If the shore is composed of clayey soils, this decreases their shearing resistance due to a drop in the angle of internal friction and apparent cohesion. Then landslides are likely to occur.

Failure of a shore due to landslides, as has been manifested by a number of observations, may be triggered by filling the reservoir, the process increasing with time. That is why marginal degradation must be invariably considered as immediate danger to structures located in the danger zone.

E.G. Kachugin divides the shore line strip into three subzones to evaluate hazard due to marginal degradation: 1—immediate danger zone: 2—subzone of likely shore line failure within 20 years: 3—subzone of ultimate degradation.

Table 43.1 shows widths of these subzones for various soils in average conditions.

Slopes composed of sandy soils are no longer scoured if their gradient attains  $2-5^\circ$ , those of Quaternary clay deposits if the gradient is  $5-8^\circ$ .

The easiest method of ensuring safety of a highway is to construct it at (or transfer to) a requisite distance from the edge of the reservoir deter-



Table 43.1

Widths of Subzones (after E.G. Kachugin)

Description of soil	Width from high-water edge, m		
	Subzone 1	Subzone 2	Subzone 3
Loess	60	160	To be calculated by rough estimation
Small-grained sand	20	40	
Medium-grained sand	15	30	
Loams	10	20	
Coarse-grained sand and gravel	5	10	

mined by proper analysis. Alignments of newly proposed river or valley crossings must then be possibly located such that bridge piers should rest on weakly erodible or practically nonerodible rocks. An alternative is to protect bridge approaches and bridge piers from scouring by appropriate means.

Lack of reliable methods of predicting rates of the process under consideration inhibits elaboration of measures for control of marginal degradation. The method of analogues relying on direct observations may prove useful for this.

Chapter 44

Landslides and Other Crustal Displacements

Sec. 44.1. Introduction

A landslide is understood to be a minor earth movement in which soil masses creep more or less slowly downslope due to gravity. This event is generally accompanied by some degree of disturbance of the natural structure of soil.

A landslide is triggered if the shearing (tangential) stresses appearing in a soil mass due to one cause or another exceed the magnitudes that the soil is able to resist.

If the soil mass supporting a structure loses stability, so does the structure itself start to be displaced.

Such a displacement, which is invariably differential, will cause deformations, structure settlement, disturbance of normal operating conditions



**Fig. 44.1.** Landslide involving some 70 000 m<sup>3</sup> of material has affected a road (Miatlinskaya Hydropower Station area)

of equipment and, regrettably, rather often, total failure and disintegration of the structure.

Landslides present a hazard for any type of engineering structure. In urban areas landslides may damage buildings and streets located on slopes, particularly, adjoining a body of water. Cases have been recorded when landslides wrecked industrial objects found on river banks and mountain slopes.

Crustal displacements have frequently interfered with the operation of railroads and highways. Rock falls and landslides have sometimes displaced the roadbed of a highway, for example, that of the Black Sea longshore highway and the Simferopol-Yalta thoroughfare. Major earth movement occurred several years ago encroaching on an approach road to the Oka River bridge in the city Gorky (Fig. 44.1).

A landslide may damage a road embankment slope (Fig. 44.2).

To ensure continuous traffic, particularly hazardous sections of railway and highway alignment had to be shifted. Such shifts sometimes called for decreased embankment heights or took road alignments out of cuts. In other instances highway alignments were transferred a few kilometres away, or tunnelling for roads and hydroengineering structures was used.

It should be kept in mind that a tunnel carrying a road or a hydro-engineering structure does not guarantee these latter from earth movement hazard. Portal sections of a tunnel piercing the mass of incompetent upper layers of soil may be endangered. Tunnel shear failures have occurred due to contact slips of bedrock stacks (for example, of crustal basalt) along a sloping surface of Tertiary marls underlying them.

Poor siting of the alignment of a river crossing without making allowance for likely slides may result in failure of bridge abutments or even piers and may sometimes cause total disintegration of bridge structures.

We may refer to a failure of a bridge across the Peace River (British Columbia). The bridge was built during World War II and operated in normal conditions during 15 years. Earth movement occurred in 1957 on one of the river banks which caused displacement of the bridge abutment and tipping toward the stream by 3.5-4 m, the foundation remaining undisturbed. The landslide destroyed the bridge abutment, the first scaffold span and two



Fig. 44.2. Slump slide on the slope of an embankment



**Fig. 44.3.** Slump slide in the Zeravshan River valley, Tajikistan. Displacement of mass of Paleozoic strata of limestones and slates overlain by sand and clay conglomerates (photograph by V. Presnukhin)

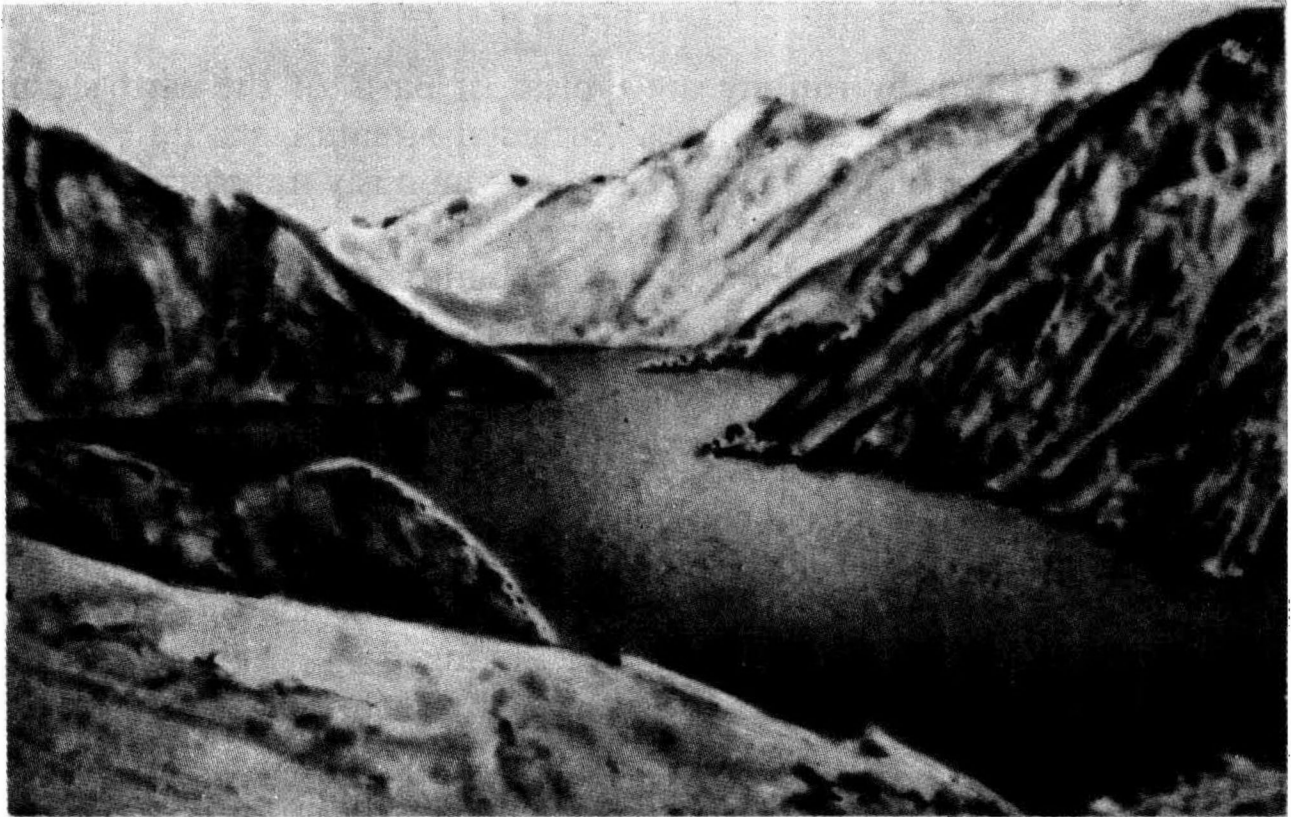


Fig. 44.4. Sarez Lake with a capacity of about 15 billion  $\text{m}^3$  formed after a mountainous river was dammed by a landslide

bridge spans totalling 153 m in length. It was deemed unreasonable to reconstruct the bridge, so another bridge was built at a different location. This decision was made on an assumption that the displacement had occurred at the contact surface of crustal rock underlain by incompetent clay slates.

We can refer to quite a number of case histories of bridge deformation induced by landslides. Landslides and rock slides may occasionally assume catastrophic scales (Fig. 44.3). A rock slide in the upper reaches of the Amu Darya River tributaries in the Pamir deserves special mention. A 2 billion  $\text{m}^3$  of material was displaced resulting in the formation of Sarez Lake with depths attaining 600 m (Fig. 44.4).

#### Sec. 44.2. Causes of Landslides

To estimate the stability of slopes we divide these into three types: denudation slopes, slopes (in particular, underwashed) of failure by rupture, and accumulation or talus slopes.

**Denudation slopes** are such relief features that form due to the action of surface denudation agents, such as meteoric water, ice, wind etc. A slope is ultimately smoothed and flattened, ideally, until it represents a plane sur-



face. In the latter case the slope must demonstrate a definite margin of stability.

**Slopes of failure by rupture** are typical of parts of the earth's crust stricken by slides or subject to slides. Particular attention should be called to eroding or littoral slopes that are being continuously transformed by the eroding and abrading action of a river, sea or lake.

Such slopes are in a state of temporary limit equilibrium that may be disturbed at slightest provocation. This can trigger mass movement. An example can be found in the riverside slope of the Volga River near the town Ulyanovsk.

**Accumulation or talus slopes**, as the name suggests, result from accumulation of erosion products at the toe of a bedrock slope. Owing to their origin, accumulation slopes are in a state of limiting equilibrium. Particular danger is presented by active *screes*, moving deposits composed mainly of coarse detrital products of weathering.

The stability of such slopes is disturbed by such factors as increased shearing forces, reduced resisting forces or both.

**An increase of active shearing forces** and, as a result, origination of a slide is associated with the shearing stresses due to the erection of an engineering structure on the slope, formation of spoil banks as well as with an increase in the weight of the soil mass, higher gradients etc.

**A reduction of resisting forces** in rocks may be induced by a drop in the shearing strength of soils composing the slope or by removal of lateral support, say, when excavating a cut across the slope.

Factors likely to cause such changes are numerous and diversified.

Weathering plays an essential role in the disturbance of slope stability. In the general case this process lowers the shearing strength of rocks and often causes cracks to be intensively formed. The stability of a slope may also be impaired by continuous slow-rate deformation induced by creep properties of materials composing the slope.

Surface and subsurface (primarily ground) waters represent even more important agents conducive to disturbance of slope stability. The effect of these waters on the stability of a soil mass subject to movement is twofold: soil layers previously found above the water table are wetted and weakened: pressure water produces an uplift effect on the soil mass. This process reduces normal effective stresses (pressure on skeletal particles of soil) and lowers the friction forces acting in the soil.

In addition, the stability of a slope may be impaired by hydrostatic pressure of the water filling the voids in the soil mass enhancing the shearing forces affecting the soil, by the tractive force of the groundwater flow influencing the soil (hydrodynamic or seepage pressure) as well as by the scouring of the sand from the lower strata.

Additional saturation of poorly wetted crustal soil layers by meteoric

and sewage water may occur both from the upper surface and from below as water is uplifted at a definite head from an aquiferous layer underlying the creeping soil mass (say, at the contact with bedrocks) and fed by this water at higher horizons of the slope. An important role is played here by the rapid rise of the water table or head in the aquifer due to more abundant water supply, say, during melting of snow or autumn rain spells.

Note that if at the toe of a creeping slope there occurs upward seepage at a pressure equal to the thickness of the creeping layer, that is, at a hydraulic gradient equal to unity, then the uplift water pressure may reduce the stability of the soil mass almost twofold. If the water head at the contact zone is twice the thickness of the creeping layer, under definite conditions the degree of slope stability may drop to zero. This is the more dangerous since slope stability very often approaches equilibrium.

Under conditions of hydrodynamic and seepage pressure of groundwater percolating downward in the body of creeping soil, the stability of a sliding slope is generally increased as the level and pressure of subsurface water are artificially lowered and vice versa.

It should be also pointed out that meteoric water saturating the topsoil increases its weight, thus reducing the stability of the slope, particularly, if the upper crustal layers are composed of sandy and similar soils whose voids are free from moisture.

A detrimental effect may be produced by the water of a stream or reservoir on the toe of a slope both by scouring and eroding, on the one hand, and by wetting the soil mass after a rise in the water level, on the other hand. Particularly adverse effect is produced by a rise of the water table during a freshet or the filling of the reservoir which weakens clayey soils under the slope.

On the other hand, a rapid drop in the water level may also complicate matters due to removal of uplift pressure increasing the weight of the soil mass and due to intensive withdrawal of groundwater (hydrodynamic or seepage pressure). These factors may appreciably impair the stability of a sliding slope.

**Man's activities** often involve additional wetting of slopes (irrigation, sewage disposal) which impairs their stability. Deleterious effect may also be induced by land cultivation facilitating percolation of meteoric water, by removal of vegetation cover from slopes reducing the binding role of root systems. Vibrations from passing traffic are also likely to disturb slope stability.

Construction on a slope can likewise reduce its stability by the excavation made in it and by the increased load on the soil mass.

Seismic events are followed by inertia forces (increased shearing stresses) acting on a slope and a drop in the shearing resistance of soil (vibration-induced liquefaction of sands, reduction of cohesion etc.).

Sec. 44.3. Possible Patterns of Disturbance of Slope Stability

To elaborate measures of slide control that would be most suitable for each particular case, knowledge is needed of the pattern and possible development of earth movement.

Clearly, the type of the slide is governed by the natural conditions and factors causing the disturbance of a slope or hill side. The natural conditions include: recent tectonics and associated alterations in the hydrologic regime resulting in the deeper cutting of rivers into the earth's surface; climate; topography of the slope; geology of the mass of soil composing the

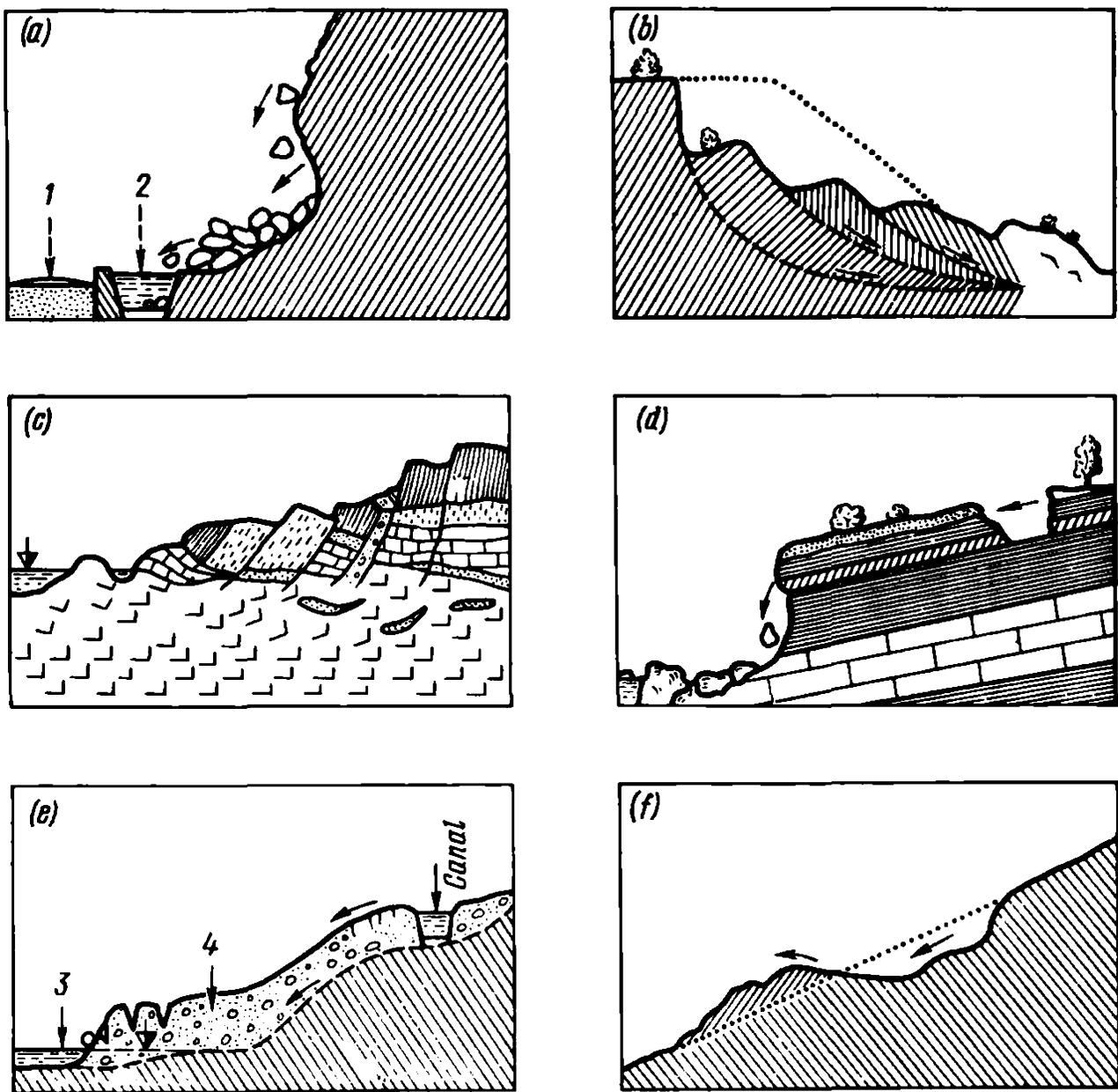


**Fig. 44.5.** Principal patterns of disturbance of stability of slopes and their deformations:  
a—rock falls and inrushes; b—rotational shear failure; c—failure by chipping followed by subsidence;  
d—landslip or slump slide; e—shallow slide; f—mudflow slide; 1—road; 2—canal; 3—river; 4—spalled  
detrital material



slope; geotechnical properties of materials making up the slope; ground-water regime; regime of the body of water washing the slope.

Knowledge of the likely pattern of earth movement and of the natural conditions makes it possible to fairly reliably determine the principal cause of movement, and, consequently, choose the most efficient remedial measures.

Figure 44.5 presents the principal types of disturbance of the stability of natural slopes and their deformations.

What makes a *rock fall* (Fig. 44.5a) peculiar is that it occurs practically unexpectedly. Rock falls involving stiff (hard and cemented argillaceous rocks) materials are particularly common on steep jointed benches. When undisturbed, the stability of such slopes and steep hill sides is due to cohesion. Yet continued weathering of the soil mass, which in mountainous country is mainly induced by frost action may appreciably reduce the stability of a slope or of individual rock blocks composing it. Rock falls will occur in the latter case (Fig. 44.6).

Moisture accumulated in the fissures, when frozen solid at night, may mean trouble. As the ice melts in the daytime, especially on southern slopes, rock avalanches may be triggered. Rock falls and avalanches may sometimes be started by slightest external provocation, such as a distant explosion or thunderclap.



Fig. 44.6. Fallen rocks blocking a road

Seismic events often cause rock falls and slides. Alternatively, these may occur if a stream scours a steep bank. This is particularly possible if the upper strata of stiff rocks are underlain by less competent materials. Rock fall and avalanche hazard is enhanced by road construction when bedding planes which are inclined toward the excavation are being undercut. Such events, as a rule, completely block traffic on roads.

Sarez Lake in the Pamir (see Fig. 44.4), already mentioned above, was formed in 1911 when a rock massif collapsed during a Richter intensity scale number 9 earthquake. As a result, the Bartang River was blocked by a natural dam 5 km long and up to 700 m high. The length of the lake is some 55 km. New mass movement which would involve 1-2 km<sup>3</sup> of material is impeding. Protective measures have been worked out.

Rotational shear failures (see Fig. 44.5b) typically occur on slopes and hill sides composed of clayey soils manifesting fairly homogeneous structure. Failure of a slope (hill side) by rupture may be compared with that of a monolith construction member owing to a load-induced excess stress. Similarly to any other body, this state is associated with the appearance in the slope soil mass of surfaces along which shear or slide of a slump of the slope occurs as if it were a monolith mass. The location and character of surfaces of sliding (surfaces of chipping) in such a slope are only governed by the relationship between the forces active in the soil mass that are conditioned by the shape of the slope.

According to laws of structural mechanics the lines of possible sliding appear on a chart as curves and may be approximated by arcs of a circle. This permits estimation of the stability of a slope by calculation. The line of sliding, curved at its upper part, transforms to a straight or zigzag line to conform to the contact surfaces of individual layers or the shape of the underlying soil mass.

Rupture failure may appear as a series of consecutive *shears* occurring along load-induced lines of sliding as demonstrated for the general case by Fig. 44.7.

Since the shear line is curved, the displacement of a slump occurs followed by rotation of the moving slump about one or several successive instantaneous centres. A one-centred rotational shear takes place if the curve of sliding is circular. As a result, the upper part of the displaced slump is invariably inclined in the opposite direction. Shear of the successive slump generally occurs very rapidly although preparatory processes take place gradually. The velocity of further sliding of the chipped-off blocks or products of their disintegration downslope is governed by conditions to be considered below.

The character of a slope failure due to *chipping induced by subsidence* (see Fig. 44.5c) may be understood from Fig. 44.8. The subsidence of a

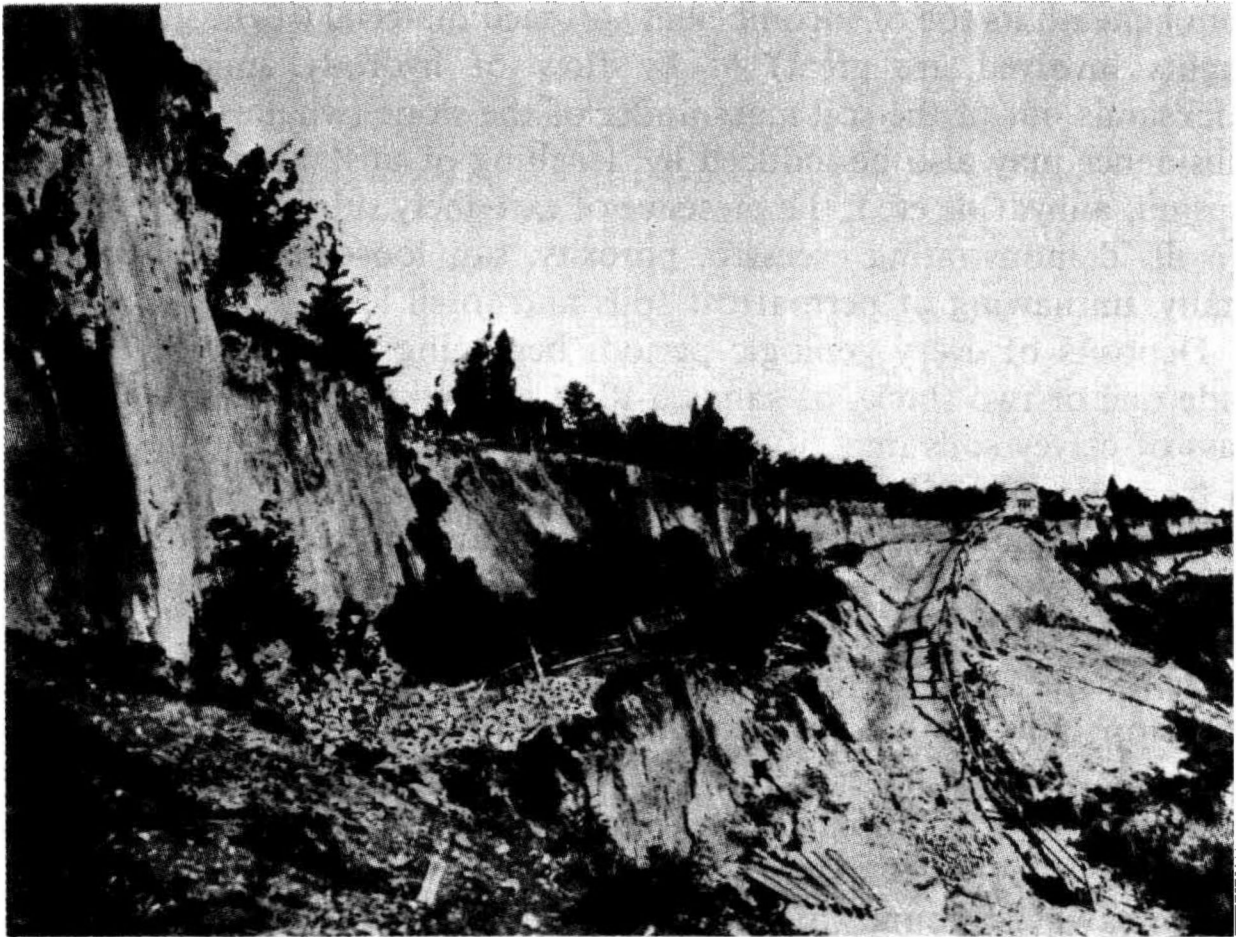


**Fig. 44.7.** River bank slope repeatedly affected by rotational shear failure

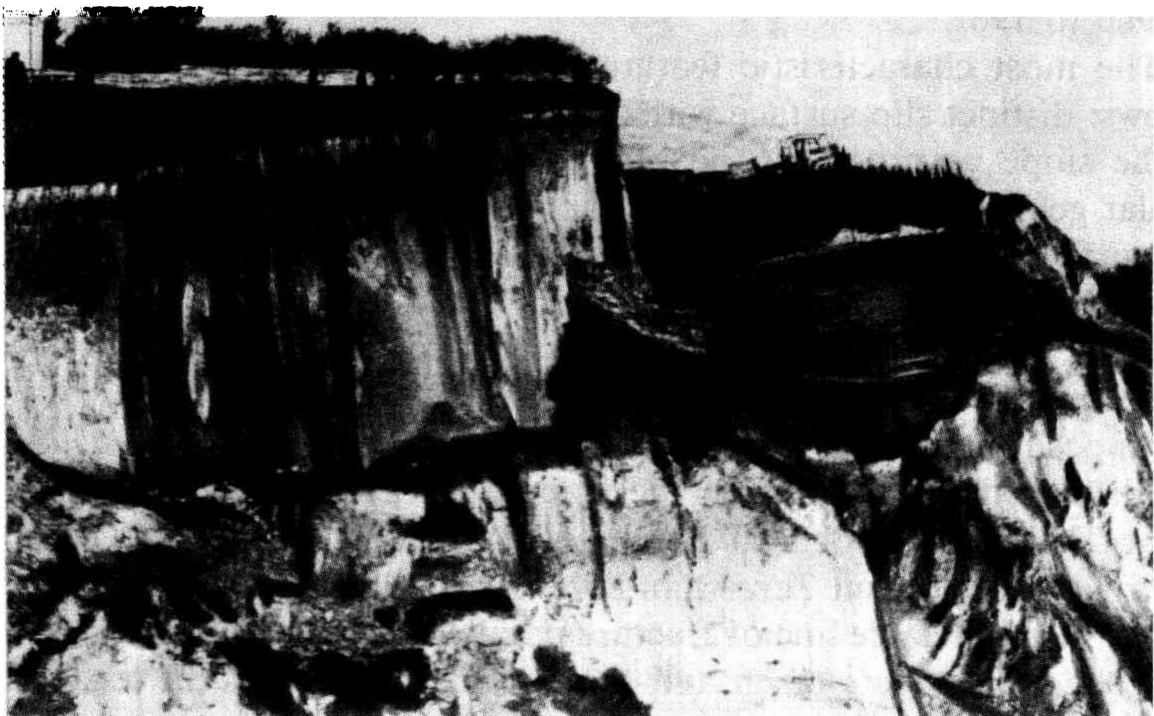


**Fig. 44.8.** Landslides caused by failure followed by subsidence of an underlying clay stratum

slope may be caused by the squeezing out of the soil mass in the slope or from beneath its toe of incompetent softened material (if the gradients and heights involved are great) or by flow of hydrodynamically unstable quicksands out of the soil mass under of the slope (whatever its gradient). Subsidence may also be induced by: leaching of unstable rocks (rock salt, gypsum, anhydride etc.); the presence of extremely subsiding loess-like soils or soils demonstrating excessive porosity, say, loose-textured sands; and, finally, unthawing of permafrost soils and fossil ice.

Deposits of every geologic period, beginning from the Devonian, include one or two stacks of sands 5-10 m, sometimes 15 m in thickness. A mass of clayey soils may often include seams of sands 1-2 m in thickness. Such seams may affect appreciably the stability of a slope. So, open-casts in the Kursk Region magnetic anomaly have demonstrated that most slides of slopes in clayey soils were caused by washing of such sands out of the soil mass by groundwater.

Being entrained by the creeping masses, the chipped off slumps move downslope at rates that are insignificant at first, although the shear occurs very rapidly. Cases have been recorded when substantial sections of banks collapsed due to chipping caused by vertical subsidence up to 10 m in amplitude in a matter of a few minutes. Chipping failures are particularly common when groundwater washes small-grained sands out of the soil mass onto a slope. This factor was responsible for a major landslide near Beketovka (Volgograd Region) in 1941. Similar events took place on a steep river bank of the Dnieper in the vicinity of Kiev, as demonstrated by investigations of the Ukrainian Hydraulic Engineering Institution conducted in 1960 to 1961.

The most characteristic features of a landslide (see Fig. 44.5*d*) are as follows: distinct slip surface with a large angle of dip toward the direction of the slope governed by the geologic structure of the soil mass; fairly regular geometry of the structure of the soil mass; displacement along the slip surface of whole blocks or stacks of rocks torn off from the mass of the slope (Fig. 44.9).

In the particular case slip surfaces are provided, as a rule, by bedding planes, relatively thin clay seams, contacts of two layer suites of unconformable occurrence, or lines of major tectonic fractures. A slide of this type that displaced some 25 million m<sup>3</sup> of material occurred near the village Oni in the Tajik Soviet Socialist Republic on April 24, 1964. This completely dammed the abundant Zeravshan River. This mass movement had occurred due to an appreciable line of fracture parallel to the river bank. Urgent corrective measures were taken and the danger to the adjacent localities was eliminated.

When started, slippage of stacks or blocks of weathered hard rocks



**Fig. 44.9.** Landslip in the slope of the river bank composed of sand and clay materials in the Kura River valley

along cleavage planes occurring obliquely invariably means trouble for bridge abutments and portal sections of tunnels constructed in such conditions.

Slippage of a stack of layers often takes place if the soil includes argillaceous, chlorite, talc and mica slates. Weathering and wetting of slip surfaces provide the decisive factor in this process. Crustal layers may sometimes slip along a wetted clay seam with an inappreciable angle of dip or, for that matter, even occurring horizontally. It is the seepage (hydrodynamic) pressure of groundwater that is responsible for mass movement under such conditions.

Crustal igneous (say, basalt) rocks frequently overlie a mass of marls or even clayey soils. Slippage of overlying layers (which, for example, took place in the Razdan River Valley in Armenia) may cause large-scale slides into a valley or an open-cast.

Joints and fissures in an active weathering zone are commonly filled by clay material and provide paths for percolation of meteoric water into a mass of soils or rocks where it circulates. That is why the weathering zone is convenient for slippage of rock stacks along fissures, particularly, if these are correspondingly oriented.

This factor has often been responsible for major rock falls and landslides. Apart from those already reported, a large-scale slide occurred on



October 9, 1963 that affected a slope of the Vaiont reservoir and involved over 250 million  $\text{m}^3$  of material. The resulting wall of water, some 260 m high rose up the opposite slope over the dam. The huge layer of mud attacked Longarone, Pirago, Fornace and Faè and, partially, Castellavazzo, Pineda and San Martino killing about two thousand inhabitants. Mention should be made of the failure of a steep slope composed of limestones that took place in 1903 in the vicinity of Franc Albert, Canada. 30 million  $\text{m}^3$  of material moved along a distinct line of fracture.

**A translational slide** (see Fig. 44.5e) is the most common form of developed creep. Unlike a rotational shear failure, this form of earth movement demonstrates the following features: absence of a surface of sliding dissecting the soil mass of the slope, the former being substituted by surfaces of bedrocks composing the slope that can be said to provide *a surface of creep*; the surface of creep has generally an irregular shape conforming to that of bedrocks; the creeping mass is disturbed (blocks, stacks) and represents spalled material from the erosion of the slope at its higher sections.

The particular form of slide of topsoil layers is common. An example can be provided by a hill side adjacent to the Volga River bank in Ulyanovsk. The decisive role is played here, as in many other instances, by the buoyancy and hydrodynamic effect induced by seasonal fluctuations of the groundwater table. If the creeping material is of substantial thickness, rotational shear failures will occur at its terminal lobe. Such failures which are very common involve soil masses erratic in shape.

Talus deposits are particularly prone to slides. If a talus deposit is of marked thickness, the earth movement may assume a very large scale. Examples can be found in talus slides on the southern sea front of the Crimea (Fig. 44.10).

Due to their inappreciable resistance to weathering, large amounts of products of weathering of clay and shales accumulate on slopes and at their toe. The action of meteoric water causes this material to soften, lose stability and slide downslope. This is the way a talus slide occurs.

If the creeping mass manifests marked viscosity (the degree of wetting being small), the velocity of movement is very low (1-2 cm a year). When the soil mass is wetted appreciably, and is travelling in a bending (if viewed in plan) bed, the process assumes the form of a plastic liquid flow. The velocity of the creep is then increased, not exceeding, however, several metres a day. Excess wetting of the creeping mass may cause liquefaction of the latter, and a mud rock flow may eventually be triggered.

**A flow slide** (see Fig. 44.5f) demonstrates features similar to a shallow slide of liquefied material. Both events involve excessively wetted soil masses moving downslope. However, there is also an important difference between these forms of earth movement. A shallow slide affects creeping

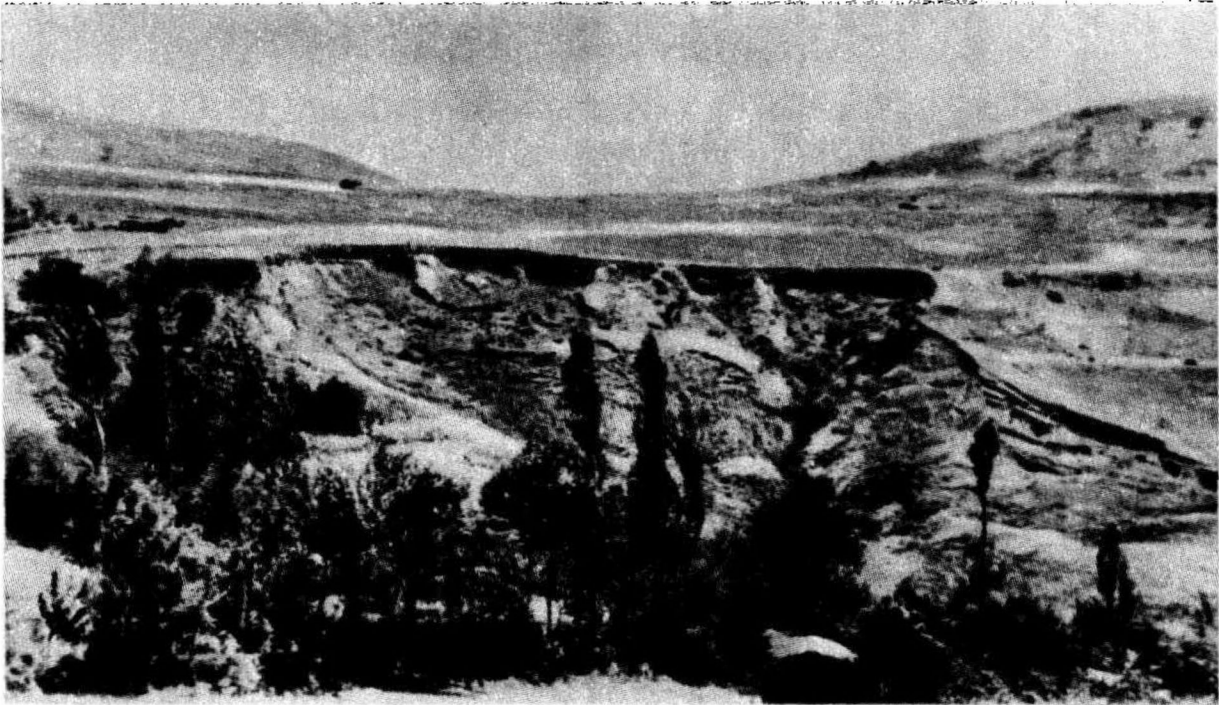


Fig. 44.10. Talus slide on the sea front line being eroded by the sea

soil mass previously detached from the bedrock material of the slope. By contrast, what is the most characteristic of a flow slide is the detachment of a definite amount of material from the soil mass under conditions of excessive local wetting. In the latter event the sliding mass does not generally demonstrate either a regular structure or, for that matter, a surface of sliding. A flow slide generally affects only the particular topsoil mass not disturbing the underlying strata. Differently speaking, it occurs locally where groundwater is discharged to the surface of the slope, say, as a spring.

Topsoil layers of slopes (Fig. 44.11) composed of loose cohesionless materials which, after excessive wetting, may pass to a quicksand condition, are very much prone to flow slides. Sand slopes sometimes liquefy suddenly due to a loss of their total stability caused by sliding over the surface of an incompetent layer underlying them. A classical example is to be found in the shear failure of a portion of the upstream face of the Fort Peck Dam (Montana) during which a large mass of sand (several million  $\text{m}^3$ ), both in the foundation and in the saturated portion of the dam, liquefied and was displaced to a distance of some 500 m.

A slope failure that occurred in the summer of 1960 in a port at the Volga riverside is very instructive. A process, similar to one described above, caused heavy concrete plates lining the slope to be displaced in a matter of a few minutes to 160 m from the bank. At this, some of the plates were covered by a 0.8-1.0 m thick layer of quicksand mass sliding from the slope.



**Fig. 44.11.** Mudflow slide induced by excessive migration of groundwater to the upper surface of the slope (photograph by V. Presnukhin)

As has been shown by analysis, it is the dynamic action on submerged sand slopes that causes such failures. Loess slopes are also prone to movement. As has been pointed out above, dry loess can stand on very high steep slopes, yet at locations where groundwater comes to the surface, saturated loess becomes very unstable and easily sloughs.

Flow slides may also occur in submerged slopes composed of rather coarse-grained sands at a river side or a bridge abutment slope after an abrupt drop in the water level of the reservoir or stream. As has already been mentioned, vibrations or other dynamic and hydrodynamic overloading may cause similar events in a saturated fine- or small-grained sand mass.

#### **Sec. 44.4. Stability Computations for a Slope or Hill Side**

It is often necessary to quantitatively evaluate the stability of a slope or hill side and find a factor of safety for the particular job.

This is usually the case when designing, say, slopes of an excavation. Similar problems are met with whenever troublesome ground is involved or slide control measures have to be elaborated.

It should be pointed out that earth movement is a complex phenomenon that has not been completely understood. Therefore precise solutions are generally hard to make, so semiempirical methods validated by actual practice have to be used.



When employing methods to be outlined below it should be borne in mind that they are only approximate and can be used as aids for general geotechnical analysis of the region. A number of failures induced by inaccurate predictions of slides led to the elaboration of a multitude of calculation methods. Careful study has revealed a very close affinity between these methods. Moreover, it has been shown that stability computations are better facilitated not so much by the choice of the method, but, rather, by how well the particular scheme fits into the actual natural conditions, and, notably, by how closely the design soil characteristics correspond to the real parameters of soil.

It should be finally emphasized that when making calculations of likely earth movement the particular type of slide should be taken into account or, at least, in view of a vast assortment of slides, we must decide to which of the two principal slide classes, viz. a rotational slide or a translational slide, the particular landslide can be referred.

*Rotational, or shear slides* are such crustal movements where a mass of soil is displaced along *a surface of sliding* appearing beneath the slope and, under conditions of general overloading of the soil in the slope, offering the least resistance.

The determination of the pattern and location of the surface of sliding in a shear slide is the most complex, and, to an extent, indeterminate task. This is what mainly makes stability computations difficult to perform.

Stability computations that involve **translational slides** are, by contrast, more determinate: we do not have to locate the surface of sliding. This latter is provided either by the geologic structure of the soil mass or the crustal surface on which, say, a road embankment is being constructed. These computations, however, include some points connected with detailed analysis of the problem.

What follows provides only principal pathways for such computations.

1. **A shear slide.** Under such conditions engineering practice generally employs a method of a circular-cylindrical surface of sliding (Fig. 44.12).

The particular method is the most convenient for stability computations of slopes in *homogeneous* materials. This is particularly valid for the most common form of earth movement, a rotational shear failure (see Fig. 44.5b).

Designing practice very often employs this method for prediction of crustal displacement of slopes composed of unhomogeneous materials as well.

Clearly, such kind of slide is produced by a shear of the soil of the slope and displacement of some of it along a surface of sliding of one shape or another. As is shown by analysis and field observations, for clayey soils this surface is invariably curvilinear. On the other hand, in the most elementary

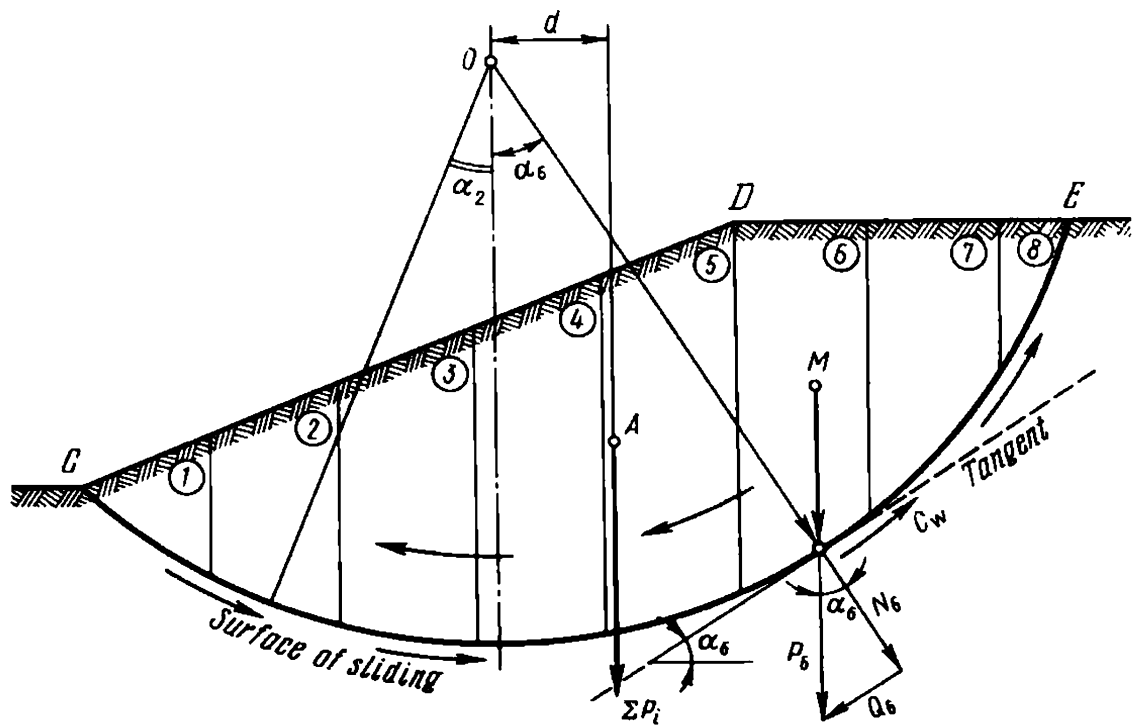


Fig. 44.12. Diagram for slope stability computations by referring to a method of circular-cylindrical surface

cases the shape of this line of sliding can be approximated by a circular arc of a radius  $R$  and centre  $O$  which are definite for each particular case (W. Fellenius, K. Terzaghi and others).

Civil engineering has now at its disposal an assortment of methods for stability computations of slopes depending on the given shape of the surface of sliding. However, as has been manifested by detailed study, the methods proposed by workers both in this country and elsewhere yield practically similar results.

The simplest, in principle, and most popular in the USSR is what is known as *the method of moments*. It is assumed that a slope may creep only if the creeping mass rotates about a centre  $O$  (Fig. 44.13). Consequently, the sliding surface  $BD$  may be represented by an arc of a circle with a radius whose centre is at  $O$ .

The sliding mass is assumed to be a solid block every part of which participates in the movement. This, of course, is only a rough approximation.

The sliding soil mass is being acted on by two moments:  $M_{rot}$ , rotating this thick block of soil, and  $M_{res}$ , resisting it. The factor of safety of the slope,  $k_{saf}$ , will be found from the ratio of these moments

$$k_{saf} = M_{res}/M_{rot} \tag{44.1}$$

What makes matters complicated in this method is a need for taking into account the variable values of friction forces  $T$  that appear at different

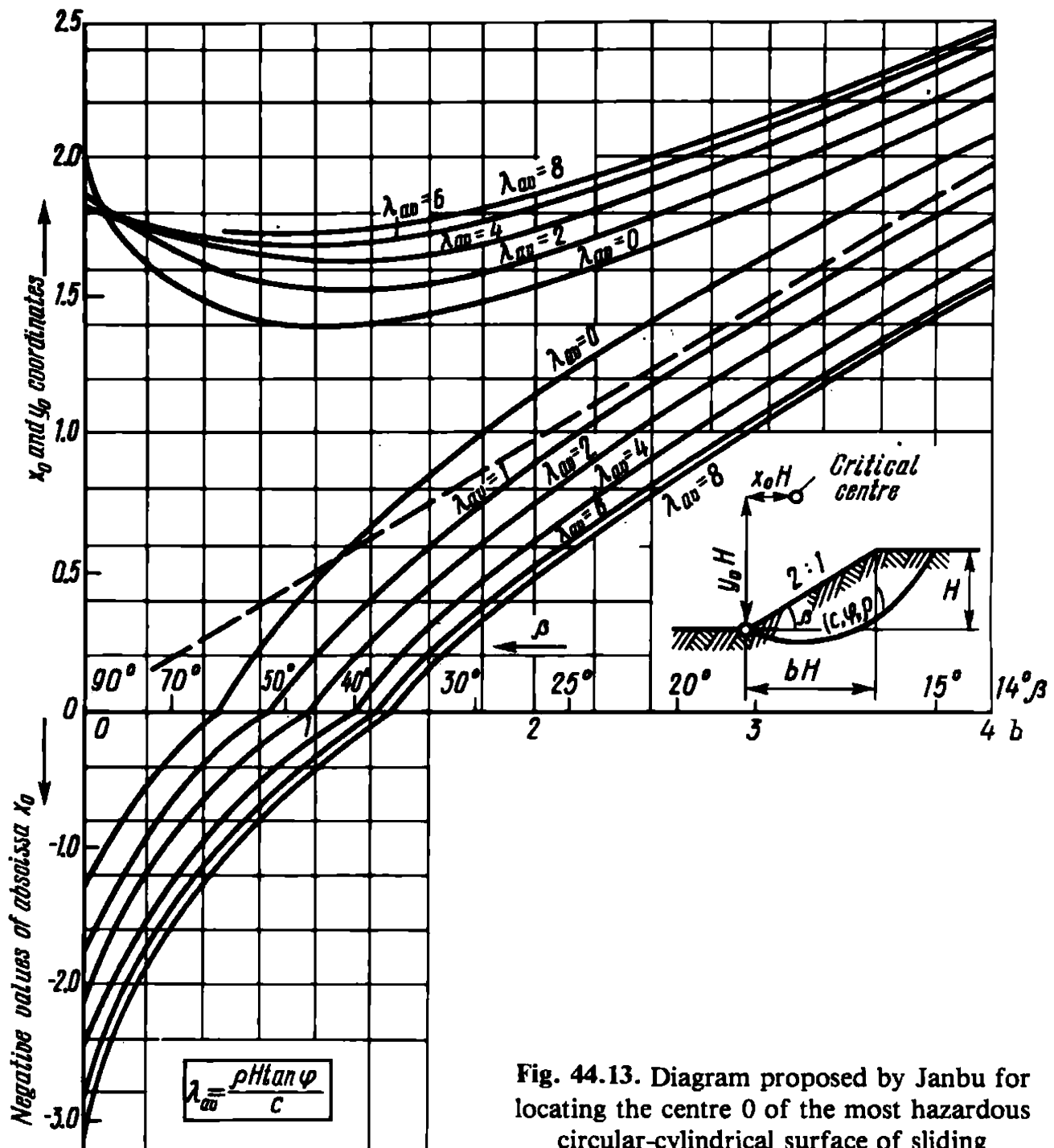


Fig. 44.13. Diagram proposed by Janbu for locating the centre  $O$  of the most hazardous circular-cylindrical surface of sliding

points of the surface of sliding during the shear. The fact is that

$$T = N \tan \varphi \quad (44.2)$$

where  $N$  is the normal component of the weight  $P$  of a definite portion of the soil block to a tangent to the surface of sliding at its particular point, say in block 6 in Fig. 44.12.

As can be seen from this diagram,

$$N_i = P_i \cos \alpha_i \quad (44.3)$$

where  $\alpha_i$  is the angle of inclination of the tangent to the surface of sliding

to the horizontal at a specified point whose numerical measure is the angle between a vertical and a radius vector  $R$  to this point.

Thus in the particular case the direction of the normal force  $N$  agrees with that of the radius vector  $R$ .

It will be concurrently noted that the shearing force  $Q_i$  at this point induced by the load  $P_i$  can be found from a straightforward relation

$$Q_i = P_i \sin \alpha_i \quad (44.4)$$

Clearly,  $Q_i$  may have different signs in the descending and ascending branch of the line of sliding.

A substitution into Eq. (44.2) of the value of  $N$  from Eq. (44.3) yields the friction force

$$T_i = P_i \cos \alpha_i \tan \varphi_i \quad (44.5)$$

Apart from the angle  $\alpha_i$ , the value of  $P_i$  may also change at different points of the line of sliding. These factors, taken together, make it possible to find the factor of safety of the slope under particular conditions from this relationship

$$k_{saf} = \Sigma M_{res} / \Sigma M_{rot} \quad (44.6)$$

Thus a need arises in slicing the hypothetical sliding mass into a number of design blocks for each of which we must determine the forces of the shearing resistance. In so doing, it must be kept in mind that the total resistance  $S_i$  appearing at the surface of sliding is made up of friction forces  $T_i$  and cohesion forces  $C_i$ . Consequently,  $S_i = T_i + C_i$ , and for each individual  $i$ -th block

$$S_i = P_i \cos \alpha_i \tan \varphi_i + c_i l_i \quad (44.7)$$

Thus the sums of the rotational and resisting moments will be equal to

$$M_{rot} = \Sigma P_i \sin \alpha_i R \quad (44.8)$$

$$M_{res} = \Sigma (P_i \cos \alpha_i \tan \varphi_i + c_i l_i) R \quad (44.9)$$

A substitution of the values of the moments from the last relationship into Eq. (44.6) after reducing the fraction by  $R$  ultimately yields

$$k_{saf} = \frac{\Sigma (P_i \cos \alpha_i \tan \varphi_i + c_i l_i)}{\Sigma P_i \sin \alpha_i} \quad (44.10)$$

Note that the values of  $\varphi_w$  and  $c_w$  in the formulae above and in what follows must typically correspond to their natural values with respect to density-moisture of soil.

If the soil is strictly homogeneous, when  $\varphi_w = \text{const}$ ,  $c_w = \text{const}$ ,  $\rho_w = \text{const}$ , the above relationship, by virtue of Eqs. (44.3) and (44.4), can be

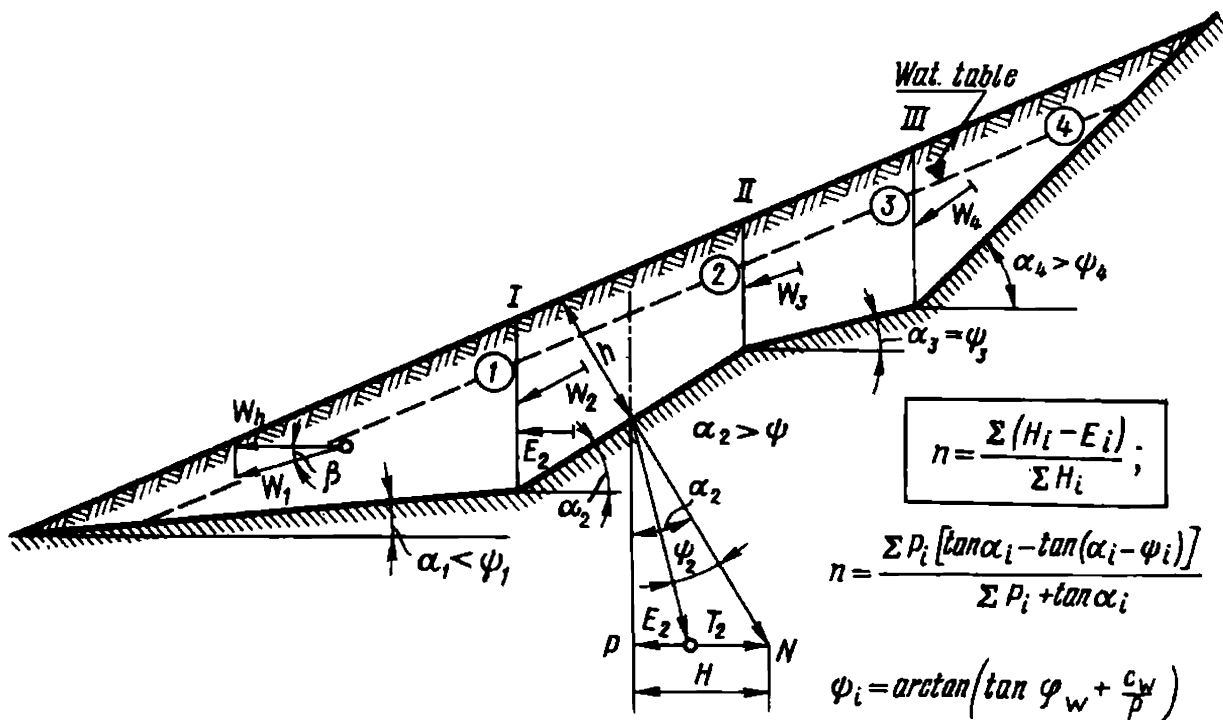


Fig. 44.14. Diagram illustrating a method of horizontal forces

rewritten as follows:

$$k_{saf} = \frac{\sum N_i \tan \varphi_w + cL}{\sum Q_i} \quad (44.11)$$

Clearly, when evaluating the stability of a slope to a definite degree submerged (e.g. a river bank) it is necessary to establish the pressure of each separate block,  $P_i$ , taking into account the buoyancy effect of the water.

If there is a structure of the slope, say, a bridge abutment, the latter's weight  $P_s$  and the horizontal force  $G_s$  (say, earth pressure imparted by the approach embankment earth pressure to the bridge abutment) must be allowed for when determining the resisting,  $M_{res}$ , and the rotational,  $M_{rot}$ , moments.

The particular method is often complicated in actual practice by the indeterminate position of the centre of rotation,  $O$ . Its coordinates and the value of the radius  $R$  must be determined such that the most disadvantageous location of  $O$  be established in order to find the least possible value of the factor of safety  $k_{saf}$  for the particular slope. The position of  $O$  is commonly found by consecutive calculations. To simplify matters, several methods for this operation are available, for example, the Janbu method (Fig. 44.14).

It is common occurrence that a slide may be triggered if the factor of safety  $k_{saf}$  is only insignificantly less than unity. To ensure requisite slope stability, it is imperative that  $k_{saf} > 1.0$ . In theory, the stability of the slope

or hill side will be guaranteed if the factor of safety only by a small margin exceeds unity.

The more indeterminate is the problem, the larger must be the value of  $k_{saf}$ . Therefore, when dealing with a slope whose stability is indeterminate, and in view of the inevitable inaccuracy of establishing the shearing strength of soil, it is plausible to use  $k_{saf} = 1.25-1.30$  or even 1.5 for stability computations. At the same time, on stabilizing a progressive slide, which makes it possible by inverse calculations (at  $k_{saf} = 1.0$ ) to check on the parameters of the shearing resistance of soils, it proves quite feasible and reasonable to adopt  $k_{saf} = 1.05-1.10$ .

Stability computations by the method under consideration in definite conditions may call for taking into account the possible effect of such factors as seepage pressure of subsurface water, sensitivity of clayey soils, slide flows of liquefied sand etc.

**Allowing for subsurface water seepage pressure.** Seepage pressure appears whenever there is a flow of subsurface water. If there is a gradient, an inclined surface of free subsurface water flow or of the piezometric level of pressure waters, it will cause a drop in the water head. This is due to the resistance offered by the soil to the flowing water. It is this very reaction force that builds up seepage pressure.

A flow of subterranean water is generally drained toward the stream valley, that is, it is directed downslope. Clearly, the soil mass beneath the slope is acted on by seepage pressure whose principal direction agrees with that of slide pressure. Consequently, in the particular case seepage pressure is a contributing factor of a slide event.

A similar picture, often much more exaggerated, can be observed in the slopes of flanks of reservoirs and canal bords after an abrupt drop in the level of water. Seepage pressure is a very important factor among those responsible for a disturbance of the stability of the slope or hill side.

Seepage pressure  $W_s$  is an active volume force acting on soil. Unit seepage pressure is found as the product of the density of water  $\rho_w$  with the hydraulic gradient at the given point  $I$ . When solving the problem in an MKS system  $\rho_w = 1 \text{ t/m}^3$ . Under such conditions, if water seeps through a definite volume of soil,  $V$ ,  $W_s = \rho_w VI$ .

In a two-dimensional case

$$W_s = \rho_w \omega I \quad (44.12)$$

where  $\omega$  is the cross-sectional area in the plane of the drawing (in particular, design block below the depression curve).

The depth of the flow of subsurface water in the soil mass constantly fluctuates which causes both  $\omega$  and  $I$  to vary simultaneously. Therefore

seepage pressure should be determined as being

$$\Sigma W_s = \Sigma q_w \omega_i I_i \quad (44.13)$$

where  $i$  is the consecutive number of the block.

The value of the hydraulic gradient  $I_i$  can be first approximated by the slope of the depression curve in the particular successive block. It can thus be seen that seepage pressure will increase with increasing the level of sub-surface water (factor  $V$ ) and gradient  $I$ . Such a state may largely arise under conditions of natural or forced increase in the discharge rate of sub-surface waters.

As is shown by studies of seepage pressure, if the surface of sliding has a circular-cylindrical shape, seepage pressure may be established if we assume soil below the depression curve as being uplifted  $P_{up}$  (numerator of the formula) and below that of active forces as  $P_i$  not acted on by uplift pressure (denominator of these formulae). Then the principal equation of the given method, Eq. (44.10), will take on this form

$$k_{saf\ s} = \frac{\Sigma P_{up} \cos \alpha_i \tan \varphi_i + \Sigma c_i l_i}{\Sigma P_i \sin \alpha_i} \quad (44.14)$$

The subscript "s" in the above formula implies that the factor of safety allows for seepage pressure; the subscript "up" suffixing  $P$  means that the weight of each of design blocks is taken allowing for the uplift pressure.

If the slope is submerged and there is no seepage through the soils (water levels in the reservoir and soil mass are equal), the active shearing forces  $Q$  (denominator of stability formulae) must be determined by taking into account the uplift pressure. To give an example

$$k_{saf} = \frac{\Sigma P_{up} \cos \alpha_i \tan \varphi_i + \Sigma c_i l_i}{\Sigma P_{up} \sin \alpha_i} \quad (44.15)$$

**2. A translational slide.** As has been mentioned above, this case is simpler to consider. The character of the surface of sliding is governed not only by the state of stress of soil, but, rather, by the natural soil conditions and structure of the soil mass. An important role may here be played by the mode of occurrence of incompetent interlayers manifesting reduced shearing resistance (sliding) or by the shape of the surface of the underlying layers along which the creeping mass slides (crustal soil displacement).

In a two-dimensional case these surfaces of sliding may be approximated in the plane of the drawing by an array of straight lines, lines of sliding (see Fig. 44.14).

*A method of horizontal forces* may be used to good advantage for evaluating the stability of a mass of soil under such conditions, as has been demonstrated by practice.

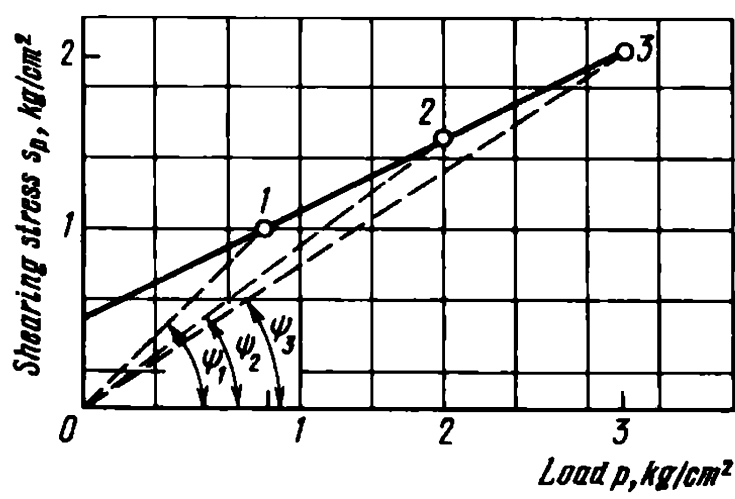


Fig. 44.15. Chart for a relationship between the shearing strength of clayey soil,  $s_p$ , and the coefficient  $F_p$  and the angle of shearing resistance  $\psi_p$

The shearing resistance of soil  $s_p$ , apart from the common expression in terms of the angle of internal friction  $\varphi$  and cohesion  $c$  may be expressed through the coefficient  $F_p$  and the angle of shearing resistance  $\psi_p$  (Fig. 44.15). In the latter case there is no need in the subdivision of the total shearing resistance into forces of internal friction  $p \tan \varphi$  and cohesion  $c$ . These index characteristics are interconnected by the relationships  $F_p = \tan \psi_p$  and  $\psi_p = \arctan F_p$ .

At the same time  $F_p = s_p/p$  where, as usual,  $s_p = p \tan \varphi + c$ . Then  $F_p = \tan \varphi + c/p$ , and  $s_p = pF_p$ .

As can be seen, the coefficient  $F_p$  and the angle of shearing resistance  $\psi_p$  are related to loading (see Fig. 44.16). In particular, if  $p = 0$ , the coefficient  $F_p$  and angle  $\psi_p$ , are, respectively, equal to infinity and the right angle. On the other hand, if the loading  $p$  is infinity,  $F_p = \tan \varphi$  and  $\psi_p = \varphi$ .

Analysis shows that the critical angle of slope equals the angle of shearing resistance of soil  $\psi_p$  if the normal stress  $p$  corresponds to the specified

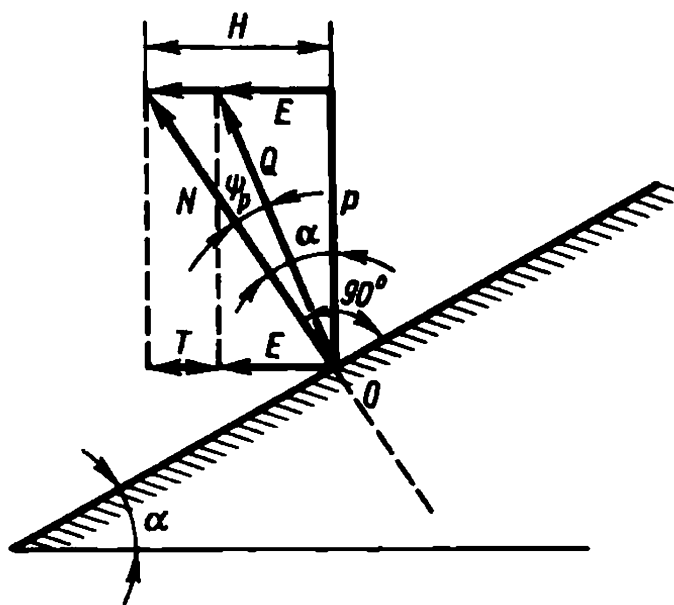


Fig. 44.16. Principles of a method of horizontal forces



condition, that is

$$\psi_p = \alpha_{cr} \quad (44.16)$$

It will be recalled that the angle of shearing resistance  $\psi_p$ , in a loose soil whose cohesion is zero ( $c = 0$ ) is equal to the angle of internal friction,  $\varphi$ . Consequently, the critical angle of slope  $\alpha_{cr}$  composed of loose soil equals the angle of internal friction, i.e.  $\alpha_{cr} = \varphi$ .

Let us now consider Fig. 44.16. Here  $N$  is a normal component of the reaction of the mass  $P$  of a definite design block selected in Fig. 44.15 to the surface of sliding on the condition that  $\psi_p = 0$ , that is, when  $\varphi = 0$  and  $c = 0$ . The force  $Q$  also represents the reaction  $P$  yet under conditions of friction and cohesion of soil active at the surface of sliding. The direction of this force is governed by the angle of internal friction  $\varphi$  or by the angle of shearing resistance  $\psi_p$  if the soil manifests cohesion ( $c \neq 0$ ).

The force  $H$ , being a projection of the force  $N$  on a horizontal axis, represents an outward thrust, that is, pressure exerted on a vertical wall by the lower soil block selected in Fig. 44.15 if the soil has no friction or cohesion. The force  $T$  is a portion of the outward thrust  $H$  that is sustained by the forces of friction and cohesion:  $E$  is the unattenuated portion of  $H$ . It is obvious that

$$H = P \tan \alpha \quad (44.17)$$

$$E = P \tan (\alpha - \psi_p) \quad (44.18)$$

$$T = H - E = P[\tan \alpha - \tan (\alpha - \psi_p)] \quad (44.19)$$

Equation (44.18) makes it possible, in principle, to establish the stability of each of the soil blocks selected in Fig. 44.15. Clearly, if  $\alpha = \psi_{\varphi p}$ , block 3 is in equilibrium; if  $\alpha > \psi_{\varphi p}$ , the stability of blocks 2 and 4 is not guaranteed and they impart pressure to the blocks underlying them. Finally, if  $\alpha < \psi_p$ , block 1 explicitly manifests a margin of stability and provides a buttress, as it were, for blocks located above.

By knowing the values of  $\Sigma(\pm H_i)$  and  $\Sigma T_i$  for soil blocks of the entire slope subject to sliding, it is possible to find the corresponding factor of safety

$$k_{saf} = \Sigma T_i / \Sigma(\pm H_i) \quad (44.20)$$

If there is seepage of water through the slope, the former imparts an additional pressure  $W_s$  to the sliding soil. The magnitude of  $W_{si}$  transmitted to each individual block is found from the familiar relationship, Eq. (44.12):

$$W_{si} = q_w \omega_i I_i$$

The direction of the seepage pressure  $W_{si}$  within each block can be as-

sumed as being parallel to the depression curve in the particular block. It is thus possible to establish the angle  $\beta_{si}$  between the direction of  $W_i$  and the horizontal.

The factor of safety  $k_{saf}$  of the sliding body in the given case, taking into account the seepage pressure, in conformity with Eq. (44.20), will be found from the relationship

$$k_{saf} = \frac{\sum T_i}{\sum (\pm H_i) + \sum W_i \cos \beta_{si}} \quad (44.21)$$

An especially important role is played by the subsurface waters in the stability of creeping soil on the slope if the contact with the bedrocks contains an aquifer with a pressure head likely to fluctuate in the course of time, say, from season to season, depending of the amount of precipitation.

A pressure head  $h_w$  is active in the contact layer which in the general case may be larger or smaller in thickness than the crustal layer  $h_s$ .

At equilibrium, with the critical value of the angle of slope,  $\alpha_{cr}$ ,  $k_{saf} = 1.0$ . Then

$$\tan \alpha_{cr} = (1 - 1/2 \times h_w/h_s) \tan \varphi_w + \frac{c_w}{q_s h_s} \quad (44.22)$$

For the particular case, if the soil in the contact layer displays no cohesion, that is, with  $c = 0$ , one obtains

$$\tan \alpha_{cr} = (1 - 1/2 \times h_w/h_s) \tan \varphi_w \quad (44.23)$$

Clearly, if  $h_w = h_s$  (practically,  $h_w$  may be greater than  $h_s$ ), in the given case the critical angle of slope is  $\alpha_{cr} = \varphi_w/2$ .

As can be seen, the presence of a pressure horizon in the contact layer appreciably reduces the stability of the sliding soil mass at the surface of sliding. If the pressure head  $h_w$  is conspicuous and exceeds the thickness of the sliding soil layer, the critical angle of slope may prove very small, and the sliding mass will move even if the rate of slope is insignificant under conditions of a substantial thickness of the soil mass,  $h_s$ , and inappreciable cohesion of soil,  $c_w$ .

**An approximate method for stability computations for an equally stable slope ( $F_p$  method).** Designing practice and engineering geology are using this method proposed by the writer in 1943 ever more extensively. Following from general concepts of slope stability, the present method relies on an assumption that at limiting equilibrium an equally stable slope, for each of its points at a depth  $z$  from the free surface, satisfies the condition

$$\alpha_z = \psi_{pz} \quad (44.24)$$

where  $\alpha_z$  is the angle of inclination of the slope to the horizontal at a depth

$z$ ;  $\psi_{pz}$  is the angle of shearing resistance characteristic of the particular horizon.

It will be recalled that the angle of shearing resistance  $\psi_{pz}$  is connected to the magnitude of the coefficient of the shearing resistance  $F_{pz}$  through the relationships

$$F_{pz} = \tan \psi_{pz} \quad (44.25)$$

$$\psi_{pz} = \arctan F_{pz} \quad (44.26)$$

At the same time, as is known,  $F_p = \tan \varphi + c/p$  is the coefficient of shear. For the given case the load  $p$  at a depth  $z$  equals the weight of the overburden, i.e.  $p = \rho z$ . Then the above equation may be rewritten as

$$F_{pz} = \tan \psi_{pz} = \tan \varphi + c/\rho z \quad (44.27)$$

If there is a uniformly distributed load  $p_0$  beyond the crest of the slope, we will have

$$F_{pz} = \tan \psi_{pz} = \tan \varphi + c/(p_0 + \rho z) \quad (44.28)$$

Clearly, if cohesion,  $c$ , is zero, the angle of shearing resistance, by virtue of Eqs. (44.25-44.28), will invariably equal

$$\psi_{pz} = \varphi \quad (44.29)$$

This is typical of loose cohesionless sands. Following from this and the above equations, it may be assumed that the angle of slope is uniform throughout its length under such conditions and is governed by the magnitude of  $\varphi_0$ , viz. the angle of repose characteristic of the particular sand variety (Fig. 44.17).

For other soils manifesting cohesion, the profile of an equally stable slope, by virtue of Eq. (44.24) and Eqs. (44.27) and (44.28), is curved, being steeper at the upper portion of the slope and flatter at the lower one.

For a subcritical state characterized by the magnitude of  $k_{saf}$ , for each horizon  $z$  we will have

$$\tan \alpha_z = (1/k_{saf}) \tan \psi_{pz} \quad (44.30)$$

The degree of stability of the entire slope is governed by the condition that at any depth  $z$

$$k_{saf} = \tan \psi_{pz} / \tan \alpha_z > 1$$

There are a graphical and an analytical methods for plotting the profile of an equally stable slope or of a slope with a specified value of  $k_{saf}$  by using Eqs. (44.24) and (44.30). The analytical method appears to be more accurate compared with the graphical one. However, if the soil mass of the slope is composed of several layers demonstrating different mechanical pro-

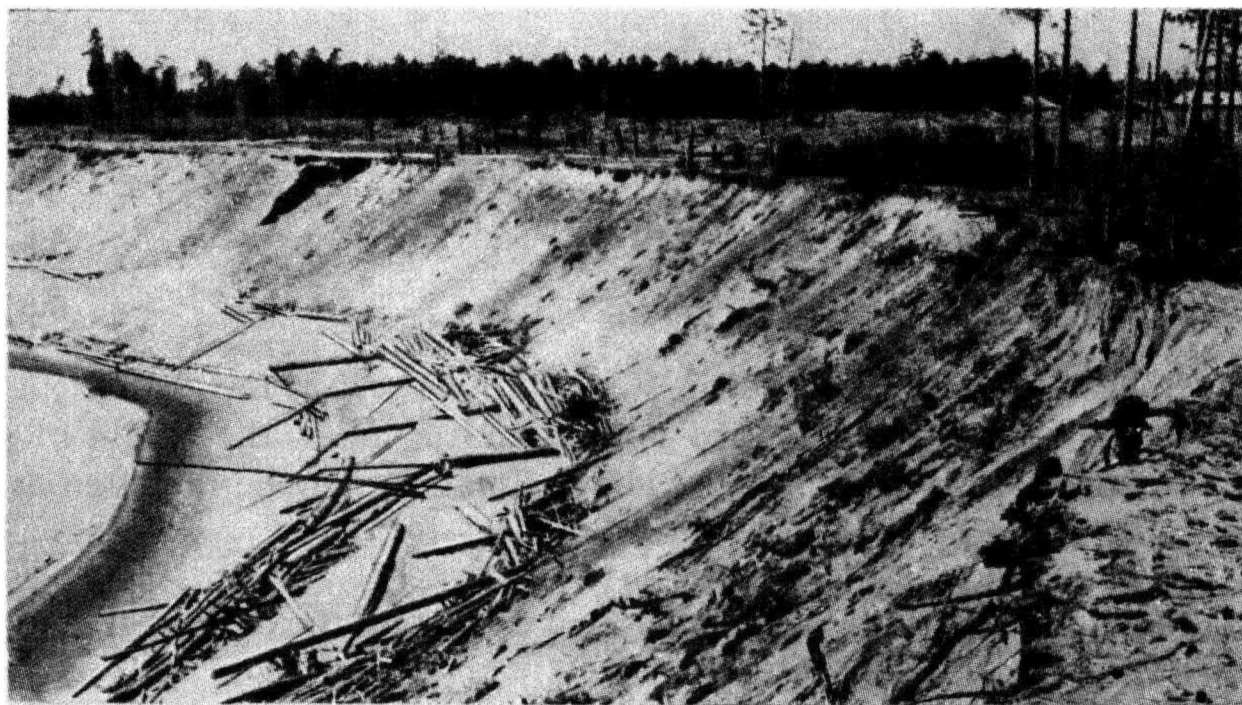


Fig. 44.17. Uniform rate or river bank slope composed of loose cohesionless sandy soils (photograph by V.M. Lashchilova)

perties, the analytical method is too bulky and preference should be given to the graphical one.

The graphical method of  $F_p$  (Fig. 44.18) is this. By referring to Eqs. (44.24) and (44.30), the slope is sliced into a series of design layers with the foot at a depth  $z_1, z_2, \dots, z_n$  from the upper surface. The larger the number of subdivisions, the greater accuracy will be attained. If the soil under the slope includes seams of different materials, the horizons corresponding to the design layers must conform to the contacts of such seams.

Find the value of the angle of shearing resistance  $\psi_{pz}$  for each of the layers with a depth  $z_i$  through the magnitude of the coefficient of shearing resistance  $F_p$  found from Eq. (44.27) or (44.28). After this, by using Eq. (44.24) or (44.30), establish the magnitudes of the angles of slope,  $\alpha_z$ , corresponding to the established values of the angles of shearing resistance  $\psi_{pz}$ , given one value of the factor of safety  $k_{saf}$  or another. At equilibrium  $k_{saf} = 1$ . If  $k_{saf}$  has this value, the slope is generally plotted by referring to Eq. (44.24).

Start the plotting from the lowest point in the slope for  $z_{max} = H$ . Measure out there the angle  $\alpha_z$ , corresponding to the particular horizon, then continue the determining line until it intersects the following horizon at a depth  $z$ . At the point of intersection measure out again the angle  $\alpha_1$  corresponding to this horizon. Find thus a new point of intersection of the determining line with the adjacent upper horizon etc. until the slope comes to

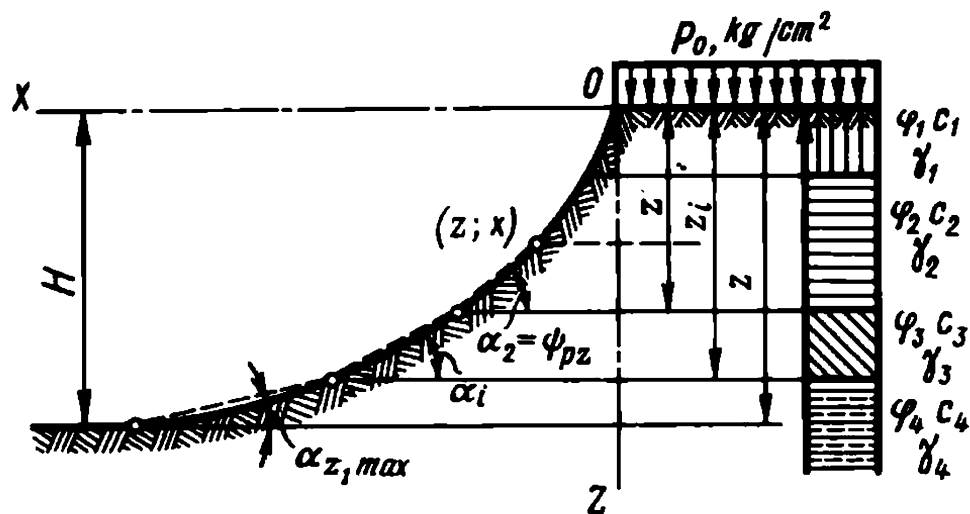


**Fig. 44.18.** Diagram for uniformly strong slope stability computations ( $F_p$  method)

the surface. Connect by a smooth curve the obtained points of intersection of the design horizons with lines determining the angles of slope  $\alpha_1$ . As is shown by practice, this method fairly adequately mirrors the actual conditions (Fig. 44.19).

Note that in the absence of a load on the surface of the soil mass beyond the crest of the slope, i.e. if  $p_0 = 0$ , and if the soil exhibits even inappreciable

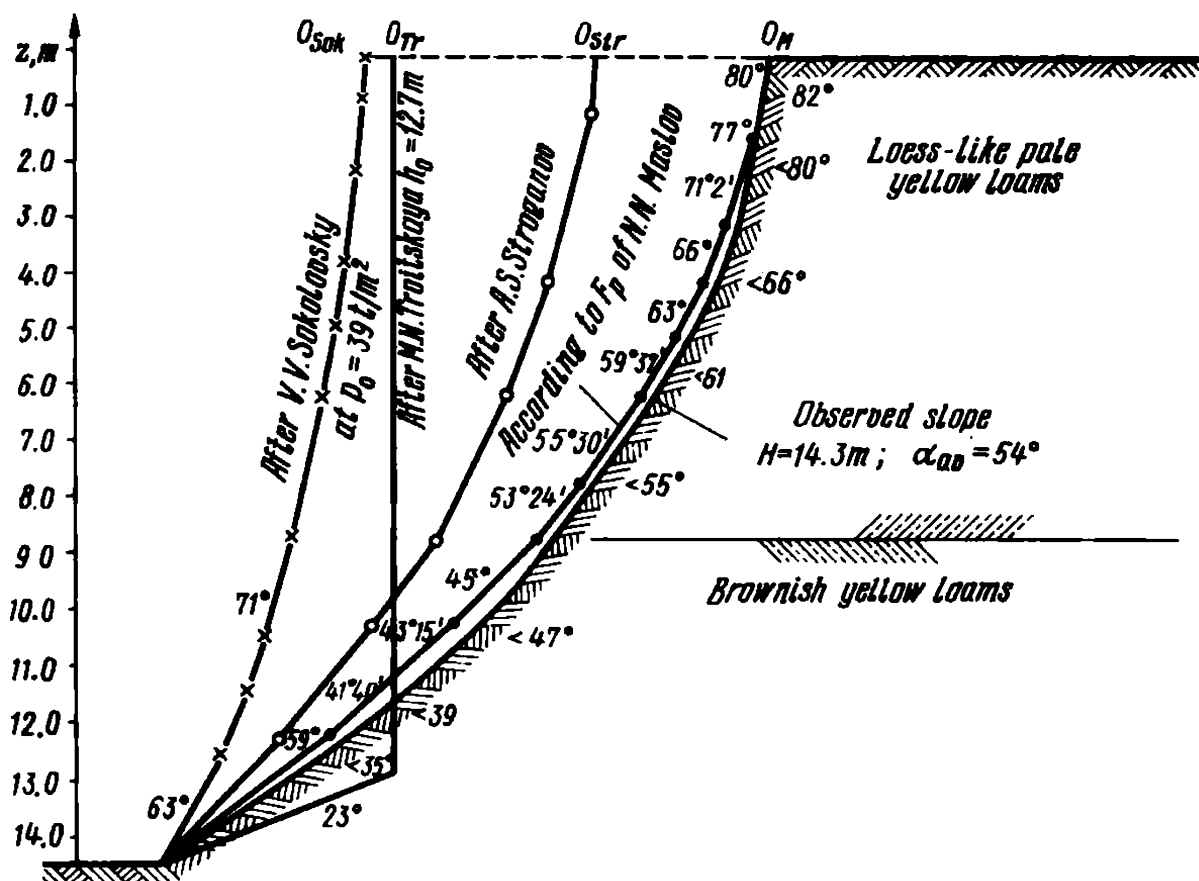


**Fig. 44.19.** Diagram permitting comparison between the actual shape of creeping slope ( $k_{saf} = 1$ ) and that plotted by referring to the  $F_d$  method

cohesion,  $c$ , the angle of slope at the surface of the soil mass becomes equal to  $90^\circ$  at  $z = 0$ . This follows from Eq. (44.27).

It is often necessary to determine the height  $H_v$  of a vertical slope that is stable, given specified parameters  $q$ ,  $\varphi$  and  $c$ . This is accomplished by referring to Eq. (32.8):

$$E_{ac} = 1/2 q H^2 \tan^2(45^\circ - \varphi/2) - 2c[H \tan(45^\circ - \varphi/2) - c/q]$$

In a vertical slope the active pressure of the soil mass is  $E_{ac} = 0$ . In discarding the second bracketed term due to its smallness, reducing the equation by the term  $H \tan(45^\circ - \varphi/2)$  and solving it with respect to  $H$  ( $H_v$  in the particular case), we find the height of a slope which is able to stand without any support:

$$H_v = \frac{4c}{q \tan(45^\circ - \varphi/2)} \quad (44.31)$$

**Evaluation of possible conditions under which washing of sands from the soil mass and creeping of the slope occur.** Such a need may arise when estimating conditions of a likely disturbance of the stability of a slope or hill side induced by a shear by rupture and subsidence (see Fig. 44.5c) and a flow slide (see Fig. 44.5f). Clearly, displacement of sand in a sand layer or on a slope is caused by liquefaction of sand or its saturation to such a degree as to enable a flow of subsurface water with a definite gradient ( $I$  of flow) to entrain it.

For this process to develop in the course of time the displaced sand mass that has lost stability should be carried away from the location of its deposition thus leaving room for new masses of sand.

If such a slope or hill side is located lower than the water table of a reservoir or stream the transport of such sand masses will be enhanced by wave disturbance and surface water currents. If the surface of a slope is free (i.e. dry) sand masses may be displaced only downslope.

Analysis of conditions of stability of upper layers of a sand mass in a slope acted on by seepage pressure (cf. Chap. 24) makes it possible to obtain this relationship:

$$k_{saf} = (1/2) \tan \varphi / \tan \alpha \quad (44.32)$$

Consequently, the critical angle of slope ( $k_{saf} = 1.0$ ) at which soil may slide downslope will be

$$\alpha = \varphi/2 \quad (44.33)$$

The angle of internal friction  $\varphi$  for sand materials is generally close to  $30^\circ$ . Consequently, if the rate of slope is  $\alpha > 15^\circ$  or its steepness is  $1/m =$

= 1/3.75, the movement of the sand washed out of the soil mass or liquefied on the surface of the slope is likely to occur.

It should be finally emphasized that stability computations call for adequate use of index characteristics, such as the angle of friction ( $\varphi_w$ ) and cohesion ( $c_w$ ).

#### Sec. 44.5. Prevention of Landslides

**Passive** measures of prevention of landslides generally consist in proper siting of structures.

The easiest, in principle, solution is to locate a road alignment or centre-line of a river crossing where a slide is not likely to occur. But, since this is not always feasible, construction often has to resort to **active preventive measures against sliding**.

Clearly for such measures to be efficient, in each particular case we must determine if the ground is troublesome at present or may become such in future. We must invariably establish the type of the slide. The classification of slides presented above may prove of service.

That **the slope is troublesome** can often be established from visual indications. These primarily include the character of the slope, presence of mounds and old slide scars (slide-induced cirques), tilted trees ("drunken forest") etc. That the ground is troublesome can often be revealed by deformations of structures and appearance of cracks.

If the degree of the stability of a slope is hard to establish from external symptoms, stability computations may be useful.

Preventive measures against sliding are numerous and diversified. The most important of these consist in drainage of soil masses prone to creep by constructing intercepting covered drains, sinks etc. Special care must be taken to lower the water table and high pore pressure. This may largely be achieved by levelling the surface of the slope to facilitate surface water run-off and reduce percolation of meteoric water. Shoreline protection measures, such as stone riprap, rockfill, dikes, to prevent slope underwashing may prove useful. Weak material likely to trigger a slide should be removed. If necessary, retaining walls can be constructed as a remedy against sliding. Transverse buttresses may be used for support, even if temporary, of buildings.

In such conditions it is essential to forbid removal of vegetation, limit construction, control the water regime.

The choice of the particular preventive measures is governed by the principal cause of the slide. So, if a debris slide has occurred it often suffices to clear the slope from loose rocks and rock blocks that are unstable. If more complicated conditions arise it may prove a particularly efficient

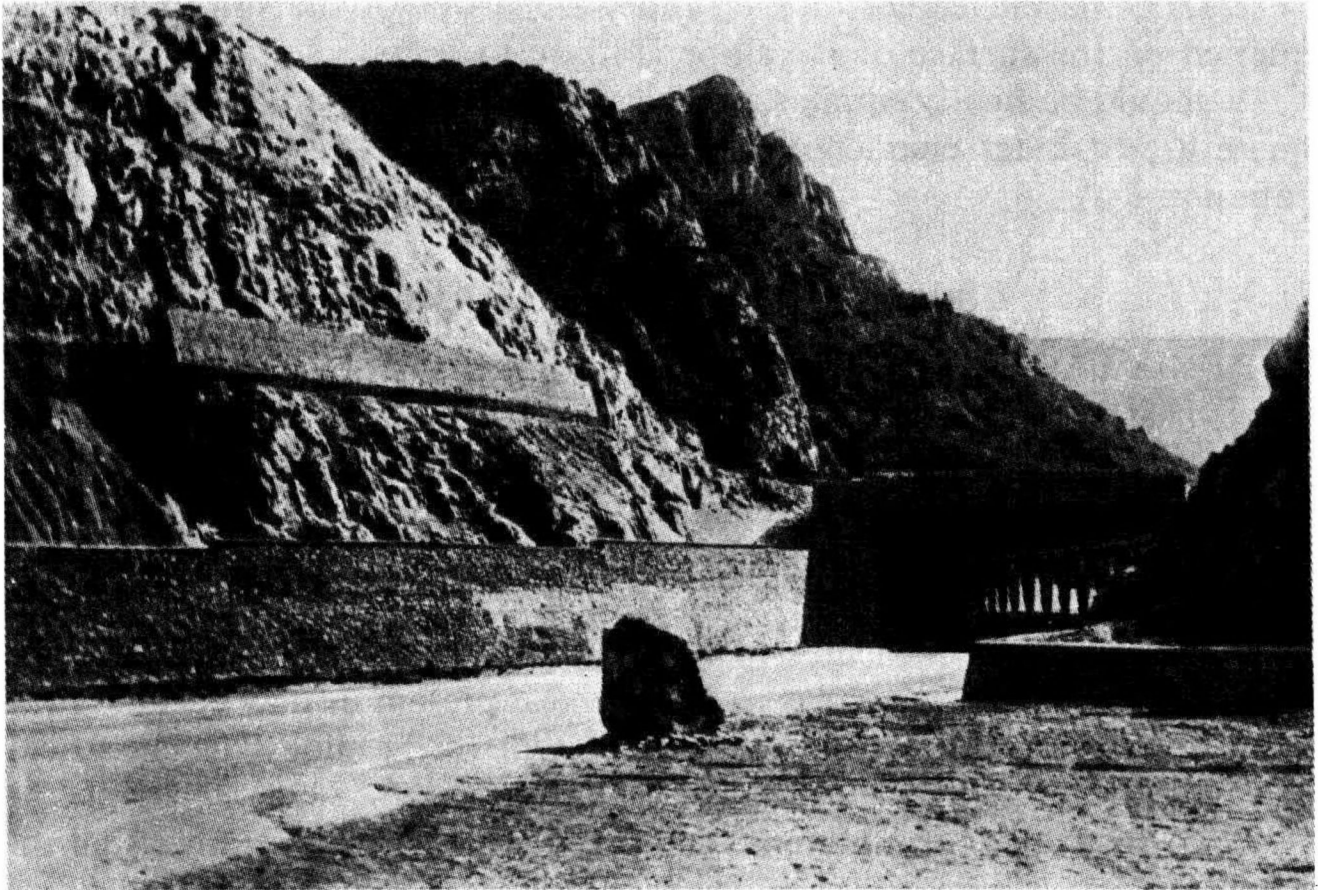


**Fig. 44.20.** Deflector walls and a gallery (right-hand side) for protecting a road from intrushes and rock falls

measure to construct retaining walls or use protective facing. Sometimes it is better to use metallic tie bars to prevent rock blocks from falling. In case of badly fissured rocks, apart from tie bars, metal nets may be used to stabilize the suspicious portions of slopes. It is invariably practicable to construct deflector walls (Fig. 44.20).

If the rocks on the slope are very much decayed, the best remedial measure against rock falls would be flattening out of the slope. This technique may also be employed if a rotational shear failure is likely to occur. Rock slides may be controlled by flattening out of the slope if the stability of the slope was mainly caused by the inadequate strength of the underlying soil strata.

If this type of slide is occasioned by the washing of sand material out of the underlying soil mass by seepage flow, slide control calls for good drainage, including transverse one, to divert the flow of subsurface water before it comes to the surface. Under similar conditions it is often convenient to provide stone drains and reciprocal filters where the groundwater is discharged to the surface of a slope composed of troublesome sand.

It is particularly difficult to control **sliding of stacks or even suites of**



**seams** if the creeping soil mass is of conspicuous thickness. On the other hand, if the soil mass losing stability is of minor thickness, thorough drainage is invariably useful. Under such conditions the sliding strata can best be anchored by concrete pillars set near the surface of sliding that are sufficiently strong to sustain the shearing forces active in this zone. If the creeping soil mass is of minor thickness, a retaining wall is generally better.

The best means of preventing slides is adequate drainage which will remove seepage pressure due to subsurface water flow. Such steps are particularly necessary when the stability of soil (usually uppermost soil) is disturbed by creep deformation, since the creeping soil mass is generally oversaturated. By somewhat reducing their water content it is possible to increase the viscosity of the creeping clayey soil thus lowering, at least, the velocity of earth movement. It should be borne in mind, that a retaining wall should be sufficiently strong and should rest on sound material, i.e. its foundation should be located below the surface of sliding. Otherwise the retaining wall may be displaced jointly with the soil under the slope.

When designing and constructing a retaining wall we must take into account a possibility that oversaturated soil may fail to impart pressure of the slide to the wall. If a retaining structure is supported by bedrock, the creeping soil will flow around or above it (Fig. 44.21). Such phenomena sometimes occur at the Sochi-Sukhumi section of the Black Sea coast highway.



**Fig. 44.21.** Tongue of creeping soil encroaches on a retaining wall (photograph by M.G. Demchishin)



**Fig. 44.22.** Structure for protecting a slope from creep deformation (photograph by L.K. Ginzburg)

As a retaining wall is being constructed on a clayey soil we should consider a likely deterioration of its material in the course of time and a possible slow deformation due to creep properties of such soils.

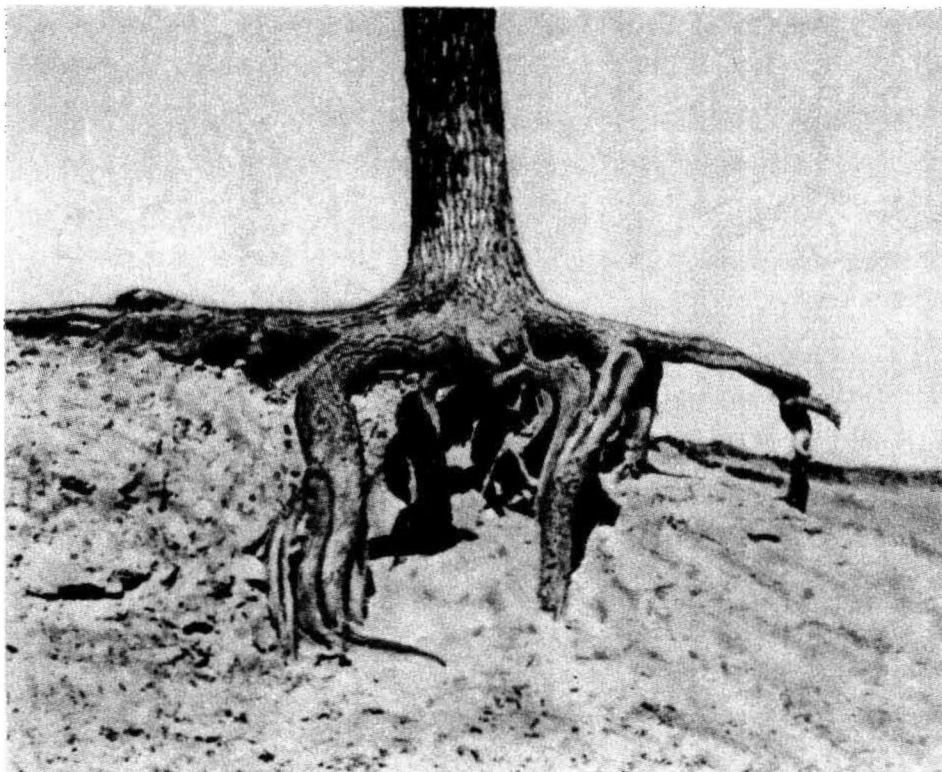


**Fig. 44.23.** Root system helps stabilize troublesome slope

Protective measures against *flow slides* of generally cohesionless soil masses below a natural slope consist mainly in drainage of the flow of subsurface waters or groundwater before it is discharged at the surface of the slope. Coarse material drainage filters operating as an inverted filter are especially useful under such conditions. The dynamic stability of a submerged sand slope is achieved by compaction of the sand or placing stone riprap.

Large diameter reinforced concrete piles (ground anchors) have been particularly popular in the last few years for stabilization of troublesome slopes. For better rigidity these anchors are interconnected by reinforced concrete plates and a network of tie bars (Fig. 44.22).

Removal of trees and shrubs from slopes will cause detrimental results. As is known, vegetation root systems are good stabilizers of troublesome ground (Fig. 44.23), so it would be unreasonable to destroy them, especially if we want to reduce the risk of a slide.

---

## Chapter 45

### Rheological Phenomena and Their Role in Creep Events

---

#### Sec. 45.1. Conditions of Occurrence

The importance of rheological phenomena is governed by the particular natural conditions. It is common occurrence that the stability of a slope or hill side is disturbed without any visible change in the loads acting on the soil mass beneath a slope or in the factors responsible for the shearing resistance of materials composing the slope.

Such events are often ascribed to rheological processes responsible for continuous and slow (at velocities of a few cm or mm in a year) deformations of slopes and hill sides (*creep*). As to the reduction in the strength of clayey soils, it is generally associated with their continuous deformation (*long-term stability*). The slide itself commonly represents a vigorous termination of a process that has been in progress for a long period of time. This is, in particular, evidenced by tension fissures and slope shear cracks often found some distance from the crest of the slope that appear long before a slide occurs. A number of examples may be found, in, say, slides in Odessa that occur every eight years on the average, or in a major slide of 1956 in Macedonia that involved 20 million m<sup>3</sup> of material and had been in preparation during a few decades. Reference may also be made to numerous landslides in England reported by A.W. Skempton.

Very interesting findings have been presented by K. Peterson. He reports on a number of failures of clay slopes of earth works that demonstrated the initial values of the factor of safety 1.5-1.7 and occurred half a year and four years after completion.

A slide may abruptly occur on a slope that seemed to be stable for quite a long period of time. The deterioration of soil in the course of time may result in any form of earth displacement (rotational shear failure, slope failure by rupture etc.). This phenomenon is to an extent associated with clayey soil characterized by bonds of cohesion  $c_s$ .

The deformations being considered partially affect the development of creep events on slope walls induced by a slow yet continuous departure of a creeping soil mass along a slide-flattened surface of the slope from the creeping bench which is in a state of excess stress (slides on the Black Sea shore of the Caucasus, in the vicinity of Odessa etc.).

## Sec. 45.2. The Evaluation of Long-Term Stability of a Slope or Hill Side

Conditions of the long-term stability of a slope are estimated in conformity with the principal criteria of creep (cf. Chap. 31) used for solving an identical problem when designing a retaining wall.

It will be recalled that in the particular case stability computations use relationships suggested for the evaluation of the total stability of one structure or another. In so doing, they rely on parameters of the bearing capacity of clayey soils ( $c_w$ ,  $\Sigma_w$ ,  $c_s$  and  $\varphi_w$ ) in various combinations. The values of the factor of safety  $k_{c_w}$ ,  $k_{\Sigma_w}$ ,  $k_{c_s}$  and  $k_\varphi$  are then determined and analysed.

For an illustration, let us follow the course of this analysis as applied to the most common form of slide, the rotational shear failure. The evaluation of the stability of the slope or hill side employs in this case a formula proposed by Karl von Terzaghi:

$$k_{saf} = \frac{\Sigma(P_i \cos \alpha_i \tan \varphi_i + c_i l_i)}{\Sigma P_i \sin \alpha_i} \quad (45.1)$$

On expansion, the formula of the total cohesion appears as  $c_i = c_w = \Sigma_w + c_s$ . Then the above relationship takes on the following form:

$$k_{saf \ c_w} = \frac{\Sigma[P_i \cos \alpha_i \tan \varphi_i + (\Sigma_w + c_s)l_i]}{\Sigma P_i \sin \alpha_i} \quad (45.2)$$

The method of procedure of computations is as usual, including the value of the total cohesion  $c_w$  and determination of the factor of safety  $k_{c_w}$ .

If  $k_{c_w} < 1$ , the object in hand is invariably insufficiently stable and requires remedial measures. If  $k_{c_w} > 1$ , additional analysis is needed to determine the long-term stability and deformation of the slope or hill side.

If calculations of  $\Sigma_w$  are omitted, then for  $k_{cs} > 1$  the long-term stability is fully ensured and no deformation is likely to occur. On the other hand, if  $k_{\varphi_w} < 1$  and  $k_{\Sigma_w} > 1$ , that is, under conditions of mobilization of  $\Sigma_w$ , the object may be prone to a creep deformation in the course of which rigid bonds of cohesion may be ruptured ( $c_s = 0$ ). In this case the long-term stability of the slope (hill side) is ensured on the condition that  $k_{\beta\Sigma_w} < 1$  and concurrently  $k_{\Sigma_w} > 1$ , yet the object will be subject to deformation. Finally, if  $k_{\varphi_w} > 1$ , the long-term stability of the slope or hill side is ensured unaccompanied by any creep-induced deformation.

### Sec. 45.3. Prediction of the Intensity of Creep Deformation of a Sliding Slope

The problem has not as yet been completely understood. Let us therefore consider the simplest slide type, a translational slide slippage of soil along a uniform plane surface of sliding.

Let us first analyse a creep deformation of a stack of bedrock strata of conspicuous thickness ( $H$ ) underlain by a weak layer of clayey soil,  $d$  in thickness (Fig. 45.1).

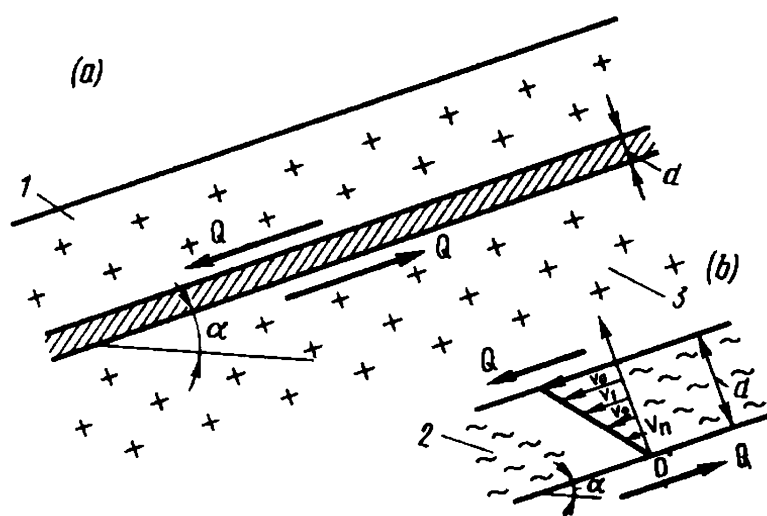
A rough idea of the intensity of crustal movement in the course of time, i.e. the velocity of displacement  $v_0$  in a subcritical state may be inferred by proceeding from the familiar equations proposed by Newton and Bingham-Schwedoff. Clearly, the velocities of displacement will be different at different horizons within the sublayer which is  $d$  in thickness. At the foot of the sublayer the velocity will be zero ( $v_d = 0$ ), and at the top maximum ( $v_0 = \max$ ) and responsible for the intensity of the crustal soil creep.

In conformity with Newton's law (yield point  $\tau_{lim} = 0$ ) we have

$$v_0 = \frac{\tau}{\eta} d \quad (45.3)$$

**Fig. 45.1.** Diagram for computations of the velocity of creep deformation,  $v_i$ , of the topsoil layers (1) along a slip surface provided by a relatively thin seam (2) of clayey soil,  $d$  in thickness:

$a$ —mode of occurrence of clay seam;  
 $b$ —detail of event; 1—immovable layer



in which rheological equation  $\eta$  is viscosity of soil, in the particular case, in the sublayer.

The value of the tangential stress  $\tau$  is found through the angle of dip of the sublayer  $\alpha$  and the weight of the overburden  $H$ :

$$\tau = \varrho_w H \sin \alpha \quad (45.4)$$

Hence

$$v_0 = 1/\eta \varrho_w H \sin \alpha d \quad (45.5)$$

Clearly, if  $\tau_{lim} = p \tan \varphi_w + c_s = 0$ , that is, if  $\varphi_w \rightarrow 0$  and  $c_s = 0$ , the topsoil layers will creep at minimum angles of dip  $\alpha$  at a velocity conditioned by the viscosity of soil in the sublayer (factor  $\eta$ ).

Things are different if  $\tau_{lim} \neq 0$ . Then, in conformity with the relationship proposed by Bingham-Schwedoff (cf. Chap. 31) the velocity of creep at the horizon  $y$  will be equal to

$$dv_y = \frac{\tau - \tau_{lim}}{\eta} dy$$

or

$$dv_y = \frac{\tau - (p \tan \varphi_w + c_s)}{\eta} dy \quad (45.6)$$

In this equation  $p$  is the normal stress induced by the weight of the overburden

$$p = \varrho_w H \cos \alpha \quad (45.7)$$

and  $\tau$  is the tangential (shear) stress found from Eq. (45.4).

In order to determine  $v_0$  let us substitute the values of  $p$  and  $\tau$  from the above relations into Eq. (45.6)

$$dv_y = \frac{\varrho_w}{\eta} H [\sin \alpha - (\cos \alpha \tan \varphi_w + c_s/\varrho_w H)] dy \quad (45.8)$$

Having integrated this equation and found the value of the constant  $C = 0$  following from the condition that at  $y = 0$  the velocity of the creep  $v_y = 0$ , we obtain

$$v_y = \frac{\varrho_w}{\eta} H \left[ \sin \alpha - \left( \cos \alpha \tan \varphi_w + \frac{c_s}{\varrho_w H} \right) \right] y \quad (45.9)$$

As to the surface of the creeping soil mass, at  $y = d$  the velocity is equal to

$$v_0 = \frac{\varrho_w}{\eta} H [\sin \alpha - (\cos \alpha \tan \varphi_w + c/\varrho_w H)] d \quad (45.10)$$



**Fig. 45.2.** Disturbed structure of soft plastic clay seam 12 cm in thickness during a creep deformation. Devonian soil mass composed of sand and clay materials

As a result of the deformation of the sublayer the true cohesion is generally disturbed in the zone of sliding determining the value of  $d$ . Figure 45.2 represents, in particular, the disturbed structure. In this case, for  $c_s = 0$ , Eq. (45.10) will take on this form

$$v_0 = \frac{q_w}{\eta} H (\sin \alpha - \cos \alpha \tan \varphi_w) d \quad (45.11)$$

Clearly, the critical value of the angle of dip of the sublayer,  $\alpha$ , at which creep may be expected, will be found from the relationship:

$$\sin \alpha_{cr} = \cos \alpha_{cr} \tan \varphi_w \quad (45.12)$$

i.e.

$$\alpha_{cr} = \varphi_w \quad (45.13)$$

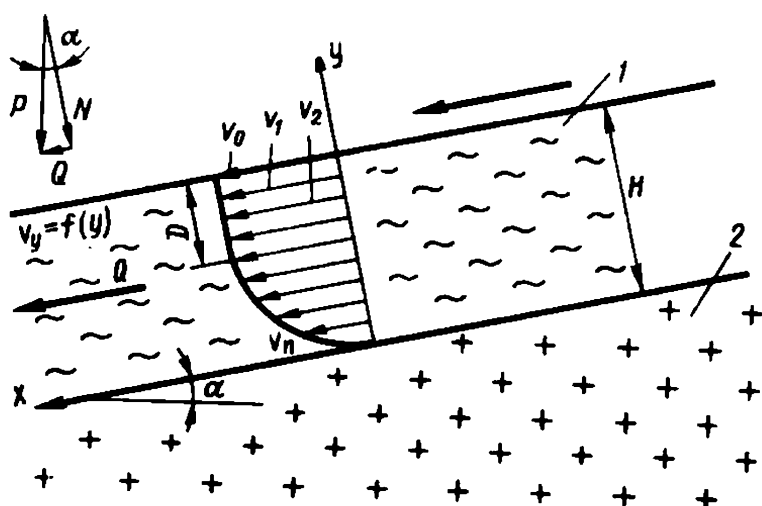


Fig. 45.3. Diagram for determining the velocity of creep of moving soil mass downslope:

1—sliding talus material; 2—bedrocks in undisturbed occurrence conditions

The events we have considered are mainly characteristic of slopes prone to sliding.

It will be recalled that for pseudoplastic clays the angle  $\varphi_w$  may be fairly small. This may cause a creeping deformation of a soil mass even if the soil layers are only mildly inclined. The mechanism of a topsoil creep is somewhat different.

The approximate velocity of downslope movement of oversaturated sliding layers may be determined by using a diagram in Fig. 45.3.

For a more general case, by taking into account the initial shearing resistance of soil or the yield point, in conformity with the equation of Bingham-Schwedoff (cf. Chap. 31) we have

$$dv_y = \frac{\tau_y - \tau_{lim}}{\eta} dy \quad (45.14)$$

We can find the weight  $P$  of an individual block of soil  $H$  for a horizon  $y$  with a cross sectional area  $\omega$  by using the relationship:

$$P = \rho_w(H - y) \omega$$

The normal,  $N$ , and tangential,  $Q$ , constituents of the weight of the block,  $P$ , for a slope whose angle of dip is  $\alpha$  are, respectively, equal to

$$N = \rho_w(H - y) \omega \cos \alpha$$

$$Q = \rho_w(H - y) \omega \sin \alpha$$

Thence the normal,  $p_y$ , and tangential (shearing),  $\tau_y$ , stresses are

$$\tau_y = \rho_w(H - y) \sin \alpha \quad (45.15)$$

$$p_y = \rho_w(H - y) \cos \alpha \quad (45.16)$$

A substitution of these values of  $\tau_y$  and  $p_y$  into the principal differential



equation (45.14) yields

$$dv_y = \frac{q_w}{\eta} \{ (H - y) \sin \alpha - [(H - y) \cos \alpha \tan \varphi_w + c_s] \} dy \quad (45.17)$$

An integration of the above equation yields the value of  $v_y = f(y)$ , given the constant of integration is  $C = 0$ , following from the condition that for  $y = 0$  and  $v_y = 0$ :

$$v_y = \frac{q_w}{\eta} \left( Hy - \frac{y^2}{2} \right) \left[ (\sin \alpha - \cos \alpha \tan \varphi_w) \right] - \frac{c_s}{\eta} y \quad (45.18)$$

The velocity of the plastic flow at the surface  $v_0$  will be found from Eq. (45.18) which for  $y = H$  and  $c_s \neq 0$  takes on this form:

$$v_0 = \frac{q_w}{\eta} \left[ H(H - D) - \frac{(H - D)^2}{2} \right] (\sin \alpha - \cos \alpha \tan \varphi_w) - \frac{c_s}{\eta} (H - D) \quad (45.19)$$

In the latter equation  $D$  is the thickness of the dead zone adjacent to the surface where, as the soil preserves the initial shearing strength, the velocity remains constant, i.e.  $v_D = \text{const.}$

The thickness of the dead zone is determined following from the condition that at a depth  $D$  the shearing stress  $\tau$  in Eq. (45.15) for  $D = H - y$  will be equal to the yield point  $\tau_{lim} = p_D \tan \varphi_w + c_s$ , where  $p_D$  is found by referring to Eq. (45.16). Then

$$D = \frac{1}{q_w} \frac{c_s}{\sin \alpha - \cos \alpha \tan \varphi_w} \quad (45.20)$$

In a particular case, when  $c_s = 0$ , Eq. (45.19) takes on a simpler form:

$$v_0 = \frac{q_w}{2\eta} H^2 (\sin \alpha - \cos \alpha \tan \varphi_w) \quad (45.21)$$

It can thus be seen that important role for the mode of occurrence of a likely slide of a conspicuous slope is played by its thickness. Clearly, for  $c_s = 0$  the critical angle of slope, given  $v_0 = 0$ , will be found from the relation

$$\alpha_{cr} = \varphi_w \quad (45.22)$$

For  $\varphi_w = 0$  and  $c_s = 0$  the yield point is  $\tau_{lim} = 0$ , and the problem is solved in conformity with Newton's law, Eq. (31.15), given the coefficient of viscosity  $\eta$  is constant in the period of time  $t$ :

$$dv = \frac{\tau}{\eta} dy$$

The solution of the above equation employs Eq. (45.18) into which the

values of  $\varphi_w = 0$  and  $c_s = 0$  are substituted. As a result we have

$$v_y = \frac{Q_w}{\eta} [Hy - y^2/2] \sin \alpha \quad (45.23)$$

The velocity of displacement,  $v_0$ , at the surface of the soil mass in the latter case will be

$$v_0 = \frac{Q_w}{2\eta} H^2 \sin \alpha \quad (45.24)$$

The coefficient of viscosity  $\eta$ , largely responsible for the rate of creep, is to a certain extent governed by the consistency of the material.

The values of  $\eta$  are generally in the range  $a(10^{10}$  to  $10^{13})$  P (poise) or  $a(10^4$  to  $10^7)$  kg  $\times$  s/cm<sup>2</sup>. It would be of interest to note that  $\eta = a \times 10^{10}$  P corresponds to the viscosity of melted glass or pitch at +9 °C.

It should be noted in conclusion that the deformation of the crustal soil layers governed by the velocities of creep ( $v_0$ ) may occur both under conditions of overall stability of the entire crustal soil mass or, alternatively, under conditions that cause crustal soil layers to slide at the contact with the roof of bedrocks.

## Chapter 46

### Seismic Events

#### Sec. 46.1. General Characteristics

Tectonic processes are still going on. The most dramatic examples of modern tectonics are seismic events or earthquakes. These occur at an annual rate of up to 10 thousands.

A number of major earthquakes have been recorded that resulted in massive losses of human lives and destruction of thousands of buildings and structures. So, the Calcutta earthquake of 1737 destroyed 300 000 lives. Portugal, Spain and northern Morocco were subjected to three strong shocks in the forenoon of November 1, 1775. The Lisbon earthquake of 1775 literally devastated Lisbon, the loss of life was heavy. The disaster was the more detrimental since the first shock was followed by a colossal whirling wall of water sweeping everybody and everything it met on its path. The major Skopje, Yugoslavia, earthquake is in the memory of every one (Fig. 46.1).

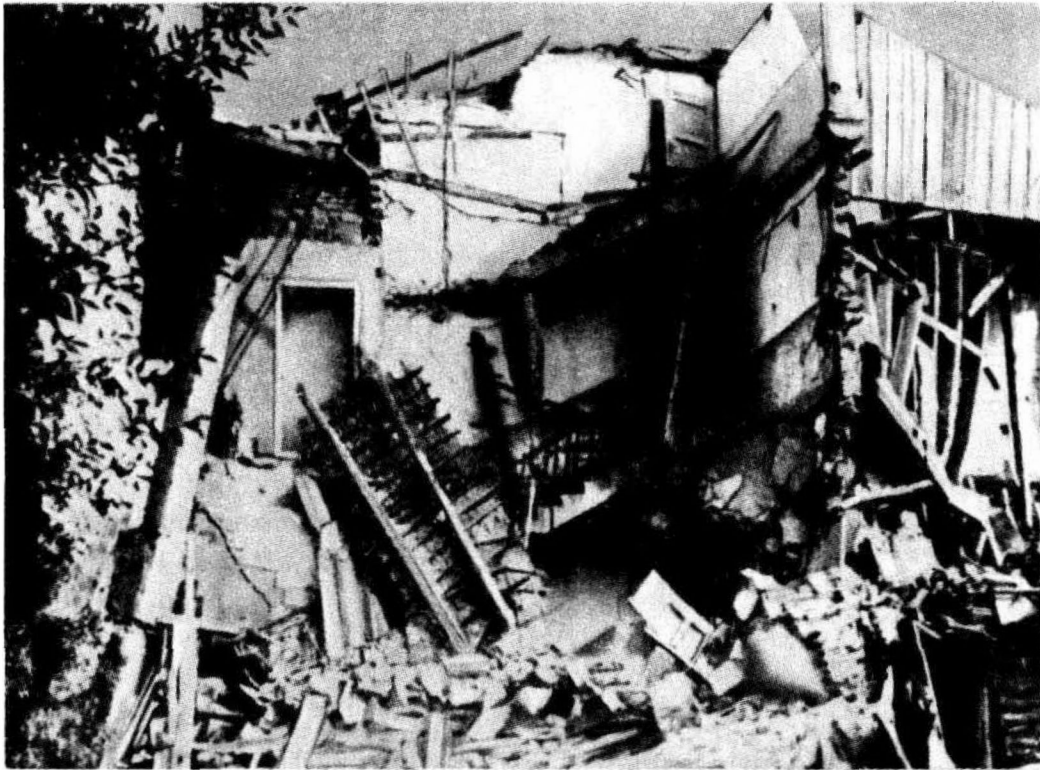


**Fig. 46.1.** Damaged buildings in the Skopje earthquake of 1963

The earthquake that literally devastated Tokyo and Yokohama on September 1, 1923, laid a heavy toll on human lives and property. 11 000 buildings were ruined and 59 000 houses burned in Yokohama as a result of the earthquake-induced fires. Throughout the area affected in Tokyo, the death toll was 100 000, while 43 000 remained missing. Over 300 000 houses were damaged. 45% of brick buildings collapsed, 10% of reinforced concrete, during that event. The 1950 Himalayas earthquake, one of the severest seismic events, recorded instrumentally, was equivalent to an energy released by explosions of 100 000 A-bombs.

An extremely severe earthquake took place on December 4, 1956 in the Mongolian People's Republic and the adjacent regions of the USSR and China and brought about vast devastations. A mountain peak was split in two. Part of a mountain, 400 m in height, collapsed and fell down a precipice. A depression, up to 18 km in length and 800 m in width, originated. Broad fissures, up to 20 m in width appeared on the ground surface. One of these broke for a length of 250 km. The intensity of the earthquake approached force 11.

The American scientists consider the 1964 Alaskan earthquake, the intensity of which was over 11, as being the most severe of all known seismic events in the world's history. However, the most violent earthquake of the present century took place in 1960, Chile. It affected an area of over 200 000 km<sup>2</sup> and caused numerous landslides.

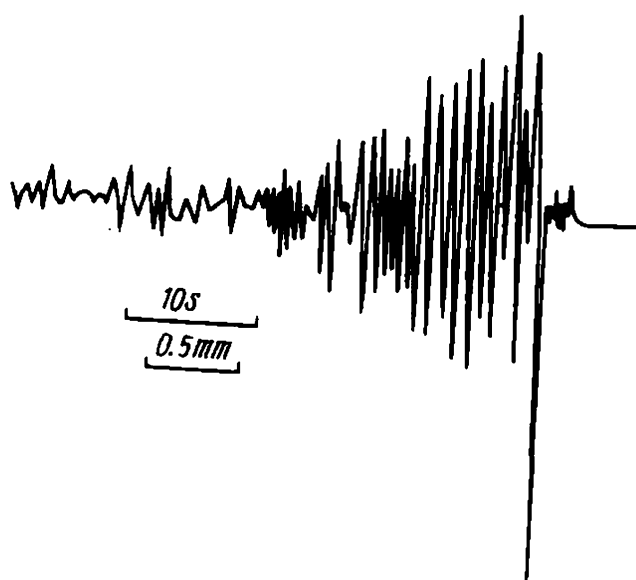


**Fig. 46.2.** Seismogram of a force 6 earthquake that affected the town of Kulyab, Tajikistan, in 1952

During the last decades several large-scale earthquakes have been recorded in this country: the Yalta earthquake of 1927; the Ashkhabad earthquake of 1948; the 1966-1967 Tashkent earthquakes and the 1976 Gazli, Uzbekistan, earthquake.

Most earth tremours are very hard to detect and can only be recorded by sensitive instruments, seismographs. Yet as many as a hundred earthquakes per annum are destructive and one catastrophic. This suggests that destructive earthquakes are violent movements of the earth crust after a period of accumulation of stress.

It may be assumed that earthquakes are caused by major and sudden discontinuities of the crust, ruptures and faults as well as displacements of the crust. They are associated with the physicochemical processes that are at work in the earth's bowels and with changes in the thermodynamic conditions in the inner reaches of the earth.

The pattern of ground surface vibrations during an earthquake can be inferred from Fig. 46.2 which presents an accelerogram of vibrational translations (or displacements) as recorded by a seismograph at a recording station.

The seismic impulse and vibrational movement caused by it often last only a few seconds. However, during a major (or strong-motion) event even this short-lived shock generally brings about catastrophic consequences. Seismic events are known that demonstrated continuous vibrations, as in the Alma-Ata earthquake of 1910 which lasted for 5 minutes. Earthquakes lasting 10-15 s or more occur the most commonly.

An examination of accelerograms shows that the seismic vibrations attain the greatest amplitude only after a weaker vibration has occurred. Dif-

ferently speaking, practically any earthquake has an initial stage. This stage is heralded by weaker seismic waves called *precursor waves*.

Seismic waves of an earthquake originate at a place in the earth crust some distance from the surface called the focus or hypocenter.

The foci of earthquakes have generally been found at depths not exceeding 20-50 km. However, we know of seismic events whose foci were located 500-600 km below the earth surface. This is convincing proof of that tectonic processes take place in the deep inner reaches of the earth\*.

The sites of the most frequent and intensive earthquakes are regions of folded mountains of recent origin. Thus seismic events are closely linked to tectonic processes, and, particularly, to modern folded mountain-building. This is the reason why the severest earthquakes in this country take place in mountainous areas of young origin, such as Transcaucasia, mountainous regions of Turkmenistan (Ashkhabad), the Crimea, Baikal region, the Far East, Kamchatka, the Kurile Isles. Rather severe (up to intensity 9) earthquakes typically occur in mountainous regions of Middle Asia.

It should be made clear that the zones of strong-motion earthquakes almost invariably coincide with zones of faults or folds of tectonic origin. In particular, the well-known severe earthquake in Transcaucasia and in the vicinity of the town of Shemakha, Azerbaijan, have taken place in the fracture zones of the Caucasian mountain range. The Crimean earthquakes are associated with tectonic disturbances at the floor of the Black Sea, about 80 km offshore from the Black Sea coast line where there is an underwater step or marginal slope and a dramatic increase in depths. Similar conditions obtained during the Alaskan earthquake of 1964 we have already reported above.

Lowland regions representing less suspicious areas of the earth crust (*continental platforms*) demonstrate inappreciable seismicity. These include the European regions of the USSR and Siberian Lowland. However, even in these areas minor seismic events do take place echoing severe earthquakes occurring in mountainous regions. So, severe Carpathian earthquakes (1940) caused minor seismic vibrations in Kiev, Kharkov, Voronezh and even Moscow. A small-scale earthquake was recorded in Moscow in 1802 and another one quite recently, in 1976. The same year saw the severest earthquakes, notably, the Guatemala earthquake that destroyed 23 000 lives and ruined 200 000 houses, the earthquakes in Northern Italy and China.

Destructive earthquakes are often occasioned by single shocks. Sometimes seismic impulses may come as successive shocks occurring during

---

\* Natural earthquakes may be classified as tectonic, plutonic or volcanic, depending on their origin (cf. D.P. Krynine and W.R. Judd, op. cit., p. 674)—*Translator's note*.

several months (the Crimean earthquake of 1927). A typical example can be found in the 1966 Tashkent earthquake that lasted during a year almost uninterrupted. In such cases we can refer to a seismic period of a particular region.

Some regions witness destructive earthquakes spaced at large (200 years or more) periods of time, whereas others experience them at relatively short intervals, as Petropavlovsk in Kamchatka. Severe earthquakes have regularly occurred in Shemakha during the last 300 years. Some 100 events have been recorded in this town in this period. This fact caused offices located in Shemakha to be moved to Baku, a town less subject to seismic hazard.

An earthquake is generally accompanied by subterranean roar, deafening thunder and involves fractures and crustal displacements. These events often cause depressions in one area and crustal upheavals in another one. For example, during the 1892 earthquake a substantial portion of Port Royal, Jamaica, went thundering down to the sea. During the Lisbon earthquake of 1755 there was a conspicuous land uplifting which appreciably altered topography of Portugal. The 1862 earthquake caused the littoral part of Baikal Lake's shore to be submerged resulting in the appearance of a gulf called Proval (Russian for depression). Alaskan earthquake of 1899 raised the continental shelf 10-15 m thus forming vast areas of land. At other places land sank and the sea flooded the littoral strip. A similar phenomenon occurred during the 1811 earthquake that affected the upper reaches of the Mississippi River. A sudden sinking of a vast tract of forested land formed a large lake there.

The downwarping of land may attain sometimes as much as several hundred metres. The sinking of the sea floor has repeatedly ruptured submarine telegraph cables. The downwarpings of the ocean floor caused by earthquakes have sometimes caused entire islands to be engulfed. The vertical displacement of the sea floor during the 1923 earthquake in Japan was a few hundred metres.

The actual location of the Phoenician city Tyros well known in antiquity was lost during the previous millennia. Aerial photographs have recently discovered the ruins of this city lying on the sea floor of the Mediterranean in the proximity to the coast of Asia Minor. Undoubtedly, the submergence of Tyros was occasioned by a catastrophic sinking of the land.

Major fractures, faults and displacements caused by an earthquake are characterised by dramatic relative deformations and shifts of the adjacent regions. Seismic faults often break for several kilometres. So, the 1891 earthquake in Japan caused fissures and crustal displacements over 100 km in extent, and formed ledges that attained 20 m in width.

Lateral displacements of individual ground surface areas are common in an earthquake. This phenomenon, in particular, was caused by the major

Californian earthquake of 1900 where the fault and shear zone broke for 500 km. The ledges that formed were not more than 6 m height. Similar events have been reported there also in the recent time.

If the epicenter of a seismic event is located on the floor of a sea or an ocean, a *submarine earthquake* occurs which produces tidal waves up to several tens of metres in height\*. These seismic waves called *tsunami* propagate from the site of their origination at velocities up to hundreds of or more than 1 000 km/h.

Tsunami waves or tsunamis are caused by sudden risings and sinkings of substantial areas of the world ocean. The tsunami wave that occurred in 1946 in Hawaii and brought about devastating results took place a few hours after the Alaskan earthquake 3 800 km north of Hawaii resulting in an abrupt rising of the sea floor.

Tsunami waves travelling many thousands of miles from the site of origination may attain tremendous heights. For example, Japan's earthquake of 1896 gave rise to waves 30 m high that attacked the coast destroying 27 000 lives and washing away more than 10 500 buildings.

Tsunami waves that attacked Kamchatka's coast in the middle 18th century and were first reported by the Russian scientist S.P. Krashenninikov attained 70 m in height. Such waves cause large-scale devastations on the sea shore.

The results of seismic events may assume diversified forms. Earthquake-induced landslides and rock falls often affect vast areas (Fig. 46.3). Mountainous rivers are then dammed by the displaced soil masses and spalled material, deep lakes are formed presenting hazard to large territories. The falling debris and soil may bury whole settlements.

The Chile earthquake of 1960 caused major deformations of relief covering an area of 200 000 km<sup>2</sup>. The Alpine regions of the country were displaced 300 m for a length of over 40 km. The San Francisco earthquake of 1906 caused a downslope sliding of moist pastures by 800 m.

The 1964 slight earthquake occasioned ground motion of some 25 million m<sup>3</sup> of material, mostly sandstone, in the Zeravshan River valley, Tajikistan, which dammed the natural channel. The natural dam was 120 m in height. A most likely rupture of the dam meant catastrophic consequences for the cities Pejikent and, in part, Samarkand. Urgent measures were taken to safely drain the large and deep reservoir formed by the dam.

Roads, especially in mountainous regions, as well as ones passing on hillside sections covered by talus deposits demonstrating only minor stabil-

---

\* In fact, seismic sea waves are generally only 1 m in height and are spaced at large intervals. However, as they approach the coast, the friction of the sea floor reduces the intervals and increases the height of the waves to 25 m or more.



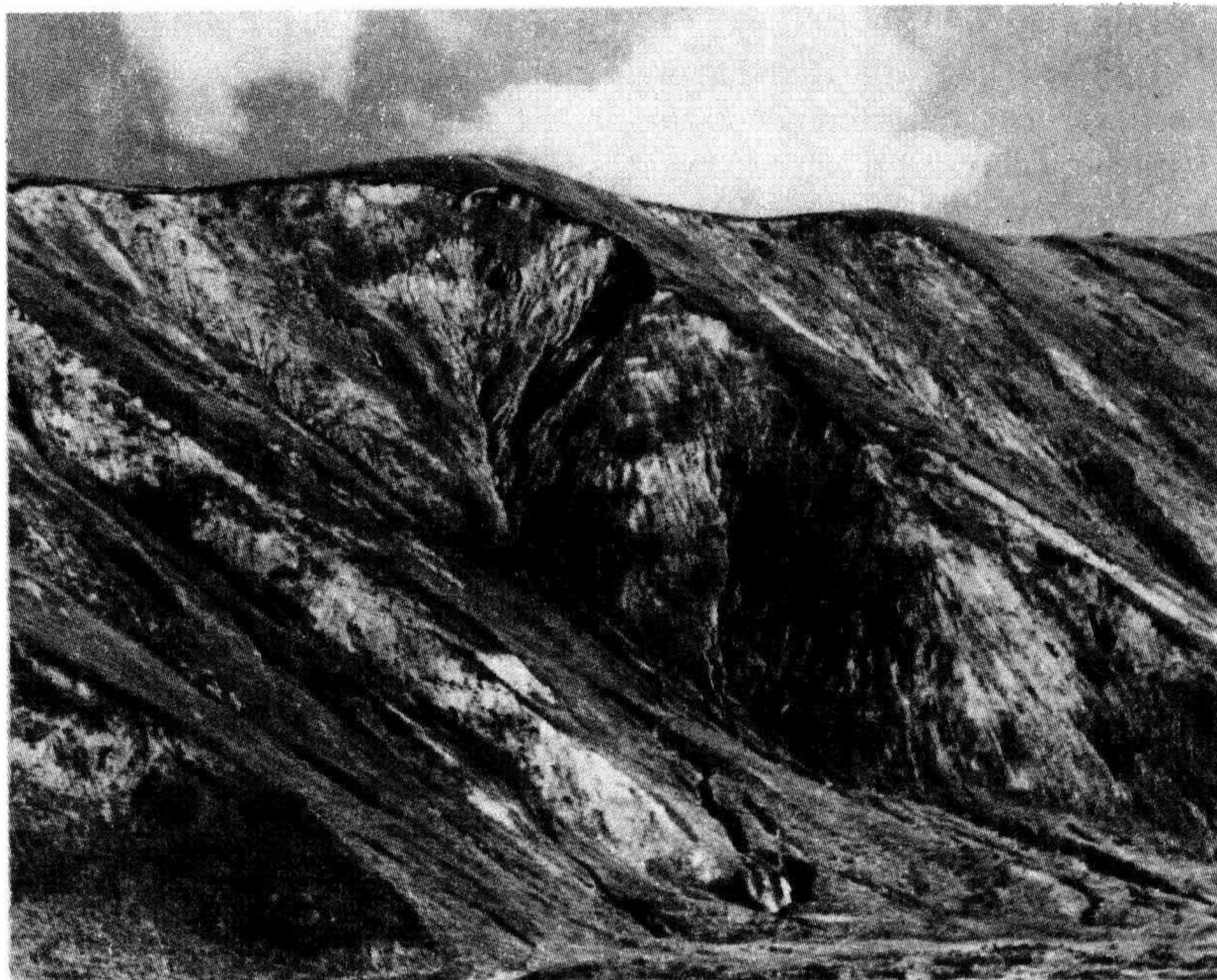


**Fig. 46.3.** Landslide in the Yasman River valley induced by the Khant earthquake of 1949  
(photograph by V. Presnukhin)

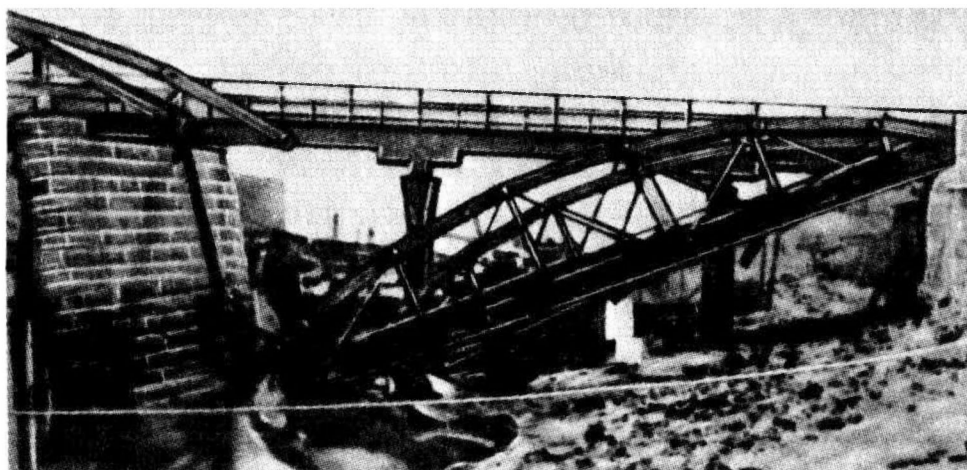


**Fig. 46.4.** Failure of a bridge on sand caused by an earthquake followed by settlement and tilting of a bridge abutment (Japan, 1923)



ity, are especially vulnerable to earthquake-induced landslide damage. On the other hand, even intermediate-intensity earthquake have repeatedly disturbed the stability of bridges and approach embankments resting on talus deposits. Such events were particularly numerous during the 1923 earthquake in Japan. Embankments were generally damaged due to subsidence by 2 m and more, cracks, ruptures and slides of slopes. The disturbed stability and deformation of piers and abutments was the principal cause of damages and often total failures of bridges. Bridge piers and abutments sometimes settled 1 m and more. Bridge abutments in all cases reported were tilted and displaced by several decimetres. This occurred even if the abutment and pier foundations were underpinned by piles. Such events were undoubtedly induced by the liquefaction of saturated sands in the foundations of structures due to the dynamic action (Fig. 46.4).

### **Sec. 46.2. Construction Conditions in Seismic Areas**

In the face of such an awesome phenomenon as an earthquake humanity was helpless even in a not very distant past.

As towns, communications, port and other facilities developed, an urgent need arose to work out measures to be able to decrease, even if in minor ways, the likely seismic effect on engineering structures.

As has already been reported, the 1923 earthquake practically devastated Tokyo. However, several buildings built to special aseismic design remained intact. This was convincing proof of a possibility to deal with the aftereffects of seismic events at relatively low costs and of the correct pathway to take into account seismic forces when designing one type of structure or another. The problems of aseismic design of buildings were the keynote of studies that followed.

Construction in seismic areas in the USSR is in conformity with the SNiP Building Code II-A.12-69\* (part II, Design Standards, 1977). This manual contains recommendations for aseismic design of apartment houses, public and industrial buildings and structures. It presents principal methods for determining seismic loads and for calculations of their effects.

Some recommendations are especially important. For example, it is proposed that in seismic regions the centre lines of roads be located some distance from precipices, sections subject to rock falls and talus slides, or marshy areas. It points to the specific features of designing a road on a hill side, warns against unrestricted use of arch-type bridges, suggests that bridge abutments be supported by bedrocks etc. All these recommendations take into account the seismicity of the particular regions gauged in intensity numbers characterizing the expected seismicity.

During an earthquake the structure may be damaged or even destroyed

due to the following principal causes: disturbance of the stability of its foundation; direct action of seismic inertia forces on the structure; possible origination of resonance in tower-type structures if the forced vibrations of the structure agree with those of the seismic wave.

The stability of the foundations under conditions being considered may be disturbed by seismic action on structures supported by a mass of *saturated sand*.

What makes the aforementioned Building Code specific is that it gives recommendations for determining, wherever necessary, the magnitudes of inertia seismic forces  $S_{ik}$  which may affect structures.

According to Sec. 2.4. (Eq. 1) of the SNiP Building Code,

$$S_{ik} = Q_k K_c \beta_i \eta_{ik}$$

where  $\beta_i$  and  $\eta_{ik}$  are quantities allowing for dynamic properties of a structure being designed that have no direct bearing on the subject of the present book.

The action of the force  $S_{ik}$  is assumed to be static, and further computations are performed in conformity with rules of statics. To simplify matters, the above quantities are taken to be equal to unity, which yields the value of the inertia force  $S_{ik}$ , the latter, being a horizontal component, in calculations must be applied to the centre of the mass of the considered element  $Q_k$  in weight:

$$S_{ik} = \pm K_c Q_k \quad (46.1)$$

The plus or minus sign in the above relation suggests a possibility of the different orientation of the force of inertia (backward—forward; upward—downward) according to the direction of the wave motion or its constituents. As in other similar cases, the value of the seismic inertia force is expressed in terms of the weight of the body  $M$  and its acceleration  $\alpha_c$ :

$$S_{ik} = \alpha_c M \quad (46.2)$$

As is known, the weight of a body is

$$Q_k = Mg \quad (46.3)$$

where  $g$  is acceleration due to gravity ( $g = 9\,810 \text{ mm/s}^2$ ). Hence the weight of the body is

$$M = (1/g) Q_k \quad (46.4)$$

and

$$S_{ik} = \frac{\alpha_c}{g} Q_k \quad (46.5)$$

Let us introduce a new index characteristic,  $K_c$ , which is the seismicity coefficient,

$$K_c = \frac{\alpha_c}{g} \quad (46.6)$$

and insert it into Eq. (46.5). This yields the already familiar relationship, Eq. (46.1),  $S_{ik} = \pm K_c Q_k$ .

For better visualization of the phenomenon it is reasonable to determine the value of the angle  $\delta_c$  as being

$$\delta_c = \arctan K_c \quad (46.7)$$

Differently speaking, it is plausible to consider the behaviour of a structure under the particular seismic conditions in terms of additional stresses appearing in the structure as its foundation and axes are inclined to the horizontal through an angle  $\delta_c$ .

The pressure of cohesionless soil on a retaining wall, allowing for the seismic action, is found from Eqs. (18) and (19) proposed by the SNiP Building Code:

$$q_c = [1 + K_c \tan (45^\circ + \varphi/2)]p$$

$$q_c^* = [1 - K_c \tan (45^\circ + \varphi/2)]p^*$$

where  $q_c$  and  $q_c^*$  are, respectively, active and passive earth pressure during a seismic event:  $p$  and  $p^*$  are active and passive static earth pressure, respectively.

In conformity with the SNiP Building Code, the value of the seismicity coefficient,  $K_c$ , is related to the seismic intensity as follows:

Design seismicity, intensity number	7	8	9
Seismicity coefficient, $K_c$	0.025	0.05	0.1

As can be seen, the value of  $K_c$  shows the seismic acceleration  $\alpha_c$  as being a fraction of the acceleration due to gravity  $g$ .

It follows from the above that one structure or another can be tested for seismicity by referring to the available methods, only provided that, by using one technique or another, the design values of  $K_c$  or the maximum values of seismic acceleration  $\alpha_{c \max}$  and, if necessary, the period of the seismic wave  $T$  have been previously established. This is the principal task to be solved when evaluating the seismicity of a particular unit area during the particular period of time.

The possible values of  $K_c$  or  $\alpha_{\max}$  for a particular region may be roughly determined by referring to seismic maps issued by official agencies (see an

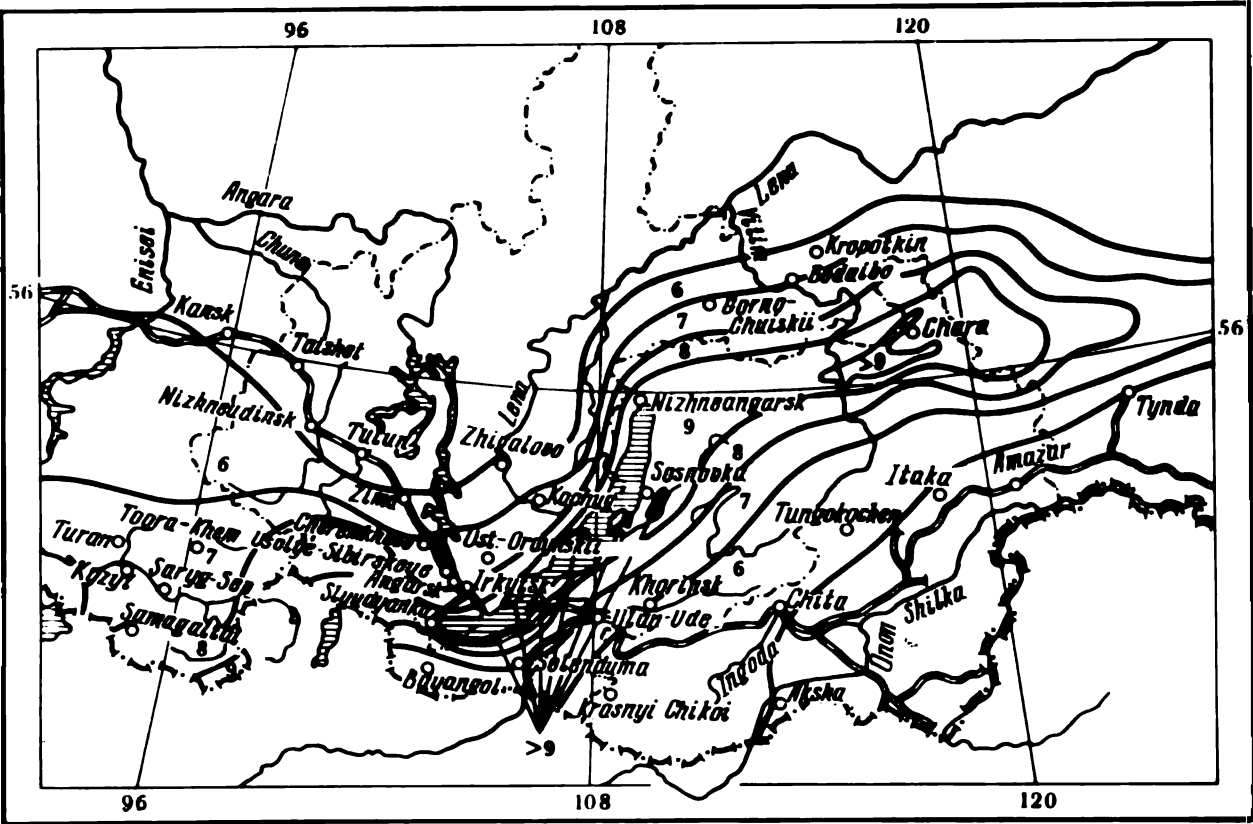


**Fig. 46.5.** Schematic map of local seismicity of the Irkutsk Region, the Buryat Autonomous Soviet Socialist Republic and the Chita Region (Supplement 1, SNiP II-A. 12-69. Construction in seismic zones. 6-9—earthquake intensity numbers)

example in Fig. 46.5 taken from the SNiP Building Code). These maps show regional seismicity gauged by using a 12 force number intensity scale, USSR St.St. GOST 6249-52 (Table 46.1). Similar maps have been compiled for many regions of the USSR. Reference may be made to a List of Populated Points of the USSR Located in Seismic Regions published as a supplement to the SNiP II-A.12-69 Building Code. However, actual observations of the earthquakes that have occurred in the last years demonstrate that the magnitudes of seismic accelerations very much exceed the values presented in Table 46.1.

Table 46.1

Design Values of Seismic Acceleration

Earthquake intensity, scale number	Design ac- celeration, mm/s <sup>2</sup>	Earthquake intensity, scale number	Design ac- celeration, mm/s <sup>2</sup>	Earthquake intensity, scale number	Design ac- celeration, mm/s <sup>2</sup>	Earthquake intensity, scale number	Design accelera- tion, mm/s <sup>2</sup>
1	Up to 2.5	4	11-25	7	100-250	10	1 000-2 500
2	2.5-5	5	26-50	8	250-500	11	2 500-5 000
3	6-10	6	51-100	9	500-1 000	12	> 5 000

Seismologists are currently elaborating an international earthquake intensity scale. The International Association of Seismology and Physics of the Earth’s Interior have recommended an MSK-1964 intensity scale according to which seismic accelerations have values given in Table 46.2 as a temporary international intensity scale.

Table 46.2

MSK-1964 Scale Seismic Acceleration Values

Earthquake intensity, scale number	Design acceleration, mm/s <sup>2</sup>	Earthquake intensity, scale number	Design acceleration, mm/s <sup>2</sup>
5	120-250	8	1000-2000
6	250-500	9	2000-4000
7	500-1000	10	4000-8000

In the 1940s it was suggested to gauge earthquakes according to their *magnitude* (M), which is an instrumentally measured quantity demonstrating the total energy released in an earthquake. The earthquake is assumed to present no hazard to human life or property until its magnitude attains 6.5 M. A cataclysmal seismic event is gauged by 8 M or more. The shock of 8.3 M that devastated San Francisco in 1906, and the 1923 earthquake in Japan is gauged by 8.9 M.

An earthquake intensity  $J_0$  at the epicenter, according to S.L. Solovyov, has a magnitude, which is roughly  $J_0 = 1.7 - 2.2$  M.

The local intensity of an earthquake is governed by relief of the terrain and, primarily, its geologic features, properties of soils, mode of their occurrence and water regime. For example, according to the data on the 1923 earthquake, the seismic acceleration in the lower districts of Tokyo resting on alluvial deposits was 1.5-2 times greater than in the elevated quarters supported by more competent soils.

Sound unweathered hard rocks, e.g. granite, of substantial thickness provide the most reliable foundations in seismic areas. Any faults or fractures dramatically increase seismic hazard. Seismicity of such areas may be 1-3 intensity numbers greater. Loose saturated soils are the most liable to seismicity.

The seismicity of a building site, in conformity with the Building Code, is determined by referring to seismic maps of town districts and villages or industrial enterprizes in compliance to a special manual.

In areas of intensity 7 or more it is permissible to decrease or increase the seismicity of intensity 1 of the building site as determined from the data of seismic prospecting and approved by the body responsible for the pro-

ject. In so doing, the following must be taken into consideration:

unweathered hard rocks and dense coarse detrital soils with low moisture content are the most convenient from the viewpoint of aseismic design;

gravelly, sandy and clayey (macroporous) saturated soils and plastic and liquid clayey (non-macroporous) soils are the most suspicious materials;

the following properties of an area are particularly conducive to seismic hazard: rugged topography (steep banks, gullies, canyons etc.) rocks weathered and decayed due to physico-geologic processes, proximity of tectonic fault lines.

Note that, when increasing earthquake intensities by 1 force number, it is necessary to increase twofold the design values of seismic acceleration  $\alpha$  and, consequently, the seismic constant  $K_c$  with the results that may follow. That is why seismic prospecting is essential.

It may be assumed that during an earthquake on large-period ( $T > 1$  s) vibrations the vibrations of a much greater frequency, possibly, that of vibrations of the soil mass proper, 15-25 Hz, are superposed. This is, in particular evidenced by the roar generally heard during an earthquake. Regrettably, seismographs and accelerographs that are currently available are unable to record these oscillations.

According to Japan's standards, the value of the seismic constant  $K_c$  is generally taken as being equal to  $1/3$  which corresponds to the horizontal component of the seismic acceleration  $\alpha_c = 3270 \text{ mm/s}^2$ .

As can be seen, the above data relating to the value of  $K_c$  fail to solve the problem completely. Moreover, it is often necessary to allow for local conditions. That is why we must elucidate the physical meaning of the seismic constant  $K_c$  characterizing the intensity of an earthquake.

Like in any other type of wave motion, there appears a *spectrum of various waves* called *seismic*. These are longitudinal, compressional, or  $P$  (for primary) waves; transverse, shear or  $S$  (for secondary) waves; and surface seismic waves.

$P$  waves are ones in which particles oscillate in the direction of propagation. In  $S$  waves particles oscillate at right angles to the direction of propagation. An example of a longitudinal wave may be found in an acoustic wave in which compression and expansion zones alternate. By contrast, light waves, by virtue of their character, refer to transverse waves.

The longest and slowest surface waves are Love and Rayleigh waves which propagate from the epicenter (a point on the surface of the earth above the seismic focus of earthquake) similarly to sea waves, travelling walls of varying height. Surface waves of a period 15-20 s cause displacements of crustal masses, particularly conspicuous in areas in the proximity to the epicenter of the earthquake. These waves induce the

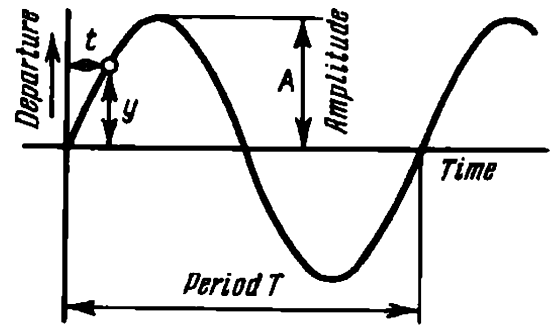


**Fig. 46.6.** Amplitude  $A$  and period  $T$  of a harmonic vibration

strongest vibrations and bring about the most devastating effects. Conversely, transverse waves produce less detrimental effects on structures compared with longitudinal waves.

Depending on the location of an object with respect to the focus of earthquake or its epicenter the soil mass may be acted on by seismic waves differently oriented to the horizontal. The most hazardous is an angle of orientation approaching the angle of internal friction of sand.

The velocity of propagation of seismic waves is conditioned by the medium, and in hard rocks the velocity of propagation of longitudinal waves is characterized by a value of 4-6 km/s. The velocity of propagation of transverse waves under identical conditions is 3-4 km/s.

The velocity of propagation of seismic waves is appreciably reduced in less dense materials. For example, in limestones this velocity is only 2.4 km/s; in loose soils it is generally within 1 km/s. At the same time the amplitude of the wave is increased, which, in turn, enhances danger to structures induced by the earthquake.

Depending on the earthquake intensity and geologic features of the building site both the period of frequency and the amplitude of seismic vibrations may vary in a very great range as will the seismic acceleration  $\alpha_c$ .

In a harmonic oscillation often used for evaluating seismic events and having the shape of a sinusoid (Fig. 46.6) the frequency departure  $y$  at a moment of time  $t$  is found from the relationship

$$y = A \sin 2\pi t/T \quad (46.8)$$

where  $A$  is the amplitude and  $T$  is the vibrational period.

The acceleration of this motion for any moment  $t$  is determined from this equation as a second derivative of the path in the course of time, the first derivative being the velocity of motion  $v$ :

$$\alpha_c = \frac{d^2 y}{dt^2} = -4 \frac{\pi^2}{T^2} \sin 2\pi \frac{t}{T} \quad (46.9)$$

We want to determine the maximum value of this acceleration  $\alpha_{c \max}$ . Clearly, it can be found from the latter equation by setting the function of

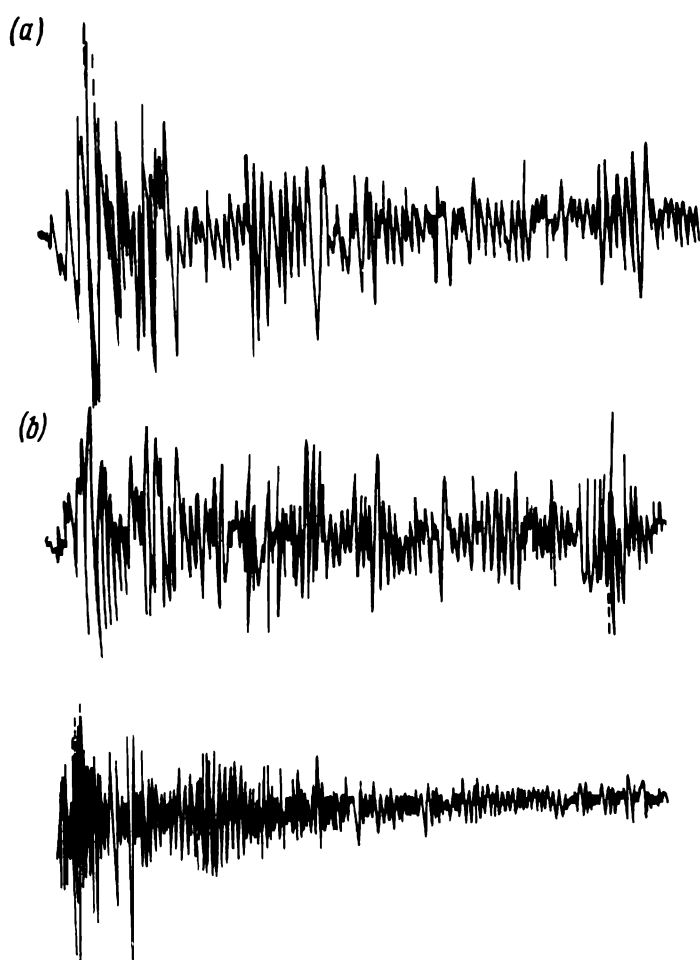


Fig. 46.7. Accelerogram of a force 8 earthquake (after S.V. Medvedev)

*a*—vertical vibrations; *b*—horizontal vibrations

sin equal to its maximum possible value, viz. unity. This yields (expressed in absolute terms)

$$\alpha_{c \max} = 4\pi^2 A/T^2 \quad (46.10)$$

If we express the time factor in terms of the vibrational frequency  $f$ , we obtain

$$\alpha_{c \max} = 4\pi^2 A f^2 \quad (46.11)$$

Thus, the design value of the seismic constant  $K_c$  can be easily established by referring to a *seismogram*.

The most useful evidence for estimating seismicity of one area or another is provided by long-term observations using seismographs that record seismic vibrations and accelerographs measuring seismic acceleration. The general shape of an accelerogram taken by using this device is presented in Fig. 46.7. Accelerograms yield the values of seismic acceleration, which are the most important quantities for the civil engineer.

A local recording station may often provide most valuable data on the intensities of earthquake, typical amplitudes, frequencies and durations of vibrations. However, the investigator does not usually have at his disposal such means though he may need to more correctly establish seismicity of



one region or another (problems relating to local seismicity). Under such conditions it is possible to roughly estimate the seismicity of the particular site by direct observations or by collection of pertinent evidence.

The criteria presented in St.St. GOST 6249-52 may prove very useful in this case. According to these criteria earthquake of different intensities have the following characteristics:

I. No damage to houses or structures. No residual disturbances in soils or groundwater and surface water regime. Earthquake not felt (classified as *unnoticeable*) and only instrumentally recorded.

II. No damage or disturbance inflicted to structures. Felt only by a few persons and classified as *very feeble*.

III. No damage or disturbance of structures. Suspended objects, such as lamps, curtains, open doors slightly swing. Standing cars rocked inappreciably. Felt as vibrations of rapidly moving vehicles. Classified as *weak*.

IV. No damage in buildings or structures. Suspended objects swing, fluids in vessels oscillate, dishes disturbed. Felt by nearly every one. Classified as *moderate*.

V. Damage slight in structures. Open doors and windows swing, window panes oscillate. Dishes and objects on shelves overturned. Felt by almost everybody; domestic animals agitated. Classified as *fairly strong*.

VI. Minor damage in many buildings. Light furniture disturbed. Many run outdoors. People move unsteadily. Animals run out of shelters. Classified as *strong*.

VII. Damage slight to considerable in many structures. Masonry fences damaged. Roads cracked; landslides, occasionally rock slides in mountainous areas. Previously existing springs disappear, new springs emerge. Some persons jump out of windows. Motion without support made difficult. Classified as *very strong*.

VIII. Damage considerable in structures, some buildings collapse. Large-scale talus slides and rock falls. Persons can hardly stand. Classified as *destructive* (see Fig. 46.8).

IX. Structures badly damaged, buildings fall. Fall of most chimneys, stacks, towers. Rails bent. Rock avalanches. Classified as *destructive*.

X. Structures often collapse. Embankments and dams badly damaged. Ground badly cracked by fissures 1 m wide. Fall of cliffs. Battering of waves of reservoirs. New lakes originate. Animals rush about. Old trees broken. The earthquake is classified as *annihilating*.

XI. Few (if any) structures remain standing. Long sections of embankments collapse. All rails warped and buckled. Numerous fissures on ground, vertical displacement of soil strata. Classified as *catastrophic*.

XII. *Major catastrophe*. Damage total. Large-scale changes of ground: overthrusts, ruptures, landslides etc. tremendous.



**Fig. 46.8.** Building in Niigata that failed by tilting due to the earthquake-induced disturbance of the bearing capacity of saturated sands

### **Sec. 46.3. Seismic Stability of Saturated Sands**

In the context of the above classification of earthquake intensities the evaluation of seismic stability of *saturated loose cohesionless soils* (primarily sands) in foundations of structures and in submerged slopes of dams, dikes, canals etc. is of particular importance.

How vulnerable to seismic action is the mass of saturated fine-grained sands and swamp deposits is illustrated by this example. The 1935 earthquake in the Ganges River Valley in India was of exceptional violence. More than 360 engineering structures (bridges and conduits) on roads were ruined; numerous buildings collapsed in the afflicted area.

Attention should be called to the fact that failures of structures were attended with their sinking (sometimes total) in the mass of completely liquefied soil. At a number of sites jets of water rose through the cracks in the crustal clayey soil mass. Vertical displacement up to 1 m of an immense area occurred.

These phenomena are easily understood if we refer to data on the behaviour of fine-grained saturated sands influenced by dynamic loads outlined in Chap. 30. We should also take into account the fact that alluvial deposits in the Ganges River Valley are 1 000 m in thickness, and the groundwater table is only 2 m below the ground surface.

The hypothesis of a possible disturbance of the stability of saturated sand due to a dynamic load was unambiguously proved by analysis of the large-scale Niigata earthquake of 1964 (Fig. 46.8). This event graphically demonstrated all the consequences of the disturbance of the stability of saturated sands (fissures, subsidences, differential settlement, structures thrown out of plumb and overturned). Similar phenomena were observed

during a recent earthquake in California. A characteristic illustration is provided by the failure of a bridge on a pile foundation supported by a mass of saturated sand (see Fig. 46.4).

The above phenomena are universally known. However, inadequate attention is being paid to them by building codes despite the importance of the problem. In particular, Table 1 of the SNiP Building Code only points to a need to increase by one intensity number the design value of the local seismicity if the groundwater table is nearer than 4 m to the ground surface. In addition, it is necessary to take into account the specific properties of the sand, its type, density, thickness of the sand deposit, the effect of surcharge, as these are essential factors responsible for the behaviour of saturated sands during seismic events.

Let us consider the problem in more detail. The stability of saturated sands sustaining a dynamic load is disturbed under conditions diagrammatically shown in Fig. 46.9. Vibrations acting on sand followed by acceleration exceeding a definite *critical value* of  $\alpha_{cr}$  tend to consolidate this material. The value of  $\alpha_{cr}$  is governed by such properties of the sand as density, uniformity, smoothness of grains etc.

As sand is being consolidated, the voids filled by water decrease in volume. The pore water which is excessive for the new density of the sand migrates upward, toward the free surface. This process involves ascending flows of water demonstrating a definite gradient, and consequently, a definite pressure head  $h_z$ .

For a one-dimensional case the value of  $h_z$  can be determined by this reasoning. Let us introduce a new quantity, *the coefficient of dynamic compaction*  $\nu_n$ . This is understood to be an index characteristic indicative of the rate of compression of sand with a specified density related to porosity  $n$  acted on by a dynamic load at a definite intensity determined by a period  $T$ , amplitude  $A$  and vibrational motion acceleration  $\alpha_c$ .

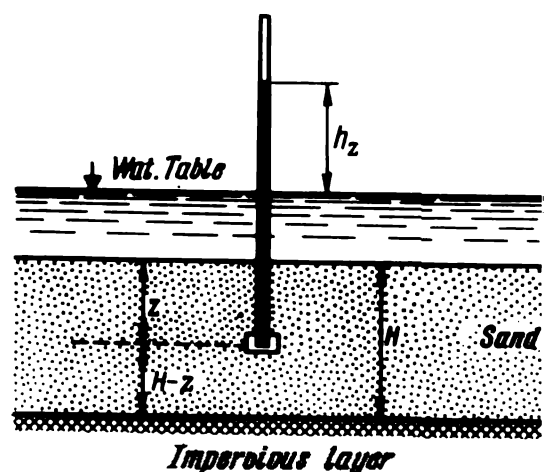


Fig. 46.9. Parameters of the dynamic regime of a submerged sand mass

By virtue of the above definition we may write:

$$\nu_n = \frac{dn}{dt} \quad (46.12)$$

Thus if all the voids are filled by water, the coefficient  $\nu$  will be indicative of the rate of compression of sand (referred to porosity  $n$ ) and of the amount of water squeezed out of the voids per unit of time following a shock acting on the sand. The coefficient of compression is measured in  $(t^{-1})$ , which is a reciprocal of time.

Let us select an elementary layer of sand which is  $dz$  in thickness in the mass of sand (Fig. 46.9). The increment of the discharge of water in the total upward flow  $dq_z$  due to the shock-induced compression of sand in the particular layer can be found from this relationship:

$$dq_z = - \frac{dn}{dt} dz \quad (46.13)$$

The minus sign in the right-hand side of this equation implies that with reducing the sand porosity the seepage of water through the sand mass increases. If we assume the cross sectional area passing water  $\omega$ , to be unity, we can write  $\omega = 1.0$ . Let us define the coefficient of permeability as  $K_p$ . Then

$$q_z = K_p \frac{dh_z}{dz} \quad (46.14)$$

In the particular case the discharge of water will be determined in conformity with Darcy's law:

$$q_z = \omega K_p I_z \quad (46.15)$$

The value of the hydraulic gradient at the horizon  $z$  will be found from the relationship:

$$I_z = \frac{dh_z}{dz} \quad (46.16)$$

By differentiating Eq. (46.14) with respect to  $z$  we obtain

$$\frac{dq_z}{dz} = K_p \frac{d^2 h_z}{dz^2} \quad (46.17)$$

Let us transform Eq. (46.13):

$$\frac{dq_z}{dz} = - \frac{dn}{dt} \quad (46.18)$$

By comparing Eqs. (46.17) and (46.18) we have

$$\frac{d^2 h_z}{dz^2} = - \frac{I}{K_p} \frac{dn}{dt} \quad (46.19)$$

In the particular case, to simplify matters, we assume that in Eq. (46.12)

$$\frac{dn}{dt} = \nu_n = \text{const}$$

whence

$$\frac{d^2 h_z}{dz^2} = - \frac{I}{K_p} \nu_n \quad (46.20)$$

Clearly,

$$h_z = - \frac{\nu_n}{K_p} \int \int dz^2 \quad (46.21)$$

At the same time

$$dh_z = - \frac{\nu_n}{K_p} \int dz \quad (46.22)$$

or

$$I_z = \frac{dh_z}{dz} = - \frac{\nu_n z}{K_p} + C_1 \quad (46.23)$$

Let us determine the constant of integration  $C_1$  proceeding from the condition that for  $z = H$ , that is, at the contact with an aquiclude in the absence of discharge ( $q_H = 0$ ), the gradient is  $I_H = 0$ . As a result, we have

$$I_z = \frac{\nu_n}{K_p} (H - z) \quad (46.24)$$

Hence it is possible to obtain a differential equation for determining the dynamic pressure head  $h_z$ :

$$dh_z = \frac{\nu_n}{K_p} (H - z) dz \quad (46.25)$$

Consequently,

$$h_z = \frac{\nu_n}{K_p} \int (H - z) dz \quad (46.26)$$

Having integrated and determined the constant of integration  $C_2$ , given that for  $z = 0$ , that is on the surface of the sand layer, the pressure head

is  $h_z = 0$ , we finally obtain

$$h_z = \frac{\nu_n}{K_p} \left( Hz - \frac{z^2}{2} \right) \quad (46.27)$$

Thence it follows that the relationship between the dynamic head and the depth  $h_z = f(z)$  is of parabolic character. On the surface layer for  $z = 0$  the dynamic head is  $h_z = 0$ . The dynamic head  $h_z$  attains its maximum value at the foot of the layer at the contact with the aquiclude for  $z = H$ .

The relationship between  $J_z$  and the depth  $z$  is linear. Given  $z = 0$ , at the upper surface of the layer, this gradient is of maximum value which indicates that the sand conditions here are the most complicated. The value of the dynamic gradient is  $J_H = 0$  at the contact with the aquiclude which is quite natural.

If the sand mass is underlain by a layer of material exhibiting good draining properties (for example, gravel) the water removed from the sand mass as this latter is compressed may percolate upwards and downwards. The above formulae hold good for the given case as well, provided the values of  $H$  substituted there are halved.

It is often necessary to allow for a reduction of the value of  $\nu_n$  with increasing the depth in the sand mass, especially, if the latter is of conspicuous thickness (several tens of metres). The first version of the solution of the problem assumes a linear relationship between the coefficient  $\nu_z$  and the depth  $z$ :

$$\nu_z = f(z); \quad \nu_z = \nu_0 \frac{L - z}{L}$$

where  $\nu_0$  is the coefficient of dynamic compaction at the surface of the sand mass;  $L$  is the depth at which  $\nu_z = 0$  where  $\alpha_z \geq \alpha_{cr}$ , viz. where the critical acceleration decreasing with depth becomes equal to  $\alpha_{cr}$ .

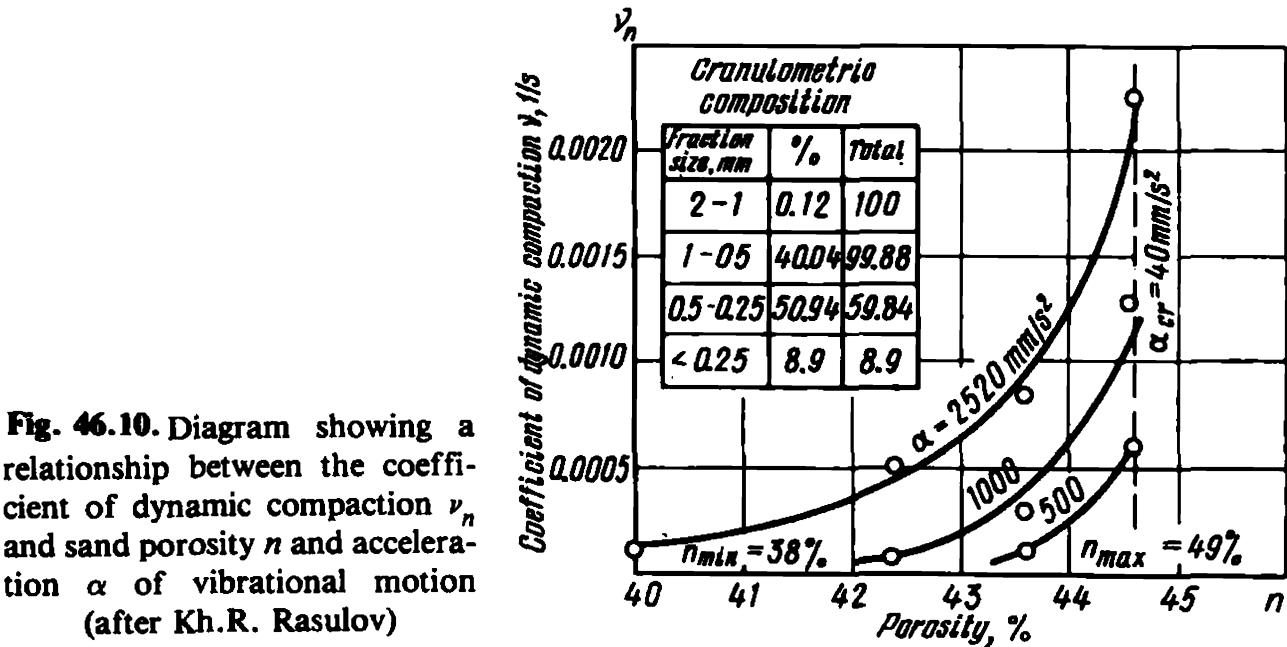
The solution of the problem for such conditions involves the following relationships for determining the dynamic heads  $h_z$  and gradients  $J_z$  acting at a depth  $z$ :

$$h_z = \frac{1}{2} \frac{\nu_0}{K_p} \left( Lz - z^2 + \frac{z^2}{3L} \right) \quad (46.28)$$

$$J_z = \frac{dh_z}{dz} = \frac{1}{2} \frac{\nu_0}{K_p} \left( L - 2z + \frac{z^2}{L} \right) \quad (46.29)$$

The reduction of the value of the coefficient of dynamic compaction accordingly decreases the values of  $h_z$ , yet the mechanism of the event remains the same.

The tests for determinations of the coefficient of dynamic compaction



use this relationship:

$$\nu_n = \Delta n / \Delta t \tag{46.30}$$

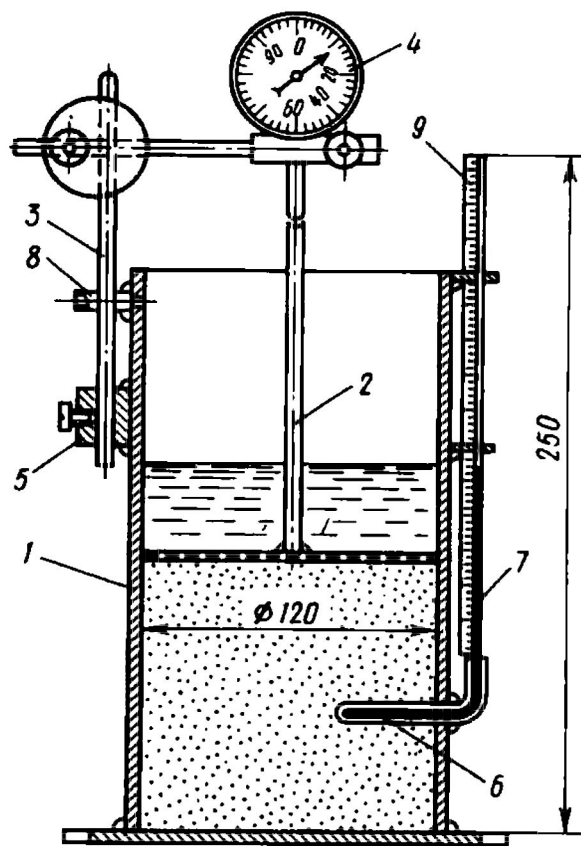
where  $\Delta n$  is the decrease of sand porosity within a discrete minor interval of time  $\Delta t$ .

With increasing sand porosity  $n$ , smoothness of its grains and intensity of the dynamic load the coefficient  $\nu_n$  increases from zero to a value corresponding to the conditions that obtain after a dynamic load. The pattern of the alteration of  $\nu$  for a definite sand variety, depending on the above factors, is presented in Fig. 46.10. The magnitude of this coefficient for the sand of interest to us must invariably be established by laboratory tests.

Thus, the evaluation of the dynamic, including seismic, stability of a mass of saturated cohesionless soils requires their index characteristics, primarily, the value of the critical acceleration  $\alpha_{cr}$ , and if  $\alpha_{des} > \alpha_{cr}$ , the coefficient of dynamic compaction  $\nu_n$ . Apart from this, it is necessary to know the value of the coefficient of the permeability of the soil  $K_p$ .

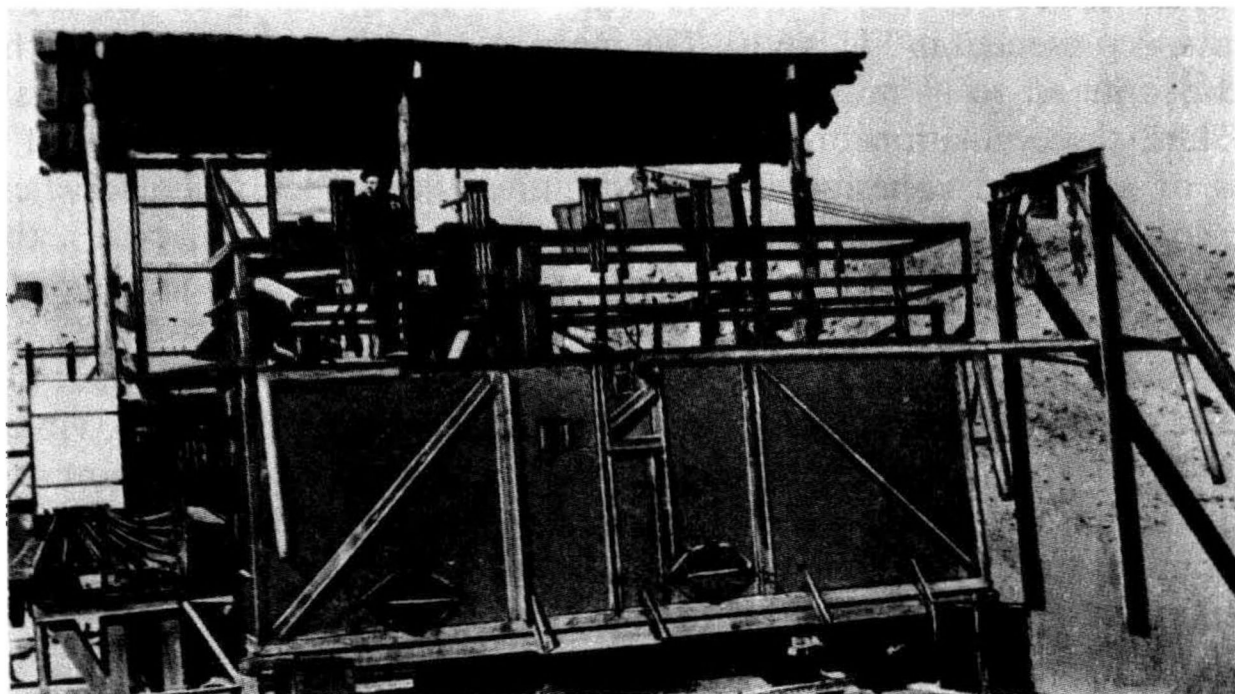
The constants  $\alpha_{cr}$  and  $\nu_n$  must be determined by taking into account the specified design seismic characteristics (acceleration  $\alpha$ , amplitude  $A$ , vibrational frequency  $f$  or period  $T$ ) and the particular density of soil (porosity  $n$ ). These parameters are determined by using special vibration machines that simulate soil vibrations under a specified dynamic regime. Such tests generally employ vibrations at a frequency close to that of the soil (15-30 Hz).

Figure 46.11 is a diagram of an elementary machine for laboratory tests. Figure 46.12 presents an installation for *in situ* horizontal vibrational and dynamic load tests of Kara Kum sands.



**Fig. 46.11.** Apparatus for laboratory tests of saturated sands under conditions of dynamic load:

1—testing pot; 2—pressure gauge rod; 3, 5, 8—elements for fixing pressure gauge 4; 6—recess for piezometric tube 7; 9—scale for measuring pressure head



**Fig. 46.12.** 25t-capacity test installation for determinations of seismic stability of submerged sands under industrial conditions



Given the soil density and vibrational frequency, the value of critical acceleration  $\alpha_{cr}$  is found for a saturated soil by gradually increasing the vibrational amplitude and, consequently, its acceleration from zero to a value at which, referring to the subsidence of the soil surface, we determine its compaction and, hence, the onset of the dynamically excited state of the sand. The relationship between  $\alpha_{cr}$  and density for a definite sand variety is graphically shown in Figs. 46.13 and 46.14.

The same installation is used to determine the value of *the coefficient of dynamic compaction* for the same conditions, allowing both for the porosity of the sand and seismic parameters ( $\alpha$ ,  $f$  or  $T$ ).

Evidently, seismic loads on a saturated sand mass at an intensity referred to the acceleration  $\alpha_p > \alpha_{cr}$  will reduce the stability of the sand.

The shearing resistance of loose sand in static conditions is found from the familiar relation

$$s_{st} = p_{st} \tan \varphi \quad (46.31)$$

where  $p_{st}$  is the normal stress at a horizon  $z$  induced by the weight of the overburden or structure (dead load);  $\varphi$  is the angle of internal friction of sand.

If the load acting on loose sand is of seismic origin, conditions change. Then we have

$$s_{dyn} = p_{dyn} \tan \varphi \quad (46.32)$$

where  $s_{dyn}$  and  $p_{dyn}$  have the previous value, yet as applied to new dynamic conditions.

The variation of the normal stress under dynamic conditions is accounted for by the buoyancy effect of *the dynamic pressure head*  $h_z$  appearing in the sand mass as it is compacted by vibrations:

$$p_{dyn} = p_{st} - \rho_w h_z \quad (46.33)$$

where  $\rho_w$  is the density of water.

If there is no dead load acting on the soil the value of  $p_{st}$  at the horizon  $z$  is determined by the weight of the overburden

$$p_{st} = \rho_s z \quad (46.34)$$

where  $\rho_s$  is the bulk density of sand, determined by taking into account, when necessary, the hydrostatic uplift pressure acting on it (in the submerged state  $\rho_w \approx 1 \text{ t/m}^3$ ). By virtue of these two relations we can rewrite Eq. (46.32) as:

$$s_{dyn} = (\rho_s \text{ uplift } z - \rho_w h_z) \tan \varphi \quad (46.35)$$

As follows from this equation, for  $z = h_z$  the shearing resistance of sand

**Fig. 46.13.** Relationship between the critical acceleration  $\alpha_{cr}$  of small-grained sands and sand porosity referred to porosity  $n$  and content of grains  $<0.25$  mm in size:  
1—with varying grain-size sand; 2—small-grained well rounded sand

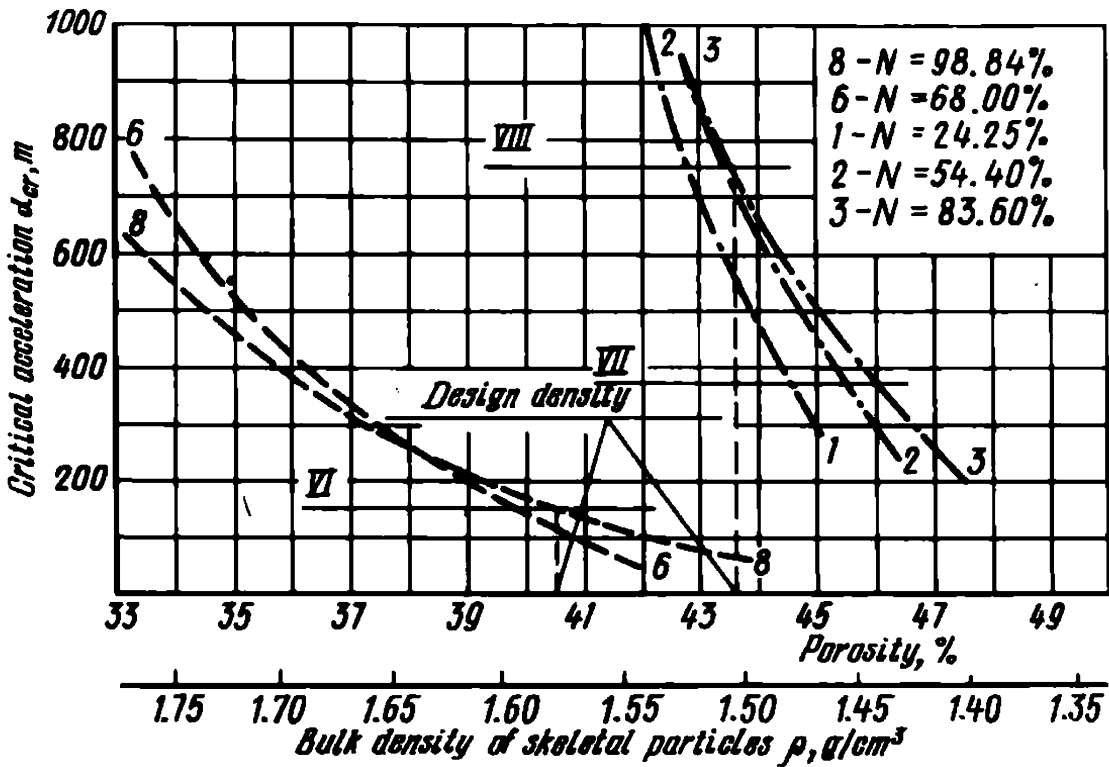
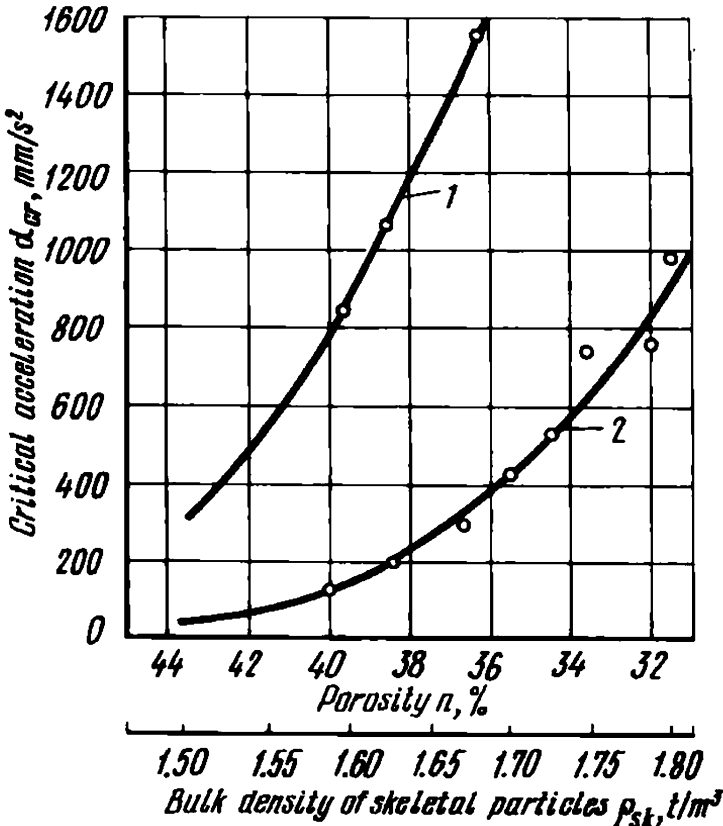


**Fig. 46.14.** Critical acceleration depending on porosity,  $n$ , of angular and well rounded sands with different contents of particles less than 0.25 mm,  $N$ :  
1-3—angular sands; 6, 8—well rounded sands

is  $s_{dyn} = 0$ . In this case sand completely loses its stability and transforms to a heavy fluid (*liquefaction of sand*).

Analysis of Eqs. (46.35) and (46.27) demonstrates that, other conditions being equal, hazard of liquefaction of sand increases with increasing its porosity  $n$ , the thickness of the sand layer  $H$ , and with decreasing the coefficient of permeability of sand  $K_p$  and, naturally, in proportion to the duration,  $t$ , of seismic action. That is why under seismic conditions the greatest hazard is presented by saturated fine- and small-grained sands exhibiting reduced permeability induced by the small value of  $K_p$  and occurring as deposits of conspicuous thickness.

When conducting dynamic tests of sands, it is often sufficient to determine only the value of the critical acceleration  $\alpha_{cr}$  corresponding to the particular conditions. In so doing the degree of aseismic stability of sand is established by direct correlation of the values of  $\alpha_{cr}$  and design acceleration  $\alpha_{c\ des}$ . Clearly, in this case matters are simplified.

If a saturated sand mass is overlain by structures or a fairly thick layer of dry sand, when determining the coefficient of dynamic compaction  $\nu_n$  or critical acceleration  $\alpha_{cr}$ , this condition must accordingly be taken into account. If the values of normal stresses are relatively small, the relationship  $\alpha_{cr} = f(p_n)$  is of a linear character.

It should be made clear that the stability and deformations of structures resting on any soil mass (dry, or, particularly, submerged sand mass) in seismic regions is generally important only if during the construction the dry sand soil is submerged (say, when excavating a pond or reservoir). It is assumed at this that the sand occurring below the table of surface or groundwater was subjected in the geologic past to dynamic action and after being compacted is already found in an inert state.

The phenomenon described above involving a reduction of the shearing strength of a submerged sand mass due to the effect of a dynamic load is one of the principal causes of failures of slopes, in particular, those of earth structures during seismic events.

The dynamic stability of sand composing submerged slopes is the smaller, the larger is the gradient of the slope.

According to a relationship proposed by Valid Canan of the Moscow Highway Engineering Institute,

$$\alpha_{cr\beta} = \mu(s_{dyn} - \tau_{max})$$

whence

$$\alpha_{cr\beta} = \alpha_{cr0}(1 - \tau_{max}/s_{st}) \quad (46.36)$$

i.e. under conditions of a transition regime of the soil mass the shearing

resistance of sand in dynamic conditions  $s_{dyn}$  may be assumed as being equal to the shearing resistance in static conditions  $s_{st}$ .

In the above equations  $\alpha_{cr\beta}$  is the critical acceleration of sand in a slope with an angle  $\beta$ ;  $\tau_{max}$  is the maximum shearing stress in a slope;  $\alpha_{cr0}$  is the critical acceleration of sand with a horizontally oriented surface;  $\mu$  is an experimentally determined parameter of sand.

It follows that if the shearing resistance of sand is exhausted ( $s_{st} = s_{dyn} = \tau_{max}$ ) the critical acceleration is  $\alpha_{cr} = 0$ . This is, in particular, what occurs if the ratio of slope  $\beta$  is equal to the angle of repose of the given sand variety, i.e. if  $\beta = \varphi_0$ . Clearly, in this critical case the stability of the slope may be disturbed by the slightest dynamic load acting on it.

Se Dinh Fe of the Leningrad Construction Engineering Institute has proposed for the case  $\beta_1 \leq \beta \leq \varphi_0$  this equation

$$\alpha_{cr} = \frac{\alpha_{cr\beta_1}}{\varphi_0 - \beta_1} (\varphi_0 - \beta) \quad (46.37)$$

where  $\beta_1$  is the angle of slope at which the critical acceleration still preserves its value corresponding to a horizontal surface  $\alpha_{cr\beta_1}$ , i.e.  $\alpha_{cr\beta_1} = \alpha_{crp0}$ .

As follows from Eqs. (46.27) and (46.36), even if the angle of slope is  $\beta = \varphi_0$ , even inappreciable dynamic load may prove critical.

The above conclusions base on an assumption that the dynamic angle of friction  $\varphi_{dyn}$  of sand following vibrations appears at accelerations lower than 0.5 g, i.e. acceleration due to gravity remains practically unaltered and equal to its values under static conditions:

$$\varphi_{dyn} = \varphi_{st}$$

If accelerations exceed due to gravity, and the normal stresses in the sand mass are completely or almost completely damped by dynamic inertia forces, then the bearing capacity of a sand foundation, even if the values of the coefficient of friction are constant, may drop to zero.

The methods of the evaluation of seismic stability of saturated sands outlined above represent, in a nutshell, a seepage theory of the dynamic stability of saturated sands proposed by the present author in 1959 that has been considerably developed in the recent period.

Compaction of sands is, in principle, the easiest way of ensuring seismic stability of saturated sands whenever it proves feasible. Compaction of sand makes it possible to increase the coefficient of dynamic compaction  $\nu$ , thus reducing the dynamic pressure head and gradient and, consequently, enhancing the resistance of sand in dynamic conditions  $s_{dyn}$ .

This method has been used, in particular, to ensure dynamic stability of the sand foundation of the Assouan dam on the Nile. The foundation of this dam is a cushion of hydraulically deposited small-grained sand 30 m

**Fig. 46.15.** Relationship between the critical acceleration,  $\alpha_{cr}$ , of well rounded sand (content of particles less than 0.25 mm,  $N = 72\%$ ) occurring in the vicinity of Volgograd and the frequency of forced vibrations at different additional loads ( $p$  in  $\text{kg}/\text{cm}^2$ ). Sand density referred to porosity  $n = 39\%$ ; relative density  $D = 0.38$

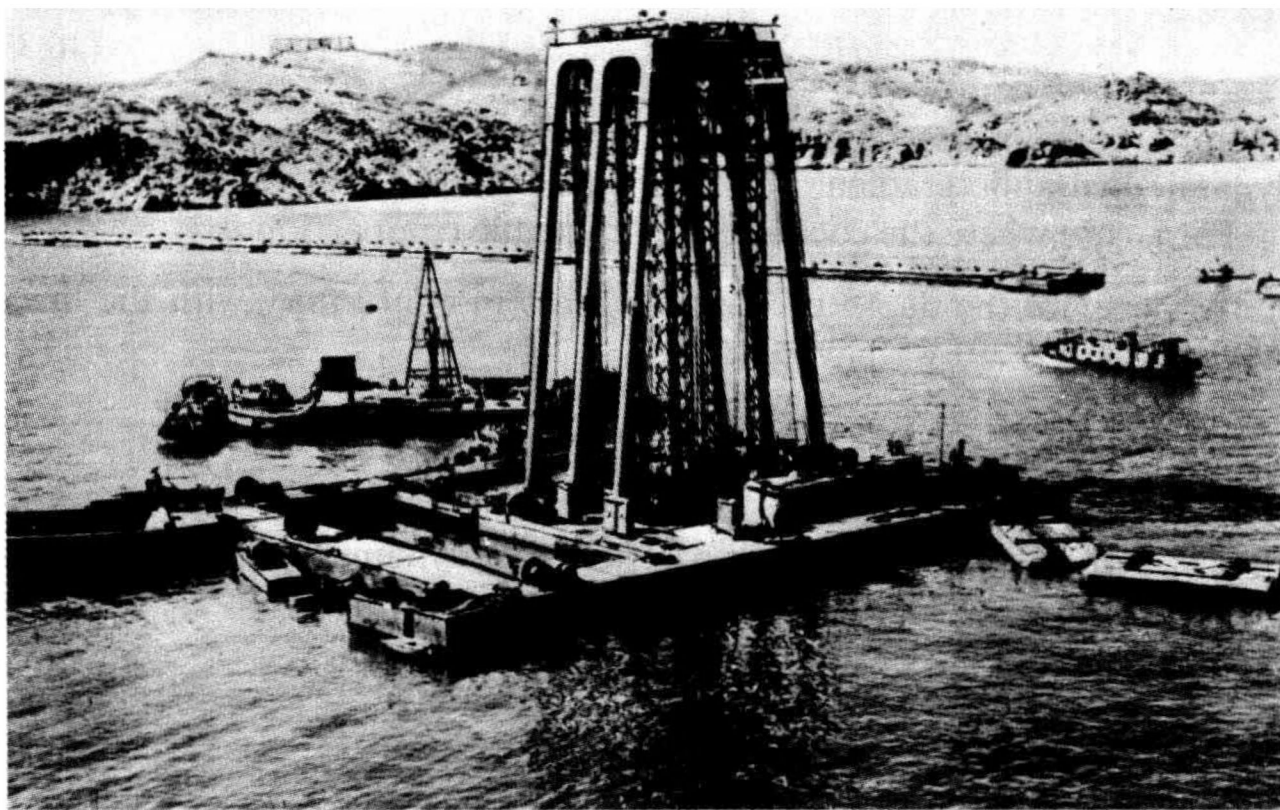
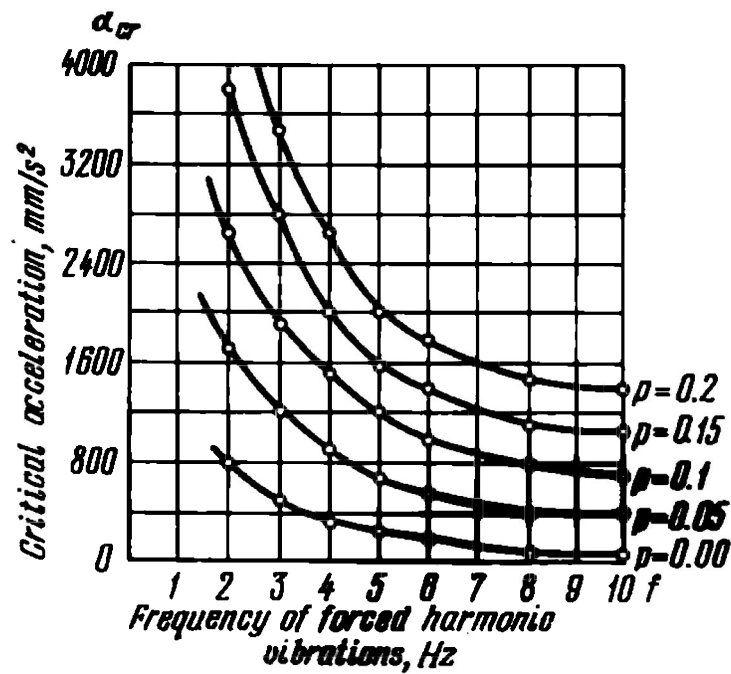


**Fig. 46.16.** Plant for deep compaction of sand foundation of the Assouan Dam

in thickness. The density of the sand in the cushion was at first insufficient (bulk density of skeletal particles was  $\rho_{sk} = 1.56-1.58 \text{ t/m}^3$ ) which is usually the case when hydraulic filling is needed. Additional compaction of the sand cushion until the bulk density was  $1.65-1.68 \text{ t/m}^3$  was achieved by using a Soviet-built compaction plant (see Fig. 46.16). The plant relied for its operation on deep compaction of the sand mass by means of large diameter hollow rods with vibrators installed inside. The sand density was achieved, referred to the bulk density  $1.68-1.70 \text{ t/m}^3$ , which was sufficient.

Additional loading of the sand mass may often prove the most efficient means of increasing the dynamic stability of sand. The critical acceleration can then be dramatically enhanced if the following relationship is satisfied:

$$\alpha_{cr\ p} = \alpha_0 + mp \quad (46.38)$$

where  $\alpha_0$  is the critical acceleration for the particular sand variety in the absence of additional loading ( $p = 0$ );  $p$  is the intensity of additional loading;  $m$  is the proportionality factor found experimentally. It is possible to eliminate dynamic conditions in the sand mass ( $h_z = 0$ ).

The advantageous effect of additional loading is reduced with increasing the vibrational frequency (Fig. 46.15).

The desired effect can be attained, however, at lower costs by attenuating only the action of the dynamic pressure head ( $h_z$ ), i.e. by working against backpressure appearing at this  $\rho_w h_z$ . The elementary buoyancy force acting in a two-dimensional case on a sand layer  $dz$  in thickness is

$$dW_z = - \Delta_w \omega J_z dz \quad (46.39)$$

where  $\omega$  is the cross sectional area of the volume concerned;  $J_z$  is the dynamic hydraulic gradient at a depth  $z$ .

For a case where the coefficient of dynamic compaction is  $\nu_z = - \frac{dn}{dt}$  and varies with the depth of the sand mass in conformity with the linear relationship (46.29) we have

$$J_z = \frac{1}{2} \frac{\nu_0}{K_p} \left( L - 2z + \frac{z^2}{L} \right)$$

where  $L$  is the depth at which the coefficient of dynamic compaction of the surface equal to  $\nu_0$  becomes zero or when  $\alpha_{des} \leq \alpha_{cr}$ .

By virtue of Eqs. (46.39) and (46.29) we can write

$$W_z = - \frac{1}{2} \rho_w \omega \frac{\nu_0}{K_p} \int_0^L \left( L - 2z + \frac{z^2}{L} \right) dz$$

By integrating the above equation between  $z = 0$  and  $z = L$  we obtain

$$W_z = -\frac{1}{6} q_w \omega \frac{\nu_0}{K_p} L^2 \quad (46.40)$$

The value of additional loading  $P$  within the same elementary area  $\omega$  for a definite thickness of the material for additional loading,  $d$ , equals

$$P = q_{add} \omega d$$

Under conditions of limiting equilibrium  $P = W_z$ . Then

$$d = \frac{1}{6} \times \frac{q_w}{q_{add}} \times \frac{\nu_0}{K_p} L^2 \quad (46.41)$$

As can be seen, apart from other known factors the efficiency of the additional loading is reduced almost twofold if it is found below the water level.

The effect of the foundation soil conditions on the seismic stability of structures had been long given inadequate attention and it was only at the 9th International Conference on Soil Mechanics that the problem was considered as being most important. It was recognized that the vertical components of seismic vibration present the greatest hazard for foundations of structures. It was also established that incompetent soils were more hazardous for light-weight wooden structures than for heavy concrete structures. No explanation of the fact was, however, given by the Conference. It appears that it is the own weight of the structure and the resultant normal stresses acting on the soil mass that produce the damping effect.

It was pointed out in the proceedings of the Third World Conference on Earthquake Engineering that the Niigata earthquake of 1963 provided classical proof of the seepage theory outlined above. This recognition is another piece of evidence suggesting the necessity of taking into account not only inertia seismic forces but also the foundation soils of structures to be designed in seismic areas.

The problem of the dynamic stability of submerged sands has to be also faced when erecting structures transmitting a dynamic load to their foundations. It becomes especially crucial when sand cushions have to be hydraulically deposited under structures, particularly, subaqueous tunnels carrying traffic that cross streams or sea gulfs in ports.

A similar event occurred, e.g. during the construction of such a tunnel in Hampton Road, USA, when it was necessary to compact the sand cushion to attain the relative density  $D = 0.80-0.85$  to avoid the failure of the tunnel foundation due to vibrations induced by passing vehicles.

## Chapter 47

### **The Purpose and Types of Geotechnical Studies and Exploration**

---

#### **Sec. 47.1. General Principles**

Geotechnical explorations for the construction of highways, bridges and airports have much in common. Yet there are important differences between these types of exploratory work. It is out of scope of the present book to consider the problem at length to meet the requirements of the syllabuses of the different college departments.

That is why what follows deals with the general principles and types of geotechnical exploration that are valid for the civil engineer, whatever his specific field.

The main purpose of geotechnical exploration is to evaluate the importance of one type of geodynamic phenomena or another (seismicity, landslides, karst etc.) which may endanger the project and dramatically increase costs due to the necessity to resort to protective measures.

**The principal and the most important objectives** of exploratory work are to determine whether the aforementioned phenomena present a hazard to the structure being designed; determine how great the hazard is, what form it will assume and what protective measures (if any) should be taken; accumulate, whenever needed, the whole spectrum of data for preparing a plan of protective measures that are the most reasonable for the particular job.

In so doing, account must be made of the geodynamic phenomena presenting a danger to the structure in hand that should be investigated according to their nature as outlined in Part Three of the book.

**The second group of problems** to be solved by geotechnical studies includes the accumulation of the relevant data for designing one type of structure or another which could characterize the lithological composition of the foundation soil, the mode of occurrence of separate soil layers and the hydrologic regime (type of subsurface waters, their table, temperature, chemistry, water bearing capacities of individual strata etc.). In addition, it is necessary to conduct analysis of the composition and conditions of materials composing the soil mass obtaining quantitative characteristics and, necessarily, index characteristics of the rocks and soils illustrating their deformability and bearing capacity.

When designing an airport it often proves necessary to carry out subsurface explorations for the construction of underground facilities and



engineering structures. The content and techniques of such investigations are very much the same as in a geotechnical exploration for a tunnel. Apart from specific operations relating to the determinations of rock pressure, gas content and temperature, an assortment of geologic survey operations are performed to study the geologic conditions of the particular rock mass and disclose all possible tectonic disturbances and karst phenomena. When performing these operations, follow the recommendations outlined in the pertinent chapters of the present book.

Such exploratory work often employs large-scale geologic surveys using geophysical methods and, sometimes, aerial photography.

To make geotechnical studies the most efficient, the program of exploratory work must be consistent with the purpose, appearance, type, design and dimensions of the structure being designed; in addition, the program and scope of exploratory work must conform to the particular stage of designing.

Depending on the type of construction and stage of designing, the geologic structure, hydrogeologic conditions and geotechnical events and processes are studied from different points of view and in different detail.

### Sec. 47.2. Types of Geotechnical Exploration

**Products of previous investigations.** The entire territory of the USSR has been by now covered by geologic surveys of one degree of detail or another. Products of these surveys are published both in periodic literature and in proceedings of institutions. Such materials are called *literature*. By contrast, results of numerous geologic, hydrogeologic and geotechnical investigations that have not been published for one reason or another are kept in the archives of the relevant agencies and institutions. They are termed *stored records*.

Inadequate attention is often paid to the utilization of literature and stored records. However, these frequently may contain data that will make it possible to dramatically reduce field work and thus considerably save time. Moreover, analysis of the available data on the previous exploratory work will provide lines to be followed in subsequent investigations. In this case geotechnical studies will be conducted the most efficiently.

**A complex engineering geologic survey.** The first stage of geotechnical exploratory work necessarily includes what is called a complex engineering geologic survey that relies on the data of the geologic survey.

The geologic survey is one of the principal methods for exploration of the geologic structure of the upper crustal layers. The intent of field investigations is the preparation of geologic maps in conformity with the relevant requirements.

It is the purpose of the complex engineering geologic survey to study the geotechnical conditions of the construction of a structure being designed. In so doing, the local geology is studied as well as hydrogeological features and a possibility of occurrence of such events as landslides, karst phenomena, seismic events etc. and engineering properties of soils of interest for the structure in hand are preliminarily evaluated.

At the same time that the geologic survey is conducted, rocks prevailing in the given locality are determined and conditions of their occurrence are established followed by the evaluation of their engineering properties.

Observations of rocks are made whenever the latter are naturally exposed (in canyons, gullies etc.) and on flanks of man-made excavations, such as road cuts, open pits and others. When necessary, sites of natural occurrence are cleared or, alternatively, small size prospect pits are excavated.

During the exploratory operations soil samples are taken for further analysis, and, when needed, their natural moisture contents are preserved (say, by paraffining). In addition, levels of water in wells are recorded and data on seasonal water level fluctuations are collected. The final product of an engineering geologic survey is an engineering geologic map.

In the course of the complex engineering geologic survey data on the practice of construction under identical conditions are collected, observations of the behaviour of the erected structures (settlements, cracks, deformations, seepage water migration, conditions of slopes) are made, data on the footings, problems encountered during the construction of foundations etc. are recorded. All these findings are carefully written down and correlated with a topographic and a geologic map.

**Mine workings.** The later geologic investigations involve reconnaissance by using one type of mine workings or another. These may include a trench 0.6-0.8 m wide and up to 1.5 m deep, a test and prospect pits, a bore hole, a shaft and an adit.

*A trench* is generally a deep excavation, usually with steep flanks. They are generally excavated on slopes and for investigations of the structure of dislocated soil masses.

*A test pit* is a vertical mine working, generally square in plan, 1.5 by 1.5 m or somewhat larger on the side, dug generally to a depth of 3 to 5 m, sometimes more. Depending on the properties of the materials involved the walls are generally braced by timber that is available. Water from test pits is removed by using buckets or by elementary pumps, depending on the amount of seeping water.

*A shaft*, similarly to a deep test pit, up to 20-30 m in depth, is excavated in particularly important cases, generally with reinforced concrete bracing and mechanical pumping and hoisting.

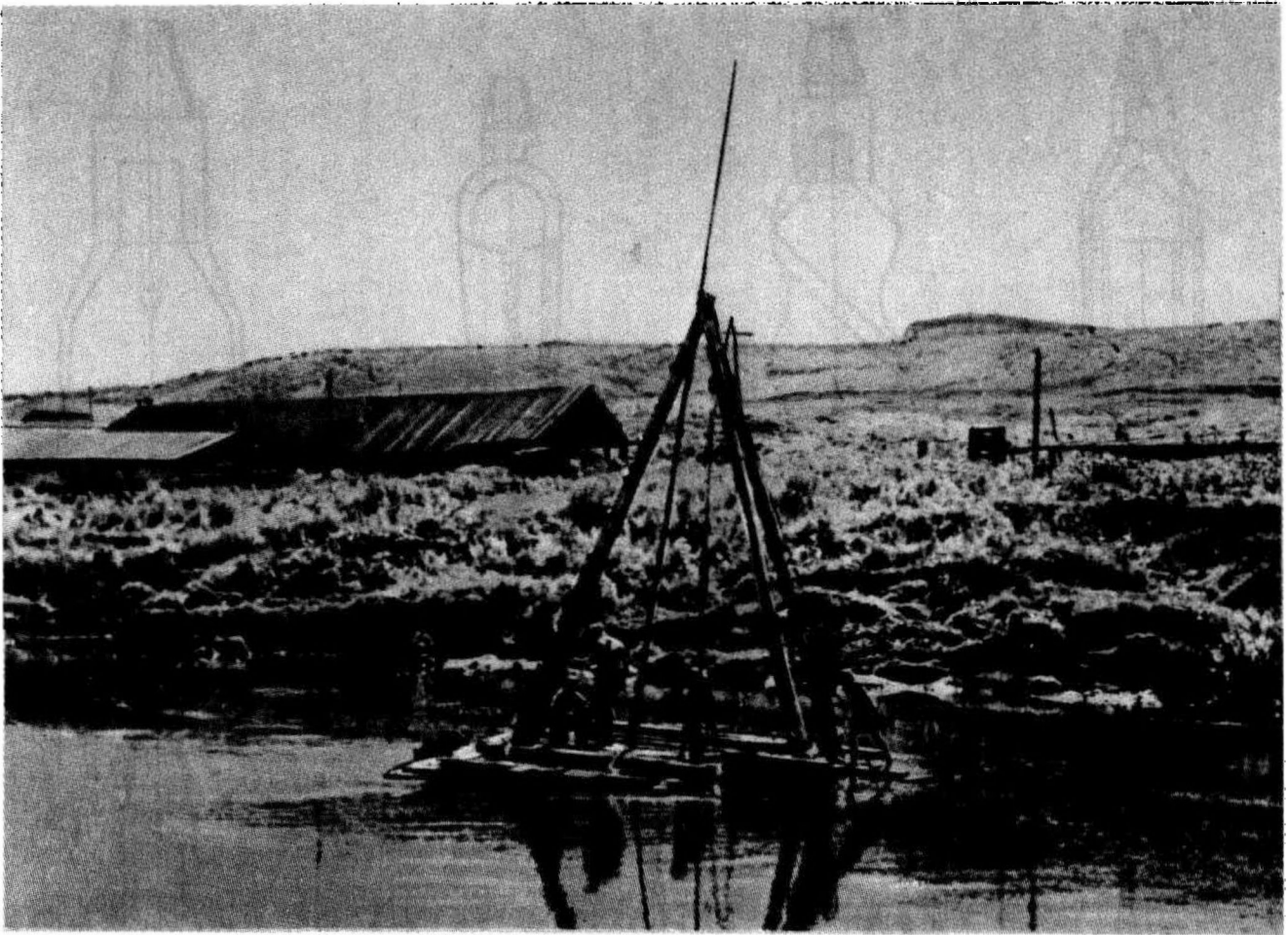


Fig. 47.1. Rig for manual percussion rotary drilling

*An adit* is a horizontal mine working one end of which comes to the ground surface. Adits (or side drifts) are commonly driven in slopes for studying their geologic structure and are inclined to the horizontal through a small angle for drainage of water. Adits are generally braced by timber sheeting, less often by concrete.

The most general procedure in making subsurface investigations is to drill exploratory borings (called bore holes or drill holes) by using different methods and instruments depending on the properties of the material and purpose in mind.

If the subsurface material is soft, the method of hand-operated *percussion rotary drilling* is commonly employed (Fig. 47.1).

Various bits (Fig. 47.2) may be used for cutting and taking soil samples. Sampling of soft permeable rocks makes use of valve tube samplers; that of soft soils (sands, plastic clays) employs sampling spoons; of denser soils, uses earth augers. For penetration into hard rock and coring of boulders that may be encountered use is made of various chopping bits. Minor charges may also be used in drill holes under such conditions. Bits are attached to drill rods which are threaded tube sections of small diameter.

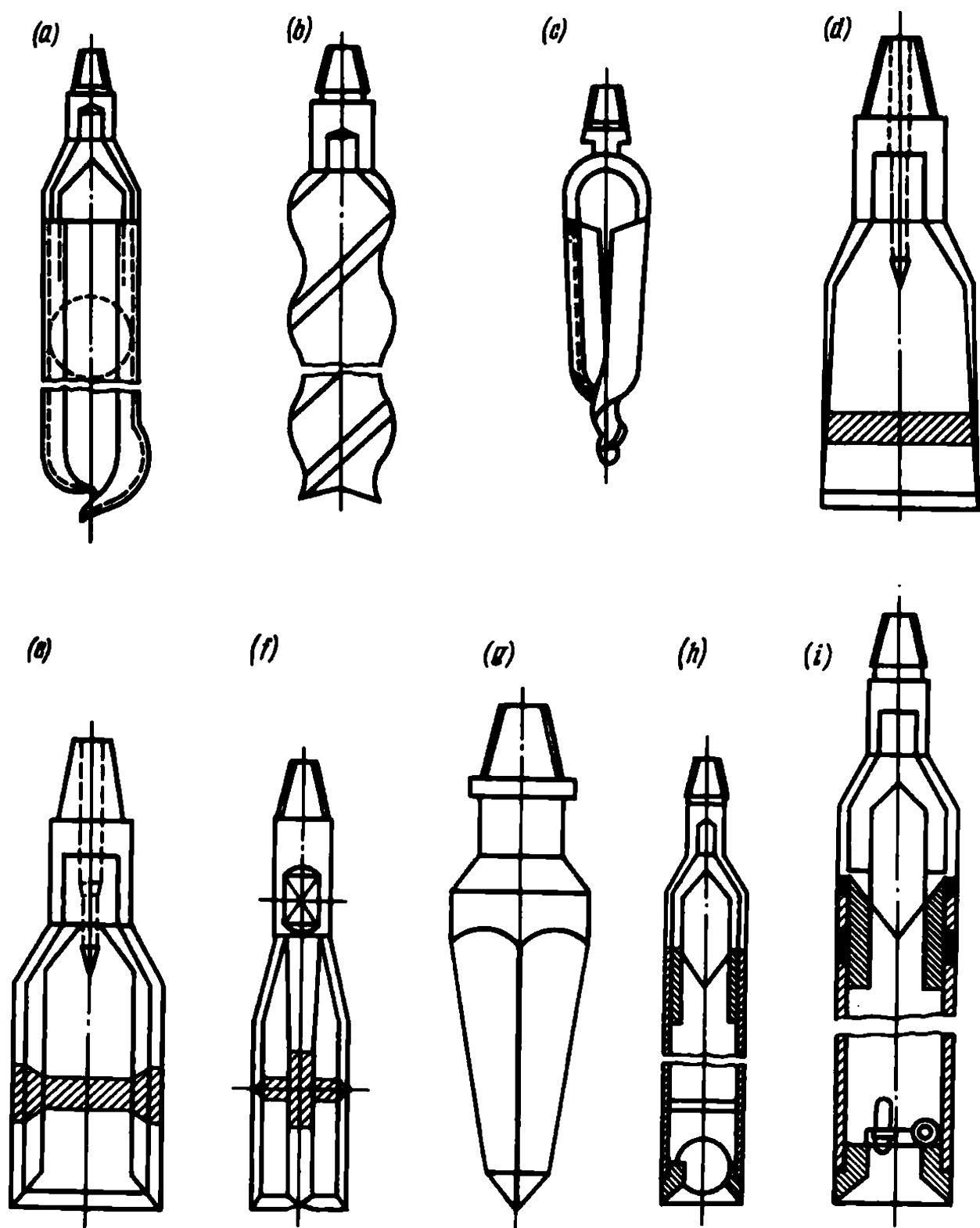


Fig. 47.2. Tools used for percussion rotary drilling:

*a*—sampling spoon; *b*—earth auger; *c*—two-blade earth auger; *d*—flat chopping bit; *e*—I-shaped chopping bit; *f*—x-shaped chopping bit; *g*—pyramidal chopping bit; *h*—ball-valve tube sampler; *i*—poppet-valve tube sampler

The general method of protecting the walls of a bore hole is by the use of casing of “pipe” of various diameter. The diameter of casing represents that of the bore hole. It is generally gauged in inches (4.6 and 8”). The hoisting and lowering of the tool are provided by means of a block system

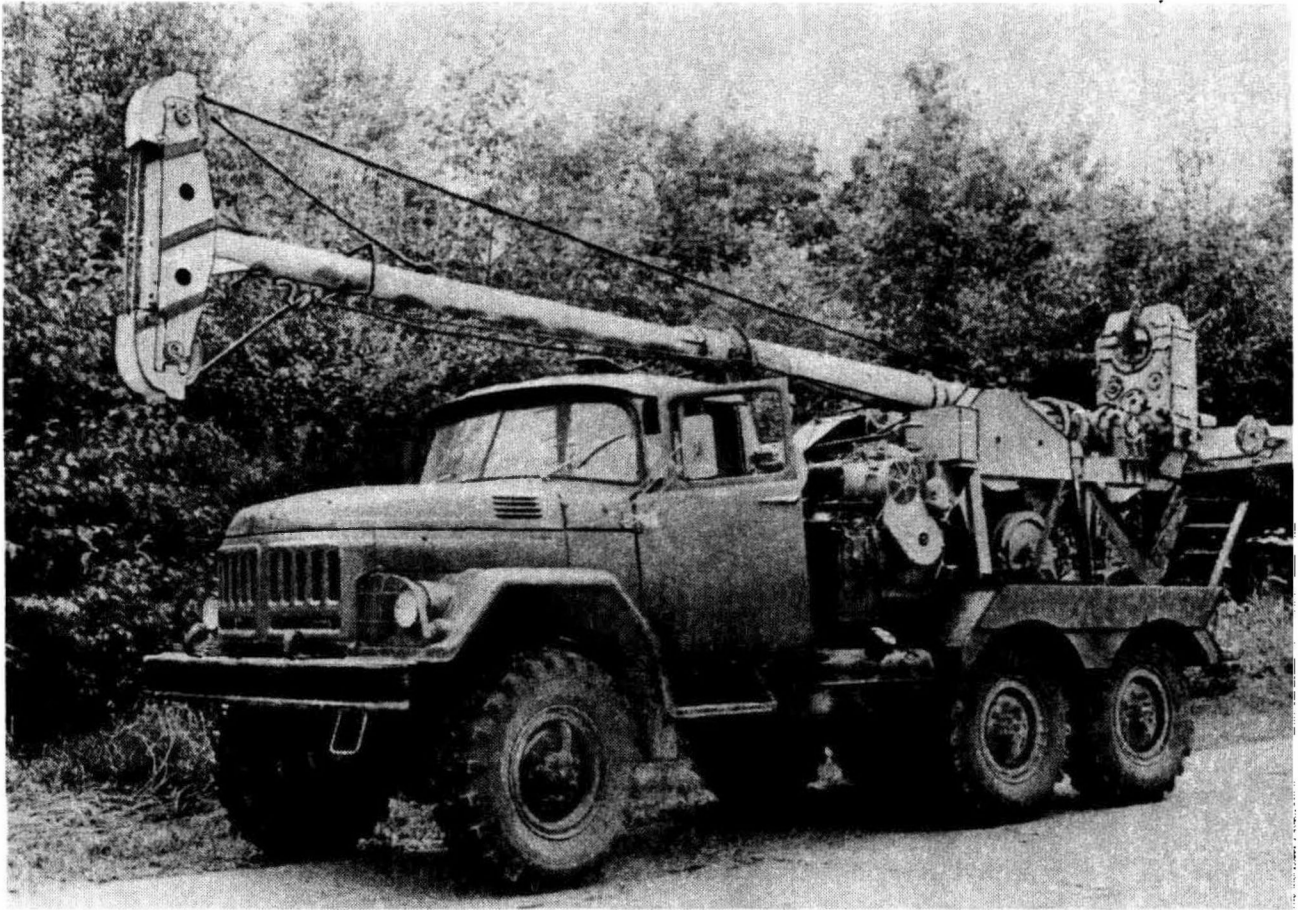


Fig. 47.3. ACYVB-75 drill rig mounted on truck (photograph courtesy of Gidroproekt Institute)

suspended from a rig and operated by a hand or mechanical winch. The entire system forms a drill rig. Instead of hand-operated, self-propelled rigs may be used (Figs. 47.3 and 47.4).

The use of a drill hole invariably yields disturbed samples. These cannot be used for determinations of Class One index characteristics (compressibility, shearing resistance etc.). As has been already pointed out, these tests require *undisturbed samples*.

Undisturbed samples (which are, in fact, disturbed) are extracted from a bore hole by means of *drive samplers*. A drive sampler is a hollow tube of a special design with fixtures for securing a sample. A drive sampler is forced into the ground by pushing (or jacking) or by rotating (a double-walled core barrel).

These recent years have been witnessing a new method of drilling, *vibrodrilling*, or *vibration drilling*. This method makes use of a drilling tool which is introduced into the ground by means of a vibrator mounted directly on the head or drill rod. This technique permits high rates of penetration into soft soils (4 to 6 m/min).

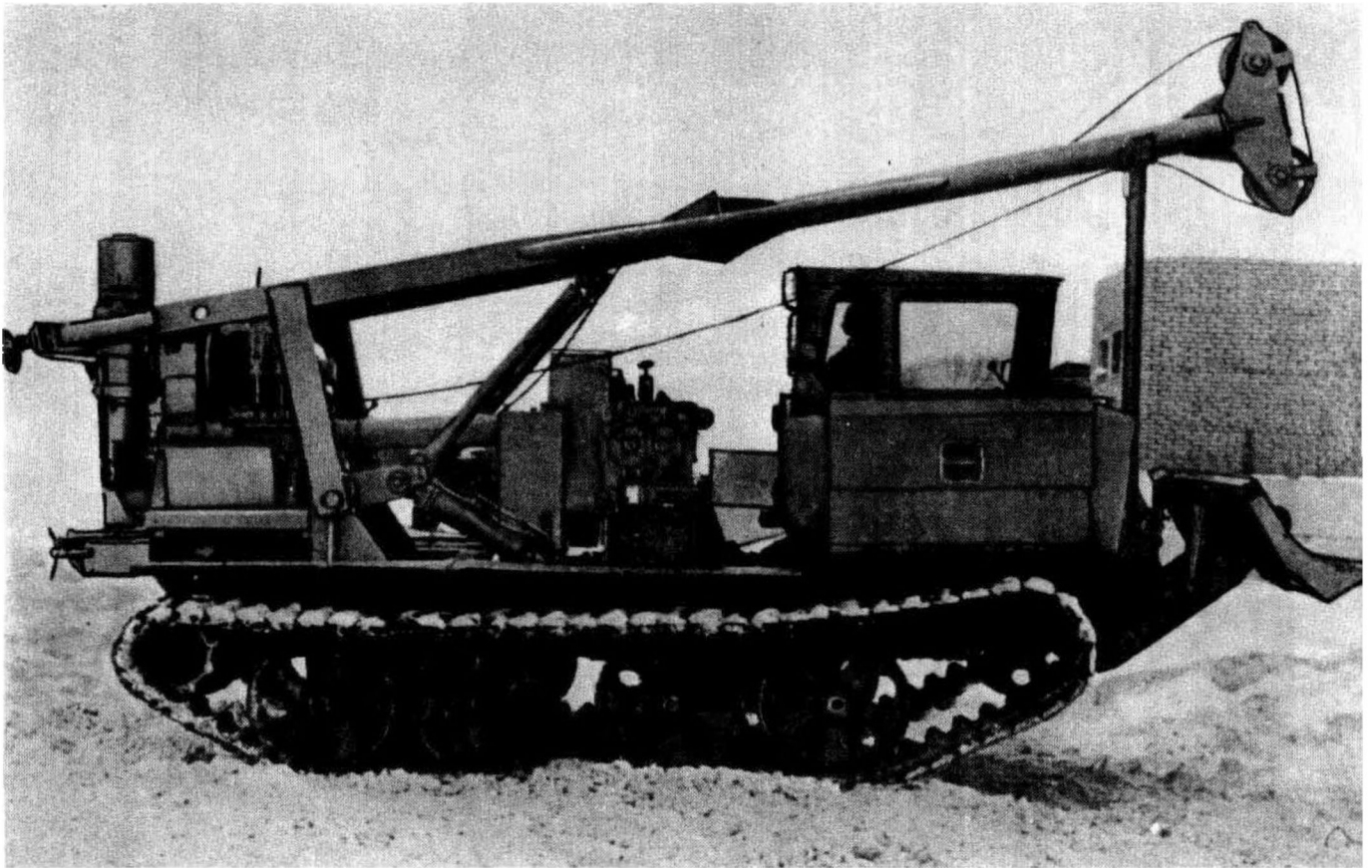


Fig. 47.4. CBA-500 drill rig mounted on caterpillar

If hard rocks have to be cored, *core drilling* is used. The core drilling or boring is done by a continuous rotational process using a mechanically driven rotary rig. The cutting tool is a bit into which teeth are fitted from a hard material such as pobedite or stellite. If a particularly hard rock must be cored, diamond bits are used.

Drilling mud pumped into the drill hole is used in core boring.

There is a tendency in these last years to drill large diameter (1-1.5 m) bore holes thus extracting rock cores of large diameter (Fig. 47.5), which permits a more detailed investigation of the material.

Sometimes (in the absence of water or using a well pump for removal of water) an observer may be lowered in a cradle down a large-diameter bore hole.\* This would permit the *in situ* observations of the conditions of occurrence of rocks to be made and photographs to be taken.

Core boring yields more or less long rock samples called *cores* (Fig. 47.6) that give a good idea of the rock drilled.

---

\* Men are known to have been asphyxiated in unvented deep test pits owing to the lack of oxygen (D.P. Krynnie and W.R. Judd, op. cit., p. 241 ff).—*Translator's note.*



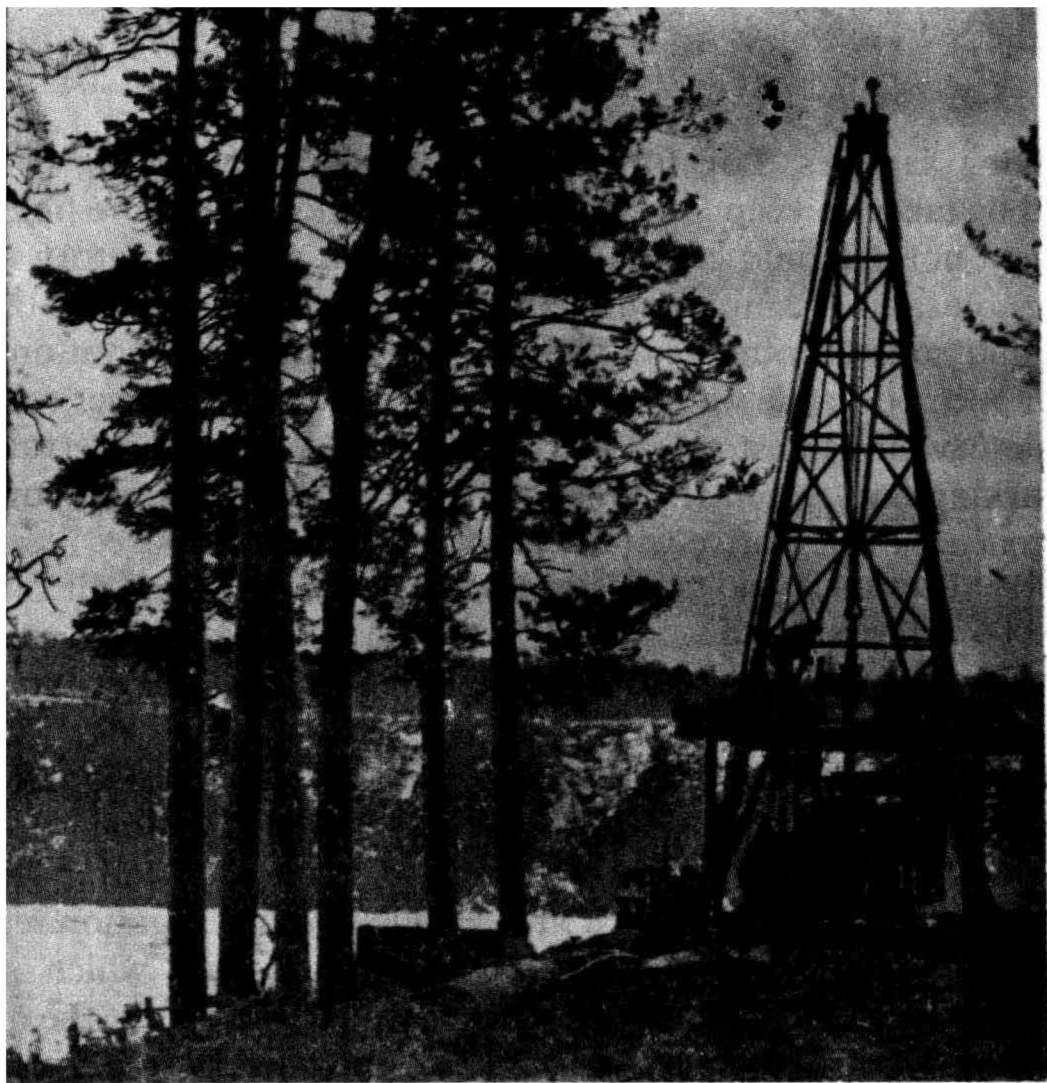
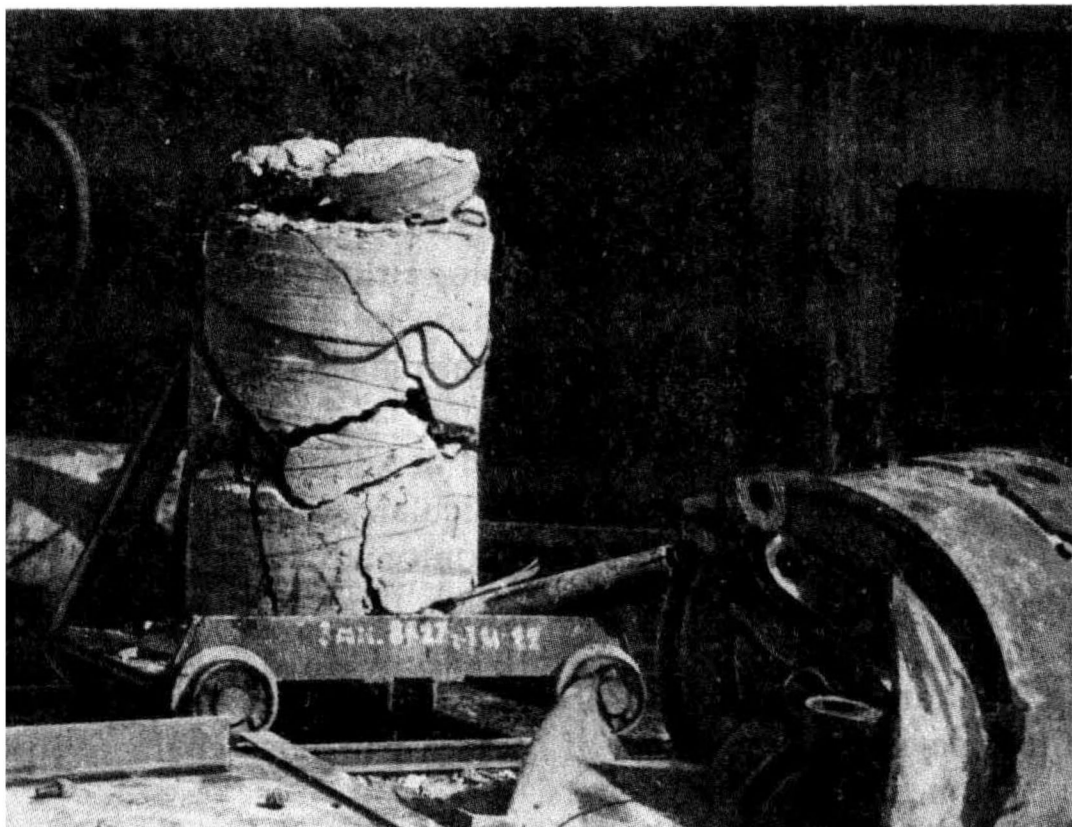


**Fig. 47.5.** Core drilling of large-diameter bore holes



**Taking samples. Log forms.** As an exploratory boring is made care should be taken to keep field notes (test pit field notes, bore hole logs etc.). The field notes should contain all the data on the exploratory working or boring, on taking samples and cores, field determinations of the types of rocks and soils encountered. They should include the elevations at which water appeared or the water table was encountered and other relevant data. When excavating a test pit, a shaft or an adit, at regular intervals sketch in the working and record the characteristics of the rocks and conditions of occurrence or, alternatively, take photographs.

All soil samples and rock cores recovered from a test pit or bore hole should be described and stored in specially designed sample boxes. Samples should be taken at each of the successive soil strata and at intervals of at least 50 cm. Undisturbed samples recovered by using drive samplers are paraffined to rule out dessication and are delivered to a laboratory with a relevant certificate.

**Investigation reports.** The data obtained by engineering geology investigations should be presented in a technical or investigation report. Such a report prepared with one degree of detail or another, which is governed by the stage of designing work, should adequately interpret the data on the stratigraphy and engineering properties of the particular construction site.

The investigation report should contain chapters presenting the following data:

(1) the local conditions (landscape, orography, climate); (2) conditions that may disturb the overall stability of the construction site (seismicity, landslides, karst phenomena etc.); (3) the geologic features and tectonics of the given locality; (4) the lithologic composition of the foundation soil of the structure being designed; (5) the hydrology of the area; (6) the results of laboratory tests; (7) the recommended design characteristics; (8) the data on events relating to engineering geology that have been detected on the construction site or that are likely to occur during the construction and operation of the structure; (9) principal remedial measures to be taken to correct the above events.

The investigation report should be accompanied by pertinent tabular and graphic materials. These, in particular, should contain geologic and hydrogeologic maps (the latter with contour lines).

An essential part of the investigation report are geologic logs of bore holes and profiles (Fig. 47.7) that are prepared for a number of directions. These facilitate interpretation of the geologic structure of the subsurface, its lithologic composition, age of rocks, their index characteristics, regime and location of subsurface waters.

Figure 47.8 represents a form of a geologic log of a bore hole. Each log,



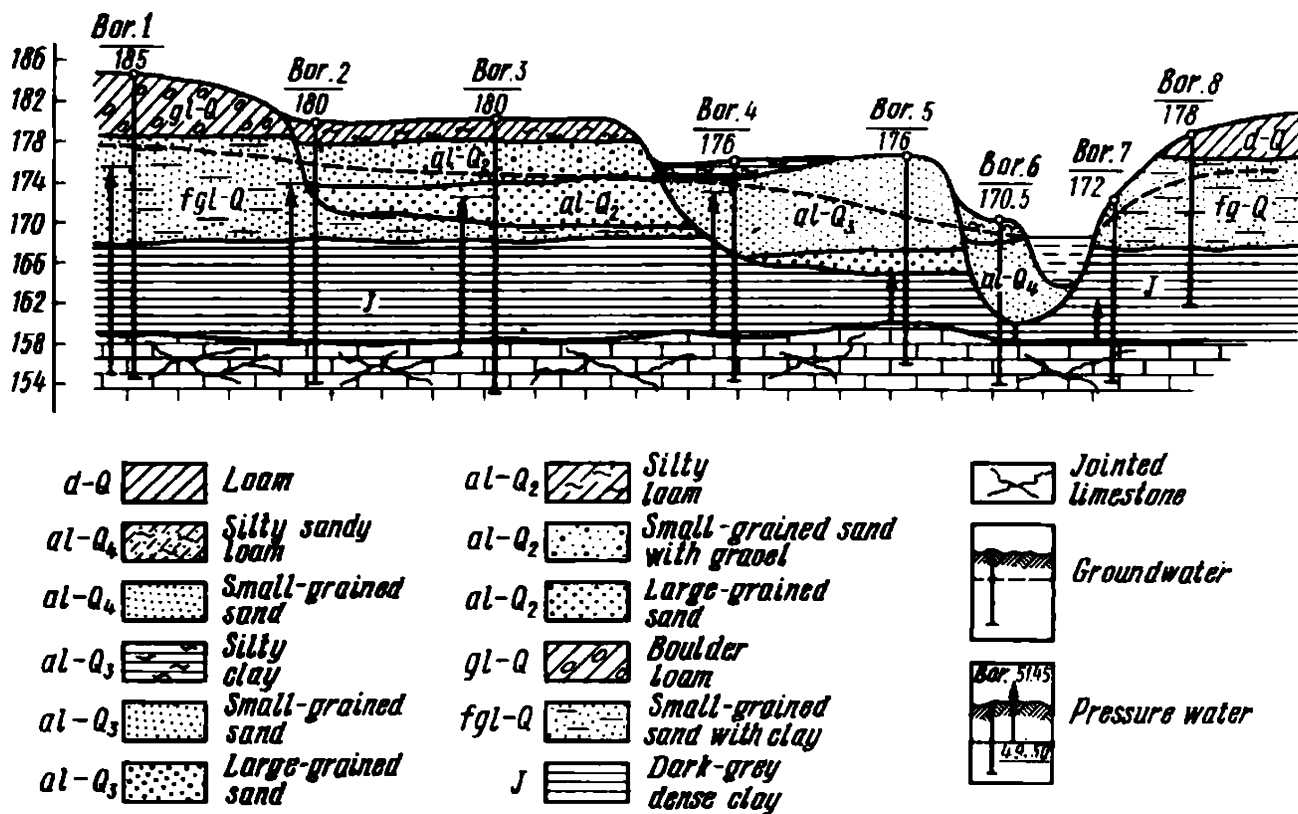


Fig. 47.7. Geologic lithologic section of overburden

Elevation of mouth of bore hole 85.4 m					Initial $d=127\text{mm}$ Final $d=89\text{mm}$		Description of rocks
Geologic age	Depth of foot of layer, m	Elevation of foot of layer, m	Thickness of layer, m	Lithologic section, water-bearing property	Level of appearance of water	Location of sampling	
$l-Q_4$	2	83.4	2		84.6	84.6	Powdered fine-grained sand
	4.4	81	2.4		82.2		Medium-clay content soft plastic loam
$gl-Q_2$	10.4	75	6		75		Moraine-heavy loam with gravel, shingle and boulders, heavy plasticity
$fgl-Q_2$	12.4	73	2				Various grain size sand with gravel and shingle
$J_2$	16	69.4	3.6				Black micaceous clay, semihard consistency
	16.5	68.9	0.5				Small-grained micaceous sand

Fig. 47.8. Geologic log of a drill hole

apart from the above data, should indicate the locations where samples are taken.

**Preliminary surveys for highways** have some specific features. It should be first of all made clear that adequate and timely surveys aid in the decision-making when designing and constructing a highway. Conversely, most faults found during the operation of a highway generally result from poor quality of the preliminary survey.

An obligatory element of such exploratory work is the study of the engineering properties of soils in the corridor that is 100-200 m wide on either side of the highway alignment. Apart from determinations of soil varieties, their properties, mode of occurrence, groundwater conditions much attention must be called to the assessment of geodynamic processes likely to present a hazard to the structure being proposed.

*A feasibility study* of the construction of a highway involves a spectrum of data that give a rough idea of the local natural conditions. A major role is played at this stage by reconnaissance of all complicated sections of the highway alignment (sites of river and valley crossings, areas prone to landslides etc.).

*A detail design stage* includes items to be determined for preparation of a detail design. *A contractor design* calls for exploration of individual sections of the highway that need to be studied in more detail.

For one version or another to be validated, additional, more detailed geotechnical studies are necessary so that the geologic conditions of characteristic sections of the alignment could be understood by referring to a large-scale map and a geologic section obtained by a detailed engineering and geological survey. Use should also be made of instrumental observations to study subsurface water conditions and creep deformations in the course of time, and to investigate properties of red (or brown) clays.

Engineering and geologic reconnaissance work makes use of the same techniques that have been listed above (shallow pits; test pits; bore holes; vibration drilling, presenting a new efficient method etc.). The results of this exploratory work are totally documented by bore hole logs, geologic logs, a plan of bore holes, geologic sections etc.

Figure 47.9 is an example of the graphic representation of the data obtained by geotechnical studies of a section of a highway. These materials all make part of a technical report covering the conditions of construction of a roadbed and containing all the data pertinent to the project.

Soil samples are tested in a laboratory to evaluate their engineering properties. Such tests are made by the use of pressuremeter probes, static and dynamic sounding methods, radiometry and others. For the description of these methods the reader is referred to pertinent manuals and instructions.



**Preliminary surveys for airports and airfields** have much in common with geotechnical studies for highway construction. This is especially so since airport construction necessarily involves the construction of roads. These operations, however, have some specific features, especially, when unpaved airfields are involved. In such cases, apart from common geotechnical studies, soil, geobotanic and agrotechnical investigations should be conducted with different degree of detail.

The objective of *soil investigations* is to determine the types of soil, their physicommechanical and chemical characteristics. Moreover, determinations of their granulometric composition, colour, moisture content, structure, density, stratification, inclusions etc. are needed.

*Geobotanic investigations* are performed to study grass vegetation so that the most tolerable and stable sod forming grass species are identified.

*Agrotechnical investigations* study conditions of sod formation. These investigations are carried out in conformity with acting instructions and manuals.

### Sec. 47.3. Special Types of Geotechnical Studies

The most common of these are aerial photography, geophysical methods of investigations and determination of physicommechanical characteristics of soils by sounding and vane shear tests.

Aerial photography and geophysical methods of investigations are auxiliary operations that must be used jointly with excavation of test pits or exploratory borings.

**Aerial photography.** Aerial photography or photogrammetry is advantageous for construction of roads and bridges when it is desired to locate a highway alignment and select the best site for a river crossing.

Aerial photographs are taken by using aerial cameras mounted on planes or helicopters. Such planimetric images of the terrain give an idea of the relief, vegetation, soils and other landscape features of the particular locality. Aerial photogrammetry is an effective means of dealing with geodynamic processes. Aerial photographs are particularly useful for studies of the *local landscape*. The method of landscape geological investigations relies on the assumption that the landscape of a given locality or region mirrors the planimetric arrangement of the underlying soil layers. It is implied that the appearance and form of the landscape are governed by environmental conditions, local geology and modern tectonic processes.

Interpretation of aerial photographs is a complex operation. There are special instructions and manuals which must be followed for the purpose in mind.

The most common *geophysical methods* of geotechnical studies are *the*

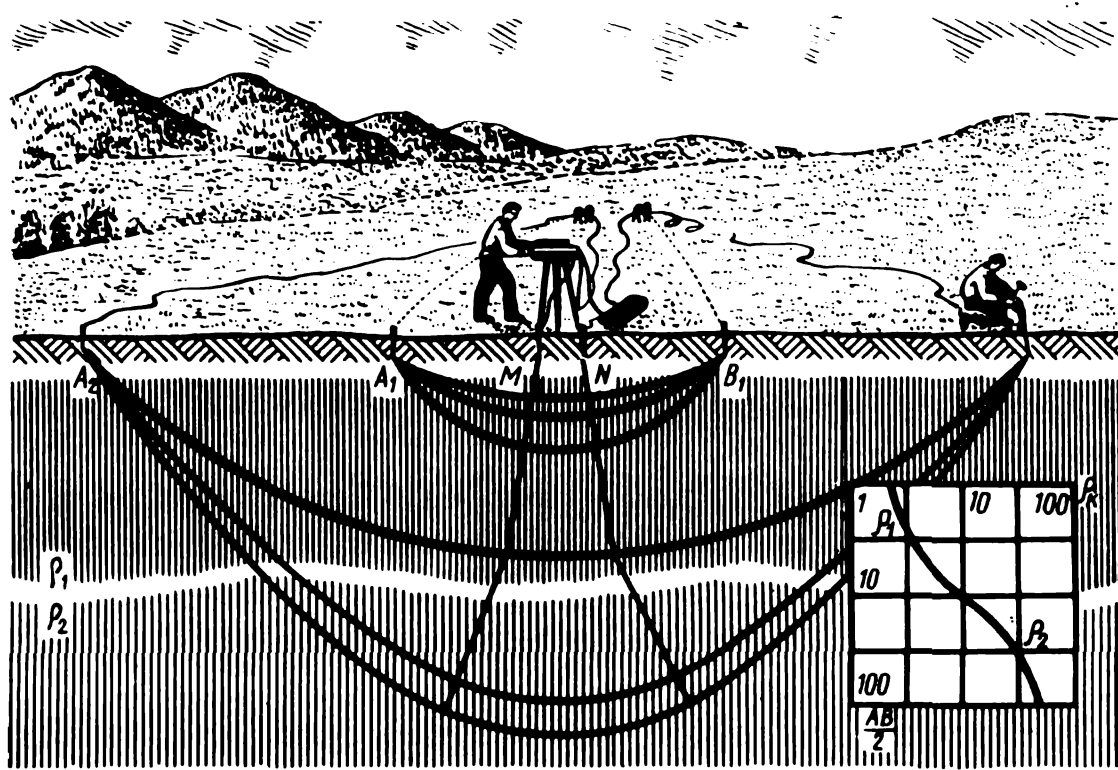


Fig. 47.10. Electrical-resistivity field method

*electrical-resistivity field method and the seismic refraction method.* Geophysical methods are very promising largely because they permit the evaluation of the geologic conditions of the given locality, character of rocks, degree of their soundness, deformability, mode of occurrence, position of the surface water table etc.

The electrical-resistivity method is used for exploration of the upper crustal layers. It is based on the different resistivity of rocks to an electric current passed through them. The electrical resistivity is mainly governed by the mineralogic composition of rocks, porosity, saturation and mineral content of subsurface waters.

Geotechnical investigations for large bridges extensively use the electrical-resistivity method. It is advantageous for locating and contouring deep river valleys of ancient origin, for determining the depths and mode of occurrence of bedrock materials, for detecting and contouring caverns in rocks etc.

Electrical sounding uses two electrodes set into the ground and an electrical field whose configuration and parameters can be varied by changing the distance between the electrodes (Fig. 47.10). The parameters of the resulting electric field are interpreted accordingly identifying elements of the geologic section that differ in electric properties. By referring to the specific electrical resistivity of the rocks composing the particular section a chart is plotted from which a geologic profile is prepared.

Consequently, the method of electrical sounding makes it possible to determine the sequence of rocks at a given point in a vertical direction, therefore this method has been called electrical drilling. By contrast, the fixed depth resistivity measurements along a line, a method, called electrical trenching, makes it possible to compile a geologic section along a given traverse horizontally.

The advantages of *seismic methods* of geophysical exploration are particularly obvious when it is necessary to determine the geologic structure of a locality involving hard rocks, particularly, for establishing the mode of occurrence, conditions and mechanical properties of rocks (modulus of deformation determinations). This method uses the different velocities of seismic waves travelling in different media. Seismic waves are sent into the ground by explosions of small charges or by the impact of a heavy drop hammer.

Other methods of geophysical exploration, including the radioactivity method, are relatively seldom used in civil engineering and only for solving special problems. In addition, their accuracy, conditioned by many factors, is generally less than desired.

That is why aerial photogrammetry and geophysical methods should be considered as most attractive techniques that are best employed jointly with test pits and test bore holes.

**Vane shear tests in bore holes** are very useful especially when testing soft clayey soils undisturbed samples of which are rather difficult to recover.

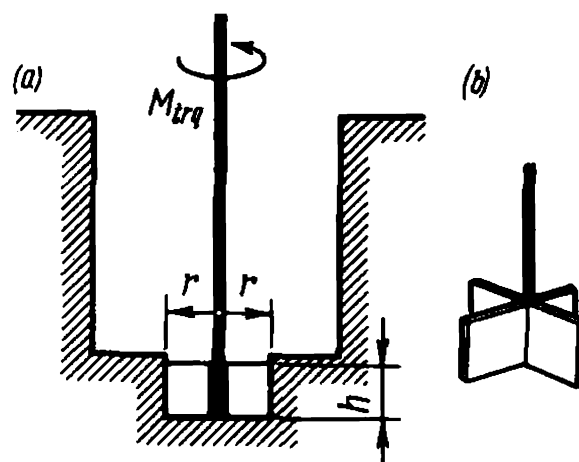
This method has been developed by now, such that it is currently possible to determine not only shear parameters of soils (angle of internal friction and cohesion) but others as well. The OBC-3n device designed by N.M. Smurov and Yu.R. Perkov which is finding ever greater use in highway engineering is of interest. Unlike other similar devices, this apparatus makes it possible to cut the soil at the contact of the surface of rotation. The device can determine the strength characteristics of soil (true angle of friction, total cohesion, apparent and true cohesion) in field conditions of occurrence or when the soil sustains a load.

The working tool of the testing device of classical design (Fig. 47.11) is a two- or four winged *vane*. This is forced into the wall of a test pit or bore hole and then is made to rotate. By knowing the force applied to the vane rotated in the bore hole it is possible to calculate the shearing strength of the soil in  $\text{kg/cm}^2$ :

$$s = \frac{M}{1.57d^2(h + d/3)} \quad (47.1)$$

where  $M$  is the torque;  $d$  is the diameter of the vane casing (in Soviet-made instruments  $d = 5.5\text{--}7.5$  cm);  $h$  is the height of the vane casing (in Soviet-made instruments  $h = 11\text{--}20$  cm).

Fig. 47.11. Vane shear test  
a—vane; b—detail



**Soil testing by sounding methods.** If the foundation of a structure is provided by a naturally occurring soil mass, the permissible load is governed by the density or consistency of the soil.

Direct determinations of soil density and consistency by laboratory tests use samples taken in a test pit or bore hole.

The determination of the field moisture content of soil presents no problem since the original soil structure needn't be preserved. To determine the field density of a loose soil is more difficult. To take an undisturbed sample of, say, sand is only possible when it occurs above the groundwater table. Even so the operation is time-taking since exploration concerns a vast area and considerable depths.

Due to the difficulties presented by direct determinations of density and consistency of the aforementioned soils numerous efforts have been made to use indirect techniques. These include *the sounding* (penetration) *method*, and radioactivity methods. The latter, however, are very rarely employed in civil engineering investigations due to their specificity.

Sounding uses a drive cone point forced into the ground. In this country cones 36 and 74 mm in diameter with the opening angle  $60^\circ$  are used.

The sounding method is an indirect technique of exploration, i.e., the results of sounding make it possible only to judge of the relative density of soils and their sequence in a vertical direction. As to the necessary geotechnical characteristics of soils, the data obtained by sounding are interpreted by referring to the definite correlation between the composition and condition of soil on the one hand, and the resistance offered by soil to the penetration of the drive point.

There are two large groups of sounding procedures, static and dynamic. In the static methods the sounding rod is pushed into the ground by static loading. In the dynamic methods the rod is driven by the impact of drop hammers.

*The static sounding technique* is generally used for soft soils without inclusions of large rock fragments. A hydraulic jack or a chain hoist etc. is

commonly employed for forcing the rod into the ground. The properties of soil in natural conditions of occurrence are determined by the depth of penetration of the conical point into the soil at one load or another.

The specific static reaction of the soil,  $\omega$ , in  $\text{kg/cm}^2$ , is correlated with the penetration of the conical point into the ground through this relationship:

$$\omega = Q/F$$

where  $Q$  is the static reaction;  $F$  is the cross sectional area of the conical point.

According to the findings of the Foundation Engineering Research Institute, the density of sands of one grain size or another, apart from the value of  $\omega$ , is governed by the sounding depth. So, if  $\omega = 90 \text{ kg/cm}^2$  at a depth 10 m, small-grained sand may be considered as being dense. On the other hand,  $\omega = 20\text{-}50 \text{ kg/cm}^2$  for a clayey soil suggests stiff plastic consistency.

*The dynamic sounding technique* uses a rod with a drive point which is driven into the ground by means of a drop hammer or a sampling spoon. The results of the dynamic sounding are much more difficult to interpret compared with static sounding, since the depth of penetration of the conical point is conditioned by the weight of the drop hammer, the height from which it is dropped, the weight of the conic point and its friction against the ground. By referring to the data of dynamic sounding tables have been prepared showing the relationship between the specific penetration resistance (or number of blows for penetration of the point by a few centimetres) and density of sand, modulus of deformation and consistency of clayey soils.

**Field tests and observations.** *Testing the bearing capacity of soils.* Taking samples for laboratory tests inevitably involves disturbance of the natural structure of soil. The natural density and apparent cohesion of a loose soil, say, sand are totally disturbed in this process.

The density of a loose soil under natural conditions of occurrence is very hard to determine and only approximately. The strength of most clayey soils is largely governed by inner bonds, particularly, true cohesion,  $c_s$ .

As samples of clayey soils are taken from a soil mass their cohesiveness is more or less disturbed. For this reason the shearing resistance of a soil which is one of the principal factors responsible for the bearing capacity of soil can be found by laboratory tests only approximately, the errors generally attaining appreciable values.

Apart from that, as has been repeatedly pointed out, determinations of the strength and critical stability of a soil from theoretical premises, by using formulae, cannot be much relied upon. Therefore, when designing an



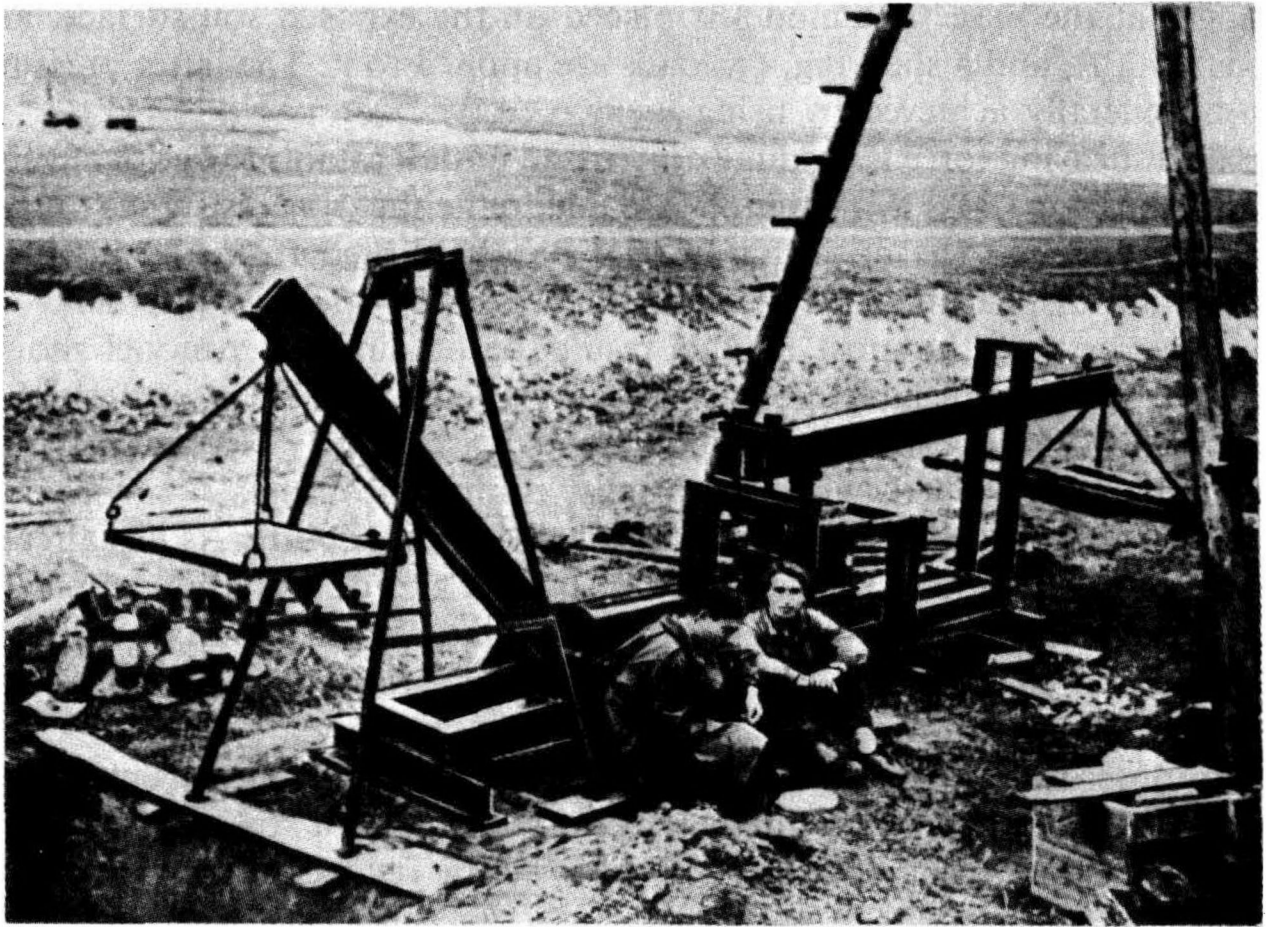


Fig. 47.12. PTIC-1 installation for shear tests of large-size undisturbed soil samples. Designed by M.I. Shmakov of the Gidroproekt Institute

important structure, control field tests often have to be made. These include *in situ* investigations of the foundation material so as to minimize computational errors.

Field tests with this purpose in mind fall into two main categories: (a) determinations of the shearing resistance of soils, and (2) tests to check on the design data when establishing the critical bearing power of the foundation of a structure.

Field tests to determine *the shearing resistance of soils* can, in turn, be divided into three groups: (1) shear tests of large undisturbed soil blocks and rock pillars left standing in an open pit or working; (2) shear tests of models of structures on the upper surface of a soil mass; (3) determinations of the strength of soil by indirect techniques.

What makes shear tests of rock pillars specific is that they require large-scale field operations where textural and structural features of the soil remain unaltered, such as to exclude laboratory tests. Such shear tests make use of special installations (Fig. 47.12).

Shear tests of models are, to a certain degree, of universal character. The model generally represents a concrete block that may differ in size with

flanges at the base. The model is placed on the exposed soil surface, and a vertical,  $P$ , and a shearing,  $Q$ , loads are applied to it. The latter pressure,  $Q$ , is generally achieved by using jacks.

The shearing force is gradually increased until it attains the critical value of the shearing stress,  $\tau_{cr}$ , taken to be equal to the shearing resistance of soil,  $s_p$ . The onset of the critical state can be established from the incipient horizontal displacement of the model recorded by special equipment.

In order that the most reliable results be obtained, the model should possibly have appreciable dimensions (1 by 1 m or more). If it is desired to determine shearing characteristics,  $\varphi$  and  $c$ , separately, several different loads must be applied, which, naturally, complicates tests.

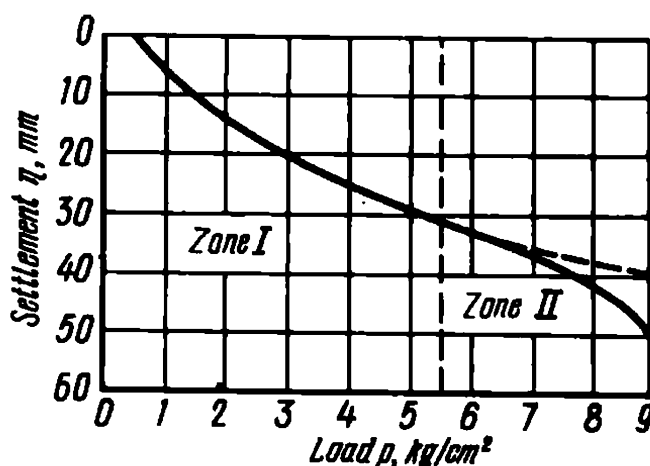
**Tests and observations to determine soil compressibility.** As has already been repeatedly noted, forecasts of settlements and deformations of structures are generally far from being very accurate. This is mainly accounted for by the disturbance of the natural structure of soil as soil samples are taken from the soil mass.

In order to avoid the disturbance of soil when important structures are involved, care is taken to estimate the compressibility of soil and determine the needed index characteristics *in situ*, i.e. in field conditions, without recovering soil samples from the soil mass. For this, a test pit is excavated at the proposed building site. Then, a bearing plate of a definite size is placed at the level of the layer of interest to us. By using special equipment a certain load is applied to the plate increasing this latter until the load is equal to the design, or even somewhat greater, magnitude. Observations of the settlement of the bearing plate should be conducted throughout the test. The next step is to plot graphs showing the relationship between the settlement of the plate in the course of time and the load transmitted to it. By referring to these graphs it is possible to determine the settlement of the plate under a given load until the settlement is completely discontinued.

Attention should be called to the fact that the determined settlement of the bearing plate may include not only the compaction-induced settlement of soil what is of most interest to us but also that due to the squeezing of the soil from beneath the bearing plate (arching). Clearly, such indeterminate settlement is of no use for the forecast of a likely settlement of the structure manifesting a fairly large foundation preventing the subsoil from arching. Hence it is necessary to make this test with a trial load such as to avoid plastic events and such that the measured subsidence of the bearing plate would only indicate the settlement of the soil due to compaction induced by the normal stresses.

In the general case this condition calls for the use of fairly large plates with sufficient penetration into the ground and fairly slow rate of growth

Fig. 47.13. Chart for determining soil compressibility at trial load. Dashed section of curve illustrates a hypothetical settlement in the absence of plastic events in soil



of load in the course of time so as to avoid harmful effects of the above events.

Tests with trial loads make use of a standard plate 5 000 cm<sup>2</sup> (70 by 70 cm) in area. Larger-size plates may be used if greater loads are applied. Bearing plates less than 50 by 50 cm in size should not be used. After the bearing plate and loading device have been installed it is best to fill the test pit by soil completely. This provides the most advantageous conditions for increasing the stability of the soil under the bearing plate against possible arching.

The observational data on the settlement of the bearing plate stabilized under one load or another are used, when needed, for plotting a diagram showing the relationship between the settlement of the plate and the magnitude of loading. Figure 47.13 illustrates such a diagram. Zone I is characteristic of the process of the ever increasing soil compaction which is evidenced by a somewhat lowered increment of the settlement of the bearing plate with increasing the load. Zone II manifesting a new increase in the settlement and greater rate of its increment corresponds to failure of the soil and arching from beneath the bearing plate. Therefore, when analysing the likely settlement of a structure being designed, no consideration is given to the section of the curve in zone II.

Thus the modulus of total deformation should be determined only for the section of the deformation (plate settlement) curve that corresponds to the phase of compaction of soil.

The observed results make it possible to establish moduli of soil compressibility necessary for calculating the possible settlements of structures. The modulus of compressibility,  $E_p$ , is calculated by referring to the familiar relationship for the settlement of a square rigid loaded plate on the side  $B$ :

$$E_p = 0.88(1 - \nu^2)pB/\eta_{in}$$

where  $E_p$  is the modulus of compressibility or total deformation in  $\text{kg/cm}^2$ ;  $p$  is the total load on the bearing plate in  $\text{kg/cm}^2$ ;  $B$  is the side of the plate used for the test (for a plate  $5\,000\text{ cm}^2$  in area  $B = 70\text{ cm}$ );  $\eta_{fin}$  is the final settlement corresponding to a load  $p$  in  $\text{cm/m}$ ;  $\nu$  is the coefficient of lateral deformation (Poisson's ratio) taken for sands and sandy loams to be equal to 0.3; for loams and plastic clays 0.35 and 0.42, respectively; for dense clays 0.20.

The design value of  $E_p$  is assumed to be equal to its average value obtained by several tests of one and the same soil layer.

Given the value of the modulus of compressibility  $E_p$  at a load  $p$ , it presents no problem to find the modulus of settlement or relative deformation  $e_p$  corresponding to this value of  $E_p$  by using the relation

$$e_p = 1\,000p/E_p \quad (47.2)$$

The modulus of compressibility  $E_p$  is only determined for the compaction phase.

It should be finally noted that a trial load used in testing for immediate determination of the magnitude of settlement of a structure at a given load without taking into account the size of the structure in terms of  $E_p$  (or  $e_p$ ) would lead to appreciable error.

It is best to obtain data on the evaluation of the compressibility of the overburden by analysing the findings on settlements of structures built under identical conditions. The values of  $e_p$  and  $E_p$  can then be found by calculations. The above characteristics will be average for a structure of conspicuous size supported by a stratified soil mass.

**Main principles of the rational organization of civil engineering investigations.** Engineering geology and soil mechanics, being interrelated as theoretical and practical disciplines, possess an impressive body of formulae able to solve all problems that are posed when building engineering structures even under the most unfavourable natural conditions. However, in order to obtain the optimum results, civil engineering investigations should be conducted taking into account all relevant requirements.

The fact that the local geology should be adequately studied before designing an engineering structure is validated by construction practice. A convincing proof of this is to be found in the numerous failures resulting from disregarding this condition. It does not make it necessary, however, to have too many exploratory borings of conspicuous depth at a building site. Regrettably, geologic sections, which are invariably needed, are often plotted by referring to the data obtained from such exploratory borings using elementary construction ("geometric geology").

It should be made clear that exploratory borings must be sited such as

to determine local geology and geologic features of the subsoil of the structure being designed relying on overall analysis of the region. A major role is played here by geologic surveys with the intent to establish conditions of formation of the particular geologic structure, facies of sedimentary rocks, and, necessarily, to determine what tectonic disturbances have occurred at the site of interest to us.

Viewed in this context, test pits and exploratory borings generally provide means of control which are needed to verify the overall picture made possible by analysing the data of geologic exploratory work. Clearly, this approach could make it possible to appreciably reduce the number of requisite test pits and exploratory borings and, concurrently, to enhance the accuracy of geologic maps and sections needed for designing a structure.

As follows from the theory of the state of stress of the foundation soil of a structure, its bearing capacity can be established by studying the geologic structure of the underlying strata, often to a conspicuous depth. Once the geologic features are known, especially when the natural mode of occurrence is disturbed, the depth of exploratory borings, if properly spaced, may be dramatically decreased. The same lines must be followed when drilling bore holes for taking soil samples to be tested in laboratory.

When analysing the hydrology of the building site, care must be taken to find the position of the groundwater table. If the groundwater table is close to the ground surface, it generally presents quite a problem to build the foundation for the structure in hand. Conversely, the low position of the water table, even if during a brief seasonal period, may prove advantageous for the above operation. Regretfully, insufficient attention is called to these points. We often fail to take into account the fact that the groundwater table may appreciably fluctuate from season to season and that it settles, after an exploratory boring has been drilled, fairly slowly. Therefore we must not be satisfied with establishing the groundwater table during the drilling process, to say nothing of the moment it is discovered. Several exploratory borings should be left for permanent observations of the groundwater table.

Valuable data on the seasonal variations of water level in the wells can be obtained from local residents. In the given case, however, these data must be referred to the water bearing horizons of interest to us. It is necessary to record the groundwater table in the bore holes some time after the drilling to allow the water level to settle down.

One of the most important aspects of civil engineering investigations is the determination of the possible action on the structure being designed of one or more geodynamic processes, such as seismicity, creep phenomena, karst, mud rock flows, erosion and others.

When conducting a geologic survey, it is always necessary to establish

whether there exists a possibility of such phenomena and to determine the degree of the risk for the structure in hand. This may possibly call for computations, e.g. of creep phenomena. However, many relevant data may also be obtained from a geologic survey.

Such an approach to the problem is the more important, since the risk of one type of geodynamic phenomenon or another to the structure may be avoided or appreciably decreased by relocation of the structure being proposed to a safer place. This is true for the selection of the centre line of a bridge if river banks are prone to landslides or erosion (scouring of river banks).

Clearly, if a structure being designed will be sited in an area whose seismicity is envisaged by relevant building codes, account should be made of the inevitable effect of seismic events on the structure. It should be noted that such a characteristic is only approximate, being averaged for the particular area. When local seismicity rates are determined, the value of the design intensity may prove to be 1-2 force numbers higher or lower which, naturally, will appreciably affect the value of seismic acceleration and seismic constant. When conducting a geologic survey which in the particular case will be very much like a civil engineering investigation the above circumstance makes it necessary to verify the design acceleration of the seismic vibration and most advantageously locate the planned project so as to minimize the effect of seismic events on the structure. The most convenient foundation would be provided by hard rocks, the least stable by swamp and silt deposits. If the subsoil should contain strata of loose saturated soils, the foundation conditions may become hazardous. In this case it is important that the position of the groundwater table at the building site be high. The determination of the design value of acceleration may be much facilitated by the inspection of destructions or damage in structures induced by seismic events. Consulting local residents may also prove useful.

Special attention must be called to the most suspicious areas, such as those adjacent to canyon walls or even fairly steep, to say nothing of submerged, slopes. It should be borne in mind that such areas are most liable to landslides during an earthquake.

The risk of slides in the general case should also be dealt with along the same lines and in the same order. It may prove useful to recall the three most important categories of slopes and hill sides (cf. Chap. 44):

*failure by rupture slopes* which are generally in a state of limiting equilibrium;

*denudation slopes* that manifest a large margin of stability;

*accumulation or talus slopes* which are commonly in a state of equilibrium.

Clearly, slopes of failure by rupture should never be used for location of foundations of structures.

Civil engineering investigations should pay particular attention to the character of river bank slopes where a bridge is being planned. Even minor symptoms may give important information. These include slide-induced scars on the topsoil, river bank erosion, tilted trees and telegraph poles, disturbed fences and deflected paths etc. Such indications unambiguously point to the inappreciable stability of the river bank slope from which fact appropriate conclusions may be made.

When a road or bridge is to be planned in mountainous country, civil engineering investigations should take into account the hazard of mud rock flows.

Apart from a survey of local residents which is invariably essential at this stage of investigations, make sure to inspect flood-land areas and river channels for rock fragments, spalled material, collapsed bridges, structures or others.

In the areas of occurrence of carbonate, to say nothing of sulfate (gypsum or anhydride), rocks civil engineering investigations must establish if karst phenomena (solution channels) may take place there. Such events can be evidenced by various tectonic disturbances, such as sink-holes, caves, caverns etc. A specific feature of karst topography is the general aridity of the area induced by the disappearance of bodies of surface water, streams and others.

It goes without saying, the geologic surveys or civil engineering investigations are unable to solve the aforementioned and similar problems. It is only skilled specialists that are capable of adequately analysing such events, once these have been disclosed by preliminary studies. In particular, all suspicious slopes and hill sides should be studied at the subsequent stages of exploratory work by referring to techniques of stability computations.

These latter require design characteristics of the soil varieties that have been encountered. It is not uncommon that mechanical properties, such as strength of deformability of rocks encountered, are characterized without relating them to the particular structure which is being designed. This practice should be warned against. The behaviour of soils in the foundation of or in the structure itself (say, a roadbed) may vary from job to job so much that without referring it to the given structure (e.g. in terms of load, scale, water regime, time) one would have to make too many unnecessary investigations, concurrently omitting ones that should necessarily be made. Such investigations, with some reservations, must have direct bearing on the structure being planned.



Determinations of design characteristics of mechanical properties of soils (strength, deformability) require undisturbed samples. These are generally available in limited quantities. Therefore it seems reasonable to relate them to Class Two index characteristics of soils by referring to soil composition and state. This stems from the property of soil to vary from point to point and the necessity to determine Class One design characteristics including mechanical properties, allowing for the generally large spread of experimental determinations. That is why it is necessary, whenever feasible, to have as many Class Two determinations as possible, at least those relating to moisture content, plasticity number of clayey soils and granulometric composition of granular soils, not omitting a single test or bore hole.

In fact, the same is true of the proportion between laboratory and field tests. No doubt, soil samples are delivered to laboratory, generally showing some disturbance in structure, decompressed to some degree and additionally wetted in the course of sampling. Therefore *in situ* bearing plate tests are better compared with laboratory investigations. The former, however, are very costly and labour-consuming, so the number of field tests is very small.

In view of the inevitable spread of experimental determinations the above circumstance prevents us from finding design characteristics of, say, soil strength relying only on the field test data. Of particular importance are data of laboratory tests that may be used for numerous determinations of, say, Class Two index characteristics of disturbed soil samples. Then field tests play the role of control tests for correlating index characteristics referred to composition and state characteristics of soils as obtained by investigations to the data of laboratory tests involving identical index characteristics.

All these remarks are valid for determinations of characteristics of soil deformability as well.

Note that disturbed soil samples often cause deformability characteristics of soils to be much exaggerated. This fact should be corrected by previously compacting soil samples at load equal to field pressure (before water is supplied to the compression machine) or by determining the value of the compressibility of the soil sample at load referring to the weight of the moisture removed from the sample.

## Conclusion

It can be seen that, whenever an important road structure is being designed, we must take into account a number of natural factors that are likely to affect the stability and strength of the structure to be constructed.



It should be the principal objective of all civil engineering investigations to disclose the possible role played by one geodynamic process or another in the operation of structures to be planned and the environmental protection. If such factors are taken into account in due time it will be possible to protect a structure from the possible harmful effects of the above events or ensure its normal service at minimum cost by using requisite protective measures.

Clearly, all the geologic features of a structure foundation should be adequately studied as hydrophysical and mechanical properties of soils and rocks composing the foundation. Disregarding these conditions and requirements may cause detrimental consequences.

We hope that the present book will be of use not only to college students but also to the beginning civil engineers in their practical work.

## SUBJECT INDEX

- Abrasion 445
- Accumulated frequency 172
- Accumulation terrace(s) 435
- Active earth pressure 342
- Active force(s) 356
- Active zone 288
- Aerial photography 532
- Amount of ice 396
- Andesite(s) 45
- Angle of dip 76
- Angle of friction 120, 143
- Angle of repose 135
- Angle of shearing resistance 146
- Anhydrite 61
- Anticline 26
- Archimedean principle 208
- Argillaceous schist(s) 63
- Argillaceous soil(s) 368
- Arrhenius's hypothesis 39
- 
- Barchanes 407
- Basalt 52
- Base-level plain 428
- Batholith 47
- Bed 75, 76
- Bench 435
- Berezantsev's formulae 227
- Boulder(s) 438
- Boulder clay 387
- Brinch-Hasen method 363
- Buissmann's formula 337
- Buried peat 376
- 
- Calcareous schist(s) 63
- Cambrian 33
- Capillary fringe 90
- Carboniferous 33
- Chalk 59
- Chipping by subsidence 458
- Cleavage 64
- Coefficient of confidence 173
- Coefficient of consolidation 156, 235
- Coefficient of dynamic compaction 513
- Coefficient of elastic semiplace 299
- Coefficient of lateral pressure 271
- Coefficient of lateral strain 284
- Coefficient of natural density 380
- Coefficient of sliding 347
- Coefficient of static consolidation 246
- Coefficient of viscosity 328
- Cohesion 122, 153
- Colloidal ageing 124
- Colloidal water pellicule(s) 124
- Compression 155
- Compression curve(s) 155
- Comglomerate(s) 57
- Continental platform(s) 493
- Contraction 22
- Creep 483
- Cretaceous 35
- Crust 13
- Cutoff(s) 370, 444
- Crystalline foundation 16
- Crystalline schist(s) 63
- 
- Darcy's law 123
- Debris cone 413
- Decompression 155
- Decrease 157
- Deep slide 355

- Deflation 66, 406
- Deformation(s) 197
- Deformation joint(s) 83
- Degree of consolidation 237
- Denudation 66
- Denudation slopes 542
- Deposit(s) 65
  - continental 65
  - eluvial 400
  - eolian 70, 407
  - fluvioglacial 390
  - glacial 71
  - marine 65
  - talus 404
- Design indices 148
- Design values 170
- Devonian 33
- Diagenesis 55
- Diatomite 61
- Diorite 52
- Dipole(s) 122
- Dispersion 103
- Displacement of structure 352
- Dolomite 59
- Drainage-free area(s) 88
- Drainage ratio 92
- Drift theory 19
- Dry sand 115
- Dynamic sounding technique 536
- Engineering geology 13
- Eolian loess 70
- Epigenesis 55
- Equivalent layer method 312
- Erosion 66, 93, 424
  - head
  - lateral
  - retrogressive
- Established creep 327
- Eustacy 69
- Exaration 66
- Expansion 155
- Failure by rupture slopes 542
- Fault(s) 24, 79
  - step 24
  - thrust 27
- Field method 533
- Field test(s) 536
- Fissure(s) 81
- Flood-plain terrace 434
- Flow slide 462, 483
- Fragment(s) 400
- Frequency rate 172
- Gabbro 52
- Gaping 81
- Genesis 14
- Geodynamic processes and phenomena 369
- Geophysical methods 532
- Geosyncline(s) 73
- Geosynclinal areas 72
- Geothermic step 96
- Glaciation 38, 387
  - Dnieper 38, 387
  - Likhvin 38, 387
  - Valdai 38, 387
- Granite 50
- Gravel 438
- Groundwater basin 91
- Groundwater contour(s) 91
- Earthquake(s) 505
  - annihilating 505
  - catastrophy 505
  - destructive 505
  - fairly strong 505
  - feeble 505
  - major catastrophe 505
  - moderate 505
  - strong 505
  - unnoticeable 505
  - very feeble 505
  - very strong 505
  - weak 505
- Effusive magmatic activity 47

- Hansen's formula 127
- Hard rock(s) 367
- High-moor peat(s) 376
- Historical geology 28
- Homogeneous material(s) 465
- Hook's law 158
- Horizontal movement(s) 26
- Hydraulic pressure gradient 243
- Hydrostatic pressure 393
  
- Impervious rock(s) 368
- Increase 157
- Initial decompression 165
- Initial gradient 244
- Intercalation 75
- Interglacial stage(s) 39
- Investigating reports 528
- Investigation(s) 532
  - agrotechnical 532
  - geobotanic 532
  - soil 532
  
- Jointing 81
  - columnar 83
  - parallelepipedal 83
- Joint(s) 85
  - bulging 85
  - decomposition 86
  - entrainment 86
  - landslide 85
  - leaching 86
  - rocking 86
  - root 86
  - subsidence 85
  - weathering 86
  
- Kandaurov's coefficient 182
- Khvalynian clay(s) 148
  
- Laccolith 47
- Landborn formula 127
- Landscape 532
  
- Landslide(s) 85, 449
- Lava field(s) 47
- Lens 75
- Lines of sliding 126
- Liparite 50
- Liquefaction of sand 515
- Lithosphere 16
- Local landscape 532
- Loess loam 377
- Log forms 528
- Long-term stability of soil 395, 483
- Loose soil(s) 368
- Loss of stability 198
  
- Magnitude 501
- Mantle 16
  - lower 16
  - upper 16
- Marble 63
- Marine regression 17
- Marine transgression 17
- Marl 59
- Marly clay(s) 147
- Mathematical statistics 171
- Meander(s) 431
- Mesozoic 35
- Metamorphism 63
  - types of 63
    - contact 63
    - dynamothermal 63
    - regional 63
- Method of circular-cylindrical surface of sliding 355
- Method of controlled deformation 355
- Method of horizontal forces 471
- Method of moments 466
- Method of sounding 535
- Microshift(s) 153
- Mine workings 522
  - adit 523
  - drilling 523
  - shaft 522
  - test 522
  - trench 522
- Mineral(s) 42

- Mineral spring(s) 88  
Mohr's circle(s) 132  
Mohr envelope 132  
Mohr rupture diagram 132  
Moraine 387  
Muck 370  
Mud rock flow(s) 412  
Mudflow slide 464
- Nahledee 393  
    common 398  
    confined-water pressure 398  
    river 398  
Neogene 37  
Normal stress 154
- Obsidian 52  
Ordovician 33  
Orogenesis 17  
    Alpine 28, 67  
    Caledonian 28, 67  
    Hercynian 28, 67  
    Kimmeridgian 28  
Oxide(s) 43
- Paleogene 37  
Paleogeography 27  
Paleozoic 33  
Passive force(s) 356  
Pauker's formula 225  
Peneplain 428  
Permafrost 391  
    dry 396  
Permeability 443  
Permian 33  
Pervious rock(s) 368  
Phenomenological theory 326  
Piezometric surface 94  
Plane footing 279  
Plastic clay(s) 332  
Plastic region(s) 196  
Poisson's ratio 266, 360
- Porosity 380  
Prandtl's scheme 224  
Pressure gradient 246  
Pressure head 93  
Prevention of landslide(s) 479  
    measures of 479  
        active 479  
        passive 479  
        troublesome 479  
Primary loess 377  
Principle of initial pressure 386  
Process(es) 17  
    denudation 22  
    endogenic 17, 20  
    exogenic 17  
    tectonic 17  
Proterozoic 33  
Pseudocreep 323  
Pseudoplastic clay(s) 332  
Pseudoquicksand(s) 129
- Quartz 50  
Quaternary 37  
Quicksand(s) 129, 390
- Rankine's equation 344  
Rectangular footing 279  
Refraction method 533  
Relative density 116  
Relaxation 323  
Residual deformation 181  
Rising source(s) 94  
River terrace(s) 434  
Rock(s) 16  
    argillaceous 368  
    chemical 55  
    clastic 55  
    clayey 55  
    continental 55  
    effusive 45  
    hypabyssal 45  
    igneous 43  
        acidic 43, 50  
        basic 43, 49

- intermediate 44
- superbasic 44
- ultraacidic 44
- intrusive 45
- magmatic 21, 43
- marine 55
- metamorphic 16, 43
- organogenic 55, 59
- plutonic 45
- sedimentary 16, 43
- Rock fall 457
- Rotational slide(s) 465
- Runoff 88, 92
- Safety factor 184
- Sample(s) 525
  - undisturbed 525
- Sand(s) 439
- Sand dune(s) 407
- Sandstone(s) 63
- Sandy loam(s) 57
- Saturation zone 89
- Seepage pressure 470
- Seismicity coefficient 499
- Seismic method(s) 534
- Seismogram 504
- Shear 178, 458
- Shear slide(s) 465
- Shearing resistance capacity 119
- Shearing resistance of soils 537
- Shield(s) 16
  - Ukrainian 16
- Silicate(s) 44
- Silurian 33
- Sinking 225
- Slichter's method 99
- Slide 342
  - contact 342
  - slab 342
- Sliding of stacks 480
- Slippage 460
- Soil(s) 408
  - brown 410
  - chernozem 409
  - chestnut-coloured 410
  - desert 410
  - grey forest 409
  - podzol 409
  - red earth 412
  - sandy 108
  - solonchak 412
  - takyrs 412
  - tundra 409
  - turf-podzol 409
  - wet 108
- Soil moisture horizon 89
- Spectrum of waves 502
- Stability 199
- Stability limit(s) 197
- Stabilometer 130
- Stage 405
- Stiff clay(s) 332
- Stock 47
- Stoke's law 335
- Strata 55
- Strike 76
- Submarine earthquake 495
- Subsidence 380
- Surface of sliding 465
- Surface runoff 88
- Syncline 26
- Syenite(s) 52
- Syneresis 334
- Swelling branch 155
- Talus *or* talus deposit(s) 404
- Talus slopes 542
- Tectonic phases 28
- Tectonic revolution 22
- Terrigene material 73
- Theory
  - Arrhenius 39
  - climatic 39
  - cosmic 39
  - Wegener 39
- Theory of filtrational consolidation 233
- Thickness 72
- Thixotropy 334

- Total moisture capacity 109
- Translational slide 462, 471
- Triassic 35
- Tsunami 495
- Tuffite(s) 54
- Types of geological exploration 521
  - literature 521
  - stored records 521
  
- Van der Waals forces 124
- Vein(s) 47
- Veined shoot 47
- Vertical movement(s) 23
- Vibrocompressor curve 308
- Vibrodrilling 525
- Vitreous texture 49
- Voids ratio 114, 115
- Volcanism 21
  
- Water
  - absorbed 123
  - adsorbed 123
  - condensation 87
  - connate 87
  - free 90
  - gravitational 123
  - hygroscopic 89
  - infiltration 87
  - juvenile 87
  - karst 87
  - pellicular 90
  - quarry 87
  - swamp 92
- Water table 91
- Water vapour 89
- Weathering 54, 400
  - biological 400, 402
  - chemical 54, 400
  - physical 54, 400
- Wegener's hypothesis 39
- Wolf's formula 311
  
- Yield point 328, 331
- Young's modulus 158
  
- Zones of fracture 27

**TO THE READER**

**Mir Publishers would be grateful  
for your comments on the content,  
translation and design of the book.  
We would also be pleased to receive  
any other suggestions you may wish  
to make.**

**Our address is:  
Mir Publishers  
2 Pervy Rizhsky Pereulok  
1-110, GSP, Moscow, 129820  
USSR**